

PHYTOCHEMICAL AND PHARMACOLOGICAL INVESTIGATION OF SELECTED PLANTS AVAILABLE IN THE WESTERN GHATS OF INDIA

A Thesis submitted in partial fulfillment for the Degree of

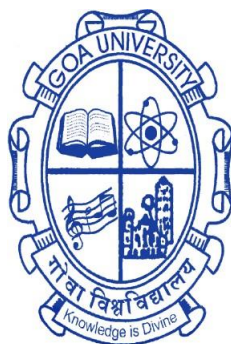
DOCTOR OF PHILOSOPHY

IN

PHARMACY

To

GOA UNIVERSITY



By

LIESL MARIA FERNANDES E MENDONÇA

Goa College of Pharmacy, Government of Goa,

Panaji - Goa.

March 2023

DECLARATION

I, Mrs. Liesl Maria Fernandes e Mendonca, hereby declare that this thesis represents work which has been carried out by me and that it has not been submitted, either in part or full, to any other University or Institution for the award of any research degree.

Place: Panaji - Goa.

Date : 28-03-2023

Mrs. Liesl Maria Fernandes e Mendonça
(M.Pharm in Pharmacology)

CERTIFICATE

I hereby certify that the work was carried out under my supervision and may be placed for evaluation.

Dr. Arun Bhimrao Joshi
(Ph.D. in Pharmaceutical sciences)
Professor and Head,
Department of Pharmacognosy,
Goa College of Pharmacy,
Government of Goa,
Panjim-Goa, 403001.

Affectionately Dedicated to

Almighty God,

My

Loving Family & baba Zayne



ACKNOWLEDGMENT

“If you believe, and have no doubt, you will receive whatever you ask for in prayer.”

Matthew 21:22

*"Ask, and it shall be given you;
Seek, and you shall find;
Knock, and it shall be opened unto you:"*

“For everyone who asks receives; who seeks finds; and who knocks, the door will be opened’.

Matthew 7:7

With immense gratitude in my heart and profound respect, I take this opportunity to acknowledge the contributions of all those who opened their doors and supported me in different ways, whenever I sought them, throughout the fruitful journey of my Ph.D. research work. I firmly believe that these are all God sent angels who helped me overcome every challenge, at times when I needed the most. Special thanks to the laboratory rats used for my study. “It takes a village to raise a child”- Hillary Clinton; Likewise, my work bears the imprint of all those who helped me at every stage to raise and nurture my research babe, and to whom I am extremely grateful.

*At the outset, I express my wholehearted gratitude to my esteemed Guide and mentor, **Dr. Arun Bhimrao Joshi**, Professor and Head, Department of Pharmacognosy, Goa College of Pharmacy for being my guiding light throughout my research tenure. As a father guides and motivates his child, Sir has walked an extra mile with me through thick and thin, accompanying and guiding me at every juncture of my research. I am indeed fortunate to have sir as my research supervisor, with his remarkable enthusiasm, passion for work, intellect, experience, dedication, patience, and pleasant personality. Your contributions will never be forgotten sir and the expertise gained has been embedded and revered forever.*

*I would like to convey my deep gratitude to **Dr. Gopal Krishna Rao** sir, Principal and Head of the Ph.D. research centre, Goa College of Pharmacy, for introducing Ph.D. in Pharmacy programme at our college and providing all the necessary amenities to carry out the research work effectively. Thank you very much sir for your support, motivation, advice and trust in my abilities to accomplish my research goal.*

*I highly acknowledge the contributions by the subject experts of my Doctoral Research Committee, **Dr. Madhusudan P. Joshi**, Professor and Head, Department of Pharmacology, Goa College of Pharmacy and **Dr. Prasanna V. Habbu**, Professor and Head, Department of Pharmacognosy and Phytochemistry, Soniya Education Trust's (SET) College of Pharmacy, Dharwad, for their critical evaluation, timely suggestions, and invaluable feedback in enhancing our research activities. The questions put forth during the periodic DRC meetings, provided an insight to understand and explore additional areas in the research domain.*

*I express my earnest thanks to **Dr. Anant Bhandarkar**, Assistant Professor, Department of Pharmacognosy and Phytochemistry, for his invaluable guidance, support, motivation and sincerity in helping me to carry out my research activities. His knowledge, aptitude, expertise and confidence has inspired me to achieve my targets better with each passing day.*

*I express my deep sense of gratitude to **Dr. Vivek Kamat**, Director, Directorate of Technical Education Goa, and all the authorities of Government of Goa for permitting me to enrol for the Ph.D. programme and granting approvals for presenting my research work at various conferences.*

*I pay special thanks to **Dr. Savita Kerkar**, Dean, School of Biological Sciences and Biotechnology; **Dr. C. Ghadi**, Vice Dean of School of Biological Sciences and Biotechnology and **Dr. Nitin Sawant**, Professor in the Department of*

Zoology for permitting me to use the facilities of the departments of Biotechnology and Zoology to carry out my research work. I would like to acknowledge the contributions of **Dr. Shamshad Shaikh**, Assistant Professor in Zoology and **Dr. Samantha Fernandes D'mello**, Assistant Professor in Biotechnology, Goa University for helping with the animal dissection and guiding me with the biochemical analysis. I am also thankful to the staff of both the departments and Ph.D. research scholars Ms. Manasi, Ms. Preeti, Ms. Noha, etc. who generously shared their utilities and made me comfortable.

I am thankful to **Dr. Sunita Garg**, Emeritus Scientist CSIR-NISCAIR, New Delhi and **Dr. Satyanarayan S. Hebbar**, Department of Botany, Government Pre-university college, Dharwad, Karnataka; for authenticating the plant material for my research work. I also pay my wholehearted gratitude to **Dr. Vijay Kumbhar** and **Dr. Kishore Bhat** from Maratha Mandal Institute of Dental sciences, Belagavi; late **Dr. Sanjay Mishra**, Ex-Professor from Dr. Prabhalkar Kore Basic science Research centre, Belagavi; **Dr. Himanshu Joshi**, Principal and Professor at College of Pharmacy Graphic Era Hill university, Uttarakhand; for facilitating and guiding with the anticancer research activities. I extend my gratitude to late **Dr. Jayadeva sir**, Ex-Professor, SJM College of Pharmacy, Chitradurga; **Dr. Shreenivas M.T** and **Dr. Harish** from Honeychem Pharma Pvt. Ltd., Bengaluru; for facilitating the purification of isolated phytoconstituents and providing the spectral data. A special thanks to **Dr. Avatar Singh** from Sophisticated Analytical Instrumentation Facility (SAIF) and Central Instrumentation Laboratory, Punjab university for assisting and providing the spectral data. A special gratitude to **Dr. Srinivas Joshi**, Professor, Department of Pharmaceutical Chemistry at SET College of Pharmacy, Dharwad; for helping me with the molecular docking activity.

I extend my humble gratitude to the Heads of Departments of Goa College of Pharmacy, **Dr. Sanjay Pai**, Department of Pharmaceutical Chemistry and

*Pharmaceutical analysis and **Dr. Prashant Bhide**, Department of Pharmaceutics for providing the laboratory facility for UV spectroscopic analysis and for motivating and encouraging me to achieve my goal. I wish to thank **Dr. Rupesh Shirodkar** (Professor) and **Dr. Rajashree Gude** (Professor), **Dr. Yogita Sardesai** (Professor), **Dr. Raghuvir Pissurlenkar** (Professor), **Ms. Lorna Silveira** (Associate Professor), **Smt. Teja Walke** (Associate Professor) and **Dr. Titiksh Devale** (Associate Professor), for their affection, care, timely help and guidance. I would also like to acknowledge the encouragement and valuable advice rendered by **Mrs. M.H.S. Godinho** and **Ms. Lilian Almeida**, retired Associate Professors of Goa College of Pharmacy, during their tenure at the institute.*

*I humbly thank **Dr. Madhusudan P. Joshi**, Head of the Department of Pharmacology, Goa College of Pharmacy for permitting me to undertake my research activities and balancing the departmental activities. I extend my deep gratitude to my department colleagues **Smt. Shailaja Mallya**, **Smt. Vedita HegdeDesai**, **Smt. Asmita Arondekar** and **Dr. Damita Cota** for their constant support, encouragement and valuable advice during the completion of my project.*

*I also thank **Dr. Anand Mahajan**, Professor in Department of Pharmaceutical Analysis for his sound advice and help in analysing the spectral data. A special word of appreciation to **Dr. Shailendra Gurav**, Professor in Department of Pharmacognosy and **Dr. Mythili Jedegunta**, Professor in Department of Pharmacognosy for their moral support, enthusiasm, guidance, and motivation throughout my study.*

*I am also grateful to my friends and colleagues **Smt. Nutan Naik** (Assistant Professor) and **Smt. Shweta Borkar** (Assistant Professor) for their motivation, help and affection rendered in times of need. I extend my sincere thanks to **Smt. Sachi Kudchadkar** (Assistant Professor), **Dr. Adison Fernandes** (Assistant Professor), **Shri Rahul Chodankar** (Assistant Professor), **Shri Vitthal Bhandare** (Assistant*

Professor), **Shri Raveendra Hulloikar** (Assistant Professor), **Smt. Seema Shet** (Assistant Professor) **Smt. Saba Jamadar** (Assistant Professor), **Shri Vaibhav Potdar** (Assistant Professor), **Shri Rohan Prabhu** (Assistant Professor) for rendering necessary help and support whenever approached.

Many thanks to my dear student and alumnus **Ms. Isha Kher**, Proprietor Brizz medicals, for going out of her way by helping in arranging and procuring the dedicated rat neurotransmitter and antioxidant enzyme kits from USA to manage complete my biochemical analysis in time. A special thanks to the research scientist at Skanda laboratories, Bengaluru for helping with the acute toxicity studies.

A special gratitude to the current and ex-non-teaching staff of Goa College of Pharmacy, **Shri. Sertorio Colaco**, **Smt. Arlette Baretto**, **Shri Ravindra Kholkar**, **Shri. Dattaraj**, **Smt. Shweta Vaigankar**, **Shri. Mohan Gaude**, **Shri. Trivikram**, **Smt. Rekha**, **Smt. Riya**, **Smt. Jennifer**, **Shri. Succor**, **Smt. Josephine**, **Shri. Vinay**, **Smt. Sarika**, **Shri. Sandesh**, **Smt. Kanchan**, **Smt. Prashanti**, **Smt. Shubhangi**, **Shri Sandip**, **Smt. Maya**, **Smt. Vaishali**, **Smt. Sujata**, **Smt. Manisha**, **Smt. Deepali**, **Smt. Swapnaja**, **Smt. Shilpa**, **Shri. Arjun**, **Smt. Subodini**, **Shri. Gabriel**, **Shri. Praveen**, **Shri. Thomas Martins**, and others for their timely help and support.

I also place on record the support and encouragement received from my fellow Ph.D. Research scholars, **Smt. Rucheera**, **Ms. Gauri**, **Smt. Reema**, **Smt. Anupriya**, **Ms. Pooja**, **Shri. Hozefa** etc. and our present and passed out **M.Pharm research**, **B.Pharm** and **D.Pharm** students.

My sincere thanks to the library staff **Mrs. Maya**, and **Mrs. Vaishali Raut** for providing the reference material, the security guards **Shri. Hitendra** and **Shri. Joseph** for staying back and keeping vigil till I complete my research work. A sincere word of appreciation to **Shri Satyanarayan**, my carpenter who tailored the Light and dark, mirror chamber and holeboard apparatus for my study.

*A special thanks to my uncle **Prof. Dr. Julio B. Fernandes** for his invaluable advice and encouragement during my research. I also remember all my teachers, staff and colleagues from, Our Lady of the Rosary high school- Dona Paula and Primrose primary school, and Goa College of Pharmacy, who have played an important role in moulding me into the person I am today.*

*Words fall short to express my love and appreciation to my family. This work is a tribute to the sacrifices made by each one of you through my Ph. D. journey and I am forever indebted to you all. With a heart filled with affection and gratitude, I would like to thank my **husband Elroy Mendonca** whose support, understanding, zeal and motivation, has helped me in achieving this accolade. To my precious **son Zayne Mendonca**, whose unending love, and support kept me going. To my affectionate and ever-loving **parents Mrs. Antonette and Dr. John Fernandes**, and **parents-in-law Mrs. Annabelle and Mr. Erasmo Mendonca**, for their unconditional love, support, motivation, selfless sacrifices, and blessings bestowed upon me throughout. To my sister **Dr. Samantha Fernandes D'mello**, my brothers in law **Mr. Algernon and Mr. Erwin**, my darling niece and God child **Kaitlyn**, my God mother **Ms. Alcina Monteiro**, and my dear friends **Mrs. Devika Dhond Parrikar and Smita Haldankar**; thank you all very much for all the love, encouragement, guidance and support always. I am also grateful to my extended family for their care and advice all along the way.*

I also place on record, my sincere gratitude to all those who have directly or indirectly lent a helping hand in my research and in the completion of my thesis and my sincere apologies to all those whom I could not mention individually.

Above all, I profoundly thank and praise Almighty GOD for being so kind and compassionate and bestowing his countless blessings upon me to successfully complete my Ph.D. research work, one day at a time...

Thank you one & all

..... MRS. LIESL MARIA FERNANDES E MENDONÇA

ABSTRACT

Plant sources have played a prominent role in research related to the discovery and development of new drugs, alleviating diseases, and improving the quality of life of patients. Polyphenols are secondary metabolites present in plants that act as antioxidants, improve health, and reduce the risk of developing degenerative diseases. The study evaluated the therapeutic potential of the selected plants *Hybanthus enneaspermus* Linn. and *Bauhinia foveolata* Dalzell. for antioxidant, anticancer and anxiolytic activities.

The powder of the whole plant of *H. enneaspermus* and leaves of *B. foveolata* were subjected to extraction with ethanol to yield the ethanolic extract of *H. enneaspermus* (EEHE) and *B. foveolata* (EEBF), respectively. EEHE and EEBF were fractionated with toluene to yield toluene soluble (TFHE, TFBF) and toluene insoluble (ITHE, ITBF) biofractions. The toluene insoluble biofractions were successively fractionated with ethyl acetate and methanol to yield ethyl acetate (EFHE, EFBF) and methanol (MFHE, MFBF) soluble biofractions, respectively. The extracts and biofractions were screened to detect the presence of phytoconstituents, total phenolic and flavonoid content and antioxidant activities using DPPH, Hydrogen peroxide, Nitric oxide and ABTS free radical scavenging assays.

The extracts and biofractions were screened for *in vitro* anticancer activity on MCF-7 (breast cancer), Hop-62 (lung cancer), and HeLa (cervical cancer) cell lines employing antiproliferative sulforhodamine assay, apoptosis, and cell cycle assays by flow cytometry. EEHE, ITHE EEBF, and ITBF were screened for anxiolytic potential using Elevated Plus Maze, Light and Dark Transition, Mirror Chamber Test, Hole board test and Optovarimex screening models at doses of 100, 200, and 400 mg/kg BW in rats. The treatment group of rats exhibiting significant anxiolytic activity after a 30-day trial were

subjected to isolation of the brain, dissection and estimation of neurotransmitters and antioxidant enzymes in the rat brain homogenates.

Column chromatography and preparative HPLC were utilized to isolate constituents from ITHE, MFBF and EBF. The structures of the compounds isolated were elucidated and characterized using IR, $^1\text{H-NMR}$, $^{13}\text{C-NMR}$, and mass spectroscopic methods. The phytoconstituents isolated from ITHE were screened for *in vitro* anticancer activity on MCF-7 (breast cancer), while those from MFBF and EBF were screened against Hop-62 (lung cancer), and HeLa (cervical cancer) cell lines employing antiproliferative sulforhodamine assay, apoptosis, and cell cycle assays by flow cytometry. The isolated phytoconstituent from *H. enneaspermus* and *B. foveolata* displaying significant pharmacological activities in all the above *in vitro* assays, were screened for *in vitro* Caspase-3 activity and DNA fragmentation studies. Molecular level gene expression studies were performed against the compound exhibiting prominent *in vitro* anticancer activity, using β -actin as an internal control reference gene and Bcl-2, Bax and p53 as target genes to confirm the mechanism of action. *In silico* molecular docking using the SYBYL program was used to investigate the binding of all isolated phytoconstituents with the crystal structure of human Caspase-3 for anticancer activity and human GABA_A-BZD receptor for the antianxiety activity to predict the mode of action.

Preliminary phytochemical screening revealed the presence of various phytoconstituents in the ethanolic extracts EEHE, EEBF and their biofractions. EEHE, ITHE, EEBF and ITBF exhibited the maximum phenolic content and flavonoid content. The total phenolic content of the EEHE, ITHE, EEBF and ITBF was found to be 19.41 ± 0.65 , 15.35 ± 0.43 , 49.12 ± 0.31 and 45.58 ± 0.83 mg GAE/g, respectively. The total flavonoid content of the EEHE, ITHE, EEBF and ITBF was found to be 6.38 ± 0.36 , 4.36 ± 0.21 , 28.75 ± 0.42 and 26.58 ± 0.69 mg QUE/g respectively. The results of the study illustrated the efficacy of the extracts and most biofractions to scavenge the DPPH,

hydrogen peroxide, nitric oxide and ABTS free radicals with IC_{50} values $< 100 \mu\text{g/mL}$.

EEHE, TFHE, and ITHE exhibited substantial antiproliferative and apoptotic activities against MCF-7 cells arresting the cells in the G_2/M phase. EEBF, TFBF, EFBF and MFBF demonstrated profound anticancer activity against Hop-62 and HeLa cell lines. MFBF induced apoptosis in Hop-62 cells with $42.24 \pm 0.57 \%$ cells in the early and $4.61 \pm 0.88 \%$ cells in the late-stage apoptosis, comparable to standard Doxorubicin. EFBF exhibited significant antiproliferative activity on HeLa cell lines. It induced significant apoptotic activity ($p < 0.001$) with $11.09 \pm 0.91 \%$ cells in early apoptosis, while $16.38 \pm 0.83 \%$ in late apoptosis after 24 h of treatment as compared to standard Cisplatin.

In the *in vivo* antianxiety studies, ITHE and ITBF at 400 mg/kg significantly reduced anxiety levels comparable to standard Diazepam, as depicted in the various experimental models. Increased levels of dopamine, nor adrenalin, GABA and serotonin and reduced glutamate neurotransmitter levels were observed in the isolated brain tissue homogenates, with a significant increase in expression of GABA levels in the cerebral cortex, hippocampus, pons, medulla oblongata and cerebellum. The extracts also potentiated endogenous antioxidant levels like superoxide dismutase, glutathione peroxidase, catalase, glutathione reductase, and glutathione-s-transferase.

Chromatographic and spectroscopic studies confirmed the isolation of Quercetin, Rutin and Hesperidin from ITHE, while Quercetin, Kaempferol, Isorhamnetin, and β -Glucogallin from MFBF and Gardenin B from EFBF. Hesperidin isolated from ITHE, displayed significant growth inhibition at GI_{50} value of $15.84 \pm 2.81 \mu\text{g/mL}$, with $16.89 \pm 0.88 \%$ and $23.18 \pm 0.43 \%$ cells in early and late apoptotic stages, compared to standard Doxorubicin. Kaempferol isolated from MFBF induced significant activity with $23.03 \pm 0.37 \%$ cells in early apoptosis, $2.11 \pm 0.55 \%$ cells in late apoptosis and $0.51 \pm 0.37 \%$ cells in the necrotic stage, producing cell cycle arrest in S phase. On the HeLa cell lines, EEBF,

TFBF, and EFBF depicted significant antiproliferative activity with $GI_{50} < 10 \mu\text{g/mL}$, and EFBF inducing early apoptosis in $11.09 \pm 0.91 \%$ cells and late apoptosis in $16.38 \pm 0.83 \%$ cells, comparable to standard Cisplatin. Gardenin B, isolated from EFBF, revealed significant antiproliferative and apoptotic activities with $16.53 \pm 1.00 \%$ and $7.22 \pm 0.86 \%$ cells in early and late apoptotic stages, respectively, inducing cell cycle arrest in S-phase. Furthermore, Hesperidin and Gardenin B significantly upregulated the Caspase -3 enzyme and DNA fragmentation in MCF -7 and HeLa cells, respectively. Gardenin B significantly downregulated Bcl-2 gene expression and upregulated p53 and Bax genes in a dose-dependent manner, confirming its apoptotic mode of action.

In silico docking studies with human Caspase-3 enzyme revealed that all compounds occupied the same binding site as standards Doxorubicin and Cisplatin, with a consensus scores between 7.00 - 2.65. Almost all the isolated compounds docked with human GABA_A-BZD receptor exhibited consensus scores between 7.75 - 5.19, indicating the same type of interaction with the GABA_A receptor as that of the standard drug Diazepam, suggesting the probable mechanism of action via GABA_A-BZD-Cl⁻ ion channel receptor. It may thus be concluded that the flavonoids present in the selected medicinal plants are largely responsible for their therapeutic virtues in treating cancer and anxiety.

Keywords: *Hybanthus enneaspermus*, *Bauhinia foveolata*, antioxidant, apoptosis cell cycle, caspase-3, DNA fragmentation, gene expression, anxiolytic, GABA_A-BZD, preparative

Contents

1	Introduction.....	1
1.1	Traditional medicine.....	1
1.1.1	History of traditional medicine.....	1
1.1.2	Advancement of traditional medicine.....	1
1.1.3	Role of natural products.....	2
1.2	Oxidative stress.....	3
1.3	Cancer	5
1.3.1	Carcinogenesis.....	5
1.3.2	Hallmarks of Cancer.....	6
1.3.3	Genes regulating apoptosis and cancer at molecular level.....	7
1.3.4	Breast cancer.....	8
1.3.5	Lung cancer	9
1.3.6	Cervical cancer.....	9
1.3.7	Oxidative stress and Cancer.....	10
1.4	Anxiety	11
1.4.1	Manifestations of anxiety.....	11
1.4.2	Types of anxiety disorders.....	12

1.4.3	Neuroanatomy of anxiety.....	14
1.4.4	GABAergic neurotransmission.....	14
1.4.5	Serotonergic neurotransmission and other neuromodulators	15
1.4.6	Oxidative stress and Anxiety.....	17
1.4.7	Conventional anxiolytic therapy versus potential herbal anxiolytics	17
1.5	Role of flavonoids as therapeutics	18
2	Plant profile.....	22
2.1	<i>Hybanthus enneaspermus</i> Linn	22
2.1.1	Botanical name	22
2.1.2	Synonym.....	22
2.1.3	Vernacular names	22
2.1.4	Taxonomic classification.....	22
2.1.5	Geographical distribution	23
2.1.6	Morphological description	23
2.1.7	Traditional uses	23
2.1.8	Phytoconstituents.....	23
2.1.9	Pharmacological activities.....	24
2.2	<i>Bauhinia foveolata</i> Dalzell	26

2.2.1	Botanical name.....	26
2.2.2	Synonym	26
2.2.3	Vernacular names.....	26
2.2.4	Taxonomic classification	26
2.2.5	Geographical distribution.....	27
2.2.6	Morphological description	27
2.2.7	Traditional uses	28
2.2.8	Phytoconstituents	28
2.2.9	Pharmacological activities	29
3	Review of Literature	30
3.1	Review of <i>Hybanthus enneaspermus</i>	30
3.2	Review of <i>Bauhinia foveolata</i>	58
3.3	Review of the Genus <i>Bauhinia</i>	59
3.4	Review of related pharmacological activities	79
4	Research Objectives	86
5	Materials and Methods	
5.1	Materials	88
5.1.1	Instrumentation.....	88
5.1.2	Chemicals and reagents	88

5.1.3	Cell cultures	89
5.2	Methods.....	90
5.2.1	Collection and authentication of selected medicinal plants..	90
5.2.2	Preparation of extracts and biofractions	90
5.2.3	Qualitative preliminary phytochemical investigation	91
5.2.4	Quantitative phytochemical analysis.....	98
5.2.5	Determination of <i>in vitro</i> antioxidant activity.....	99
5.2.6	Determination of <i>in vitro</i> anticancer activity of extracts and biofractions	101
5.2.7	Acute toxicity studies	104
5.2.8	<i>In vivo</i> antianxiety activity	106
5.2.9	Biochemical estimations in rats' brain homogenates	114
5.2.10	Isolation of Phytoconstituents	118
5.2.11	Determination of <i>in vitro</i> anticancer activity of isolated compounds	126
5.2.12	<i>In silico</i> molecular docking studies: isolated compounds	129
5.2.13	Statistical analysis	130
6	Results	131
6.2.1	Collection and authentication of <i>H. enneaspermus</i> and <i>B. foveolata</i>	131
6.2.2	Preparation of extracts and biofractions	131

6.2.3	Qualitative preliminary phytochemical investigation.....	131
6.2.4	Quantitative phytochemical analysis.....	131
6.2.5	Determination of <i>in vitro</i> antioxidant activity	132
6.2.6	<i>In vitro</i> anticancer activities of the ethanolic extracts and biofractions	136
6.2.7	Acute toxicity studies.....	164
6.2.8	<i>In vivo</i> antianxiety studies.....	166
6.2.9	Biochemical estimation.....	184
6.2.10	Isolation and structural elucidation of phytoconstituents	194
6.2.11	<i>In vitro</i> anticancer activities of the isolated compounds.....	297
6.2.12	<i>In silico</i> molecular docking studies.....	331
7	Discussion.....	354
8	Conclusion.....	374
9	Future Prospective	376
10	References	377
11	Annexures	
	I. Authentication Certificate of <i>Hybanthus enneaspermus</i>	
	II. Authentication Certificate of <i>Bauhinia foveolata</i>	
	III. IAEC approval for antianxiety studies	
	IV. IAEC approval for acute toxicity studies	

V. Publications

VI. Presentations

LIST OF ABBREVIATIONS

5-HT:	5-Hydroxytryptamine
ABTS:	2,2'azino-bis (3-ethylbenzothiozoline-6-sulfonic acid)
Ach:	Acetylcholine
ACTH:	Adrenocorticotropic hormone
AgNO ₃ :	Silver nitrate
ALA:	Alanine
ALT:	Alanine amino transaminase
ANOVA:	Analysis of variance
APC:	Antigen presenting cell
APX:	Ascorbate peroxidase
ARG:	Arginine
ASN:	Asparagine
ASP:	Aspartic acid
AST:	Aspartate aminotransferase
AT:	Ambulatory Time
ATP:	Adenosine triphosphate
BAX:	BCL-2 associated x protein
BBB:	Blood-brain barrier
BLC:	B lymphoblastic cell
BLM:	Basolateral membrane
BPAE:	<i>B. purpurea</i> alcoholic extract
BRCA:	Breast Cancer gene
BSA:	Bovine serum albumin

BW:	Body weight
BZD:	Benzodiazepines
¹³ C:	Carbon-13 isotope
CAT:	Catalase
CB:	Cerebellum
CC:	Cerebral cortex
CK:	Creatine kinase
Cl ⁻ :	Chloride
Cm ⁻¹ :	Waves per centimeter
CNS:	Central nervous system
Conc.:	Concentrated
CPCSEA:	Committee for the Purpose of Control and Supervision of Experiments on Animals
CT:	Computed tomography
CuO:	Cupric oxide
DAL:	Dalton's ascitic lymphoma
DAPI:	4-,6-diamidino-2-phenylindole
DLS:	Dynamic light scattering
DMBA:	Dimethylbenzanthracene
DMEM:	Dulbecco's Modified Eagle Media
DMSO:	Dimethyl sulfoxide
DNA:	Deoxyribonucleic acid
DPPH:	2,2-diphenyl-1-picrylhydrazyl
DT:	Distance Travelled
DW:	Distilled water
EAC:	Ehrlich Ascites Carcinoma
EBV:	Ethanollic extract of <i>B. variegata</i> .
EDTA:	Ethylenediaminetetraacetic acid

EDX:	Energy-dispersive X-ray
EEBF:	Ethanollic leaf extract of <i>Bauhinia foveolata</i> Dalzell.
EFBF:	Ethylacetate soluble fraction of ethanolic extract of <i>Bauhinia foveolata</i> Dalzell.
ELISA:	Enzyme-linked immunosorbent assay
EO:	<i>Emblica officinalis</i>
EPM:	Elevated plus maze
ER:	Estrogen receptor
FBS:	Fetal bovine serum
FITC:	Fluorescein isothiocyanate
FRAP:	Ferric reducing antioxidant power
FTIR:	Fourier transform infrared spectroscopy
g:	Gram
G6PDH:	Glucose-6-phosphate dehydrogenase
GAD:	Generalized Anxiety Disorder
GAE:	Gallic acid equivalent per gram
GCMS:	Gas chromatography mass spectrometry
GI ₅₀ :	Growth inhibitory 50%
GLU:	Glutamic acid
GPx:	Glutathione peroxidase
GR:	Glutathione reductase
GS:	Glutathione synthetase
GSH:	Glutathione
GST:	Glutathione S-transferase
h:	Hours
¹ H NMR:	Proton nuclear magnetic resonance
H ₂ O ₂ :	Hydrogen peroxide
H ₂ SO ₄ :	Sulphuric acid

HBT:	Hole Board Test
HCl:	Hydrochloric acid
HCT-15:	Human colon cancer cell lines
HeLa:	Human cervical adenocarcinoma cell line
HER2:	Human epidermal growth factor receptor 2
HIS:	Histidine
Hop-62:	Human lung cancer cell line
HP:	Hippocampus
HPLC:	High-performance liquid chromatography
HPV:	Human papillomavirus
HR-ESI-MS:	High-resolution Electrospray Ionization Mass Spectrometry
HSV-I:	<i>Herpes simplex</i> virus type I
HT-29:	Human colorectal adenocarcinoma cell line
IBM© SPSS:	International business machine statistical package for the social sciences
IC ₅₀ :	Half maximal inhibitory concentration
ICP-OES:	Inductively coupled plasma- Optical emission spectrometry
<i>i.p.</i> :	Intraperitoneal
IR:	Infrared
IU:	International Unit
KBr:	Potassium bromide
Kg:	Kilogram
KVAT:	Krishna Valley Agro Tech
L:	Litre
LC-MS:	Liquid chromatography-mass spectrometry
LD ₅₀ :	Lethal Dose, 50%

LDH:	Lactate dehydrogenase
L-Dopa:	Levodopa
LDT:	Light and dark transition
LYS:	Lysine
M:	Molar
MABA:	Microplate Alamar Blue assay
MBC:	Metastatic breast cancer
MCF-7:	Human breast cancer cell line
MCT:	Mirror chamber Test
MFBF:	Methanol soluble fraction of ethanolic extract of <i>Bauhinia foveolata</i> Dalzell
µg:	Microgram
µL:	Microliter
µM:	Micromolar
mg:	Milligram
MIC:	Minimal inhibitory concentration
Min:	Minute(s)
mL:	Milliliter
mM:	Millimolar
MTT:	3- (4, 5-dimethylthiazol-2-yl)-2, 5 (diphenyltetrazolium bromide)
N:	Normality
NAA:	1-Naphthaleneacetic acid
NaCl:	Sodium Chloride
NADPH:	Nicotinamide Di phosphate
NE:	Norepinephrine
ng:	Nanogram
NJE:	<i>Nardostachys jatamansi</i> extract

NLE:	Number of light box entries
nm:	Nanometer
NME:	Number of mirrored chamber entries
NMR:	Nuclear magnetic resonance
NO:	Nitric oxide
NOE:	Number of open arm entries
NSCLC:	Non-small cell lung cancer
OD:	Optical density
OECD:	Organization for Economic Cooperation and Development
OGTT:	Oral glucose tolerance test
OPV:	Optovarimex model
PBS:	Phosphate buffer saline
PDB:	Protein Data bank
PFA:	Paraformaldehyde
pg:	Picogram
PHE:	Phenylalanine
PI:	Propidium iodide
PKM2:	Pyruvate kinase M2
PM:	Pons and Medulla Oblongata
p.o.:	Per oral
PR:	Progesterone receptor
PTEN:	Phosphatase and tensin homolog
PTSD:	Post-Traumatic Stress Disorder
PTSL:	Percent time spent in light box
PTSM:	Percent time spent in the mirrored chamber
PTSO:	Percent time spent in open arm
RAPD:	Random amplified polymorphic DNA

RB:	Retinoblastoma protein
RME:	Remaining methanol extract
RNA (hTR):	Ribonucleic acid (Human telomerase RNA)
<i>rolB</i> and <i>rolC</i> :	Root oncogenic loci (<i>rol</i>) genes
ROS:	Reactive oxygen species
Rpm:	Rotations per minute
RPMI:	Roswell Park Memorial Institute
RT:	Room temperature
RT-PCR:	Reverse transcription-polymerase chain reaction
s:	Seconds
SD:	Standard deviation
SDS-PAGE:	Sodium dodecyl-sulfate polyacrylamide gel electrophoresis
SER:	Serine
SGOT:	Serum glutamate oxaloacetic transaminase
SGPT:	Serum glutamate pyruvate transaminase
SOD:	Superoxide dismutase
<i>Sp.</i> :	<i>Species</i>
SRB:	Sulforhodamine B
SSRIs:	Selective serotonin reuptake inhibitors
STZ:	Streptozotocin
SOD:	Super oxide dismutase
TAC:	Total antioxidant capacity
TBRAS:	Thiobarbituric acid reactive substances
TCA:	Trichloroacetic acid
TEM:	Transmission electron microscopy
TFBF:	Toluene soluble fraction of ethanolic extract of <i>Bauhinia foveolata</i> Dalzell.

THR:	Threonine
TiO ₂ :	Titanium dioxide
TLC:	Thin layer chromatography
TMB:	Tetramethylbenzidine
TRH:	Thyrotropin-releasing hormone
TRP:	Tryptophan
TSH:	Thyroid stimulating hormone
TYR:	Tyrosine
UPLC:	Ultra performance liquid chromatography
UV-Vis:	Ultraviolet - Visible
WBC:	White blood cell
WHO:	World Health Organization
XRD:	X-ray diffraction
ZnO:	Zinc oxide

List of Tables

1.1	Types of anxiety disorders.	13
1.2	Flavonoids and their possible pharmacological activities.	20
2.1	Traditional uses of <i>H. enneaspermus</i>	24
5.1	Experimental design for acute toxicity activity.	105
5.2	Experimental design for antianxiety activity.....	107
5.3	Optimisation of solvent system for separation of ITHE phytoconstituents.	118
5.4	Instrumental conditions for purification of LMH by Preparative HPLC.	119
5.5	Gradient elution programme for purification of LMH by Preparative HPLC.	120
5.6	Optimisation of solvent system for separation of phytoconstituents in MFBF.	121
5.7	Instrumental conditions for purification of LMF by Preparative HPLC.	122
5.8	Gradient elution programme for purification of LMF by Preparative HPLC.	123
5.9	Optimisation of solvent system for separation of phytoconstituents in EFBF.	123
5.10	Instrumental conditions for purification of LME by Preparative HPLC.	125
5.11	Gradient elution programme for purification of LME by Preparative HPLC.	125
6.1	Preliminary phytochemical screening of EEHE and its	

	biofractions.	133
6.2	Preliminary phytochemical screening of EEBF and its biofractions. ..	133
6.3	Free radical scavenging analysis of EEHE and biofractions.	134
6.4	Free radical scavenging analysis of EEBF and biofractions.	135
6.5	Antiproliferative of EEHE and its biofractions on MCF-7 cell lines.	136
6.6	Apoptosis analysis of EEHE and its biofractions on MCF-7 cell lines.	138
6.7	Cell cycle analysis of EEHE and its biofractions on MCF-7 cell lines.	140
6.8	Growth control of Hop-62 cells by EEHE and its biofractions.	142
6.9	Growth control of HeLa cell lines by EEHE and biofractions..	144
6.10	Growth control of MCF-7 cells by EEBF and its biofractions	146
6.11	Growth control of Hop-62 cells by EEBF and its biofractions.	148
6.12	Apoptosis analysis of EEBF and its biofractions on Hop-62 cell lines	150
6.13	Cell cycle analysis of EEBF and biofractions on Hop-62 cell lines.	152
6.14	Growth control of HeLa cell by EEBF and its biofractions.	154
6.15	Apoptosis analysis of EEBF and its biofractions on HeLa cell lines.	156
6.16	Cell cycle analysis of EEBF and its biofractions on HeLa cell lines.	158
6.17	Growth control of normal cell lines by EEHE and its biofractions.....	160
6.18	Growth control of normal cell lines by EEBF and its biofractions.	162
6.19	Summary of clinical signs and mortality in animals during 14 days observation period.	164
6.20	Summary of body weight of animals in Mean \pm SD (gm).	165

6.21	Summary of weekly feed consumption in animals.	165
6.22	Effect of EEHE, ITHE, control and Diazepam on NOE in EPM.	166
6.23	Effect of EEBF, ITBF, control and Diazepam on NOE in EPM.	167
6.24	Effect of EEHE, ITHE, control and Diazepam on PTSO in EPM.	168
6.25	Effect of EEBF, ITBF, control and Diazepam on PTSO in EPM.	169
6.26	Effect of EEHE, ITHE, control and Diazepam on NLE in LDT.	170
6.27	Effect of EEBF, ITBF, control and Diazepam on NLE in LDT.	171
6.28	Effect of EEHE, ITHE, control and Diazepam on PTSL in LDT.	172
6.29	Effect of EEBF, ITBF, control and Diazepam on PTSL in LDT.	173
6.30	Effect of EEHE, ITHE, control and Diazepam on NME in MCT.	174
6.31	Effect of EEBF, ITBF, control and Diazepam on NME in MCT.	175
6.32	Effect of EEHE, ITHE, control and Diazepam on PTSM in MCT.	176
6.33	Effect of EEBF, ITBF, control and Diazepam on PTSM in MCT.	177
6.34	Effect of EEHE, ITHE, control and Diazepam on head dips in HBT.	178
6.35	Effect of EEBF, ITBF, control and Diazepam on head dips in HBT.	179
6.36	Effect of EEHE, ITHE, control and Diazepam on DT (cm) in OVT.	180
6.37	Effect of EEBF, ITBF, control and Diazepam on DT (cm) in OVT.	181
6.38	Effect of EEHE, ITHE, control and Diazepam on ST (s) in OVT.	182
6.39	Effect of EEBF, ITBF, control and Diazepam on AT (s) in OVT.	183
6.40	Effect of ITHE, ITBF, control and Diazepam treatments on Catalase enzyme levels (U/mg of protein) in rats' brain.	184
6.41	Effect of ITHE, ITBF, control and Diazepam treatments on Superoxide enzyme levels (U/mg of protein) in rats' brain.	185
6.42	Effect of ITHE, ITBF, control and Diazepam treatments on Glutathione-S-transferase enzyme levels (U/mg of protein) in rats' brain.	186
6.43	Effect of ITHE, ITBF, control and Diazepam treatments on Glutathione peroxidase enzyme levels (U/mg of protein)	

	in rats' brain.	187
6.44	Effect of ITHE, ITBF, control and Diazepam treatments on Glutathione reductase enzyme levels (U/mg of protein) in rats' brain.	188
6.45	Effect of ITHE, ITBF, control and Diazepam treatments on Nor adrenaline levels (ng/g of wet tissue) in rats' brain.	189
6.46	Effect of ITHE, ITBF, control and Diazepam treatments on Dopamine levels (ng/g of wet tissue) in rats' brain.	190
6.47	Effect of ITHE, ITBF, control and Diazepam treatments on Serotonin levels (ng/g of wet tissue) in rats' brain.	191
6.48	Effect of ITHE, ITBF, control and Diazepam treatments on GABA levels ($\mu\text{g/g}$ of wet tissue) in rats' brain.	192
6.49	Effect of ITHE, ITBF, control and Diazepam treatments on Glutamate levels ($\mu\text{g/g}$ of wet tissue) in rats' brain.	193
6.50	$^1\text{H-NMR}$ data of isolated compound LMH1.	197
6.51	$^{13}\text{C-NMR}$ data of isolated compound LMH1.	198
6.52	$^1\text{H-NMR}$ data of isolated compound LMH2.	209
6.53	$^{13}\text{C-NMR}$ data of isolated compound LMH2.	209
6.54	$^1\text{H-NMR}$ data of isolated compound LMH3.	223
6.55	$^{13}\text{C-NMR}$ data of isolated compound LMH3.	224
6.56	$^1\text{H-NMR}$ data of isolated compound LMF1.	240
6.57	$^{13}\text{C-NMR}$ data of isolated compound LMF1.	241
6.58	$^1\text{H-NMR}$ data of isolated compound LMF2.	249
6.59	$^{13}\text{C-NMR}$ data of isolated compound LMF2.	250
6.60	$^1\text{H-NMR}$ data of isolated compound LMF3.	260
6.61	$^{13}\text{C NMR}$ of the isolated compound LMF3	261
6.62	$^1\text{H-NMR}$ data of isolated compound LMF4.	273
6.63	$^{13}\text{C-NMR}$ data of isolated compound LMF4.	274

6.64	¹ H-NMR data of isolated compound LME1.	286
6.65	¹³ C-NMR data of isolated compound LME1.	287
6.66	Growth control of MCF-7 cell lines by ITHE isolates.	297
6.67	Apoptosis analysis of ITHE isolates on MCF-7 cell lines.	299
6.68	Cell cycle analysis of ITHE isolates on MCF-7 cell lines	301
6.69	Growth control of Hop-62 cell lines by EFBF isolates.	303
6.70	Apoptosis analysis of MFBF isolates on Hop-62 cell lines.	305
6.71	Cell cycle analysis of MFBF isolates on Hop-62 cell lines.	307
6.72	Growth control of Hop-62 cell lines by EFBF isolate (LME1).	309
6.73	Apoptosis analysis EFBF isolate (LME1) on Hop-62 cell lines.	309
6.74	Cell cycle analysis of EFBF isolate (LME1) against Hop-62 cells. ...	310
6.75	Growth control of HeLa cell lines by MFBF isolates.	312
6.76	Apoptosis analysis of MFBF isolated compounds on HeLa cell lines.	314
6.77	Cell cycle analysis of MFBF isolated compounds on HeLa cell lines.	316
6.78	Growth control of HeLa cell lines by EFBF isolate (LME1).....	318
6.79	Apoptosis analysis of EFBF isolate (LME1) against HeLa cell lines.	318
6.80	Cell cycle analysis of EFBF isolate (LME1) against HeLa cell lines.	319
6.81	Growth control of normal cell lines by ITHE isolates.	321
6.82	Growth control of normal cell lines by MFBF and EFBF isolates	323
6.83	Gene expression analysis using Real Time PCR.	327
6.84	Surflex Docking score (Kcal/mol) of the isolated compounds with Caspase-3 enzyme.....	343
6.85	Surflex Docking score (Kcal/mol) of isolated compounds with GABA _A receptor.....	353

List of Figures

2.1	Morphological parts of <i>Hybanthus enneaspermus</i>	25
2.2	Morphological parts of <i>Bauhinia foveolata</i>	29
5.1	<i>Hybanthus enneaspermus</i> Linn. - Extraction and fractionation	92
5.2	<i>Bauhinia foveolata</i> Dalzell. - Extraction and fractionation	92
5.3	Elevated Plus Maze apparatus.	109
5.4	Light and Dark apparatus.....	109
5.5	Mirror chamber apparatus.....	110
5.6	Holeboard apparatus.	110
5.7	Optovarimex (Autotrack) apparatus.	111
5.8	Isolation of rats in individual cages.	111
5.9	Biochemical estimation of antioxidant enzymes and neurotransmitters in rats, brain.	117
6.1	Free radical scavenging activities of EEHE and biofractions.	134
6.2	Free radical scavenging activities of EEBF and biofractions.....	135
6.3	Antiproliferative activity of EEHE and its biofractions against MCF-7 cell lines.	136
6.4	Morphological changes of MCF-7 cells treated with EEHE and its biofractions... ..	137
6.5	Apoptosis activity of EEHE and its biofractions against MCF-7 cell lines.....	138
6.6	Apoptosis analysis of EEHE and biofractions against MCF-7 cell lines.	139
6.7	Cell cycle activity of EEHE and its biofractions against MCF-7 cell lines.....	140
6.8	Cell cycle analysis of EEHE and biofractions on MCF-7 cell lines.....	141
6.9	Antiproliferative activity of EEHE and its biofractions against Hop-62 cell lines.	142
6.10	Morphological changes of Hop-62 cells treated with EEHE and its biofractions. .	143
6.11	Antiproliferative activity of EEHE and biofractions against HeLa cell lines.	144
6.12	Morphological changes of HeLa cells treated with EEHE and its biofractions. ...	145

6.13	Antiproliferative analysis of EEBF and biofractions against MCF-7 cell lines. ...	146
6.14	Morphological changes of MCF-7 cells treated with EEBF and biofractions.	147
6.15	Antiproliferative activity of EEBF and biofractions against Hop-62 cell lines. ...	148
6.16	Morphological changes of Hop-62 cells treated with EEBF and its biofractions.	149
6.17	Apoptosis assay of EEBF and biofractions against Hop-62 cell lines.	150
6.18	Apoptosis analysis of EEBF and biofractions against Hop-62 cell lines.	151
6.19	Cell cycle assay of EEBF and biofractions against Hop-62 cell lines.	152
6.20	Cell cycle analysis of EEBF and biofractions against Hop-62 cell lines.	153
6.21	Antiproliferative activity of EEBF and its biofractions against HeLa cell lines. ..	154
6.22	Morphological changes of HeLa cells treated with EEBF and its biofractions. ...	155
6.23	Apoptosis activity of EEBF and its biofractions against HeLa cell lines.	156
6.24	Apoptosis analysis of EEBF and its biofractions against HeLa cell lines.	157
6.25	Cell cycle activity of EEBF and its biofractions against HeLa cell lines.	158
6.26	Cell cycle analysis of EEBF and its biofractions against HeLa cell lines.	159
6.27	Antiproliferative activity of EEHE and its biofractions against normal cell lines.	160
6.28	Morphological changes of normal cells treated with EEHE and its biofractions. .	161
6.29	Antiproliferative activity of EEBF and its biofractions against normal cell lines.	162
6.30	Morphological changes of normal cells treated with EEBF and its biofractions. .	163
6.31	Effect of EEHE, ITHE controls and Diazepam on number of open arm entries (NOE) using Elevated Plus Maze model.	166
6.32	Effect of EEBF, ITBF, control and Diazepam on number of open arm entries (NOE) using Elevated Plus Maze model.	167
6.33	Effect of EEHE, ITHE, control and Diazepam on percent time spent in open arm (PTSO) using Elevated Plus Maze model.	168
6.34	Effect of EEBF, ITBF, control and Diazepam on percent time spent in open arm (PTSO) using Elevated Plus Maze model.	169
6.35	Effect of EEHE, ITHE, control and Diazepam on number of light box entries (NLE) using Light and Dark transition model.	170

6.36	Effect of EEBF, ITBF, control and Diazepam on number of light box entries (NLE) using Light and Dark transition model.	171
6.37	Effect of EEHE, ITHE, control and Diazepam on percent time spent in light box (PTSL) using Light and Dark transition model.	172
6.38	Effect of EEBF, ITBF, control and Diazepam on percent time spent in light box (PTSL) using Light and Dark transition model.	173
6.39	Effect of EEHE, ITHE, control and Diazepam on number of mirrored chamber entries (NME) using Mirror chamber test model.	174
6.40	Effect of EEBF, ITBF, control and Diazepam on number of mirrored chamber entries (NME) using Mirror chamber test model.	175
6.41	Effect of EEHE, ITHE, control and Diazepam on percent time spent in mirror chamber (PTSM) using Mirror chamber test model.	176
6.42	Effect of EEBF, ITBF, control and Diazepam on percent time spent in mirror chamber using (PTSM) Mirror chamber test model.	177
6.43	Effect of EEHE, ITHE, control and Diazepam on number of head dips using Hole board test model.	178
6.44	Effect of EEBF, ITBF, control and Diazepam on number of head dips using Hole board test model.	179
6.45	Effect of EEHE, ITHE, control and Diazepam on distance travelled (DT) using Optovarimex model.	180
6.46	Effect of EEBF, ITBF, control and Diazepam on distance travelled (DT) using Optovarimex model.	181
6.47	Effect of EEHE, ITHE, control and Diazepam on ambulatory time (AT) using Optovarimex model.	182
6.48	Effect of EEBF, ITBF, control and Diazepam on ambulatory time (AT) using Optovarimex model.	183
6.49	Effect of ITHE, ITBF, control and Diazepam on Catalase enzyme levels in rats' brain.	184

6.50	Effect of ITHE, ITBF, control and Diazepam on Superoxide enzyme levels in rats' brain.	185
6.51	Effect of ITHE, ITBF, control and Diazepam on Glutathione-S-transferase enzyme levels in rats' brain.	186
6.52	Effect of ITHE, ITBF, control and Diazepam on Glutathione peroxidase enzyme levels in rats' brain.	187
6.53	Effect of ITHE, ITBF, control and Diazepam on Glutathione reductase enzyme levels in rats' brain.	188
6.54	Effect of ITHE, ITBF, control and Diazepam on Nor adrenaline levels in rats' brain.	189
6.55	Effect of ITHE, ITBF, control and Diazepam on Dopamine levels in rats' brain.	190
6.56	Effect of ITHE, ITBF, control and Diazepam on Serotonin levels in rats' brain.	191
6.57	Effect of ITHE, ITBF, control and Diazepam on GABA levels in rats' brain.	192
6.58	Effect of ITHE, ITBF, control and Diazepam on Glutamate levels in rats' brain.	193
6.59	Isolation of phytoconstituents from ITHE.	194
6.60	Preparative HPLC chromatogram of LMH (ITHE purified fraction).	195
6.61	Structure of Quercetrin.	196
6.62	IR spectrum of LMH1 (Quercetrin).	199
6.63	¹ H-NMR spectrum of LMH1 (Quercetrin).	200
6.64	Resolution of ¹ H-NMR spectrum of LMH1 (Quercetrin).	201
6.65	Resolution of ¹ H-NMR spectrum of LMH1 (Quercetrin).	202
6.66	Resolution of ¹ H-NMR spectrum of LMH1 (Quercetrin).	203
6.67	¹³ C-NMR spectrum of LMH1 (Quercetrin).	204
6.68	Resolution of ¹³ C-NMR spectrum of LMH1 (Quercetrin).	205

6.69	Resolution of ¹³ C-NMR spectrum of LMH1 (Quercetrin).	206
6.70	Mass spectrum of LMH1 (Quercetrin).	207
6.71	Structure of Rutin.	208
6.72	IR spectrum of LMH2 (Rutin).	211
6.73	¹ H-NMR spectrum of LMH2 (Rutin).	212
6.74	Resolution of ¹ H-NMR spectrum of LMH2 (Rutin).	213
6.75	Resolution of ¹ H-NMR spectrum of LMH2 (Rutin).	214
6.76	Resolution of ¹ H-NMR spectrum of LMH2 (Rutin).	215
6.77	Resolution of ¹ H-NMR spectrum of LMH2 (Rutin).	216
6.78	Resolution of ¹ H-NMR spectrum of LMH2 (Rutin).	217
6.79	¹³ C-NMR spectrum of LMH2 (Rutin).	218
6.80	Resolution of ¹³ C-NMR spectrum of LMH2 (Rutin).	219
6.81	Resolution of ¹³ C-NMR spectrum of LMH2 (Rutin).	220
6.82	Mass spectrum of LMH2 (Rutin).	221
6.83	Structure of Hesperidin.	222
6.84	IR spectrum of LMH3 (Hesperidin).	226
6.85	¹ H-NMR spectrum of LMH3 (Hesperidin).	227
6.86	Resolution of ¹ H-NMR spectrum of LMH3 (Hesperidin).	228
6.87	Resolution of ¹ H-NMR spectrum of LMH3 (Hesperidin).	229
6.88	Resolution of ¹ H-NMR spectrum of LMH3 (Hesperidin).	230
6.89	¹³ C-NMR spectrum of LMH3 (Hesperidin).	231
6.90	Resolution of ¹³ C-NMR spectrum of LMH3 (Hesperidin).	232
6.91	Resolution of ¹³ C-NMR spectrum of LMH3 (Hesperidin).	233
6.92	Resolution of ¹³ C-NMR spectrum of LMH3 (Hesperidin).	234
6.93	Resolution of ¹³ C-NMR spectrum of LMH3 (Hesperidin).	235
6.94	Mass spectrum of LMH3 (Hesperidin).	236
6.95	Isolation of phytoconstituents from MFBF.	237
6.96	Preparative HPLC chromatogram of LMF (MFBF purified fraction).	238

6.97	Structure of Quercetin.	239
6.98	IR spectrum of LMF1 (Quercetin).	242
6.99	¹ H-NMR spectrum of LMF1 (Quercetin).	243
6.100	Resolution of ¹ H-NMR spectrum of LMF1 (Quercetin).	244
6.101	Resolution of ¹ H-NMR spectrum of LMF1 (Quercetin).	245
6.102	¹³ C-NMR spectrum of LMF1 (Quercetin).	246
6.103	Mass spectrum of LMF1 (Quercetin).	247
6.104	Structure of Kaempferol.	248
6.105	IR spectrum of LMF2 (Kaempferol).	251
6.106	¹ H-NMR spectrum of LMF2 (Kaempferol).	252
6.107	Resolution of ¹ H-NMR spectrum of LMF2 (Kaempferol).	253
6.108	Resolution of ¹ H-NMR spectrum of LMF2 (Kaempferol).	254
6.109	¹³ C-NMR spectrum of LMF2 (Kaempferol).	255
6.110	Resolution of ¹³ C-NMR spectrum of LMF2 (Kaempferol).	256
6.111	Resolution of ¹³ C-NMR spectrum of LMF2 (Kaempferol).	257
6.112	Mass spectrum of LMF2 (Kaempferol).	258
6.113	Structure of Isorhamnetin.	259
6.114	IR spectrum of LMF3 (Isorhamnetin).	262
6.115	¹ H-NMR spectrum of LMF3 (Isorhamnetin).	263
6.116	Resolution of ¹ H-NMR spectrum of LMF3 (Isorhamnetin).	264
6.117	Resolution of ¹ H-NMR spectrum of LMF3 (Isorhamnetin).	265
6.118	Resolution of ¹ H-NMR spectrum of LMF3 (Isorhamnetin).	266
6.119	¹³ C-NMR spectrum of LMF3 (Isorhamnetin).	267
6.120	Resolution of ¹³ C-NMR spectrum of LMF3 (Isorhamnetin).	268
6.121	Resolution of ¹³ C-NMR spectrum of LMF3 (Isorhamnetin).	269
6.122	Resolution of ¹³ C-NMR spectrum of LMF3 (Isorhamnetin).	270
6.123	Mass spectrum of LMF3 (Isorhamnetin).	271
6.124	Structure of β -Glucogallin.	272

6.125	IR spectrum of LMF4 (β -Glucogallin).	275
6.126	^1H -NMR spectrum of LMF4 (β -Glucogallin).	276
6.127	Resolution of ^1H -NMR spectrum of LMF4 (β -Glucogallin).	277
6.128	Resolution of ^1H -NMR spectrum of LMF4 (β -Glucogallin).	278
6.129	^{13}C -NMR spectrum of LMF4 (β -Glucogallin).	279
6.130	Resolution of ^{13}C -NMR spectrum of LMF4 (β -Glucogallin).	280
6.131	Resolution of ^{13}C -NMR spectrum of LMF4 (β -Glucogallin).	281
6.132	Mass spectrum of LMF4 (β -Glucogallin).	282
6.133	Isolation of phytoconstituent from EFBF.	283
6.134	Preparative HPLC chromatogram of LME (EFBF purified fraction).	284
6.135	Structure of Gardenin B	285
6.136	IR spectrum of LME1 (Gardenin B).	288
6.137	^1H -NMR spectrum of LME1 (Gardenin B).	289
6.138	Resolution of ^1H -NMR spectrum of LME1 (Gardenin B).	290
6.139	Resolution of ^1H -NMR spectrum of LME1 (Gardenin B).	291
6.140	^{13}C -NMR spectrum of LME1 (Gardenin B).	292
6.141	Resolution of ^{13}C -NMR spectrum of LME1 (Gardenin B).	293
6.142	Resolution of ^{13}C -NMR spectrum of LME1 (Gardenin B).	294
6.143	Resolution of ^{13}C NMR spectrum of LME1 (Gardenin B).	295
6.144	Mass spectrum of LME1 (Gardenin B).	296
6.145	Antiproliferative activity of ITHE isolates against MCF-7 cell lines.	297
6.146	Morphological changes of MCF-7 cells treated with ITHE isolates.	298
6.147	Apoptosis activity of ITHE isolates against MCF-7 cell lines.	299
6.148	Apoptosis analysis of ITHE isolates against MCF-7 cell lines.	300
6.149	Cell cycle activity of ITHE isolates against MCF-7 cell lines.	301
6.150	Cell cycle analysis of ITHE isolates against MCF-7 cell lines.	302
6.151	Antiproliferative assay of MFBF isolates against Hop-62 cell lines.	303
6.152	Morphological changes of Hop-62 cells treated with MFBF isolates.	304

6.153	Apoptosis activity of MFBF isolates against Hop-62 cell lines.	305
6.154	Apoptosis analysis of MFBF isolates against Hop-62 cell lines.	306
6.155	Cell cycle assay of MFBF isolates against Hop-62 cell lines.	307
6.156	Cell cycle analysis of MFBF isolates against Hop-62 cell lines.	308
6.157	Apoptosis activity of EFBF isolate (LME1) against Hop-62 cell lines.	309
6.158	Cell cycle activity of EFBF isolate (LME1) against Hop-62 cell lines.	310
6.159	Morphological changes of Hop-62 cells treated with EFBF isolate (LME1).	311
6.160	Apoptosis analysis of EFBF isolate (LME1) against Hop-62 cell lines.	311
6.161	Cell cycle analysis of EFBF isolate (LME1) against Hop-62 cell lines.	311
6.162	Antiproliferative activity of MFBF isolates against HeLa cell lines.	312
6.163	Morphological changes of HeLa cells treated with MFBF isolates.	313
6.164	Apoptosis activity of MFBF isolates against HeLa cell lines.	314
6.165	Apoptosis analysis of MFBF isolates against HeLa cell lines.	315
6.166	Cell cycle activity of MFBF isolates against HeLa cell lines.	316
6.167	Cell cycle analysis of MFBF isolates against HeLa cell lines.	317
6.168	Apoptosis activity of EFBF isolate (LME1) against HeLa cell lines.	318
6.169	Cell cycle activity of EFBF isolate (LME1) against HeLa cell lines.	319
6.170	Morphological changes of HeLa cells treated with EFBF isolate (LME1).	320
6.171	Apoptosis analysis of EFBF isolate (LME1) against HeLa cell lines.	320
6.172	Cell cycle analysis of EFBF isolate (LME1) against HeLa cell lines.	320
6.173	Antiproliferative activity of ITHE isolates against normal cell lines.	321
6.174	Morphological changes of normal cells treated with ITHE isolates.	322
6.175	Antiproliferative activity of MFBF and EFBF isolates against normal cell lines.	323
6.176	Morphological changes of normal cells treated with MFBF and EFBF isolates.	324
6.177	<i>In vitro</i> Caspase-3 activity of LMH-3 (Hesperidin) on MCF-7 cell lines.	325
6.178	<i>In vitro</i> Caspase-3 activity of LME-1 (Gardenin B) on HeLa cell lines.	325
6.179	<i>In vitro</i> DNA fragmentation of LMH-3 (Hesperidin) on MCF-7 cell lines.	326
6.180	<i>In vitro</i> DNA fragmentation of (Gardenin B) on HeLa cell lines.	326

6.181	Effect of LME-1 on Bcl-2, p53, Bax gene expression in HeLa cells.	328
6.182	Amplification plots of the genes expressed.	329
6.183	Melting temperatures of the reference and target genes.	330
6.184	Docked view of all the compounds at the active site of the Caspase-3 enzyme (PDB ID: 1QX3).	331
6.185	Interaction of Doxorubicin at the binding site of the enzyme (PDB ID: 1QX3)....	332
6.186	Interaction of Cisplatin at the binding site of the enzyme (PDB ID: 1QX3).....	332
6.187	Interaction of LMH1 (Quercetrin) at the binding site of the enzyme (PDB ID:1QX3).	333
6.188	Interaction of LMH2 (Rutin) at the binding site of the enzyme (PDB ID:1QX3).	333
6.189	Interaction of LMH3 (Hesperidin) at the binding site of the enzyme (PDB ID: 1QX3).	334
6.190	Interaction of LMF1 (Quercetin) at the binding site of the enzyme (PDB ID: 1QX3).	334
6.191	Interaction of LMF2 (Kaempferol) at the binding site of the enzyme (PDB ID: 1QX3).	335
6.192	Interaction of LMF3 (Isorhamnetin) at the binding site of the enzyme (PDB ID: 1QX3).	335
6.193	Interaction of LMF4 (β -Glucogallin) at the binding site of the enzyme (PDB ID: 1QX3).	336
6.194	Interaction of LME1 (Gardenin B) at the binding site of the enzyme (PDB ID: 1QX3).	336
6.195	Docked view of all the compounds at the BZD binding site of GABA-A receptor (PDB ID: 6D6T).	343
6.196	Interaction of Diazepam at the BZD binding site of the GABA-A receptor (PDB ID: 6D6T).	344
6.197	Interaction of LMH1 (Quercetrin) at the BZD binding site of the GABA-A receptor (PDB ID: 6D6T).	344

6.198	Interaction of LMH2 (Rutin) at the BZD binding site of the GABA _A receptor (PDB ID: 6D6T).	345
6.199	Interaction of LMH3 (Hesperidin) at the BZD binding site of the GABA _A receptor (PDB ID: 6D6T).	345
6.200	Interaction of LMF1 (Quercetin) at the BZD binding site of the GABA _A receptor (PDB ID: 6D6T).	346
6.201	Interaction of LMF2 (Kaempferol) at the BZD binding site of the GABA _A receptor (PDB ID: 6D6T).	346
6.202	Interaction of LMF3 (Isorhamnetin) at the BZD binding site of the GABA _A receptor (PDB ID: 6D6T).	347
6.203	Interaction of LMF4 (β -Glucogallin) at the BZD binding site of the GABA _A receptor (PDB ID: 6D6T).	347



CHAPTER – I

INTRODUCTION

1. INTRODUCTION

1.1. Traditional medicine

1.1.1. History of traditional medicine

Medicinal plants have played a vital role in the folklore of ancient cultures and have an essential place in the therapeutic armory of humankind.^[1] In addition to food and spices, plants were used as medicine for over 5000 years. It is estimated that 70 - 95% of the population in developing countries continue to use traditional medicines in the healing and prevention of various ailments in man and animals.^[2] Ten percent of all vascular plants are used as medicinal plants, with an estimated half a million species, as essential source of compounds for drugs and cosmetic products.^[3]

The great civilizations of the ancient Indians, Chinese, and North Africans provided written evidence of man's ingenuity in utilizing plants to treat a wide variety of diseases.^[4] In ancient Greece, scholars classified plants and described them, thus aiding the identification process. Many natural substances that were extracted from the higher plants before World War II are still in use today as clinical drugs. Quinine from *Cinchona* bark, morphine and codeine from the latex of the opium poppy, digoxin from *Digitalis* leaves, atropine (derived from hyoscyamine) and hyoscine from species of the Solanaceae family continue to be in clinical use. After the war, there were relatively few discoveries of new drugs from higher plants, with the notable exception of reserpine from the *Rauwolfia* species marking the age of the tranquillizers and vinblastine and vincristine from *Catharanthus roseus*, which were effective in cancer chemotherapy.^[5]

1.1.2. Advancement of traditional medicine

During recent years, the attention of the pharmaceutical industry has switched once more to the natural world, and this may be illustrated by reference to three clinical drugs, taxol, etoposide and artemisinin. Taxol isolated from the bark of the Western Pacific Yew, *Taxus brevifolia*, was active against cancer cells, by promoting the assembly of

tubulin into microtubules. The resin podophyllin obtained from the root of the mayapple, *podophyllum peltatum*, is toxic and used clinically to remove warts. The major constituent of the resin is the lignan podophyllotoxin which inhibits cell division. Artemisinin, isolated from *Artemisia annua* is an effective antimalarial used in treatment of multi-drug resistant strains of *Plasmodium falciparum*, the cause of human malignant cerebral malaria. Natural compounds like caffeine, codeine, morphine, nicotine, reserpine etc already have a proven record for central nervous system activities; but there still remains an urgent need to develop new clinical drugs. [5]

In the present scenario, the review of different national pharmacopoeia reveals that at least 120 distinct chemical products or moieties from herbal sources have been utilized as lifesaving drugs. Indian traditional medicinal systems believe in a holistic and logical approach to diagnosis, which is based on rational observation, and the use of potent herbal preparations, thus being important targets for medical research. The growing demand for several Indian formulations displays the strategy for the advancement and integration of traditional herbal medicine into modern medicine. [6]

1.1.3. Role of natural products

Research has evolved from the screening of medicinal plants for bioactive agents to the development of drugs and dosage forms for natural products of merit. [7] Medicinal plant drugs can be placed into two broad categories. Complex mixtures containing a wide variety of compounds (e.g., infusions, essential oils, tinctures, or extracts) and pure, chemically defined active principles. Pure compounds are used when the activity is strong and specific and/or has a small therapeutic index. [8]

Phytochemicals are naturally occurring chemical compounds that possess biological properties viz. antioxidant, antimicrobial, modulation of detoxification of enzymes, stimulation of the immune system, decrease of platelet aggregation and modulation of

hormone metabolism, anticancer and other properties. Numerous studies are being conducted to determine the effectiveness of phytochemicals and comprehend the underlying mechanism of their action.^[9] Most of the phytochemicals from plant sources, namely phenolics and flavonoids, have been reported to have a positive impact on health and the prevention of various ailments.^[10]

1.2. Oxidative stress

Oxidative stress has been associated as a causative factor in the etiology of a variety of pathological conditions that can initiate or propagate the development of degenerative diseases.^[11] Reactive free radicals contribute to oxidative stress in living cells by damaging the lipids, proteins, DNA and other macromolecular components. Altered cellular changes and excitotoxicity play a specific role in the pathogenesis of degenerative diseases like cancer, neurodegenerative disorders, cardiovascular diseases, cataract and inflammation.^[12]

In healthy cells, only a very small percentage (3 %) of the total oxygen consumed by the cell is changed into reactive oxygen species. There is a direct correlation between generation of reactive oxygen species and metabolic rate of living organisms. Reduction in metabolism, causes accumulation of toxic oxygen radicals, as these radicals cannot be eliminated easily and ultimately leading to cell damage by mitochondrial injury.^[13]

Free radicals are unstable molecules having unpaired electrons, making them extremely reactive. To achieve stability, the electrons often pair up with electrons from other atoms and molecules. Environmental, chemical, and biological factors could be responsible for generation of free radicals. Environmental factors include exposure to ultraviolet sunlight, X-rays and gamma rays, radiation, smoking, pollution, ozone and certain drugs, chemicals, or pesticides. Numerous biological and chemical processes, such as digestion and respiration, occur during the normal functioning of the human body. These result in production of free radicals as a by-product of metabolic reactions. Additionally,

exposure of free radicals to biomolecules such as proteins, lipids, and nucleic acids through redox reactions causes injuries to the organs or tissues or cells by damaging the cell wall and cell contents. Under normal conditions, the body's defence mechanisms like antioxidant enzymes neutralise or eliminate the free radicals. However, excess of free radicals in the body builds up oxidative stress due to shift in the balance between pro-oxidant and antioxidant reactions. [14,15]

Reactive oxygen species (ROS), like O_2^- , $H_2O_2^-$, and OH^- are constantly produced *in vivo* under aerobic conditions. The most important intracellular sources of ROS in eukaryotic cells are the mitochondrial respiratory chain, microsomal cytochrome P450 enzymes, flavoprotein oxidases, and peroxisomal fatty acid metabolism. A family of plasma membrane-associated enzymes known as NADPH oxidases uses NADPH as an electron donor to trigger the oxidation of oxygen to generate O_2^- . These can result in changing the fluidity of the membrane, increasing its permeability due to lipid peroxidation, loss of protein conformation and enzyme function, and genomic harm from DNA scission. [15,16]

There are four types of defense mechanisms against oxidative stress brought about by free radicals: (i) preventive mechanisms, (ii) repair mechanisms (iii) physical defenses, and (iv) antioxidant defenses. Enzymatic antioxidant defenses include three primary enzymes, namely glutathione peroxidase (GPx), catalase (CAT), superoxide dismutase (SOD), that are involved in the direct elimination of ROS, and secondary enzymes, namely glutathione reductase (GR), glutathione-S-transferase (GST), glucose-6-phosphate dehydrogenase (G6PDH) and ascorbate peroxidase (APx), which help in the detoxification of ROS by decreasing peroxide levels or by maintaining a steady supply of metabolic intermediates (glutathione, NADPH) that are necessary for optimum functioning of the primary antioxidant enzymes. Ascorbic acid (vitamin C), α -tocopherol (vitamin E), glutathione (GSH), carotenoids, flavonoids, and other antioxidants that exhibit a

homoeostatic or protective role against ROS are examples of nonenzymatic antioxidants. ^[17]

1.3. Cancer

Cancer is a complex life-threatening disease and ranked the second-highest cause of death, accounting for about 10 million deaths in 2020. ^[18] Cancer is one of the prominent causes of morbidity and mortality worldwide, with current treatment regimens being costly, triggering intolerable side effects and ultimately dramatically reducing the quality of life of the individual. ^[2]

Cancer cells are considered immortal as they have infinite potential for replication, growth, and proliferation by disturbing the normal cell cycle and apoptotic mechanisms. Cancer cells mainly show cell cycle deregulation, leading to uncontrolled proliferation. ^[19] The disease is characterized by uncontrolled cell division. Cell growth in cancer is categorized into four stages such as stage I, stage II, stage III and stage IV or metastases condition. Among these, metastases condition or stage IV is responsible for significant death. Several typical cellular functions are evaded as cancer cells multiply. The multistep development of human tumours results in the acquisition of numerous biological abilities, such as maintaining proliferative signaling, eluding growth inhibitors, and resisting cell death, highlighting the hallmarks of cancer. ^[20]

1.3.1. Carcinogenesis

Various etiological factors lead to cancer through a multi-step process termed as carcinogenesis. It involves initiation, promotion, progression and malignant conversion. ^[21]

1. Initiation: Occurs when a carcinogen interacts with DNA, producing a strand break or an altered nucleotide called an adduct. Then if the genome is replicated before repair enzymes can correct the damage. A DNA polymerase may misrepair the damaged sequence and permanently fix a heritable error in the genome.

2. Promotion: Tumour promotion involves activation of cell surface receptors, activation/inhibition of cytosolic enzymes and nuclear transcription factors, stimulation of proliferation, inhibition of apoptotic cell death etc.
3. Progression: Progression is accelerated by additional exposure to genotoxic agents, and it is due to genetic instability and non-random sequential chromosomal aberrations. The stage of progression involves irreversible genetic changes within cells, leading to immediate structural changes in the genome of the cell, like the initiation stage.
4. Malignant conversion: It involves a multifocal change in premalignant lesions. There will be upregulation of transcriptional activity and expression of modified cell surface molecules, gene amplification, alterations in cell-cycle regulatory genes, secreted proteases and methylation of DNA. All these changes facilitate migration and invasion.

1.3.2. Hallmarks of Cancer

Genes control normal cellular growth, while in cancer, these controlling genes are altered, typically by mutations. Some of these genes are common in many tumours (e.g. p53 or TP53), while others are specific to particular tumours. ^[13,22]

The genetic basis of cancer include: ^[13,22]

- Excessive and autonomous growth by growth-promoting oncogenes.
- Refractoriness to growth inhibition by growth suppressing anti-oncogenes.
- Escaping cell death by apoptosis by genes regulating apoptosis and cancer.
- Avoiding cellular ageing by telomeres and telomerase in cancer.
- Continued perfusion of cancer by angiogenesis.
- Invasion and distant metastasis by cancer dissemination.
- DNA damage and repair system by mutator genes and cancer.
- Cancer progression and tumour heterogeneity by clonal aggressiveness.

- Cancer a sequential multistep molecular phenomenon
- MicroRNAs in cancer: OncomiRs.

1.3.3. Genes Regulating Apoptosis and Cancer at Molecular level

Besides the role of mutant forms of growth-promoting oncogenes and growth-suppressing anti-oncogenes, another mechanism of tumour growth is by escaping cell death by apoptosis. Apoptosis in a normal cell is guided by a cell death receptor, CD95, resulting in DNA damage. Besides, there is the role of some other proapoptotic factors (Bad, Bax, Bid and p53) and apoptosis-inhibitors (viz. Bcl-2, Bcl-x etc.).^[13,22]

In cancer cells, apoptosis is interfered, due to mutations in the above genes that regulate apoptosis in the normal cell. The examples of tumours by this mechanism are as under:

a) Bcl-2 gene is seen in normal lymphocytes, but its mutant form with characteristic translocation (t14;18) (q32;q21) was first described in B-cell lymphoma and hence the name Bcl. It is also seen in many other human cancers, such as the breast, thyroid, and prostate. Mutation in the Bcl-2 gene removes the apoptosis-inhibitory control on cancer cells. Thus, more live cells undergoing mitosis contribute to tumour growth. Myc oncogene and the p53 tumour suppressor genes are also connected to apoptosis. While Myc allows cell growth, Bcl-2 inhibits cell death; thus, Myc and Bcl-2 together allow cell proliferation. Normally, p53 activates the proapoptotic gene Bax but mutated p53 (i.e., absence of p53) reduces apoptotic activity and thus allows cell proliferation.

b) p53 gene (TP53) is normally present in very small amounts and accumulates only after DNA damage. The two major functions of p53 in the normal cell cycle are,

i) In blocking mitotic activity, p53 inhibits the cyclins and Cyclin-dependent kinases (CDKs) and prevents the cell from entering the G₁ phase transiently, allowing the cell to repair DNA damage.

ii) In promoting apoptosis, p53 and the Rb genes (retinoblastoma) work together to identify the genes that have DNA damage that the body's natural system is incapable of repairing. P53 directs such cells to apoptosis by inducing the Bax gene and eliminating the defective cells. This process operates in the cell cycle at G₁ and G₂ phases before the cell enters the S (DNA synthesis) or M (mitosis) phase. Because of these significant roles in the cell cycle, p53 is called the 'protector of the genome'. The mutation of the p53 gene ceases the protective or growth suppressor action while promoting the effect of oncogenes. Homozygous loss of the p53 gene helps, keep the genetically damaged and unrepaired cells surviving and proliferating, resulting in malignancy. More than 70 % of human cancers have a homozygous loss of p53 by acquired mutations in somatic cells, e.g., cancers of the lung, head and neck, colon, and breast.

The important tumour-suppressor anti-oncogenes are Rb, p53 (TP53), Transforming Growth Factor - β (TGF- β), APC and β -catenin proteins and BRCA 1 and 2 etc. that are responsible for several cancers like retinoblastoma, osteosarcoma, cancers of the lung, head and neck, colon, breast, cervical, pancreas, colon, stomach etc. [13,22]

1.3.4. Breast cancer

Breast cancer is a growing concern in the present days, as it is the main cause of cancer mortalities amongst women worldwide, with 0.68 million deaths in 2020. [18] Breast cancer usually arises in the epithelial cells lining the ducts or lobules in the glandular tissues of the breast. It could be caused due to germ-line mutations in high-penetrance breast cancer susceptibility genes like BRCA1, BRCA2, p53 and Phosphatase and tensin homolog (PTEN) gene. Fibro-adenosis with severe dysplasia and epitheliosis are pre-malignant and increases the risk of breast cancer. Based on the underlying molecular mechanisms breast cancer can be clinically sub-classified on gene expression, human epidermal growth factor receptor 2 [HER2], estrogen receptor [ER], progesterone receptor [PR], and proliferation

status. HER-2/neu proto-oncogene was over-expressed in 20 - 30 % of invasive breast cancers and reduces the chances of survival. [23, 24]

1.3.5. Lung cancer

Lung cancer accounted for 1.8 million deaths in 2020, accrediting it as the most common cause of cancer-related mortalities globally. [18] Chronic exposure to tobacco smoke is the single most predominant cause of around 80 % of lung cancers. Four major histologic types comprise most lung cancers, including small cell lung cancer (SCLC) and the three non-small cell lung cancer (NSCLC) types. Squamous and SCLC arise mainly from the central airways, while adenocarcinomas (including bronchioloalveolar cancer) are peripherally located. Large cell lung cancer represents less differentiated forms of the other NSCLC types. Adenocarcinomas arise from the progenitor cells of the bronchioles (Clara cells), alveoli (Type II pneumocytes), or mucin-producing cells and are the most common types of lung cancer. Oncogenes c-Myc, mutated K-ras, overexpressed Epidermal growth factor receptor (EGFR), cyclin D1, and Bcl-2 mainly contribute to the pathogenesis of lung cancer. Telomerase RNA (hTR), the catalytic component human Telomerase reverse transcriptase (hTERT) and the mutated forms of tumour suppressor genes p53, Rb and p16 are commonly expressed in lung cancer. [18, 25]

1.3.6. Cervical cancer

It is a sexually transmitted disease resulting from the infection with oncogenic human papillomavirus (HPV). Oncogenic HPV DNA is found in over 95% of invasive cervical cancers worldwide. It is the fourth most frequent cancer types in women globally, with 3,42,000 deaths in 2020. [18] HPVs are small, non-enveloped DNA tumour viruses. Their genomes encode eight genes (E1, E2, E4, E5, E6, E7, L1 and L2 open reading frames). HPV has a predilection for cervix epithelial cells that are stratified into a non-differentiated basal monolayer and a suprabasal differentiated non-proliferating epidermis. Basal cells of the cervix infected with HPV continue to divide and are maintained by HPV

early proteins that stimulate and propagate cell growth via the actions of the E5, E6 and E7 genes. E6 oncoprotein induces cellular transformation by interacting primarily with the p53 tumour suppressor protein and with other cell cycle regulators like Bak, Blk and cell adhesion proteins etc. E6 of high-risk HPV type has disrupted the extrinsic apoptotic pathway by binding to TNFR-1 (tumour necrosis factor receptor), Fas, CD95 ligand and TNF related apoptosis inducing ligand (TRAIL) receptors, thus inhibiting the downstream release of caspase 8 and caspase 10 and inhibiting the formation of the death-inducing signalling complex (DISC).^[26]

1.3.7. Oxidative stress and Cancer

In almost all cancers, the high level of ROS has been detected, making it one of the best-characterized phenotypes in cancer.^[27] One of the most important pathways associated with oxidative stress and cancer is the Ras pathway, wherein the main mechanism of Ras activation in tumors involves point mutations. Around 30% of human tumors contain activating mutations in the Ras family of oncogenes, rendering a protein constitutively active. Many genes are implicated in the modulation of energy metabolism and cancer. One of the most frequently mutated genes in human cancers is p53, which modulates the balance between glycolysis and the utilization of the respiratory chain in the mitochondria.^[28]

In breast cancer, the tumor suppressor gene breast cancer gene 1 (BRCA1) that is responsible for repairing DNA, is mutated. The gene is mutated in 40 - 50% of hereditary types and either absent or expressed at low levels in 30 - 40% of sporadic breast cancers.^[29] Estrogens, are important in the development and progression of human breast cancer because they can be transformed into the carcinogenic metabolite 4-hydroxyestradiol by cytochrome P4501B1.^[30] Both metabolites can be further oxidized into a reactive quinone that can react with DNA. The compounds 4-OHE₂ and 2-OHE₂ and their quinone derivatives are able to generate oxidative stress.^[31]

In lung cancer, the levels of ROS are increased, since the endogenous Pyruvate kinase isozymes (PKM2), responsible for detoxification of ROS, gets mutated through cysteine 358 oxidation, directing glucose to the pentose phosphate pathway. The lung cancer cells thus exhibit increased sensitivity to oxidative stress. [28]

Cervical cancer cells depend on the oxidative phosphorylation pathway to produce ATP instead of glycolysis. The end product of lipid peroxidation, Malondialdehyde (MDA), is significantly increased in cervical cancer. MDA is highly cytotoxic, acting as a tumor promoter and increasing the levels of oxidative stress. [27]

1.4. Anxiety

Anxiety is a common psychological disorder affecting several people worldwide. It is an unpleasant emotional or fearful state of mind where the subject fears a defined or an undefined threat. [32] Anxiety is a cardinal symptom and an almost inexorable component of many medical and surgical conditions. [33]

During the history of psychology, anxiety has been associated with adverse consequences; therefore, in this field many studies have been carried out and huge financial and human resources have been allocated to treat anxiety. According to the World Health Organization, anxiety is one of the top psychological disorders, its prevalence is increasing in developing countries, with a population of 500 million suffering worldwide. [34]

1.4.1. Manifestations of anxiety

Stress and anxiety are common psychiatric manifestations of the modern world and lifestyles. Persistent and unrelenting stress often leads to anxiety and unhealthy behaviours. [35]

Normally, anxiety is an adaptive, emotional response to stressful physiological, psychological, and social stimuli that every person may experience in life. ^[36] Slight anxiety can motivate people to perform at their best and become more productive. Anxiety becomes a medical concern, when it becomes more intense, and interferes with day-to-day activities. Pathological anxiety is one of the most prevalent psychological disorders that has debilitating effects on the quality of life of many people. This neurological disorder is characterized by excessive ponderings, worrying, restlessness, nervousness and fear about future uncertainties based on real or imagined events. ^[37] It is often found in conjunction with psychiatric (depression and substance abuse disorders) as well as nonpsychiatric (chronic fatigue, cardiac diseases, or respiratory compromise) disorders. Anxiety may impair homeostasis; typical symptoms include increased heart rate, palpitations, blood pressure, rapid breathing, chest pain, sweating, irritability, and increased muscle tension, significantly affecting both physical and psychological health of an individual. ^[38] Anxiety may be caused by several factors like stress, alcohol, substance abuse, drug induced and genetic abnormalities etc. ^[37]

1.4.2. Types of anxiety disorders

There are several types of anxiety disorders, each with its own distinct profile and set of clinical symptoms. ^[39] These are listed in Table 1.1.

Table 1.1: Types of anxiety disorders. ^[39]

Sr. No.	Anxiety Disorder	Short Description
1.	Obsessive Compulsive Disorder (OCD)	It is an anxiety disorder characterised by recurrent, unwanted thoughts (obsessions) and/or repetitive behaviours (compulsions).
2.	Acute Stress disorder	An anxiety disorder that develops within one month after a severe traumatic event or experience.
3.	Separation anxiety disorder	A disorder over real or threatened separation from people to whom one is attached.
4.	Social phobia	An excessive, persistent fear of social or performance situations.
5.	Phobic disorders	A disorder in which the affected person experiences an excessive or irrational fear of a specific situation, an object that disrupts their ability to function in normal daily activities.
6.	Post-Traumatic Stress Disorders (PTSD)	It is a complex health condition that can develop in response to a traumatic experience - a life-threatening or extremely distressing situation that causes a person to feel intense fear, horror or a sense of helplessness.
7.	Panic disorders	This usually makes the person believe that they are either seriously ill or about to die and can leave them distressed for quite a while.
8.	Tourette's Syndrome	An inherited, neurological disorder characterized by repeated and involuntary body movements and uncontrollable vocal sounds.
9.	Anxiety due to a physical disorder or a substance	It is associated with direct physiological effects of intoxication or withdrawal from a substance.
10.	Generalised Anxiety Disorder (GAD)	Persistent worry and anxiety about health, work, money, family etc. lasts for at least six months, even when there are no signs of trouble in life.

1.4.3. Neuroanatomy of anxiety

Human anxiety is accompanied by changes in neural systems that coordinate distinct defensive responses to threats. It includes areas such as the medial prefrontal cortex (mPFC), amygdaloid, hypothalamic nuclei, hippocampus, basal ganglia and midbrain regions. [40]

There is a wide role of neurochemical systems in the phenomenon of anxiety. Neurotransmitters like monoamines (dopamine, noradrenaline and serotonin), GABA, Corticotropin-releasing factor (CRF), Melanocyte stimulating hormone (MSH), neuropeptides (galanin, neuropeptide Y, arginine vasopressin, tachykinin and substance P), neurosteroids and cytokines act as modulators of anxiety. [41] GABAergic and serotonergic systems are most frequently associated with anxiety. GABA is the primary inhibitory neurotransmitter in the CNS. It is the most abundant inhibitory neurotransmitter released at approximately 50% of the brain synapses. [42,43] The presence of GABAergic neurons in the brain facilitates the inhibition of neuronal activity by differing ongoing excitatory input. [44,45] The GABAergic neurotransmission is responsible for a variety of inhibitory activities, such as anxiolysis, muscle relaxant, anticonvulsant etc. and dysfunction within this system leads to several diseases like anxiety, seizures, motor impairment, neurodegenerative disorders, pain, insomnia etc. [46]

1.4.4. GABAergic neurotransmission

GABA acts via two main types of receptors

- 1) Fast-acting ion-gated or 'ionotropic' receptors - GABA_A
- 2) Slow-acting G-protein coupled 'metabotropic' receptor - GABA_B

GABA_A receptor is the predominant receptor type in the brain. In addition to its fast synaptic inhibitory role, it regulates the excitatory tone of dopaminergic, serotonergic neurons etc. [47-49,50]

GABA_A receptor

The $\alpha 1$ - $\beta 2$ - $\gamma 2$ subtype represents the most abundant form of GABA_A receptor in the CNS. ^[51] The α subunits provide sensitivity to GABA on the GABA_A receptor and also determine its pharmacological specificity towards a number of allosteric modulators, *viz.* benzodiazepines (BZDs) etc. BZDs (Diazepam, Chlordiazepoxide, Oxazepam, Lorazepam, Alprazolam etc.) facilitate GABAergic inhibition by potentiating the GABA_A receptor complex in the CNS. Binding of BZDs to the GABA_A receptor ($\alpha 1$ - $\beta 2$ - $\gamma 2$ subtype), within the interface between the α and γ subunits, enhances the probability of chloride ion channel opening in response to GABA, thus inducing the opening of the ion channels, and further causing inhibition and hyperpolarization of neurons. Abnormality in the expression and function of this receptor leads to anxiety. Studies reveal that benzodiazepines (BZDs) and other GABA_A modulators reduce anxiety; however, competitive, and non-competitive GABA_A receptor antagonists and benzodiazepine inverse agonists produce anxiety. ^[48,49,52]

1.4.5. Serotonergic neurotransmission and other neuromodulators

Noradrenaline is responsible for arousal, vigilance, attention, motivation, reward, learning and memory, blood pressure regulation etc. and is mainly present in the locus coeruleus nucleus, brain stem, cerebral cortex, hypothalamus, hippocampus, cerebellum, adrenals, substantia nigra, corpus striatum, amygdaloid nucleus etc. The actions of noradrenaline are mainly inhibitory (β -receptors), but some are excitatory (α - or β -receptors). Dopamine regulates mood, motor control, learning, the reward system, compulsion, behaviour, joy, euphoria and endocrine functions. It is primarily found in the corpus striatum, cortex, limbic system, hypothalamus, hippocampus, and nucleus accumbent in the brain. Dopaminergic neurons form three main systems namely, nigrostriatal pathway, mesolimbic or mesocortical pathways and tuberohypophyseal system. There are two main types of dopaminergic receptors, D₁ and D₂. The D₁ family

includes D₁ and D₅, while D₂ family is pharmacologically prominent in the CNS and consists of D₂, D₃ and D₄.^[48,49,53]

5-Hydroxytryptamine controls mood, sleep, wakefulness, behaviour, emotions, feeding, appetite, regulates body temperature, blood pressure, sexual function, intestinal motility etc. It is found in the cortex, brainstem, enterochromaffin cells, limbic system, hippocampus etc. 5-HT acts on several subtypes of 5-HT (5HT₁₋₇) receptors. In most areas of the CNS, 5-HT has a strong inhibitory action. Their action is mediated by 5-HT_{1A} receptors and is associated with membrane hyperpolarization caused by an increase in potassium conductance. Some cell types are slowly excited by 5-HT owing to its blockade of potassium channels via 5-HT₂ or 5-HT₄ receptors. Glutamate is an excitatory neurotransmitter and is present throughout the central nervous system (CNS), *viz.* cerebral cortex, hippocampus, Brain stem, midbrain, basal ganglia etc. and is involved in neurodevelopment, learning and memory, mood regulation, formation of neuronal networks, acute and chronic neurodegenerative processes.^[48,49,53]

Selective Serotonin Reuptake Inhibitors (SSRIs) like Fluoxetine, Fluvoxamine, Paroxetine, Sertraline, Citalopram etc. regulate the levels of serotonin in the brain and are reported to be useful in managing anxiety disorders like panic disorder, social anxiety, obsessive compulsive disorder, generalized anxiety, PTSD etc. Studies have postulated that dopamine also plays an essential role in the pharmacotherapy of anxiety. Recognizing anxiolytic effects of non-benzodiazepine azapirone agents (buspirone, gepirone, and ipsapirone), which act as 5HT_{1A} partial agonists and their therapeutic role in clinical anxiety and mood disorders, has further focused attention on the 5-HT_{1A} receptor. Buspirone appears to only interact with the dopaminergic system with reasonable potency and exhibits properties of both a dopamine agonist and a dopamine antagonist. Dopamine can stimulate ACTH secretion by the pituitary, and this neurotransmitter plays a role in reducing anxiety.^[39,48,53]

1.4.6. Oxidative stress and Anxiety

Anxiety disorders can also be due to free radical-induced damage to GABAergic and serotonergic systems. In recent studies, oxidative stress is associated with nervous system impairment and neurobehavioral disorders such as anxiety and depression. [54] Patients with anxiety disorders have reported to exhibit higher lipid peroxidation activity, thus increasing the workload of enzymes like superoxide dismutase, glutathione peroxidase etc. Hence oxidative metabolism is also considered a plausible pathway that can affect anxiety regulation. [41]

Cells utilize oxygen to produce ATP, which drives multiple cellular processes such as biosynthesis and locomotion. Maintaining oxygen homeostasis is crucial for the survival and proper function of cells and organisms. Reduced oxygen levels (hypoxia) initiate physiological changes in cells to adapt to the hypoxic environment, and the failure of this process results in cell death and organ dysfunction. It has been documented that multiple organ systems are highly affected by hypoxia, particularly the brain. Molecular responses to hypoxia play a causal role in multiple human diseases such as cancer, stroke, pulmonary oedema, inflammation, and nervous system diseases (schizophrenia, anxiety, depression etc.). [55] Studies have revealed that antioxidants are vital as adjuvant therapy in patients with generalized anxiety disorder and depression. [56]

1.4.7. Conventional anxiolytic therapy versus potential herbal anxiolytics

Benzodiazepines (indirect GABA_A receptor agonists) and selective serotonin reuptake inhibitors (SSRIs) are the choices of drugs and the mainstay of pharmacological treatment for anxiety disorders. However, the chronic use of benzodiazepines produces tolerance, dependency, sleepiness, and lethargy and can induce a drug withdrawal syndrome if the drug is discontinued. On the other hand, chronic use of SSRIs can produce considerable side effects. Therefore, the screening for new leads with anxiolytic properties and less adverse effects continues. [57] Conventional drug therapy has a narrow margin of

safety between the anxiolytic effect and unwanted side effects, thus prompting researchers to evaluate new compounds, especially plant-based drugs having less undesirable effects. ^[56]

Many medicinal plants have stimulating or calmative effects on the central nervous system, and the plant kingdom provides hundreds of CNS active substances covering the whole spectrum of activity, such as psycho-analeptic, psycholeptic, analgesic, antiepileptic, psychodysleptic (hallucinogenic) effects. ^[58] Medicinal plants exerted sedative and anxiolytic effects via potentiation of the inhibitory or decreasing the excitatory neurotransmission. However, in general, the mechanisms of action of the medicinal plants used for the treatment of psychiatric disorders involved modulation of neuronal communication via specific plant metabolites binding to neurotransmitter or neuromodulator receptors, stimulating, or sedating CNS activity, and regulating or supporting the healthy function of the endocrine system. The beneficial effects of medicinal plants in neuroprotective disorders were mediated via their antioxidant activity, anti-excitotoxic effect, apoptotic inhibition, neurotrophic effects, enhancing protective signalling, altering membrane microstructures, decreasing inflammation, and preventing accumulation of polyubiquitinated protein aggregates in critical regions of the brain. ^[59]

1.5. Role of flavonoids as therapeutics

Flavonoids are the most common plant polyphenols that also form an important component of our diet. Their complex molecular structures are related to biological functions in the human body. Plants and dietary foods rich in polyphenolics like flavonoids, tannins, gallic acid, etc., act as natural antioxidants that can improve health and reduce the risk of cancers and other degenerative diseases. ^[60] Plant flavonoids are extensively studied for their anticancer activities, along with other biological functions. Flavonoids derived from higher plants are successful in killing cancer cells, and some of them are in different phases of clinical trials. A total of twenty-two Phase II clinical trials and one Phase

III clinical trial investigated flavonoids alone or combined with other therapeutics either on hematopoietic/lymphoid or solid tumours. [61] These phytochemicals have demonstrated anticancer activity by inhibiting tumour cell proliferation, inducing apoptosis, suppressing cell cycle, metastasis, angiogenesis, etc. [62]

Some plants that contain flavonoids and demonstrate antianxiety activity are *Abies pindrow*, *Calotropis gigantean*, *Matricaria recutita*, *Gelsemium sempervirens*, *Medicago sativa*, *Passiflora coerulea*, *Passiflora incarnate*, *Tilia Americana*, *Turnera aphrodisiaca*. Flavonoids possessing anxiolytic effects include apigenin, chrysin, kaempferol, quercetin etc. Flavonoids are also reported to be potent antioxidants. [56] Polyphenolic flavonoids like anthocyanins, quercetin etc., cross the blood-brain barrier and localize in various brain regions such as the cerebellum, cortex, hippocampus, or striatum and like other flavonoids, they can act centrally. The flavonoids have been shown to exert a benzodiazepine-like pharmacological activity due to binding affinity to GABA_A receptors and have advantageous potential as anxiolytics as they rarely have any side effects. [63]

Extracts from the plant show the presence of flavonoids, and the flavonoids exert antianxiety activity through GABA receptors. Anxiolytic activity of several flavones has been attributed to their affinity for the central benzodiazepine site on the GABA_A receptor resulting in sedation, anxiolytic or anti-convulsive effects. [64]

Table 1.2: Flavonoids and their possible pharmacological activities. ^[61]

Subclass	Flavonoids	Possible Bioactivity
Flavonol	Quercetin	Anticancer, antioxidant, antimicrobial, antidiabetic, anti-inflammatory, neuroprotective, antianxiety, hepatoprotective
	Myricetin	Anticancer, antidiabetic, anti-infectious, antioxidant, anti-inflammatory, anti-obesity, neuroprotective
	Kaempferol	Anticancer, antioxidant, anti-inflammatory, antidiabetic, neuroprotective, antianxiety.
	Rutin	Anticancer, antioxidant, antimicrobial, antidiabetic, anti-inflammatory, neuroprotective, antianxiety, cardioprotective, hepatoprotective, nephroprotective
	Morin	Anticancer, antioxidant, anti-microbial, antidiabetic, neuroprotective, anti-arthritis, anti-inflammatory, nephroprotective, cardio protective, hepatoprotective
Flavanol	Catechin	Anticancer, antioxidant, antimicrobial, anti-allergenic, anti-inflammatory, UV protection activity
	Epicatechin	Anticancer, antioxidant, antidiabetic, anti-inflammatory, cardio-protective, neuroprotective
	Epigallocatechingallate	Anticancer, antioxidant, antimicrobial, anti-allergic, antidiabetic, anti-inflammatory, cardio-protective, neuroprotective
Flavone	Apigenin	Anticancer, antidiabetic, neuroprotective, antianxiety anti-arthritis, anti-depressant, anti-inflammatory
	Luteolin-7-glucoside	Anticancer, anti-inflammation, anti-allergy and antioxidant
	Dimethoxy flavone	Anticancer, antifungal
Isoflavone	Genistein	Anticancer, antioxidant, antimicrobial, antidiabetic, cardioprotective
	Daidzein	Anticancer, antidiabetic, anti-osteoporosis, anti-aging, antioxidant, anti-microbial, anti-inflammatory
Flavanone	Naringenin	Anticancer, antioxidant, antimicrobial, anti-inflammatory, antiadipogenic, anti-diabetic, cardioprotective, eye-protective
	Hesperidin	Anticancer, anti-allergic, anti-oxidant and anti-inflammatory
Flavanonol	Dihydro-quercetin	Anticancer, antioxidant, anti-bacterial

In line with the small-molecule synthetic drugs, several components from herbal sources are being continuously screened as prospective therapeutic agents to combat various ailments. Phytochemicals have demonstrated anticancer activities by various mechanisms and also exhibit promising potential in the treatment of several psychological ailments including anxiety disorders.

Two indigenous plants viz. *Hybanthus enneaspermus* Linn. (F.) Muell and *Bauhinia foveolata* Dalzell. available in the Western Ghats of India were selected for the study as the genera *Hybanthus* and *Bauhinia* are established to possess a rich reservoir of phytoconstituents that may be beneficial as antioxidants and help mitigate or cure various ailments including cancer and nervous system disorders. The current study was thus focussed on evaluating the potential of *Hybanthus enneaspermus* Linn. (F.) Muell and *Bauhinia foveolata* Dalzell. for antioxidant activities and further assessing their ability as anticancer and anxiolytic agents and subsequently deducing their probable mode of action thereof.



CHAPTER – II

PLANT PROFILE

2. PLANT PROFILE

The plants selected for the study were *Hybanthus enneaspermus* Linn. (F.) Muell and *Bauhinia foveolata* Dalzell.

2.1. *Hybanthus enneaspermus* Linn. (F.) Muell

2.1.1. Botanical name

Hybanthus enneaspermus Linn. [65]

2.1.2. Synonym

Ionidium suffruticosum (Ging.) [65]

2.1.3. Vernacular names [65-67]

- Common name Spade flower, pink ladies slipper, ratan purush, purusharathna.
- Sanskrit Lakshmisheshta, padmucharini, purusharathna, rathnapurusha.
- English Spade flower, ladies pink slipper
- Hindi Ratan purush
- Malayalam Orilathamatai
- Marathi Rathanparas
- Tamil Orilai thamarai
- Kannada Purusharatna

2.1.4. Taxonomic Classification [65-67]

- Kingdom Plantae
- Sub-kingdom Tracheophyta
- Division Magnoliophyta

- Class Magnoliopsida
- Order Malpighiales
- Family Violaceae
- Genus *Hybanthus*
- Species *enneaspermus*

2.1.5. Geographical distribution

It is a small suffrutescent perennial herb found mostly in the tropical and subtropical regions of the world, particularly in places like tropical Asia, Africa, Australia, Arabia, Sri Lanka, Indochina, Philippines, Borneo, Java, Guinea, Taiwan, and in India. In India, the genus is mainly found in warmer parts of the Deccan peninsula, Western Ghats and also in southern India. ^[65-67]

2.1.6. Morphological Description

H. enneaspermus is a small erect perennial herb, pubescent in nature and grows to a height of 60 cm and forms many diffuse or ascending branches. It has been noticed that the flowering season of this plant occurs from August to September. Its Root is spindle-shaped, cylindrical, rough, and light yellow in colour. Stem is sparingly branched with a woody base. Leaves are simple, alternate, sub-sessile, linear, to lanceolate. The base is attenuated, and margins serrate with nectiferous glands. Flowers are 8 to 10 mm across, pink, axillary and solitary. Fruits are 5mm across, capsule, sub-globose with ribbed seeds. The seeds are ovoid, acute, longitudinally striate, yellowish-white, and about 1.5 mm long. The leaves are seen as tender stalks. ^[65-67]

2.1.7. Traditional Uses

The traditional uses of *H. enneaspermus* have been listed in Table 2.1. ^[65-67]

2.1.8. Phytoconstituents

Alkaloids, Flavonoids, Steroids, Terpenoids, Phenols, Tannins, Saponins, Cardiac glycosides, Cyanogenic glycosides, Anthraquinone glycosides, Dipeptides, Sugars, Amino acids, Aurantiamide acetate etc. ^[65-67]

2.1.9. Pharmacological activities

Antioxidant, Antiproliferative, Anticonvulsant, Antidiabetic, Aphrodisiac, Hepatoprotective, Antiplasmodial, Antimicrobial, Antibacterial, Antifungal, Antiviral, Anti-Inflammatory, Nephroprotective, Antiarthritic, Antisecretory, Anti-Nociceptive, Antiallergic, Antihyperlipidemic, Neuroprotective, Cardioprotective, Anticancer etc. ^[65-67]

Table 2.1: Traditional uses of *H. enneaspermus*.

Part of the plant	Traditional Use
Whole plant	Used in the treatment of kapha and pitta, urinary calculi, stangury, pain, dysentery, vomiting, burning, wandering of the mind, urethral discharge, blood troubles, asthma, epileptic fits, cough, cold, fever, malaria, cholera , stomach problems and skin diseases. It provides tone to the breast. Also used as a nutritive and tonic. Its formulations have been used externally for the treatment of wounds and syphilis. Whole plant juice when consumed with cow's milk provides relief from diabetes and improves the sexual vigor in males. Provides strength to the newborns when consumed by mothers during pregnancy and parturition.
Leaves and stalks	Aphrodisiac, Tonic, Demulcent and a Liniment for headache.
Leaves and Fruits	Antidotes for Scorpion stings and Cobra bites by Tribals.
Roots	Antigonorrhoeic, Diaphoretic, Diuretic, for Bowel complaints and Urinary Problems.

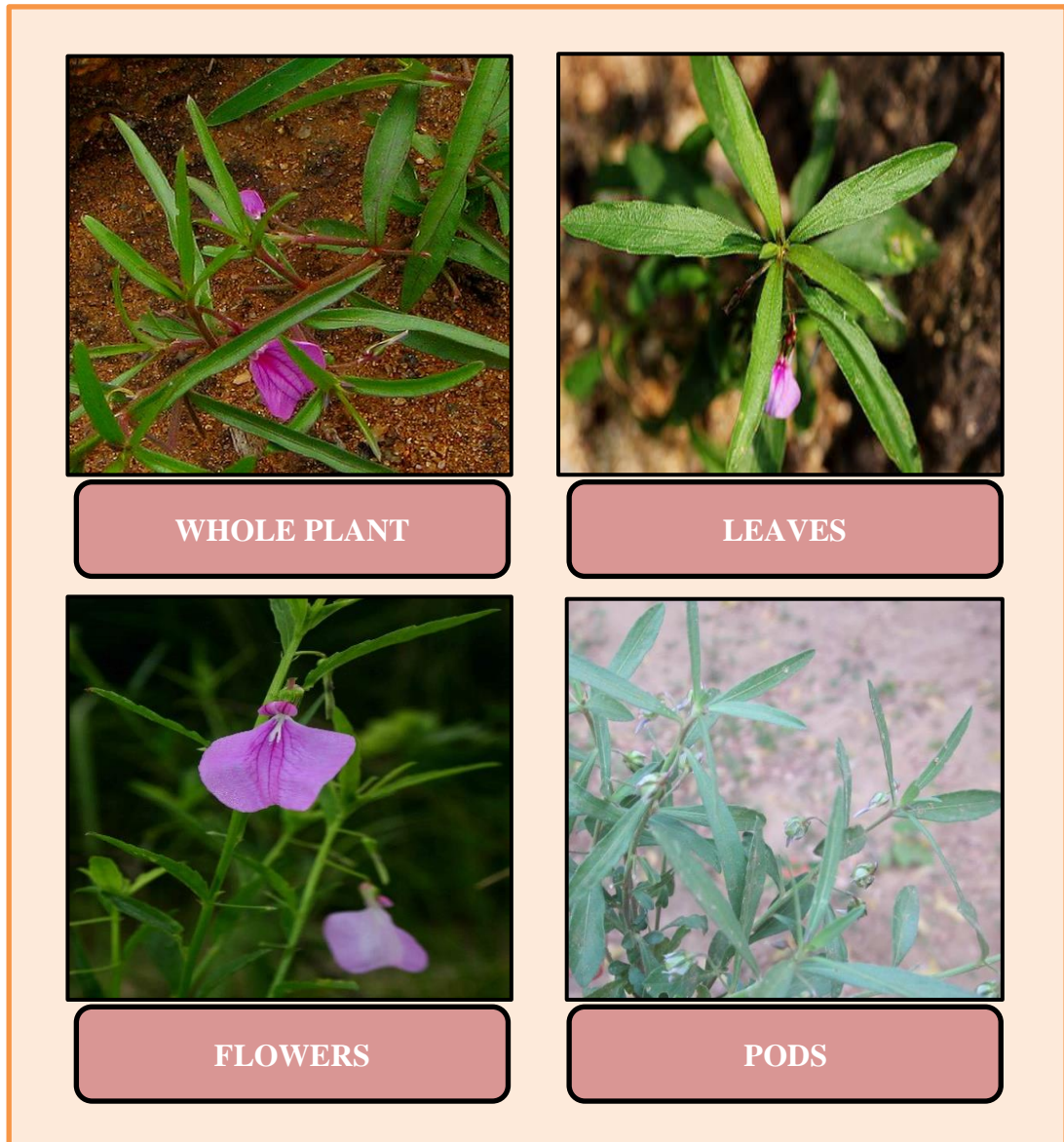


Figure 2.1: Morphological parts of *Hybanthus enneaspermus* [69-70]

2.2. *Bauhinia foveolata* Dalzell.

2.2.1. Botanical name

Bauhinia foveolata Dalzell. [71-74,78]

2.2.2. Synonyms

Bauhinia lawii, *Piliostigma foveolatum* [71-74,78]

2.2.3. Vernacular names [71-74]

- Common name Pore Leaved *Bauhinia*
- Sanskrit Kachnar, Gandari
- Hindi Kachnar
- Marathi Chamoli, Moti chambuli
- Kannada Basvanapada

2.2.4. Taxonomic classification [73,74]

- Kingdom Plantae
- Sub-kingdom Tracheophyta
- Super division Embryophyta
- Division Magnoliopsida
- Class Magnoliophyta
- Order Fabales
- Family Fabaceae / Leguminosae
- Subfamily Caesalpinioideae
- Genus *Bauhinia*
- Species *foveolata*

2.2.5. Geographical distribution

Pore-leaved *Bauhinia* is an endemic tree, native to the Western Ghats of India. It reaches up to a height of 25 m. The trees are found growing between 450 and 1000 m. in the semi-evergreen forests of Gujarat, Dadra & Nagar Haveli, Maharashtra and Dandeli, Karnataka. They are widely distributed in most tropical countries, including Africa, Asia and South America; their leaves and stem bark have been used frequently in folk medicine as a remedy for different pathologies, particularly diabetes, infections, pain and inflammatory processes.^[71,72,75,78]

2.2.6. Morphological Description ^[71,72,76,78]

The genus *Bauhinia* (Fabaceae, Leguminosae) constitutes nearly 300 - 400 species, out of which most studied are *B. racemosa*, *B. variegata*, *B. purpurea*, *B. forficata*, *B. mondara* etc., which are commonly known as 'cow's paw' or 'cow's hoof', because of the shape of their leaves.

The leaves of *B. foveolata* are probably the largest of all *Bauhinia* species in India. The leaves can be over a foot across. The species name *foveolata* is derived from the fact that the underside of the leaves is covered with minute pores (foveoli), each of which has a sort of stopper or plug retained in position by a slender thread coming from the middle of the pore. These pores are somewhat like chained plugs in kitchen sinks.

The leaves are sub-orbicular, deeply cordate at the base, glabrous above, pubescent beneath, and nerve slightly pitted beneath. Leaves are alternate, 2-6 inches long, 3-7 inches wide, bifurcated and rounded. They are suborbicular to broadly ovate, subacute to broadly obtuse lobes at apex, cordate at base, glabrous above, pubescent beneath with numerous closely situated fine pits within areolae of reticulations and each pit with a hyaline inflated trichome; petioles 3 cm - 7.2 cm long, shallowly grooved and pubescent.

The flowers are not very showy compared to other *Bauhinia* species. They are white in colour and about a cm or so across. Flower buds are obovoid, obtuse at the apex, and densely pubescent. The hypanthium is 3-5 mm long, turbinate, and pubescent. Bracts are minute, ovate, pubescent; bracteoles similar, situated near the pedicel base. The petals are white, 12-16 mm x 3-4 mm in size, oblong to obovate shape, obtuse at the apex, veined, glabrous inside, with inflated trichomes on outer side. Flowers are small, unisexual, in dense with branched panicles, 5-lobed calyx tomentose, and white-to-light cream corolla with alternate long and short stamens, densely hairy ovary, linear-oblong pods, and red tomentose. Gynophore is 1.5-2 mm long, free, pubescent; ovary is 8-10 x 1.5-2 mm, densely pubescent; stigma is 2.5 mm across and peltate. The bark and stem have terminal or axillary panicles, often as aggregates on the common peduncle, and its reflexed branches are pubescent. The pods are up to 48 x 3.5 cm, linear-oblong, tapering towards the apex, twisted, ligneous, finely pitted, and pubescent. Pods appear as linear-oblong-tomentose, reddish brown in colour. The seeds are 5-8 mm across, oblong to suborbicular in shape.

The traditional uses, phytoconstituents and pharmacological activities reported are of the species of the *Bauhinia* genus, since no much literature has been reported on *Bauhinia foveolata* Dalzell.

2.2.7. Traditional Uses

In treatment of dysmenorrhea, menorrhagia, tuberculosis, asthma, bronchitis, diabetes, pain and inflammation, haemorrhage, leprosy, tumors, epilepsy, ulcers, carminative, laxative, tonic, astringent, anthelmintic etc. ^[73,78]

2.2.8. Phytoconstituents

Alkaloids, Flavonoids, Steroids and Triterpenes, Phenolics, Catechins, Tannins, Anthraquinones etc. ^[77,78]

2.2.9. Pharmacological activities

Antioxidant, Anti-inflammatory, Anticarcinogenic, Antimicrobial, Antihyperlipidemic, Hepatoprotective, Hypoglycaemic, Nephroprotective, Proteinase Inhibitor, Wound healing activity, Antiulcer, Immunomodulatory. [77,78]

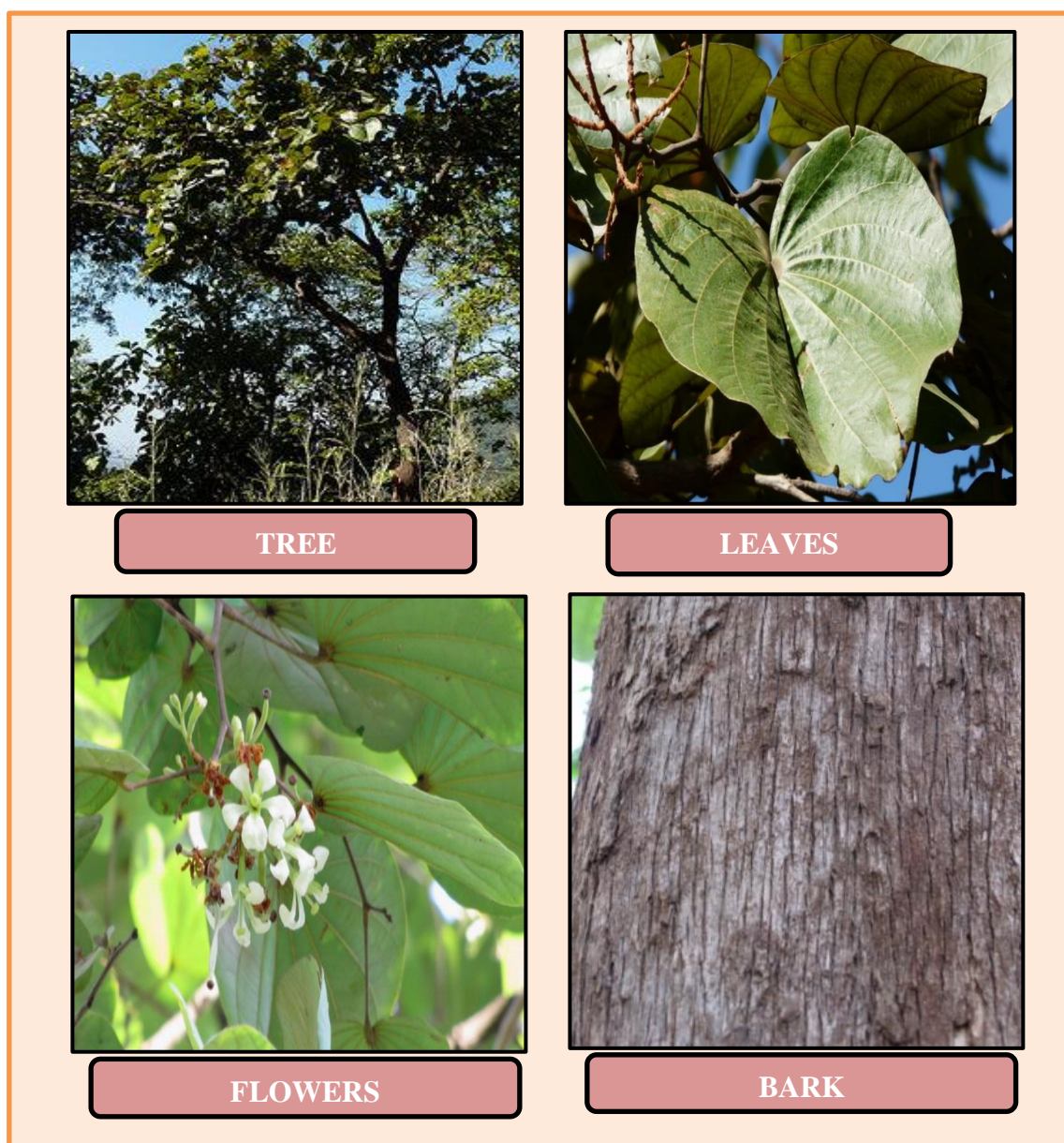
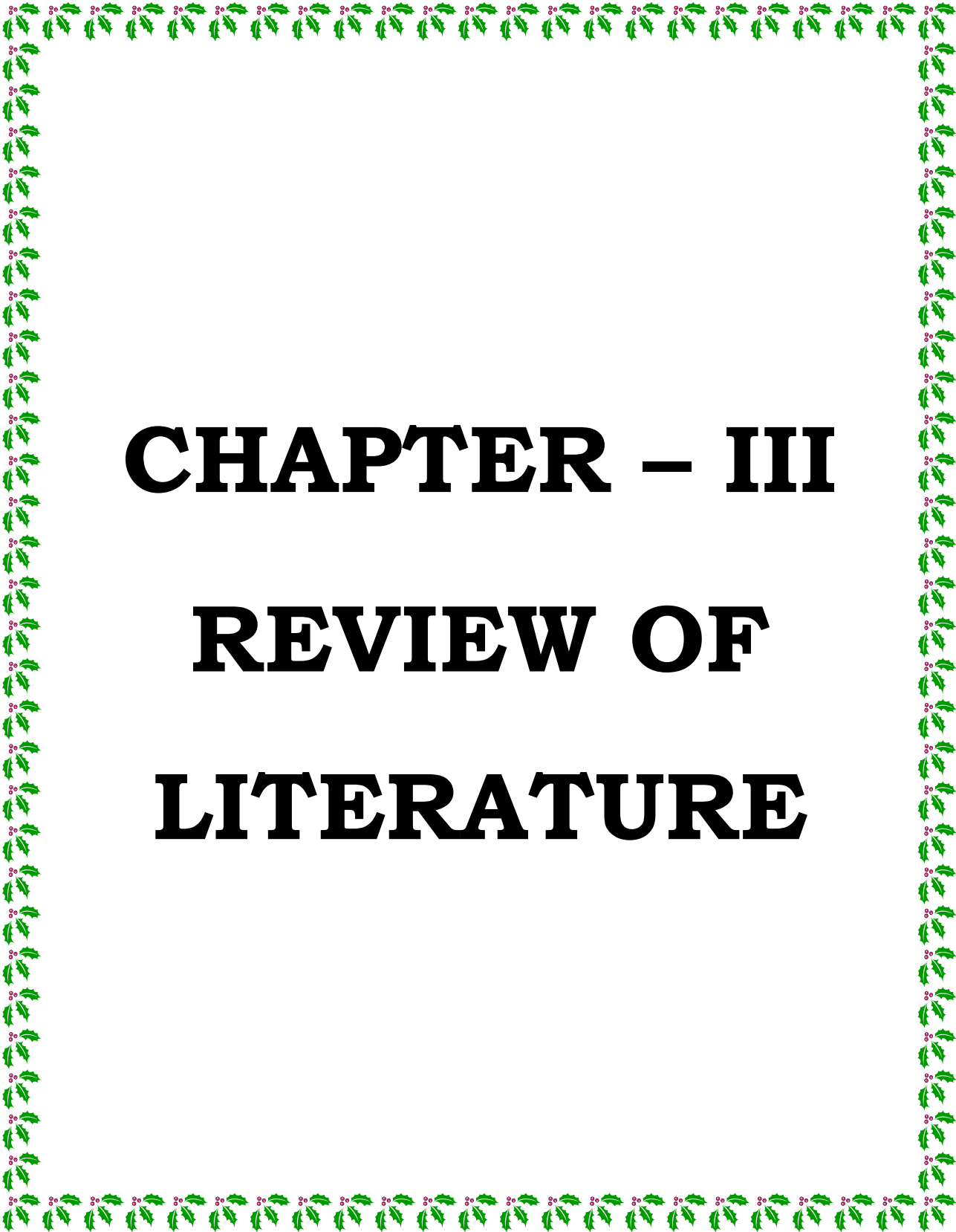


Figure 2.2: Morphological parts of *Bauhinia foveolata* [75-76]



CHAPTER – III

REVIEW OF

LITERATURE

3. REVIEW OF LITERATURE

3.1. Review of *Hybanthus enneaspermus*

Mohanty et al. (2023) ^[79] described the phytoremediation potential of *Agrobacterium*-mediated transformed hairy roots of *H. enneaspermus* adsorbed with toxic metals like selenium (Se) and lanthanum (La) and compared it with plantlets under *in-vitro* conditions. *Agrobacterium rhizogenes* A4RS induced hairy roots with higher biomass in 5-7 days of infection on *in-vitro* leaves of *H. enneaspermus*. Inductively coupled plasma optical emission spectrometry (ICP-OES) data indicated that the hairy roots could accumulate both selenium and lanthanum more efficiently than plantlets. The hairy roots and plantlets demonstrated optimum absorption at 50 ppm under individual and combined metal supply. The metal accumulation performances of La were increased by 13.6 % and Se by 10.9 % in hairy roots with combined metal supply (La and Se) compared to individual supply (La or Se) conditions. The Se accumulated more than La, but the La accumulation percentage increased considerably under combined metal supply conditions, displaying the suitability and potential of hairy roots for the phytoremediation of La and Se.

Sathish et al. (2023) ^[80] reported the precursor-feeding enhancement of L-Dopa production in the hairy root culture of *H. enneaspermus*. An efficient and reproducible protocol for *Agrobacterium rhizogenes*-mediated hairy root was efficiently induced from *in vitro* grown leaf explants of *H. enneaspermus*. Among the various factors analysed, acetosyringone (100 μ M), sonication (40 s), and vacuum infiltration (2 min) followed by two day co-cultivation period revealed a maximal percentage of hairy root induction using A4 strain (29.6 %). Polymerase chain reaction (PCR) analysis confirmed the transgenic status of the hairy root by using the *rol B* gene-specific primer. The highest amount of fresh weight (17.71 g) and dry weight (2.14 g) was noted in the 40-day-old *A. rhizogenes*-induced hairy root cultures. The optimal production of L-Dopa (32.71 mg/g dry weight) was observed when the hairy roots were treated with the precursor L-tyrosine (100 μ M), as

compared with the control culture. The research enabled to design the procedure to transfer the gene of interest for secondary metabolism into the hairy roots of *H. enneaspermus*.

Maheswari et al. (2022) ^[81] investigated pure titanium dioxide (TiO₂) and their composite nanostructures [Cupric oxide (CuO-) and Zinc oxide (ZnO-) loaded TiO₂] prepared by the modified hydrothermal cum green synthesis method. Various analyses like structural, surface and morphology, chemical functional groups and optical analysis of the prepared nanostructures were conducted. The XRD pattern confirmed the anatase phase structure of TiO₂, and the aggregated spherical-shaped particles were observed from Field Emission Scanning Electron Microscopy (FESEM) image analysis. The various functional groups related to TiO₂ were observed from FTIR and Raman analysis. The optical band gap of TiO₂ and CuO- and ZnO-loaded TiO₂ composites were calculated as 3.2 eV, 2.64 eV and 2.60 eV. The nanostructures prepared were examined using methylene blue dye for photocatalytic performance and rhodamine dye at different times of UV irradiations (60, 120, 180 min) for three pH values (4, 6 and 8). It was observed that among the three samples, CuO- and ZnO-loaded TiO₂ composite nanostructures showed excellent dye degradation for the pH of 6. The antioxidant activity of TiO₂/CuO/ZnO composites was enhanced (55.10 ± 0.20 %) as compared to other compounds.

Sathish et al. (2022) ^[82] evaluated the impact of silver nanoparticles on the micropropagation of *H. enneaspermus* and assessed the genetic fidelity using Random Amplified Polymorphic DNA (RAPD) and Start Codon Targeted (SCoT) markers. Clonal propagation of *H. enneaspermus* was carried out using shoot tips as explants, induced on Murashige and Skoog (MS) medium enriched with different levels of 6-benzyl amino purine (BAP), kinetin (Kin) and thiadiazuron (TDZ) and silver nanoparticles (AgNPs). The optimum concentration of BAP (1.5 mg/L) with AgNPs (3 mg/L) exhibited a determined response of 90.66 % and created a maximum of 77.23 shoots with a maximum shoot length of 3.72 cm after four weeks. The vigorous shoots were embedded on an MS medium

modified with optimum concentration of Indole-3-butyric acid (IBA, 1 mg/L) and AgNPs (1 mg/L), exhibiting the highest number of roots (9.65) with an average root length of 4.77 cm and 87 % response. The rooted plantlets were efficiently acclimatized in the soil. Genetic homogeneity analysis revealed that the regenerated plants were genetically uniform, and no detectable genetic difference was observed when compared to the mother plant. The study helped in providing a new protocol for targeted gene editing in *H. enneaspermus*.

Al-Owaisi et al. (2022) ^[83] assessed the ability of aqueous extracts of 13 medicinal herbs to detoxify aflatoxin B1 (AFB1), a potent and commonly occurring carcinogen in foods. The herbal extracts of *H. enneaspermus*, *Eclipta prostrata* and *Centella asiatica* exhibited over 70 % detoxification of AFB1. LC-MS and TLC analysis confirmed the degradation of AFB1. Two purified fractions from *H. enneaspermus* (R_f 0.75 and 0.87) using TLC displayed *in vitro* AFB1 detoxifying properties. The analysis of the active fractions by GC-MS revealed the presence of linalool and bornyl acetate as significant components. These results suggest the possible involvement of volatile compounds of *H. enneaspermus* in the detoxification of AFB1.

Katta et al. (2022) ^[84] reported the pathophysiology of diabetic cataracts to formulate and develop novel and effective anti-cataract agents. The study explored the protective role of *Piper longum* and *H. enneaspermus* in preventing oxidative damage of lens protein in glucose-induced cataracts in goats. Cataractogenesis in diabetes is mainly due to the generation of free radicals causing the oxidation of long-lived proteins. Various study parameters, *viz.* malondialdehyde (MDA), total soluble lens proteins, and protein carbonyl level as a measure of lens protein oxidation, were measured in the lens homogenates. Both the extracts of *Piper longum* and *H. enneaspermus* exhibited a significant reduction in the concentration of protein carbonyl levels, preserved the total soluble proteins and lowered the MDA content ($p < 0.001$). The aqueous seed extract

of *Piper longum* exhibited better anti-cataract activity compared to *H. enneaspermus* against glucose-induced cataract formation in the organ culture model. This can be attributed to its antioxidant activities which might help inhibit the peroxidation of lipids and oxidation of lens proteins.

Sankareswaran (2021) ^[85] analyzed the *in silico* molecular docking of Anti-Human Immunodeficiency Virus-1 Reverse Transcriptase (Anti-HIV-1 RT) from *H. enneaspermus*. A blended docking and neural framework approach was used to screen against HIV-1 inhibitors of HIV-1 RT from active compounds from *H. enneaspermus*. Five bioactive compounds, namely, Apigenin, Quercetin, Luteolin, Quercetin 3-o- α -d-rhamnoside, Kaempferol-3-o- α -rhamnoside, were used for molecular docking studies in the direction of drug improvement towards HIV-1 RT (PDB -1FK9) by Autodock software. Among the five biomolecules screened, Apigenin exhibited the highest dock score of -7.21, indicating a great scope in designing novel anti-HIV drugs.

Kumari et al. (2021) ^[86] evaluated the anti-urolithiasis activity of ethanolic extract of *H. enneaspermus* by *in silico* and *in vitro* approaches. The *in vitro* anti-urolithiasis study was conducted with ethanolic extract and standard drug, Cystone, using five assays viz. crystal dissolution, crystallization, nucleation, aggregation, and growth assay of crystal. *In silico* studies were done using AutoDock 4.2 tools to determine the binding energy and affinity of chemical constituents (Rutin and Quercetin) against the adenine phosphoribosyltransferase, oxalate oxidase, glycolate oxidase with their PDB ID: 1L1Q, 2ETE, 2RDT. Compared with cystone, the plant extract can prevent and inhibit the crystal dissolution, crystallization, nucleation, aggregation and growth of the crystal. *H. enneaspermus* also exhibited strong binding energy and affinity towards the targets Adenine phosphoribosyltransferase, Oxalate oxidase, and Glycolate oxidase in *in-silico* studies. The study thus proved that the ethanolic extract of *H. enneaspermus* has a potent urolithiasis activity.

Suchithra et al. (2021) ^[87] reported the *in vitro* antioxidant, antidiabetic and antiurolithiatic activity of synthesised silver nanoparticles using stem bark extracts of *H. enneaspermus*. Silver nanoparticles of the stem bark extracts were characterised using UV-Vis, FTIR, TEM, XRD and DLS methods for further confirmation. TEM analysis revealed that the silver nanoparticles formed were spherical. X-ray diffraction confirmed that the silver nanostructure exhibited a face-centred cubic crystal structure. DLS showed that the size of the nanoparticles is 644.2 nm. By increasing the concentration of silver nanoparticles, the weight of the formed crystals reduced from 0.94 g to 0.13 g in struvite crystals and was analysed by FTIR analyses. This multidisciplinary approach showed a better percentage of inhibition, thus indicating the antioxidant, antidiabetic and antiurolithiatic activity of silver nanoparticles.

Du et al. (2020) ^[88] evaluated the *in vivo* aphrodisiac activity of the herbal powder, extract, and the most abundant cyclotide, hyen D, extracted from *H. enneaspermus* on rats in a single dose regimen. The results indicated that the extract and hyen D significantly decreased the intromission latency of sexually naïve male rats, and the extract improved a range of other measured sexual parameters *viz.*, first behavior latency, mount frequency, ejaculation latency, and ejaculation post interval. The results suggested that the extract could enhance libido and facilitate erectile function in male rats and that the cyclotide hyen D could contribute to the libido-enhancing activity of this ethnomedicinal herb.

Nivethitha et al. (2020) ^[89] assessed the cytotoxic and antioxidant activity of *H. enneaspermus* silver nanoparticles using brine shrimps. They reported a proportionate increase in antioxidant and cytotoxic activities with increasing concentrations of the silver nanoparticles. Silver nanoparticles produce reactive oxygen species and free radicals, causing apoptosis (cell death) and thereby preventing their replication. Antioxidants have resistance against oxidative stress by scavenging free radicals, thereby preventing many

diseases. The antioxidant activity was analysed by the DPPH method. The percentage of the lethality of brine shrimps and antioxidant activity increased as the concentration of the silver nanoparticle increased, thus indicating that silver nanoparticles of *H. enneaspermus* possess both cytotoxic and antioxidant activities.

Sathish et al. (2020) ^[90] reported the effect of elicitors in enhancing the L-Dopa production from adventitious root cultures of *H. enneaspermus*. The adventitious root culture was established from the leaf explants of *H. enneaspermus*. Highest root induction frequency of 70.66 % with 17.76 roots per explant was recorded in explants inoculated on MS medium supplemented with IBA 0.5 mg/L. The effect of elicitors on the biosynthesis of L-Dopa content was evaluated by exposure of adventitious roots to different durations and concentrations of salicylic acid (SA), yeast extract (YE), methyl jasmonate (MeJA) and silver nitrate (AgNO₃). The elicitor salicylic acid at 100 µM dosage for 6 h enhanced L-Dopa yield to 12.64 mg/g dry weight compared to the control culture. The above findings revealed that the elicitation experiment could improve the production of L-Dopa in adventitious root cultures of *H. enneaspermus*. It may also serve as a source for commercially producing these essential secondary metabolites.

Patel (2020) ^[91] evaluated the antidiabetic, antioxidant and nephroprotective activity of a flavonoid-rich fraction of *H. enneaspermus* in diabetic rats along with *in-silico* molecular docking studies for SOD, CAT, GPx, xanthine oxidase and nuclear factor kappa B (NF-KB). The flavonoid-rich fraction was prepared using ethyl acetate. The oral glucose tolerance test normoglycemic effect of the flavonoid-rich fraction of *H. enneaspermus* (EHE) was evaluated orally at 45 mg/Kg and 90 mg/Kg doses. The effect of EHE on blood glucose, BW, enzymes such as SOD, CAT and thiobarbituric acid reactive substances (TBARS) and lipid parameters were estimated out at 45 and 90 mg/Kg orally daily for 21 days in streptozotocin-induced type-2 diabetic rats. A molecular docking technique was also performed against SOD, CAT, GPx, xanthine oxidase and nuclear factor

kappa B (NF-KB) for selected phytoconstituents. EHE showed a significant amount of phenolic, tannin, flavonoid and saponin. EHE significantly decreased blood glucose levels in diabetic rats. All the tested lipid parameters and enzyme levels of SOD, CAT and GPx were significantly restored to the normal level in the EHE-treated rats. Moreover, there was a significant increase in BW in the EHE-treated rats. The docking study showed the best binding affinity and interaction of phytoconstituents with xanthine oxidase, and NF-KB signified their role in kidney disorders. Thus the authors concluded that EHE has an imposing profile as an antidiabetic, antioxidant and nephroprotective drug in treating kidney disorders in hyperglycemia.

Amrithaa et al. (2020) ^[92] assessed the anti-inflammatory and antimicrobial properties of *H. enneaspermus* mediated silver nanoparticles. The AgNPs were synthesized using *H. enneaspermus*, acting as a capping and reducing agent at room temperature. It was further subjected to evaluation of antimicrobial and anti-inflammatory activity. Antimicrobial activity was evaluated using Minimum inhibitory concentration (MIC) and Minimum bactericidal concentration (MBC) by diffusion method. Anti-inflammatory activity was evaluated using diclofenac sodium in different concentrations and served as a standard. *H. enneaspermus*-mediated AgNPs demonstrated a proportionate increase in activity with increasing dose concentration for their antimicrobial and antioxidant properties. Thus, the study concluded that *H. enneaspermus*-mediated AgNPs demonstrated substantial antimicrobial and antioxidant activity.

Patel (2019) ^[93] evaluated the flavonoid-rich extract of *H. enneaspermus* in Streptozotocin-Nicotinamide-induced diabetic rats along with antioxidant enzymes. The flavonoid-rich fraction was isolated using ethyl acetate solvent, and phytochemical analysis was carried out to detect the presence of chemical compositions. Male Charles Foster rats were used in this study. The effect of ethyl acetate fraction of *H. enneaspermus* (EHE) was evaluated at a dose of 45 mg/Kg and 90 mg/Kg orally per day for 21 days in diabetic rats.

The effect of ethyl acetate fraction on blood glucose, BW the enzymatic activity of superoxide dismutase (SOD), catalase (CAT) and thiobarbituric acid reactive substance (TBARS) were analyzed in the supernatant of the 10 % liver tissue homogenate in 0.025 M Tris-HCl buffer (pH 7.5). Lipid parameters such as total cholesterol (TC), triglycerides (TG), High-density lipoprotein cholesterol (HDL-C), Very low-density lipoprotein-cholesterol (VLDL-C), Low-density lipoprotein-cholesterol (LDL-C), atherogenic index (AI) etc. were determined. The effect of EHE on glucose uptake by rat hemidiaphragm was also investigated. EHE exhibited significant content of phenolic, tannin, flavonoid, flavonol and saponins. All the tested lipid parameters (TC, TG, HDL-C, VLDL-C, AI) and antioxidant enzyme (SOD, CAT, and TBARS) levels were significantly restored to the normal level in the EHE-treated rats, with a significant increase in the BW and glycogen content. Glucose uptake by the hemidiaphragm was also enhanced in the presence of EHE. The study indicated that EHE is a strong antioxidant and hypolipidemic agent candidate.

Patel (2019) ^[94] investigated the aldose reductase inhibitory (ARI) potential of phytoconstituents rich principles from the whole plant of *H. enneaspermus*. Hot extraction technique with ethanol was used to prepare the ethanolic extract of *H. enneaspermus* and screened to detect the phytoconstituents present by standard official methods. Total phenol, flavonoid and flavonol content were determined using Folin-ciocalteu reagent and aluminium trichloride. Healthy adult Wistar albino rats were used to evaluate the aldose reductase inhibitory potential. The study revealed the presence of various secondary metabolites and a significant amount of phenol, flavonoid and flavanol content in the ethanolic extract. The extract reported significant ARI activity with IC_{50} of 49.46 ± 2.26 $\mu\text{g/mL}$ but was less compared to standard quercetin (IC_{50} 3.326 ± 0.11 $\mu\text{g/mL}$). The authors inferred that the ethanolic extract of *H. enneaspermus* exhibited significant ARI activity, attributing to high levels of phenols and flavonoids.

Shekhawat et al. (2018) ^[95] reported the *in vitro* multiplication, micromorphological studies and *ex vitro* rooting of *H. enneaspermus*. Surface-sterilized nodal segments were cultured on Murashige and Skoog (MS) medium with different concentrations of 6-benzyl amino purine (BAP) and kinetin (Kin). Shoots were further proliferated maximally on MS medium augmented with BAP and Kin within 4 - 5 weeks. The shoots were rooted *in vitro* on a half-strength MS medium containing IBA. The cloned shoots were pulse-treated with IBA and cultured on soil rite in a greenhouse. About 96 % of the IBA-pulsed shoots were rooted *ex-vitro* in soil rite. The *ex-vitro* rooted plantlets showed a better rate of survival (92 %) in a field study than *in vitro* rooted plantlets (86 %). A comparative foliar micromorphological study of *H. enneaspermus* was performed from *in vitro* to *in vivo* conditions to understand the micromorphological changes during plant developmental processes concerning variations in stomata, vein structures and spacing, and trichomes. The authors concluded that the *ex-vitro* rooting in *H.enneaspermus* could be exploited for conservation and large-scale propagation of this medicinally important plant.

Aigbe et al. (2018) ^[96] evaluated the analgesic activity of the aqueous leaf extract of *H. enneaspermus* (ALHE) at 50, 100 and 200 mg/Kg, BW orally in rodents. Acetic acid and acetylcholine-induced mouse writhing tests, formalin-induced pain and tail clip tests in mice were used to determine analgesic activity. Naloxone, glibenclamide or pilocarpine were administered to some animals 30 min before ALHE prior to induction of pain. Open field and phenobarbitone-induced sleep tests were the parameters used to evaluate the CNS activity of the extract in addition to its analgesic action. The extract (50 - 200 mg/Kg) significantly inhibited writhing in the acetic acid- and acetylcholine-induced mouse writhing tests. It was most effective at 100 mg/Kg, producing 97.6 % and 96.5 % inhibition in both tests. Naloxone, glibenclamide and pilocarpine significantly ($p < 0.001$) altered this analgesic effect of the extract. The extract also significantly ($p < 0.001$) increased the pain threshold in the tail clip test and reduced reaction time in both phases of the formalin-

induced pain test. The extract significantly reduced the locomotive and exploratory activities of mice in the open field test. However, it did not significantly affect the hexobarbitone-induced sleep test in mice. The results thus indicated that the aqueous extract of *H. enneaspermus* probably acts through mechanisms likened to those of opioid receptor antagonists, muscarinic receptor antagonists, and potassium channel openers.

Muthu et al. (2017) ^[97] isolated and characterized the active compounds derived from the whole plant of *I. suffruticosum*. The plant was extracted with various solvents (petroleum ether, ethyl acetate and methanol) and subjected to preliminary phytochemical screening. The methanolic extract of *I. suffruticosum* was chromatographed using different solvent fractions. FTIR, NMR and mass spectrophotometric methods characterized the structures of the isolated compounds. The preliminary phytochemical screening results revealed the presence of coumarins, flavonoids and amino acids as active constituents from the methanolic extract of *I. suffruticosum*. Three compounds were isolated from the methanolic extract by column chromatography. The structural elucidation led to the characterization of 3-amino-6-hydroxy-4-(4-methylphenyl)-2H-chromen-2-one (145 mg), 1-amino-1-ethoxypropan-2-ol (135 mg) and methyl-2-hydroxy-4-methoxy benzoate (110 mg).

Afolabi et al. (2017) ^[98] determined the mechanisms involved in the analgesia produced by ethanol extract of *H. enneaspermus* leaves. Forty-two male Wistar rats were used for the analgesic study by tail immersion and formalin test models. Animals were segregated into seven sets of six rats each. Group I (control) received distilled water (10 mL/Kg), while groups II and III received acetaminophen (the reference drug, 100 mg/Kg *i.p.*) and EEHE (1000 mg/Kg orally), respectively. Groups IV-VII were pretreated with cimetidine (50 mg/Kg *i.p.*), naloxone (5 mg/Kg *i.p.*), propranolol (0.15 mg/Kg *i.p.*), and prazosin (0.15 mg/Kg *i.p.*), respectively, 1 h before EEHE treatment. The results indicated that EEHE-induced increase in tail-flick latency, was reduced by the blockade of histamine

and adrenergic receptors, However, this action was prevented by the blockade of opiate receptors in the tail-flick test. Also, the EEHE-induced decrease in paw-licking time and increase in tail-flick latency was prevented by the blockade of opiate receptors but unaffected by histamine and adrenergic receptor blockers. The authors concluded that the analgesic effect of EEHE in different pain types may involve different neural mechanisms and that the opioidergic pathway contributes more to EEHE-induced analgesia than the other pathways.

Jayanthi et al. (2017) ^[99] determined the total phenolic and flavonoid content of ethanolic extracts of stem and root of *H. enneaspermus* by Folin-Ciocalteu and Aluminium Chloride methods, respectively. In the present study, the *H. enneaspermus* stem and root were powdered and extracted with ethanol to yield the ethanolic extract. Total phenolic content in stem and roots was 18.497 ± 0.976 and 15.459 ± 0.787 , and total flavonoid content was 2.321 ± 0.787 and 1.671 ± 0.487 respectively. It was noted that the phenol and flavonoid contents in the stem were higher than in the root extract.

Chenniappan et al. (2017) ^[100] evaluated the therapeutic and fertility restoration effects of *I. suffruticosum* on sub-fertile male Wistar albino rats. The effects were observed on testis and caudal spermatozoa. The ethanol lyophilized fraction of the leaf extract of *I. suffruticosum* was administered orally on carbendazim-induced sub-fertility rats (250 mg/Kg BW for 28 days). The effects of fractions on rat's fertility parameters, i.e., body and testes weight, sperm motility, sperm vitality, epididymal sperm counts, its morphology, enzyme and antioxidant stress and histopathology, were studied and compared with clomiphene citrate. The sub-fertile male rats treated with *I. suffruticosum* leaf extract increased their BW by 7 g, testis weight of 97 mg, increased cauda epididymal sperm counts of 34.2×10^6 sperms/mL. The motility of the sperm and vitality were increased by 46% and 28 %, respectively, while the normal sperm morphology improved up to 32%. The

carbendazim-treated group showed a loss in BW of 33 g, testis weight of 851 mg, and decreased epididymal sperm counts of 15×10^6 sperm/mL, with sluggish motility. A significant fall in the live sperms of about 57 % was observed. Thus, the leaf fraction of *I. suffruticosum* increased the testicular weight, spermatogenesis, sperm counts, lessened sperm agglutination, and increased testicular oxidative biomarkers, SOD, and CAT. Thus, the study effectively supported the traditional claim of *I. suffruticosum* in treating infertility.

Jaikumar et al. (2016) ^[101] evaluated the anticancer potential of ethanolic leaf extract of *H. enneaspermus* against Hep-2 cell lines. The ethanolic fraction of *H. enneaspermus* was subjected to GC-MS analysis, which revealed the presence of eight new compounds viz. Coumarine, 7- formyl-4-methyl, Cycloheptene,4- methoxy2-phenyl, alpha Cuvebene, Cromaril, 4H-1-Benzopyran-4-one, 7-hydroxy-2-(4- hydroxyphenyl), 4'5,7-Trihydroxy isoflavone, 16-Octadecenoic acid, methyl ester and 4H-1-Benzopyran-4-one, 2-(3,4- dimethoxyphenyl)- 5-hydroxy-3,7- dimethoxy. The ethanolic extract indicated potent growth inhibitory activity against the Hep-2 cell line with an IC₅₀ value of 19.75µg/mL, confirming the potential use of *H. enneaspermus* anti-proliferative agents against hepatocellular carcinoma.

Anupa et al. (2016) ^[102] carried out the phytochemical and *in vitro* antioxidant activity of *H. enneaspermus*. Dried leaves of the plant were extracted with hexane, chloroform, ethyl acetate, ethanol and distilled water. Preliminary phytochemical screening was performed using a standard protocol. DPPH, reducing power and hydrogen peroxide free radical scavenging methods were used to evaluate the antioxidant activity of the ethanolic extract. The preliminary phytochemical screening demonstrated the presence of flavonoids, terpenoids, tannins, phenols and saponins. The ethanolic extract exhibited maximum free radical scavenging activity in the DPPH model (24.32 %) compared to the standard (45.41 %) at 60 mg/mL. The reducing power assay exhibited maximum

absorbance of 1.038 at 60 mg/mL, while the percentage inhibition of hydrogen peroxide radicals was 35.11 %. Thus ethanolic leaf extract exhibited significant antioxidant activity, serving as a better source of natural antioxidants and thus preventing the progress of oxidative stress.

Suman et al. (2016) ^[103] assessed the bioactive components from the whole plant of *H. enneaspermus* by GC-MS analysis, biosynthesized its silver nanoparticles at room temperature and then evaluated its larvicidal activity. The AgNPs were synthesized using *H. enneaspermus* L. extract, acting as a reducing and capping agent at room temperature. The synthesized AgNPs were characterized by UV-Vis spectroscopy, XRD, FTIR, Zeta potential, DLS, TEM and EDX. The silver surface plasmon resonance was measured at 420 nm in the UV-Vis spectrum. FTIR revealed that the AgNPs were capped with plant compounds of alcohol, phenols, carbonyl, amines, and amide functional groups. TEM image showed that the particles were spherical, hexagonal, and triangular in shape, and the size range was 16 - 26 nm. DLS study showed an average size of 25.2 nm, and the zeta values were measured (-27.1 mV), proving the nanoparticles' stability. The biosynthesized AgNPs showed larvicidal activity with LC₅₀ values of 17.24 and 13.12 mg/L against the fourth-instar larvae of *Anopheles subpictus* and *Culex quinquefasciatus*, respectively. The GC-MS analysis of the plant extract revealed the presence of 39 bioactive phytochemical compounds possessing a wide range of activities that may be responsible for treating incurable diseases.

Behera et al. (2016) ^[104] evaluated the genetic stability and coumarin content of transformed rhizoclones and regenerated plants of *H. enneaspermus*. The transformed nature of *Agrobacterium rhizogenes*-transformed hairy root somaclones (rhizoclones) was verified by PCR amplification of *rolA-B* and *mas2* genes. Clonal fidelity among rhizoclones was revealed by RAPD analysis exhibiting DNA monomorphism. Transformed leafy shoots exhibited maximum coumarin content (3.25 mg/g dry weight) significantly

higher than natural aerial part samples. Genetic stability of selected fast-proliferating rhizoclones and their respective *in vitro* shoot regenerants in terms of RT-PCR based expression of *rolB* and *rolC* genes and coumarin content was maintained through 16 successive multiplication cycles. This investigation indicated the possibility of harnessing the genetically stable biosynthetic potential of hairy root clones and transformed shoot regenerants of *H. enneaspermus in vitro* towards maintainable production of coumarin and other medicinally essential phytochemicals.

Thiru et al. (2015) ^[105] assessed the regulation of the ROS defence system by *H. enneaspermus* in carbon tetrachloride (CCl₄) to induce cardiac damage. Administration of CCl₄ induces damage in the rats' heart with a reduction in antioxidant enzymes such as SOD, CAT, GPx, GR, GST. However, treatment with ethanolic extract of *H. enneaspermus* (HEE) in CCl₄-intoxicated rats was found to protect the heart, as indicated by the enzyme levels in the serum. A significant increment of serum enzyme levels such as SOD, CAT, GPx, GR and GST were observed following HEE treatment during CCl₄ intoxication. However, Malondialdehyde (MDA) levels in HEE-treated rats were reduced. Thus the results suggested that treatment of HEE may be the remedy for the adverse effect of CCl₄ on heart function.

Sundaram et al. (2015) ^[106] studied and compared the antioxidant activity of crude and alkaloid extracts of *H. enneaspermus*. Antioxidants such as catalase, peroxidase, superoxide dismutase, vitamin C, vitamin E and lipid peroxidation assays were analyzed in both extracts. The content of total tannins, phenols, flavonoids, carotenoids and alkaloids was estimated using standard procedures. Free radical scavenging activity was assayed using DPPH, ABTS, superoxide radical, nitric oxide, hydroxyl radical, hydrogen peroxide, H₂O₂, FRAP and reducing power methods. The results confirm that the crude and alkaloid extracts of *H. enneaspermus* revealed a high level of secondary metabolites and antioxidant activities. *H. enneaspermus* showed significant antioxidant properties, acting as a good

source of natural antioxidants that may be beneficial in preventing the destructive process of various oxidative stress.

Velayutham et al. (2015) ^[107] investigated the bioactive compounds from the methanolic leaf extracts of *in vivo*, *in vitro* and fungal elicited *in vitro* plants of *H. enneaspermus* through GC-MS analysis. The leaf explants were cultured on MS (Murashige and Skoog) medium complemented with different concentrations of NAA (1-naphthalene acetic acid) for callus induction. The calli were treated with four different fungal elicitors, namely, *Mucor prayagensis*, *Trichoderma viride*, *Fusarium moniliformis* and *Aspergillus niger*, on suspension culture containing the same growth regulators for two weeks. The GC-MS analysis revealed that the leaves of *in vivo* and *in vitro* plants contained 16 different phytochemicals, whereas the fungal treated *in vitro* plants showed more phytochemicals, i.e., 22 (*Mucor prayagensis*), 26 (*Trichoderma viride*), 19 (*Fusarium moniliformis*) and 21 (*Aspergillus niger*) compounds. The study demonstrated that the fungal species could be used to elicit and enhance the secondary metabolites in medicinal plants.

Afolabi et al. (2014) ^[108] assessed the antinociceptive effect of ethanolic leaf extract of *H. enneaspermus* in rats. Seventy-two male rats were randomly divided in a blinded fashion into four groups, each for the tail immersion test (n=12) and formalin test (n=6). Group 1 (control) received 0.6 mL of distilled water. Group 2 received 100 mg/Kg of acetaminophen (paracetamol). Groups 3 and 4 received 500 mg/Kg and 1000 mg/Kg of ethanolic extract of *H. enneaspermus* leaf (EEHE), respectively. In the formalin test, oral administration of 500 mg/Kg and 1000 mg/Kg EEHE caused inhibitions of 62.48% and 72% in the early phase and 70.54% and 78.63% in the late phase, respectively. The 1000 mg/Kg dose significantly reduced the paw-licking time compared to the standard drug (acetaminophen) in the formalin test. The 500 mg/Kg and 1000 mg/Kg doses significantly

increased the tail-flick latency in a manner comparable to acetaminophen, thus evaluating the antinociceptive effect of the leaf extract.

Ragavan et al. (2014) ^[109] evaluated the qualitative and quantitative analysis of phytochemicals and minerals, free radical scavenging, total antioxidant reduction potential, HPTC analysis and *in vitro* cytotoxic effect of hydroethanolic extract of *H. enneaspermus*. The results revealed the presence of alkaloids, flavonoids, carbohydrates, protein, phenols, steroids, tannins, glycosides and terpenoids. Iron content was reported to be 42 mg/g, and phosphorus (3.4 mg/g) among the minerals. Amongst the various methods used to evaluate free radical scavenging activity, the hydroethanolic extract of *H. enneaspermus* (HEEHE) exhibited significant antioxidant potential with IC₅₀ values of 78.49, 254.51, 210.52, 112.56 and 236.51 µg/mL by DPPH, superoxide, nitric oxide, hydroxyl and reducing power assays respectively. High-performance thin-layer chromatography (HPTLC) chromatogram showed the presence of flavonoids and glycosides in the *H. enneaspermus* extract.

Vamsi et al. (2014) ^[110] described the antibacterial activity of *H. enneaspermus* against *Enterococcus faecalis* - a root canal organism. The aqueous extract of *H. enneaspermus* was tested against the most resistant bacteria of the root canal system *E. faecalis*, using a microbiological agar diffusion test. The aqueous herbal extract exhibited a significant inhibitory effect on the root canal organism, thus confirming its possible use as a root canal irrigant.

Patel et al. (2013) ^[111] investigated the glucose utilization capacity of bioactivity-guided fractions (petroleum ether, chloroform, and aqueous) of *H. enneaspermus* and *Pedaliium murex* in isolated rat hemidiaphragm. *In vitro* glucose uptake by hemidiaphragm study showed increased utilization of the glucose by hemidiaphragm in the presence of different fractions, thus concluding that different fractions of both plants had extra pancreatic mechanisms like glucose uptake by peripheral tissues.

Vetriselvan et al. (2013) ^[112] evaluated the antihyperlipidemic potential of hydroalcoholic extract of *H. enneaspermus* against high-fat diet-induced Wistar albino rats. The animals were dosed with 100 mg/Kg, 200 mg/Kg, and 400 mg/Kg BW, of the hydroalcoholic extract of *H. enneaspermus* and standard Atorvastatin at a dose of 1.2 mg/Kg, BW. Significant antihyperlipidemic effects were obtained, as evidenced by restoring biochemical parameters altered by cholesterol towards the normal. An almost normal histological appearance of the liver was observed in treated groups. 400 mg/Kg showed better activity but less than the standard Atorvastatin. The results indicated that the hydroalcoholic extract of *H. enneaspermus* has a potential hypolipidemic effect along with recovery of liver functions.

Mozhi et al. (2013) ^[113] evaluated the anti-allergic and analgesic activity of aerial parts of *H. enneaspermus*. The petroleum ether and ethanolic extract of aerial parts of *H. enneaspermus* were screened for analgesic activity using the hot plate, tail immersion, and tail flick methods. The anti-allergic activity was screened by milk-induced eosinophilia and leukocyte methods. The ethanolic extract showed more significant activities than the petroleum ether extract. The activities may be attributed to phytochemical constituents like flavonoids and polar constituents.

Sadasivam et al. (2013) ^[114] evaluated the antimicrobial and phytochemical analysis of leaves of *I. Suffruticosum*. The antimicrobial activity was carried out on four clinically isolated bacteria viz. *Enterobacter sp.*, *Klebsiella pneumoniae*, *Staphylococcus sp.* and *E.coli* and fungi *Candida sp.* and *Aspergillus sp.* using the disc diffusion method. A promising antifungal activity against *Candida sp.* was reported at 25 mg/mL. Moderate activity was observed against *Enterobacter sp.* and *E.coli*. The phytochemical analysis was done using GCMS, wherein 22 compounds were identified, among which 9, 12, 15-Octadecatrienolic acid was identified as a major component.

Kumar et al. (2013) ^[115] evaluated the antioxidant potential of the aqueous extract from the whole plant of *I. Suffruticosum*. The freeze-dried extract was subjected to hydroxyl radical, FRAP, and iron chelating activity. Ascorbic acid was the standard used to determine hydroxyl radical and FRAP assays, while Ethylenediaminetetraacetic acid (EDTA) was used as a standard in the iron chelation assay. The results indicated that IC₅₀ values of aqueous extract were reported to be 120 µg/mL, 163 µg/mL and 430 µg/mL by hydroxyl free radical, by iron chelation and FRAP methods, respectively, as against the standards used.

Olubajo et al. (2013) ^[116] assessed the impact of maternal consumption of aqueous leaf extract of *H. enneaspermus* (HEaq) on pregnancy in Sprague Dawley rats. The control group received distilled water, while the test group received 2 g/Kg BW of HEaq orally. Blood samples collected after oral administration of aqueous leaf extract of *H. enneaspermus* were tested for total blood count, serum thyroid hormone, thyroid stimulating hormone (TSH) and thyrotropin-releasing hormone (TRH) assay. 50% of rats in each group were sacrificed on day nineteen of pregnancy, and the placenta and foetus were removed and weighed, while the remaining rats carried their pregnancy to term. The number and weights of litter and post-natal survival rate were recorded. It was observed that HEaq significantly decreased ($p < 0.05$) foetal weight, placenta weight, foetal growth and survival, number and weights of litter at birth, maternal serum triiodothyronine T3 and TSH level. Mean corpuscular haemoglobin, white blood cell count, platelet count and lipid profile were significantly increased ($p < 0.05$). It increased the frequency and percentage contraction of the gravid myometrial muscle in a dose-dependent manner. Thus, maternal consumption of aqueous leaf extract of *H. enneaspermus* adversely affected pregnancy and development of the foetus, as it precipitated resorption of developing foetus and reduced size and weight of litter at term.

Nathiya et al. (2013) ^[117] evaluated the anti-infertility effect of *H. enneaspermus* on endosulfan-induced toxicity in male rats. Ethanolic extract of *H. enneaspermus* was used to determine the effect and various parameters such as MDA, GSH, α -Tocopherol (vitamin E), Ascorbic acid (vitamin C) antioxidant enzyme of ALT (SGPT), AST (SGOT), Urea, Total cholesterol, Hemoglobin, total protein, sperm count, sperm motility were analysed. *H. enneaspermus* was observed to be beneficial in recovering infertility in endosulfan-induced toxicity in male albino rats.

Mishra et al. (2012) ^[118] evaluated the wound-healing activity of different extracts (aqueous, chloroform and methanolic) of *H. enneaspermus* in albino rats. Formulations of crude aqueous, chloroform and methanolic extracts of the *H. enneaspermus* were applied topically over the wound. It was found that ointment-treated rats showed accelerated healing than the control, suggesting that *H. enneaspermus* powder could be developed as a therapeutic agent for wound healing.

Sailaja et al. (2012) ^[119] assessed the effect of acrylamide and *H. enneaspermus* leaf extract (HE) active principles on mice testis glutathione-S-transferases. This enzyme helps in the biotransformation of electrophilic compounds, that cause damage to cells by conjugating with the substrate glutathione. Acrylamide is a neurotoxicant that causes damage to almost all cells, including the liver, testis, brain and kidney. The GSTs were purified from mice testis using glutathionyl linked agarose affinity chromatography, analyzed by SDS-PAGE and were resolved into four subunits, i.e. Yc, Yb, Y β & Y δ . The expression of these subunits was confirmed by Western blot analysis. The mice were subjected to acrylamide (AC) and a combination of HE and AC to evaluate the effect of *H. enneaspermus*. This exposure significantly altered the specific activity of mice GSTs in testis. On immunoblot analysis, polyclonal antibodies produced against purified GSTs of mice testis showed a significant increase of μ class GSTs (Yb & Y β) based on dose and time-dependent manner. The regulation of synthesis of μ -GSTs was dependent upon the

dose of acrylamide and active principles of HE. The authors thus proposed that μ -GSTs may be used as tumour markers for testis carcinoma.

Anand et al. (2012) ^[120] assessed the effect of *H. enneaspermus* on the kidney and heart mitochondrial Na^+/K^+ ATPase, Ca^{2+} ATPase and Mg^{2+} ATPase activities against carbon tetrachloride-induced oxidative stress in rats. Wistar strain male albino rats were segregated into four groups, wherein group I served as normal control, Group II served as vehicle control, Group III received a single dose (29th day) of CCl_4 in corn oil (3mL/Kg, *i.p.*) and Group IV was treated with ethanolic extract of *H. enneaspermus* (500 mg/Kg BW, orally). The activities of kidney and heart mitochondrial Na^+/K^+ ATPase, Ca^{2+} ATPase and Mg^{2+} ATPase were restored after treatment with CCl_4 , and *H. enneaspermus* extracts treated group, proving that *H. enneaspermus* extract acts as a potent regulator for membrane-bound enzymes in mitochondria on carbon tetrachloride-induced oxidative stress in rats.

Vuda et al. (2012) ^[121] evaluated the hepatoprotective and antioxidant activity of *H. enneaspermus* against carbon tetrachloride (CCl_4) induced liver injury in rats, using silymarin as a standard drug. Rats were treated with an aqueous extract of *H. enneaspermus* at either 200 or 400 mg/Kg dose after segregation into pre-treatment (once daily for 14 days before CCl_4 intoxication) and post-treatment (2, 6, 24 and 48 h after CCl_4 intoxication) groups. Pre-treatment and post-treatment with the aqueous extract showed significant hepatoprotection by reducing the aspartate transaminase, alanine transaminase and alkaline phosphatase enzymatic activities and raised total bilirubin levels. It significantly decreased hepatic lipid peroxidation and correspondingly increased tissue total thiols. Post-treatment with aqueous extract improved ceruloplasmin levels, thus suggesting the potential therapeutic use of *H. enneaspermus* as an alternative for patients with acute liver diseases.

Satheeshkumar et al. (2012) ^[122] evaluated the *in vivo* antioxidant and lipid peroxidation effects of the various extracts of the whole plant of *Iondium suffruticosum* in rats fed with a high-fat diet. Successive petroleum ether, ethyl acetate, and methanolic extracts were administered orally at a daily dose of 200 mg/Kg, BW for nine weeks. The group treated with methanolic extract reported a significant increase in the antioxidant tissue enzymes (TBRAS, GSH, SOD, CAT, GPx, GR). The results were compared with the standard Atorvastatin (1.2 mg/Kg, BW). The study concluded that the methanolic extract of *Iondium suffruticosum* is a rich source of natural antioxidants that may be beneficial in combating oxidative stress.

Muthu et al. (2012) ^[123] evaluated the hypolipidemic activity of flavone isolated from *Mucuna pruriens* and coumarin isolated from *I. suffruticosum* in rats fed with a high-fat diet. The powdered drug plant was successively extracted with petroleum ether, ethyl acetate and methanol to yield the petroleum ether, ethyl acetate and methanolic extracts, respectively. The methanolic extracts of *M. pruriens* and *I. suffruticosum* were subjected to column chromatography to isolate flavones and coumarins, respectively. The acute toxicity study was conducted using Wistar albino rats and further subjected to induction of hyperlipidemia and evaluation of antihyperlipidemic activity. Flavone fraction (265 mg) was obtained by eluting the methanolic extract of *M. pruriens* with ethyl acetate: methanol (80:20 v/v). Similarly, the coumarin derivative (245 mg) was obtained by eluting the methanolic extract of *I. suffruticosum* with benzene: chloroform (70:30, v/v). The acute toxicity revealed that the flavone (*M.pruriens*) and coumarin (*I.suffruticosum*) were safe up to 100 mg/Kg; hence one-tenth of the dose (10 mg/Kg) was considered as an evaluation dose. The rats fed with a high fat demonstrated significant ($p < 0.001$) elevation in plasma total and LDL-cholesterol, triglycerides and phospholipids. Administration of flavone (*M. pruriens*) and coumarin isolated from (*I.suffruticosum*) at the dose of 10 mg/Kg BW/day along with a high-fat diet significantly ($p < 0.001$) prevented the rise in the total plasma and LDL-cholesterol, triglycerides and phospholipids. However, treatment of coumarin isolated

from (*I.suffruticosum*) showed more cardioprotective effects against hyperlipidemia than that of flavone (*M.pruriens*).

Anand et al. (2012) ^[124] carried out the GC-MS analysis and antimicrobial evaluation of bioactive components of *H. enneaspermus*. The study revealed the existence of more than ten compounds, such as D-mannitol, tetradecanediol, phytol, monolonoleoylglycerol trimethylsilyl ether, silane etc. The anti-microbial activity of ethanolic and aqueous extracts was evaluated against *Staphylococcus aureus*, *Bacillus subtilis*, *Escherichia coli*, *Pseudomonas aeruginosa*, *Shigella shigae*, *Salmonella typhi*, *Proteus vulgaris*, *Candida albicans*, and *Aspergillus niger* by using agar disc diffusion method. The ethanolic extract of *H. enneaspermus* exhibited more significant activity against the microbes than the aqueous extract.

Anand et al. (2012) ^[125] characterized the bioactive constituents present in the ethanolic extract of *H. enneaspermus* using UV-Vis, FTIR and GC-MS spectroscopic methods. The crude extract was scanned in the wavelength ranging from 300-1100 nm using a Perkin Elmer spectrophotometer, and the characteristic peaks were detected. FTIR spectrum confirmed the presence of phenols, alcohols, alkanes, alkyl halides, carboxylic acids, aromatics, nitro compounds, and amines in the extract. GC-MS analysis exhibited the presence of phytochemical compounds detected using the NIST Ver - 2.0 2005 library, demonstrating different therapeutic activities. The biological activity evaluation was based on Dr. Duke's Phytochemical and Ethnobotanical Databases. The significant phytoconstituents were (5E,13E)-5,13-Docosadienoic acid (20.90 %) and Cedran-diol (13.02 %), possessing many biological activities. The study provides a platform to screen many bioactive components for various ailments.

Arumugam et al. (2012) ^[126] assessed the *in-vitro* antifungal activity of *H. enneaspermus*. Petroleum ether, chloroform and methanolic extracts of *H.*

enneaspermus were subjected to preliminary phytochemical screening using established methods and tested against *Aspergillus flavus*, *Aspergillus fumigatus* and human pathogenic fungi *Candida albicans* and *Candida tropicalis* by well diffusion method. Preliminary phytochemical screening revealed the presence of triterpenoids and steroids in petroleum ether, only steroids in chloroform extract and alkaloids, flavonoids, saponins and phenolic compounds in methanolic extract. The methanolic extract exhibited significant activity against all tested fungal strains, followed by petroleum ether and chloroform extract.

Sahoo et al. (2012) ^[127] evaluated the antiulcer and antisecretory activity of the alcoholic and aqueous extracts of the whole plants of *H. enneaspermus*. Acute oral toxicity studies of the ethanolic and aqueous extracts were carried out in Swiss albino mice up to a dose of 5000 mg/Kg. The efficacy study of the extracts was performed by a pyloric ligation-induced gastric ulcer model with a dose of 25 mg/Kg, 50 mg/Kg and 100 mg/Kg BW orally in rats. The parameters evaluated include pH of the gastric juice, ulcer sores, ulcer index, total acidity, free acidity and % protection conferred by the extracts, as against the standard ranitidine (50 mg/Kg). The alcoholic extract at 100 mg/Kg exhibited higher potency than the aqueous extract. It reduced gastric acid secretion and ulcer index with induction of neutralizing activity, thus indicating substantial antiulcer and antisecretory potential.

Radhika et al. (2011) ^[128] evaluated the cardioprotective activity of *H. enneaspermus* extract against isoproterenol (20 mg/100 g, subcutaneously) induced myocardial infarction in rats. The positive inotropic and chronotropic response of isoproterenol caused severe oxidative stress in the myocardium through increased lipid peroxidation. *H. enneaspermus* was administered orally at 500 mg/Kg BW for 4 weeks. Histological examination of the rat's heart section confirmed myocardial injury with isoproterenol. The plant extract of *H. enneaspermus* reduced the oxidative stress by decreasing lipid peroxidation, increasing GSH and normalising the levels of cardiac marker

enzymes such as CK, LDH, SGOT, SGPT and cardiac-specific protein Troponin I in the blood of both treatment groups. In histopathological studies, *H. enneaspermus* extract treated animals showed less cellular infiltration and enhanced cardioprotective activity.

Thyagaraju et al. (2011) ^[129] investigated the hepatoprotective activity of the ethanolic extract of *H. enneaspermus* by suppressing paracetamol toxicity by its antioxidant principles in mice blood and liver. The hepatoprotective and antioxidant activity of the ethanolic extract of *H. enneaspermus* was evaluated by the catalase, superoxide dismutase, glutathione s-transferase, glutathione reductase and lipid peroxidation enzyme assays in mice. The paracetamol toxicity-treated mice stimulated serum transaminases and alkaline phosphatases while reducing liver glutathione content and elevating lipid peroxidation and antioxidant enzymes. However, the ethanolic extract of *H. enneaspermus* restored the normal activities of enzymes and protected the hepatocytes by depleting the liver's necrotic cells and lipid peroxidation.

Patel et al. (2011) ^[130] evaluated the hypoglycaemic and antioxidant potential of *H. enneaspermus*. The parameters used to evaluate anti-diabetic activity were the oral glucose tolerance test (OGTT) and normoglycaemic effect of alcoholic extract of *H. enneaspermus* at a dose of 125 mg/Kg, 250 mg/Kg and 500 mg/Kg per orally. The hypoglycaemic activity and effect on BW were tested at 250 and 500 mg/Kg orally daily for 21 days in Streptozotocin-induced diabetic rats (STZ). The glucose uptake by the hemidiaphragm was also evaluated. Total phenolic and flavonoid content were assessed, and their correlation with various antioxidant assays was also determined. Alcoholic extract was reported to have high phenolic and flavonoid content, total antioxidant capacity and free radical scavenging activity. There was a significant increase in BW and a decrease in blood sugar levels on treatment with the extract. The alcoholic extract increased glucose uptake on isolated rat hemidiaphragm compared to the control, thus proving to reduce blood glucose levels in the STZ-induced diabetic model.

Ramamoorthy et al. (2011) ^[131] investigated the phytochemical and anti-inflammatory activity of *I. suffruticosum*. The leaves of *H. enneaspermus* were extracted successively with hexane and chloroform. Aurantamide, Indole-3-butyric acid, β -sitosterol, and n-6 benzyladenine were isolated and characterized. The antipyretic activity was carried out using yeast induced hyperpyrexia method. Significant activity was reported with hexane extract in comparison with chloroform extract.

Kannan et al. (2011) ^[132] studied the anxiolytic behaviour of the hydroalcoholic extract of the dried whole plant of *H. ennespermus* (HAEHE) in swiss albino mice. The elevated plus maze elevated T-maze, Vogel conflict test and isolation-induced aggression models were used to assess Anxiolytic activity. The efficacy of the extract (200 mg/Kg and 400 mg/Kg) was compared with the standard anxiolytic drugs Diazepam (2 mg/Kg) and Fluoxetine (10 mg/Kg). Significant increase in the number of entries and time spent in open arm depicted in the Elevated plus maze model, increased baseline latency and decreased avoidance and escape in the elevated T-maze, decreased number of shocks licks in the Vogel conflict test, fighting and biting in the isolation-induced aggression models, suggested that the HAEHE has potent anxiolytic activity.

Arumugam et al. (2011) ^[133] reported the antifungal activities of the different extracts (petroleum ether, chloroform and methanolic) of *H. enneaspermus* on wet clothes. Three fungi were identified on wet clothes, viz. *Aspergillus niger*, *Aspergillus flavus* and *Aspergillus fumigatus*. The antifungal activities of different extracts were screened and graded based on the inhibition zones. Among the three extracts used for the studies, the methanolic extract exhibited maximum growth inhibition, followed by chloroform and petroleum ether extract.

Awobajo et al. (2010) ^[134] evaluated the hypoglycemic activities of aqueous and methanolic leaf extracts of *H. enneaspermus* and *Paquetina nigricense* in normal and alloxan-induced diabetic female Sprague Dawley rats. The effective hypoglycemic dose (EHD) for HE(aq) and HE(meth) was found to be 80 mg/Kg and 180 mg/Kg BW, respectively. This produced a percentage reduction of whole blood glucose levels of 44.15 ± 0.46 at 7 h and 44.94 ± 0.32 at 10 h, respectively. The aqueous and methanolic extracts of *P. nigricense* have displayed EHD of 80 mg/Kg and 160 mg/Kg BW, respectively, along with reduction in whole blood glucose of 46.59 ± 0.35 and 48.03 ± 0.44 at 4 h and 9 h, respectively. All animals in this test were administered 1.071 g/Kg BW of glucose after 12 h of fasting, along with the corresponding effective dose of the extracts. Aqueous leaf extract of *H. enneaspermus* revealed potential hypoglycaemic activities equivalent to the standard hypoglycemic drug Glibenclamide.

Kar et al. (2010) ^[135] evaluated the central nervous system activity of aerial parts of *H. enneaspermus*. Ethanolic and aqueous extracts of the plant were subjected to preliminary phytochemical analysis. Extracts of *H. enneaspermus* at doses of 250 and 500 mg/Kg were administered orally along with standard drugs Diazepam (1 mg/Kg), Chlorpromazine (5 mg/Kg), Imipramine (30 mg/Kg) and screened for behavioural profiles like maze test, barbiturate and alcohol-induced sleeping time, tail suspension test, despair test, head dip test, locomotor and motor coordination test. The phytochemical evaluation confirmed the presence of carbohydrates, phenols, flavonoids, amino acids, tannins, alkaloids, anthraquinones, glycosides, saponins and steroids. Aqueous and alcoholic extracts showed significant CNS activity at both doses. The results showed that *H. enneaspermus* extracts exhibited significant anxiolytic activity. It also significantly decreased the sleeping latency and increased the sleeping time. Tail suspension, head dip and despair test showed that *H. enneaspermus* extracts (250 mg/Kg and 500 mg/Kg) were able to induce a significant increase in the immobility time, like the standard drug, Imipramine.

Tripathy et al. (2009) ^[136] evaluated the anti-arthritic potential of alcoholic and aqueous extracts of the whole plant of *H. enneaspermus* in Freund's adjuvant-induced arthritis in mice. The yield of alcoholic and aqueous extracts was 12.8 % and 10.6 %, respectively. Alkaloids, flavonoids, glycosides, phenols, carbohydrates, and tannins were present in both extracts. Both extracts significantly decreased the paw thickness ($p < 0.001$) at the end of 30 days of treatment. The results indicated that the alcoholic extract exhibited a pronounced reduction in inflammation (59.4 %) compared to the aqueous extract (57.4 %). The above findings suggest that the selected plants support the folklore use of *H. enneaspermus* against inflammatory conditions like arthritis.

Setty et al. (2007) ^[137] analysed the free radical scavenging and nephroprotective activity of *H. enneaspermus*. The ethanolic and aqueous extracts of *H. enneaspermus* at 250 mg/Kg and 500 mg/Kg doses were administered orally. Cisplatin at 5 mg/Kg was administered intraperitoneally to induce renal injury in rats by increasing the blood urea and serum creatinine levels. The alcoholic and aqueous extracts of *H. enneaspermus* showed a dose-dependent reduction in the elevated blood urea and serum creatinine levels. The extracts also increased GSH, GST and SOD levels and inhibited lipid peroxidation induced by cisplatin in kidney homogenates. Thus, both extracts of *H. enneaspermus* possess significant curative and preventive nephroprotective activity.

Narayanswamy et al. (2007) ^[138] reported preliminary aphrodisiac activity of ethanolic and aqueous extracts of *H. enneaspermus* at doses of 300 mg/Kg BW, orally in rats, in a single-dose regime and chronic dose regime daily for 28 days as against the standard L-dopa at 100 mg/Kg BW. The parameters used for assessing sexual arousal and performance were mount latency, number of mounts, intromission latency, number of intromissions, ejaculation latency, number of ejaculations, and post-ejaculation pause. Single-dose administration of the aqueous extract exhibited a decrease in mounts and intromission latency, while an increase in ejaculation and intromission frequency was

observed. In the chronic model, both the extracts, i.e. alcoholic and aqueous, increased the number of mounts, ejaculations and intromissions with decreased mounting and intromission latency. It was also observed that treatment with aqueous extract elevated testosterone levels in sexually inactive male rats. The findings thus revealed that *H. enneaspermus* might exert aphrodisiac activity in sexually inactive male rats.

Weniger et al. (2004) ^[139] determined the *in vitro* antiplasmodial potential of *H. enneaspermus* against *Plasmodium falciparum* K1 chloroquine-resistant and 3D7 chloroquine-sensitive strains for twenty extracts from nine Benin traditionally used to treat malaria. All the plants exhibited antiplasmodial activity below 10 µg/mL. Nine extracts displayed IC₅₀ values below 5 µg/mL towards one or both strains. The methanolic extract of aerial parts of *Croton lobatus* was active against the sensitive 3D7 strain with an IC₅₀ value of 0.38 µg/mL. Methylene chloride extract of *H. enneaspermus* exhibited significant inhibition of the growth of *Plasmodium falciparum* resistant K1 strain was observed with the IC₅₀ value of 2.57 µg/mL. In comparison, the methanolic extract of *Croton lobatus* roots exhibited an IC₅₀ value of 2.80 µg/mL.

Hemalatha et al. (2003) ^[140] reported the anticonvulsant and free radical scavenging potential of *H. enneaspermus*. The anticonvulsant activity was assessed employing maximal electric shock and strychnine-induced convulsions using aqueous and ethanolic extracts of *H. enneaspermus* (200 mg/Kg and 400 mg/Kg BW, orally). Aqueous extract (200 mg/Kg and 400 mg/Kg orally) showed significant protection in both models with no neurotoxicity. The activity was equipotent to phenobarbitone sodium (30 mg/Kg *i.p.*). The aqueous extract exhibited free radical scavenging activity against DPPH free radicals.

3.2. Review of *Bauhinia foveolata*

Habbu et al. (2020) [78] reported the isolation, characterisation, and cytotoxic studies of secondary metabolites from the leaves of *B. foveolata*. The powdered leaves were extracted with 95 % ethanol using Soxhlet apparatus. The ethanolic extract was further fractionated with ethyl acetate and n-butanol to yield the ethyl acetate and n-butanol fractions, respectively. These fractions were further subjected to the isolation of phytoconstituents using column chromatography. The isolated compounds were characterised using IR, ¹H-NMR, ¹³C-NMR and mass spectroscopic methods and also by comparison with the reported values. The isolated compounds were further subjected to *in vitro* antiproliferative MTT assay using human colon cancer cell lines (HT-29 and HCT-15). Column chromatography led to the isolation of 13-Docosenamide from ethyl acetate fraction and quercetin, isorhamnetin, and odoratin-7-glucoside from the butanol fraction of ethanolic leaf extract of *B. foveolata*. Among all the tested compounds against colon cancer cell lines, quercetin and odoratin-7-glucoside exhibited antiproliferative potential with IC₅₀ of 75.33 ± 10.01 µg/mL and 95.00 ± 5.56 µg/mL towards HT-29 cancer cell line and 105.06 ± 6.52 µg/mL and 102.45 ± 10.22 µg/mL towards HCT-15 cancer cell lines, thus proving their cytotoxic effect in treating colon cancer.

Gamit et al. (2018) [141] reported the antimicrobial and antimalarial activities of eight medicinal plants traditionally used by tribal communities of Tapi District, Gujarat. The powdered leaves, bark, and whole plants of eight species of ethnomedicinal plants were separately extracted with five solvents, viz. ethyl acetate, acetone, petroleum ether, chloroform, and hexane, to yield the respective extracts. The extracts were further subjected to *in vitro* antimicrobial and antimalarial activities. Antibacterial activity was assessed against two gram-positive bacterial strains (*Staphylococcus aureus*, *Streptococcus pyogenes*), two gram-negative bacterial strains (*Escherichia coli*, *Pseudomonas aeruginosa*) with Ampicillin, Ciprofloxacin, and Chloramphenicol as standard drugs.

The *in vitro* antifungal activity of plant extracts was determined against *Candida albicans*, *Aspergillus niger*, and *Aspergillus clavatus* by agar dilution method, with Nystatin and Griseofulvin as standards. *In vitro* antimalarial activity was performed by the microassay protocol against the *Plasmodium falciparum* strain, with Quinine and Chloroquine as standards. Acetone extract of *B. foveolata* bark and *Bridelia spinosa* bark demonstrated the most effective antibacterial activity and antifungal activity, respectively, in comparison with standard drugs. Ethyl acetate extracts of *Bridelia spinosa* leaf and *B. foveolata* bark exhibited significant antimalarial activity, respectively, which is superior to the standard drug. The study provides support for the traditional use of plants by tribal people to cure various ailments.

3.3. Review of the Genus *Bauhinia*

Khanna et al. (2022) ^[142] assessed the anticancer activities of *Bauhinia variegata* bark extracts on lung carcinoma cells A549 and H460. Bark extracts of *Bauhinia variegata* were prepared by different solvents using Soxhlet apparatus and tested for their antioxidant potential by DPPH assay. The lung cancer cell lines were treated with *Bauhinia variegata* bark extracts and viability of cells was measured by MTT assay; metastatic ability was determined through Scratch assay and effect on DNA integrity was shown by gel electrophoresis. Petroleum Ether Bark Extract (PEBE) inhibited proliferation (A549, IC₅₀ = 1.5 mg/mL) at 48 h treatment. DNA damage was observed in A549 cells by agarose gel electrophoresis. The Chloroform Bark Extract (CBE) inhibited proliferation of H460 (IC₅₀ = 1 mg/mL) with DNA damage after 24 h treatment. Soft agar assay indicated decreased ability to form colonies and scratch test showed impaired migration of A549 and H460 to PEBE and CBE treatment respectively. Apoptosis was detected using fluorescent dye staining in A549 and H460 cells. Caspase-3 activity was increased significantly in A549 and H460 cells. PEBE and CBE decrease the mitochondrial membrane potential gradient of A549 and H460 cells respectively. This study categorically proved the cytotoxic activity of *Bauhinia variegata* bark extracts on A549 and H460 cells.

Chávez-Bustos et al. (2022) ^[143] evaluated the hypoglycemic, antioxidant, and genoprotective activities of a methanolic extract of *B. forficata* leaves and stems in mice treated with streptozotocin (STZ). Secondary metabolites were determined by qualitative phytochemical procedures. *In vitro* antioxidant activity was determined by the DPPH method. The genoprotective activity was evaluated in 3 groups of mice: control, anthracene (10 mg/kg), and anthracene and *B. forficata* (500 mg/kg) and the presence of micronuclei in peripheral blood was measured for 2 weeks. For hypoglycemic activity, the crude extract was prepared in a suspension and administered (500 mg/kg, *i.p.*) in previously diabetic mice with STZ (120 mg/kg, *i.p.*), measuring blood glucose levels every week as well as the animals' BW for six weeks. The extract indicated good antioxidant activity and caused a decrease in the number of micronuclei. The diabetic mice treated with *B. forficata* presented hypoglycemic effects in the third week of treatment, perhaps due to its secondary metabolites. Thus, *B. forficata* was confirmed to be good a candidate as an adjuvant to allopathic therapy.

Phonghanpot et al. (2021) ^[144] evaluated the antiproliferative, antibacterial, and antioxidant activities of aqueous (root and stem) extracts of *B. strychnifolia* in gut and liver cells. The biological activity was assessed using MTT assay, microscopic analysis, disc diffusion, and broth microdilution against various strains and cell lines. The free radicals scavenging assays (ABTS and GSH) and LC-MS analysis were also performed. The extracts inhibited the growth of human hepatocellular carcinoma (Hep-G2) and colon adenocarcinoma (HT-29) cell lines. The extracts inhibited the growth of *Bacillus cereus* and *Staphylococcus aureus*. It also exhibited moderate antioxidant activity with increased GSH production in Hep-G2 cell lines compared to the control. LC-MS analysis revealed that 3,5,7,3',5'-pentahydroxyflavanonol-3-O- α -L-rhamnopyranoside was a major phytoconstituent in the root extract, while β -sitosterol was a major phytoconstituent, in the stem extract. 3,5,7,3',5'-pentahydroxyflavanonol-3-O- α -L-rhamnopyranoside and β -sitosterol exhibited potent cytotoxicity against the cancer cell lines. Thus, the study

supported the folklore use of *B. strychnifolia* root and stem decoction in the treatment of liver and colon cancer.

Vijayan et al. (2019) ^[145] evaluated the anticancer, antimicrobial, antioxidant, and catalytic potential of green-synthesized silver and gold nanoparticles of *B. purpurea* aqueous leaf extract. The green-synthesized silver and gold nanoparticles were characterized by UV-Vis, FT-IR, XRD, TEM and EDX analysis. The synthesized silver and gold nanoparticles were analyzed for anticancer activity using A549 cell lines. The antimicrobial activity was evaluated by agar well diffusion method against six microbial strains viz. *Staphylococcus aureus*, *Bacillus subtilis*, *Escherichia coli*, and *Pseudomonas aeruginosa*. The fungal strains used were *Aspergillus flavus* and *Aspergillus nidulans*. The antioxidant potential was evaluated by DPPH assay. The catalytic activities of synthesized AgNPs-*purpurea* and AuNPs-*purpurea* were analyzed using reduction dyes methylene blue and rhodamine B by sodium borohydride. The formations of silver and gold nanoparticles were confirmed by observing the surface plasmon resonance peaks at 430 nm and 560 nm, respectively, in the UV-Vis absorption spectrum. FTIR analysis revealed that the silver and gold nanoparticles were capped with plant compounds of alcohol, phenols, carbonyl etc., functional groups. XRD analysis revealed the formation of planes of a face-centred cubic structure of the nanoparticles. HR-TEM study showed clear lattice fringes confirming the crystallinity of synthesized nanoparticles. EDX spectrum of AgNPs-*purpurea* displayed a peak at 3 keV, which is typical of the absorption of metallic silver nanocrystallites due to surface plasmon resonance, while peaks of gold at 2–2.5 keV, 8–8.5 keV, and 9.5–10 keV were confirmed in the EDX spectrum of AuNP-*purpurea* nanoparticles. A significant anticancer effect against lung carcinoma cell line A549 was observed in a dose-dependent manner with IC₅₀ values of 27.97 µg/mL and 36.39 µg/mL, respectively. AgNPs-*purpurea* and AuNPs-*purpurea* showed a considerable antimicrobial effect on all tested microorganisms than the leaf extract. The synthesized silver and gold nanoparticles exhibited significant antioxidant potentials with IC₅₀ values of 42.37 µg/mL and 27.21

µg/mL, respectively. The nanoparticles also served as good catalysts to reduce the organic dyes.

Santos et al. (2019) ^[146] investigated the two native species of *Bauhinia* from Argentina namely, *B. uruguayensis* (BU) and *B. forficata* (subsp. *Pruinose*, BF). The dried powdered leaves of *B. forficata* and *B. uruguayensis* were extracted with varying concentrations of water and methanol to yield the hydro-methanolic extract. The leaf extract was analysed by high-performance liquid chromatography (HPLC) mass spectrometry (MS/MS). The chromatographic analysis yielded five main compounds in BF, corresponding to rutosides and rhamnosides derivatives of kaempferol and quercetin. As per the literature, these compounds are considered to be chemotaxonomic markers and possess antioxidant potentials. Kaempferitrin, an antidiabetic agent, was also confirmed in BF extracts. The extracts of BU confirmed the presence of four major compounds viz. rhamnosides and galloyl derivatives from quercetin and kaempferol by HPLC-MS/MS analysis. One of these compounds, quercetin-3-rhamnoside, may bestow anti-inflammatory and analgesic properties to BU extracts.

Sharmila et al. (2018) ^[147] synthesised the zinc oxide nanoparticles (ZnO NPs) using *B. tomentosa* leaf extract as a bioreducing agent. Powdered leaves of *B. tomentosa* were extracted with distilled water to yield the aqueous extract. The extract was mixed with ZnSO₄ solution to yield the ZnO NPs, which were further characterised by UV-Vis, TEM, EDX, XRD and FTIR analytical methods. The synthesised ZnO NPs were evaluated for antibacterial activity against two Gram-positive bacteria (*Bacillus subtilis* and *Staphylococcus aureus*) and Gram-negative bacteria (*Escherichia coli* and *Pseudomonas aeruginosa*) by the well-diffusion method. UV-Vis spectroscopy analysis confirmed the formation of ZnO NPs by a characteristic surface plasmon resonance (SPR) peak at 375 nm. TEM analysis revealed that the synthesized ZnO NPs were in the nanoscale range. The hexagonal structure of the ZnO NPs was confirmed by XRD analysis.

FTIR spectrum validated that the phenolics or proteins may be involved in the bioreduction process for nanoparticle synthesis. ZnO NPs exhibited significant antibacterial activity against Gram-negative bacteria, *P. aeruginosa* and *E. coli*, than Gram-positive bacteria. The results of this study demonstrated that the phytoconstituents present in *B. tomentosa* leaf extract could be responsible for the bioreducing property of ZnO NPs.

Pandey (2017) ^[148] evaluated the *in vivo* antitumour potential of extracts from various parts (leaf, stem bark and flower) of *B. variegata* against b16f10 melanoma tumour model in c57bl/6 mice. Hydromethanolic extract prepared from the leaf, stem bark and flower of *B. variegata* was assessed for their antitumour activity. The extracts at doses of 500 and 750 mg/Kg BW were given orally along with cyclophosphamide (chemotherapeutic drug) for 40 days. Inhibition of tumour growth, increased survival time of the treated group, histopathological studies and antioxidant parameters were used to ascertain antitumour activity. The group treated with *B. variegata* extract and cyclophosphamide exhibited remarkable results for all the measured parameters compared to the control tumour group. A dose-dependent response was observed in tumour volume, inhibition rate, life span time and antioxidant parameter of extracts. Thus the authors concluded that *B. variegata* hydromethanolic extract has potential therapeutic significance due to the bioactive compounds present, confirming its anticancer use in folk medicine.

Rahman et al. (2016) ^[149] assessed the cytotoxic and apoptotic potential of the methanolic extract of *B. racemosa* (MEBR) against the HeLa cell line. The cytotoxic activity and apoptotic effects of MEBR were evaluated by MTT and DAPI staining tests, respectively, on HeLa cell lines. Changes in mitochondrial membrane potential and intracellular reactive oxygen species (ROS) level were also assessed by 5,5',6,6'-tetrachloro-1,1',3,3'-tetraethylbenzimidazol-carbocyanine iodide and dichlorodihydrofluorescein diacetate staining tests respectively. Total phenolic content was determined by colorimetric method using gallic acid calibration curve. MEBR exposure to

HeLa cells significantly decreased the cell viability ($p < 0.001$, $IC_{50} = 80 \mu\text{g/mL}$) comparable to that of tamoxifen ($p < 0.001$, $IC_{50} = 48 \mu\text{g/mL}$) in a concentration-dependent manner. It also led to the depolarization of mitochondria and induced the production of ROS, initiating the apoptotic effect in a concentration-dependent manner. The total phenolic content was 886.83 mg GAE/g dried extract. The authors concluded that MEBR possessed potent cytotoxic activity against HeLa cell lines with induction of apoptosis.

Sharma et al. (2015) ^[150] evaluated the protective effect of *B. variegata* leaf extracts against oxidative damage, cell proliferation and bacterial growth. The powdered leaf sample was sequentially extracted with hexane (HX), benzene (BZ), chloroform (CH), ethyl acetate (EA), acetone (AC), ethanol (ET) and water (AQ) in Soxhlet apparatus to yield their respective extracts. Evaluation of antioxidant activity was performed using FRAP assay, Beta-carotene bleaching and Lipid peroxidation inhibition (LPOI) assay. Anticancer activity was assessed using SRB assay against colon (Colo-205; HCT-116), prostate (PC-3), lung (A-549; NCI-H322), and breast (T-47D) cell lines. Antimicrobial activity was determined using Kirby-Bauer disc diffusion method against gram-negative bacteria *Proteus vulgaris*, *Salmonella typhi* and *Bordetella bronchiseptica* and gram-positive bacteria *Bacillus cereus* and *Streptococcus mutans*. Ethyl acetate, acetone, and aqueous extracts exhibited appreciable ferric-reducing antioxidant power. Aqueous and benzene extracts accounted for significant free radical scavenging activity in the beta-carotene bleaching assay. Inhibition of lipid peroxidation was also displayed by aqueous extract in rat liver homogenate. Aqueous fraction demonstrated remarkable antiproliferative activity (91-99 %) against colon (Colo-205 and HCT-116) and lung (A549) cancer cell lines. However, lower activity was observed against prostate (PC-3), breast (T47D) and lung (NCI-H322) cancer cell lines. Low to moderate antibacterial activity was manifested by hexane, benzene, ethyl acetate and aqueous extracts against *Proteus vulgaris*, *Salmonella typhi*, *Bordetella bronchiseptica*, *Bacillus cereus* and *Streptococcus mutans*. The study thus revealed considerable antioxidant, free

radical scavenging, anticancer and antibacterial activity by *B. variegata* leaf extracts.

Garbi et al. (2015) ^[151] reported the anticancer activity of *B. rufescens* leaf extracts on MCF-7 human breast cancer cells. Petroleum ether and methanolic extracts were prepared using the Soxhlet apparatus. MCF-7 cells were cultured in a complete medium consisting of 10% fetal bovine serum and 90% minimal essential medium and incubated with different concentrations of the extracts viz. 31.25, 62.50, 125, 250 and 500 µg/mL for 72 h and subjected to MTT assay. Petroleum ether and methanolic extracts exhibited a significant reduction in cell mortality of MCF-7 cells in a dose-dependent manner. The GI₅₀ values of petroleum ether and methanolic extracts were reported to be 23.77 µg/mL and 14.75 µg/mL, respectively. The study thus revealed that petroleum ether and methanolic leaf extracts of *B. rufescens* induced an antiproliferative effect against MCF-7 cell lines.

Ajiboye et al. (2015) ^[152] reported the antioxidant and antimicrobial potentials of the leaf extract of *B. monandra*. The powdered leaves were extracted with 95% ethanol to yield ethanolic extract. The ethanolic extract was partitioned with n-hexane and ethyl acetate to yield the n-hexane (HFBM) and ethyl acetate (EFBM) fractions. The preliminary phytochemical screening was performed on the ethanolic extract and EFBM adopting established procedures. The antioxidant activity of HFBM and EFBM was assessed using DPPH free radical scavenging assay against the standard ascorbic acid. The antibacterial activity of EFBM and HFBM against three gram-negative bacterial strains (*Escherichia coli*, *Pseudomonas aeruginosa* and *Klebsiella oxytoca*) was also evaluated. GC-MS analysis was performed on HFBM and EFBM fractions to assess the phytoconstituents present in the fractions. The phytochemical analysis of the ethanolic extract and EFBM revealed the presence of flavonoids, cardiac glycosides, tannins, steroids, phenolics, terpenoids, alkaloids, and saponins. *In vitro* antioxidant activity studies revealed that EFBM exhibited maximum antioxidant (IC₅₀ µg/mL=0.010) activity than HFBM (IC₅₀ µg/m = 5.564) and reference standard ascorbic acid (IC₅₀ µg/mL=30). In the *in vitro* antimicrobial

studies, EFBM exhibited the highest antibacterial potential, while HFBM showed negligible activity against all the bacteria strains. GC-MS analysis of EFBM displayed the presence of oleic acid as a major component, classified as monounsaturated omega-9-fatty acid with 40.76% concentration. In the case of HFBM, the major component identified was 4-hydroxy-5-methyl-3-propyl-2-hexanone with 42.70% concentration. The results of these studies demonstrated that EFBM possesses compounds with antioxidant and antimicrobial properties and can be used in modern medicine to combat pathogenic microorganisms.

Kumar et al. (2014) ^[153] evaluated the apoptosis and cell cycle studies of the ethanolic bark extract of *B. variegata* (BBEE) on HeLa cell lines. Thin-layer chromatographic (TLC) studies confirmed the presence of flavonoids. The flavonoid-rich extract was further subjected to *in vitro* anticancer activity using MTT and SRB assays. The extract-treated HeLa cell lines were subjected to apoptosis assay by Ethidium bromide/Acridium orange fluorescent staining method. Flow cytometric analysis was also performed to analyse the effect of plant extract on cell cycle progression. The IC₅₀ values of the extract against HeLa cell lines were found to be 184 ± 6.16 µg/mL and 199 ± 3.34 µg/mL by MTT and SRB assays, respectively. BBEE extract induced apoptotic cell death in HeLa cell lines. The flow cytometric analysis on BBEE-treated HeLa cell lines exhibited the cell cycle arrest in G₀/G₁ phase, confirming the cytotoxic activity of *B. variegata* bark extract on cervical cancer.

Jatav et al. (2014) ^[154] assessed the nootropic potential of ethanolic extract of *B. variegata* in rats. The extract was subjected to the estimation of total flavonoid content by the aluminium chloride method. Flavonoid-rich extract of *B. variegata* was subjected to acute oral toxicity and efficacy studies. The extract was found to be safe up to 2000 mg/Kg. The activity was determined using 200 mg/Kg and 400 mg/Kg BW of the extract and compared with the standards Piracetam (200 mg/Kg BW, orally), Baclofen (5 mg/Kg, *i.p.*) and Diazepam (5 mg/Kg BW, *i.p.*). The activity models used were elevated plus maze,

rotating rod apparatus, baclofen-induced catatonia, and diazepam-induced amnesia. A significant decrease in transfer latency with no alteration in locomotor activity was observed with a 400 mg/Kg BW flavonoid-rich fraction of *B. variegata*, thus indicating its cognitive enhancement effect. In rotarod studies, the flavonoid-rich fraction of *B. variegata* increased the time of fall compared to Diazepam. In Baclofen-induced catatonia, administration of flavonoid-rich fraction demonstrated a protective effect on rats. Thus, demonstrating its nootropic potential with enhanced performance in murine models.

Jash et al. (2014) ^[155] reported the chemical investigation of methanolic extract of the stems of *B. variegata*. The stem powder was extracted using methanol in a Soxhlet apparatus to yield the methanolic stem extract, which was subjected to preliminary phytochemical investigation. The methanol soluble fraction was subjected to column chromatography for isolation of phytoconstituents. The isolated compounds were characterised using UV-Vis, IR, ¹H-NMR, ¹³C-NMR and mass spectrometric methods. The phytochemical investigation of the methanolic stem extract of *B. variegata* led to the isolation and characterisation of four bioactive phytoconstituents viz., Lupeol, β -Sitosterol, Kaempferol and Quercetin. The authors concluded that the constituents isolated from this extract could account for the biological activities exhibited by the methanolic extract.

Chaudhari et al. (2013) ^[156] evaluated the *in vitro* anti-diabetic and anti-inflammatory activity of the stem bark of *B. purpurea*. Dried (crude) petroleum ether and hexane extracts of stem bark of *B. purpurea* were subjected to anti-diabetic activity, and petroleum ether and methanol extracts were subjected to anti-inflammatory activity. *In vitro* anti-diabetic activity was evaluated using non-enzymatic glycosylation of haemoglobin assay, glucose uptake in yeast cells and alpha-amylase inhibition assay. *In vitro* anti-inflammatory activity was evaluated using inhibition of albumin denaturation, membrane stabilization test, preparation of red blood cells, heat-induced hemolytic assay, and protein inhibitory action. All the extracts exhibited anti-diabetic and anti-inflammatory activity; however, at the highest concentration, the extracts exhibited significant activity.

Kuo et al. (2013) ^[157] reported the isolation and identification of twenty-two components from the heartwood of *B. purpurea* and analyzed their structures by spectroscopic methods. Among the isolated and characterized compounds, six were steroids, two triterpenoids, three fatty alcohol, acid and ester, two glycerols, five flavonoids, two phenols, one chromone, and one sugar. A new compound, 6'-(β -sitosteryl-3-O- β -glucopyranosidyl)tetraeicosanoate was reported for the first time.

Kang et al. (2013) ^[158] reported the free radical scavenging activity from different solvents of leaves of *B. vahlii*. The powdered plant samples were extracted by Soxhlet extraction sequentially with petroleum ether, chloroform (BLC), acetone (BLA) and methanol (BLM) and the air-dried residue was further extracted with hot water (BLH). Folin Ciocalteu and Aluminium trichloride were used to evaluate total phenolic and flavonoid contents. The *in vitro* antioxidant potential of the extracts was evaluated using *in vitro* assays like FRAP, ABTS, DPPH, Metal chelating activity, Phosphomolybdenum assay, Hydroxyl radical, and β -carotene/linoleic acid antioxidant activity. The highest yield was obtained from the hot water extract (6.3%), while the chloroform extract yielded the least (2.1%). The methanolic extract exhibited higher content of total phenolics (48.7 ± 0.7 g GAE/100 g extract), tannins (21.7 ± 0.7 g GAE/100 g extract) and flavonoids (10.3 ± 0.2 RE/100 g extract). The methanolic extract of *B. vahlii* leaves exhibited a strong antioxidant potential compared to other extracts. Thus, these extracts can be considered potential sources of natural antioxidants, providing a basis for developing a valuable food additive to enhance human nutrition.

Jain et al. (2013) ^[159] reported the isolation of pentacyclic phenols from the ethanolic root bark of *B. racemosa*. The dried powdered roots were extracted with ethanol to yield the ethanolic root bark extract, which was further treated with hexane, chloroform and ethyl acetate to yield the respective fractions of the extract. The hexane and chloroform fractions exhibited similar TLC profiles and hence were combined and chromatographed

over silica, while the ethyl acetate fraction was chromatographed separately. Column chromatography led to the isolation of compounds and the structures were elucidated and characterised by UV-Vis, IR, HR-ESI-MS, 1D and 2D-NMR spectral studies and finally confirmed by the single crystal X-ray analysis. The results of the study revealed that one novel phenolic compound, racemosolone, was isolated along with 10 known compounds (n-tetracosane, β -sitosteryl stearate, eicosanoic acid, stigmasterol, β -sitosterol, racemosol, octacosyl ferulate, de-O-methyl racemosol, lupeol and 1,7,8,12b-tetrahydro-2,2,4-trimethyl-2H-benzo[6,7]cyclohepta [1,2,3] benzopyran-5,10,11 triol) from the root bark of *B. racemosa*. The presence of racemosolone was confirmed for the first time in the root bark of *B. racemosa* and naturally.

Santos et al. (2012) ^[160] reported the chemical composition and anxiolytic-like effects of *B. platyptala*. The study involved the preparation of the extract and its fractions, phytochemical and GC-MS analysis and biological evaluation. The powdered drug was extracted with ethanol and subjected to fractionation with diethyl ether, ethyl acetate and water to yield the respective fractions. These were subjected to qualitative phytochemical screening using standard procedures and GC-MS analysis. *In vivo* biological evaluation was performed using behavioural, anxiolytic, and antidepressant models *viz.* Open field test (spontaneous motor activity, total motility, locomotion, rearing and grooming behaviour), Elevated-plus-maze test (EPM), Forced swimming test etc. The ethanolic extract of *B. platyptala* and its ethereal, aqueous and ethyl acetate fractions were administered intraperitoneally in male Swiss mice. The results revealed that the ethereal fraction (50 mg/Kg, *i.p.*) significantly decreased total motility, locomotion and rearing. A single dose of ethanolic extract and ethereal fractions (50 mg/Kg, *i.p.*) increased the exploration of the elevated plus-maze open arms similar to that of diazepam (2 mg/Kg, *i.p.*). In the forced swimming test, the ethanolic extract and its fractions (12.5 mg/Kg, 25 mg/Kg or 50 mg/Kg) did not display considerable activity compared to the standards Paroxetine (10 mg/Kg or 20 mg/Kg, *i.p.*) and Imipramine (25 mg/Kg or 50 mg/Kg, *i.p.*) in reducing

immobility. The phytoconstituents p-cymene, phytol, D-lactic acid, and hexadecanoic acid are present as per GCMS analysis of the ethanolic extract and the ethereal fraction from *B. platyptala* may be responsible for the anxiolytic-like properties.

Annegowda et al. (2012) ^[161] described the effect of extraction techniques on the phenolic content, antioxidant and antimicrobial activity of *B. purpurea*. The leaves of *B. purpurea* were extracted by soxhlet, ultrasonication and maceration methods using ethanol (99.5 %, v/v) to obtain Soxhlet (SBE), ultrasonicated (UBE) and macerated (MBE) *B. purpurea* leaf extract. The effects of different extracting methods on the polyphenolic content and antioxidant activities using DPPH, ABTS, FRAP and TAC were investigated. Disc diffusion and broth dilution methods were performed to evaluate the antibacterial activity of these extracts. The results indicated that UBE possessed significant ($p < 0.05$) polyphenolic constituents, followed by MBE and SBE. All the extracts exhibited potential DPPH and ABTS radical scavenging and potential reducing ability in TAC and FRAP methods. UBE possessed significant ($p < 0.05$) radical scavenging activity and reducing ability, followed by MBE and SBE. The antibacterial efficacy was maximum with UBE, followed by MBE and SBE. The extracts were subjected to thin layer chromatography bioautography followed by high-performance thin layer chromatography (HPTLC) densitometric determination. The results depicted that extraction using the ultrasonication method yields the highest amount of antioxidant compounds among the three methods. The study thus confirms that the ultrasonic extraction is an ideal, simple, and rapid method to obtain antioxidant and antibacterial-enriched *B. purpurea* leaf extract.

Gerenutti et al. (2011) ^[162] evaluated the central nervous system (CNS) activities of the aqueous extract of *B. forficata* using behavioural anxiety models in rats. An acute toxicity study of the extract was carried out by administering doses up to 5000 mg/Kg BW. The pharmacological evaluation was performed using the behavioural Open field assay, Pluz maze assay and Pentobarbital sleep time. Acute toxicity study revealed that the

aqueous extract was safe up to 5000 mg/Kg BW. The result indicated that the administration of *B. forficata* aqueous extract (5.0 g/Kg) in the open field test showed a decrease in locomotion frequency and an increase in time of immobility, suggesting reduced general activity. Open-field grooming duration was increased by the extract. In the elevated plus maze, the extract exhibited an increase in open-arm entries and time into open arms. The aqueous extract significantly augmented pentobarbital-induced sleep, reflected by increased sleeping time assessed with the loss-of-righting reflex. The results thus suggested that *B. forficata* aqueous extract induced anxiolytic effect.

Zakaria et al. (2011) ^[163] reported the antiproliferative and antioxidant activities of various extracts (aqueous, chloroform and methanolic) of the leaves of *B. purpurea*. *In vitro* antiproliferative activity was carried out using MTT assay for 3T3 (normal mouse fibroblast), MCF-7 (estrogen-dependent human breast adenocarcinoma), MDA-MB-231 (human breast carcinoma), Caov-3 (human ovarian adenocarcinoma), HL-60 (acute promyelocytic leukaemia), CEMss (T-lymphoblastic leukaemia) and HeLa (human cervical adenocarcinoma). The antioxidant activity was assessed using DPPH and superoxide anion-free radical assays. The aqueous and chloroform extracts successfully inhibited the proliferation of all cancer cells. In contrast, the methanol extract inhibited the proliferation of all cells except the CEMss cells. The aqueous extract was effective against MCF-7 (IC₅₀ = 9 µg/mL), MDA-MB 231 (IC₅₀ = 17 µg/mL) and Caov-3 (IC₅₀ = 16 µg/mL) cell lines. The chloroform extract was effective against the CEMss (IC₅₀ = 18 µg/mL) and HeLa (IC₅₀ = 21 µg/mL); while the methanolic extract was highly effective only against the HL-60 (IC₅₀ = 12 µg/mL) cell lines. No proliferation inhibition of 3T3 cells was observed in all the extracts. Aqueous and methanolic extracts of *B. purpurea* (20, 100 and 500 µg/mL) exhibited concentration-dependent antioxidant activity only in the superoxide scavenging assay due to their high phenolic content. Thus, the *B. purpurea* leaf possesses potential antiproliferative and concentration-dependent antioxidant activities.

Zakaria et al. (2011) ^[164] evaluated the *in vivo* antiulcer activity of the aqueous leaf extract of *B. purpurea* (BP AE) using absolute ethanol and indomethacin-induced gastric ulcer and pyloric ligation models. Acute toxicity was performed to evaluate the safety profile of the extract. BP AE, at the dose of 5000 mg/Kg BW, did not exhibit any signs of toxicity to rats when given orally. Hence, 100, 500 and 1000 mg/Kg BW doses were administered orally to evaluate the antiulcer activity of the extract in all models. However, the dose-dependent activity was observed only in the absolute ethanol-induced gastric ulcer model. Histological studies supported the observed antiulcer activity of BP AE. In the pyloric ligation assay, BP AE increased the gastric wall mucus secretion ($p < 0.05$). The authors concluded that BP AE exhibited potential antiulcer activity, attributing to the presence of saponins or sugar-free polyphenols, thus validating the traditional use of *B. purpurea* in treating ulcers.

Ananth et al. (2010) ^[165] evaluated the wound-healing potential of methanolic and chloroform *B. purpurea* leaf extracts in rats. Formulations of methanolic and chloroform extracts were prepared in carbopol and simple ointment base at concentrations of 2.5% and 5%. These were applied to the experimentally induced wounds of Sprague Dawley rats induced by excision, incision, burn and dead space wound models. In the excision and burn wound models, animals treated with high doses of methanolic and chloroform extracts displayed a significant reduction in epithelization and wound contraction (50%) compared to the control. In comparison to their respective bases, the incision wound model showed a significant increase in breaking strength with methanolic and chloroform extracts. In the dead space wound model, methanolic and chloroform extract treatment (100 mg/Kg and 500 mg/Kg BW) orally produced a significant increase in the breaking strength, dry tissue weight and hydroxyproline content of the granulation tissue when compared to the control. Methanolic extract exhibited significant activity, followed by the chloroform extract, thus indicating the potent wound-healing activity of *B. purpurea* leaves.

Lakshmi et al. (2009) ^[166] evaluated the protective effect of the ethanolic leaf and unripe pod extracts of *B. purpurea* on gentamicin-induced nephrotoxicity in Wistar rats. Nephrotoxicity was induced in rats by intraperitoneal administration of gentamicin 100 mg/Kg daily for eight days. The ethanolic extract of *B. purpurea* from leaves and unripe pods was administered concurrently at 300 mg/Kg daily by oral route. Serum creatinine, serum uric acid, blood urea nitrogen and serum urea were used as indicators to analyse kidney damage. The study revealed that the ethanolic extract of leaves and unripe pods of *B. purpurea* significantly protected the rat kidneys from gentamicin-induced histopathological changes, viz., glomerular congestion, blood vessel congestion, accumulation of inflammatory cells, epithelial desquamation and necrosis of the kidney cells. The extracts also normalised the gentamicin-induced increase in serum creatinine, serum uric acid and blood urea nitrogen levels, thus confirming its nephroprotective effect.

Shreedhara et al. (2009) ^[167] screened the ethanolic stem extract of *B. purpurea* for analgesic and anti-inflammatory activities. Wistar albino rats and mice were used as the experimental animals, for the respective activities. The ethanolic extract of *B. purpurea* was administered at a dose of 50 mg/Kg and 100 mg/Kg BW, intraperitoneal and subjected to efficacy studies. The analgesic activity was evaluated using Eddy's hot plate method and acetic acid-induced writhing method and compared against the standard analgin (150 mg/Kg, BW). The anti-inflammatory activity was determined by carrageenan-induced paw oedema using a plethysmometer and compared against the standard Diclofenac sodium (5 mg/Kg, BW). The analgesic and anti-inflammatory activities of ethanolic extracts of *B. purpurea* were significant ($p < 0.001$). The maximum analgesic effect was observed at 120 min at the dose of 100 mg/Kg (*i.p.*) and was comparable to that of standard. The percentage of oedema inhibition was reported as 46.4% and 77% for 50 mg/Kg and 100 mg/Kg (*i.p.*), respectively, compared to the standard. Ethanolic extract of *B. purpurea* displayed significant analgesic and anti-inflammatory activities at the dose of 100 mg/Kg, comparable to the standard drugs.

Agrawal et al. (2009) ^[168] evaluated the anticarcinogenic and antimutagenic potential of methanolic extract of *B. variegata* using Swiss albino mice. The biological activities of the extract were assessed using a skin carcinogenesis and melanoma tumour model, along with micronucleus and chromosomal aberration tests. 7,12-Dimethylbenzanthracene (DMBA) was used as a carcinogen. In the skin papilloma model, significant prevention, with delayed appearance and reduction in the cumulative number of papillomas, was observed in the group treated with DMBA, extract and croton oil as compared to the group treated with DMBA and croton oil. C57 Bl mice that received the methanolic extract of *B. variegata* at the doses of 500 mg/Kg and 1000 mg/Kg BW for 30 days exhibited a significant increase in life span with a decrease in tumour size as compared to controls. During the antimutagenicity studies, a single application of the extract at doses of 300, 600 and 900 mg/Kg dry weight, was administered 24 hours prior to the *i.p.* administration of cyclophosphamide (50 mg/Kg). The results significantly prevented micronucleus formation and chromosomal aberrations in bone marrow cells of mice, in a dose-dependent manner. The authors thus confirmed that the methanolic extract of *B. variegata* exerts anticarcinogenic and antimutagenic activity.

Raj Kapoor et al. (2009) ^[169] evaluated the cytotoxic activity of a flavanone from the stems of *B. variegata*. The powdered stems of *B. variegata* were extracted with ethanol to yield the ethanolic extract. The extract was partitioned in water and extracted with benzene, diethyl ether, ethyl acetate and butanol to yield respective fractions. The ethyl acetate fraction was subjected to column chromatography to isolate a flavanone. The structure was elucidated using UV-Vis, ¹H-NMR, ¹³C-NMR, and mass spectroscopic methods. The isolated flavanone was tested for cytotoxic activity against 57 human tumour cell lines, representing leukemia, non-small cell lung, colon, central nervous system, melanoma, ovarian, renal, prostate and breast cancers. The structure of the isolated compound was identified as 5,7,4'-trimethoxy flavanone, exhibiting cytotoxic activity with

the range of 4.06–4.81 μM . The compound was more selective against OVCAR-5 and SKOV-3 cell lines of ovarian cancer. Thus, the authors concluded that the isolated flavanone has cytotoxic activity against human tumour cell lines.

Jain et al. (2008) ^[170] reported the bioactivities of polyphenolics from the roots of *B. racemosa*. Air-dried roots of *B. racemosa* were pulverised and extracted with n-hexane, diethyl ether, and methanol successively to give the hexane (6.77 g), diethyl ether (65.66 g), and methanolic (67.82 g) extracts, respectively. The diethyl ether extract was subjected to column chromatography using gradient elution with petroleum ether, benzene, ethyl acetate, and methanol to obtain various phytoconstituents. The isolated compounds were characterised using IR, ¹H-NMR and mass spectrometric methods. The compounds were further subjected to antibacterial activity using *Bacillus thuringiensis*, *Enterobacter cloacae*, *Escherichia coli*, *Klebsiella pneumoniae*, *Pseudomonas aeruginosa*, and *Staphylococcus aureus* by employing the disc diffusion method. Antifungal activity by disc diffusion method was used to screen *Aspergillus flavus*, *A. fumigatus*, *A. niger*, *Penicillium chrysogenum*, and *Rhizopus stolonifer*. The efficacy against *Herpes simplex* virus type I (HSV-I), *Poliomyelitis* virus type I (Polio I) and *Vesicular stomatitis* virus (VSV) was evaluated by the plaque inhibition method for antiviral activity.

Kaewamatawong et al. (2008) ^[171] reported the isolation of seven flavonols from the methanolic leaf extract of *B. malabarica*. The isolated compounds were characterised and identified as 6, 8-di-C- methylkaempferol-3-methyl ether, kaempferol, afzelin, quercetin, isoquercitrin, quercitrin, and hyperoside by comparison of physical and spectrometric data with the values reported in the literature.

Boonphong et al. (2007) ^[172] reported the isolation of eleven new secondary metabolites along with two known flavanones and five known bibenzyls, bioactive

compounds from the root extract of *B. purpurea*. The new compounds reported include eight dihydrodibenzoxepin, a dihydrobenzofuran, a novel spirochromane-2,1'-hexenedione, and a new bibenzyl. The isolated compounds were further subjected to antimycobacterial, antimalarial, antifungal, cytotoxic, and anti-inflammatory activities using *in vitro* assays. The antimycobacterial activity was assessed against *Mycobacterium tuberculosis* H37Ra using the Microplate Alamar Blue assay (MABA) and compared against the standard drugs, isoniazid and kanamycin sulfate. The antimalarial activity was determined using the microculture radioisotope technique against *Plasmodium falciparum* and compared against the standard, Dihydroartemisinin. Antifungal activity was assessed against *Candida albicans*, using a colorimetric method with Amphotericin B and 10% DMSO as positive and negative controls, respectively. Cytotoxicity was determined using SRB assay and compared against the reference compound, ellipticine. Anti-inflammatory activity was determined by measuring the inhibition of COX enzymes using the radioimmunoassay method, using Aspirin as a positive control. All the isolated compounds depicted substantial pharmacological activities in the models mentioned above.

Aderogba et al. (2006) ^[173] reported the isolation of two flavonoids from *B.mondara* leaves and their antioxidant activity. The powdered leaves were extracted with methanol to yield the methanolic extract. The extract was successively partitioned with hexane, dichloromethane, ethyl acetate and butanol to yield the respective fractions. The ethyl acetate fraction was subjected to column chromatography. The isolated compounds were characterised by ¹H-NMR, ¹³C-NMR and mass spectroscopic methods. Antioxidant activity was evaluated using the DPPH scavenging assay. Bioassay-directed fractionation of the ethyl acetate soluble leaf extract led to the isolation of two active compounds, characterised and identified as Quercetin-3-O-rutinoside (rutin) and Quercetin. Quercetin displayed maximum antioxidant activity when compared to rutin. The higher antioxidant

activity of Quercetin could be due to the presence of a free hydroxyl group in position 3, as both compounds have catechol groups (3' and 4' di-OH) on ring B.

Gupta et al. (2004) ^[174] evaluated the antitumour and antioxidant activity of the methanolic stem bark extract of *B. racemosa* (MEBR). The antitumour and antioxidant activity of the extract was evaluated at a dose of 50, 100, and 200 mg/Kg BW *i.p.*, against Ehrlich ascites carcinoma (EAC) tumour in Swiss albino mice. Acute and short-term toxicity studies were performed to confirm the safety of MEBR. The tumour was inoculated for 24 h, and the extract was administered daily for 14 days. On the last day, mice were sacrificed to observe the antitumour activity. The effect of MEBR on the growth of the transplantable murine tumor, alterations in the hematological profile, the life span of EAC-bearing hosts and alterations in liver biochemical parameters (lipid peroxidation, antioxidant enzymes) were determined. MEBR was safe to 200 mg/Kg in acute and short-term toxicity studies. It exhibited a decrease in tumour volume, packed cell volume and viable cell count. The non-viable cell count and mean survival time were increased, which resulted in an increase in the life span of EAC tumour-bearing mice. The haematological profile reverted to almost normal levels in extract-treated mice. MEBR decreased the levels of lipid peroxidation while increasing the levels of GH, SOD and CAT. Thus, the authors concluded that MEBR displayed a profound antitumour effect by regulating lipid peroxidation and supporting the antioxidant defense system in EAC-bearing mice.

Raj Kapoor et al. (2003) ^[175] evaluated and reported the antitumour activity of the ethanolic extract of *B. variegata* (EBV) against Ehrlich Ascites Carcinoma (EAC) in Swiss albino mice. The oral acute toxicity study of the extract was carried out in Swiss albino mice. EAC cells were maintained by weekly *i.p.* inoculation of 10^6 cells/mouse. The parameters used to evaluate antitumour activity were, Median survival time (MST), effect on the solid tumor, effect on haematological parameters, and *in vitro* cytotoxicity against EAC cells. The results indicated that the extract was safe up to 2.5 g/Kg. A

significant enhancement in the mean survival time of EBV-treated tumour-bearing mice was reported compared to the control group. EBV treatment enhanced peritoneal cell counts. EBV could reverse the alterations in haematological parameters, protein, and PCV brought on by tumour inoculation after 14 days. EBV effectively reduced solid tumour mass development induced by EAC cells, thus confirming its cytotoxic effect towards EAC tumour cells.

Raj Kapoor et al. (2003) ^[176] assessed and reported the antitumour activity of the ethanolic extract of *B. variegata* (EBV) on Dalton's ascitic lymphoma (DAL) cells. DAL cells were maintained by weekly *i.p* inoculation of 10^6 cells/mouse. The parameters used to evaluate antitumour activity were, Median survival time (MST), effect on the solid tumour and effect on haematological parameters. The effect of EBV on the survival of tumor-bearing mice exhibited MST of 23 days in the control group, while MST was 32 days (139.13%) and 40 days (173.9%) for the groups treated with EBV (250 mg/Kg orally) and 5-Fluoro Uracil (20 mg/Kg, *i.p.*), respectively, daily. EBV treatment was found to enhance peritoneal cell counts. It was able to reverse the changes in the haematological parameters, protein and PCV after tumour inoculation. The percent of neutrophils was reported to be increased while the lymphocyte count was reduced, as observed in differential WBC count. The authors concluded that the ethanolic extract of *B. variegata* could be a novel and potential agent in cancer chemotherapy.

Yadava et al. (2000) ^[177] isolated a novel flavone glycoside from the chloroform-soluble fraction of the ethanolic extract of *B. purpurea* stems. The powdered stem was extracted with ethanol to yield the ethanolic stem extract of *B. purpurea*. The extract was successively partitioned with n-hexane, chloroform, and methanol to yield the respective fractions of the extract. The chloroform-soluble fraction of the extract was subjected to column chromatography. The isolated compound was characterized using UV-Vis, IR, ¹H-NMR, ¹³C-NMR and mass spectroscopic methods. The compound was identified as 5,6-

dihydroxy-7-methoxyflavone 6-O- β -D-xylopyranoside. Column chromatography resulted in the isolation of polyphenolics, which were characterised and identified as 1,7,8,12b-tetrahydro-2,2,4-trimethyl-10-methoxy-2H-benzo [6,7] cyclohepta[1,2,3-de][1]benzopyran-5,9-diol (racemosol), 1,7,8,12b-tetrahydro-2,2,4-trimethyl-2H-benzo[6,7]cyclohepta[1,2,3-de][1]benzopyran-5,10,11-triol, and 1,7,8,12b-tetrahydro-2,2,4-trimethyl-2H-benzo[6,7] cyclohepta [1,2,3-de][1]benzopyran-5,9,10-triol (de-O-methyl racemosol). The isolated compounds exhibited profound antibacterial, antifungal, and antiviral activities against all strains. The methanol extract displayed significant efficacy against Herpes simplex virus.

3.4. Review of other related pharmacological activities

Talebi *et al.* (2021) ^[178] explained the role of flavonoids for the prevention of neurodegenerative diseases by several clinical studies. Chrysin, a natural flavonoid is isolated from diverse fruits, vegetables, and mushrooms, and has several pharmacological activities comprising of antioxidant, anti-inflammatory, antiapoptotic, anticancer, and neuroprotective effects. The role of chrysin was evaluated in depression, anxiety, neuroinflammation, Alzheimer's disease, Parkinson's disease, Huntington's disease, epilepsy, cerebral ischemia, spinal cord injury, neuropathy, multiple sclerosis, and Guillain-Barré's Syndrome. The study revealed that chrysin has protective effects and is effective against neurological diseases by modulating oxidative stress, inflammation, and apoptosis in animal models.

Yazan *et al.* (2022) ^[179] evaluated the anti-cancer activity of the lead bioactive compound present kernel extract of *Mangifera pajang* against human breast cancer cell lines with positive estrogen receptor (MCF-7). The methanolic extract of the dried powder of *Mangifera pajang* was subjected to column chromatography for isolation of

phytoconstituent. The isolated phytoconstituent was characterised using IR, ¹H-NMR, ¹³C-NMR and mass spectroscopic methods. The cytotoxicity, morphological changes, flow cytometry and cell cycle arrest analyses were performed to examine the mechanism of anti-proliferation and apoptosis against the MCF-7 cell lines. Column chromatography led to the isolation of methyl gallate; the structure was confirmed by spectral analysis. Methyl gallate demonstrated induction of apoptosis in MCF-7 cells with three concentrations (1,10 and 100 µM) after 48 h of treatment. The cell cycle arrest showed a significant ($p < 0.05$) decrease in cell progression at G₂/M phase of MCF-7 after treatment with 100 µM of methyl gallate. The cell percentage of early and late apoptosis was significant at 10 and 100 µM of methyl gallate. Methyl gallate treatment also induced up-regulation of reactive oxygen species levels in MCF-7 cells with a reduction in superoxide dismutase levels, via up-regulating oxidative stress pathway. The study displayed the efficacy of methyl gallate in mammary tumor therapy.

Farrag *et al.* (2021) ^[180] assessed the antiproliferative, apoptotic and oxidative stress suppression activities of quercetin against induced toxicity in lung cancer cells of rats. The lung cancer cell lines used for the study were A549 and H69 cancer cells and two genes Bax and Bcl-2 that play an important role in apoptosis pathways were investigated. Immunohistochemical study for caspase-3 that is considered as indicator for apoptosis was performed. Molecular docking studies of Quercetin with anti-oxidative stress enzymes (GSPH and SOD) were also studied. The study revealed that Quercetin exhibited prominent antiproliferative activity against tested lung cancer cell lines, with IC₅₀ values of 8.65, 7.96 and 5.14 µg/ml on A549 at 24, 48 and 72 h respectively. Significant effects of quercetin on Bax, Bcl-2 and caspase-3 were observed, proving its ability to induce apoptosis. *In silico* studies revealed that, Quercetin exhibited reduction in MDA and elevation of levels SOD and glycogen phosphorylase, indicating its ability in suppressing oxidative stress.

Razack et al. (2018) ^[181] studied the anxiolytic action of the ethanolic extract of *Nardostachys jatamansi* extract (NJE) in mice. Elevated plus maze, Open field test, Light dark box test, and Vogel's conflict test were used as screening models to evaluate *in vivo* anxiolytic activity. The rats were treated orally with NJE (250 mg/Kg) for 3, 7 and 14 days or diazepam (1 mg/Kg) and flumazenil (0.5 mg/Kg *i.p*) before behavioral assessment. The mice were sacrificed by cervical dislocation and brain tissues were collected for further estimation of monoamine neurotransmitters, GABA, and antioxidant enzymes. The biodistribution experiment was carried out using radiolabelled extract (technetium-99m at hydroxyl groups of identified metabolites using stannous chloride as reducing agent). The *in vivo* activity and blood kinetics were further evaluated in rabbits. Treatment of mice for 7 days caused an increase in time spent in open arms in elevated plus maze, number of line crossings in open field test, increased time spent in lit compartment of light-dark box test, an increase in number of licks made and shocks accepted in Vogel's conflict test, with results comparable to diazepam and this treatment also caused a significant increase in monoamine dopamine, noradrenaline and serotonin neurotransmitters and GABA in brain and tissue antioxidants like Glutathione S-transferase (GST), Superoxide dismutase, catalase, Glutathione reductase etc.

Co-treatment of NJE with flumazenil (GABA-benzodiazepine antagonist) antagonised the anxiolytic actions of NJE and exhibited significant reduction in time spent in open arms of elevated plus maze, and decrease in number of line crossing in open field test and also number of shocks and licks accepted in Vogel's conflict test. The blood kinetics and *in vivo* biodistribution studies indicated that the labelled compound was cleared rapidly from blood (within 24 h) and accumulated majorly in kidneys (11.65 ± 1.33), liver (6.07 ± 0.94), and blood (4.03 ± 0.63) after 1 h. Only, a small amount was observed in brain (0.1 ± 0.02) probably because of its inability to cross blood-brain barrier. These results highlight biodistribution pattern of NJE, and also indicated that a 7-day treatment with NJE produced significant anxiolytic effects in mice and also a significant increase in brain

monoamine and GABA neurotransmitter levels, suggesting its anxiolytic effects are primarily mediated by activating GABAergic receptor complex.

Singh et al. (2017) ^[182] reported the antianxiety activity guided isolation and characterization of bergenin from *Caesalpinia digyna* Rottler roots. The ethanolic extract of the roots were successively fractionated with petroleum ether, chloroform, methanol, The authors, earlier reported that the ethylacetate fraction exhibited significant anxiolytic activity. Hence this fraction was subjected to column chromatography, for isolation of compounds. Elution was done with petroleum ether, chloroform and methanol, to give 158 fractions and one pure compound CD1. Identical fractions showing similar spots on TLC were pooled together to get five fractions F1-F5. These were further subjected for anxiolytic activity, using elevated plus maze, open field, and mirror chamber test. Percent yield of fractions was F1 (1.7), F2 (4.1), F3 (4.9), F4 (49.0) and F5 (36.1). F4 exhibited significant anxiolytic activity, and hence were further subjected to column chromatography to yield three sub fractions F4.1–F4.3. A pure compound CD₂ was precipitated from fraction F4.3. CD₁ and CD₂ were characterised by IR, ¹H-NMR, ¹³C-NMR and mass spectroscopic methods. Spectral analysis confirmed that both compounds CD₁ and CD₂ were bergenin. The sub fractions F4.1–F4.3 and CD₁ were further subjected to anxiolytic activity using EPM, open field and mirror chamber tests. Bergenin, isolated from roots of *C. digyna*, exhibited significant antianxiety activity at 80 mg/Kg, per orally in three models for antianxiety activity.

Pemminati et al. (2010) ^[183] evaluated the antianxiety effect of aqueous extract of fruits of *Embllica officinalis* (EO) on acute and chronic administration in rats. Male Wistar albino rats weighing 150-180 g were divided into five groups (n = 6) for acute and chronic study separately. Diazepam (1.0 mg/Kg) and EO (0.8, 2.0 & 4.0 mg/Kg) were suspended in 1 % gum acacia and administered orally. In acute study, vehicle/drugs were given 60 min before, while in chronic study they were given once daily for 10 days and the last dose was

given 60 min prior to exposure to the experimental paradigms *viz.*, elevated plus maze and bright and dark arena. EO significantly increased the number of entries into, time spent and rears in the open arms and percent ratio of open arm to total arm entries in elevated plus maze paradigm in both acute and chronic administration. In the bright and dark arena paradigm, EO on acute and chronic administration significantly increased the number of entries, time spent and rears in the bright chamber, and reduced the duration of immobility. These behavioural changes were comparable to that produced by the standard anxiolytic drug Diazepam. The behavioural disinhibition produced by EO was suggestive of its anxiolytic activity.

Latha *et al.* (2015) ^[184] evaluated the anxiolytic activity of aqueous extract of *Coriandrum sativum* (CS) Linn. in mice. Swiss albino mice (18-25 g) of either sex were randomly divided into five groups of six animals each. Dried powder of CS leaves was boiled with distilled water, cooled, filtered, placed on a hotplate for complete evaporation, finally weighed and stored. The control group, test group, and standard drugs group received saline, CS extract (50, 100, and 200 mg/Kg), diazepam (3 mg/Kg), respectively, by oral feeding. The antianxiety effect was assessed by elevated plus maze (EPM) in mice. In the EPM, CS 50 mg/Kg, 100 mg/Kg, and 200 mg/Kg significantly ($p < 0.001$) increased the number of entries in open arms compared to control. The time spent in open arms also increased in all the doses of CS extract, thus demonstrating statistically significant dose-dependent antianxiety activity of CS leaves.

Dutt *et al.* (2010) ^[185] evaluated the antianxiety activity of *Gelsemium sempervirens*. Petroleum ether, chloroform, methanol, and water extracts of *G. sempervirens* were prepared by successive extractions using a soxhlet apparatus, and subsequently evaluated for antianxiety activity using the elevated plus maze model, using Diazepam (2.5 mg/Kg) as standard drug. Acute toxicity study was performed upto 1g/Kg BW.

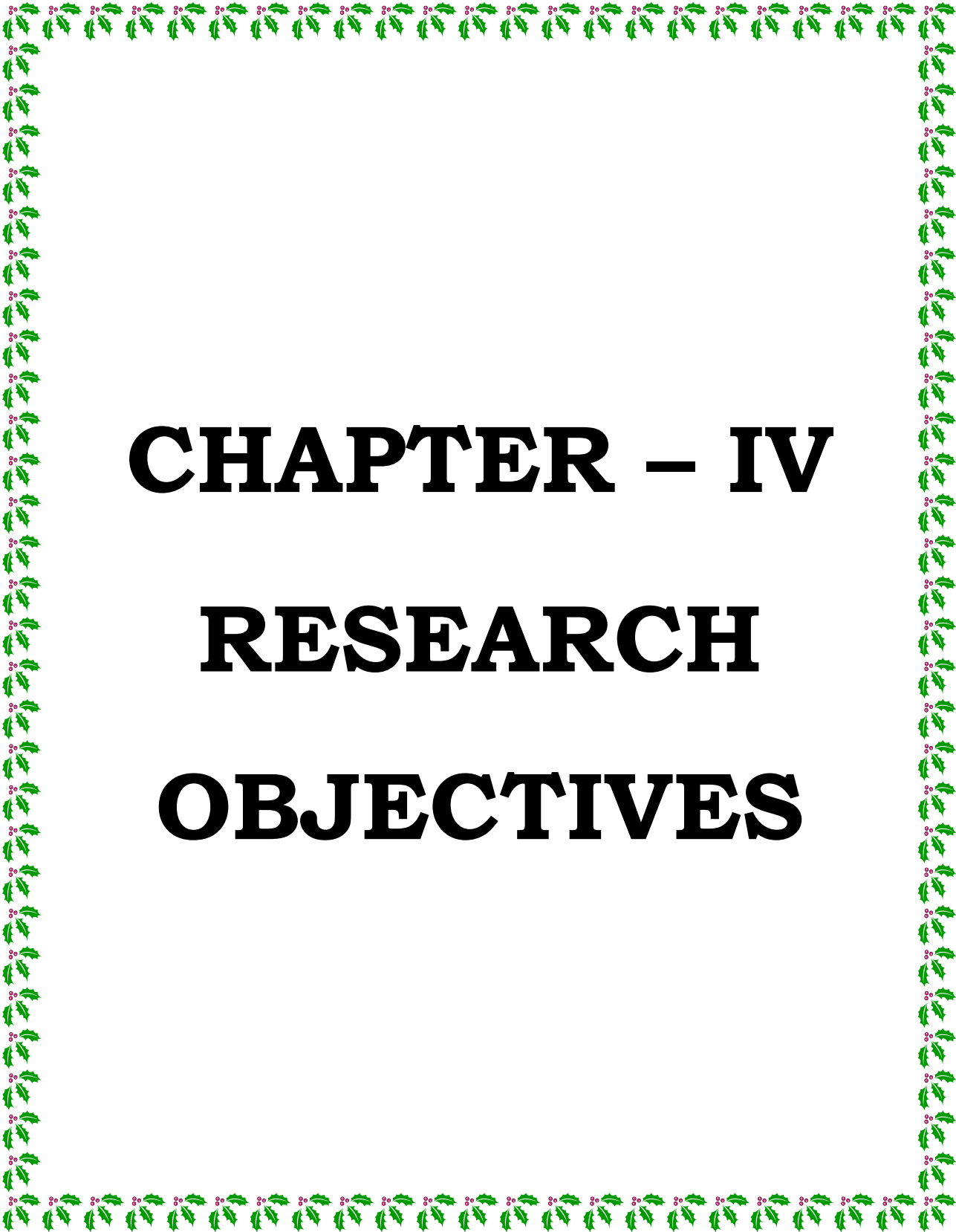
Among various extracts, the methanol extract of *G. sempervirens* exhibited significant increase in open arm entries and mean time spent in open arms at the dose of 150 mg/Kg. This was subjected to column chromatography to yield 11 fractions. All the pooled fractions (F1–11) were screened for anxiolytic activity at various doses (5, 10, 15 and 25 mg/Kg, p.o.) given to the mice, using the EPM apparatus. Fraction (F9.4) derived from the methanol extract exhibited significant anxiolytic activity at the dose level of 10 mg/Kg in the elevated plus maze test.

Kumar et al. (2005) ^[186] evaluated the anti-anxiety activity studies of various extracts of *Turnera aphrodisiaca*. Petroleum ether, chloroform, methanol, and water extracts of *T. aphrodisiaca* aerial parts were screened for anxiolytic potential (at doses of 25, 50, 75, 100, or 125 mg/Kg BW) in mice using elevated plus-maze apparatus. Among all the extracts, only methanol exhibited significant anxiolytic activity at a dose of 25 mg/Kg when compared to control as well as standard (diazepam, 2 mg/Kg BW). 15 g of methanolic extract was treated with petroleum ether, chloroform, and *n*-butyl alcohol by shaking successively, and all the shakings as well as the residual methanolic extract (RME) were further evaluated for anxiolytic activity in mice. The doses of fractions used were 10, 20, 30, 40, or 50 mg/Kg and those of RME were 10, 25, 50, 75, or 100 mg/Kg. Butanol fraction at a dose of 10 mg/Kg and RME at a dose of 75 mg/Kg were found to exhibit anxiolytic activity.

Bhandari et al. (2014) ^[187] evaluated the anti-anxiety activity of thymol using 5, 10, 20 mg/Kg. *i.p.* in Swiss albino mice. Behavioral testing was performed in animal models after 30 min of all treatment, time spent in light area and open space was observed for 5 min duration (300 s). A significant increase in percentage of time spent in open arms of EPM and significant increase in percentage of time spent in light compartment of LDT indicate anxiolytic-like effect respectively. A significant decrease in above parameters indicated anxiogenic effect. Thymol 20 mg/Kg significantly increased percentage of time

spent in open arms of EPM and light compartment of LDT as compared to their vehicle treated group. Thymol (20 mg/Kg) produced significant anti-anxiety effect as compared to vehicle (0.01 % ethanol) treated mice in both EPM and LDT behavioral models.

Sahoo *et al.* (2005) ^[188] investigated the anxiolytic activity of *C. sativum* L. seeds aqueous extract (CSE) induced by chronic restraint stress and its effect on the neurotransmitter system. The phytoconstituents were extracted using soxhlet apparatus and identified using LC-MS. The mice were orally administered with the standard drug diazepam and CSE daily and exposed to restraint stress for two weeks. Anxiolytic activity was assessed using elevated plus maze and light and dark transition test models on day 1 and 16 after chronic restraint stress. On the 16th day, the mice were euthanized by cervical dislocation. The brain was dissected and the cerebral cortex, hippocampus, and the remaining brain tissue (cerebellum and brain stem) was individually weighed and homogenized in 1 mL of ice cold 0.1 M perchloric acid. Monoamine, GABA and glutamate levels in cerebral cortex, hippocampus, and remaining brain tissue (cerebellum and brain stem) was estimated using HPLC. The results indicated that CSE treatment improved exploratory activity in the EPM and LDT models of anxiety, and restored monoamines and GABA levels to the respective baseline levels. Moreover, CSE reduced excitotoxic levels of glutamate in the hippocampus region.



CHAPTER – IV

RESEARCH

OBJECTIVES

4. RESEARCH OBJECTIVES

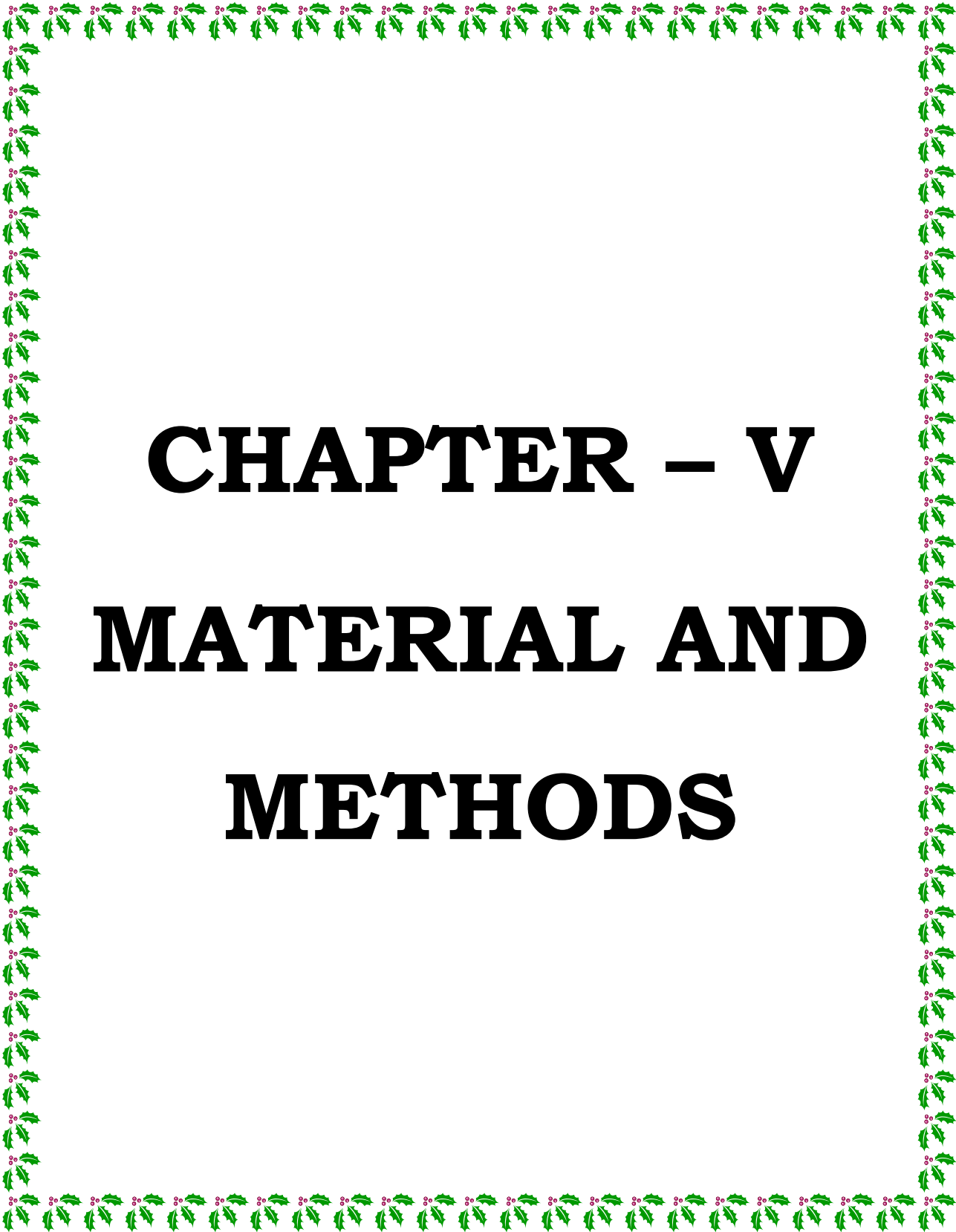
The objectives of the research were as follows.

- Collection and authentication of the plants *Hybanthus enneaspermus* Linn. and *Bauhinia foveolata* Dalzell.
- Extraction and preparation of various fractions of the extracts.
- Preliminary phytochemical and *in vitro* antioxidant activity screening of the bioactive fractions.
- Screening of the bioactive fractions for Pharmacological activity.
- Isolation and characterization of phytoconstituent from the fraction showing significant pharmacological activity.

To accomplish the above objectives, the following investigation were carried out.

- Collection and authentication of *H. enneaspermus* and *B. foveolata*.
- Preparation of the extracts of *H. enneaspermus* (EEHE) and *B. foveolata* (EEBF) and their biofractions (TFHE, ITHE, EFHE, MFHE, TFBF, ITBF, EFBF and MFBF).
- Qualitative preliminary phytochemical screening of the extracts and biofractions using established procedures.

- Quantitative phytochemical investigation - Total phenolic and total flavonoid content of the extracts and biofractions.
- Pharmacological investigation for *in vitro* antioxidant activity - DPPH, hydrogen peroxide, nitric oxide and ABTS free radical scavenging assays of the extracts and biofractions.
- Pharmacological investigation for *in vitro* anticancer activity - antiproliferative, apoptosis, cell cycle assays of the extracts and biofractions.
- Acute toxicity study of EEBF and pharmacological investigation for *in vivo* antianxiety activity. EEHE, ITHE, EEBF and ITBF were subjected to antianxiety behavioural methods using Elevated plus maze (EPM), Light and dark transition, Mirror chamber, Hole board and Open field - Optovarimex (Autotrack) tests.
- Biochemical estimations in rats' brain homogenates - Isolation of brain from the group of rats exhibiting significant antianxiety activity, dissection into various parts and estimation of antioxidant enzymes and neurotransmitters levels.
- Isolation and characterisation of phytoconstituents from the fractions showing significant pharmacological activity.
- Pharmacological investigation for *in vitro* anticancer activity - antiproliferative, apoptosis, cell cycle assays of the isolated compounds. *In vitro* caspase-3, DNA fragmentation and gene expression of the compound exhibiting significant activity.
- *In silico* molecular docking - evaluation of the isolated phytoconstituents for anticancer (caspase -3 enzyme) and antianxiety (BZD-GABA_A receptor) activity.



CHAPTER – V

MATERIAL AND

METHODS

5. MATERIAL AND METHODS

5.1. Material

5.1.1. Instrumentation

Double beam UV-Vis spectrophotometer (LABINDIA Analytical UV 3092) was used for spectroscopic analysis, Acquity UPLC (Waters, USA), Xevo G2 XS QTof (Waters, USA) were used for Liquid chromatography-Mass spectrometry, Bruker Avance Neo 500 MHz NMR spectrometer and SA Agilent 400 MHz NMR spectrometer were used Nuclear magnetic resonance (NMR) spectrometry, 2545 Binary Gradient Module (Waters, USA) for preparative High-performance liquid chromatography (HPLC), Cytomics FC500 Flow cytometer (Beckman Coulter, USA) for flow cytometry, Realplex Master cyler (Eppendorf, Germany), Elevated Plus Maze (Columbus), Optovarimex (Columbus), Light and dark, Mirror chamber and Holeboard apparatus for anxiolytic activity were used. The other apparatus used for the study were Microplate reader (Bio-rad), cooling centrifuge (Eltec), spinwin microspin (Tarsons), UV chamber (Desaga Sarstedt - Gruppe Cabuvis), Incubator (Tempo T1-90E) Weighing balance (Wensar Mab 220, Scale-Tec, Essae DS-450), Rotary evaporator (Equitron), heating mantle (Thermo scientific), electrical thermostat water bath (Thermo scientific), Hot Air Oven (Quality instrument and equipment), 5ml sterile centrifuge tubes and FACS tubes - Tarsons, India etc. were used for the study.

5.1.2. Chemicals and reagents

High purity analytical grade solvents and chemicals were used for the study. Folin ciocalteau reagent, aluminium chloride, DPPH, sodium nitroprusside, ABTS and sulphanimide were purchased from Molychem (Mumbai, India). Potassium persulfate was purchased from Himedia (India). 1,10-phenanthroline and hydrogen peroxide solution were purchased from Merck (Bangalore, India). Silica gel 60G F₂₅₄ plates were procured from Merck (Bangalore, India), silica 60-120 mesh and propidium iodide (PI) were obtained from Sigma Chemical Co (St. Louis, Mo., USA). AnnexinV-FITC Kit was

obtained from Beckman Coulter (Indianapolis, USA). Dulbecco's Modified Eagle Media (DMEM) with low glucose and Fetal bovine serum (FBS) were procured from Gibco, Invitrogen (USA). Antibiotic - Antimycotic 100 X solution was obtained from Thermofisher Scientific (USA), phosphate buffered saline (PBS), 2% paraformaldehyde solution, 0.5% BSA in 1X PBS, 0.1% Triton-X 100 in 0.5% BSA solution was obtained from HiMedia (USA). Potassium persulfate, DPBS and NEDD were obtained from Himedia (India), while Naphthyethylene diamine and DMSO was procured from Qualigens (Mumbai, India). FITC Rabbit anti-active Caspase-3 IgG Antibody kit and APO-DIRECT™ kit were procured from Pharmingen, BD Biosciences (USA), Primescript RT reagent kit (Cat No. RR037A) was procured from Takara (Japan). Primers for β -actin, Bcl-2, Bax and p53 genes were obtained from GCC Biotech, West Bengal, India. Diazepam HCl was procured from Centaur Pharmaceuticals Pvt. Ltd., Mumbai, India. Tween 80 was purchased from Merck, Pvt. Ltd., Mumbai, India. Rat neurotransmitter (Dopamine, Serotonin, GABA, Nor adrenaline, Glutamic acid) and rat antioxidant enzyme estimation kits (Catalase, SOD, Glutathione-S-transferase, Glutathione peroxidase, Glutathione reductase) estimation kits were purchased from Bioelsa (Chino, CA, USA). Reference standards were procured from Sigma-Aldrich (St. Louis, Mo., USA).

5.1.3. Cell cultures

The cell lines that were required for our study were obtained from National Centre for Cell Science, Pune, India. The stock cells were cultured in RPMI 1640 media supplemented with 10 % FBS and 2 mM L-glutamine. DMEM was supplemented with inactivated FBS (10%), penicillin (100 IU/mL), and streptomycin (100 μ g/mL) in 5 % CO₂ at 37 °C until confluent. TPVG solution that consisted of 0.2 % trypsin, 0.02 % EDTA, and 0.05 % glucose in PBS, was used to separate the cells. Before the start of the experiment, the cultures from the stock solution were transferred to 96-well microtiter plates for plating.

5.2. METHODS

5.2.1. Collection and authentication of *H. enneaspermus* and *B. foveolata*

Fresh whole plants of *H. enneaspermus* were collected from Mangalore, Karnataka, during August 2017. The sample specimen was prepared and submitted for authentication to Council of Scientific and Industrial Research - National Institute of Science Communication and Information Resources (CSIR-NISCAIR), New Delhi. The voucher specimen was deposited in the department of Pharmacognosy (GCPDOP-06), Goa College of Pharmacy, Panaji-Goa. The plants were washed to remove the extraneous matter, air-dried in the shade, cut into small pieces, powdered using a mechanical grinder, packed in a tightly closed container and stored for phytochemical and pharmacological investigation.

Fresh leaves of *B. foveolata* were collected from the forests of Dandeli, Karnataka, India, in August-September 2017. The sample specimen was prepared and submitted for authentication to Department of Botany, Government Pre-university college, Dharwad, Karnataka. The voucher specimen was deposited in the department of Pharmacognosy (GCPDOP-07), Goa College of Pharmacy, Panaji-Goa. After authentication of the sample, the leaves were dried in the shade, reduced to fine powder, packed in a tightly closed container and stored for phytochemical and pharmacological studies.

5.2.2. Preparation of extracts and biofractions ^[189]

5.2.2.1. Preparation of ethanolic extract of *H. enneaspermus* (EEHE) and its biofractions

3 Kg of the powdered drug was macerated with 4.5 L of absolute alcohol thrice for 4 days with occasional stirring. After 4 days, the ethanolic layer was decanted. The process was repeated thrice with fresh solvent. The solvent was filtered using the Whatmann filter paper (No.1), distilled off using a rotary evaporator and then evaporated to dryness to yield the extract. The ethanolic extract of *H. enneaspermus* Linn. (EEHE) was stored at 4 °C.

250 g of EEHE was refluxed successively with toluene thrice for one and half an hour, filtered using Whatmann filter paper (No.1). The solvent was recovered using a rotary evaporator, and the toluene (TFHE) and insoluble toluene (ITHE) fractions of ethanolic leaf extract of *H. enneaspermus* were obtained. 15 g of ITHE was further fractionated with ethyl acetate and methanol successively to yield ethyl acetate (EFHE) and methanol soluble (MFHE) fractions of EEHE and stored at 4 °C.

5.2.2.2. Preparation of ethanolic extract of *B. foveolata* (EEBF) and its biofractions

3 Kg of dried powdered leaves were defatted by refluxing with 3.5 L of Petroleum ether thrice. The defatted drug (1.78 Kg) was refluxed with absolute ethanol (4.5 L) for 90 min, thrice. The alcoholic extract was filtered using the Whatmann filter paper (No.1). The solvent from the extract was distilled off using a rotary evaporator, which was evaporated to dryness to yield the ethanolic extract of *B. foveolata* (EEBF), which was stored at 4 °C.

110 g of EEBF was refluxed successively with toluene, ethyl acetate and methanol thrice for one and half an hour each time and filtered using Whatmann filter paper (No.1). The solvent was separated off using a rotary evaporator and the toluene soluble (TFBF) and toluene insoluble (ITBF) fractions of EEBF were obtained. 45 g of ITBF was refluxed with ethyl acetate and methanol successively to yield the ethyl acetate (EFBF) and methanol soluble (MFBF) fractions of EEBF and stored at 4 °C.

5.2.3. Qualitative Preliminary Phytochemical Investigation

The preliminary phytochemical screening of the extracts (EEHE, EEBF) and biofractions (TFHE, ITHE, EFHE, MFHE, TFBF, ITBF, EFBF, MFBF) was performed to detect the presence of phytoconstituents using established procedures.^[190-192]

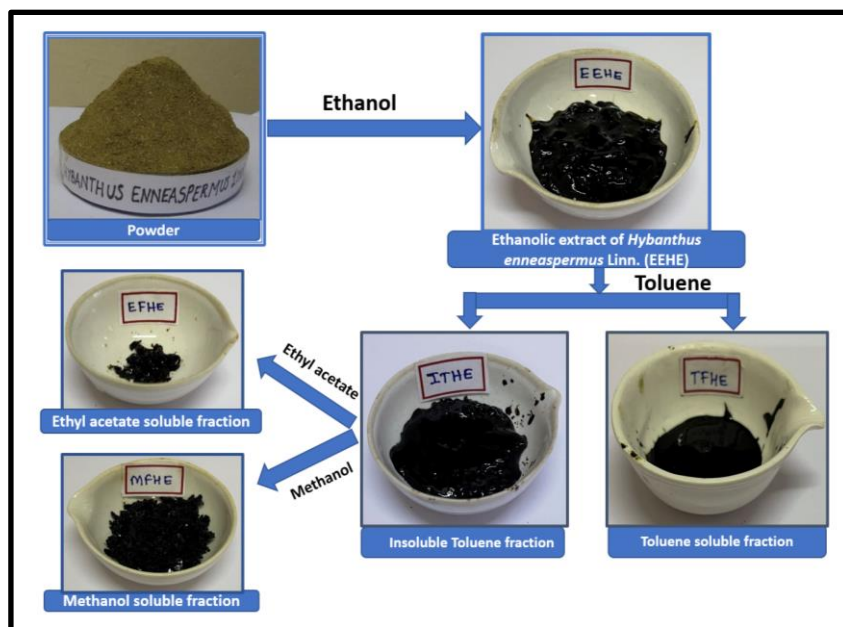


Figure 5.1: *Hybanthus enneaspermus* - Extraction and fractionation

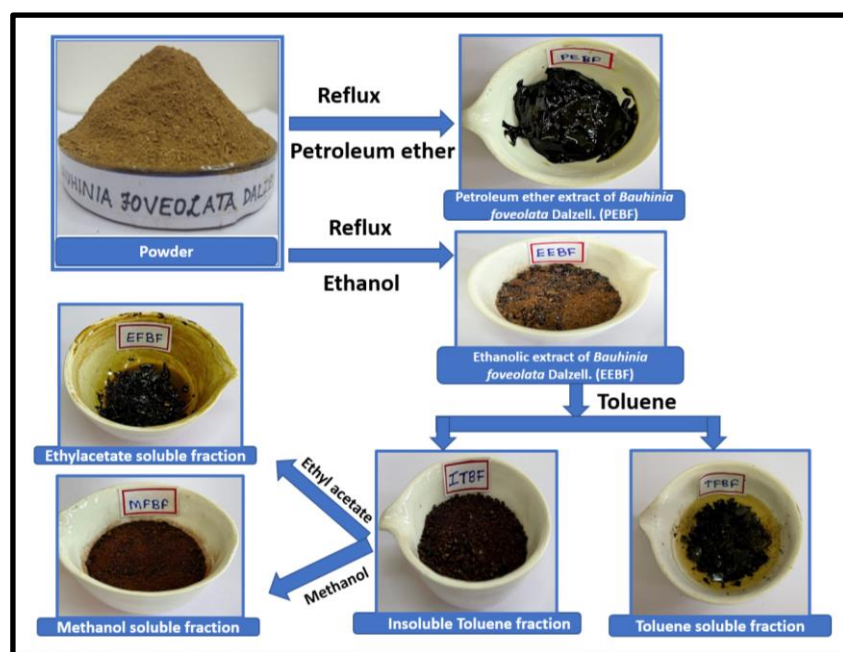


Figure 5.2: *Bauhinia foveolata* - Extraction and fractionation

5.2.3.1. Test for Alkaloids

5.2.3.1.1. Dragendroff's test

To 2 mg of the extract/biofraction, 5 mL of distilled water and 2 M HCl were added until an acid reaction occurred. To this, 1 mL of Dragendroff's reagent was added. The formation of orange - red precipitate indicated the presence of alkaloids.

5.2.3.1.2. Mayer's Test

To 2 mg of the extract/biofraction, a few drops of Mayer's reagent were added. A cream precipitate indicated the presence of alkaloids.

5.2.3.1.3. Wagner's Test

To 2 mg of the extract/biofraction, 1 mL of dilute HCl and two drops of Wagner's reagent were added. A reddish brown precipitate indicated the presence of alkaloids.

5.2.3.1.4. Hager's Test

To 2 mg of the extract/biofraction, a few drops of Hager's reagent were added. A yellow precipitate indicated the presence of alkaloids.

5.2.3.2. Tests for Glycosides

5.2.3.2.1. Test for cardiac glycosides

-

- Baljet's Test: The extract/biofraction was treated with picric acid. An orange colour indicated the presence of cardiac glycosides.
- Legal's Test: 1 mL of pyridine and 1 mL of sodium nitroprusside were added to the extract/biofraction. A pink-red colour indicated the presence of cardiac glycosides.

- Keller- Killiani Test: To 2 mL of extract/biofraction, 2 mL of glacial acetic acid, one drop of 5 % FeCl_3 and 1 mL of conc. H_2SO_4 were added. A brown ring at the interface is characteristic of cardenolide deoxysugar. The appearance of violet ring below the brown ring and greenish ring in acetic acid layer indicated the presence of cardiac glycosides.

5.2.3.2.2. Test for Anthraquinone glycosides

- Borntrager's test for O- glycosides

To 3 mL of extract/biofraction, 5 mL of 5 % dilute H_2SO_4 was added. It was boiled and filtered. An equal volume of chloroform was added and shaken. The organic solvent was separated, and then ammonia was added. A pink or red colour in the ammonical layer indicated the presence of anthraquinone glycosides.

- Modified Borntrager's test for C- glycosides

To 3 mL of extract/biofraction, 5 mL of 5 % dilute HCl and few drops of FeCl_3 were added. It was then heated in a boiling water bath for 5 min and cooled. An equal volume of chloroform was added. It was shaken well. The organic solvent was separated, and ammonia was added. A pink or red colour in the ammonical layer indicated the presence of C-glycosides.

5.2.3.2.3. Test for Coumarin glycosides.

- Fluorescence test

The extract/biofraction was moistened and taken in a test tube. The tube was covered with filter paper, soaked in dilute NaOH , and kept in a water bath. Later the filter paper was exposed to UV light. The appearance of yellowish - green fluorescence indicated the presence of coumarin glycosides.

- FeCl₃ test

To the extract/biofraction, a few drops of alcoholic FeCl₃ solution were added. Formation of deep green colour, which turned yellow on the addition of conc. HNO₃ indicated the presence of coumarins.

5.2.3.3. Test for Saponins

5.2.3.3.1. Foam test (Froth formation test)

Water was added to 2 mL of the extract/biofraction and shaken vigorously. The appearance of persistent foam indicated the presence of saponins.

5.2.3.4. Tests for Carbohydrates

5.2.3.4.1. Molisch's Test (General Test)

To 2 mL of extract/biofraction, 2 drops of freshly prepared 20 % alcoholic solution of α -naphthol were added. 2 mL of conc. H₂SO₄ was added to form a layer below the mixture. The appearance of a red-violet ring which disappeared with the addition of an excess of alkali, indicated the presence of carbohydrates.

5.2.3.4.2. Test for reducing sugars

- Fehlings's Test

To 2 mL of extract/biofraction, 1 mL mixture of equal parts of Fehling's solution A and B were added, and it was boiled for a few min. The formation of red or brick-coloured precipitate indicated the presence of reducing sugar.

- Benedict's Test

To 0.5 mL of extract/biofraction, 5 mL of benedict's solution was added and boiled

for 5 min. The formation of brick red-coloured precipitate indicated the presence of carbohydrates.

5.2.3.5. Test for Flavanoids

5.2.3.5.1. Shinoda test

To 0.5 mL of extract/biofraction, 10 drops of dilute HCl and a piece of magnesium were added. The formation of pink, reddish or brown colour indicated the presence of flavonoids.

5.2.3.5.2. Lead acetate test

To 2 mg of extract/biofraction, 1 mL of lead acetate solution was added. A yellow precipitate indicated the presence of flavonoids.

5.2.3.5.3. Vanillin- hydrochloric acid test

To 2 mg of extract/biofraction, vanillin HCl was added. The formation of pink colour indicated the presence of flavonoids.

5.2.3.6. Test for Proteins

5.2.3.6.1. Biuret's test (General test)

To 1 mL of extract/biofraction, 5 - 8 drops of 10 % w/v NaOH solution were added, followed by 1 or 2 drops of 3 % w/v copper sulphate solution. The formation of pink colour indicated the presence of proteins.

5.2.3.6.2. Millon's test (For proteins)

1 mL of extract/biofraction was dissolved in 1 mL of distilled water, and 5-6 drops of Millon's reagent were added. The formation of a white precipitate, which turns red on heating, indicated the presence of proteins.

5.2.3.7. Test for Tannins and phenolic compounds

5.2.3.7.1. Lead acetate test

To 1-2 mL of extract/biofraction, add lead acetate solution. White precipitate indicated the presence of tannins and phenolic compounds.

5.2.3.7.2. Ferric chloride (FeCl₃) test

To 1-2 mL of extract/biofraction, a few drops of 5 % w/v FeCl₃ solution were added. The green colour indicated the presence of gallotannins, the blue colour indicated the presence of hydrolysable tannins, and while brown colour indicated the presence of pseudo tannins.

5.2.3.8. Test for Resins

1 mL of extract/biofraction was dissolved in acetone, and the solution was poured into distilled water. The formation of turbidity indicated the presence of resins.

5.2.3.9. Test for Steroids and Triterpenoids

5.2.3.9.1. Salkowski's test

2 mg of extract/biofraction was shaken with CHCl₃, and to the chloroform layer, H₂SO₄ was added slowly by the side of the test tube. The formation of red colour in the lower layer indicated the presence of steroids, and the formation of yellow colour in the lower layer indicated the presence of triterpenoids.

5.2.3.9.2. Lieberman - Burchard's test

2 mg of dry extract/biofraction was dissolved in acetic anhydride, heated to boiling, and cooled and then 1 mL of concentrated H₂SO₄ was added along the sides of the test tube. A brown ring was formed at the junction of 2 layers. The formation of a deep red colour in

the upper layer indicated the presence of triterpenoids, and the turning of the upper layer to green indicated the presence of steroids.

5.2.3.10. Test for Starch

0.01 g of Iodine and 0.075 g of potassium iodide were dissolved in 5 mL of distilled water, and 2 - 3 mL of extract/biofraction were added. A blue colour indicated the presence of starch.

5.2.4. Quantitative Phytochemical Analysis

The extracts (EEHE, EEBF) and biofractions (TFHE, ITHE, EFHE, MFHE, TFBF, ITBF, EFBF, MFBF) were subjected to the determination of total phenolic content and total flavonoid content, with slight modifications to the referenced procedures.

5.2.4.1. Total Phenolic Content

The extracts and biofractions were analysed for their total content of phenolics using Folin ciocalteau method with slight modifications to the technique explained by Oliveira *et al.* ^[193] The intensity of blue colour formed due to the polyphenol content in different concentrations (10 - 1000 µg/mL) of extracts/biofractions was measured at 760 nm using UV-Vis spectrophotometer. Various concentrations (10 - 100 µg/mL) of gallic acid were used to plot the standard curve. The total phenolic content of the extracts and biofractions was stated as mg of GAE/g of samples.

5.2.4.2. Total Flavonoid content

The extracts and biofractions were assessed for their total content of flavonoids using the aluminium chloride colorimetry method as described by Meda *et al.* ^[194] Reactions of varying concentrations (10 - 1000 µg/mL) of experimental samples were analyzed at an absorbance of 415 nm using a UV-Vis spectrophotometer. The standard graph was plotted with a series of concentrations (10-100 µg/mL) of quercetin on the X-axis and absorbance

on the Y-axis. The total flavonoid content was estimated from the standard graph and expressed as mg of QUE/g of samples.

5.2.5. Determination of *in vitro* antioxidant activity

According to the procedures described below, the antioxidant activity of the extracts (EEHE, EEBF) and biofractions (TFHE, ITHE, EFHE, MFHE, TFHE, ITBF, EFHE, MFBF) was assessed using different *in vitro* free radical scavenging assays.

5.2.5.1. DPPH radical scavenging assay

The antioxidant activity of the extracts, biofractions and standard was studied using DPPH free radicals with slight modifications of the technique portrayed by Chanda *et al.*, Ghagane *et al.*, Chen *et al.* [195-197] The reaction mixture (3 mL) consists of 1 mL of DPPH in methanol (0.3 mM), 1 mL of varying concentrations of extracts/biofractions (10 - 1000 µg/mL) and standard ascorbic acid (2 - 20 µg/mL) solution separately and 1 mL of methanol. It was incubated for 30 min in the dark at RT, and then the absorbance was measured at 517 nm. The degree of DPPH purple decolorization to DPPH yellow indicated the scavenging efficiency of the extracts/biofractions. The lower absorbance of the reaction mixture indicated higher free radical-scavenging activity. The control reaction mixture consisted of 1 mL of ethanol with 1 mL of DPPH solution. The results were analyzed in triplicate.

The percentage of DPPH scavenged was calculated using the formula

$$\% \text{ DPPH scavenged} = \left[\frac{\text{Absorbance of control} - \text{Absorbance of sample}}{\text{Absorbance of control}} \right] \times 100$$

5.2.5.2. Hydrogen peroxide radical scavenging assay

Hydrogen peroxide free radicals were used to estimate the scavenging activity of the extracts, biofractions and standard by adopting the assays performed by Raju *et al.* with slight modifications. ^[198-199] To a series of test tubes, 0.3 mL of $\text{Fe}(\text{SO}_4)(\text{NH}_4)_2(\text{SO}_4)$ was added. Then 1.5 mL of different concentrations of the extracts/biofractions (10 - 100 $\mu\text{g}/\text{mL}$) or standard drug ascorbic acid (10 -100 $\mu\text{g}/\text{mL}$) was added and mixed. Hydrogen peroxide at a concentration of 5 mM, 0.1mL was added and subsequently incubated at RT in the dark for 5 min. After incubation, 1.5 mL of 1,10-phenanthroline (1mM) was added to each tube, mixed well and incubated for 15 min at RT. Finally, absorbance was measured at 510 nm using a UV-Vis spectrophotometer.

Hydrogen Peroxide radical scavenging activity was calculated using the formula

$$\% \text{H}_2\text{O}_2 \text{ scavenged} = \left[\frac{\text{Absorbance of sample}}{\text{Absorbance of control}} \right] \times 100$$

5.2.5.3. Nitric Oxide Radical Scavenging (NO) Assay

The assay evaluated the ability of the extracts and biofractions to scavenge the nitric oxide free radicals generated by sodium nitroprusside and measured by the Griess reaction against the standard Ascorbic acid. This assay was performed in accordance with the procedures described by Green *et al.* with slight modifications. ^[200-202] To a series of test tubes, 1 mL of sodium nitroprusside solution was added. Then 1 mL of different concentrations of extracts/biofractions were added and mixed. The test tubes were incubated in the dark for 150 min at RT. 2 mL of Griess reagent was added to all the test tubes and again incubated in the dark for 20 min at RT. A UV-Vis spectrophotometer was used to determine the absorbance at 540 nm.

Nitric oxide free radical scavenging activity was calculated using the formula

$$\% \text{ Nitric oxide scavenged} = \left[\frac{\text{Absorbance of control} - \text{Absorbance of sample}}{\text{Absorbance of control}} \right] \times 100$$

5.2.5.4. ABTS Radical Scavenging Assay

The ABTS free radical was produced using ABTS radical cation decolorization assay, by treating 10 mg of ABTS with 2 mg potassium persulfate in water, and the ability of the extracts and biofractions to scavenge these free radicals as against the standard ascorbic acid was determined using the methods described by Seena *et al.*, Prior *et al.* and Salama *et al.* with slight modifications. [203-205] The ABTS solution was kept in the dark at RT for approximately 12-16 h before use. Then, 1 mL of ABTS solution was diluted with 60 mL of methanol. Briefly, one mL of this solution was mixed with the same volume of different concentrations (100, 50, 25, 12.5, 6.25, 3.125 µg/mL) of the extracts/biofractions and standard ascorbic acid solution separately. The mixture was incubated for 30 min in the dark at RT, and the absorbance was measured at 734 nm.

The percentage of ABTS free radical scavenged was calculated using the formula

$$\% \text{ ABTS scavenged} = \left[\frac{\text{Absorbance of control} - \text{Absorbance of sample}}{\text{Absorbance of control}} \right] \times 100$$

5.2.6. Determination of *in vitro* anticancer activity of extracts and biofractions

The *in vitro* anticancer activity of the extracts (EEHE, EEBF) and biofractions (TFHE, ITHE, EFHE, MFHE, TFBF, ITBF, EFBF, MFBF) was determined using various methods as described below.

5.2.6.1. Antiproliferative assessment

The antiproliferative activity of the extracts and biofractions were determined against Hop-62, HeLa, MCF-7 cell lines using SRB assay, following the technique employed by Keepers *et al.* and Vichai *et al.* [206, 207] The cell lines were grown in RPMI 1640 medium containing 10 % fetal bovine serum and 2 mM L-glutamine. Cells were inoculated into 96-well microtiter plates in 100 μ L at plating densities of 1×10^3 cells/well and incubated at 37 °C, 5 % CO₂, 95 % air and 100 % relative humidity for 24 h prior to the addition of experimental samples or standard drug Doxorubicin.

The extracts/biofractions and standard drugs were initially solubilized in dimethyl sulfoxide at 100 mg/mL, diluted to 1 mg/mL with water, and stored frozen before use. An aliquot of the frozen concentrate (1 mg/mL) was thawed and diluted to 100 μ g/mL, 200 μ g/mL, 400 μ g/mL and 800 μ g/mL with a complete medium containing test article. Aliquots of 10 μ L of these different drug dilutions were added to the appropriate microtiter wells already containing 90 μ L of the medium, resulting in the required final drug concentrations, i.e. 10 μ g/mL, 20 μ g/mL, 40 μ g/mL and 80 μ g/mL. The plates were then incubated at standard conditions for 48 h, and the assay was terminated by adding cold Trichloroacetic acid (TCA). Cells were fixed *in situ* by gently adding 50 μ L of cold 30 % (w/v) TCA (final concentration, 10 % TCA) and incubated for 60 min at 4 °C. The supernatant was discarded; the plates were washed five times with tap water and air-dried. Sulforhodamine B (SRB) solution (50 μ L) at 0.4 % (w/v) in 1 % acetic acid was added to each of the wells, and plates were incubated for 20 min at RT. After staining, the unbound dye was recovered, and the residual dye was removed by washing it five times with 1% acetic acid. The plates were air-dried. The bound stain was subsequently eluted with 10 mM trizma base, and the absorbance was measured on a plate reader at a wavelength of 540 nm. Percent cell growth was calculated plate-by-plate for test wells relative to control wells.

$$\text{Percent cell growth} = \left[\frac{\text{Average absorbance of the test well}}{\text{Average absorbance of the control well}} \right] \times 100$$

$$\text{Percent growth inhibition} = 100 - \text{Percent cell growth}$$

The effect of extracts and biofractions on normal cell lines were also evaluated using SRB assay at a concentration between 12.5 µg/mL - 100 µg/mL.

5.2.6.2. Apoptosis assay by flow cytometry

The extract and biofractions exhibiting substantial antiproliferative activity were subjected to apoptosis assay at their GI₅₀ concentrations to evaluate their possible mode of action as per the procedure described by Bhagwat *et al.* and analysed by flow cytometry using FlowJo X 10.0.7 software (2).^[208] Cells were seeded in a 6-well flat bottom microplate and incubated at 37 °C with 5% CO₂, 95% air, and 100 % relative humidity for 24 h. The GI₅₀ concentrations of each sample were treated and maintained at 37 °C in a CO₂ incubator for 24 h. After incubation, cells were washed with phosphate buffer saline and centrifuged (500 x g) for 5 min at 4 °C. The supernatant was washed off, and cell pellets were resuspended in ice-cold binding buffer (1 x 10⁶ per mL). 5 µl of AbFlour™ 488 Annexin V and 2 µL PI were added, mixed gently, and incubated on ice for 15 min in the dark. The cell preparations were treated with 400 µL of ice-cold 1X binding buffer, mixed gently, and analysed by flow cytometry.

5.2.6.3. Cell cycle analysis by flow cytometry

The potential of the extract, biofractions and isolated compounds to induce cell cycle arrest was studied using cell cycle assay as per the method described by Pozarowski *et al.* and analysed by flow cytometry using FlowJo X 10.0.7 software.^[209] The cells were seeded in a 24-well flat-bottom microplate containing coverslips and maintained at 5 % CO₂, 95% air, and 100% relative humidity for 24 h. The cells were treated with GI₅₀

concentrations of the samples and incubated for 12 h. Post incubation, the plate was washed with PBS and centrifuged (200 x g) for 5 min at 4 °C. The supernatant was removed, cell pellets (1×10^5 cells) were resuspended in 0.5 mL PBS, 4.5 mL of ice-cold 70 % ethanol was added, and cells were fixed for 2 h on ice. The ethanol-suspended cells were centrifuged for 5 min (200 x g) at 4 °C. The supernatant ethanol was decanted, and cell pellets were suspended in 5 mL PBS and centrifuged (200 x g) for 5 min at 4 °C. The supernatant was decanted, and cell pellets were resuspended in 1 mL propidium iodide staining solution for 15 min at 37 °C and analysed by flow cytometry.

5.2.7. Acute toxicity studies

5.2.7.1. Acute toxicity study of ethanolic extract of *H. enneaspermus* (EEHE)

The acute toxicity study on EEHE was carried out up to 5000 mg/Kg BW, as reported by Patel *et al.* [65]

5.2.7.2. Acute toxicity study of ethanolic extract of *B. foveolata* (EEBF) [210]

The study on EEBF was carried out up to 5000 mg/Kg under protocol No. IAEC-SLS-2021-037 at Skanda Life Sciences Pvt Ltd, as per OECD guidelines 423.

5.2.7.3. Procurement of animals and ethics approval for acute toxicity studies

Sprague Dawley female rats (weighing 190 ± 20 g) from Skanda Life Sciences, Bidadi, Ramanagar, India, were used for the study. The study was certified by the Institutional Animal Ethics Committee of Skanda Life Sciences organisation (IAEC-SLS-2021-037). The animals were housed in Perspex cages and maintained under controlled animal house conditions (21 ± 1 °C temperature and 50 % - 60 % Relative humidity with 12 h : 12 h light and dark illumination cycle). The animals were fed with a commercial rat maintenance diet from Amrut laboratory animal feed manufactured by Krishna Valley Agro Tech (KVAT), Sangli and provided with purified drinking water *ad libitum*. The grouping of animals was done on the last day of the acclimatisation period by BW stratification and

randomisation method. The study was performed in compliance with the guidelines of the CPCSEA, Government of India.

5.2.7.4. Experimental design

Animals were distributed into four groups based on the individual animal body weight.

Table 5.1: Experimental design for acute toxicity activity.

Group No.	Groups (n = 6)	Route
	Treatment Dose (mg/kg BW)	
I	Normal saline	Oral
II	EEBF 50	Oral
III	EEBF 300	Oral
IV	EEBF 2000	Oral
V	EEBF 5000	Oral

5.2.7.5. Procedure

After the acclimatisation period, the animals were equally distributed into 4 groups of 3 animals per group. Animals were fasted overnight (12 h) prior to dosing (feed but not water was withheld). The test item was administered orally to groups II, III, IV and V animals on Day 1 of the study at 50 mg/kg, 300 mg/kg, 2000 mg/kg and 5000 mg/kg BW, respectively. Group I animals were treated as control and were administered with vehicle only. After dosing, animals were monitored individually for the first 30 min and then periodically for the first 24 hours.

5.2.8. *In vivo antianxiety activity*

5.2.8.1. *Procurement of animals and ethics approval for efficacy studies*

Wistar albino rats (weighing 200 ± 20 g) of either sex, purchased from the National Institute of Biosciences, Pune (CPCSEA Reg No.: 1091/GO/Bt/07/CPCSEA), India, were used for the efficacy studies to evaluate anxiolytic activity.

The efficacy study was approved by the Institutional Animal Ethics Committee of Goa College of Pharmacy, Panaji-Goa (CPCSEA/IAEC/2020/08). The animals were housed in Perspex cages and maintained under controlled animal house conditions (25 ± 2 °C temperature and 50 % - 60 % Relative humidity with 12 h: 12 h light and dark illumination cycle). Prior to the trial, the rats were acclimatised to the laboratory conditions for a week. The trials were performed in compliance with the guidelines of the CPCSEA, Government of India.

5.2.8.2. *Experimental design*

To investigate the anxiolytic-like effects of EEHE, ITHE, EEBF, and ITBF, the rats were divided into groups ($n = 6$) as tabulated in Table 5.2 and treated with three doses of the extracts and biofractions at 100 mg/kg, 200 mg/kg, and 400 mg/kg BW for 30 days. The vehicle control group received 1% Tween 80, and the standard group received 2 mg/kg diazepam.

The groups of rats were subjected to individual isolation for 2 h each day, during a five-week trial period. The rats were dosed with the respective drug, vehicle control or standard treatments 1 h before exposure to the behavioural paradigm models.

Table 5.2: Experimental design for antianxiety activity.

Group. No.	Groups (n = 6) Treatment Dose		Route
I	Control (1 % tween 80)		Oral
II	Positive Control Diazepam (2 mg/Kg)		<i>i.p.</i>
III - V	EEBF (mg/Kg BW)	100	Oral
		200	
		400	
VI - VIII	ITBF (mg/Kg BW)	100	Oral
		200	
		400	
IX - XI	EEHE (mg/Kg BW)	100	Oral
		200	
		400	
XII - XIV	ITHE (mg/Kg BW)	100	Oral
		200	
		400	

After dosing and isolation, the groups of rats were exposed to each apparatus once during each week in a chronological sequence (Elevated Plus Maze apparatus, Light and Dark apparatus, Mirror chamber apparatus, Holeboard apparatus and Optovarimex) to screen for potential anxiolytic activity. The activity was performed through the first week (T1), second week (T2), third week (T3), fourth week (T4) and fifth week (T5) during the 30 - day trial.

5.2.8.3. Screening models to evaluate anxiolytic behaviour

The behavioural parameters monitored using the various screening models were as follows

5.2.8.3.1. Elevated plus maze Test (EPM)

- Number of open arm entries (NOE)
- Percent time spent in open arm (PTSO)

5.2.8.3.2. Light and dark transition Test (LDT)

- Number of light box entries (NLE)
- Percent time spent in light box (PTSL)

5.2.8.3.3. Mirror chamber Test (MCT)

- Number of mirrored chamber entries (NME)
- Percent time spent in the mirrored chamber (PTSM)

5.2.8.3.4. Holeboard Test (HBT)

- Number of head dips (Nos.)

5.2.8.3.5. Optovarimex (OPV)/Autotrack Test

- Distance Travelled (cm)
- Ambulatory Time (s)

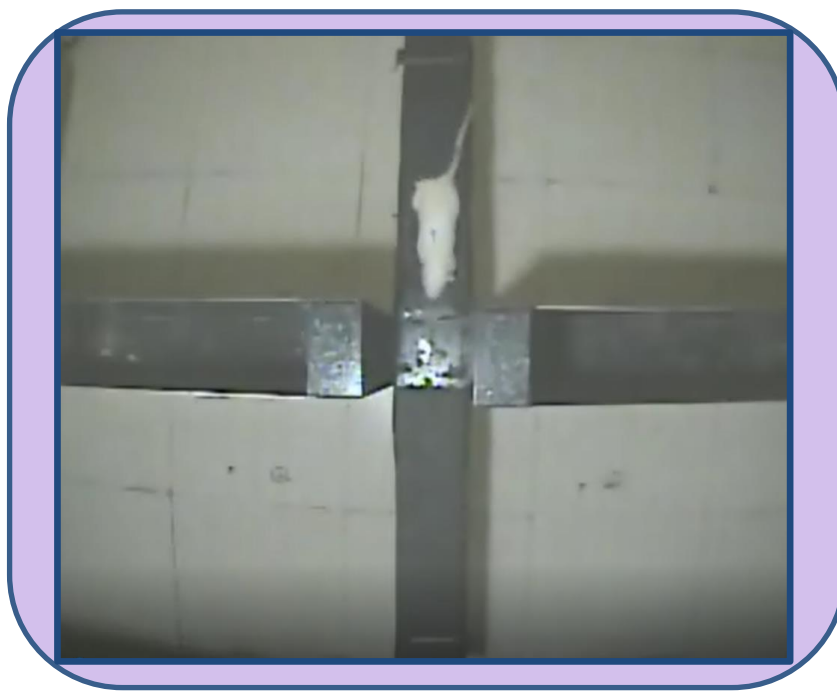


Figure 5.3: Elevated Plus Maze apparatus.



Figure 5.4: Light and Dark apparatus.



Figure 5.5: Mirror chamber apparatus

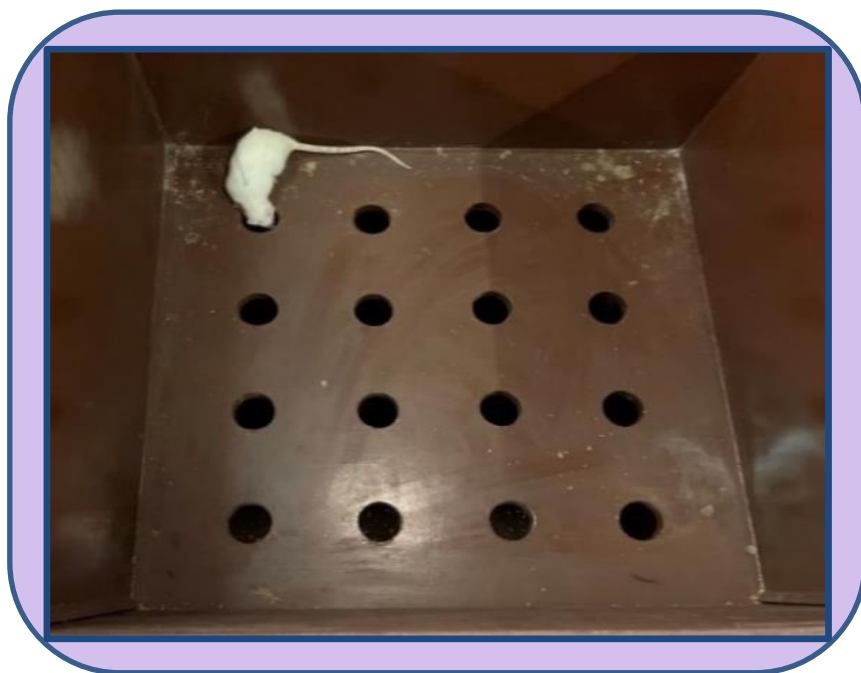


Figure 5.6: Holeboard apparatus.



Figure 5.7: Optovarimex (Autotrack) apparatus.



Figure 5.8: Isolation of rats in individual cages.

5.2.8.3.1. Elevated Plus Maze (EPM) test

Behaviour in the EPM is used as a means for assessing exploratory, anxious, and motor behaviours. The preference of the rats to open arms was studied using the elevated plus maze (EPM) test. The increased open arm entries and time spent in open arm were considered as indices for anxiolytic potential as per the method explained by Sinnathambi *et al.* [211] The EPM consists of four arms, two open ($30 \times 5 \text{ cm}^2$) and two closed ($30 \times 5 \text{ cm}^2$), arranged in such a way that the two arms of each type are opposite to each other. The maze is elevated 50 cm above the floor. The walls of the closed arms are 50 cm in height. The rat was positioned at the centre of the EPM, confronting one of the enclosed arms during each test. During a 5 min test period, the number of entries and time spent in open and enclosed arms were recorded, and analyses were carried out using Smart Version 3.0.02 Panlab Havard Apparatus software. The percentage of open-arm entries and percent time spent in open arms were calculated as indices of anxiolytic activity.

5.2.8.3.2. Light and dark transition test

The preference of the rats for the lightbox arena was assessed using the light and dark transition test, to evaluate the number of lightbox entries and time spent in the light box as per the procedure described by Guillen-Ruiz *et al.* [212] The light and dark apparatus consisted of a box ($80 \text{ cm} \times 40 \text{ cm}$ base with 40 cm high walls). The box consisted of two equal chambers ($40 \text{ cm} \times 40 \text{ cm} \times 40 \text{ cm}$) that were connected by a central doorway ($10 \text{ cm} \times 10 \text{ cm}$) that allowed the rats to freely cross from one chamber to the other. The light compartment was completely white in colour and illuminated by a 40-watt white light. The dark compartment was completely black and not illuminated. On the test day, the rats were individually placed in the dark compartment facing the doorway. During a 5 min test period, the activity was recorded, and analyses were carried out using Smart Version 3.0.02 Panlab Havard Apparatus software. The number of entries into the light compartment and time (s) spent in the light compartment were selected as reliable indices of anxiolytic activity.

5.2.8.3.3. Mirror chamber test

The preference of rats for the mirror chamber area was assessed using the mirror chamber test, to evaluate the increased mirror chamber entries and time spent in the mirror chamber as per the procedure depicted by Walf *et al.* and Paterson *et al.* ^[213,214] The mirror-chambered apparatus consisted of an open field chamber (76 cm × 57 cm × 35 cm) with four mirrored walls and one mirrored floor that were connected to a non-mirrored alleyway (57 cm × 12 cm × 35 cm) using modified methods. The activity was recorded during a 5 min test period, and analyses were carried out using Smart Version 3.0.02 Panlab Havard Apparatus software. The number of mirrored chamber entries and the time spent by the rats in the mirrored part of the chamber during the 5 min test were selected as indices to measure anti-anxiety behaviour.

5.2.8.3.4. Hole board test

The anxiolytic potential of the extracts and biofractions was assessed by evaluating the number of head dips using the hole-board apparatus as per the method expressed by Brown *et al.* ^[215] The hole-board apparatus comprised of a wooden box measuring 68 cm × 68 cm. The walls were 40 cm high, and the box was raised 28 cm above the ground. Four holes (4 cm in diameter) were cut into the floor of the apparatus; each hole was 28 cm from a corner of the box along the diagonal from the corner to the centre. Each rat was placed at the centre of the apparatus, and the number of head dips was monitored, which was taken as an index of anxiolytic activity. During a 5 min test period, the activity was recorded, and analyses were carried out using Smart Version 3.0.02 Panlab Havard Apparatus software.

5.2.8.3.5. Open field - Optovarimex (Autotrack) test

The locomotor behaviour of the rats was measured based on distance travelled (cm), ambulatory time (s), etc., using optovarimex apparatus that could be associated with potential anxiolytic activity as per the procedure described by Vogel and Kulkarni. ^[216,217]

The apparatus consisted of a central chamber (plexiglass cage, 44 cm length × 33 cm width × 20 cm height) with light sources and photocells at the base of two opposite walls. The light of each source is focused on a photocell. Any interruption in the path of light activates the photocells, and a count is measured as the horizontal locomotor activity of the rats kept in the chamber. The activity was recorded during a 5 min test period, and analyses were carried out using optovarimex software. The locomotor activity can be measured based on distance travelled (cm), ambulatory time etc. and can be associated with anxiolytic activity.

5.2.9. Biochemical estimations in rats' brain homogenates

5.2.9.1. Removal, isolation, and homogenization of brain regions

After the 30 - day behavioural examination, the rats were euthanized immediately by cervical dislocation. The brain was removed quickly and dropped in ice-cold saline on a petri plate. The brain was dissected, and the cerebral cortex, hippocampus, cerebellum, pons and medulla oblongata and the remaining brain tissues were individually weighed and homogenized in ice-cold Phosphate buffer saline (PBS) and preserved at - 80 °C until analysis.^[218]

5.2.9.2. Preparation of rat brain tissue homogenates

After brain isolation, the tissues were rinsed in ice-cold PBS to eliminate the excess blood and weighed before homogenization. These were then minced into small pieces and homogenized in fresh lysis buffer and with a microtissue grinder on ice. An ultrasonic cell disrupter was used to sonicate the resulting suspension till the solution was clarified. The homogenates were centrifuged (8000 × g) for 10 min. The supernatant was collected, and aliquots were prepared and stored at ≤ -20 °C.

5.2.9.3. Estimation of antioxidant enzymes

Antioxidant enzymes levels in the rat brain homogenates were estimated by using commercially available Bioelsa kits dedicated for rats, *viz.* rat catalase (Product No HR1E6097), rat glutathione peroxidase (Product No HR1E3333), rat superoxide dismutase (Product No HR1E9289), rat glutathione s transferase (Product No HR1E0403) and rat glutathione reductase (Product No EELR11277).

All reagents and samples were equilibrated to RT before use. The wells for the diluted standard, blank and sample were determined. 100 µL of standard/ test sample was added into the appropriate wells and covered with a plate sealer, and incubated for 80 min at 37 °C. After incubation, the liquid from each well was removed, aspirated and washed with 200 µL of wash buffer thrice to remove the solution completely by snapping the plate onto absorbent paper. The remaining wash buffer was aspirated, and the plate was inverted and blotted against absorbent paper. 100 µL of biotinylated antibody was added to each well, covered with the plate sealer and incubated for 50 min at 37 °C. Post incubation, the plate was thoroughly washed thrice with wash buffer, and 100 µL of Streptavidin-HRP was added to each well, sealed and incubated for 50 min at 37 °C. After 50 min, the plate was removed, washed 5 times and dried. 90 µL of TMB substrate solution was added to each well to give a blue colour, covered and incubated for 20 min at 37 °C, protected from light. The stop reagent (50 µL) was added to each well and mixed well, turning the liquid yellow. The plate was read using a microplate reader at 450 nm immediately.

5.2.9.4. Estimation of neurotransmitters

Neurotransmitter levels in the rat brain homogenates were estimated by using commercially available Bioelsa kits dedicated for rats *viz.* Noradrenaline (Product No HR1E9067), rat Dopamine (Product No HR1E9064), rat serotonin (5-Hydroxytryptamine) (Product No HR1E9065), rat GABA (Gamma-Aminobutyric acid) (Product No HR1E0278) and rat glutamic acid (Product No HR1E9345).

All reagents and samples were equilibrated to RT before use. The wells for the diluted standard, blank and sample were determined. 50 μL of standard/ test sample and 50 μL of Biotinylated - Conjugate (1x) were added into each appropriate well, covered with a plate sealer and incubated (at 37 °C) for 60 min. After incubation, the liquid from each well was removed, aspirated and washed with 200 μL of wash buffer thrice to remove the solution completely by snapping the plate onto absorbent paper. The remaining wash buffer was aspirated, and the plate was inverted and blotted against absorbent paper. 100 μL of Streptavidin-HRP (1x) antibody was added to each well, covered with the plate sealer and incubated (at 37 °C) for 60 min. After incubation, the plate was removed, washed 5 times and dried. 90 μL of TMB substrate solution was added to each well to give a blue colour, covered and incubated for 20 min at 37 °C, protected from light. The stop reagent (50 μL) was added to each well and mixed thoroughly, changing the colour from blue to yellow. The plate was read using a microplate reader at 450 nm immediately.

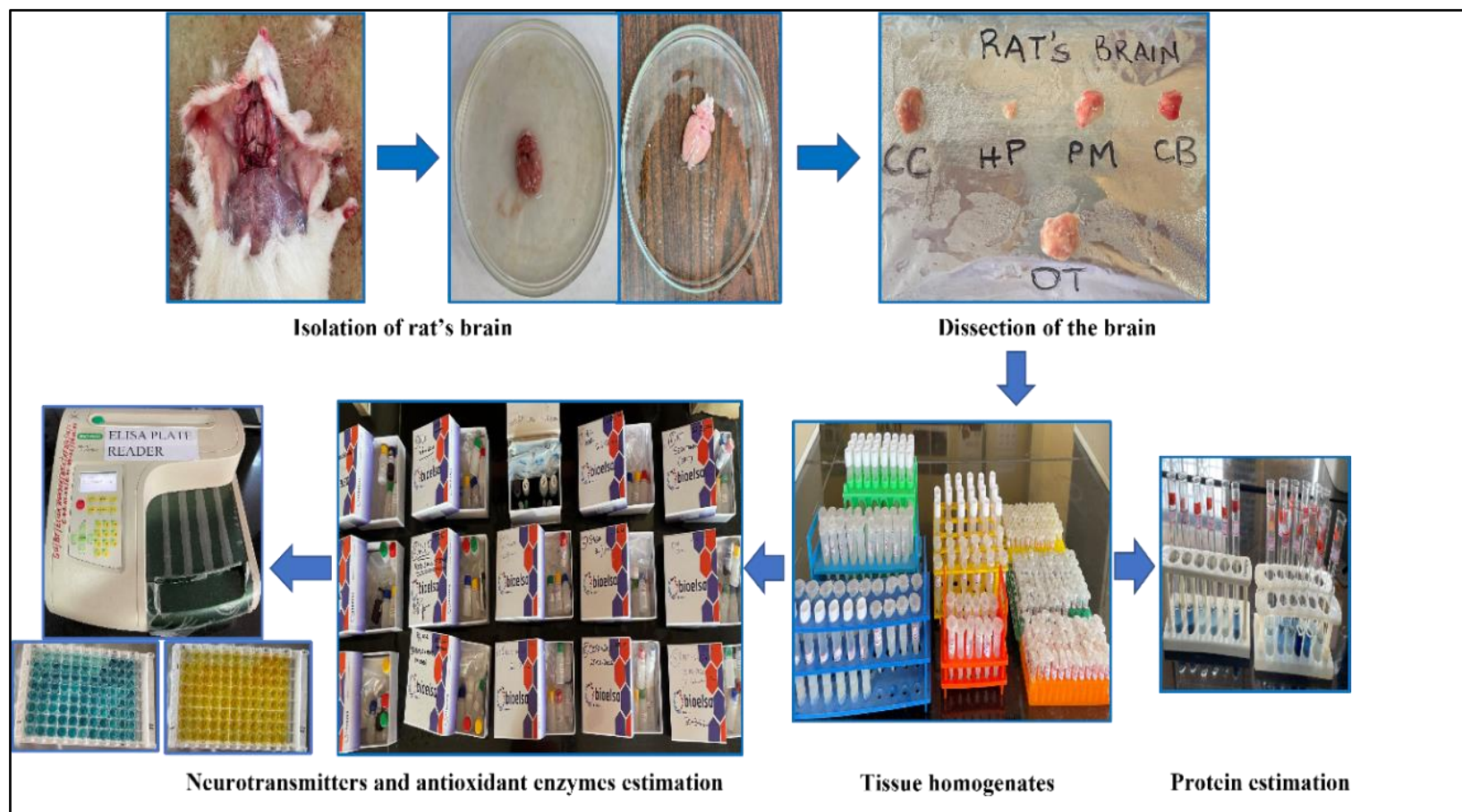


Figure 5.9: Biochemical estimation of antioxidant enzymes and neurotransmitters in rats' brain.

5.2.10. Isolation of Phytoconstituents

5.2.10.1. Isolation of phytoconstituents from ITHE ^[189, 219]

5.2.10.1.1. Thin layer chromatographic studies of ITHE

Thin layer chromatography (TLC) is a very effective technique for separating and identifying chemical constituents in mixtures. The separation of compounds between two phases is based on differences in the affinity of compounds in the two phases. Components are separated by the differential migration of solute between two phases—a stationary phase and a mobile phase. Depending on the stationary phase and using different solvents, separation can be achieved based on the partition or a combination of partition and adsorption. ITHE was subjected to TLC studies as listed in Table 5.3.

Table 5.3: Optimisation of solvent system for separation of ITHE phytoconstituents.

Sample preparation	1mg of extract was dissolved in 1 mL of ethanol.	
Stationary Phase	Silica gel GF ₂₅₄ for TLC	
Detection	Ultraviolet (254 and 366 nm)	
	Anisaldehyde sulphuric acid and alcoholic ferric chloride	
Solvent systems tried	Dichloromethane: Methanol	9.5:0.5, 9.3:0.7, 9:1, 8:2
	Butanol: Acetic acid: water	3:1:6
	Ethyl acetate: Formic acid: Acetic acid: Water	100:11:11:13.5
	Butanol: Methanol: Water	6:3:1, 7:2:1, 8:1:1
Optimised solvent system	Butanol: Methanol: Water	8:1:1

5.2.10.1.2. Column chromatography of ITHE

15 g of ITHE was dissolved in 30 mL of ethanol and mixed with 30 g of silica (#60-120) in a mortar. The resultant mixture was stirred continuously by keeping the porcelain dish in the water bath. The column was previously washed and rinsed with acetone. The

length of the column was 3 feet with an outer diameter of 5 inches. A wet packing method was used to pack the column. Glass wool was affixed at the bottom, and the column was filled with 500 mL ethyl acetate. The sample was then placed onto the column packed with 200 g of silica (60-120) and prepared in 500 mL of ethyl acetate. The column was subjected to elutions with various solvent mixtures with increasing order of polarity of ethyl acetate and methanol, starting first with ethyl acetate (100 %) and then ethyl acetate: methanol graded mixture (99:1, 98:2, 97:3, 96:4, 95:5, 94:6, 93:7, 92:8, 91:9, 90:10, 80:20, 70:30, 60:40, 50:50). The sample was finally eluted with 100 % methanol. Each time 10 mL of the elutes were collected and monitored by TLC (Silica gel GF₂₅₄, visualised by UV 254 nm and sprayed with anisaldehyde). Identical elutes were combined and concentrated to dryness at RT. Elutions carried out with ethyl acetate: methanol graded mixture (90:10, 80:20 and 70:30) resulted in an identical mixture of spots as monitored on TLC. After removing the solvent, a brown-coloured fraction (LMH) was obtained. LMH was further subjected to purification by preparative HPLC.

5.2.10.1.3. Purification of column fraction LMH by Preparative HPLC

The instrumental parameters and elution programme for the purification process are listed in Tables 5.4 and 5.5.

Table 5.4 : Instrumental conditions for purification of LMH by Preparative HPLC.

Sample preparation	150 mg of LMH was dissolved in HPLC grade methanol, filtered through millipore, and 500 μ L was injected each time. The process was repeated to obtain sufficient yield for the structural elucidation of the compounds.
Mobile Phase-A	0.1 % Formic acid in water
Mobile Phase-B	Methanol
Column	Capcell Pak C18, 250 x 10 mm ID, 5 μ Particle size
Detector	W 2998 Photo Diode Array detector
Elution	Gradient mode

Table 5.5: Gradient elution programme for purification of LMH by Preparative HPLC.

Time (min)	Flow (mL/min)	% A	% B
Initial	4.0	90.0	10.0
5.0	4.0	90.0	10.0
30.0	4.0	20.0	80.0
60.0	4.0	20.0	80.0
65.0	4.0	90.0	10.0
80.0	4.0	90.0	10.0

5.2.10.1.4. Spectral analysis of the isolated compounds

The isolated compounds of ITHE were subjected to IR, ¹H-NMR, ¹³C-NMR and LCMS spectral analysis.

5.2.10.2. Isolation of phytoconstituents from MFBF ^[189, 219]

5.2.10.2.1. Thin layer chromatographic studies of MFBF

Methanolic fraction of the ethanolic extract of *Bauhinia foveolata* Dalzell. (MFBF) was subjected to TLC studies as listed in Table 5.6.

Table 5.6: Optimisation of solvent system for separation of phytoconstituents in MFBF.

Sample preparation	1mg of extract was dissolved in 1 mL of ethanol.	
Stationary Phase	Silica gel GF ₂₅₄ for TLC	
Detection	Ultraviolet (254 and 366 nm)	
	Anisaldehyde sulphuric acid and alcoholic ferric chloride	
Solvent systems tried	Dichloromethane: Methanol	9.5:0.5, 9.3:0.7, 9:1, 8:2
	Butanol: Acetic acid: water	3:1:6
	Ethyl acetate: Formic acid: Acetic acid: Water	100:11:11:13.5
	Butanol: Methanol: Water	6:3:1, 7:2:1, 8:1:1
Optimised solvent system	Butanol: Methanol: Water	8:1:1

5.2.10.2.2. Column chromatography of MFBF

20 g of MFBF was dissolved in 40 mL of ethanol and mixed with 40 g of silica gel (#60-120) in a mortar. The resultant mixture was stirred continuously by keeping the porcelain dish in the water bath. The column was previously washed and rinsed with acetone. The length of the column was 3 feet with an outer diameter of 5 inches. A wet packing method was used to pack the column. Glass wool was affixed at the bottom, and the column was filled with 500 mL ethyl acetate. The sample was then placed onto the column packed with 200 g of silica gel (60-120) and prepared in 500 mL of ethyl acetate. The column was subjected to elutions with various solvent mixtures with increasing order of polarity of ethyl acetate and methanol, starting first with ethyl acetate (100 %) and then

ethyl acetate: methanol graded mixture (99:1, 98:2, 97:3, 96:4, 95:5, 94:6, 93:7, 92:8, 91:9, 90:10, 80:20, 70:30, 60:40, 50:50). The sample was finally eluted with 100 % methanol. Each time 10 mL of the elutes were collected and monitored by TLC (Silica gel GF₂₅₄, visualized by UV 254 nm and sprayed with anisaldehyde). Identical elutes were combined and concentrated to dryness at RT.

Elutions carried out with ethyl acetate: methanol graded mixture (90:10, 80:20, 70:30 and 60:40) resulted in an identical mixture of spots as monitored on TLC and detected with UV 254 nm and spraying with ANS. After removing the solvent, a brown-coloured fraction (LMF) was obtained. LMF was further subjected to purification by preparative HPLC.

5.2.10.2.3. Purification of column fraction LMF by Preparative HPLC

The instrumental parameters and elution programme were recorded in Tables 5.7 and 5.8.

Table 5.7 : Instrumental conditions for purification of LMF by Preparative HPLC.

Sample preparation	150 mg of LMF was dissolved in HPLC grade methanol, filtered through millipore, and 500 μ L was injected each time. The process was repeated to obtain sufficient yield for the structural elucidation of the compounds.
Mobile Phase-A	0.1 % Trifluoroacetic acid in Water
Mobile Phase-B	Methanol
Column	Waters Spherisorb S5 ODS2, 10 x 250 mm Semi Prep Column
Detector	W 2998 Photo Diode Array detector
Elution	Gradient mode

Table 5.8: Gradient elution programme for purification of LMF by Preparative HPLC.

Time (min)	Flow (mL/min)	% A	% B
Initial	5.0	70.0	30.0
45.0	5.0	20.0	80.0
50.0	5.0	20.0	80.0
51.0	5.0	70.0	30.0
60.0	5.0	70.0	30.0

5.2.10.2.4. Spectral analysis of the isolated compounds:

The isolated compounds of MFBF were subjected to IR, ¹H-NMR, ¹³C-NMR and LCMS spectral analysis.

5.2.10.3. Isolation of phytoconstituents from EFBF ^[189, 219]

5.2.10.3.1. Thin layer chromatographic studies of EFBF

Ethylacetate fraction of the ethanolic extract of *Bauhinia foveolata* Dalzell. (EFBF) was subjected to TLC studies as listed in Table 5.9.

Table 5.9: Optimisation of solvent system for separation of phytoconstituents in EFBF.

Sample preparation	1 mg of extract was dissolved in 1 mL of ethanol.
Stationary Phase	Silica gel GF ₂₅₄ for TLC
Detection	Ultraviolet (254 and 366 nm)
	Anisaldehyde sulphuric acid and alcoholic ferric chloride

Solvent systems tried	Dichloromethane: Methanol	9.5:0.5, 9.3:0.7, 9:1, 8:2
	Butanol: Acetic acid: water	3:1:6
	Ethyl acetate: Formic acid: Acetic acid: Water	100:11:11:13.5
	Butanol: Methanol: Water	6:3:1, 7:2:1, 8:1:1
	Chloroform: Ethyl acetate	9:1, 8:2, 7:3, 6:4
Optimised solvent system	Chloroform: Ethyl acetate	8:2

5.2.10.3.2. Column chromatography of EFBF

10 g of EFBF was dissolved in 20 mL of ethanol and mixed with 20 g of silica gel (#60-120) in a mortar. The resultant mixture was stirred continuously by keeping the porcelain dish in the water bath. The column was washed and rinsed with acetone. A wet packing method was used to pack this column. Glass wool was affixed at the bottom, and the column was filled with 500 mL ethyl acetate. The sample was then placed onto the column packed with 200 g of silica gel (60-120) and prepared in 500 mL of ethyl acetate. The column was subjected to elutions with various solvent mixtures with increasing order of polarity of chloroform, ethyl acetate and methanol, starting with chloroform (100%), chloroform: ethyl acetate graded mixture (99:1, 98:2, 97:3, 96:4, 95:5, 94:6, 93:7, 92:8, 91:9, 90:10, 80:20, 70:30, 60:40, 50:50), ethyl acetate (100 %), ethyl acetate: methanol graded mixture (99:1, 98:2, 97:3, 96:4, 95:5, 94:6, 93:7, 92:8, 91:9, 90:10, 80:20, 70:30, 60:40, 50:50) and finally eluted with 100 % methanol. Each time 10 mL of the elutes were collected and monitored by TLC (Silica gel GF₂₅₄, visualized by UV 254 nm and sprayed with anisaldehyde). Identical elutes were combined and concentrated to dryness at RT. Elutions carried out with ethyl acetate: methanol graded mixture (95:05, 80:20 and 70:30) resulted in identical mixture of spots as monitored on TLC and detected with UV 254 nm and spraying with ANS. After eliminating the solvent, a brown-coloured fraction (LME) was obtained. LME was further subjected to purification by preparative HPLC.

5.2.10.3.3. Purification of column fraction LME by Preparative HPLC

The instrumental parameters and elution programme for the purification process are listed in Tables 5.10 and 5.11.

Table 5.10: Instrumental conditions for purification of LME by Preparative HPLC.

Sample preparation	150 mg of LME was dissolved in HPLC grade methanol, filtered through millipore, and 500 μ L was injected each time. The process was repeated to obtain sufficient yield for the structural elucidation of the compounds.
Mobile Phase-A	0.1 % Formic acid in water
Mobile Phase-B	Methanol
Column	Waters Spherisorb S5 ODS2, 10 x 250 mm Prep Column
Detector	W 2998 Photo Diode Array detector
Elution	Gradient mode

Table 5.11: Gradient elution programme for purification of LME by Preparative HPLC.

Time (min)	Flow (mL/min)	% A	% B
Initial	5.0	60.0	40.0
50.0	5.0	5.0	95.0
60.0	5.0	5.0	95.0
61.0	5.0	60.0	40.0
75.0	5.0	60.0	40.0

5.2.10.3.4. Spectral analysis of the isolated compounds:

The isolated compounds of EFBF were subjected to IR, $^1\text{H-NMR}$, $^{13}\text{C-NMR}$ and LCMS spectral analysis.

5.2.11. Determination of *in vitro* anticancer activity of isolated compounds

The *in vitro* anticancer activity of the isolated compounds from ITHE (LMH1, LMH2, LMH3), MFBF (LMF1, LMF2, LMF3 and LMF4) and EFBF (LME1) was determined using various methods as described below.

5.2.11.1. Antiproliferative assessment

The antiproliferative activity of the isolated compounds against MCF-7, Hop-62, and HeLa cell lines was evaluated by SRB assay following the technique employed by Keepers *et al.* and Vichai *et al.*, as listed in subsection 5.2.6.1. [206,207] The effect of the isolated compounds on normal cell lines were also evaluated using SRB assay at a concentration between 12.5 µg/mL - 100 µg/mL.

5.2.11.2. Apoptosis assay by flow cytometry

The isolated compounds were subjected to apoptosis analysis at their respective GI₅₀ concentrations to evaluate their possible mode of action as per the procedure described by Bhagwat *et al.* (listed in subsection 5.2.6.2.) and analysed by flow cytometry using FlowJo X 10.0.7 software. [208]

5.2.11.3. Cell cycle analysis by flow cytometry

The ability of the isolated compounds to induce cell cycle arrest was analysed using cell cycle assay as per the method described by Pozarowski P *et al.* (listed in subsection 5.2.6.3.) and analysed by flow cytometry using FlowJo X 10.0.7 software. [209]

5.2.11.4. *In vitro* caspase-3 analysis

The compounds LMH3 and LME1 isolated from *H. enneapermus* and *B. foveolata* respectively, exhibited significant apoptotic activity against MCF-7 and HeLa cell lines respectively. These were further analysed for *in vitro* caspase-3 expression upon treatment with GI₅₀ concentration of each compound as per the procedure depicted by Crowley *et al.* and analysed by flow cytometry using FlowJo X 10.0.7 software. [220] The cells were seeded

in a 6-well flat bottom microplate containing coverslips and maintained at 37 °C in a CO₂ incubator overnight. The IC₅₀ concentrations of each sample were treated at 24 h. Post incubation, the cells were rinsed with PBS twice and centrifuged (500 x g) for 5 min at 4 °C. The supernatant was discarded and resuspended in 2 % PFA for 20 min and subsequently washed with PBS. The tubes were centrifuged (300 x g) for 5 min at 25 °C. The supernatant was decanted and washed with PBS twice. BSA (0.5 %) was added in PBS and 20 µL anti-Caspase-3 antibody. This was mixed thoroughly and incubated in the dark at RT (25 °C) for 30 min. The cells were then washed with PBS, mixed and analysed within 30 min by flow cytometry. The analysis was done using FlowJo X 10.0.7 software.

5.2.11.5. *In vitro* DNA fragmentation analysis

Since LMH3 and LME1 demonstrated significant apoptotic activity, these were further analysed for *in vitro* DNA fragmentation analysis in MCF-7 and HeLa cell lines respectively. GI₅₀ concentration of each compound were treated as per the procedure described by Darzynkiewicz *et al.* and analysed by flow cytometry using FlowJo X 10.0.7 software. ^[221] The cells were seeded in a 6-well flat bottom microplate containing coverslips and maintained overnight at 37 °C in a CO₂ incubator. The IC₅₀ concentrations of each sample were treated at 24 h. Post incubation, the cells were washed with PBS twice and centrifuged (500 x g) for 5 min at 4 °C. The supernatant was discarded and resuspended in 2% PFA for 20 min. The cells were washed with PBS. Centrifuged for 5 min (300 x g) at 25 °C, the supernatant was decanted and washed with 1X wash buffer twice. The cells were resuspended in 50 µL of the DNA labeling solution, mixed thoroughly and incubated for 60 min at 25 °C in the dark and washed with rinsing buffer. The cell pellets were resuspended in 0.5 mL of the PI/RNase Staining buffer, incubated for 30 min at RT and analysed within 30 min by flow cytometry.

5.2.11.6. Gene expression studies

5.2.11.6.1. RNA extraction

The RNA extraction procedure was carried out as per the method described by Hummon *et al.* [222] Treated and untreated cells (Control) were collected (10^5 to 10^7 cells) in a microcentrifuge tube. 400 μ l of Trizol reagent was added, vortexed and incubated at RT for 5 min. 200 μ L of chloroform was added to the mixture, vortexed and incubated at RT for 5 min. This was centrifuged at 12000 rpm for 10 min, to separate the upper aqueous layer and isopropyl alcohol and was further incubated on ice for 10 min. It was centrifuged (12000 rpm) for 5 min at 4 °C, the supernatant was later discarded, and the sample was washed with 25 μ L of molecular grade water. RNA was freeze stored at - 80 °C until cDNA conversion.

5.2.11.6.2. cDNA conversion

The cDNA conversion was done using a Primescript RT reagent kit (Cat No. RR037A, Takara, Japan). The tubes were centrifuged and incubated at 37 °C for 15 min for the reverse transcription process, followed by 85 °C for 5 s for inactivation of reverse transcriptase with heat treatment and further stored at 4 °C.

5.2.11.6.3. Real-time Polymerase Chain Reaction

The real-time PCR was carried out by using TB GreenPremix Ex Taq II (Tli RNaseH Plus). β -actin was the reference gene (internal control), while Bcl-2, Bax and p53 were the target genes used.

β -actin primers:

Forward primer: 5'- GCCCTGGCACCCAGCACAAAT -3'

Reverse primer: 5'- GGAGGGGCCGGACTCGTCAT -3'

Bcl-2 primers:

Forward primer: 5'- TTTTCTCCTTCGGCGGG -3'

Reverse primer: 5'-GGTGGTCATTCAGGTAAGTGGC-3'

TP53 primers:

Forward primer: 5'-TGGATCCTCTTGCAGCAGCC-3'

Reverse primer: 5'-AACCCCTTGCCTTACCAGAA-3'

Bax primers:

Forward primer: 5'-GGTTGTCGCCCTTTTCTA-3'

Reverse primer: 5'-CGGAGGAAGTCCAATGTC-3'

The reaction mixture was prepared on ice and the tubes were centrifuged and placed in a Realplex Master cycler (Eppendorf, Germany). The following PCR conditions were set up in the master cycler. Initial denaturation started at 95 °C for three min, followed by 40 cycles of 95 °C for 20 s, 60 °C for 20 s, and 72 °C for 30 s. Finally, a melting curve (dissociation curve) was performed from 60 °C to 95 °C for 20 min. A positive reaction was detected by strengthening a fluorescent signal in the form of an amplification plot obtained using the Realplex software. The number of cycles needed for the fluorescent signal to pass the threshold is known as the Ct (cycle threshold) (i.e. exceeds the background level). The amount of target nucleic acid in the sample is inversely correlated with the Ct values (i.e. the lower the Ct level, the greater the amount of target nucleic acid in the sample). Ct values were obtained for the reference gene (β -actin gene) and target genes (Bcl-2, p53 and Bax gene). The $2^{-\Delta\Delta Ct}$ (Livak) method calculated relative gene expression. Gene expression was calculated as fold change increase/decrease in the gene expression.

5.2.12. *In silico* molecular docking studies: isolated compounds. ^[223-225]

5.2.12.1. Anticancer activity

To investigate the mechanism and intermolecular interactions between the isolated molecules, molecular docking studies were performed on the crystal structure of Human caspase-3 (PDB ID 1QX3, 1.90 Å, X-ray Diffraction), extracted from the Brookhaven

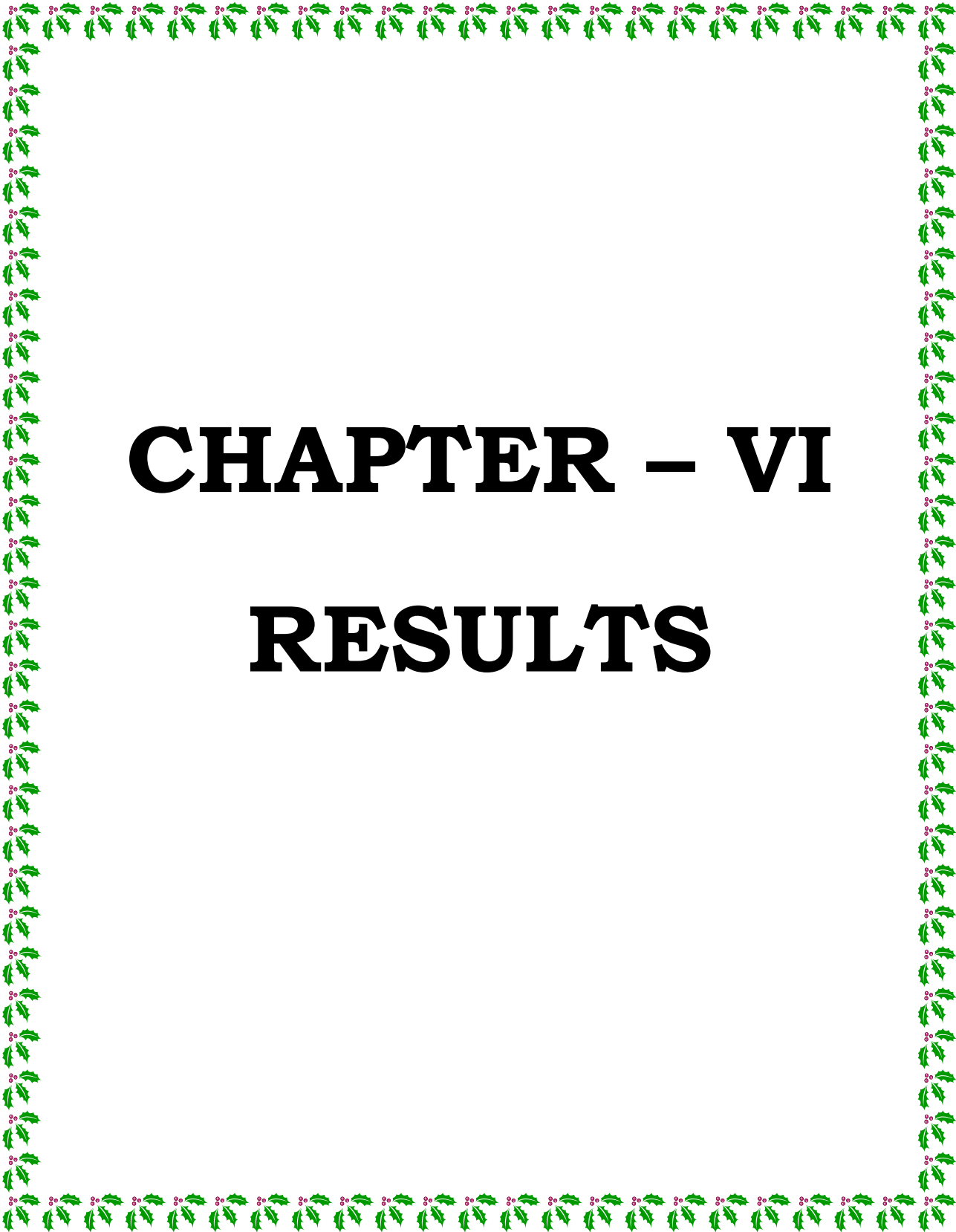
Protein Database (PDB). The proteins were prepared for docking by adding polar hydrogen atoms with Gasteiger-Huckel charges, and water molecules were removed. The 3D structure of the ligands was generated by the SKETCH module implemented in the SYBYL program (Tripos Inc., St. Louis, USA). Its energy-minimized conformation was obtained with the help of the Tripos force field using Gasteiger-Huckel charges as per Gasteiger and Marsili 1980, and molecular docking was performed with the Surflex-Dock program that is interfaced with Sybyl-X 2.0. software.

5.2.12.2. Antianxiety activity

The crystal structure of the Human GABA_A receptor alpha1-beta2-gamma2 subtype in complex with GABA and Diazepam (GABA_A-BZD, PDB ID 6D6T, 3.86 Å, ELECTRON MICROSCOPY) was extracted from the Brookhaven Protein Database (PDB). The proteins were prepared for docking by adding polar hydrogen atoms with Gasteiger-Huckel charges and removing water molecules. The 3D structure of the ligands was generated by the SKETCH module implemented in the SYBYL program (Tripos Inc., St. Louis, USA) and its energy-minimized conformation was obtained with the help of the Tripos force field using Gasteiger-Huckel charges and molecular docking was performed with Surflex-Dock program that is interfaced with Sybyl-X 2.0. Moreover, other miscellaneous parameters were assigned with the default values given by the software.

5.2.13. Statistical analysis

Analyses were performed in triplicate for *in vitro* and with 6 animals per group for *in vivo* activities. Each value is stated as the mean \pm Standard deviation (n = 3 or n = 6). The statistical study was conducted using IBM SPSS version 23.0 software (IBM Corporation, New York, USA). The statistical significance was measured using One way ANOVA along with Duncan's multiple range test, indicating that at each concentration, stage or trial, the means with different superscript letters are statistically significant with $p < 0.05$ (antiproliferative, antianxiety and biochemical activities) and $p < 0.01$, $p < 0.001$ (antiproliferative, apoptotic, cell cycle arrest, gene expression and biochemical activities).



CHAPTER – VI

RESULTS

6. RESULTS

6.2.1. Collection and authentication of *H. enneaspermus* and *B. foveolata*

The sample of *H. enneaspermus* was authenticated by Dr. Sunita Garg, Emeritus Scientist CSIR-NISCAIR, New Delhi (NISCAIR/RHMD/Consult/2017/3101-50). The certificate is enclosed as Annexure-I.

The sample of *B. foveolata* was authenticated by Dr. Satyanarayan S. Hebbar, Department of Botany, Government Pre-university college, Dharwad, Karnataka. The certificate is enclosed as Annexure-II.

6.2.2. Preparation of extracts and biofractions

6.2.2.1. The yield of EEHE was reported to be 268.37 g (8.95 % w/w), while that of TFHE, ITHE, EFHE and MFHE were 149.28 g (59.71 % w/w), 53.42 g (21.37 % w/w), 3.16 g (21.06 % w/w) and 7.81 g (52.06 % w/w) respectively.

6.2.2.2. The yield of EEBF was reported to be 151.29 g (5.04 % w/w), while that of TFBF, ITBF, EBF and MFBF were 27.99 g, (25.45 % w/w), 77.09 g, (70.08 % w/w), 13.79 g, (30.64 % w/w), and 28.68 g, (59.29 % w/w) respectively.

6.2.3. Qualitative Preliminary Phytochemical Investigation

The preliminary phytochemical analysis of *H. enneaspermus* revealed the presence of various active phytoconstituents as reported in Tables 6.1 and 6.2.

6.2.4. Quantitative Phytochemical Analysis

6.2.4.1. Total Phenolic Content

The total phenolic content of the EEHE was found to be 19.41 ± 0.65 mg GAE/g, while its biofractions TFHE, ITHE, EFHE, MFHE were reported to be 5.27 ± 0.18 ,

15.35 ± 0.43, 6.75 ± 0.27 and 8.20 ± 0.62 mg GAE/g, respectively.

The total phenolic content of the EEBF was found to be 49.12 ± 0.31 mg GAE/g, while its biofractions TFBF, ITBF, EFBF, MFBF were reported to be 3.27 ± 0.35, 45.58 ± 0.83, 21.01 ± 0.35, and 25.65 ± 0.21 mg GAE/g, respectively.

6.2.4.2. Total Flavonoid Content

The total flavonoid content of the EEHE was found to be 6.38 ± 0.36 mg QUE/g, while its biofractions TFHE, ITHE, EFHE, MFHE were reported to be 1.17 ± 0.25, 4.36 ± 0.21, 2.20 ± 0.17 and 3.02 ± 0.24 mg QUE/g, respectively.

The total flavonoid content of the EEBF was found to be 28.75 ± 0.42 mg QUE/g, while its biofractions TFBF, ITBF, EFBF, MFBF were reported to be 1.14 ± 0.28, 26.58 ± 0.69, 11.12 ± 0.46 and 14.83 ± 0.31 mg QUE/g, respectively.

6.2.5. Determination of *in vitro* antioxidant activity

Four *in vitro* free radical scavenging assays were used to assess the antioxidant activity of the ethanolic extract of *H. enneaspermus* and its biofractions. IC₅₀ value indicates the concentration of the sample, at which 50 % of the free radicals are scavenged.

The comparative results of the *in vitro* free radical scavenging activity of EEHE and its biofractions (TFHE, ITHE, EFHE, MFHE) have been listed in Figure 6.1 and Table 6.3. The results of the *in vitro* antioxidant activity of EEBF and its biofractions (TFBF, ITBF, EFBF, MFBF) have been given in Figure 6.2 and Table 6.4.

6.2.6. Determination of *in vitro* anticancer activities of the ethanolic extracts and biofractions.

The *in vitro* antiproliferative, apoptotic and cell cycle analysis of EEHE, EEBF and their biofractions against the MCF-7, Hop-62 and HeLa cell lines have been depicted in Figures 6.3 - 6.30 and Tables 6.5 - 6.18.

Table 6.1: Preliminary phytochemical screening of EEHE and its biofractions.

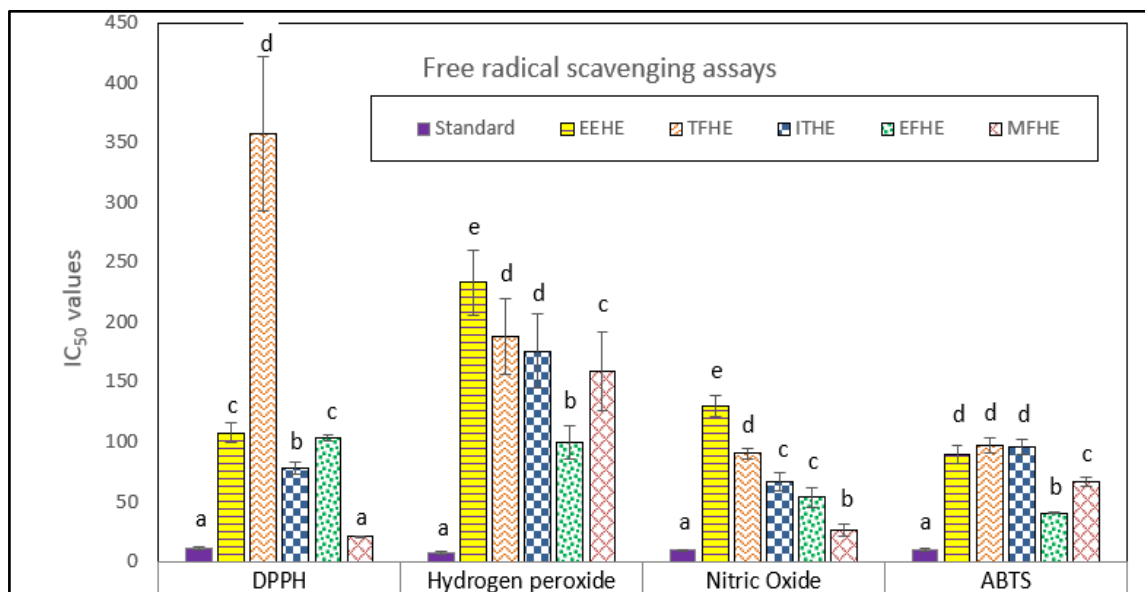
TESTS	EEHE	TFHE	ITHE	EFHE	MFHE
Alkaloids	+	-	+	+	+
Glycosides	+	-	+	-	+
Saponins	+	-	+	-	+
Carbohydrates	+	-	+	-	+
Flavanoids	+	+	+	+	+
Proteins	+	-	+	-	+
Tannins	+	+	+	+	+
Resins	-	-	-	-	-
Steroids	+	+	-	-	-
Triterpenoids	+	+	-	-	-
Starch	-	-	-	-	-

+ indicates present, - indicates absent.

Table 6.2: Preliminary phytochemical screening of EEBF and its biofractions.

TESTS	EEBF	TFBF	ITBF	EFBF	MFBF
Alkaloids	+	-	+	+	+
Glycosides	+	-	+	-	+
Saponins	+	-	+	-	+
Carbohydrates	+	-	+	-	+
Flavanoids	+	+	+	+	+
Proteins	+	-	+	-	+
Tannins	+	+	+	+	+
Resins	-	-	-	-	-
Steroids	+	+	-	-	-
Triterpenoids	+	+	-	-	-
Starch	-	-	-	-	-

+ indicates present, - indicates absent.

6.2.5. *In vitro* antioxidant activities of the ethanolic extracts and biofractions

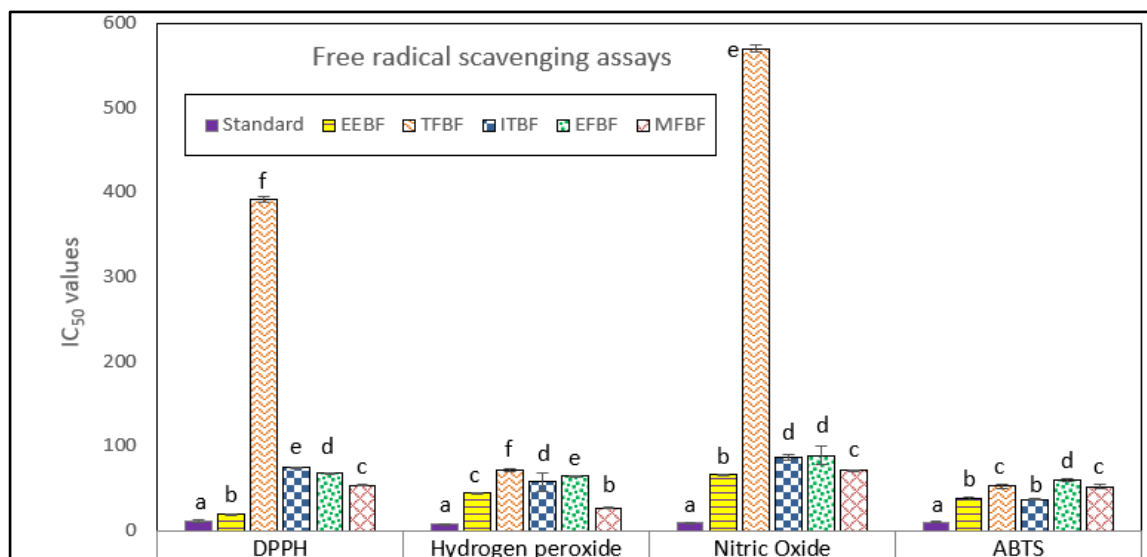
Each value is represented as the mean \pm SD (n = 3). Within each stage, the means with different superscript letters (a - e) are statistically significant (ANOVA, $p < 0.05$, and subsequent post hoc multiple comparisons with Duncan's test).

Figure 6.1: Free radical scavenging activities of EEHE and biofractions.

Table 6.3: Free radical scavenging analysis of EEHE and biofractions.

Samples	Free radical scavenging assays (IC ₅₀ = $\mu\text{g/mL}$)			
	DPPH	Hydrogen peroxide	Nitrogen Oxide	ABTS
EEHE	107.45 \pm 8.62 ^c	233.27 \pm 27.14 ^e	129.93 \pm 9.21 ^e	89.16 \pm 7.61 ^d
TFHE	357.4 \pm 64.47 ^d	188.23 \pm 31.75 ^d	90.15 \pm 4.06 ^d	97.1 \pm 6.45 ^d
ITHE	78.3 \pm 5.1 ^b	175.83 \pm 31.4 ^d	66.67 \pm 7.24 ^c	95.65 \pm 6.01 ^d
EFHE	103.5 \pm 2.66 ^c	99.11 \pm 13.59 ^b	53.42 \pm 7.87 ^c	40.38 \pm 0.88 ^b
MFHE	21.1 \pm 0.39 ^a	158.93 \pm 32.46 ^c	25.99 \pm 4.66 ^b	66.8 \pm 3.96 ^c
Standard (Ascorbic acid)	11.19 \pm 1.09 ^a	6.91 \pm 1.52 ^a	9.3 \pm 0.26 ^a	10.17 \pm 1.33 ^a

Each value is represented as the mean \pm SD (n = 3). Within each stage, the means with different superscript letters (a - e) are statistically significant (ANOVA, $p < 0.05$, and subsequent post hoc multiple comparisons with Duncan's test).



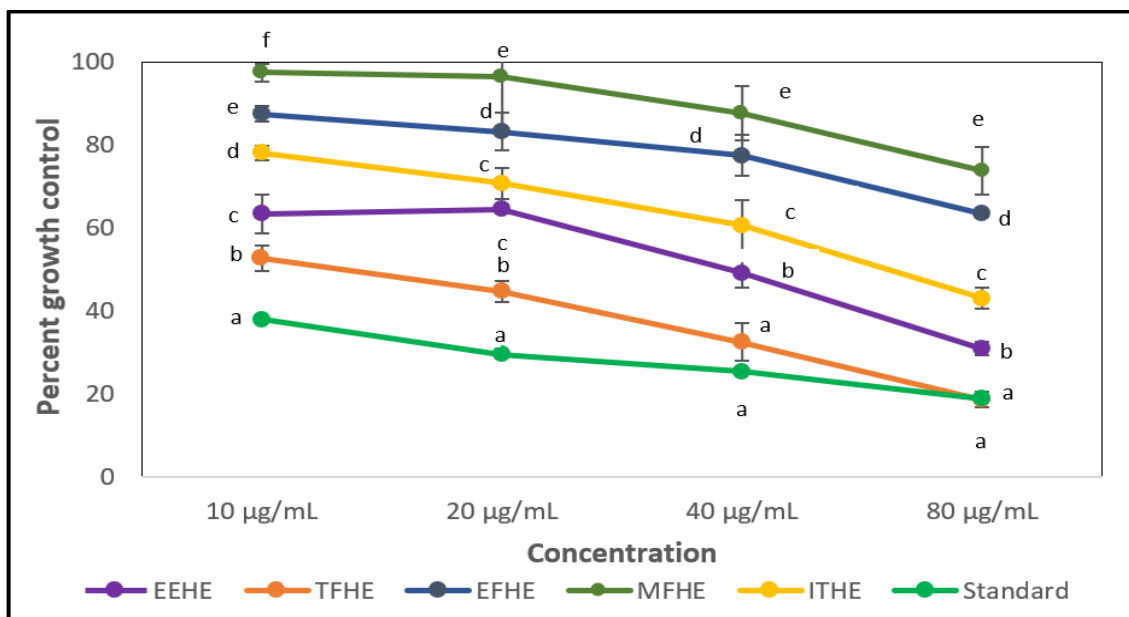
Each value is represented as the mean \pm SD (n = 3). Within each stage, the means with different superscript letters (a - f) are statistically significant (ANOVA, $p < 0.05$, and subsequent post hoc multiple comparisons with Duncan's test).

Figure 6.2: Free radical scavenging activities of EEBF and biofractions.

Table 6.4: Free radical scavenging analysis of EEBF and biofractions.

Samples	Free radical scavenging assays (IC ₅₀ = $\mu\text{g/mL}$)			
	DPPH	Hydrogen peroxide	Nitrogen Oxide	ABTS
EEBF	19.04 \pm 0.24 ^b	43.96 \pm 0.92 ^c	65.85 \pm 1.22 ^b	38.3 \pm 1.51 ^b
TFBF	391.5 \pm 3.32 ^f	71.45 \pm 1.03 ^f	569.67 \pm 4.19 ^e	52.66 \pm 2.22 ^c
ITBF	74.62 \pm 0.66 ^e	57.89 \pm 10.92 ^d	86.38 \pm 3.33 ^d	36.75 \pm 0.72 ^b
EFBF	68.39 \pm 0.27 ^d	64.66 \pm 0.43 ^c	88.67 \pm 10.61 ^d	59.83 \pm 1.27 ^d
MFBF	53.44 \pm 0.83 ^c	26.76 \pm 0.75 ^b	71.63 \pm 0.19 ^c	52.01 \pm 2.28 ^c
Standard (Ascorbic acid)	11.19 \pm 1.09 ^a	6.91 \pm 1.52 ^a	9.3 \pm 0.26 ^a	10.17 \pm 1.33 ^a

Each value is represented as the mean \pm SD (n = 3). Within each stage, the means with different superscript letters (a - f) are statistically significant (ANOVA, $p < 0.05$, and subsequent post hoc multiple comparisons with Duncan's test).

6.2.6. *In vitro* anticancer activities of the ethanolic extracts and biofractions

Each value is represented as the mean \pm SD (n = 3). Within each stage, the means with different superscript letters (a - f) are statistically significant (ANOVA, $p < 0.05$, and subsequent post hoc multiple comparisons with Duncan's test).

Figure 6.3: Antiproliferative activity of EEHE and its biofractions against MCF-7 cell lines.

Table 6.5: Growth control of MCF-7 cell lines by EEHE and its biofractions.

Experimental sample	GI ₅₀ (µg/mL)
EEHE	41.42 \pm 3.74
TFHE	10.22 \pm 6.72
EFHE	120.21 \pm 6.08
MFHE	166.08 \pm 52.92
ITHE	64.37 \pm 7.07
Standard (Doxorubicin)	5.77 \pm 0.13

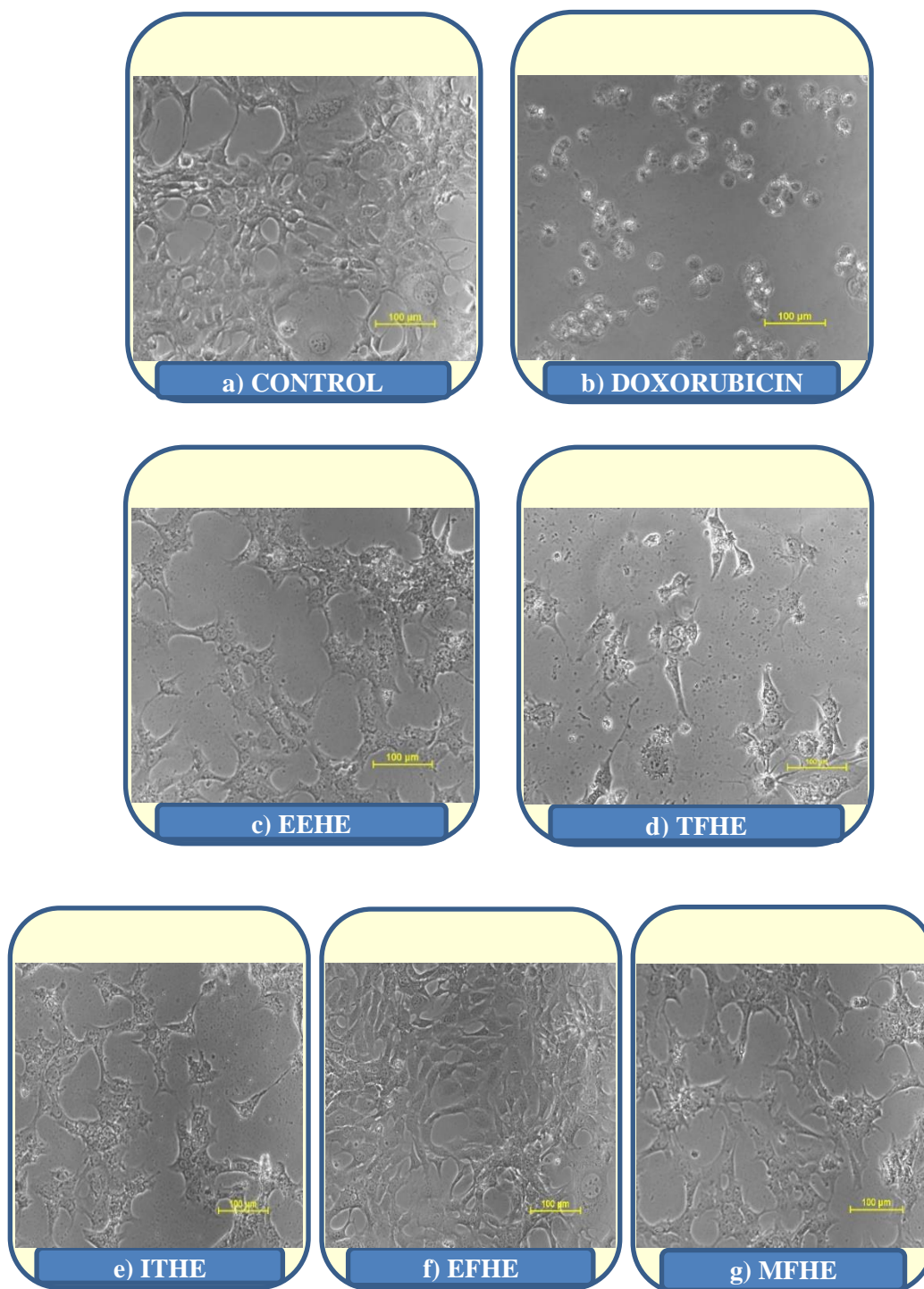
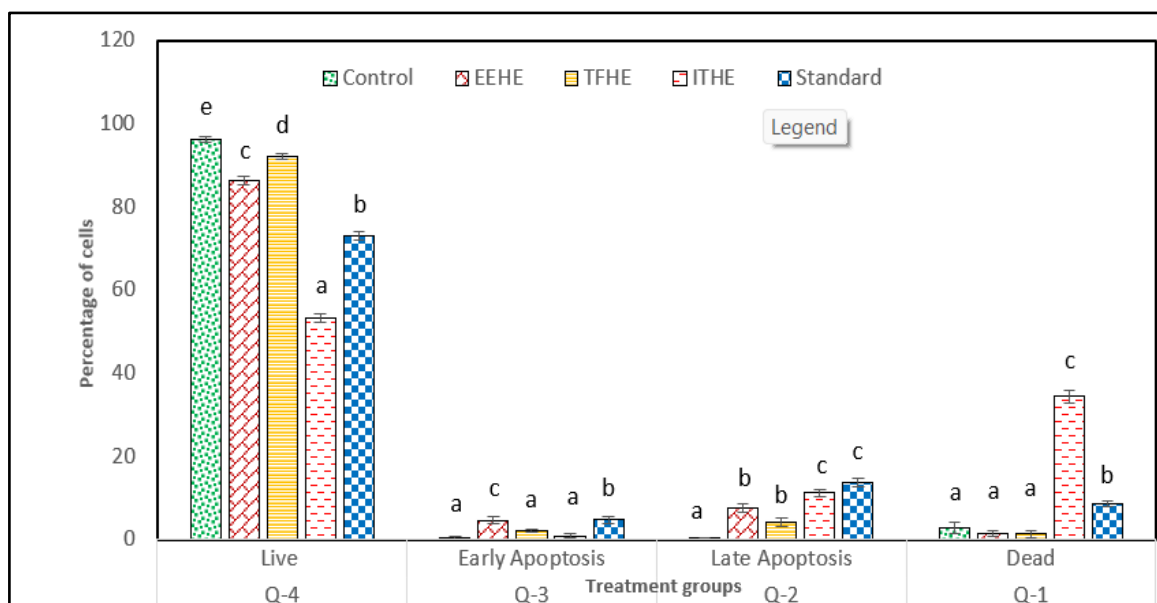


Figure 6.4: Morphological changes of MCF-7 cells treated with EEHE and its biofractions.



Each value is represented as the mean \pm SD (n = 3). Within each stage, the means with different superscript letters (a - e) are statistically significant (ANOVA, $p < 0.001$, and subsequent post hoc multiple comparisons with Duncan's test).

Figure 6.5: Apoptosis activity of EEHE and its biofractions against MCF-7 cell lines.

Table 6.6: Apoptosis analysis of EEHE and its biofractions on MCF-7 cell lines

Groups	Q-4 Live (%)	Q-3 Early Apoptosis (%)	Q-2 Late Apoptosis (%)	Q-1 Dead (%)
Control	96.3 \pm 0.76 ^e	0.44 \pm 0.44 ^a	0.41 \pm 0.25 ^a	2.86 \pm 1.29 ^a
EEHE	86.33 \pm 0.96 ^c	4.63 \pm 0.84 ^c	7.59 \pm 1.04 ^b	1.61 \pm 0.72 ^a
TFHE	92.13 \pm 0.74 ^d	2.06 \pm 0.32 ^a	4.31 \pm 1.05 ^b	1.42 \pm 0.77 ^a
ITHE	53.34 \pm 1.09 ^a	0.89 \pm 0.46 ^a	11.31 \pm 0.82 ^c	34.48 \pm 1.57 ^c
Standard (Doxorubicin)	73.2 \pm 0.96 ^b	4.81 \pm 0.83 ^b	13.67 \pm 1.02 ^c	8.58 \pm 0.65 ^b

Each value is represented as the mean \pm SD (n = 3). Within each stage, the means with different superscript letters (a - e) are statistically significant (ANOVA, $p < 0.001$, and subsequent post hoc multiple comparisons with Duncan's test).

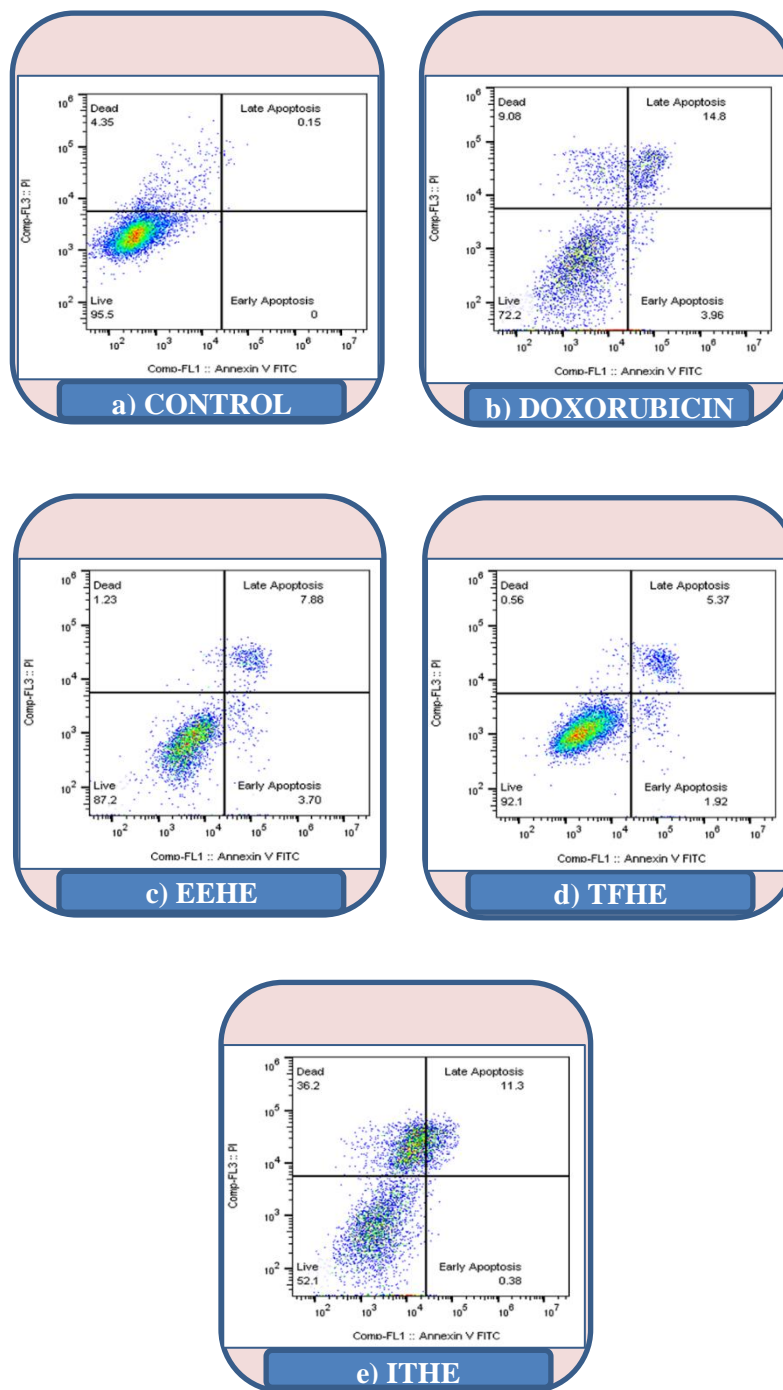
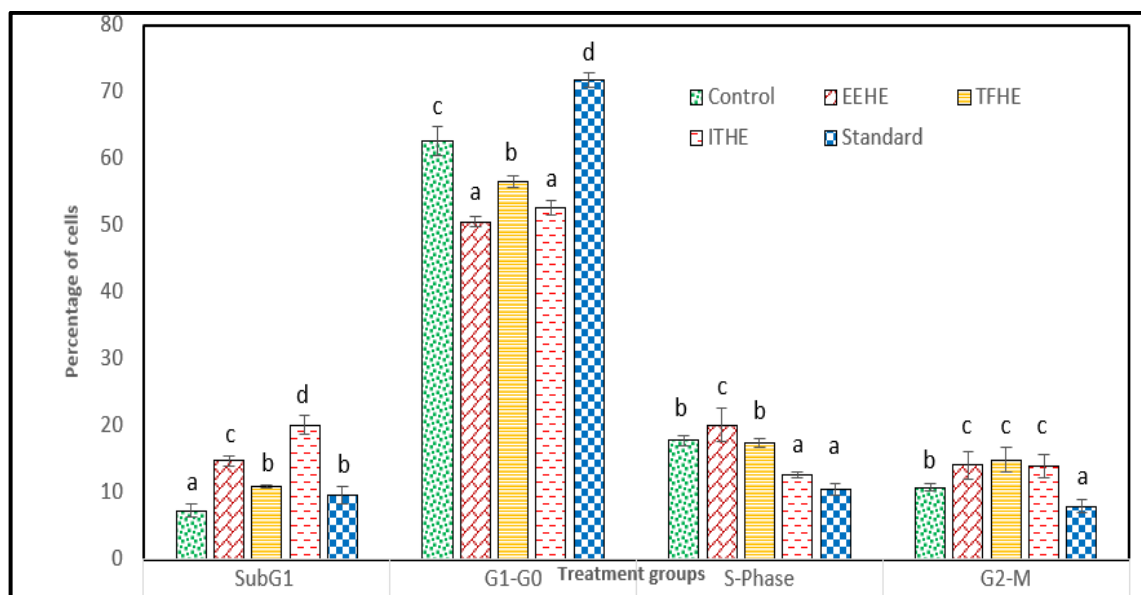


Figure 6.6: Apoptosis analysis of EEHE and biofractions against MCF-7 cell lines.



Each value is represented as the mean \pm SD (n = 3). Within each stage, the means with different superscript letters (a - d) are statistically significant (ANOVA, $p \leq 0.001$, and subsequent post hoc multiple comparisons with Duncan's test).

Figure 6.7: Cell cycle activity of EEHE and its biofractions against MCF-7 cell lines.

Table 6.7: Cell cycle analysis of EEHE and its biofractions on MCF-7 cell lines

Groups	SubG ₁ (%)	G ₁ -G ₀ (%)	S-Phase (%)	G ₂ -M (%)
Control	7.27 \pm 1.00 ^a	62.6 \pm 2.22 ^c	17.81 \pm 0.74 ^b	10.79 \pm 0.61 ^b
EEHE	14.78 \pm 0.76 ^c	50.58 \pm 0.82 ^a	20.15 \pm 2.52 ^c	14.15 \pm 2.07 ^c
TFHE	10.95 \pm 0.24 ^b	56.62 \pm 0.86 ^b	17.49 \pm 0.58 ^b	14.86 \pm 1.84 ^c
ITHE	20.15 \pm 1.37 ^d	52.66 \pm 1.14 ^a	12.71 \pm 0.37 ^a	13.99 \pm 1.65 ^c
Standard (Doxorubicin)	9.68 \pm 1.28 ^b	71.72 \pm 1.13 ^d	10.5 \pm 0.9 ^a	7.99 \pm 1.00 ^a

Each value is represented as the mean \pm SD (n = 3). Within each stage, the means with different superscript letters (a - d) are statistically significant (ANOVA, $p \leq 0.001$, and subsequent post hoc multiple comparisons with Duncan's test).

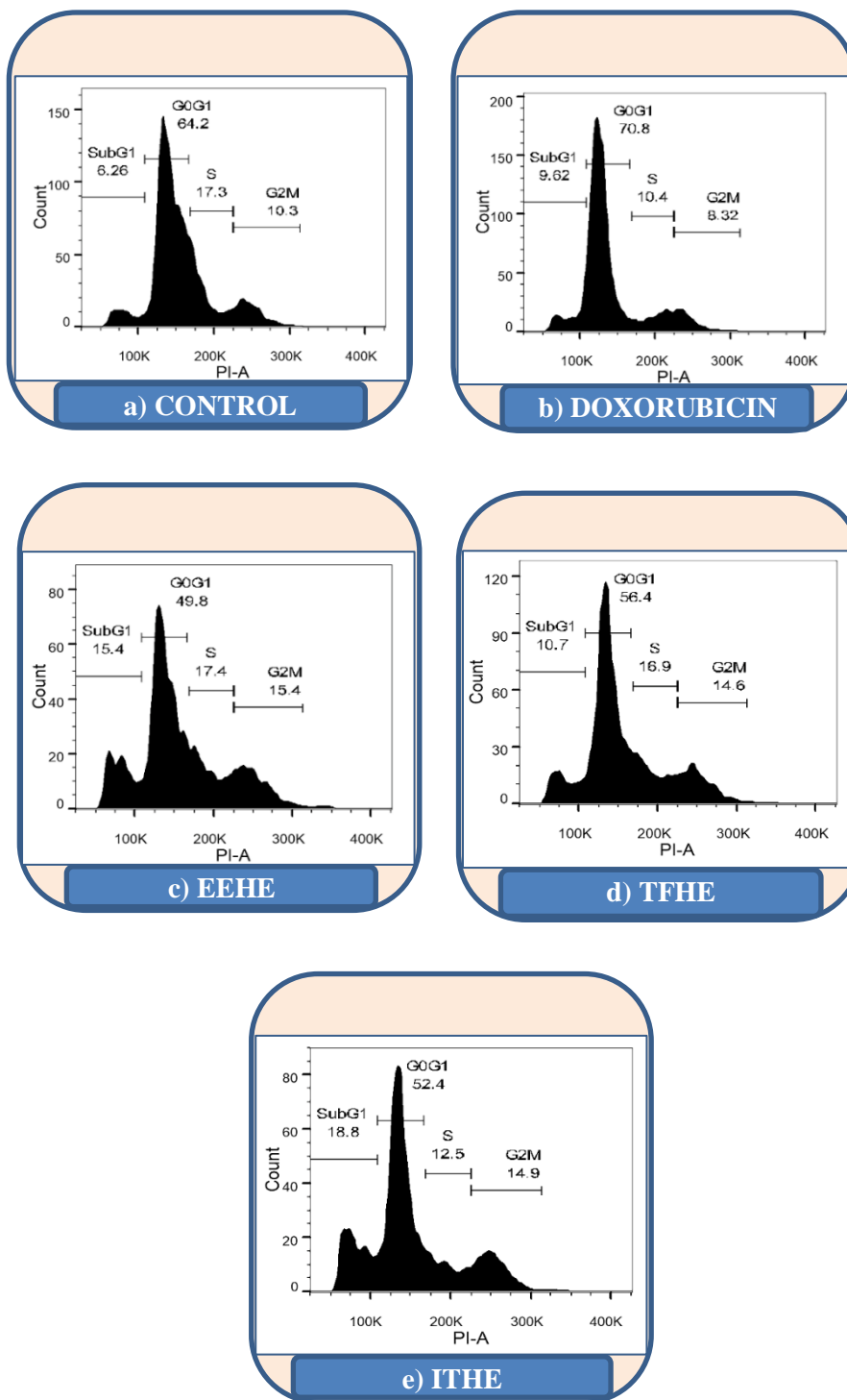
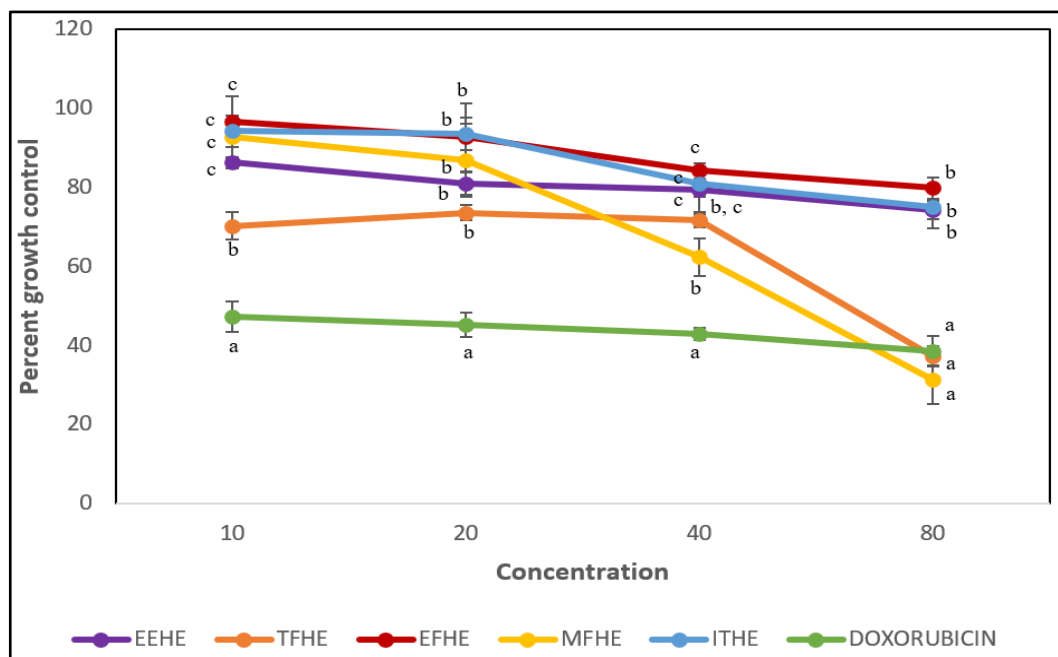


Figure 6.8: Cell cycle analysis of EEHE and biofractions on MCF-7 cell lines.



Each value is represented as the mean \pm SD (n = 3). Different superscript letters (a - c) are statistically significant (ANOVA, $p < 0.01$, and subsequent post hoc multiple comparisons with Duncan's test).

Figure 6.9: Antiproliferative activity of EEHE and its biofractions against Hop-62 cell lines.

Table 6.8: Growth control of Hop-62 cells by EEHE and its biofractions.

Experimental sample	GI ₅₀ ($\mu\text{g/mL}$)
EEHE	> 80
TFHE	63.5 \pm 8.34
EFHE	>80
MFHE	58.5 \pm 9.86
ITHE	>80
Standard (Doxorubicin)	10.63 \pm 0.90

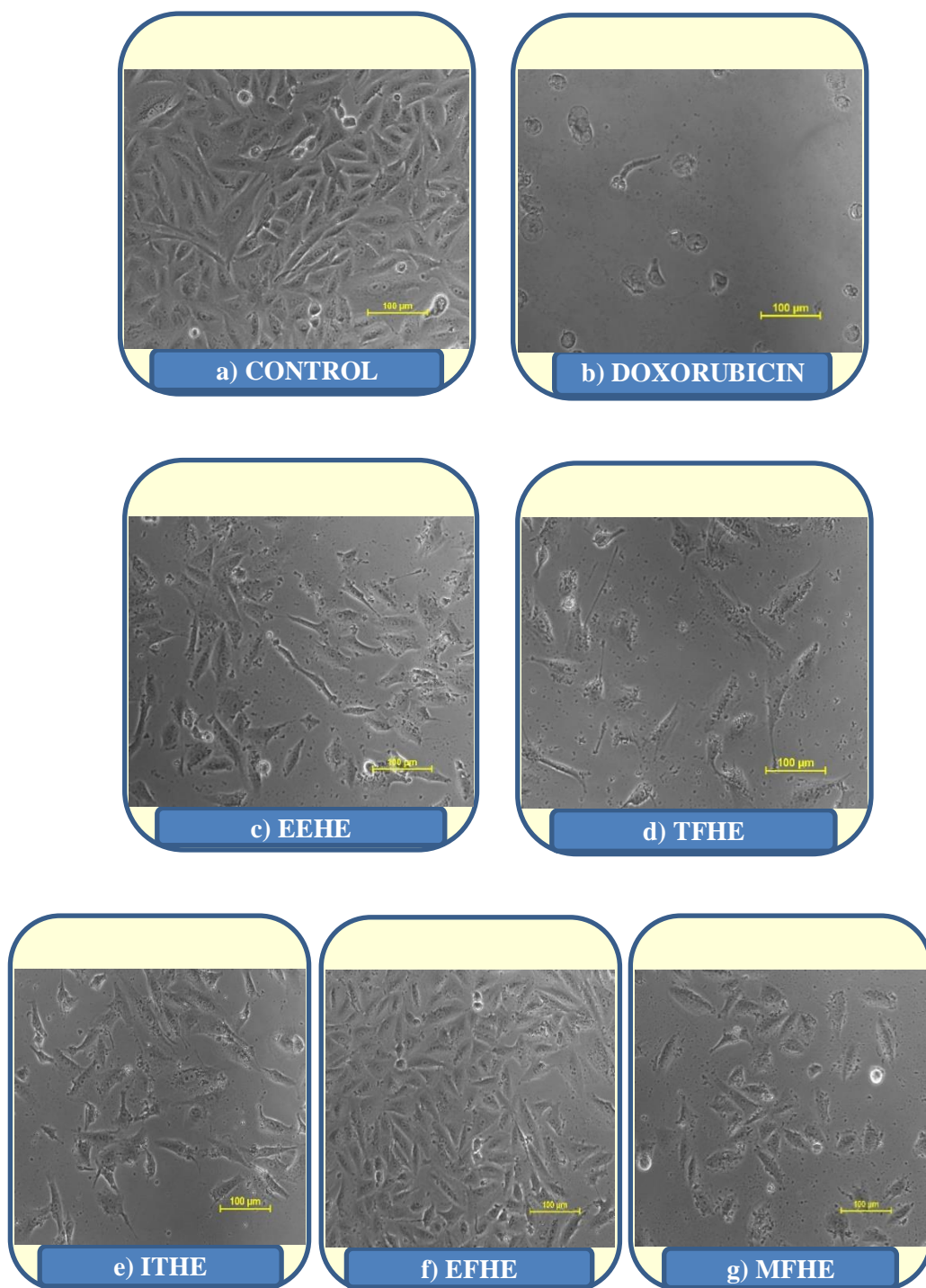
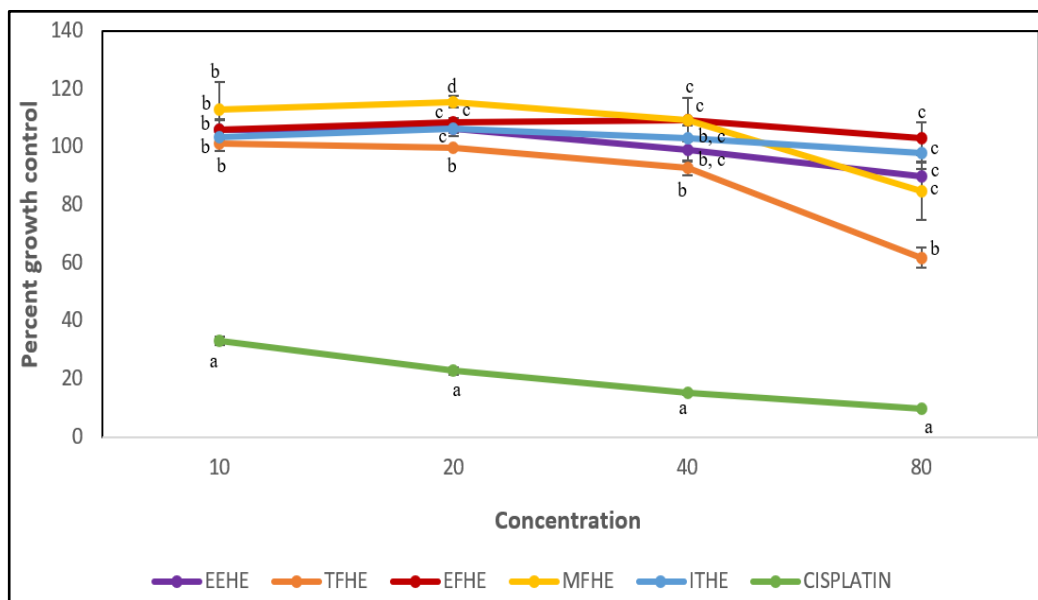


Figure 6.10: Morphological changes of Hop-62 cells treated with EEHE and its biofractions.



Each value is represented as the mean \pm SD (n = 3). Different superscript letters (a - c) are statistically significant (ANOVA, $p < 0.01$, and subsequent post hoc multiple comparisons with Duncan's test).

Figure 6.11: Antiproliferative activity of EEHE and biofractions against HeLa cell lines.

Table 6.9: Growth control of HeLa cell lines by EEHE and biofractions.

Experimental sample	GI ₅₀ ($\mu\text{g/mL}$)
EEHE	>80
TFHE	>80
EFHE	>80
MFHE	>80
Standard (Cisplatin)	1.29 ± 0.10

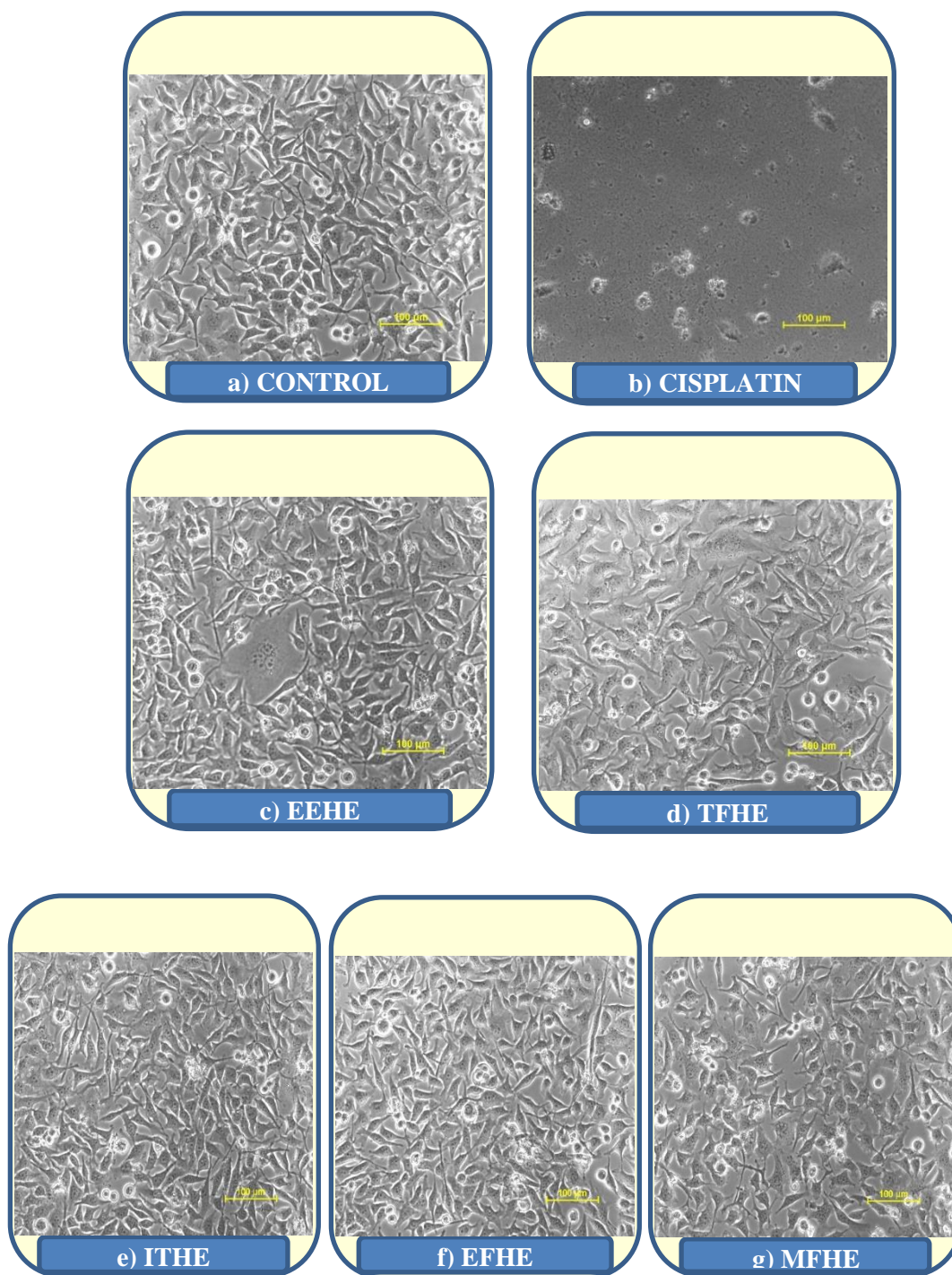
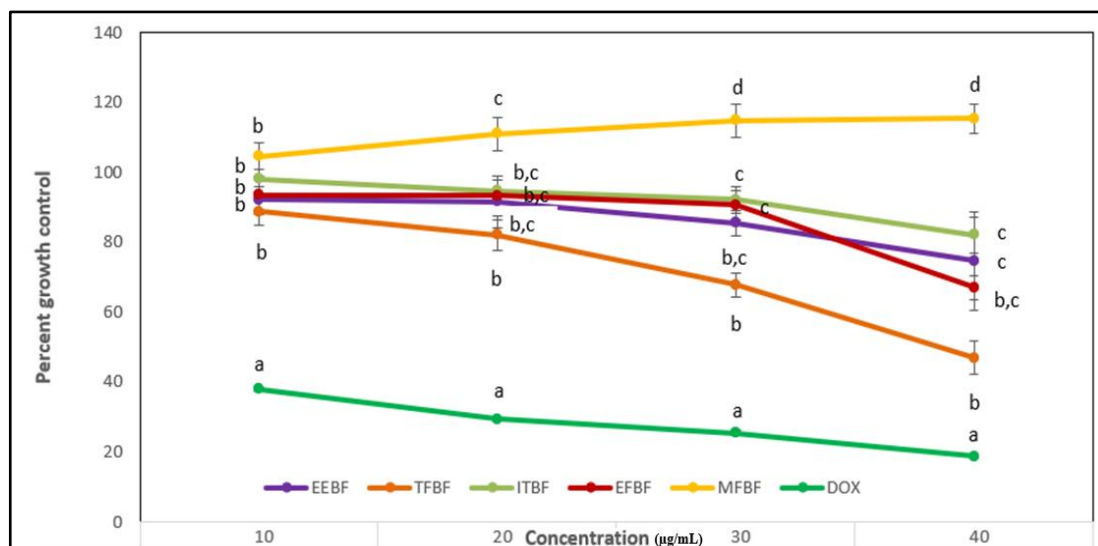


Figure 6.12: Morphological changes of HeLa cells treated with EEHE and its biofractions.



Each value is represented as the mean \pm SD (n = 3). Different superscript letters (a - d) are statistically significant (ANOVA, $p < 0.01$, and subsequent post hoc multiple comparisons with Duncan's test).

Figure 6.13: Antiproliferative analysis of EEBF and biofractions against MCF-7 cell lines.

Table 6.10: Growth control of MCF-7 cells by EEBF and its biofractions.

Experimental sample	GI ₅₀ (µg/mL)
EEBF	>80
TFBF	73.5 \pm 11.96
ITBF	>80
EFBF	>80
MFBF	>80
Standard (Doxorubicin)	5.77 \pm 0.13

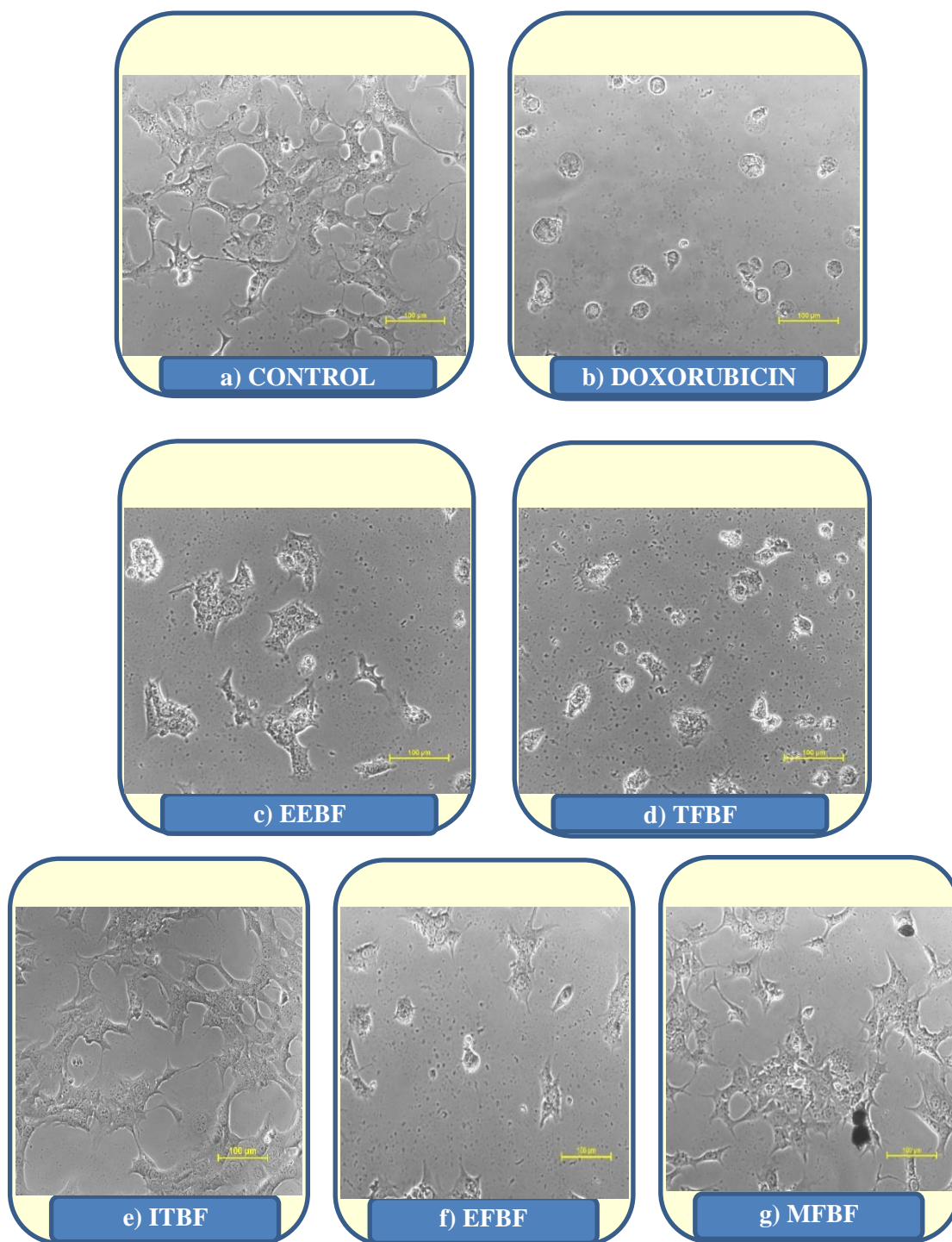
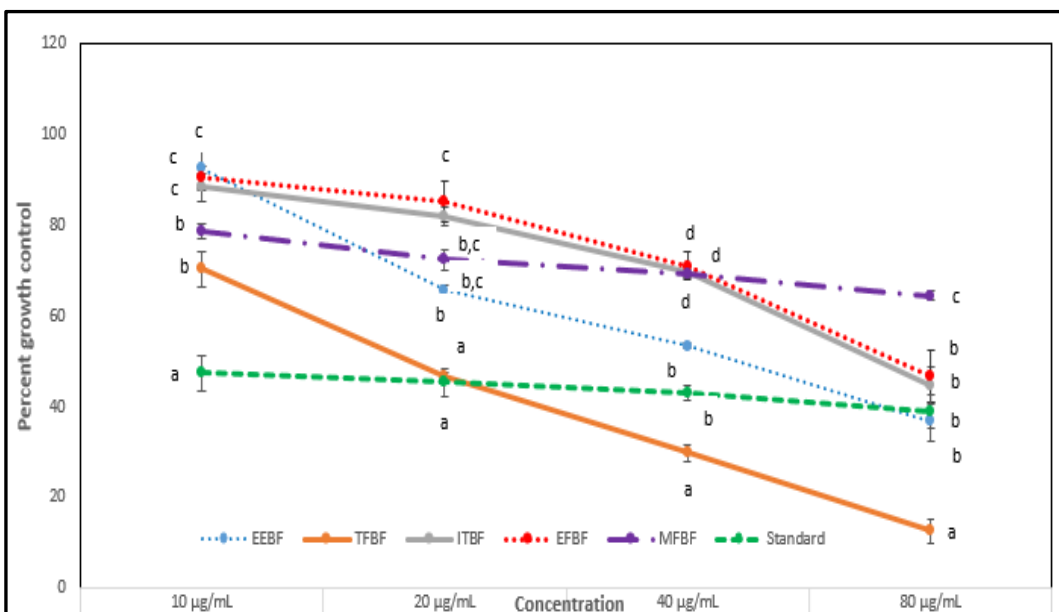


Figure 6.14: Morphological changes of MCF-7 cells treated with EEBF and biofractions.



Each value is represented as the mean \pm SD ($n = 3$). Different superscript letters (a - d) are statistically significant (ANOVA, $p < 0.01$, and subsequent post hoc multiple comparisons with Duncan's test).

Figure 6.15: Antiproliferative activity of EEBF and biofractions against Hop-62 cell lines.

Table 6.11: Growth control of Hop-62 cells by EEBF and its biofractions.

Experimental sample	GI ₅₀ (µg/mL)
EEBF	54.8 \pm 3.08
TFBF	23.7 \pm 2.54
ITBF	74.7 \pm 2.91
EFBF	74.4 \pm 5.43
MFBF	84.9 \pm 1.45
Standard (Doxorubicin)	10.63 \pm 0.90

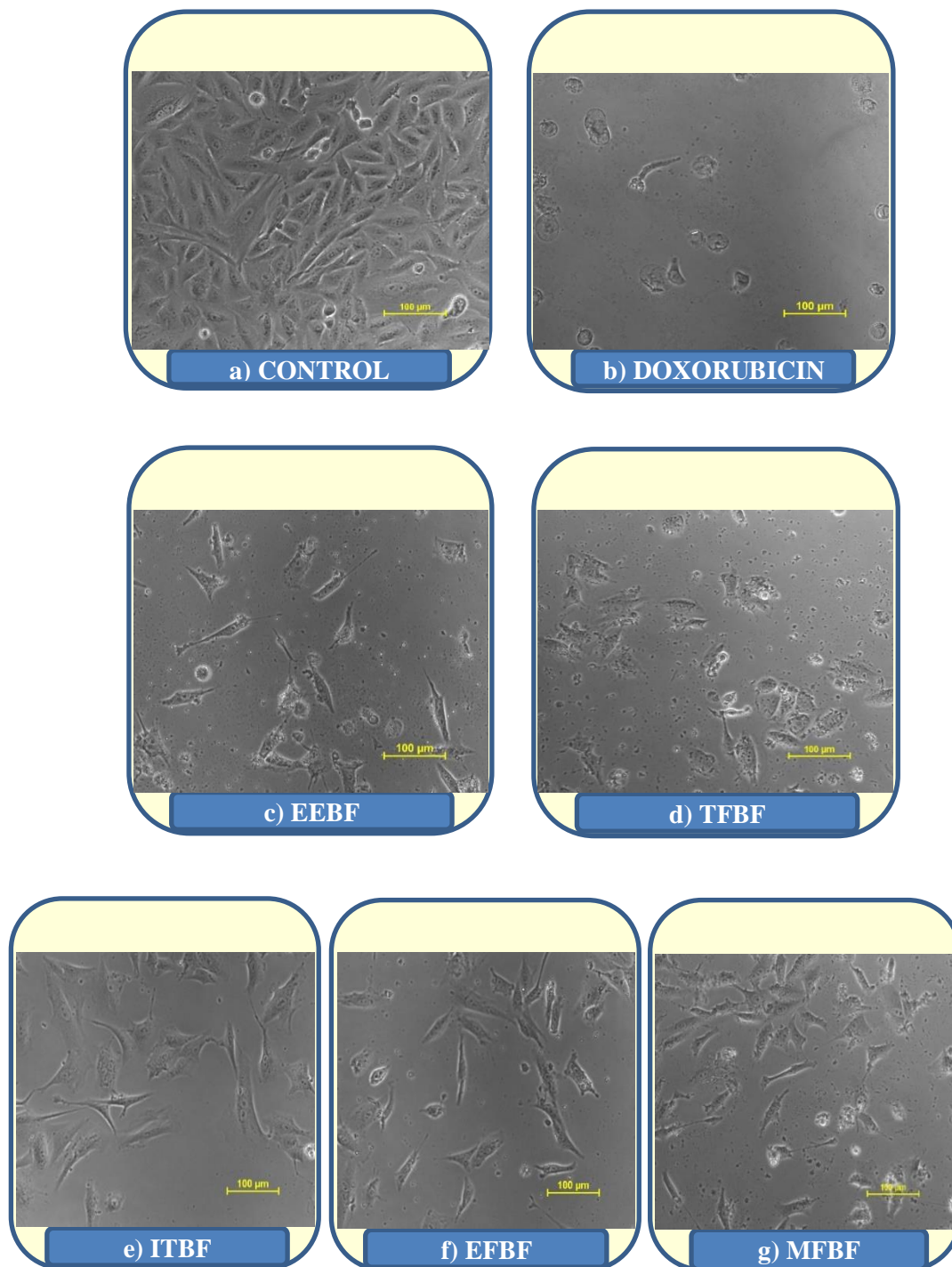
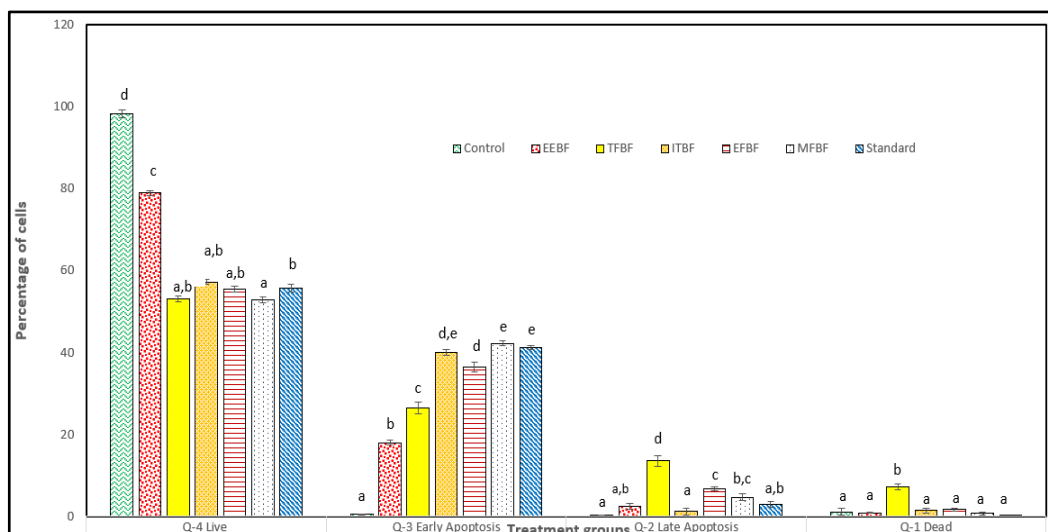


Figure 6.16: Morphological changes of Hop-62 cells treated with EEBF and its biofractions.



Each value is represented as the mean \pm SD (n = 3). Different superscript letters (a - e) are statistically significant (ANOVA, $p < 0.001$, and subsequent post hoc multiple comparisons with Duncan's test).

Figure 6.17: Apoptosis assay of EEBF and biofractions against Hop-62 cell lines.

Table 6.12: Apoptosis analysis of EEBF and its biofractions on Hop-62 cell lines

Groups	Q-4 Live (%)	Q-3 Early Apoptosis (%)	Q-2 Late Apoptosis (%)	Q-1 Dead (%)
Control	98.27 \pm 0.87 ^d	0.43 \pm 0.07 ^a	0.28 \pm 0.06 ^a	1.02 \pm 0.82 ^a
EEBF	78.98 \pm 0.7 ^c	17.95 \pm 0.51 ^b	2.33 \pm 0.66 ^{a,b}	0.79 \pm 0.17 ^a
TFBF	53.09 \pm 0.61 ^{a,b}	26.38 \pm 1.36 ^c	13.51 \pm 1.32 ^d	7.16 \pm 0.69 ^b
ITBF	57.16 \pm 0.60 ^{a,b}	40.02 \pm 0.73 ^{d,e}	1.11 \pm 0.76 ^a	1.33 \pm 0.56 ^a
EFBF	55.39 \pm 0.7 ^{a,b}	36.42 \pm 1.15 ^d	6.71 \pm 0.5 ^c	1.58 \pm 0.45 ^a
MFBF	52.79 \pm 0.7 ^a	42.24 \pm 0.57 ^e	4.61 \pm 0.88 ^{b,c}	0.61 \pm 0.4 ^a
Standard (Doxorubicin)	55.8 \pm 0.97 ^b	41.25 \pm 0.45 ^e	2.93 \pm 0.75 ^{a,b}	0.06 \pm 0.02 ^a

Each value is represented as the mean \pm SD (n = 3). Different superscript letters (a - e) are statistically significant (ANOVA, $p < 0.001$, and subsequent post hoc multiple comparisons with Duncan's test).

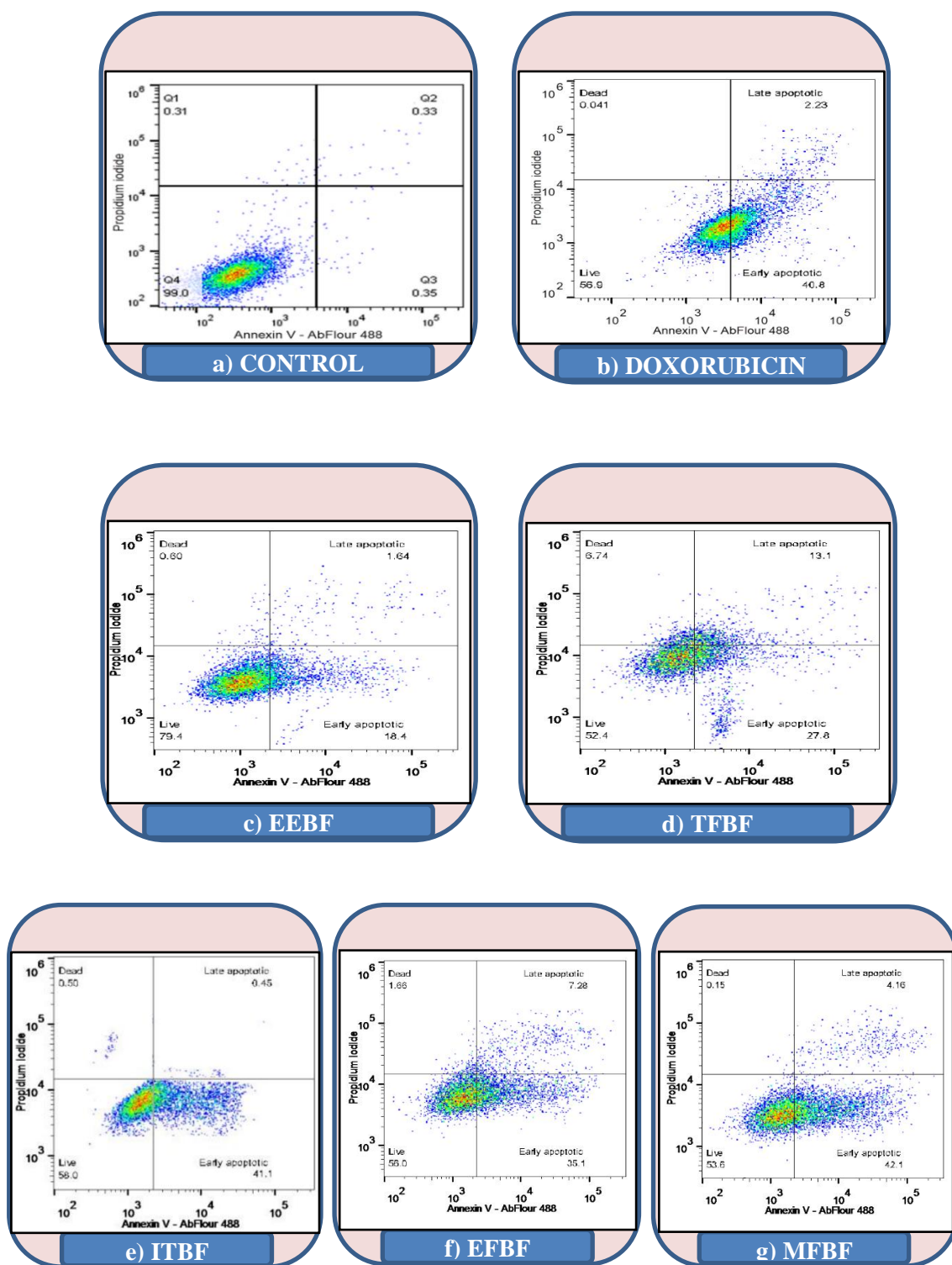
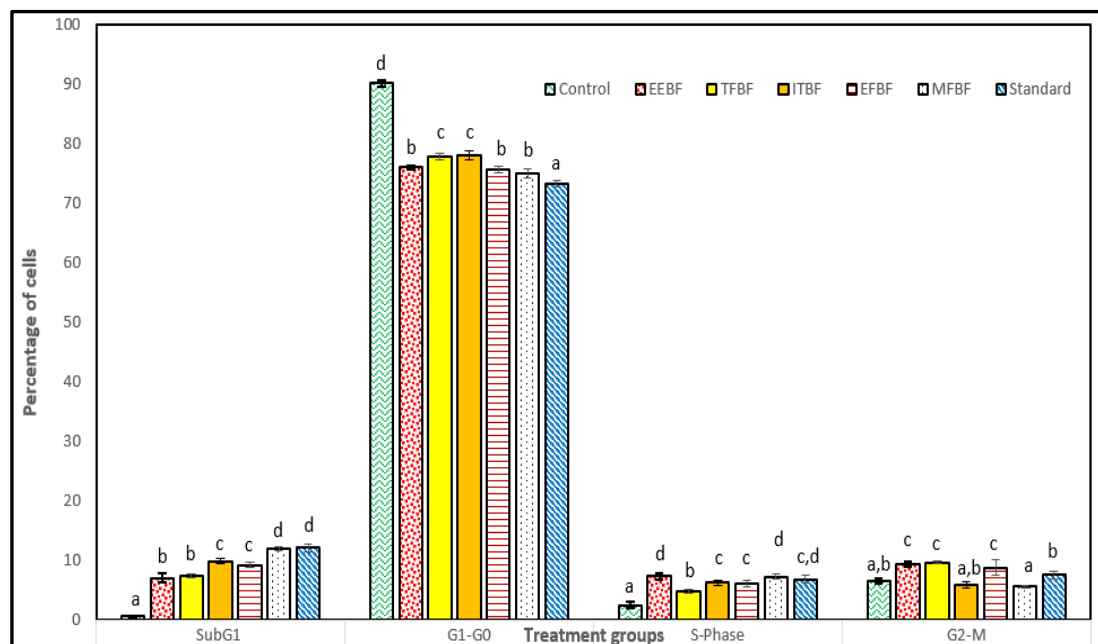


Figure 6.18: Apoptosis analysis of EEBF and biofractions against Hop-62 cell lines.



Each value is represented as the mean \pm SD (n = 3). Different superscript letters (a - d) are statistically significant (ANOVA, $p < 0.001$, and subsequent post hoc multiple comparisons with Duncan's test).

Figure 6.19: Cell cycle assay of EEBF and biofractions against Hop-62 cell lines.

Table 6.13: Cell cycle analysis of EEBF and biofractions on Hop-62 cell lines.

Groups	SubG ₁ (%)	G ₁ -G ₀ (%)	S-Phase (%)	G ₂ -M (%)
Control	0.68 \pm 0.13 ^a	90.13 \pm 0.55 ^d	2.57 \pm 0.52 ^a	6.55 \pm 0.4 ^{a,b}
EEBF	7.11 \pm 0.8 ^b	76.05 \pm 0.27 ^b	7.42 \pm 0.5 ^d	9.41 \pm 0.47 ^c
TFBF	7.49 \pm 0.37 ^b	77.88 \pm 0.52 ^c	4.88 \pm 0.26 ^b	9.75 \pm 0.17 ^c
ITBF	9.95 \pm 0.36 ^c	78.01 \pm 0.73 ^c	6.31 \pm 0.38 ^c	5.99 \pm 0.49 ^{a,b}
EFBF	9.28 \pm 0.41 ^c	75.68 \pm 0.62 ^b	6.21 \pm 0.59 ^c	8.86 \pm 1.33 ^c
MFBF	11.95 \pm 0.33 ^d	75.08 \pm 0.79 ^b	7.35 \pm 0.39 ^d	5.63 \pm 0.27 ^a
Standard (Doxorubicin)	12.2 \pm 0.62 ^d	73.3 \pm 0.46 ^a	6.88 \pm 0.61 ^{c,d}	7.63 \pm 0.65 ^b

Each value is represented as the mean \pm SD (n = 3). Different superscript letters (a - d) are statistically significant (ANOVA, $p < 0.001$, and subsequent post hoc multiple comparisons with Duncan's test).

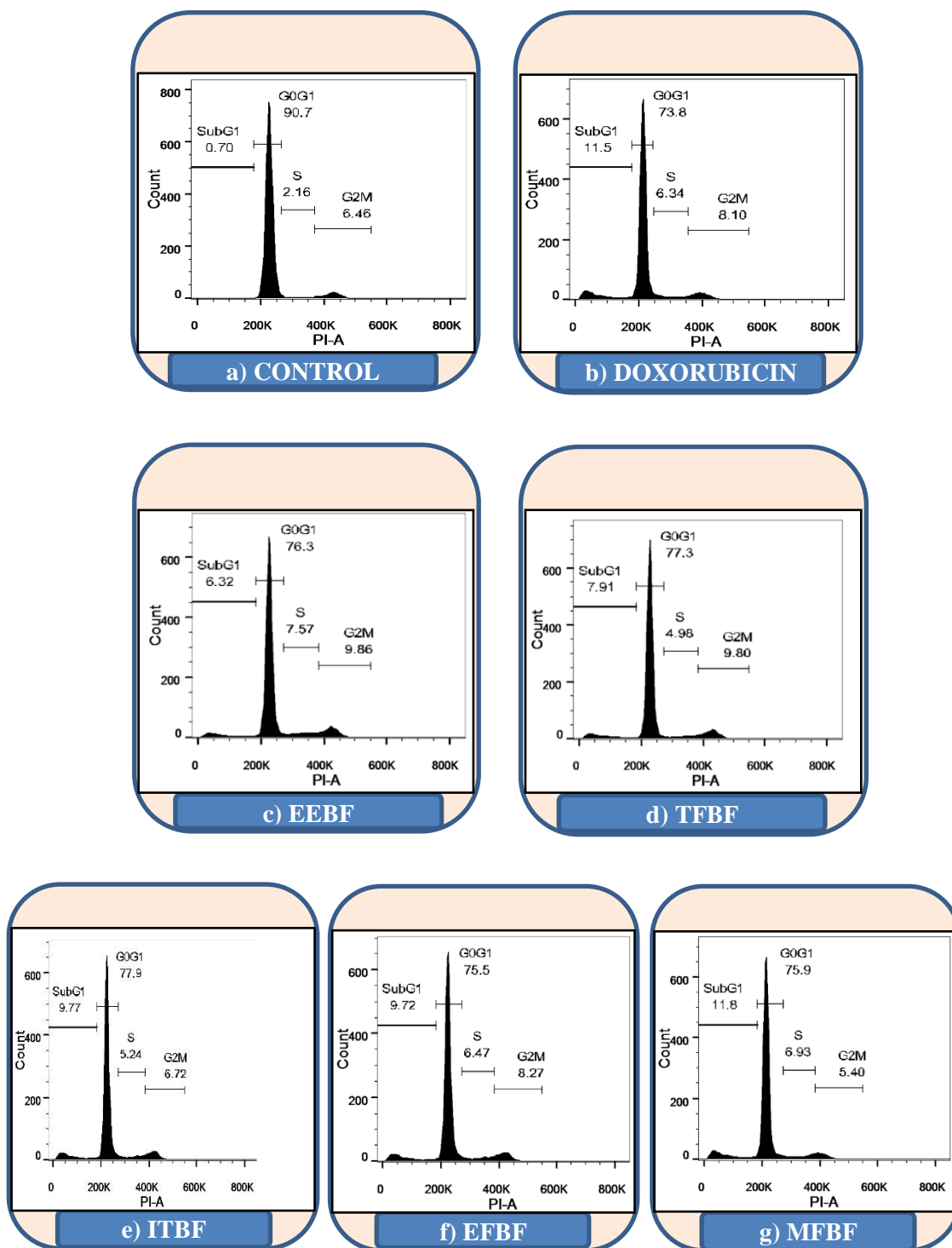
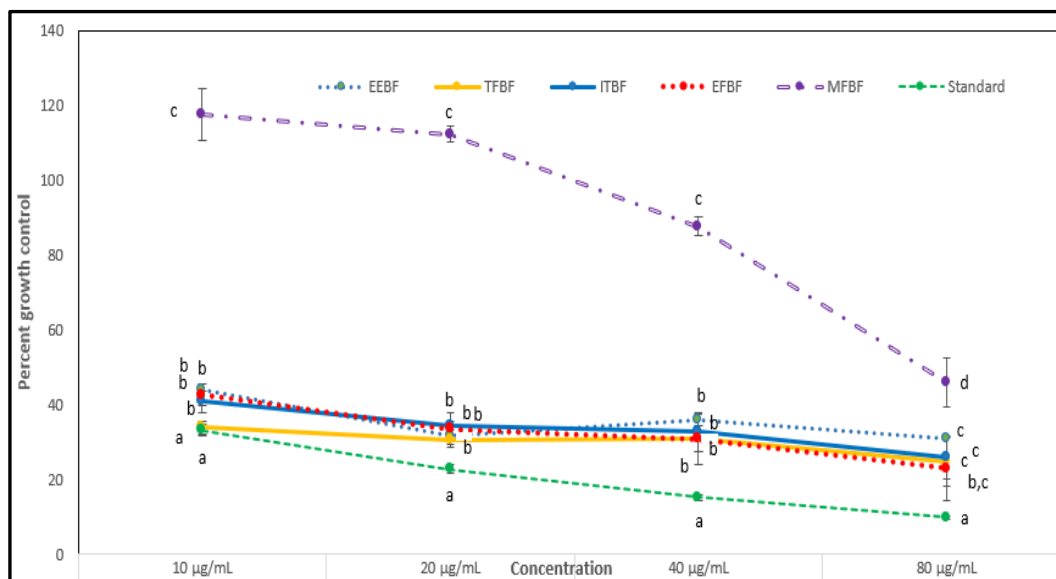


Figure 6.20: Cell cycle analysis of EEBF and biofractions against Hop-62 cell lines.



Each value is represented as the mean \pm SD ($n = 6$). Different superscript letters (a - d) are statistically significant (ANOVA, $p < 0.05$, and subsequent post hoc multiple comparisons with Duncan's test).

Figure 6.21: Antiproliferative activity of EEBF and its biofractions against HeLa cell lines.

Table 6.14: Growth control of HeLa cell by EEBF and its biofractions.

Experimental sample	GI ₅₀ ($\mu\text{g/mL}$)
EEBF	< 10
TFBF	< 10
ITBF	< 10
EFBF	< 10
MFBF	76.3 ± 1.45
Standard (Cisplatin)	1.29 ± 0.10

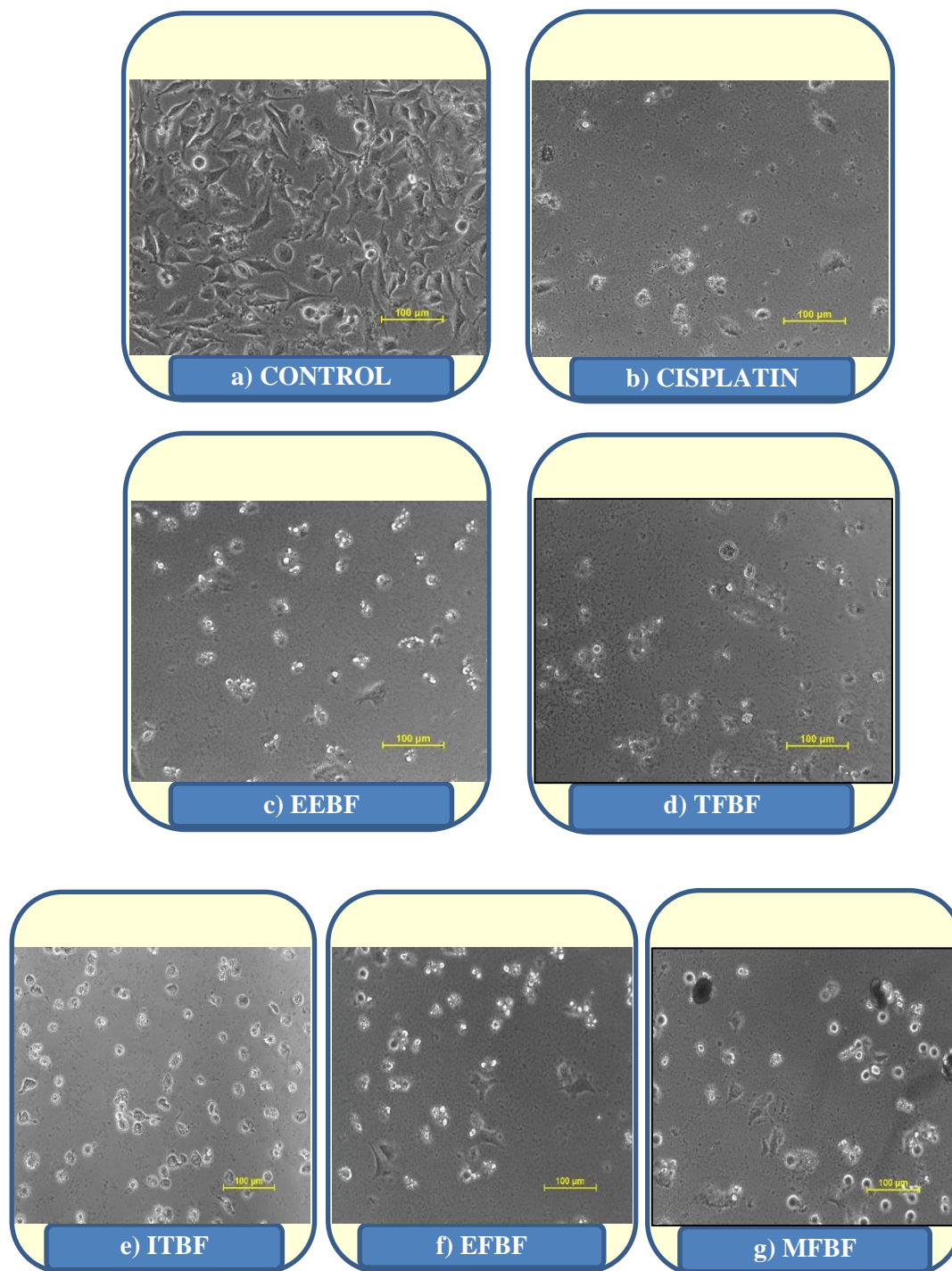
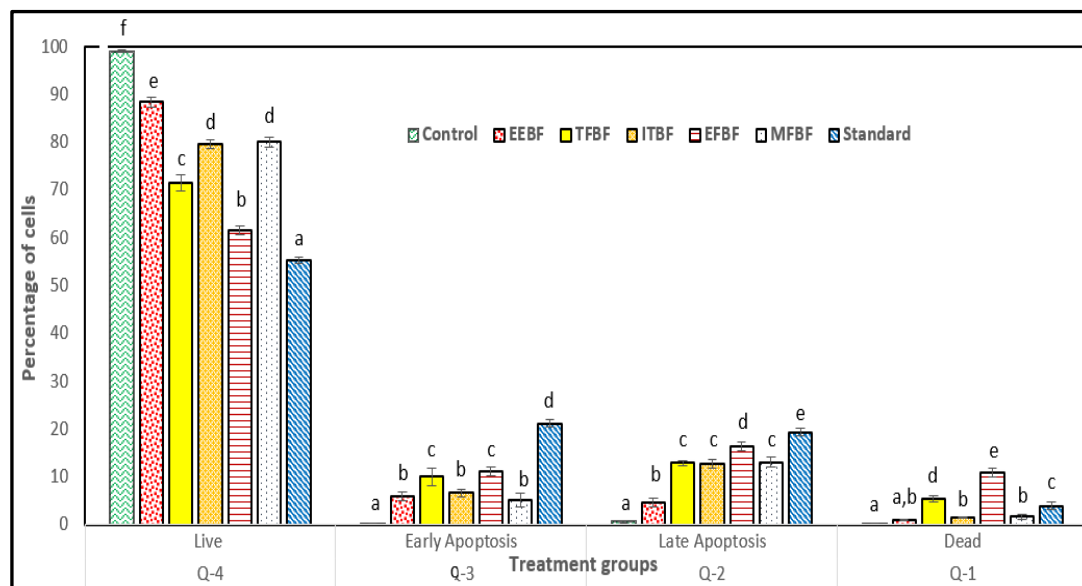


Figure 6.22: Morphological changes of HeLa cells treated with EEBF and its biofractions.



Each value is represented as the mean \pm SD (n = 3). Different superscript letters (a - f) are statistically significant (ANOVA, $p < 0.001$, and subsequent post hoc multiple comparisons with Duncan's test).

Figure 6.23: Apoptosis activity of EEBF and its biofractions against HeLa cell lines.

Table 6.15: Apoptosis analysis of EEBF and its biofractions on HeLa cell lines.

Groups	Q-4 Live (%)	Q-3 Early Apoptosis (%)	Q-2 Late Apoptosis (%)	Q-1 Dead (%)
Control	99.06 \pm 0.20 ^f	0.22 \pm 0.20 ^a	0.63 \pm 0.26 ^a	0.16 \pm 0.05 ^a
EEBF	88.43 \pm 1.07 ^c	5.93 \pm 0.87 ^b	4.69 \pm 0.89 ^b	0.97 \pm 0.22 ^{a,b}
TFBF	71.63 \pm 1.67 ^c	10.06 \pm 1.83 ^c	12.98 \pm 0.53 ^c	5.40 \pm 0.71 ^d
ITBF	79.67 \pm 1.01 ^d	6.67 \pm 0.86 ^b	12.73 \pm 0.96 ^c	1.53 \pm 0.24 ^b
EFBF	61.62 \pm 1.04 ^b	11.09 \pm 0.91 ^c	16.38 \pm 0.83 ^d	10.96 \pm 0.85 ^e
MFBF	80.09 \pm 0.98 ^d	5.17 \pm 1.39 ^b	13.07 \pm 1.03 ^c	1.70 \pm 0.49 ^b
Standard (Cisplatin)	55.40 \pm 0.66 ^a	21.23 \pm 0.85 ^d	19.37 \pm 0.76 ^e	3.99 \pm 0.72 ^c

Each value is represented as the mean \pm SD (n = 3). Different superscript letters (a - f) are statistically significant (ANOVA, $p < 0.001$, and subsequent post hoc multiple comparisons with Duncan's test).

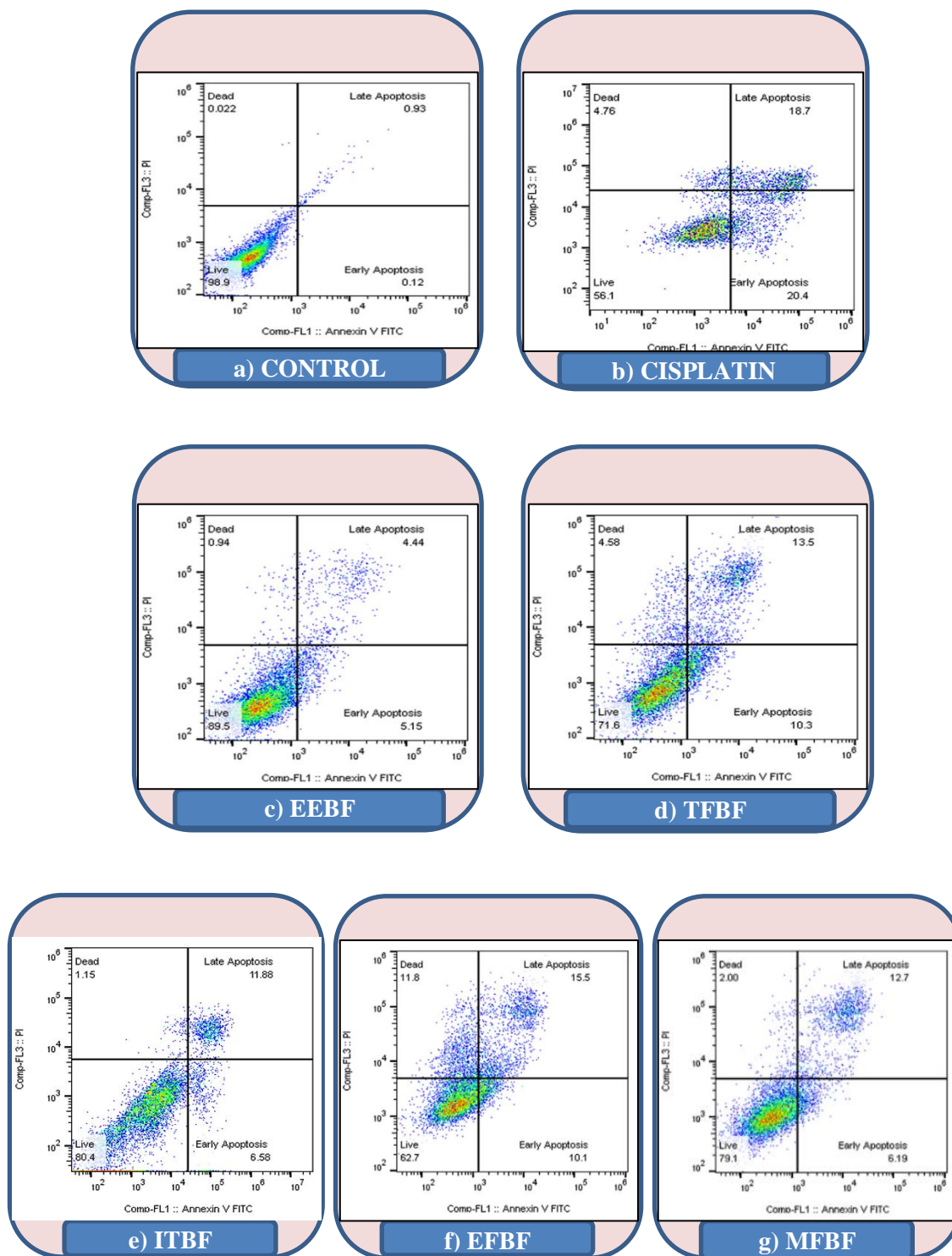
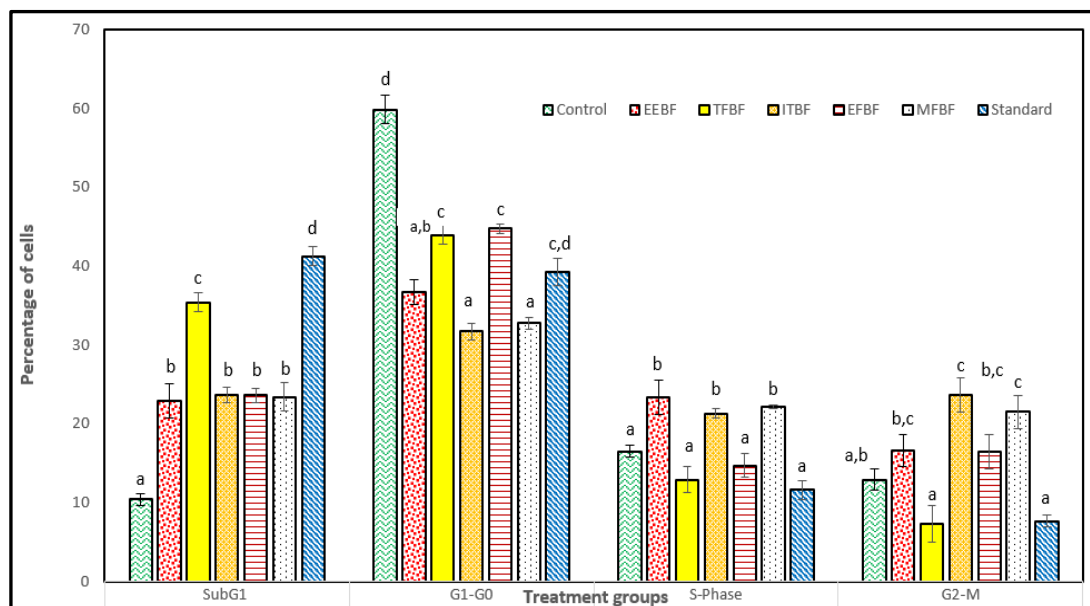


Figure 6.24: Apoptosis analysis of EEBF and its biofractions against HeLa cell lines.



Each value is represented as the mean \pm SD (n = 3). Different superscript letters (a - d) are statistically significant (ANOVA, $p < 0.001$, and subsequent post hoc multiple comparisons with Duncan's test).

Figure 6.25: Cell cycle activity of EEBF and its biofractions against HeLa cell lines.

Table 6.16: Cell cycle analysis of EEBF and its biofractions on HeLa cell lines.

Groups	SubG ₁ (%)	G ₁ -G ₀ (%)	S-Phase (%)	G ₂ -M (%)
Control	10.45 \pm 0.74 ^a	59.84 \pm 1.74 ^d	16.54 \pm 0.80 ^a	12.94 \pm 1.36 ^{a,b}
EEBF	22.87 \pm 2.21 ^b	36.67 \pm 1.53 ^{a,b}	23.34 \pm 2.13 ^b	16.65 \pm 2.03 ^{b,c}
TFBF	35.42 \pm 1.25 ^c	43.96 \pm 1.15 ^c	12.90 \pm 1.68 ^a	7.33 \pm 2.27 ^a
ITBF	23.67 \pm 1.03 ^b	31.74 \pm 1.05 ^a	21.33 \pm 0.53 ^b	23.65 \pm 2.16 ^c
EFBF	23.62 \pm 0.92 ^b	44.75 \pm 0.6 ^c	14.74 \pm 1.55 ^a	16.48 \pm 2.19 ^{b,c}
MFBF	23.41 \pm 1.76 ^b	32.74 \pm 0.75 ^a	22.14 \pm 0.26 ^b	21.49 \pm 2.07 ^c
Standard (Cisplatin)	41.25 \pm 1.25 ^d	40.57 \pm 3.04 ^{c,d}	11.64 \pm 1.18 ^a	7.65 \pm 0.74 ^a

Each value is represented as the mean \pm SD (n = 3). Different superscript letters (a - d) are statistically significant (ANOVA, $p < 0.001$, and subsequent post hoc multiple comparisons with Duncan's test).

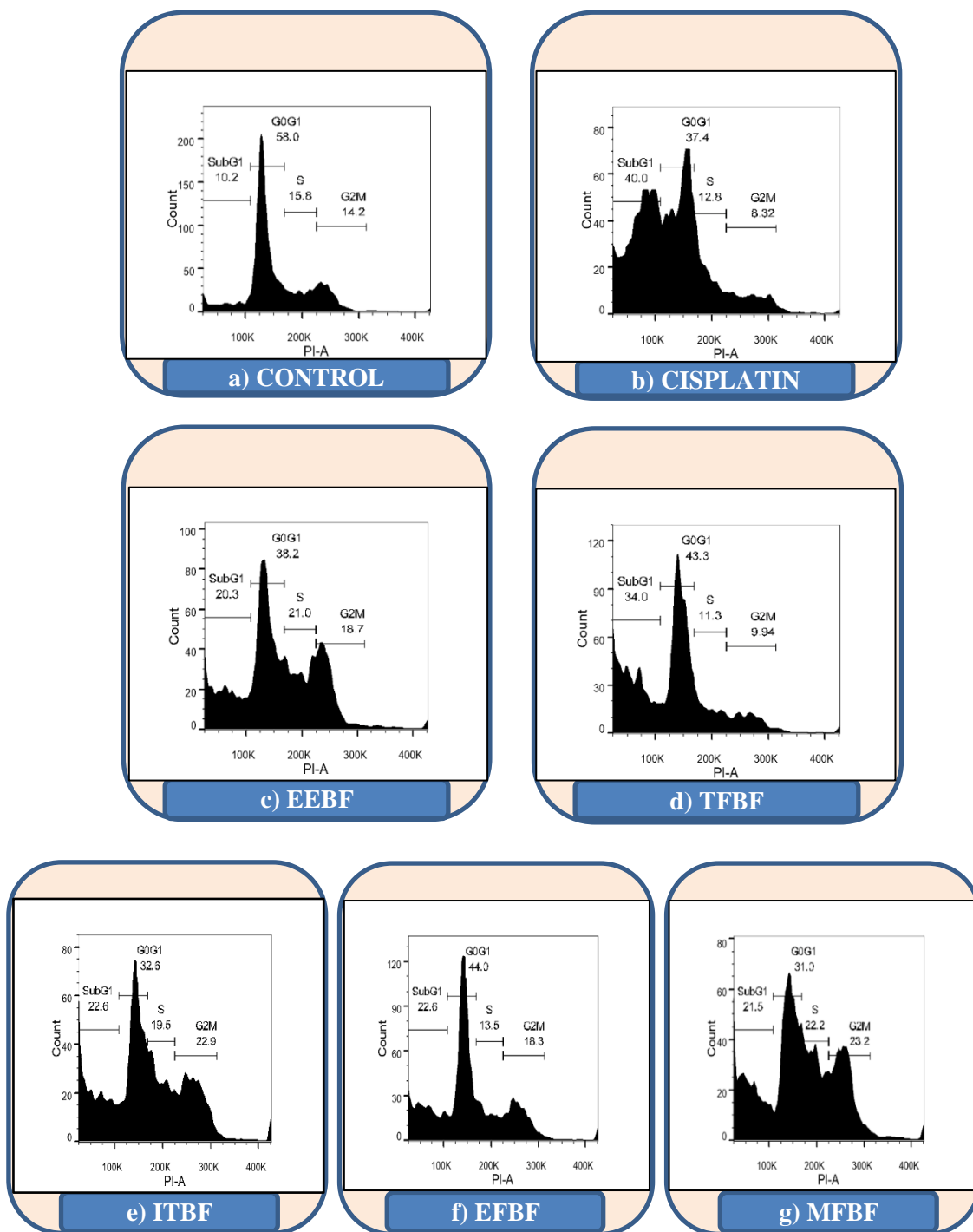
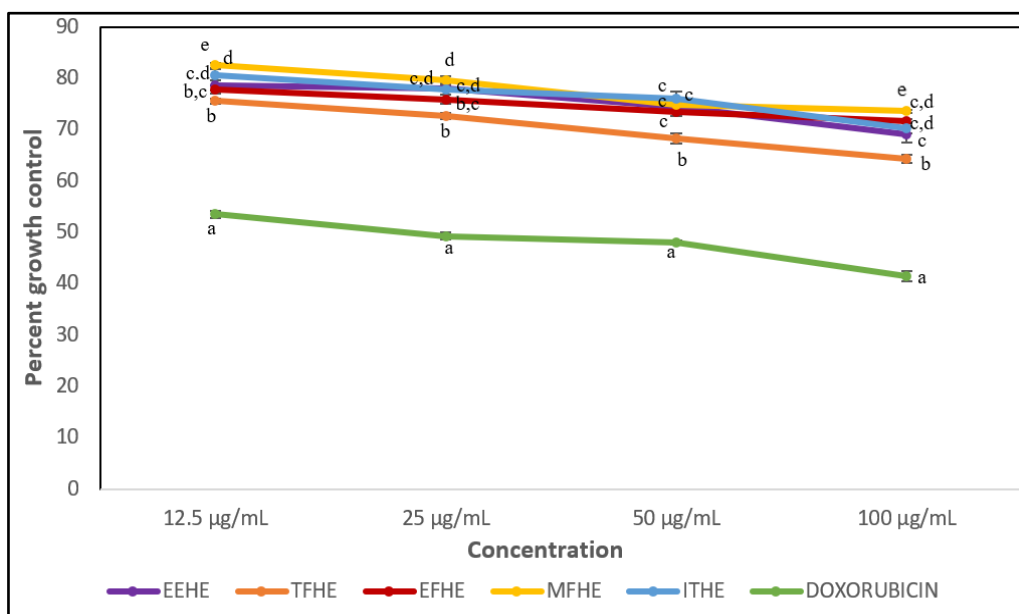


Figure 6.26: Cell cycle analysis of EEBF and its biofractions against HeLa cell lines.



Each value is represented as the mean \pm SD ($n = 3$). Within each stage, the means with different superscript letters (a - e) are statistically significant (ANOVA, $p < 0.01$, and subsequent post hoc multiple comparisons with Duncan's test).

Figure 6.27: Antiproliferative activity of EEHE and its biofractions against normal cell lines.

Table 6.17: Growth control of normal cell lines by EEHE and its biofractions.

Experimental sample	GI ₅₀ (µg/mL)
EEHE	138.8 \pm 7.35
TFHE	115.5 \pm 1.42
EFHE	139.53 \pm 1.96
MFHE	171 \pm 4.12
ITHE	160.12 \pm 2.29
Standard (Doxorubicin)	19.42 \pm 0.30

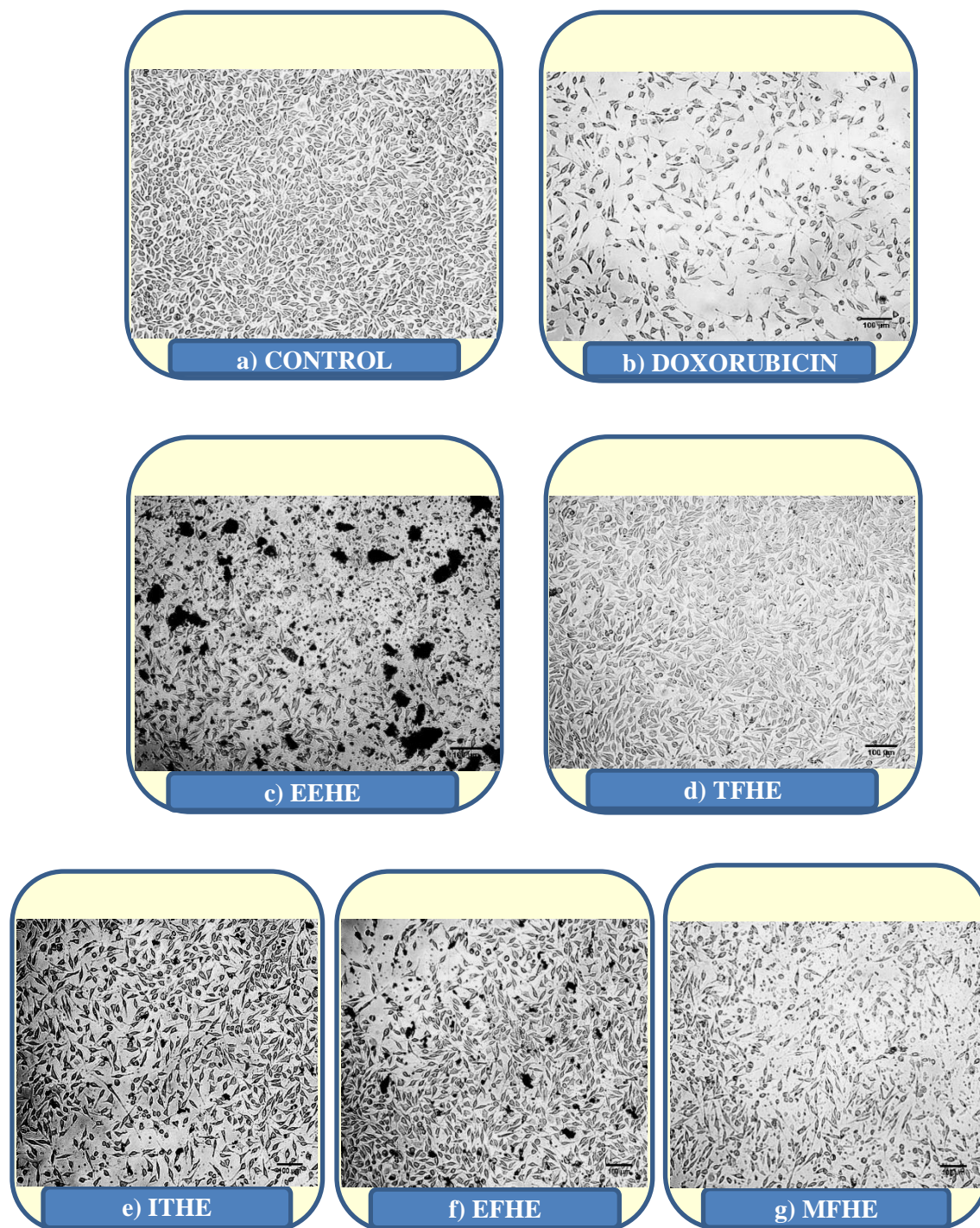
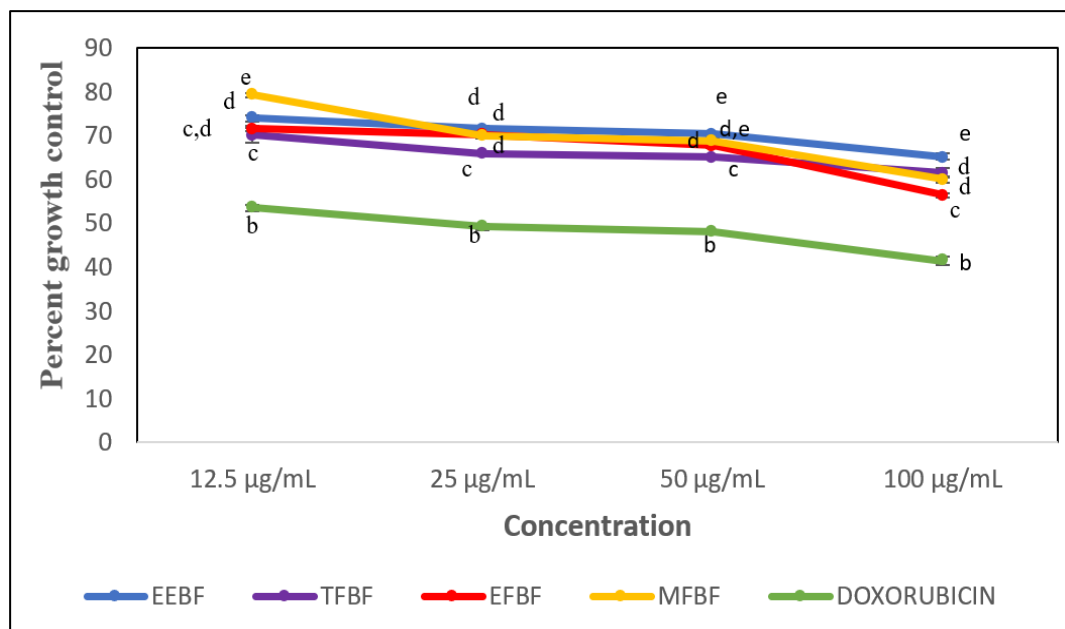


Figure 6.28: Morphological changes of normal cells treated with EEHE and its biofractions.



Each value is represented as the mean \pm SD (n = 3). Within each stage, the means with different superscript letters (a - e) are statistically significant (ANOVA, $p < 0.01$, and subsequent post hoc multiple comparisons with Duncan's test).

Figure 6.29: Antiproliferative activity of EEBF and its biofractions against normal cell lines.

Table 6.18: Growth control of normal cell lines by EEBF and its biofractions.

Experimental sample	GI ₅₀ (µg/mL)
EEBF	111.33 \pm 2.89
TFBF	135.17 \pm 2.3
ITBF	141.63 \pm 3.14
EFBF	108.2 \pm 1.64
MFBF	104.09 \pm 3.19
Standard (Doxorubicin)	19.42 \pm 0.30

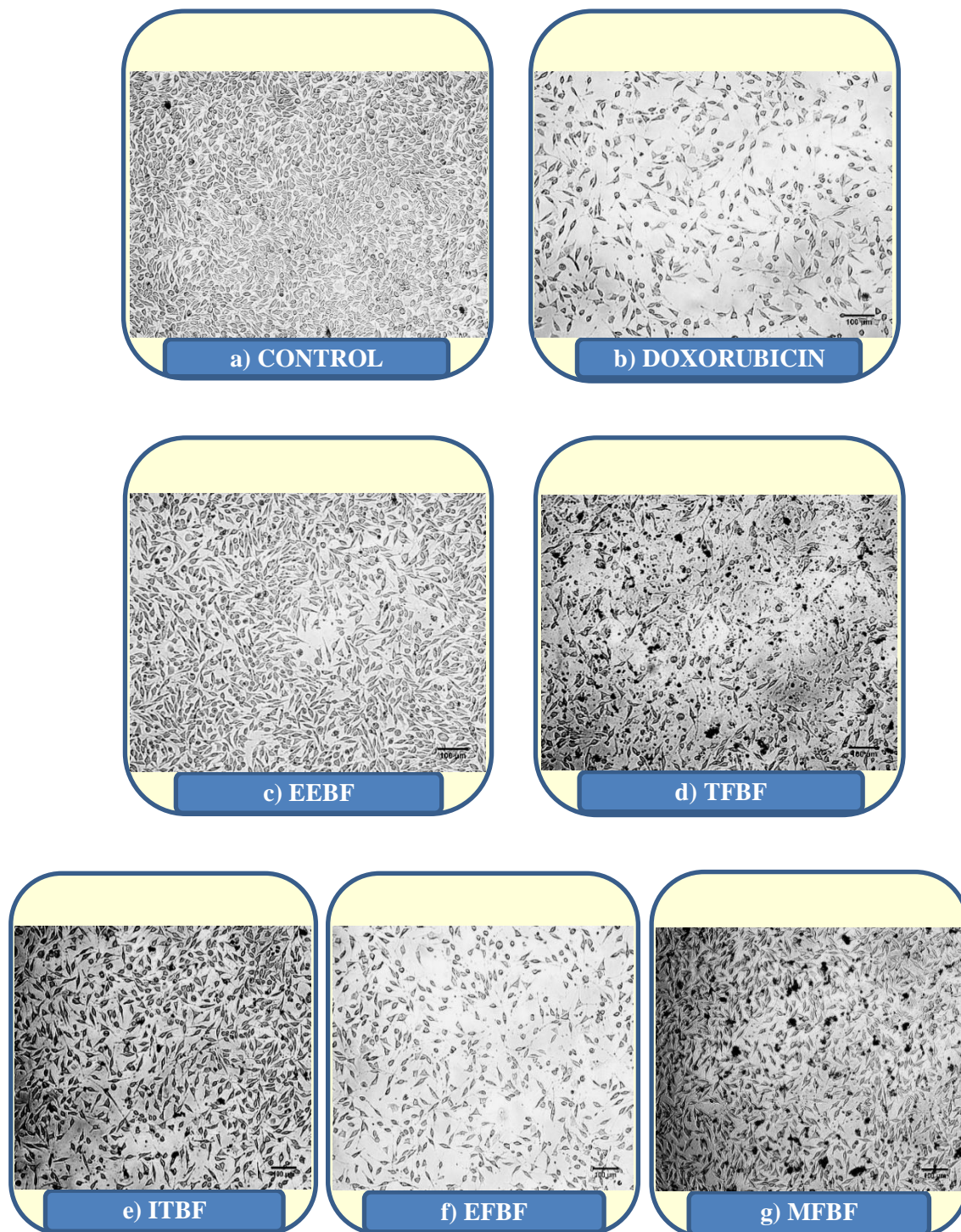


Figure 6.30: Morphological changes of normal cells treated with EEBF and its biofractions.

6.2.7. ACUTE TOXICITY STUDIES

6.2.7.1. *Hybanthus enneaspermus* Linn.

Ethanollic extract of *Hybanthus enneaspermus* Linn. was reported to be safe upto 5000 mg/kg BW as per literature. ^[65]

6.2.7.2. *Bauhinia foveolata* Dalzell.

Ethanollic extract of *Bauhinia foveolata* Dalzell. was reported to be safe upto 5000 mg/Kg BW per our study carried out under protocol No. IAEC-SLS-2021-037.

6.2.7.2.1. Clinical observations and Mortality record

Post administration of the test samples, animals were monitored for any clinical symptoms. During the first 24 h, animals in GV presented slight lethargic behavior; however there was no symptoms observed after 24 h from the dosage. During the study, no clinical or pathological symptoms were observed in any of the treatment groups.

Table 6.19: Summary of clinical signs and mortality in animals during 14 days observation period.

Group	Treatment and Dose (mg/kg BW)	Mortality
I	Normal Control	Nil
II	50	Nil
III	300	Nil
IV	2000	Nil
V	5000	Nil

6.2.7.2.2. Body weight

The body weight of all animals was recorded on Day 1, Day 7, and Day 14 of study.

Table 6.20: Summary of body weight of animals in mean \pm SD (g).

Group	Treatment and Dose (mg/kg BW)	Day		
		Day 1	Day 7	Day 14
I	Control	195.8 \pm 16.22	226.45 \pm 22.46	240.28 \pm 17.81
II	50	195.92 \pm 19.36	236.7 \pm 19.98	248.28 \pm 16.78
III	300	205.77 \pm 11.04	262.5 \pm 10.84	272.1 \pm 10.9
IV	2000	198.3 \pm 12.35	256.58 \pm 16.75	269.18 \pm 25.29
V	5000	200.87 \pm 7.78	258.82 \pm 9.45	274.36 \pm 12.1

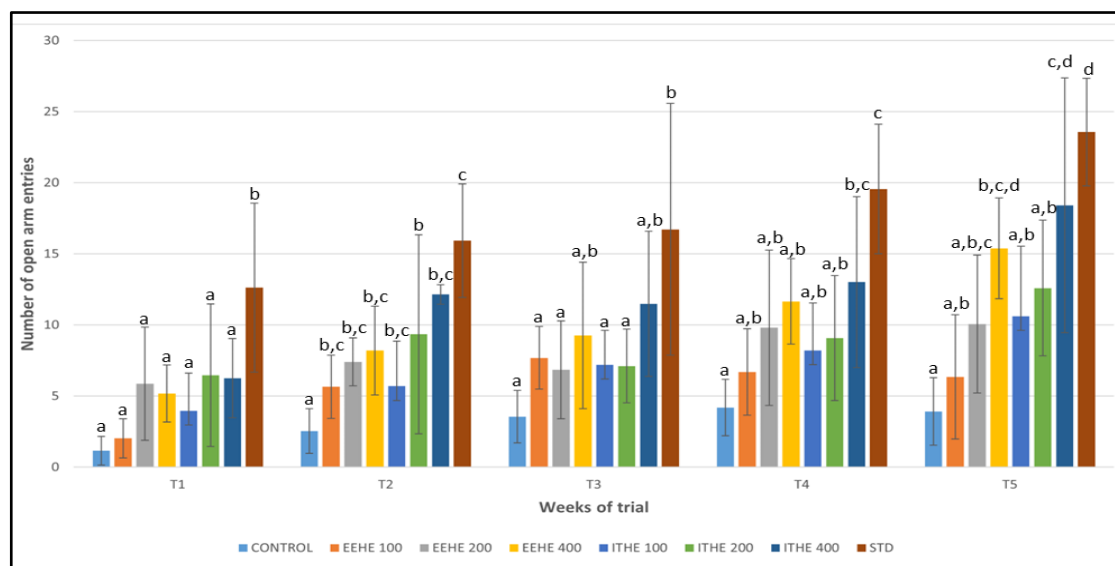
n=6; Values are Mean \pm Standard Deviation

6.2.7.2.3. Feed Consumption –

Rats were group housed in cages as per dosage regimen and were provided with *ad libitum* feed and water. Feed consumption was recorded weekly in animals group wise.

Table 6.21: Summary of weekly feed consumption in animals.

Group	Treatment and Dose (mg/kg BW)	Feed intake (g)	
		Day 1 - 7	Day 8 - 14
I	Control	236.80	322.09
II	50	278.40	313.36
III	300	325.93	307.79
IV	2000	330.80	333.46
V	5000	310.90	309.94

6.2.8. *In vivo* antianxiety studies

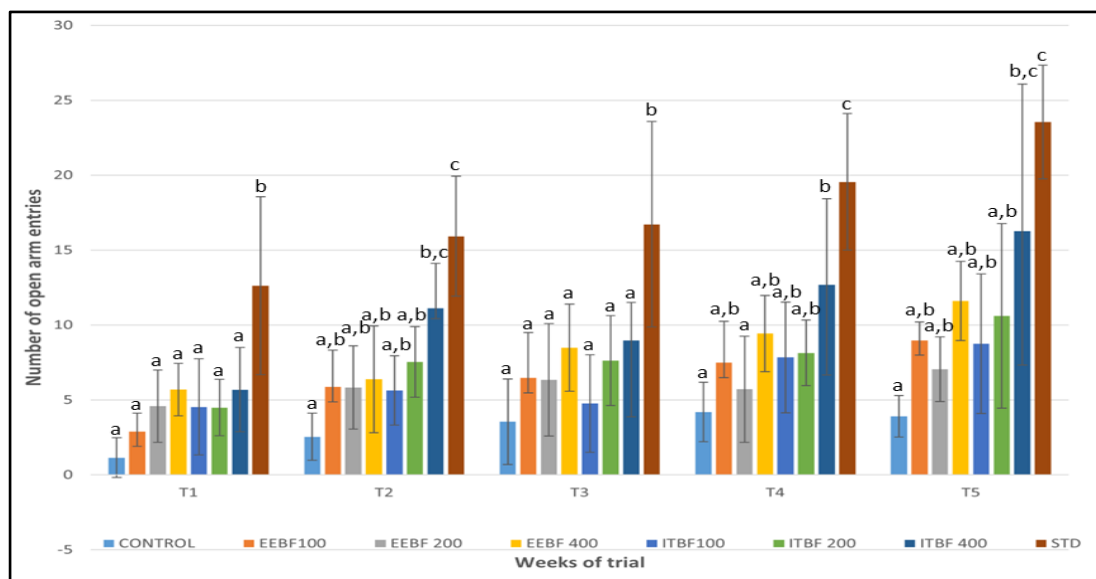
Each value is expressed as the mean \pm SD (n = 6). Different superscript letters (a - d) are statistically significant (ANOVA, $p < 0.05$, and subsequent post hoc multiple comparisons with Duncan's test).

Figure 6.31: Effect of EEHE, ITHE control and Diazepam on number of open arm entries (NOE) using Elevated Plus Maze model.

Table 6.22: Effect of EEHE, ITHE, control and Diazepam on NOE in EPM (Nos.).

Group	T1	T2	T3	T4	T5
Control	1.16 \pm 1.00 ^a	2.54 \pm 1.57 ^a	3.55 \pm 1.85 ^a	4.20 \pm 1.99 ^a	3.92 \pm 2.38 ^a
EEHE 100	2.03 \pm 1.38 ^a	5.65 \pm 2.22 ^{b,c}	7.68 \pm 2.20 ^a	6.69 \pm 3.04 ^{a,b}	6.34 \pm 4.37 ^{a,b}
EEHE 200	5.86 \pm 3.98 ^a	7.41 \pm 1.68 ^{b,c}	6.84 \pm 3.44 ^a	9.80 \pm 5.47 ^{a,b}	10.06 \pm 4.85 ^{a,b,c}
EEHE 400	5.18 \pm 2.01 ^a	8.20 \pm 3.12 ^{b,c}	9.27 \pm 5.15 ^{a,b}	11.65 \pm 3.01 ^{a,b}	15.39 \pm 3.54 ^{b,c,d}
ITHE 100	3.96 \pm 2.65 ^a	5.69 \pm 3.18 ^{b,c}	7.19 \pm 2.42 ^a	8.21 \pm 3.34 ^{a,b}	10.61 \pm 4.92 ^{a,b}
ITHE 200	6.46 \pm 5.02 ^a	9.34 \pm 7.00 ^b	7.11 \pm 2.60 ^a	9.07 \pm 4.39 ^{a,b}	12.59 \pm 4.77 ^{a,b}
ITHE 400	6.26 \pm 2.79 ^a	12.15 \pm 0.69 ^{b,c}	11.49 \pm 5.10 ^{a,b}	13.01 \pm 6.00 ^{b,c}	18.41 \pm 8.95 ^{c,d}
Standard (Diazepam)	12.62 \pm 5.94 ^b	15.93 \pm 4.00 ^c	16.72 \pm 8.85 ^b	19.56 \pm 4.55 ^c	23.56 \pm 3.79 ^d

Each value is expressed as the mean \pm SD (n = 6). Different superscript letters (a - d) are statistically significant (ANOVA, $p < 0.05$, and subsequent post hoc multiple comparisons with Duncan's test).



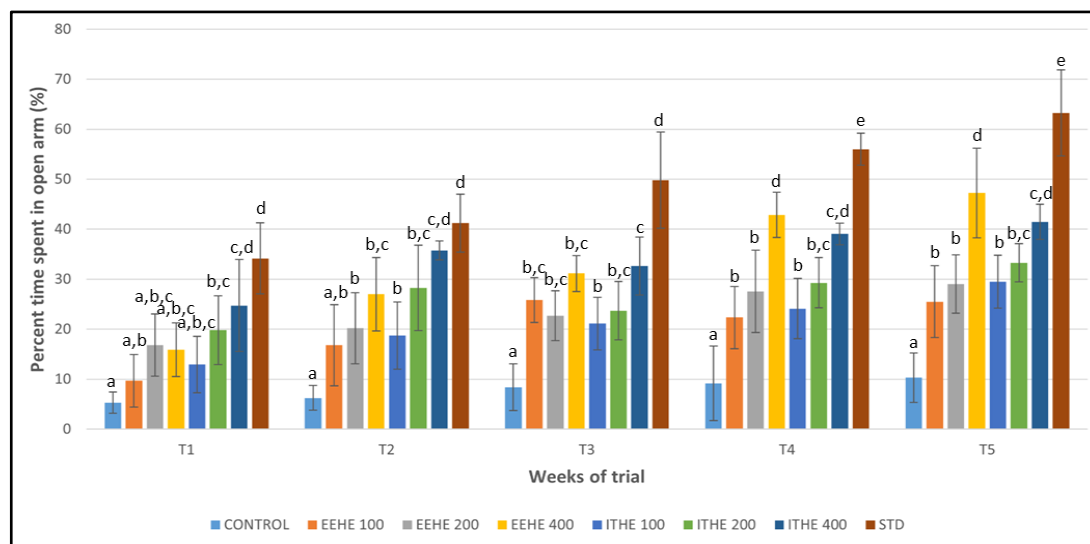
Each value is expressed as the mean \pm SD (n = 6). Different superscript letters (a - c) are statistically significant (ANOVA, $p < 0.05$, and subsequent post hoc multiple comparisons with Duncan's test).

Figure 6.32: Effect of EEBF, ITBF, control and Diazepam on number of open arm entries (NOE) using Elevated Plus Maze model.

Table 6.23: Effect of EEBF, ITBF, control and Diazepam on NOE in EPM (Nos.).

Group	T1	T2	T3	T4	T5
Control	1.16 \pm 1.32 ^a	2.54 \pm 1.57 ^a	3.55 \pm 2.85 ^a	4.20 \pm 1.99 ^a	3.92 \pm 1.38 ^a
EEBF 100	2.90 \pm 1.21 ^a	5.88 \pm 2.43 ^{a,b}	6.47 \pm 3.02 ^a	7.49 \pm 2.76 ^{a,b}	8.98 \pm 1.23 ^{a,b}
EEBF200	4.59 \pm 2.41 ^a	5.83 \pm 2.78 ^{a,b}	6.34 \pm 3.74 ^a	5.72 \pm 3.54 ^a	7.06 \pm 2.16 ^{a,b}
EEBF 400	5.70 \pm 1.75 ^a	6.38 \pm 3.56 ^{a,b}	8.49 \pm 2.90 ^a	9.43 \pm 2.54 ^{a,b}	11.61 \pm 2.65 ^{a,b}
ITBF 100	4.54 \pm 3.21 ^a	5.64 \pm 2.31 ^{a,b}	4.77 \pm 3.25 ^a	7.84 \pm 3.6 ^{a,b}	8.76 \pm 4.66 ^{a,b}
ITBF 200	4.49 \pm 1.87 ^a	7.55 \pm 2.35 ^{a,b}	7.63 \pm 2.99 ^a	8.15 \pm 2.18 ^{a,b}	10.61 \pm 6.15 ^{a,b}
ITBF 400	5.67 \pm 2.84 ^a	11.12 \pm 3.00 ^{b,c}	8.98 \pm 2.52 ^a	12.68 \pm 5.76 ^b	16.28 \pm 9.8 ^{b,c}
Standard (Diazepam)	12.62 \pm 5.94 ^b	15.93 \pm 4.00 ^c	16.72 \pm 6.85 ^b	19.56 \pm 4.55 ^c	23.56 \pm 3.79 ^c

Each value is expressed as the mean \pm SD (n = 6). Different superscript letters (a - c) are statistically significant (ANOVA, $p < 0.05$, and subsequent post hoc multiple comparisons with Duncan's test).



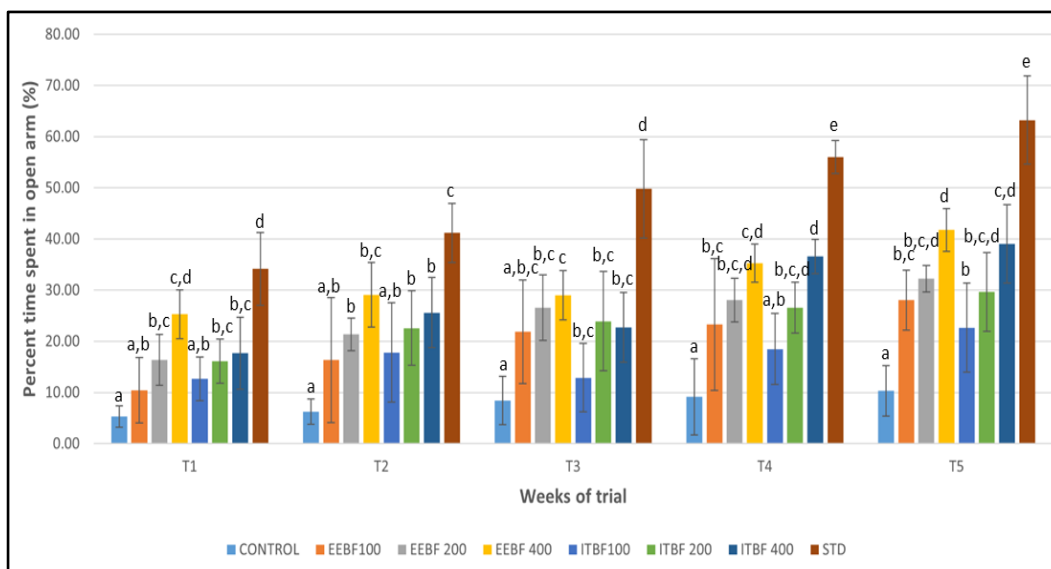
Each value is expressed as the mean \pm SD (n = 6). Different superscript letters (a-e) are statistically significant (ANOVA, $p < 0.05$, and subsequent post hoc multiple comparisons with Duncan's test).

Figure 6.33: Effect of EEHE, ITHE, control and Diazepam on percent time spent in open arm (PTSO) using Elevated Plus Maze model.

Table 6.24: Effect of EEHE, ITHE, control and Diazepam on PTSO in EPM (%).

Group	T1	T2	T3	T4	T5
Control	5.31 \pm 2.11 ^a	6.25 \pm 2.48 ^a	8.41 \pm 4.69 ^a	9.15 \pm 7.47 ^a	10.31 \pm 4.95 ^a
EEHE 100	9.67 \pm 5.23 ^{a,b}	16.79 \pm 8.10 ^{a,b}	25.82 \pm 4.50 ^{b,c}	22.33 \pm 6.22 ^b	25.50 \pm 7.18 ^b
EEHE 200	16.83 \pm 6.23 ^{a,b,c}	20.19 \pm 7.10 ^b	22.71 \pm 4.99 ^{b,c}	27.55 \pm 8.23 ^b	29.02 \pm 5.82 ^b
EEHE 400	15.89 \pm 5.40 ^{a,b,c}	26.97 \pm 7.37 ^{b,c}	31.15 \pm 3.59 ^{b,c}	42.88 \pm 4.52 ^d	47.22 \pm 8.94 ^d
ITHE 100	12.91 \pm 5.66 ^{a,b,c}	18.71 \pm 6.76 ^b	21.14 \pm 5.25 ^b	24.10 \pm 6.01 ^b	29.47 \pm 5.28 ^b
ITHE 200	19.79 \pm 6.87 ^{b,c}	28.25 \pm 8.56 ^{b,c}	23.70 \pm 5.85 ^{b,c}	29.28 \pm 5.00 ^{b,c}	33.29 \pm 3.84 ^{b,c}
ITHE 400	24.72 \pm 9.19 ^{c,d}	35.76 \pm 1.91 ^{c,d}	32.62 \pm 5.77 ^c	39.06 \pm 2.17 ^{c,d}	41.45 \pm 3.52 ^{c,d}
Standard (Diazepam)	34.15 \pm 7.09 ^d	41.19 \pm 5.77 ^d	49.81 \pm 9.62 ^d	56.01 \pm 3.23 ^e	63.23 \pm 8.61 ^e

Each value is expressed as the mean \pm SD (n = 6). Different superscript letters (a-e) are statistically significant (ANOVA, $p < 0.05$, and subsequent post hoc multiple comparisons with Duncan's test).



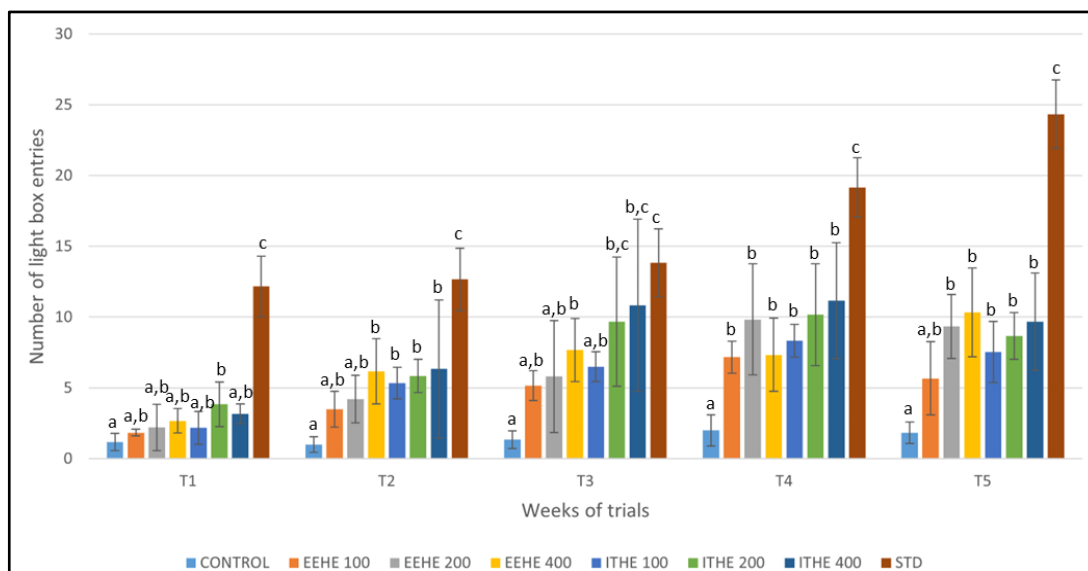
Each value is expressed as the mean \pm SD (n = 6). Different superscript letters (a - e) are statistically significant (ANOVA, $p < 0.05$, and subsequent post hoc multiple comparisons with Duncan's test).

Figure 6.34: Effect of EEBF, ITBF, control and Diazepam on percent time spent in open arm (PTSO) using Elevated Plus Maze model.

Table 6.25: Effect of EEBF, ITBF, control and Diazepam on PTSO in EPM (%).

Group	T1	T2	T3	T4	T5
Control	5.31 \pm 2.11 ^a	6.25 \pm 2.48 ^a	8.41 \pm 4.69 ^a	9.15 \pm 7.47 ^a	10.31 \pm 4.95 ^a
EEBF 100	10.42 \pm 6.43 ^{a,b}	16.32 \pm 2.21 ^{a,b}	21.86 \pm 0.11 ^{a,b,c}	23.31 \pm 2.88 ^{b,c}	28.06 \pm 5.85 ^{b,c}
EEBF 200	16.38 \pm 4.97 ^{b,c}	21.37 \pm 3.19 ^b	26.57 \pm 6.41 ^{b,c}	28.05 \pm 4.26 ^{b,c,d}	32.24 \pm 2.58 ^{b,c,d}
EEBF 400	25.29 \pm 4.77 ^{c,d}	29.08 \pm 6.30 ^{b,c}	29.00 \pm 4.84 ^c	35.26 \pm 3.71 ^{c,d}	41.77 \pm 4.21 ^d
ITBF 100	12.68 \pm 4.27 ^{a,b}	17.82 \pm 9.73 ^{a,b}	12.88 \pm 6.70 ^{b,c}	18.49 \pm 6.98 ^{a,b}	22.65 \pm 8.70 ^b
ITBF 200	16.12 \pm 4.34 ^{b,c}	22.58 \pm 7.27 ^b	23.93 \pm 9.70 ^{b,c}	26.60 \pm 4.98 ^{b,c,d}	29.66 \pm 7.70 ^{b,c,d}
ITBF 400	17.66 \pm 7.00 ^{b,c}	25.58 \pm 6.88 ^b	22.73 \pm 6.81 ^{b,c}	36.57 \pm 3.36 ^d	39.03 \pm 7.65 ^{c,d}
Standard (Diazepam)	34.15 \pm 7.09 ^d	41.19 \pm 5.77 ^c	49.81 \pm 9.62 ^d	56.01 \pm 3.23 ^e	63.23 \pm 8.61 ^e

Each value is expressed as the mean \pm SD (n = 6). Different superscript letters (a - e) are statistically significant (ANOVA, $p < 0.05$, and subsequent post hoc multiple comparisons with Duncan's test).



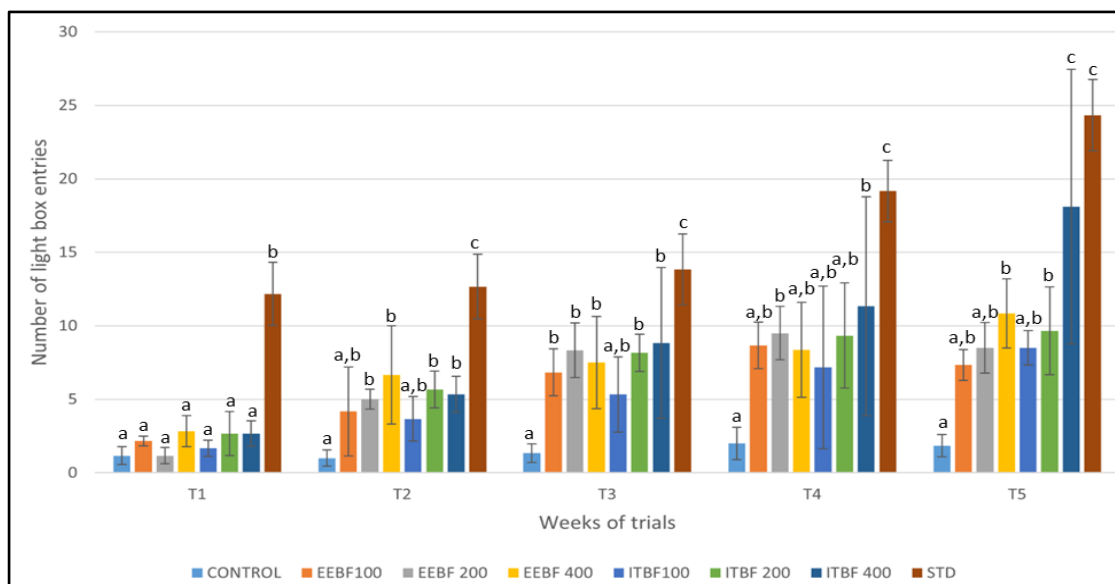
Each value is expressed as the mean \pm SD (n = 6). Different superscript letters (a - c) are statistically significant (ANOVA, $p < 0.05$, and subsequent post hoc multiple comparisons with Duncan's test).

Figure 6.35: Effect of EEHE, ITHE, control and Diazepam on number of light box entries (NLE) using Light and Dark transition model.

Table 6.26: Effect of EEHE, ITHE, control and Diazepam on NLE in LDT (Nos.).

Group	T1	T2	T3	T4	T5
Control	1.17 \pm 0.60 ^a	1.00 \pm 0.55 ^a	1.33 \pm 0.63 ^a	2.00 \pm 1.10 ^a	1.83 \pm 0.75 ^a
EEHE 100	1.83 \pm 0.24 ^{a,b}	3.50 \pm 1.26 ^{a,b}	5.17 \pm 1.06 ^{a,b}	7.17 \pm 1.13 ^b	5.67 \pm 2.58 ^{a,b}
EEHE 200	2.20 \pm 1.64 ^{a,b}	4.20 \pm 1.68 ^{a,b}	5.80 \pm 3.95 ^{a,b}	9.83 \pm 3.93 ^b	9.33 \pm 2.24 ^b
EEHE 400	2.67 \pm 0.86 ^{a,b}	6.17 \pm 2.31 ^b	7.67 \pm 2.24 ^b	7.33 \pm 2.58 ^b	10.33 \pm 3.14 ^b
ITHE 100	2.17 \pm 1.16 ^{a,b}	5.33 \pm 1.12 ^b	6.50 \pm 1.06 ^{a,b}	8.33 \pm 1.16 ^b	7.53 \pm 2.17 ^b
ITHE 200	3.83 \pm 1.56 ^b	5.83 \pm 1.17 ^b	9.67 \pm 4.56 ^{b,c}	10.17 \pm 3.60 ^b	8.67 \pm 1.64 ^b
ITHE 400	3.17 \pm 0.69 ^{a,b}	6.33 \pm 4.87 ^b	10.83 \pm 6.08 ^{b,c}	11.17 \pm 4.08 ^b	9.67 \pm 3.44 ^b
Standard (Diazepam)	12.17 \pm 2.14 ^c	12.67 \pm 2.20 ^c	13.83 \pm 2.40 ^c	19.17 \pm 2.10 ^c	24.33 \pm 2.42 ^c

Each value is expressed as the mean \pm SD (n = 6). Different superscript letters (a - c) are statistically significant (ANOVA, $p < 0.05$, and subsequent post hoc multiple comparisons with Duncan's test).



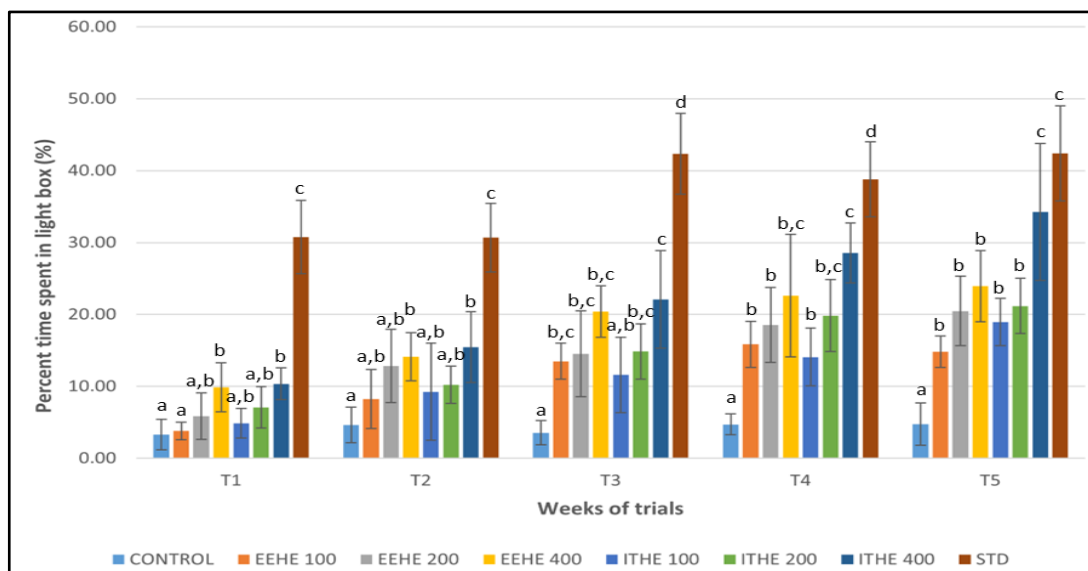
Each value is expressed as the mean \pm SD (n = 6). Different superscript letters (a - c) are statistically significant (ANOVA, $p < 0.05$, and subsequent post hoc multiple comparisons with Duncan's test).

Figure 6.36: Effect of EEBF, ITBF, control and Diazepam on number of light box entries (NLE) using Light and Dark transition model.

Table 6.27: Effect of EEBF, ITBF, control and Diazepam on NLE in LDT (Nos.).

Group	T1	T2	T3	T4	T5
Control	1.17 \pm 0.60 ^a	1.00 \pm 0.55 ^a	1.37 \pm 0.63 ^a	2.00 \pm 1.10 ^a	1.83 \pm 0.75 ^a
EEBF 100	2.17 \pm 0.33 ^a	4.17 \pm 3.03 ^{a,b}	6.83 \pm 1.60 ^b	8.67 \pm 1.59 ^{a,b}	7.33 \pm 1.03 ^{a,b}
EEBF 200	1.17 \pm 0.54 ^a	5.00 \pm 0.67 ^b	8.33 \pm 1.86 ^b	9.50 \pm 1.81 ^b	8.50 \pm 1.72 ^{a,b}
EEBF 400	2.83 \pm 1.07 ^a	6.67 \pm 3.34 ^b	7.50 \pm 3.15 ^b	8.37 \pm 3.22 ^{a,b}	10.83 \pm 2.36 ^b
ITBF 100	1.67 \pm 0.55 ^a	3.67 \pm 1.51 ^{a,b}	5.33 \pm 2.56 ^{a,b}	7.17 \pm 5.54 ^{a,b}	8.50 \pm 1.18 ^{a,b}
ITBF 200	2.67 \pm 1.51 ^a	5.67 \pm 1.25 ^b	8.17 \pm 1.26 ^b	9.33 \pm 3.57 ^{a,b}	9.65 \pm 2.99 ^b
ITBF 400	2.67 \pm 0.86 ^a	5.33 \pm 1.23 ^b	8.83 \pm 5.14 ^b	11.33 \pm 7.44 ^b	18.11 \pm 9.34 ^c
Standard (Diazepam)	12.17 \pm 2.14 ^b	12.67 \pm 2.20 ^c	13.83 \pm 2.40 ^c	19.17 \pm 2.10 ^c	24.33 \pm 2.42 ^c

Each value is expressed as the mean \pm SD (n = 6). Different superscript letters (a - c) are statistically significant (ANOVA, $p < 0.05$, and subsequent post hoc multiple comparisons with Duncan's test).



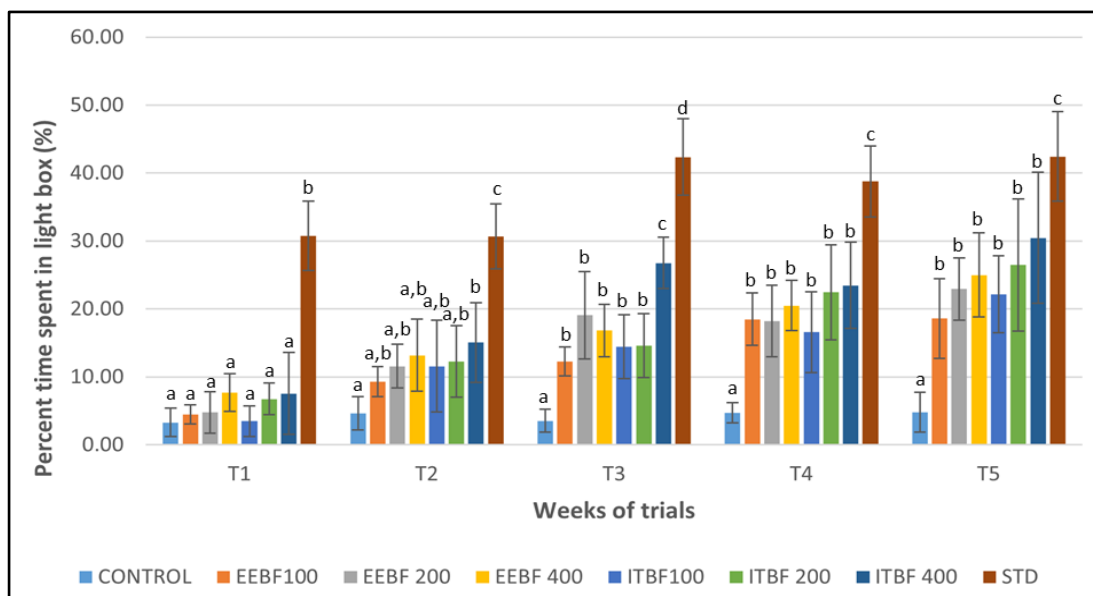
Each value is expressed as the mean \pm SD (n = 6). Different superscript letters (a-d) are statistically significant (ANOVA, $p < 0.05$, and subsequent post hoc multiple comparisons with Duncan's test).

Figure 6.37: Effect of EEHE, ITHE, control and Diazepam on percent time spent in light box (PTSL) using Light and Dark transition model.

Table 6.28: Effect of EEHE, ITHE, control and Diazepam on PTSL in LDT (%).

Group	T1	T2	T3	T4	T5
Control	3.29 \pm 2.11 ^a	4.63 \pm 2.48 ^a	3.53 \pm 1.69 ^a	4.71 \pm 1.47 ^a	4.77 \pm 2.95 ^a
EEHE 100	3.80 \pm 1.23 ^a	8.25 \pm 4.10 ^{a,b}	13.50 \pm 2.50 ^{b,c}	15.83 \pm 3.22 ^b	14.80 \pm 2.18 ^b
EEHE 200	5.83 \pm 3.23 ^{a,b}	12.86 \pm 5.10 ^{a,b}	14.53 \pm 5.99 ^{b,c}	18.55 \pm 5.23 ^b	20.48 \pm 4.82 ^b
EEHE 400	9.89 \pm 3.40 ^b	14.11 \pm 3.37 ^b	20.40 \pm 3.59 ^{b,c}	22.60 \pm 8.52 ^{b,c}	23.94 \pm 4.94 ^b
ITHE 100	4.84 \pm 2.06 ^{a,b}	9.25 \pm 6.76 ^{a,b}	11.60 \pm 5.25 ^{a,b}	14.08 \pm 4.01 ^b	18.96 \pm 3.28 ^b
ITHE 200	7.08 \pm 2.87 ^{a,b}	10.22 \pm 2.56 ^{a,b}	14.86 \pm 3.85 ^{b,c}	19.84 \pm 5.00 ^{b,c}	21.17 \pm 3.84 ^b
ITHE 400	10.36 \pm 2.19 ^b	15.45 \pm 4.91 ^b	22.10 \pm 6.77 ^c	28.57 \pm 4.17 ^c	34.24 \pm 9.52 ^c
Standard (Diazepam)	30.75 \pm 5.09 ^c	30.69 \pm 4.77 ^c	42.36 \pm 5.62 ^d	38.79 \pm 5.23 ^d	42.43 \pm 6.61 ^c

Each value is expressed as the mean \pm SD (n = 6). Different superscript letters (a-d) are statistically significant (ANOVA, $p < 0.05$, and subsequent post hoc multiple comparisons with Duncan's test).



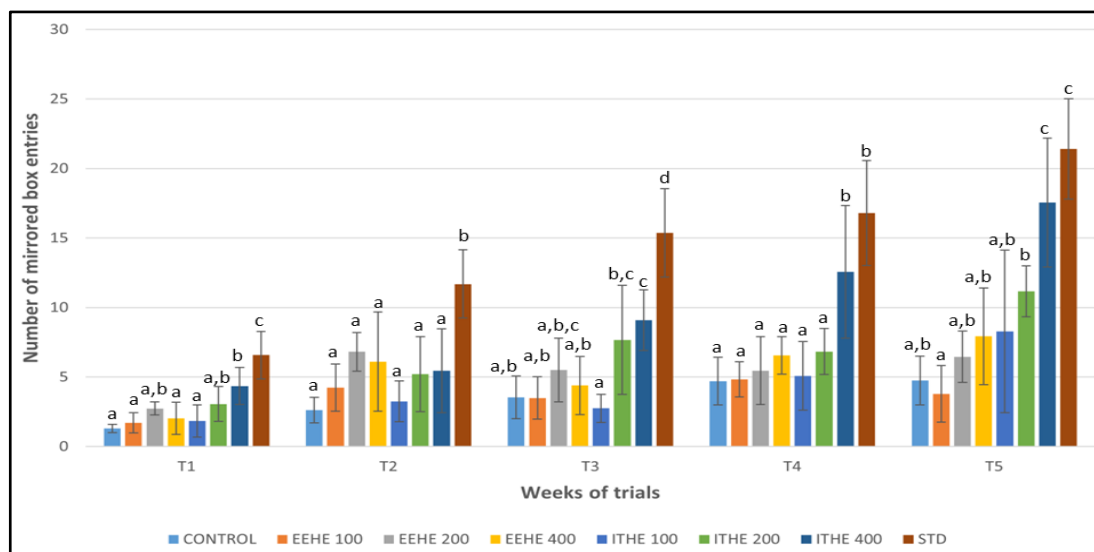
Each value is expressed as the mean \pm SD (n = 6). Different superscript letters (a - d) are statistically significant (ANOVA, $p < 0.05$, and subsequent post hoc multiple comparisons with Duncan's test).

Figure 6.38: Effect of EEBF, ITBF, control and Diazepam on percent time spent in light box (PTSL) using Light and Dark transition model.

Table 6.29: Effect of EEBF, ITBF, control and Diazepam on PTSL in LDT (%).

Group	T1	T2	T3	T4	T5
Control	3.29 \pm 2.11 ^a	4.63 \pm 2.48 ^a	3.53 \pm 1.69 ^a	4.71 \pm 1.47 ^a	4.77 \pm 2.95 ^a
EEBF 100	4.46 \pm 1.43 ^a	9.32 \pm 2.21 ^{a,b}	12.29 \pm 2.11 ^b	18.49 \pm 3.88 ^b	18.58 \pm 5.85 ^b
EEBF 200	4.75 \pm 3.06 ^a	11.57 \pm 3.19 ^{a,b}	19.08 \pm 6.41 ^b	18.22 \pm 5.26 ^b	22.92 \pm 4.58 ^b
EEBF 400	7.67 \pm 2.77 ^a	13.18 \pm 5.30 ^{a,b}	16.83 \pm 3.84 ^b	20.49 \pm 3.71 ^b	24.99 \pm 6.21 ^b
ITBF 100	3.48 \pm 2.27 ^a	11.58 \pm 6.73 ^{a,b}	14.42 \pm 4.70 ^b	16.57 \pm 5.98 ^b	22.15 \pm 5.70 ^b
ITBF 200	6.75 \pm 2.34 ^a	12.26 \pm 5.27 ^{a,b}	14.57 \pm 4.70 ^b	22.45 \pm 6.98 ^b	26.46 \pm 9.70 ^b
ITBF 400	7.56 \pm 6.00 ^a	15.06 \pm 5.88 ^b	26.77 \pm 3.81 ^c	23.46 \pm 6.36 ^b	30.46 \pm 9.65 ^b
Standard (Diazepam)	30.75 \pm 5.09 ^b	30.69 \pm 4.77 ^c	42.36 \pm 5.62 ^d	38.79 \pm 5.23 ^c	42.43 \pm 6.61 ^c

Each value is expressed as the mean \pm SD (n = 6). Different superscript letters (a - d) are statistically significant (ANOVA, $p < 0.05$, and subsequent post hoc multiple comparisons with Duncan's test).



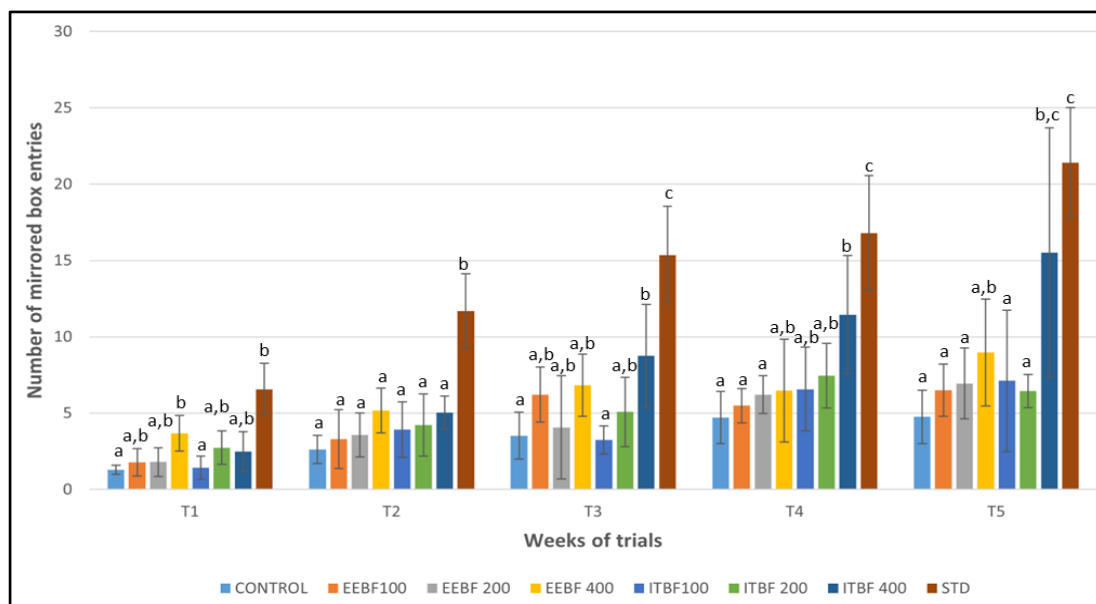
Each value is expressed as the mean \pm SD (n = 6). Different superscript letters (a - d) are statistically significant (ANOVA, $p < 0.05$, and subsequent post hoc multiple comparisons with Duncan's test).

Figure 6.39: Effect of EEHE, ITHE, control and Diazepam on number of mirrored chamber entries (NME) using Mirror chamber test model.

Table 6.30: Effect of EEHE, ITHE, control and Diazepam on NME in MCT (Nos.).

Group	T1	T2	T3	T4	T5
Control	1.29 \pm 0.29 ^a	2.62 \pm 0.92 ^a	3.53 \pm 1.53 ^{a,b}	4.71 \pm 1.71 ^a	4.76 \pm 1.76 ^{a,b}
EEHE 100	1.70 \pm 0.72 ^a	4.24 \pm 1.69 ^a	3.50 \pm 1.51 ^{a,b}	4.83 \pm 1.27 ^a	3.79 \pm 2.05 ^a
EEHE 200	2.73 \pm 0.48 ^{a,b}	6.82 \pm 1.39 ^a	5.51 \pm 2.28 ^{a,b,c}	5.46 \pm 2.45 ^a	6.46 \pm 1.85 ^{a,b}
EEHE 400	2.02 \pm 1.15 ^a	6.11 \pm 3.58 ^a	4.39 \pm 2.09 ^{a,b}	6.56 \pm 1.35 ^a	7.93 \pm 3.48 ^{a,b}
ITHE 100	1.84 \pm 1.16 ^a	3.25 \pm 1.48 ^a	2.75 \pm 1.01 ^a	5.08 \pm 2.47 ^a	8.28 \pm 5.85 ^{a,b}
ITHE 200	3.07 \pm 1.24 ^{a,b}	5.21 \pm 2.69 ^a	7.67 \pm 3.93 ^{b,c}	6.84 \pm 1.65 ^a	11.17 \pm 1.83 ^b
ITHE 400	4.35 \pm 1.33 ^b	5.45 \pm 3.02 ^a	9.09 \pm 2.18 ^c	12.56 \pm 4.77 ^b	17.55 \pm 4.64 ^c
Standard (Diazepam)	6.57 \pm 1.70 ^c	11.69 \pm 2.45 ^b	15.36 \pm 3.18 ^d	16.79 \pm 3.77 ^b	21.40 \pm 3.61 ^c

Each value is expressed as the mean \pm SD (n = 6). Different superscript letters (a - d) are statistically significant (ANOVA, $p < 0.05$, and subsequent post hoc multiple comparisons with Duncan's test).



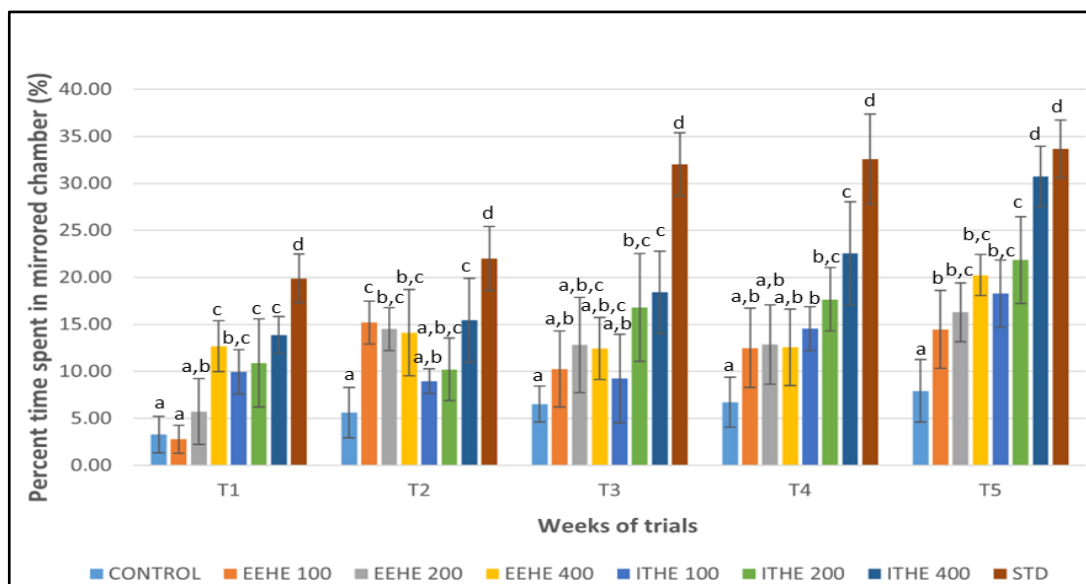
Each value is expressed as the mean \pm SD (n = 6). Different superscript letters (a - c) are statistically significant (ANOVA, $p < 0.05$, and subsequent post hoc multiple comparisons with Duncan's test).

Figure 6.40: Effect of EEBF, ITBF, control and Diazepam on number of mirrored chamber entries (NME) using Mirror chamber test model.

Table 6.31: Effect of EEBF, ITBF, control and Diazepam on NME in MCT (Nos.).

Group	T1	T2	T3	T4	T5
Control	1.29 \pm 0.29 ^a	2.62 \pm 0.92 ^a	3.53 \pm 1.53 ^a	4.71 \pm 1.71 ^a	4.76 \pm 1.76 ^a
EEBF 100	1.77 \pm 0.89 ^{a,b}	3.30 \pm 1.92 ^a	6.22 \pm 1.79 ^{a,b}	5.49 \pm 1.12 ^a	6.50 \pm 1.72 ^a
EEBF200	1.80 \pm 0.93 ^{a,b}	3.57 \pm 1.44 ^a	4.07 \pm 3.38 ^{a,b}	6.22 \pm 1.24 ^a	6.95 \pm 2.32 ^a
EEBF 400	3.67 \pm 1.17 ^b	5.18 \pm 1.47 ^a	6.82 \pm 2.04 ^{a,b}	6.48 \pm 3.37 ^{a,b}	8.98 \pm 3.50 ^{a,b}
ITBF 100	1.43 \pm 0.77 ^a	3.92 \pm 1.82 ^a	3.25 \pm 0.92 ^a	6.57 \pm 2.74 ^{a,b}	7.12 \pm 4.63 ^a
ITBF 200	2.74 \pm 1.09 ^{a,b}	4.21 \pm 2.03 ^a	5.08 \pm 2.27 ^{a,b}	7.45 \pm 2.12 ^{a,b}	6.45 \pm 1.09 ^a
ITBF 400	2.49 \pm 1.30 ^{a,b}	5.04 \pm 1.07 ^a	8.75 \pm 3.37 ^b	11.45 \pm 3.88 ^b	15.52 \pm 8.16 ^{b,c}
Standard (Diazepam)	6.57 \pm 1.70 ^b	11.69 \pm 2.45 ^b	15.36 \pm 3.18 ^c	16.79 \pm 3.77 ^c	21.40 \pm 3.61 ^c

Each value is expressed as the mean \pm SD (n = 6). Different superscript letters (a - c) are statistically significant (ANOVA, $p < 0.05$, and subsequent post hoc multiple comparisons with Duncan's test).



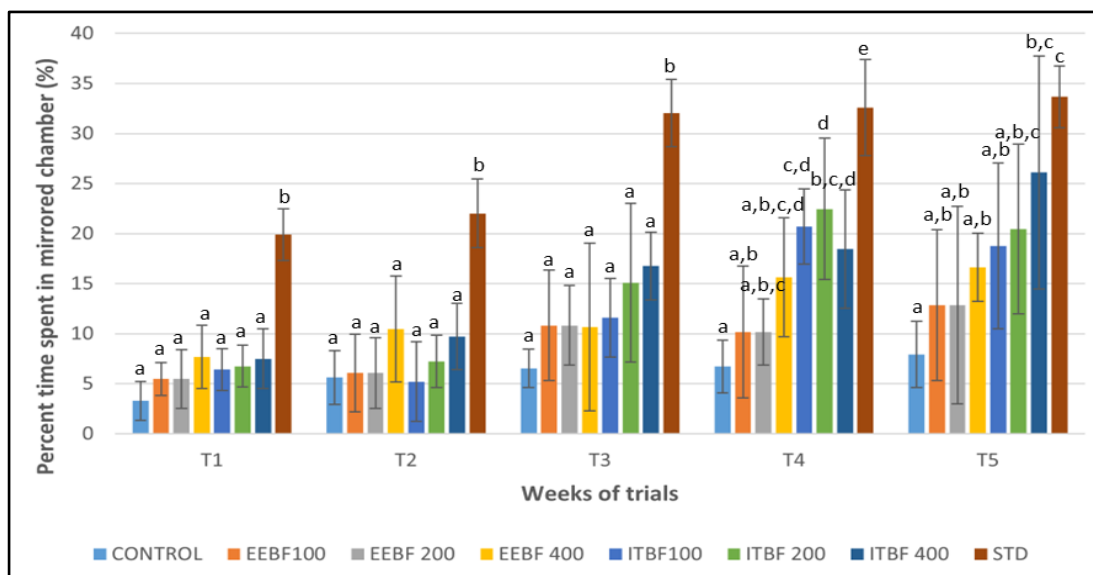
Each value is expressed as the mean \pm SD (n = 6). Different superscript letters (a - d) are statistically significant (ANOVA, $p < 0.05$, and subsequent post hoc multiple comparisons with Duncan's test).

Figure 6.41: Effect of EEHE, ITHE, control and Diazepam on percent time spent in mirror chamber (PTSM) using Mirror chamber test model.

Table 6.32: Effect of EEHE, ITHE, control and Diazepam on PTSM in MCT (%).

Group	T1	T2	T3	T4	T5
Control	3.29 \pm 1.94 ^a	5.62 \pm 2.69 ^a	6.53 \pm 1.93 ^a	6.71 \pm 2.65 ^a	7.92 \pm 3.32 ^a
EEHE 100	2.79 \pm 1.48 ^a	15.21 \pm 2.28 ^c	10.24 \pm 4.06 ^{a,b}	12.50 \pm 4.23 ^{a,b}	14.46 \pm 4.13 ^b
EEHE 200	5.73 \pm 3.48 ^{a,b}	14.51 \pm 2.28 ^{b,c}	12.82 \pm 5.06 ^{a,b,c}	12.86 \pm 4.23 ^{a,b}	16.29 \pm 3.13 ^{b,c}
EEHE 400	12.69 \pm 2.72 ^c	14.11 \pm 4.58 ^{b,c}	12.43 \pm 3.32 ^{a,b,c}	12.56 \pm 4.06 ^{a,b}	20.23 \pm 2.19 ^{b,c}
ITHE 100	9.96 \pm 2.37 ^{b,c}	8.96 \pm 1.33 ^{a,b}	9.25 \pm 4.71 ^{a,b}	14.56 \pm 2.34 ^b	18.28 \pm 3.58 ^{b,c}
ITHE 200	10.90 \pm 4.71 ^c	10.21 \pm 3.33 ^{a,b,c}	16.80 \pm 5.71 ^{b,c}	17.67 \pm 3.37 ^{b,c}	21.84 \pm 4.62 ^c
ITHE 400	13.85 \pm 1.96 ^c	15.45 \pm 4.48 ^c	18.43 \pm 4.37 ^c	22.56 \pm 5.47 ^c	30.73 \pm 3.21 ^d
Standard (Diazepam)	19.88 \pm 2.58 ^d	22.01 \pm 3.42 ^d	32.04 \pm 3.37 ^d	32.58 \pm 4.80 ^d	33.66 \pm 3.09 ^d

Each value is expressed as the mean \pm SD (n = 6). Different superscript letters (a - d) are statistically significant (ANOVA, $p < 0.05$, and subsequent post hoc multiple comparisons with Duncan's test).



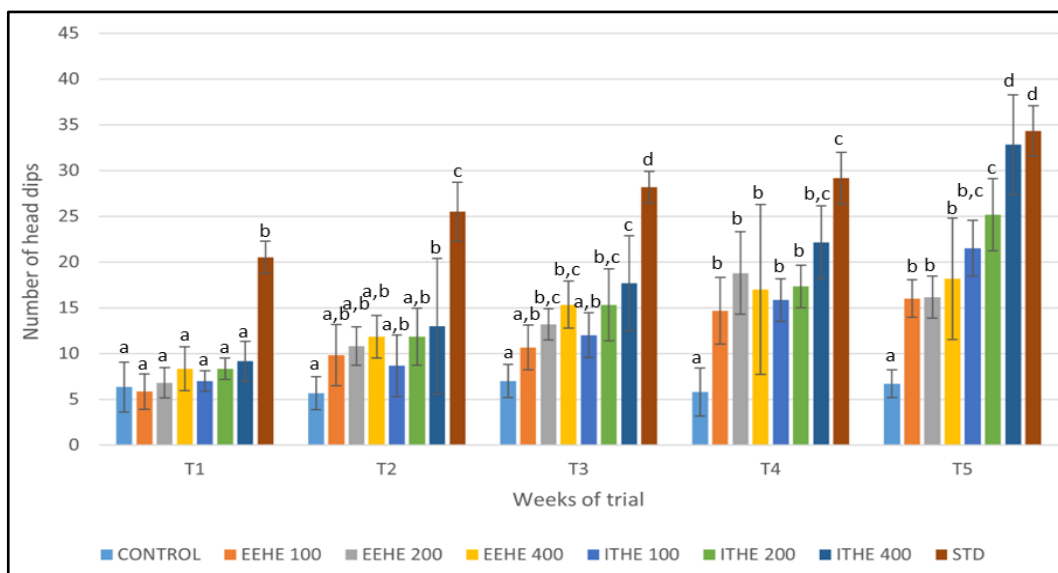
Each value is expressed as the mean \pm SD ($n = 6$). Different superscript letters (a - e) are statistically significant (ANOVA, $p < 0.05$, and subsequent post hoc multiple comparisons with Duncan's test).

Figure 6.42: Effect of EEBF, ITBF, control and Diazepam on percent time spent in mirror chamber (PTSM) using Mirror chamber test model.

Table 6.33: Effect of EEBF, ITBF, control and Diazepam on PTSM in MCT (%).

Group	T1	T2	T3	T4	T5
Control	3.29 \pm 1.94 ^a	5.62 \pm 2.69 ^a	6.53 \pm 1.93 ^a	6.71 \pm 2.65 ^a	7.92 \pm 3.32 ^a
EEBF 100	5.46 \pm 1.65 ^a	6.07 \pm 3.88 ^a	10.83 \pm 5.50 ^a	10.16 \pm 6.59 ^{a,b}	12.83 \pm 7.53 ^{a,b}
EEBF200	4.80 \pm 2.93 ^a	5.06 \pm 3.54 ^a	8.78 \pm 3.99 ^a	12.46 \pm 3.29 ^{a,b,c}	13.61 \pm 9.86 ^{a,b}
EEBF 400	7.67 \pm 3.17 ^a	10.46 \pm 5.29 ^a	10.66 \pm 8.37 ^a	15.64 \pm 5.93 ^{a,b,c,d}	16.64 \pm 3.40 ^{a,b}
ITBF 100	6.43 \pm 2.00 ^a	5.21 \pm 3.98 ^a	11.58 \pm 3.94 ^a	20.70 \pm 3.76 ^{c,d}	18.78 \pm 8.28 ^{a,b}
ITBF 200	6.74 \pm 2.09 ^a	7.21 \pm 2.62 ^a	15.08 \pm 7.94 ^a	22.45 \pm 7.06 ^d	20.45 \pm 8.48 ^{a,b,c}
ITBF 400	7.50 \pm 2.99 ^a	9.71 \pm 3.32 ^a	16.75 \pm 3.40 ^a	18.45 \pm 5.92 ^{b,c,d}	26.12 \pm 1.64 ^{b,c}
Standard (Diazepam)	19.88 \pm 2.58 ^b	22.01 \pm 3.42 ^b	32.04 \pm 3.37 ^b	32.58 \pm 4.80 ^e	33.66 \pm 3.09 ^c

Each value is expressed as the mean \pm SD ($n = 6$). Different superscript letters (a - e) are statistically significant (ANOVA, $p < 0.05$, and subsequent post hoc multiple comparisons with Duncan's test).



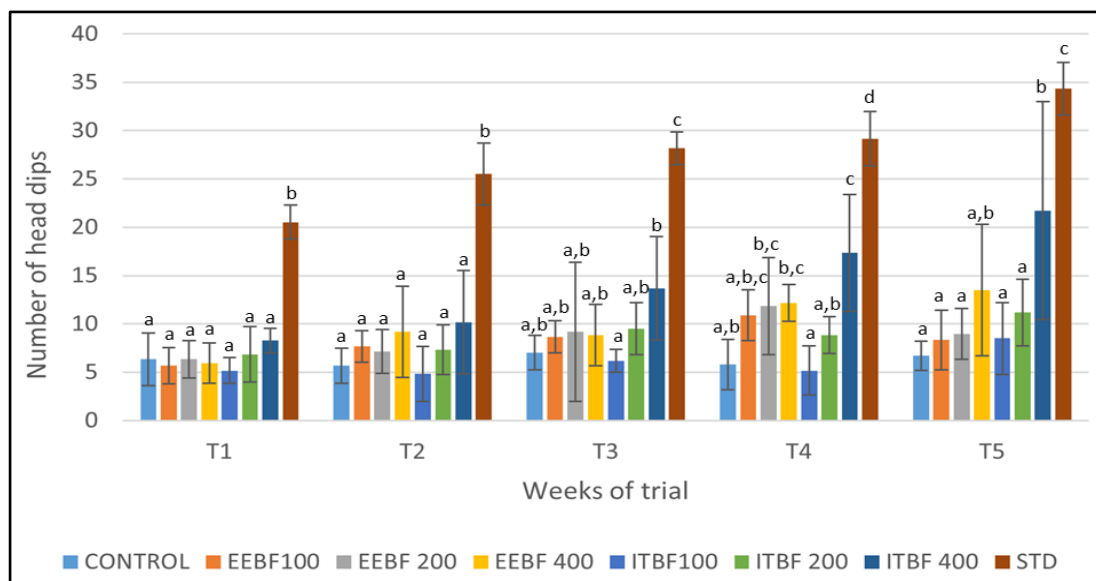
Each value is expressed as the mean \pm SD (n = 6). Different superscript letters (a - d) are statistically significant (ANOVA, $p < 0.05$, and subsequent post hoc multiple comparisons with Duncan's test).

Figure 6.43: Effect of EEHE, ITHE, control and Diazepam on number of head dips using Hole board test model.

Table 6.34: Effect of EEHE, ITHE, control and Diazepam on head dips in HBT (No.)

Group	T1	T2	T3	T4	T5
Control	6.33 \pm 2.73 ^a	5.67 \pm 1.80 ^a	7.00 \pm 1.79 ^a	5.79 \pm 2.61 ^a	6.70 \pm 1.51 ^a
EEHE 100	5.83 \pm 1.91 ^a	9.83 \pm 3.34 ^{a,b}	10.67 \pm 2.46 ^{a,b}	14.67 \pm 3.64 ^b	16.00 \pm 2.05 ^b
EEHE 200	6.80 \pm 1.64 ^a	10.80 \pm 2.10 ^{a,b}	13.20 \pm 1.70 ^{b,c}	18.80 \pm 4.49 ^b	16.17 \pm 2.30 ^b
EEHE 400	8.33 \pm 2.42 ^a	11.83 \pm 2.32 ^{a,b}	15.33 \pm 2.56 ^{b,c}	17.00 \pm 9.27 ^b	18.17 \pm 6.64 ^b
ITHE 100	7.00 \pm 1.10 ^a	8.67 \pm 3.37 ^{a,b}	12.00 \pm 2.43 ^{a,b}	15.83 \pm 2.31 ^b	21.50 \pm 3.06 ^{b,c}
ITHE 200	8.33 \pm 1.18 ^a	11.83 \pm 3.12 ^{a,b}	15.33 \pm 3.94 ^{b,c}	17.33 \pm 2.34 ^b	25.17 \pm 3.92 ^c
ITHE 400	9.17 \pm 2.18 ^a	13.00 \pm 7.42 ^b	17.67 \pm 5.21 ^c	22.17 \pm 3.95 ^{b,c}	32.83 \pm 5.45 ^d
Standard (Diazepam)	20.53 \pm 1.76 ^b	25.50 \pm 3.23 ^c	28.17 \pm 1.71 ^d	29.17 \pm 2.82 ^c	34.33 \pm 2.73 ^d

Each value is expressed as the mean \pm SD (n = 6). Different superscript letters (a - d) are statistically significant (ANOVA, $p < 0.05$, and subsequent post hoc multiple comparisons with Duncan's test).



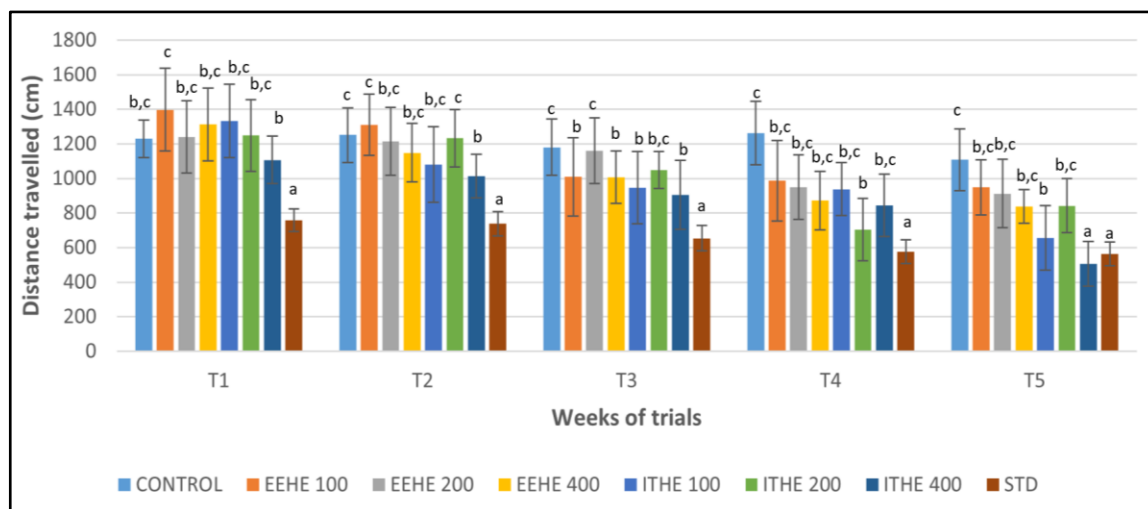
Each value is expressed as the mean \pm SD (n = 6). Different superscript letters (a - c) are statistically significant (ANOVA, $p < 0.05$, and subsequent post hoc multiple comparisons with Duncan's test).

Figure 6.44: Effect of EEBF, ITBF, control and Diazepam on number of head dips using Hole board test model.

Table 6.35: Effect of EEBF, ITBF, control and Diazepam on head dips in HBT (No.).

Group	T1	T2	T3	T4	T5
Control	6.33 \pm 2.73 ^a	5.67 \pm 1.80 ^a	7.00 \pm 1.79 ^{a,b}	5.79 \pm 2.61 ^{a,b}	6.70 \pm 1.51 ^a
EEBF 100	5.67 \pm 1.88 ^a	7.67 \pm 1.63 ^a	8.67 \pm 1.67 ^{a,b}	10.88 \pm 2.62 ^{a,b,c}	8.33 \pm 3.07 ^a
EEBF200	6.33 \pm 1.93 ^a	7.17 \pm 2.26 ^a	9.17 \pm 7.22 ^{a,b}	11.83 \pm 4.99 ^{b,c}	8.94 \pm 2.62 ^a
EEBF 400	5.95 \pm 2.10 ^a	9.17 \pm 4.72 ^a	8.83 \pm 3.19 ^{a,b}	12.17 \pm 11.92 ^{b,c}	13.50 \pm 6.81 ^{a,b}
ITBF 100	5.17 \pm 1.33 ^a	4.83 \pm 2.83 ^a	6.17 \pm 1.17 ^a	5.17 \pm 2.54 ^a	8.50 \pm 3.72 ^a
ITBF 200	6.83 \pm 2.86 ^a	7.33 \pm 2.56 ^a	9.50 \pm 2.68 ^{a,b}	8.83 \pm 1.93 ^{a,b}	11.17 \pm 3.43 ^a
ITBF 400	8.28 \pm 1.26 ^a	10.17 \pm 5.36 ^a	13.67 \pm 5.35 ^b	17.33 \pm 6.02 ^c	21.71 \pm 11.27 ^b
Standard (Diazepam)	20.53 \pm 1.76 ^b	25.50 \pm 3.23 ^b	28.17 \pm 1.71 ^c	29.17 \pm 2.82 ^d	34.33 \pm 2.73 ^c

Each value is expressed as the mean \pm SD (n = 6). Different superscript letters (a - c) are statistically significant (ANOVA, $p < 0.05$, and subsequent post hoc multiple comparisons with Duncan's test).



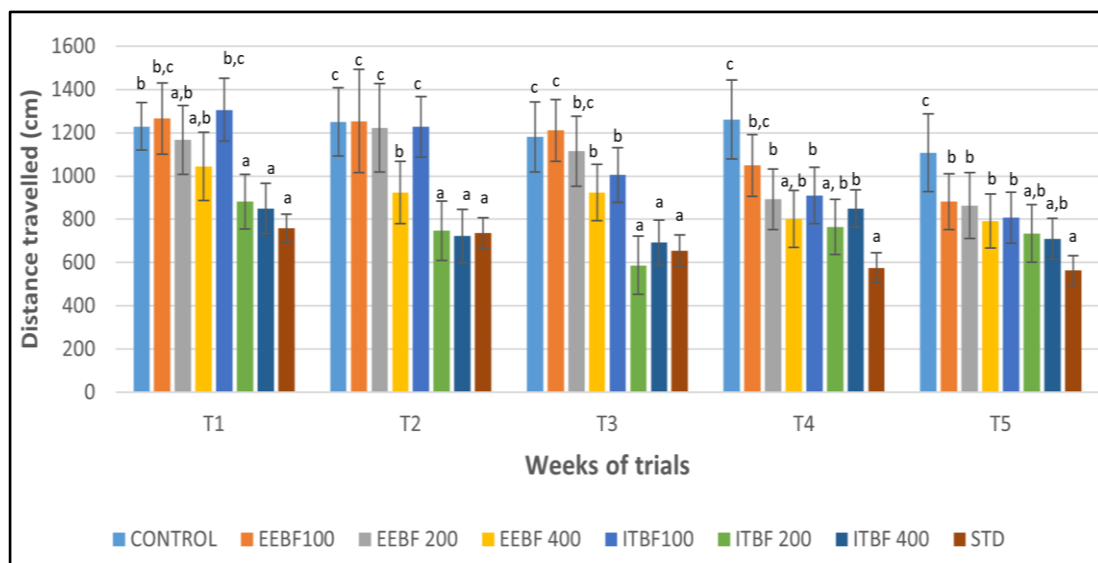
Each value is expressed as the mean \pm SD (n = 6). Different superscript letters (a - c) are statistically significant (ANOVA, $p < 0.05$, and subsequent post hoc multiple comparisons with Duncan's test).

Figure 6.45: Effect of EEHE, ITHE, control and Diazepam on distance travelled (DT) using Optovarimex model.

Table 6.36: Effect of EEHE, ITHE, control and Diazepam on DT (cm) in OPV.

Group	T1	T2	T3	T4	T5
Control	1228.50 \pm 109.08 ^{b,c}	1250.83 \pm 158.06 ^c	1180.17 \pm 162.12 ^c	1262.17 \pm 182.44 ^c	1107.33 \pm 178.76 ^c
EEHE 100	1397.50 \pm 239.41 ^c	1309.33 \pm 177.57 ^c	1008.33 \pm 227.38 ^b	987.33 \pm 233.21 ^{b,c}	948.00 \pm 160.69 ^{b,c}
EEHE 200	1240.33 \pm 209.84 ^{b,c}	1214.26 \pm 197.85 ^{b,c}	1160.17 \pm 191.14 ^c	950.67 \pm 186.88 ^{b,c}	912.17 \pm 198.13 ^{b,c}
EEHE 400	1312.17 \pm 202.34 ^{b,c}	1148.50 \pm 168.85 ^{b,c}	1007.16 \pm 152.14 ^b	871.17 \pm 16.89 ^{b,c}	838.00 \pm 98.13 ^{b,c}
ITHE 100	1333.33 \pm 12.02 ^{b,c}	1080.17 \pm 217.12 ^{b,c}	946.17 \pm 209.54 ^b	937.67 \pm 152.55 ^{b,c}	655.67 \pm 185.77 ^b
ITHE 200	1247.67 \pm 207.10 ^{b,c}	1232.00 \pm 167.10 ^c	1047.80 \pm 107.82 ^{b,c}	704.40 \pm 180.65 ^b	841.20 \pm 156.22 ^{b,c}
ITHE 400	1106.00 \pm 137.10 ^b	1013.00 \pm 127.10 ^b	905.67 \pm 199.82 ^b	844.50 \pm 185.50 ^{b,c}	505.00 \pm 130.22 ^a
Standard (Diazepam)	758.33 \pm 66.02 ^a	737.17 \pm 69.19 ^a	653.60 \pm 72.48 ^a	575.63 \pm 68.60 ^a	562.83 \pm 69.11 ^a

Each value is expressed as the mean \pm SD (n = 6). Different superscript letters (a - c) are statistically significant (ANOVA, $p < 0.05$, and subsequent post hoc multiple comparisons with Duncan's test).



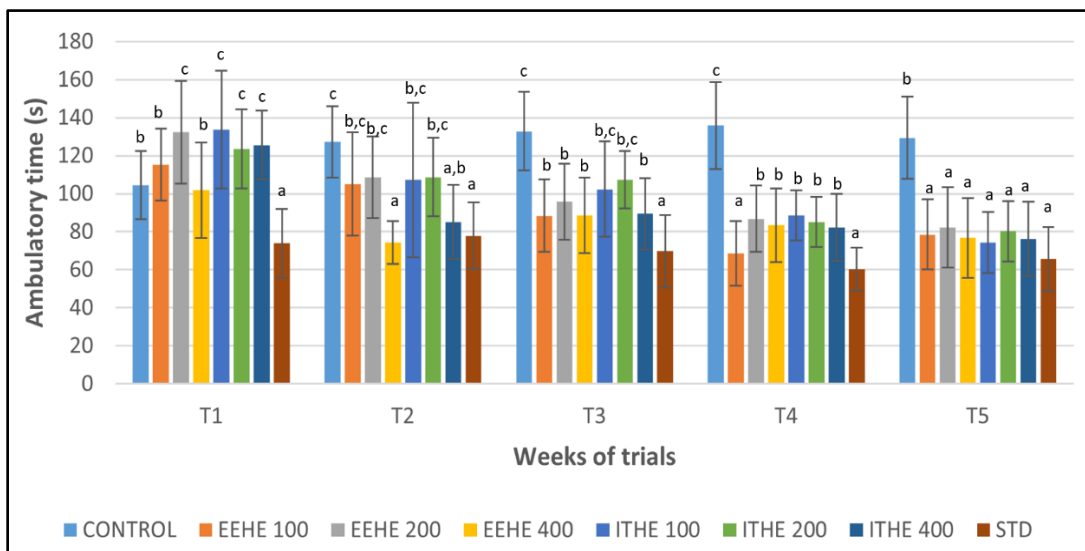
Each value is expressed as the mean \pm SD (n = 6). Different superscript letters (a - d) are statistically significant (ANOVA, $p < 0.05$, and subsequent post hoc multiple comparisons with Duncan's test).

Figure 6.46: Effect of EEBF, ITBF, control and Diazepam on distance travelled (DT) using Optovarimex model.

Table 6.37: Effect of EEBF, ITBF, control and Diazepam on DT (cm) in OPV.

Group	T1	T2	T3	T4	T5
Control	1228.50 \pm 109.08 ^b	1250.83 \pm 158.06 ^c	1180.17 \pm 162.12 ^c	1262.17 \pm 182.44 ^c	1107.33 \pm 178.76 ^c
EEBF 100	1265.33 \pm 164.93 ^{b,c}	1253.83 \pm 239.39 ^c	1210.83 \pm 143.12 ^c	1048.83 \pm 143.17 ^{b,c}	881.83 \pm 129.50 ^b
EEBF200	1166.67 \pm 158.15 ^{a,b}	1222.50 \pm 205.11 ^c	1114.50 \pm 161.67 ^{b,c}	892.00 \pm 140.47 ^b	862.17 \pm 152.27 ^b
EEBF 400	1043.83 \pm 157.15 ^{a,b}	923.50 \pm 145.11 ^b	923.50 \pm 130.47 ^b	801.33 \pm 132.47 ^{a,b}	791.17 \pm 125.41 ^b
ITBF 100	1305.83 \pm 145.40 ^{b,c}	1227.00 \pm 139.95 ^c	1005.45 \pm 126.08 ^b	909.50 \pm 130.59 ^b	807.17 \pm 117.28 ^b
ITBF 200	881.00 \pm 125.93 ^a	746.67 \pm 138.22 ^a	586.67 \pm 134.50 ^a	763.83 \pm 126.77 ^{a,b}	735.33 \pm 132.96 ^{a,b}
ITBF 400	849.50 \pm 117.09 ^a	721.83 \pm 124.37 ^a	691.83 \pm 104.30 ^a	849.67 \pm 85.48 ^b	710.17 \pm 94.34 ^{a,b}
Standard (Diazepam)	758.33 \pm 66.02 ^a	737.17 \pm 69.19 ^a	653.60 \pm 72.48 ^a	575.63 \pm 68.60 ^a	562.83 \pm 69.11 ^a

Each value is expressed as the mean \pm SD (n = 6). Different superscript letters (a - d) are statistically significant (ANOVA, $p < 0.05$, and subsequent post hoc multiple comparisons with Duncan's test).



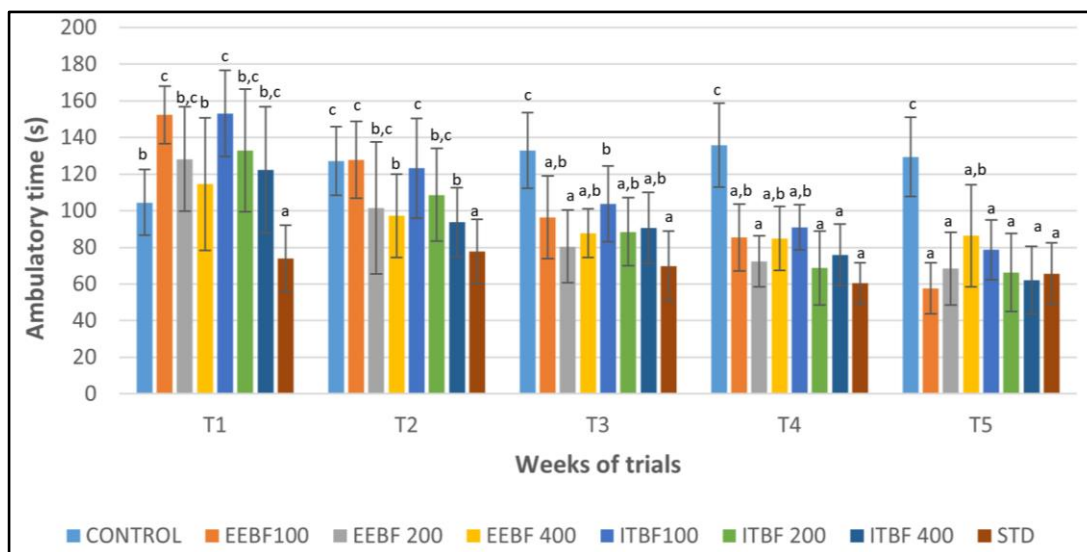
Each value is expressed as the mean \pm SD (n = 6). Different superscript letters (a - b) are statistically significant (ANOVA, $p < 0.05$, and subsequent post hoc multiple comparisons with Duncan's test).

Figure 6.47: Effect of EEHE, ITHE, control and Diazepam on ambulatory time (AT) using Optovarimex model.

Table 6.38: Effect of EEHE, ITHE, control and Diazepam on AT (s) in OPV.

Group	T1	T2	T3	T4	T5
Control	104.50 \pm 17.97 ^b	127.24 \pm 18.71 ^c	132.83 \pm 20.66 ^c	135.83 \pm 22.94 ^c	129.33 \pm 21.64 ^b
EEHE 100	115.33 \pm 18.93 ^b	105.17 \pm 27.16 ^{b,c}	88.33 \pm 19.09 ^b	68.70 \pm 17.02 ^a	78.56 \pm 18.45 ^a
EEHE 200	132.26 \pm 27.06 ^c	108.59 \pm 21.37 ^{b,c}	95.86 \pm 20.00 ^b	86.80 \pm 17.46 ^b	82.17 \pm 20.00 ^a
EEHE 400	101.89 \pm 25.06 ^b	74.33 \pm 11.37 ^a	88.59 \pm 19.68 ^b	83.33 \pm 19.76	76.67 \pm 21.10 ^a
ITHE 100	133.67 \pm 30.91 ^c	107.17 \pm 40.65 ^{b,c}	102.37 \pm 25.19 ^{b,c}	88.70 \pm 15.19 ^b	74.34 \pm 15.94 ^a
ITHE 200	123.56 \pm 20.36 ^c	108.67 \pm 20.65 ^{b,c}	107.33 \pm 15.18 ^{b,c}	85.17 \pm 13.15 ^b	80.17 \pm 11.37 ^a
ITHE 400	125.56 \pm 18.01	85.17 \pm 19.47 ^{a,b}	89.40 \pm 18.76 ^b	82.17 \pm 17.66 ^b	76.17 \pm 19.52 ^a
Standard (Diazepam)	73.88 \pm 18.14 ^a	77.91 \pm 17.46 ^a	69.78 \pm 19.11 ^a	60.34 \pm 11.26 ^a	65.56 \pm 16.78 ^a

Each value is expressed as the mean \pm SD (n = 6). Different superscript letters (a - b) are statistically significant (ANOVA, $p < 0.05$, and subsequent post hoc multiple comparisons with Duncan's test).



Each value is expressed as the mean \pm SD (n = 6). Different superscript letters (a - c) are statistically significant (ANOVA, $p < 0.05$, and subsequent post hoc multiple comparisons with Duncan's test).

Figure 6.48: Effect of EEBF, ITBF, control and Diazepam on ambulatory time (AT) using Optovarimex model.

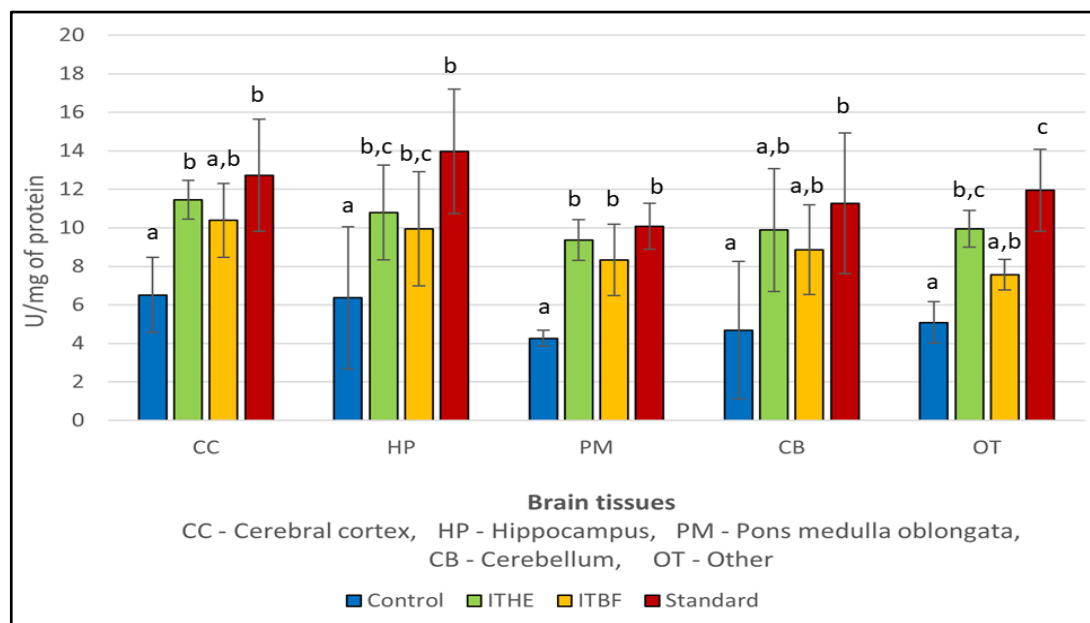
Table 6.39: Effect of EEBF, ITBF, control and Diazepam on AT (s) in OPV.

Group	T1	T2	T3	T4	T5
Control	104.50 \pm 17.97 ^b	127.24 \pm 18.71 ^c	132.83 \pm 20.66 ^{a,b}	135.83 \pm 22.94 ^c	129.33 \pm 21.64 ^c
EEBF 100	152.33 \pm 15.70 ^c	127.67 \pm 20.93 ^c	96.38 \pm 22.66 ^a	85.37 \pm 18.27 ^{a,b}	57.67 \pm 14.02 ^a
EEBF200	128.17 \pm 28.48 ^{b,c}	101.50 \pm 36.17 ^{b,c}	80.50 \pm 19.91 ^{a,b}	72.37 \pm 13.93 ^a	68.36 \pm 19.72 ^a
EEBF 400	114.50 \pm 36.26 ^b	97.24 \pm 22.66 ^b	87.83 \pm 13.27 ^b	84.83 \pm 17.39 ^{a,b}	86.33 \pm 27.84 ^{a,b}
ITBF 100	153.17 \pm 23.53 ^c	123.17 \pm 27.27 ^c	103.67 \pm 20.70 ^{a,b}	91.00 \pm 12.27 ^{a,b}	78.67 \pm 16.36 ^a
ITBF 200	132.83 \pm 33.53 ^{b,c}	108.67 \pm 25.29 ^{b,c}	88.50 \pm 18.70 ^{a,b}	68.67 \pm 20.27 ^a	66.33 \pm 21.36 ^a
ITBF 400	122.33 \pm 34.49 ^{b,c}	93.67 \pm 18.99 ^b	90.65 \pm 19.35 ^{a,b}	75.83 \pm 16.77 ^a	62.17 \pm 18.32 ^a
Standard (Diazepam)	73.88 \pm 18.14 ^a	77.91 \pm 17.46 ^a	69.78 \pm 19.11 ^a	60.34 \pm 11.26 ^a	65.56 \pm 16.78 ^a

Each value is expressed as the mean \pm SD (n = 6). Different superscript letters (a - c) are statistically significant (ANOVA, $p < 0.05$, and subsequent post hoc multiple comparisons with Duncan's test).

6.2.9. Biochemical Estimation

6.2.9.1. Estimation of levels of antioxidant enzymes in rats' brain homogenates



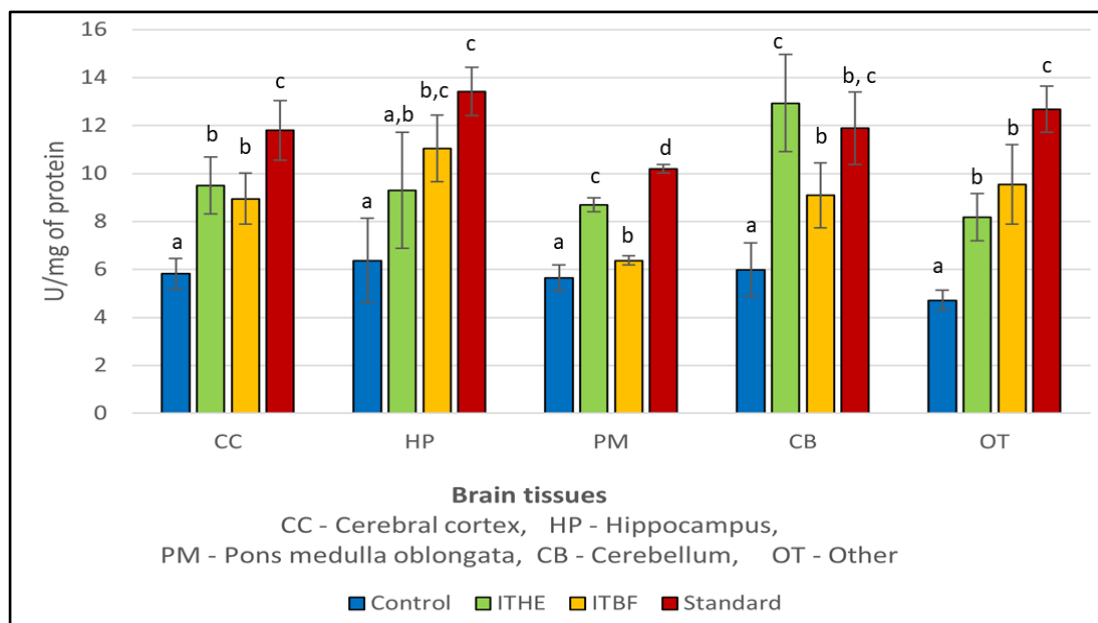
Each value is expressed as the mean \pm SD (n = 6). Different superscript letters (a - c) are statistically significant (ANOVA, $p < 0.05$, and subsequent post hoc multiple comparisons with Duncan's test).

Figure 6.49: Effect of ITHE, ITBF, control and Diazepam on Catalase enzyme levels in rats' brain.

Table 6.40: Effect of ITHE, ITBF, control and Diazepam on Catalase enzyme levels (U/mg of protein) in rats' brain.

Group	CC	HP	PM	CB	OT
Control	6.52 \pm 1.95 ^a	6.37 \pm 3.69 ^a	4.27 \pm 0.41 ^a	4.69 \pm 3.57 ^a	5.09 \pm 1.06 ^a
ITHE	11.45 \pm 1.01 ^b	10.79 \pm 2.46 ^{b,c}	9.37 \pm 1.06 ^b	9.89 \pm 3.19 ^{a,b}	9.95 \pm 0.96 ^{b,c}
ITBF	10.39 \pm 1.92 ^{a,b}	9.94 \pm 2.96 ^{b,c}	8.33 \pm 1.85 ^b	8.86 \pm 2.32 ^{a,b}	7.56 \pm 0.79 ^{a,b}
Standard Diazepam	12.73 \pm 2.92 ^b	13.97 \pm 3.23 ^b	10.08 \pm 1.18 ^b	11.27 \pm 3.66 ^b	11.95 \pm 2.13 ^c

Each value is expressed as the mean \pm SD (n = 6). Different superscript letters (a - c) are statistically significant (ANOVA, $p < 0.05$, and subsequent post hoc multiple comparisons with Duncan's test).



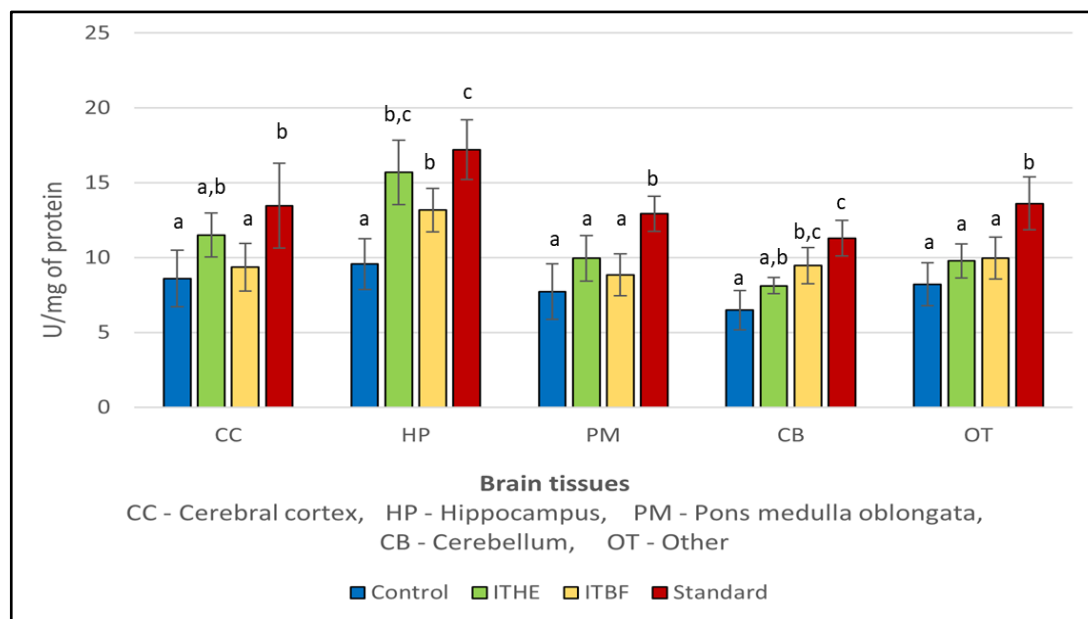
Each value is expressed as the mean \pm SD (n = 6). Different superscript letters (a - d) are statistically significant (ANOVA, $p < 0.05$, and subsequent post hoc multiple comparisons with Duncan's test).

Figure 6.50: Effect of ITHE, ITBF, control and Diazepam on Superoxide dismutase enzyme levels in rats' brain.

Table 6.41: Effect of ITHE, ITBF, control and Diazepam on Superoxide dismutase enzyme levels (U/mg of protein) in rats' brain.

Group	CC	HP	PM	CB	OT
Control	5.82 \pm 0.65 ^a	6.37 \pm 1.75 ^a	5.64 \pm 0.55 ^a	5.99 \pm 1.12 ^a	4.71 \pm 0.4 ^a
ITHE	9.50 \pm 1.19 ^b	9.30 \pm 2.42 ^{a,b}	8.68 \pm 0.29 ^c	12.93 \pm 2.02 ^c	8.18 \pm 0.99 ^b
ITBF	8.94 \pm 1.07 ^b	11.05 \pm 1.39 ^{b,c}	6.37 \pm 0.20 ^b	9.08 \pm 1.35 ^b	9.54 \pm 1.65 ^b
Standard Diazepam	11.80 \pm 1.24 ^c	13.41 \pm 1.01 ^c	10.20 \pm 0.18 ^d	11.88 \pm 1.52 ^{b,c}	12.68 \pm 0.96 ^c

Each value is expressed as the mean \pm SD (n = 6). Different superscript letters (a - d) are statistically significant (ANOVA, $p < 0.05$, and subsequent post hoc multiple comparisons with Duncan's test).



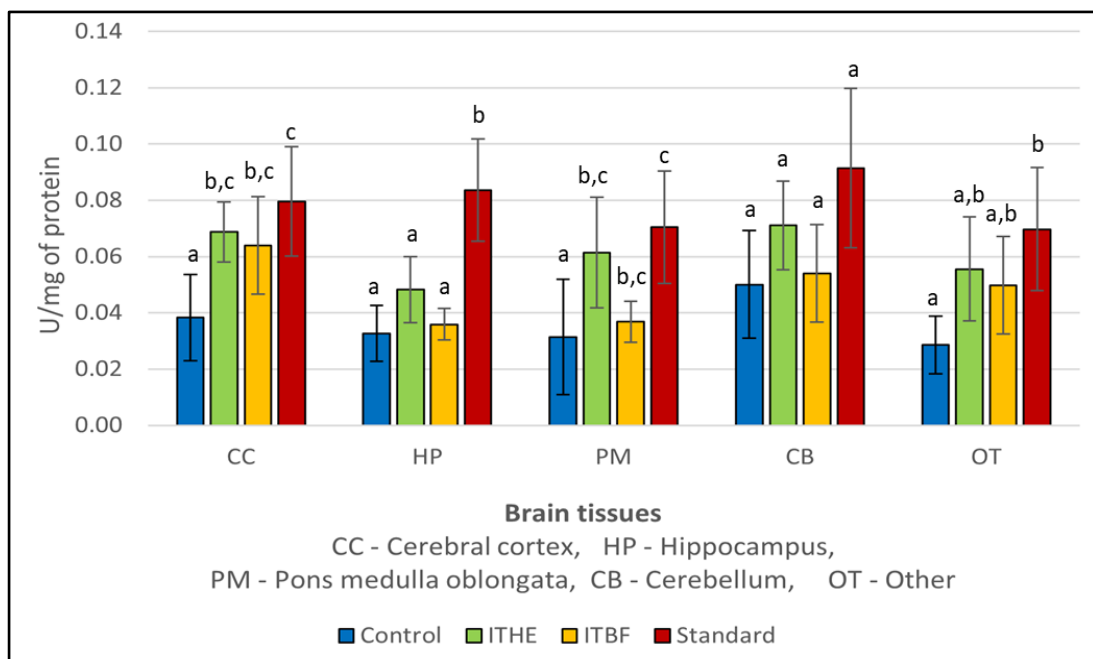
Each value is expressed as the mean \pm SD (n = 6). Different superscript letters (a - c) are statistically significant (ANOVA, $p < 0.05$, and subsequent post hoc multiple comparisons with Duncan's test).

Figure 6.51: Effect of ITHE, ITBF, control and Diazepam on Glutathione-S-transferase enzyme levels in rats' brain.

Table 6.42: Effect of ITHE, ITBF, control and Diazepam on Glutathione-S-transferase enzyme levels (U/mg of protein) in rats' brain.

Group	CC	HP	PM	CB	OT
Control	8.60 \pm 1.90 ^a	9.58 \pm 1.70 ^a	7.73 \pm 1.85 ^a	6.49 \pm 1.32 ^a	8.22 \pm 1.44 ^a
ITHE	11.51 \pm 1.47 ^{a,b}	15.69 \pm 2.14 ^{b,c}	9.96 \pm 1.52 ^a	8.13 \pm 0.55 ^{a,b}	9.78 \pm 1.14 ^a
ITBF	9.36 \pm 1.58 ^a	13.17 \pm 1.45 ^b	8.85 \pm 1.40 ^a	9.47 \pm 1.20 ^{b,c}	9.97 \pm 1.39 ^a
Standard Diazepam	13.47 \pm 2.83 ^b	17.21 \pm 2.01 ^c	12.93 \pm 1.18 ^b	11.30 \pm 1.20 ^c	13.62 \pm 1.76 ^b

Each value is expressed as the mean \pm SD (n = 6). Different superscript letters (a - c) are statistically significant (ANOVA, $p < 0.05$, and subsequent post hoc multiple comparisons with Duncan's test).



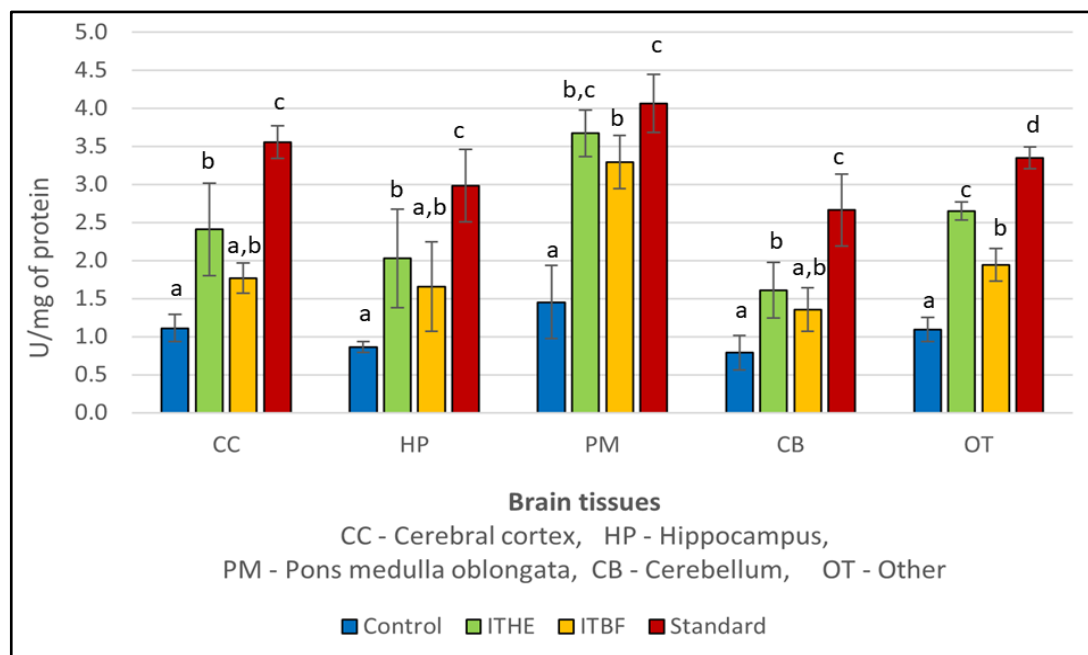
Each value is expressed as the mean \pm SD (n = 6). Different superscript letters (a - c) are statistically significant (ANOVA, $p < 0.05$, and subsequent post hoc multiple comparisons with Duncan's test).

Figure 6.52: Effect of ITHE, ITBF, control and Diazepam on Glutathione peroxidase enzyme levels in rats' brain.

Table 6.43: Effect of ITHE, ITBF, control and Diazepam on Glutathione peroxidase enzyme levels (U/mg of protein) in rats' brain.

Group	CC	HP	PM	CB	OT
Control	0.04 \pm 0.02 ^a	0.03 \pm 0.01 ^a	0.03 \pm 0.02 ^a	0.05 \pm 0.02 ^a	0.03 \pm 0.01 ^a
ITHE	0.07 \pm 0.01 ^{b,c}	0.05 \pm 0.01 ^a	0.06 \pm 0.02 ^{b,c}	0.07 \pm 0.02 ^a	0.06 \pm 0.02 ^{a,b}
ITBF	0.06 \pm 0.02 ^{b,c}	0.04 \pm 0.01 ^a	0.04 \pm 0.01 ^{b,c}	0.05 \pm 0.02 ^a	0.05 \pm 0.02 ^{a,b}
Standard Diazepam	0.08 \pm 0.02 ^c	0.08 \pm 0.02 ^b	0.07 \pm 0.02 ^c	0.09 \pm 0.03 ^a	0.07 \pm 0.02 ^b

Each value is expressed as the mean \pm SD (n = 6). Different superscript letters (a - c) are statistically significant (ANOVA, $p < 0.05$, and subsequent post hoc multiple comparisons with Duncan's test).



Each value is expressed as the mean \pm SD (n = 6). Different superscript letters (a - d) are statistically significant (ANOVA, $p < 0.05$, and subsequent post hoc multiple comparisons with Duncan's test).

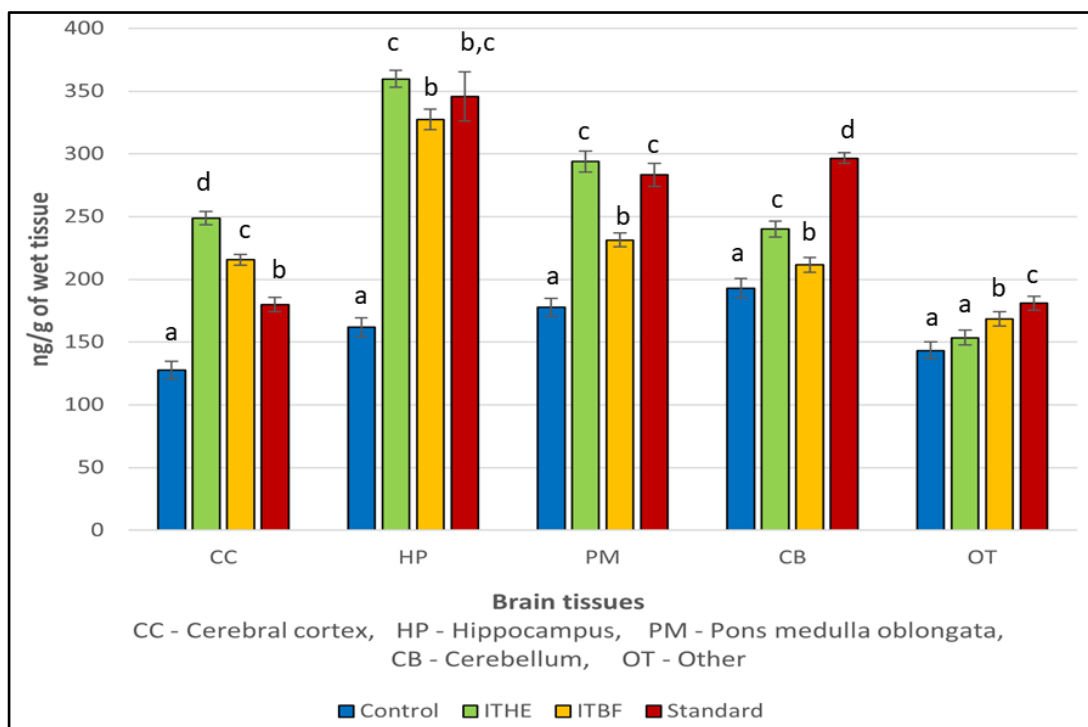
Figure 6.53: Effect of ITHE, ITBF, control and Diazepam on Glutathione reductase enzyme levels in rats' brain.

Table 6.44: Effect of ITHE, ITBF, control and Diazepam on Glutathione reductase enzyme levels (U/mg of protein) in rats' brain.

Group	CC	HP	PM	CB	OT
Control	1.11 \pm 0.18 ^a	0.86 \pm 0.07 ^a	1.45 \pm 0.48 ^a	0.79 \pm 0.23 ^a	1.09 \pm 0.16 ^a
ITHE	2.41 \pm 0.61 ^b	2.03 \pm 0.65 ^b	3.67 \pm 0.31 ^{b,c}	1.61 \pm 0.37 ^b	2.65 \pm 0.12 ^c
ITBF	1.77 \pm 0.20 ^{a,b}	1.66 \pm 0.59 ^{a,b}	3.29 \pm 0.35 ^b	1.35 \pm 0.29 ^{a,b}	1.94 \pm 0.21 ^b
Standard Diazepam	3.56 \pm 0.21 ^c	2.99 \pm 0.48 ^c	4.07 \pm 0.38 ^c	2.66 \pm 0.47 ^c	3.35 \pm 0.14 ^d

Each value is expressed as the mean \pm SD (n = 6). Different superscript letters (a - d) are statistically significant (ANOVA, $p < 0.05$, and subsequent post hoc multiple comparisons with Duncan's test).

6.2.9.2. Estimation of levels of neurotransmitters in rats' brain homogenates



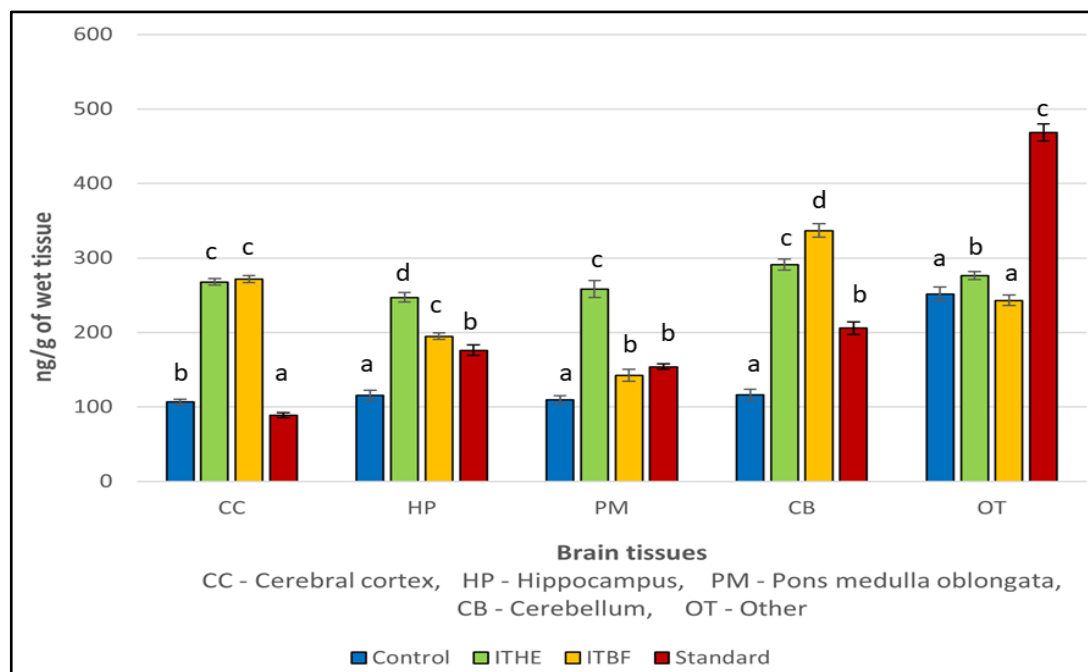
Each value is expressed as the mean \pm SD (n = 6). Different superscript letters (a - d) are statistically significant (ANOVA, $p < 0.01$, and subsequent post hoc multiple comparisons with Duncan's test).

Figure 6.54: Effect of ITHE, ITBF, control and Diazepam on Nor Adrenaline levels in rats' brain.

Table 6.45: Effect of ITHE, ITBF, control and Diazepam on Nor adrenaline levels (ng/g of wet tissue) in rats' brain.

Group	CC	HP	PM	CB	OT
Control	127.81 \pm 6.98 ^a	161.84 \pm 7.52 ^a	177.75 \pm 7.15 ^a	192.85 \pm 7.73 ^a	143.33 \pm 6.68 ^a
ITHE	248.60 \pm 5.33 ^d	359.74 \pm 6.85 ^c	293.77 \pm 8.24 ^c	239.97 \pm 6.21 ^c	153.47 \pm 5.99 ^a
ITBF	215.55 \pm 4.14 ^c	327.39 \pm 8.29 ^b	231.30 \pm 5.48 ^b	211.55 \pm 5.90 ^b	168.56 \pm 5.62 ^b
Standard Diazepam	179.88 \pm 5.64 ^b	345.63 \pm 19.51 ^{b,c}	283.21 \pm 9.03 ^c	296.56 \pm 4.34 ^d	181.02 \pm 5.48 ^c

Each value is expressed as the mean \pm SD (n = 6). Different superscript letters (a - d) are statistically significant (ANOVA, $p < 0.01$, and subsequent post hoc multiple comparisons with Duncan's test).



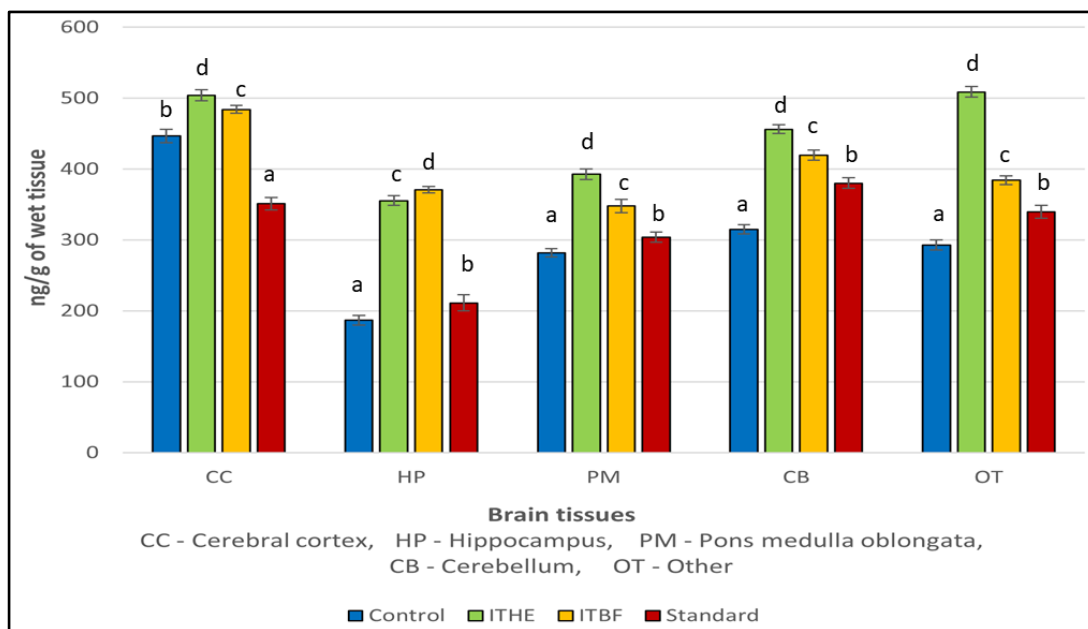
Each value is expressed as the mean \pm SD (n = 6). Different superscript letters (a - d) are statistically significant (ANOVA, $p < 0.01$, and subsequent post hoc multiple comparisons with Duncan's test).

Figure 6.55: Effect of ITHE, ITBF, control and Diazepam on Dopamine levels in rats' brain.

Table 6.46: Effect of ITHE, ITBF, control and Diazepam on Dopamine levels (ng/g of wet tissue) in rats' brain.

Group	CC	HP	PM	CB	OT
Control	106.60 \pm 3.78 ^b	115.69 \pm 6.86 ^a	109.43 \pm 5.79 ^a	116.36 \pm 7.42 ^a	251.44 \pm 9.22 ^a
ITHE	267.96 \pm 4.59 ^c	247.20 \pm 6.17 ^d	258.38 \pm 1.59 ^c	291.31 \pm 7.46 ^c	276.58 \pm 5.40 ^b
ITBF	271.66 \pm 4.89 ^c	194.94 \pm 4.53 ^c	142.22 \pm 8.01 ^b	336.73 \pm 8.95 ^d	243.11 \pm 6.86 ^a
Standard Diazepam	88.67 \pm 3.27 ^a	176.22 \pm 7.12 ^b	154.09 \pm 3.57 ^b	205.86 \pm 8.27 ^b	468.55 \pm 1.17 ^c

Each value is expressed as the mean \pm SD (n = 6). Different superscript letters (a - d) are statistically significant (ANOVA, $p < 0.01$, and subsequent post hoc multiple comparisons with Duncan's test).



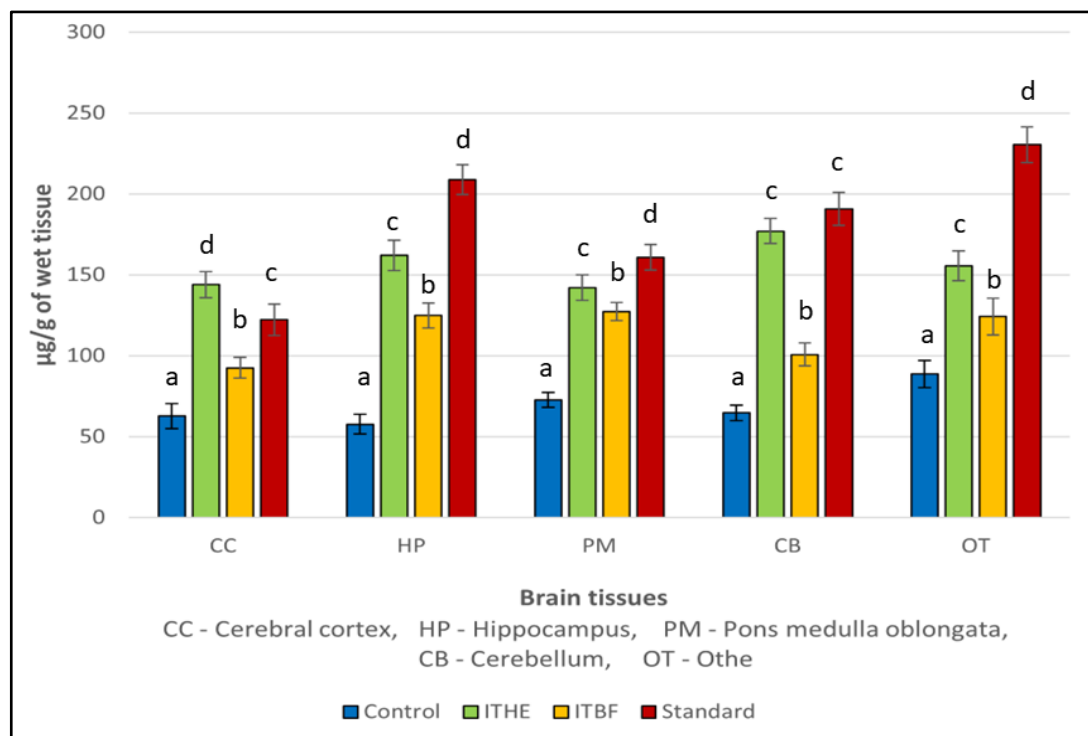
Each value is expressed as the mean \pm SD (n = 6). Different superscript letters (a - d) are statistically significant (ANOVA, $p < 0.01$, and subsequent post hoc multiple comparisons with Duncan's test).

Figure 6.56: Effect of ITHE, ITBF, control and Diazepam on Serotonin levels in rats' brain.

Table 6.47: Effect of ITHE, ITBF, control and Diazepam on Serotonin levels (ng/g of wet tissue) in rats' brain.

Group	CC	HP	PM	CB	OT
Control	446.95 \pm 9.42 ^b	186.95 \pm 6.68 ^a	281.86 \pm 5.79 ^a	314.861 \pm 6.54 ^a	292.78 \pm 7.23 ^a
ITHE	504.12 \pm 8.00 ^d	355.50 \pm 6.78 ^c	392.78 \pm 7.31 ^d	456.18 \pm 6.08 ^d	508.84 \pm 7.31 ^d
ITBF	484.24 \pm 5.58 ^c	371.21 \pm 4.52 ^d	348.00 \pm 9.24 ^c	419.86 \pm 7.28 ^c	384.45 \pm 6.26 ^c
Standard Diazepam	351.27 \pm 8.80 ^a	211.27 \pm 11.44 ^b	303.90 \pm 6.99 ^b	380.17 \pm 7.53 ^b	339.75 \pm 9.06 ^b

Each value is expressed as the mean \pm SD (n = 6). Different superscript letters (a - d) are statistically significant (ANOVA, $p < 0.01$, and subsequent post hoc multiple comparisons with Duncan's test).



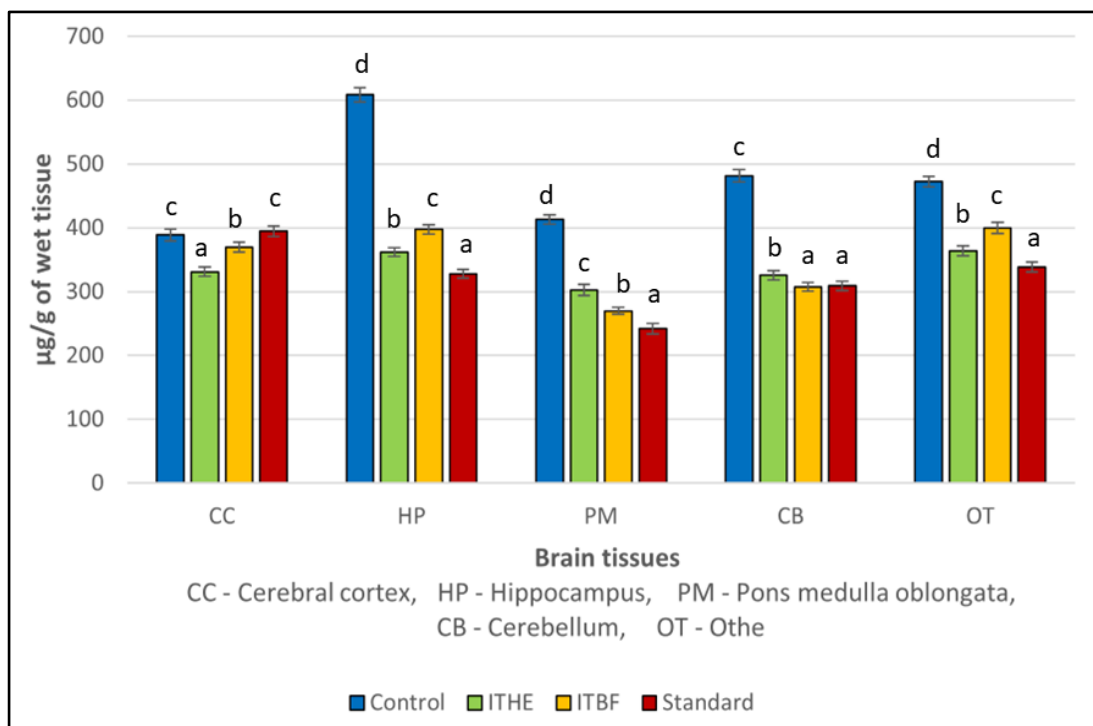
Each value is expressed as the mean \pm SD (n = 6). Different superscript letters (a - d) are statistically significant (ANOVA, $p < 0.01$, and subsequent post hoc multiple comparisons with Duncan's test).

Figure 6.57: Effect of ITHE, ITBF, control and Diazepam on GABA levels in rats' brain.

Table 6.48: Effect of ITHE, ITBF, control and Diazepam on GABA levels ($\mu\text{g/g}$ of wet tissue) in rats' brain.

Group	CC	HP	PM	CB	OT
Control	62.74 \pm 7.80 ^a	57.59 \pm 6.07 ^a	72.72 \pm 4.52 ^a	64.66 \pm 4.64 ^a	88.70 \pm 8.40 ^a
ITHE	143.87 \pm 8.16 ^d	162.02 \pm 9.40 ^c	142.05 \pm 7.97 ^c	177.00 \pm 7.75 ^c	155.60 \pm 9.13 ^c
ITBF	92.54 \pm 6.42 ^b	124.87 \pm 7.79 ^b	127.27 \pm 5.62 ^b	100.70 \pm 7.09 ^b	124.17 \pm 11.47 ^b
Standard Diazepam	122.20 \pm 9.75 ^c	208.81 \pm 9.35 ^d	160.81 \pm 7.96 ^d	190.73 \pm 0.34 ^c	230.36 \pm 11.08 ^d

Each value is expressed as the mean \pm SD (n = 6). Different superscript letters (a - d) are statistically significant (ANOVA, $p < 0.01$, and subsequent post hoc multiple comparisons with Duncan's test).



Each value is expressed as the mean \pm SD (n = 6). Different superscript letters (a - d) are statistically significant (ANOVA, $p < 0.01$, and subsequent post hoc multiple comparisons with Duncan's test).

Figure 6.58: Effect of ITHE, ITBF, control and Diazepam on Glutamate levels in rats' brain.

Table 6.49: Effect of ITHE, ITBF, control and Diazepam on Glutamate levels ($\mu\text{g/g}$ of wet tissue) in rats' brain.

Group	CC	HP	PM	CB	OT
Control	388.81 \pm 9.04 ^c	608.51 \pm 11.34 ^d	412.93 \pm 7.47 ^d	481.80 \pm 9.73 ^c	472.17 \pm 8.52 ^d
ITHE	330.94 \pm 7.46 ^a	361.75 \pm 6.72 ^b	302.47 \pm 8.79 ^c	325.66 \pm 7.18 ^b	363.78 \pm 7.59 ^b
ITBF	369.35 \pm 7.62 ^b	397.67 \pm 7.36 ^c	269.85 \pm 5.57 ^b	307.20 \pm 6.89 ^a	399.66 \pm 8.78 ^c
Standard	394.52 \pm 8.04 ^c	328.00 \pm 7.11 ^a	241.98 \pm 8.03 ^a	308.89 \pm 7.45 ^a	338.24 \pm 7.69 ^a

Each value is expressed as the mean \pm SD (n = 6). Different superscript letters (a - d) are statistically significant (ANOVA, $p < 0.01$, and subsequent post hoc multiple comparisons with Duncan's test).

6.2.10. Isolation and structural elucidation of phytoconstituents

6.2.10.1. Isolation and characterisation of phytoconstituents from ITHE

The yield of the column fraction LMH obtained was 2.16 g. Purification of LMH by preparative HPLC led to the isolation of three compounds LMH1, LMH2, and LMH3 that had yield of 87.06 mg (4.03 %), 29.2 mg (1.35 %), and 19.3 mg (0.89 %) respectively.

The structural elucidation and characterization of the isolated compounds *viz.* LMH1, LMH2, LMH3 from ITHE are listed as follows.

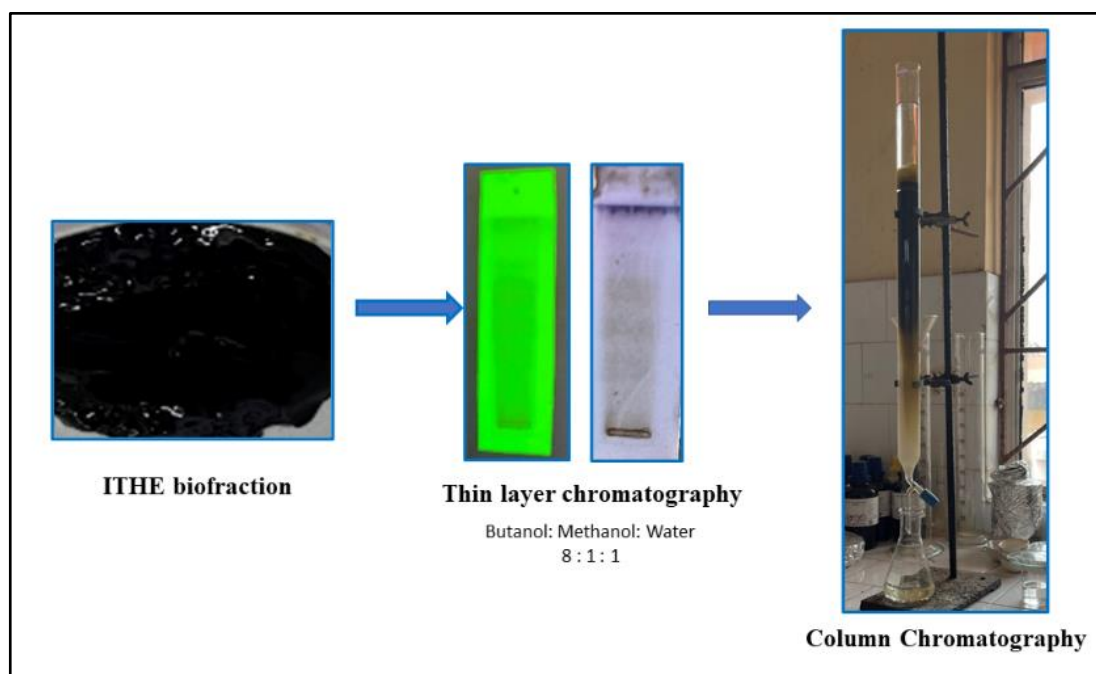


Figure 6.59: Isolation of phytoconstituents from ITHE.

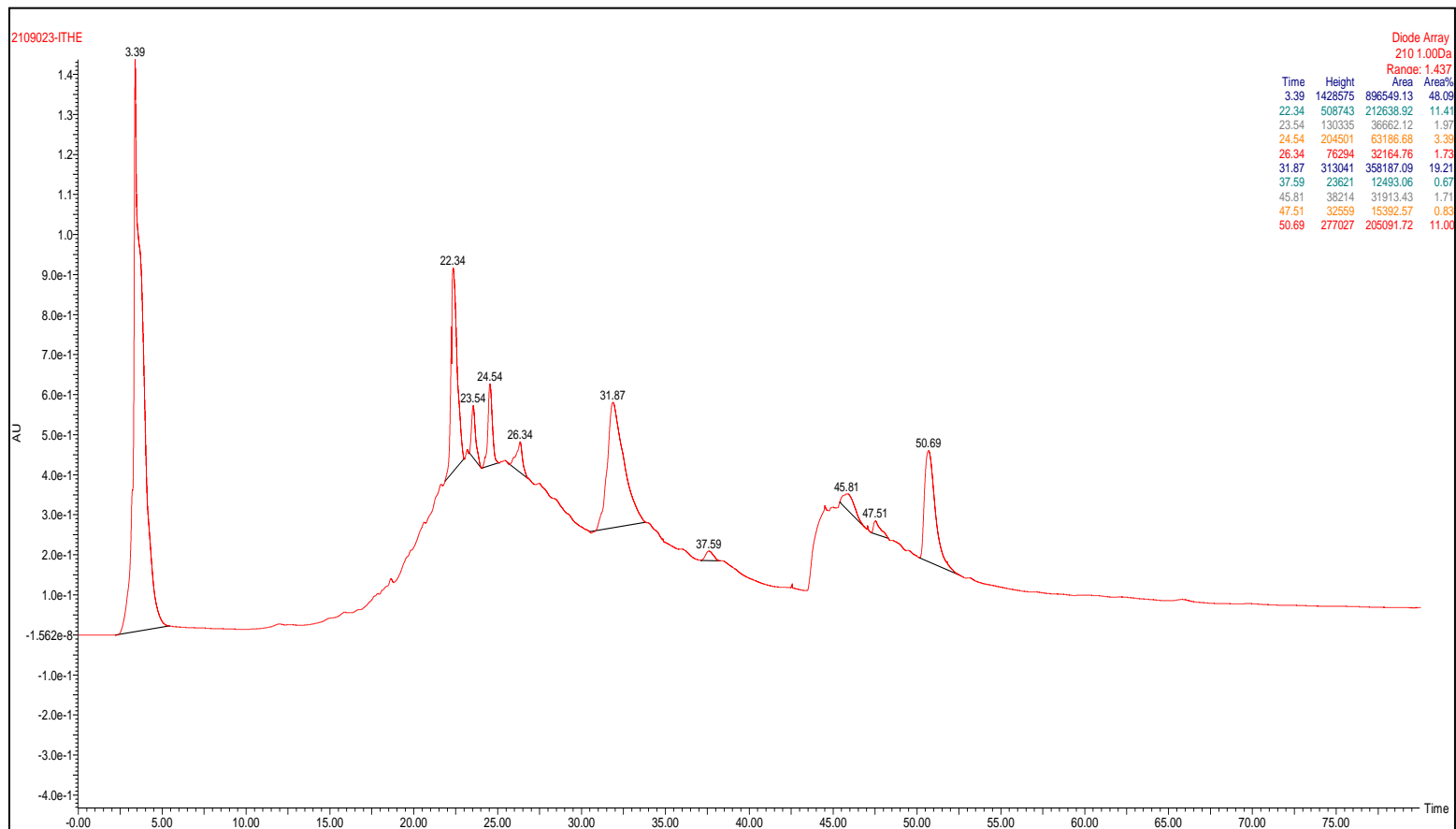


Figure 6.60: Preparative HPLC chromatogram of LMH (ITHE purified fraction).

6.2.10.1.1. CHARACTERISATION OF COMPOUND LMH1

Physical parameters of the compound

Physical state Yellowish coloured compound

Melting point 180 °C (*lit.* 176 - 189 °C) [226]

The compound LMH1 gave a positive response for shinoda test for flavonoids.

Spectral characteristics of the compound

IR (KBr) 3222 cm⁻¹ (br, OH str.)
 1652 cm⁻¹ (C=O str.)
 1380 cm⁻¹ (C-O str)
 1005 cm⁻¹ (C-O str. of 2° alc)

¹H-NMR and ¹³C-NMR Tables 6.50 and 6.51.

Mass spectra

LC-MS (m/z) 449.57 [M+H]⁺, other peaks appeared at 301.18, 241.59

Molecular formula C₂₁H₂₀O₁₁

Molecular weight 448.37 g/mol

From the m.p., IR, ¹H-NMR, ¹³C-NMR and mass spectral data, the compound was identified as **Quercetrin**.

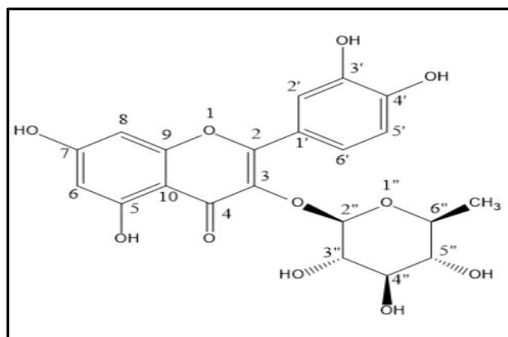


Figure 6.61: Structure of Quercetrin.

Table 6.50: ¹H-NMR data of the isolated compound LMH1.

Position	Quercetrin (DMSO-d ₆ , 400 MHz, δ ppm, J, Hz) Reported values ^[227]	LMH1 (DMSO-d ₆ , 400 MHz, δ ppm, J, Hz) Spectral values
H-6	6.21 (d, 1H, J = 2.0 Hz)	6.209 (d, 1H, J = 2 Hz)
H-8	6.40 (d, 1H, J = 2.0 Hz)	6.394 (d, 1H, J = 2 Hz)
OH-5	-	12.660 (s, 1H)
OH-7	-	10.878 (s, 1H)
H-2'	7.30 (d, 1H, J = 2.0 Hz)	7.301 (d, 1H, J = 2.4 Hz)
H-5'	6.87 (d, 1H, J = 8.6 Hz)	6.875 (d, 1H, J = 8 Hz)
H-6'	7.26 (dd, 1H, J = 8.6, 2.0 Hz)	7.266 (dd, 1H, J = 6.4, 2 Hz)
OH-3'	-	9.717 (s, 1H)
OH-4'	-	9.349 (s, 1H)
H-1''-R	5.26 (d, 1H, J = 1.6 Hz)	5.253 (d, 1H, J = 1.2 Hz)
H-2''	3.12-3.32 (m, 4H)	3.112- 3.984 (m, 4H)
H-3''		
H-4''		
H-5''		
H-6''-CH ₃	0.82 (d, 3H, J = 5.9 Hz)	0.820 (d, 3H, J = 6 Hz)

Table 6.51: ^{13}C -NMR data of the isolated compound LMH1.

Position	Quercitrin (DMSO-d ₆ , 100 MHz, δ ppm) Reported values ^[227]	LMH1 (DMSO-d ₆ , 100 MHz, δ , ppm) Spectral values
C-2	156.89	156.421
C-3	134.65	134.194
C-4	178.38	177.730
C-5	161.73	161.280
C-6	99.15	98.659
C-7	164.64	164.164
C-8	94.10	93.603
C-9	157.76	157.287
C-10	104.5	104.064
C-1'	121.17	121.091
C-2'	115.90	115.626
C-3'	145.64	145.186
C-4'	148.88	148.420
C-5'	116.09	115.436
C-6'	121.58	120.704
C-1''-R	102.26	101.817
C-2''	70.90	70.321
C-3''	71.00	70.571
C-4''	71.62	71.148
C-5''	70.70	70.032
C-6''-CH₃	17.94	17.478

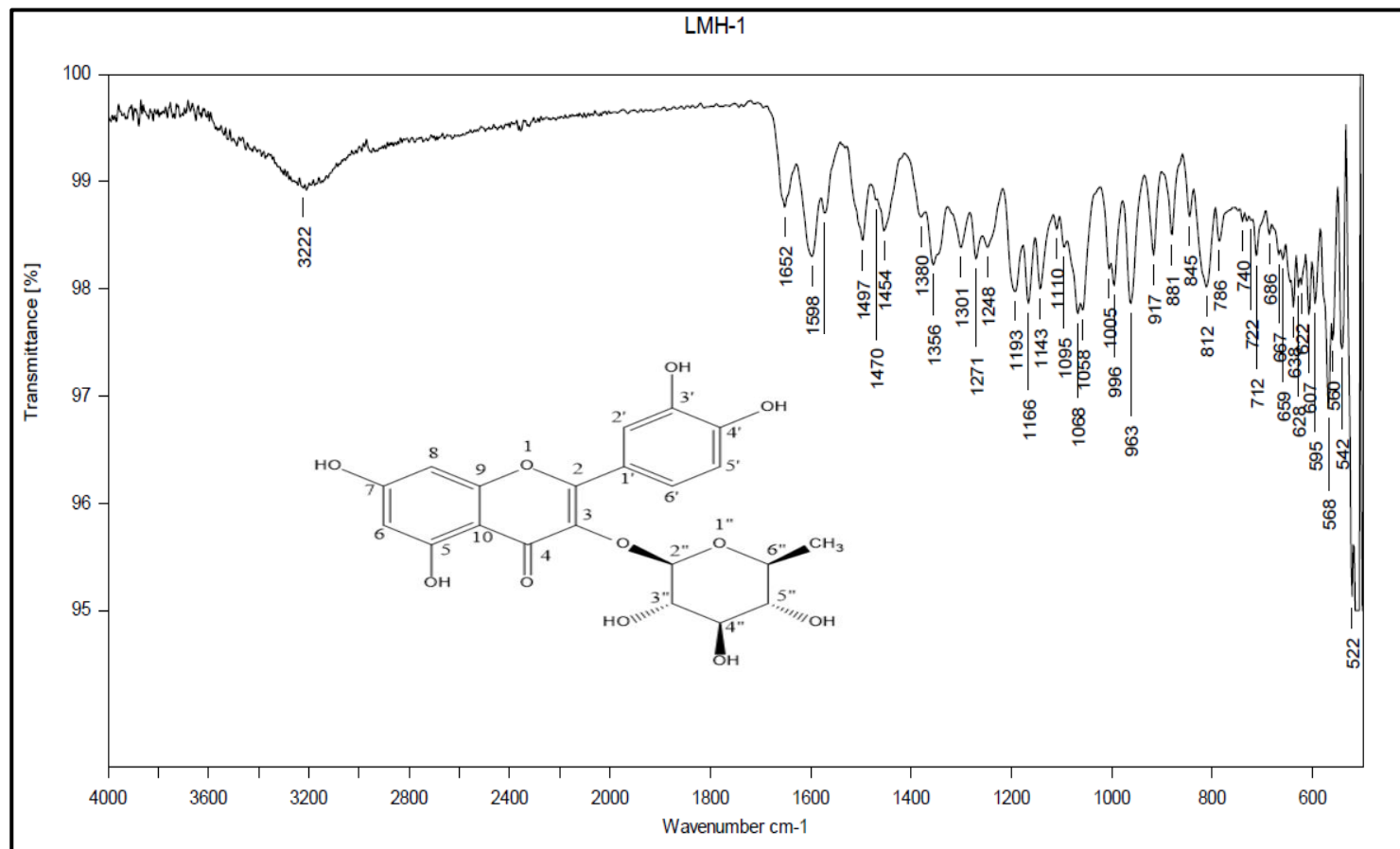
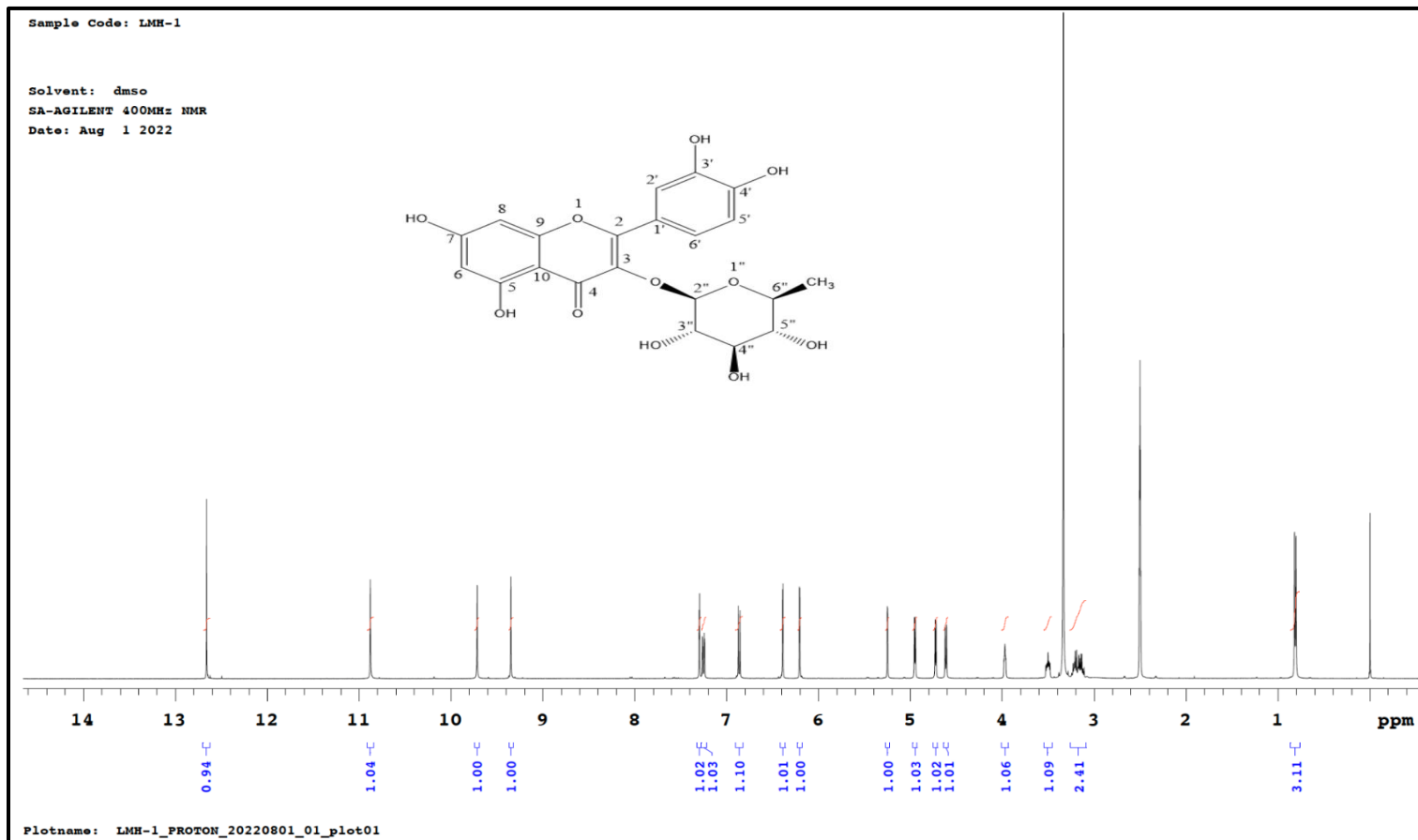


Figure 6.62: IR spectrum of LMH1 (Quercetrin).

Figure 6.63: ¹H-NMR spectrum of LMH1 (Quercetin).

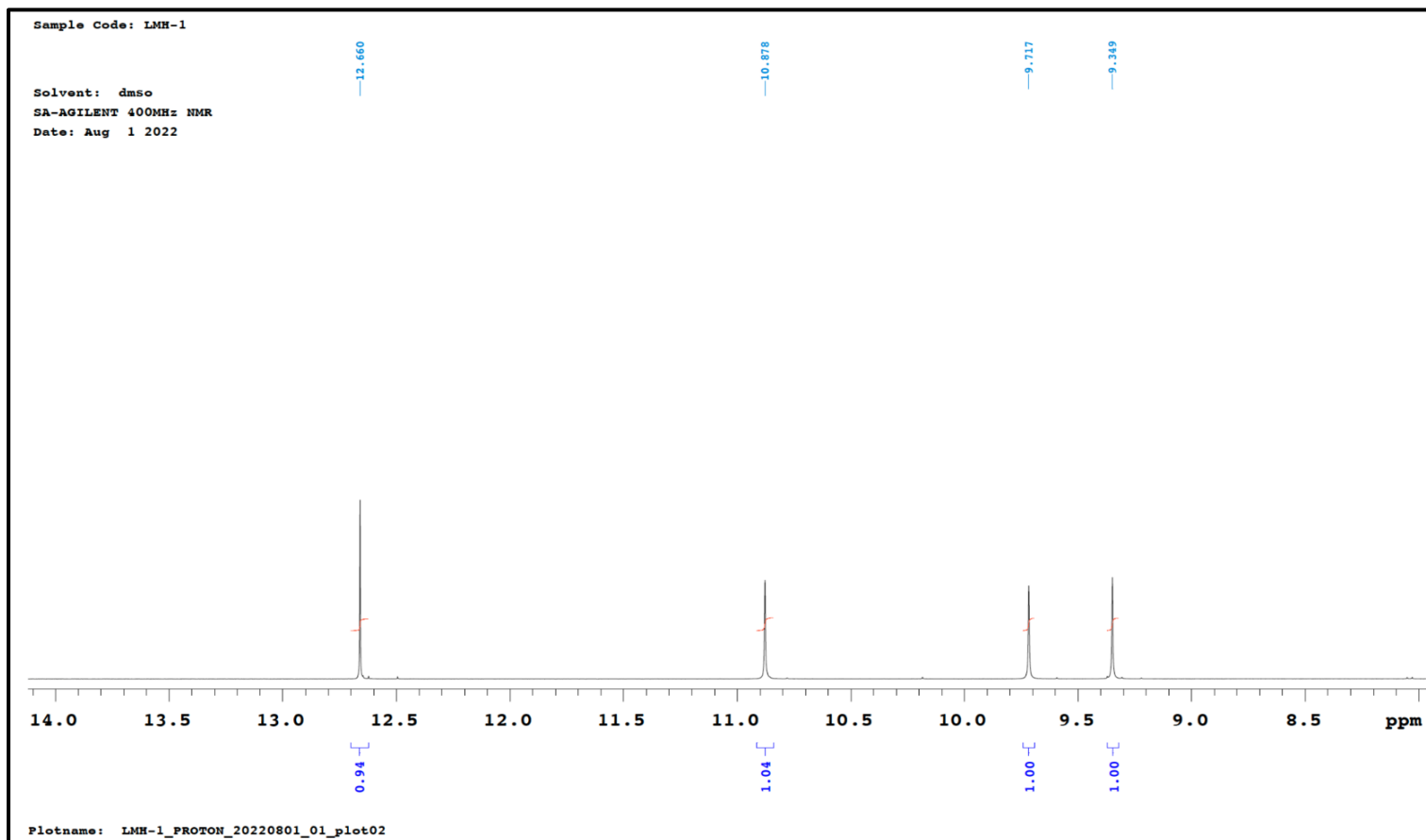


Figure 6.64: Resolution of ^1H -NMR spectrum of LMH1 (Quercetrin).

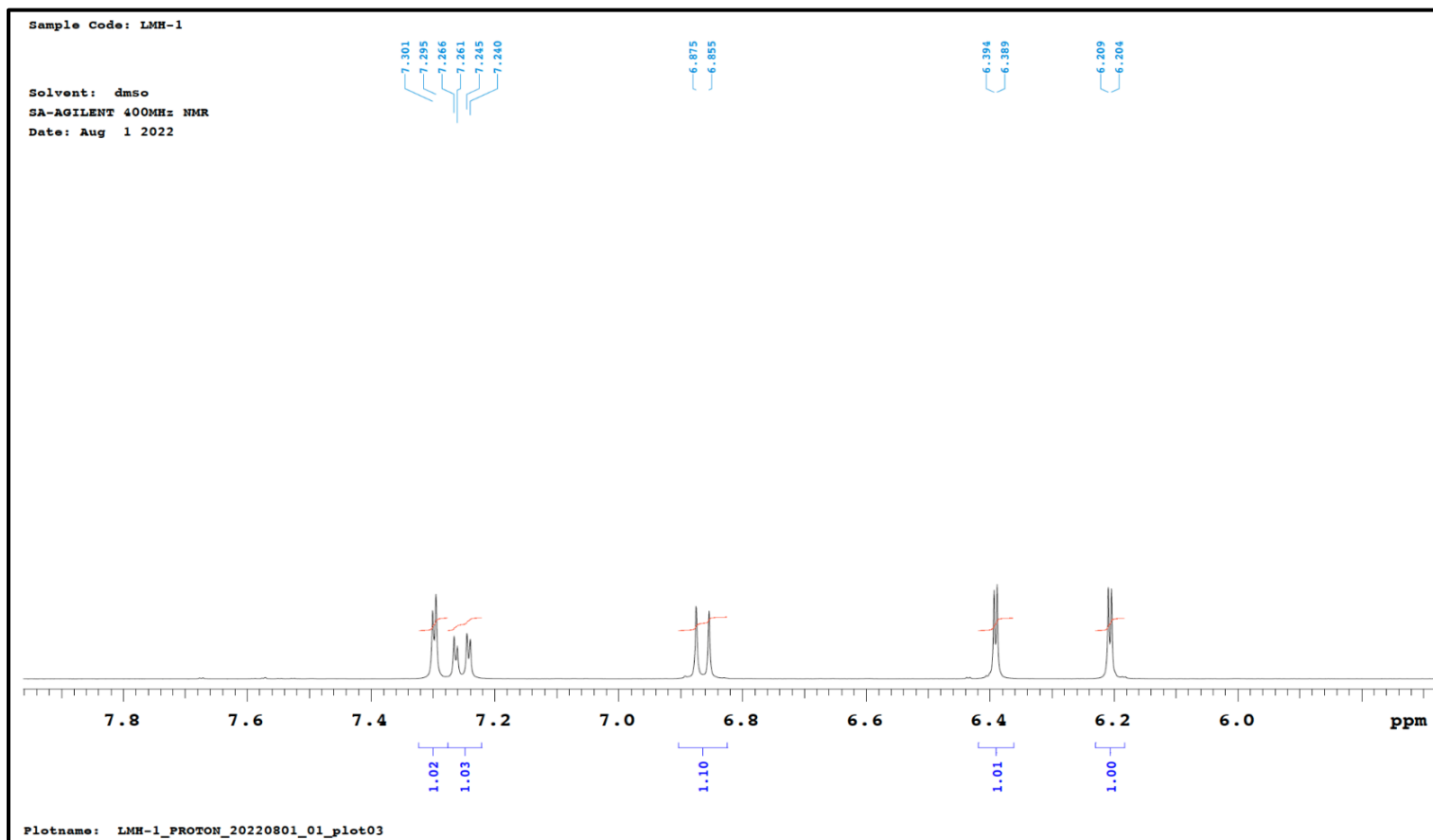


Figure 6.65: Resolution of ^1H -NMR spectrum of LMH1 (Quercetrin).

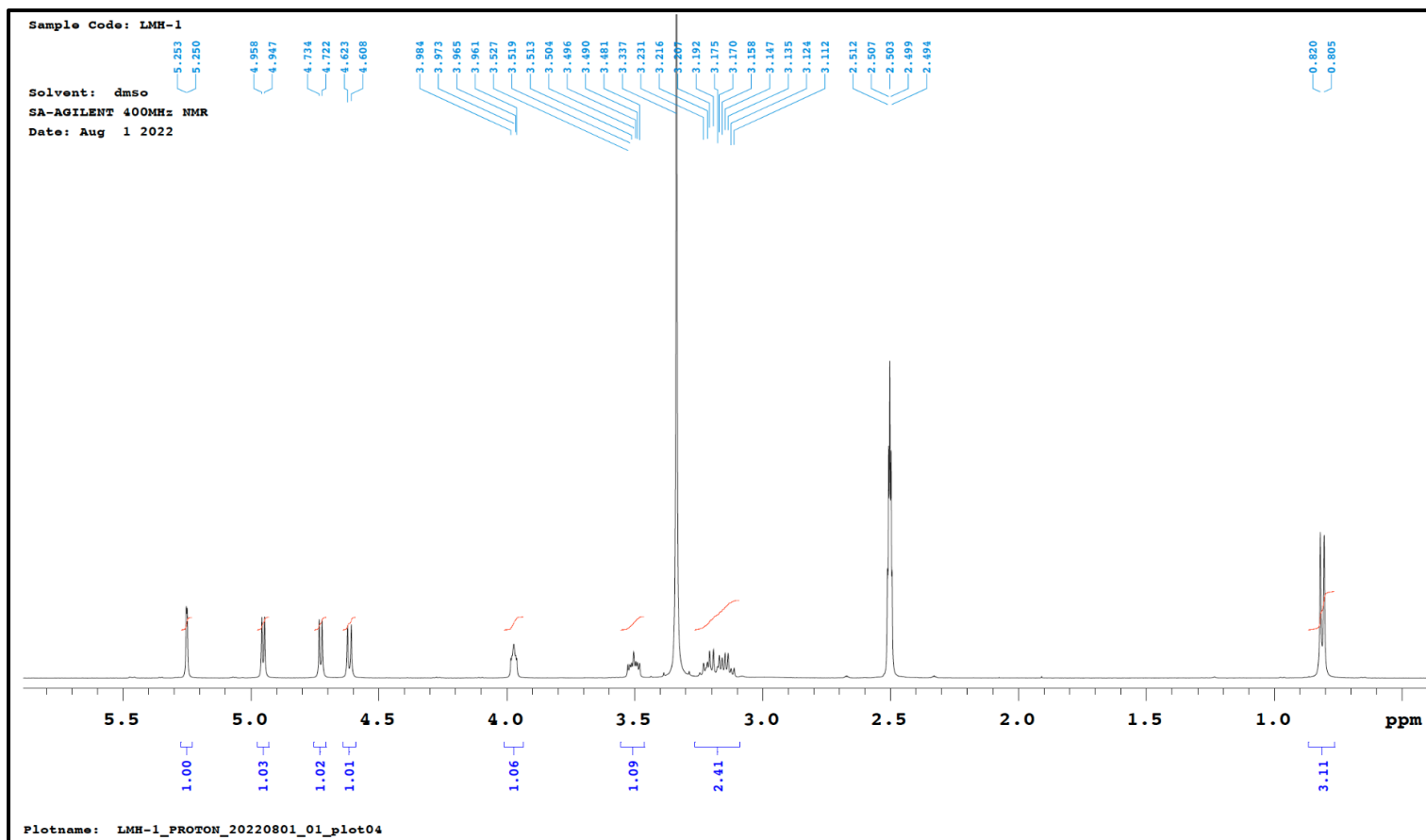
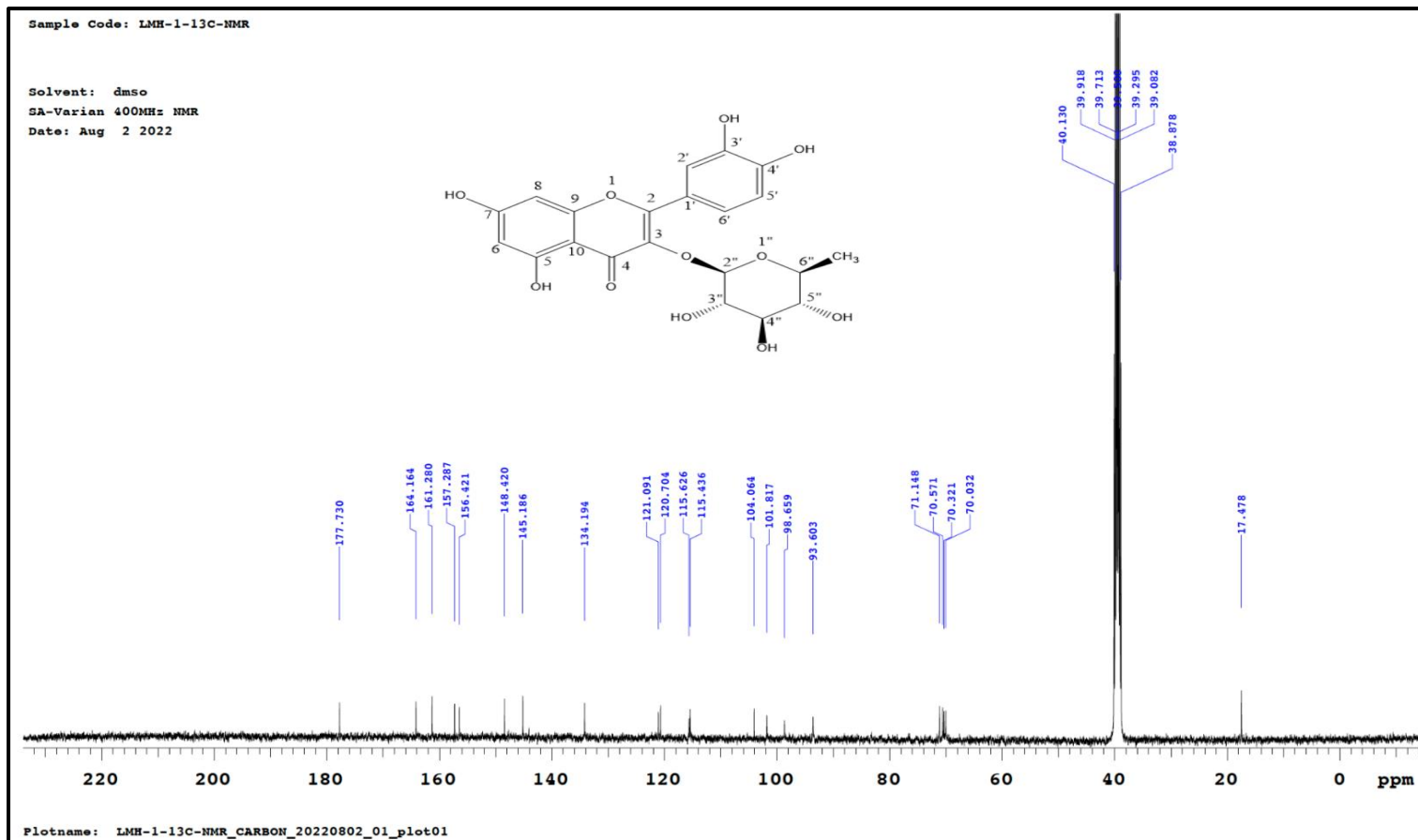


Figure 6.66: Resolution of ^1H -NMR spectrum of LMH1 (Quercetin).

Figure 6.67: ^{13}C -NMR spectrum of LMH1 (Quercetin).

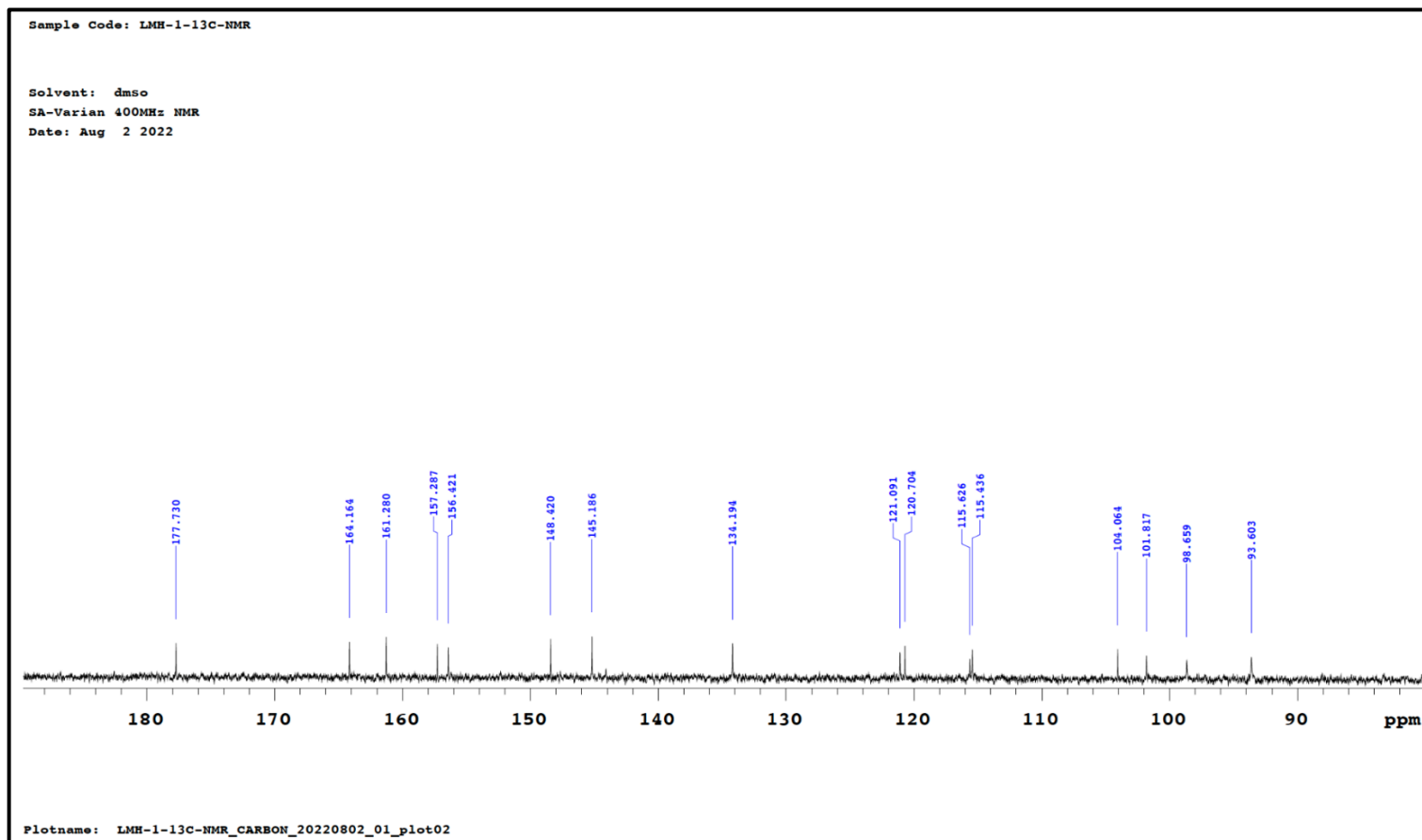


Figure 6.68: Resolution of ^{13}C -NMR spectrum of LMH1 (Quercetin).

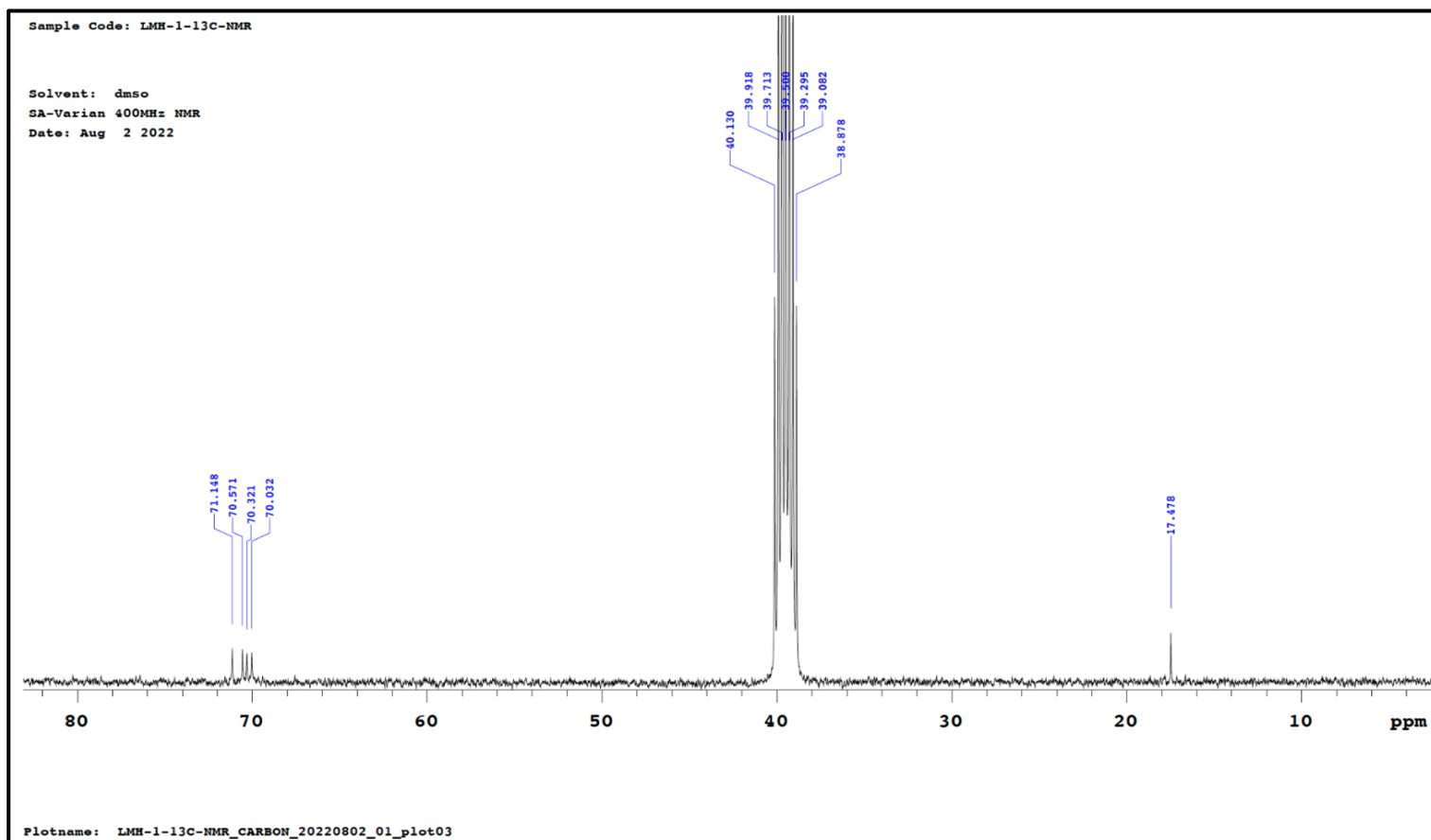


Figure 6.69: Resolution of ^{13}C -NMR spectrum of LMH1 (Quercetin).

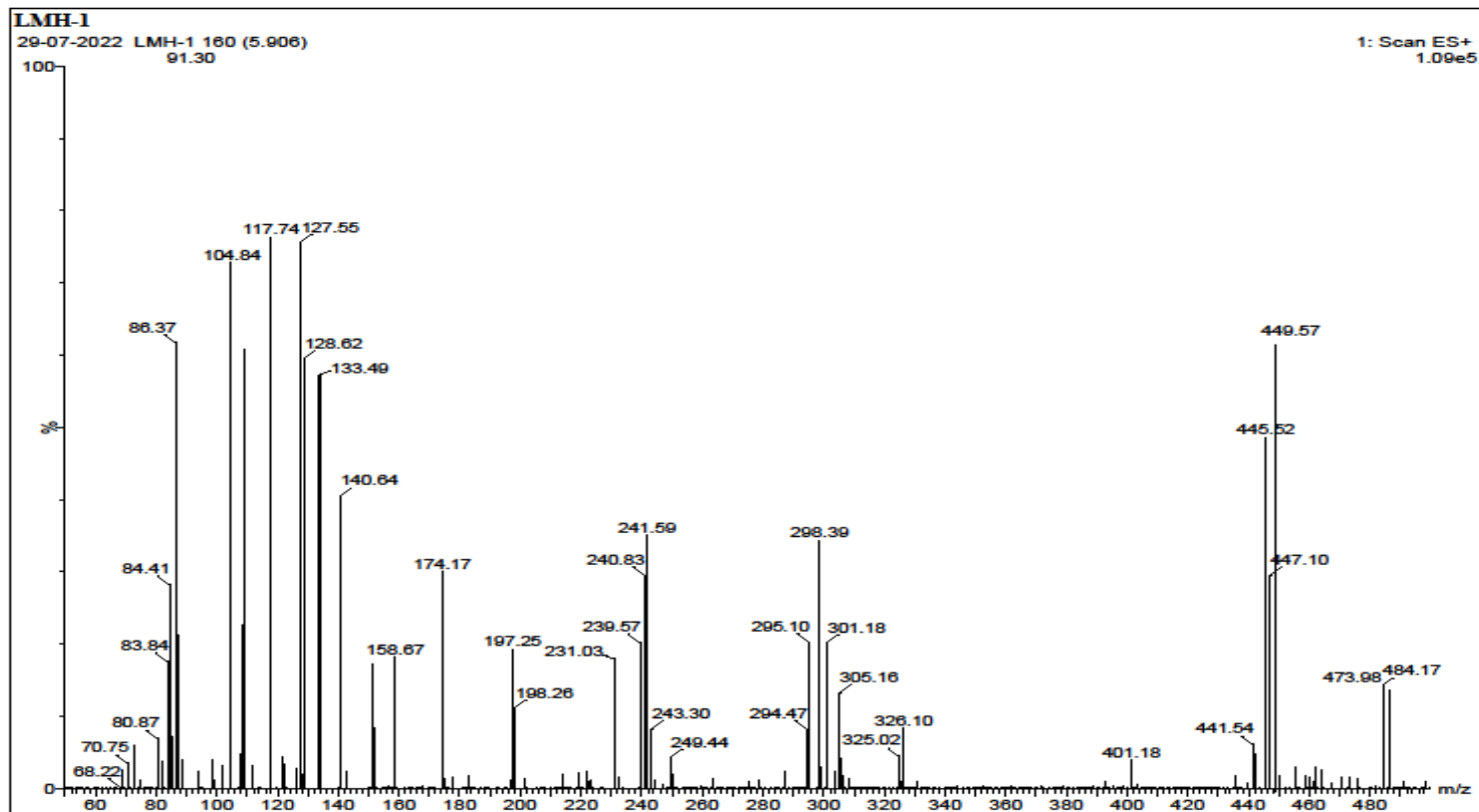


Figure 6.70: Mass spectrum of LMH1 (Quercetin).

6.2.10.1.2. CHARACTERISATION OF COMPOUND LMH2

Physical parameters of the compound

Physical state Yellowish coloured compound

Melting point 181 °C (*lit.* 179 - 185 °C) [228]

The compound LMH2 gave a positive response for shinoda test for flavonoids.

Spectral characteristics of the compound

IR (KBr) 3413.77 cm⁻¹ (OH str.)
 1641.13 cm⁻¹ (C=O str.)
 1506.72 cm⁻¹ (C=C str. in aromatic ring)
 1362.06 cm⁻¹ (C-O str.)

¹H-NMR and ¹³C-NMR Tables 6.52 and 6.53**Mass spectra****LC-MS (m/z)** 611.09 [M+H]⁺, other peaks appeared at 465.04, 303.01**Molecular formula** C₂₇H₃₀O₁₆**Molecular weight** 610.52 g/mol

From the m.p., IR, ¹H-NMR, ¹³C-NMR and mass spectral data, the compound was identified as **Rutin**.

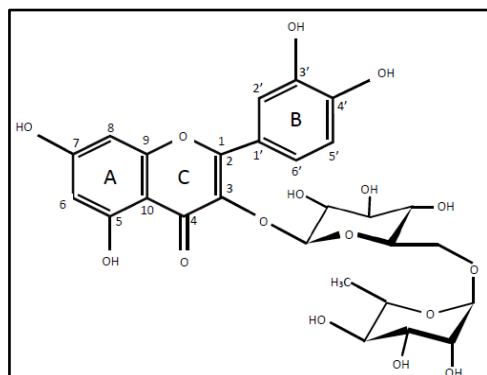
**Figure 6.71: Structure of Rutin.**

Table 6.52: ¹H-NMR data of the isolated compound LMH2.

Position	Rutin (DMSO-d ₆ , 500 MHz, δ ppm, J, Hz) Reported values ^[229]	LMH2 (DMSO-d ₆ , 500 MHz, δ ppm, J, Hz) Spectral values
H-6	6.21 (d, 1H, J = 2 Hz)	6.2075 (d, 1H, J = 1.95 Hz)
H-8	6.40 (d, 1H, J = 2 Hz)	6.3994 (d, 1H, J = 1.95 Hz)
H-2'	7.55 (d, 1H, J = 2.1 Hz)	7.5438 (s, 1H),
H-5'	6.86 (d, 1H, J = 9 Hz)	6.8643 (d, 1H, J = 9 Hz)
H-6'	7.56 (dd, 1H, J = 9, 2.1 Hz)	7.5619 (d, 1H, J = 2 Hz)
H-1''-G	5.35 (d, 1H, J = 7.4 Hz)	5.3614 (t, 1H, J = 7.3 Hz)
H-1'''-R	5.12 (d, 1H, J = 1.9 Hz)	5.1203 (d, 2H, J = 13.35 Hz)
CH ₃ -R	1.00 (d, 3H, J = 6.1 Hz)	1.0068 (d, 1H, J = 6.2)
OH-5	12.62 (s, 1H)	12.5750 (s, 1H)
OH-7	10.86 (s, 1H)	10.8508 (s, 1H)
OH-3'	9.21 (s, 1H)	9.1887 (s, 1H)
OH-4'	9.71 (s, 1H)	9.6792 (s, 1H)

Table 6.53: ¹³C-NMR data of the isolated compound LMH2.

Position	Rutin (DMSO-d ₆ , 50 MHz, δ ppm) Reported values ^[229]	LMH2 (DMSO-d ₆ , 125 MHz, δ, ppm) Spectral values
C-2	157.3	156.44
C-3	134.1	133.31
C-4	178.2	177.38

C-5	157.5	156.65
C-6	99.5	98.71
C-7	164.9	164.08
C-8	94.5	93.62
C-9	162.1	161.22
C-10	104.8	103.99
C-1'	122.5	121.62
C-2'	116.1	115.25
C-3'	145.6	144.75
C-4'	149.3	148.41
C-5'	117.1	116.30
C-6'	122.0	121.20
C-1''-G	101.6	100.75
C-2''	74.9	74.08
C-3''	77.3	76.45
C-4''	72.7	71.86
C-5''	76.7	75.90
C-6''	67.9	67.01
C-1'''-R	102.2	101.20
C-2'''	70.8	70.02
C-3'''	71.2	70.39
C-4'''	71.4	70.58
C-5'''	69.1	68.25
C-6'''- CH₃	18.6	17.73

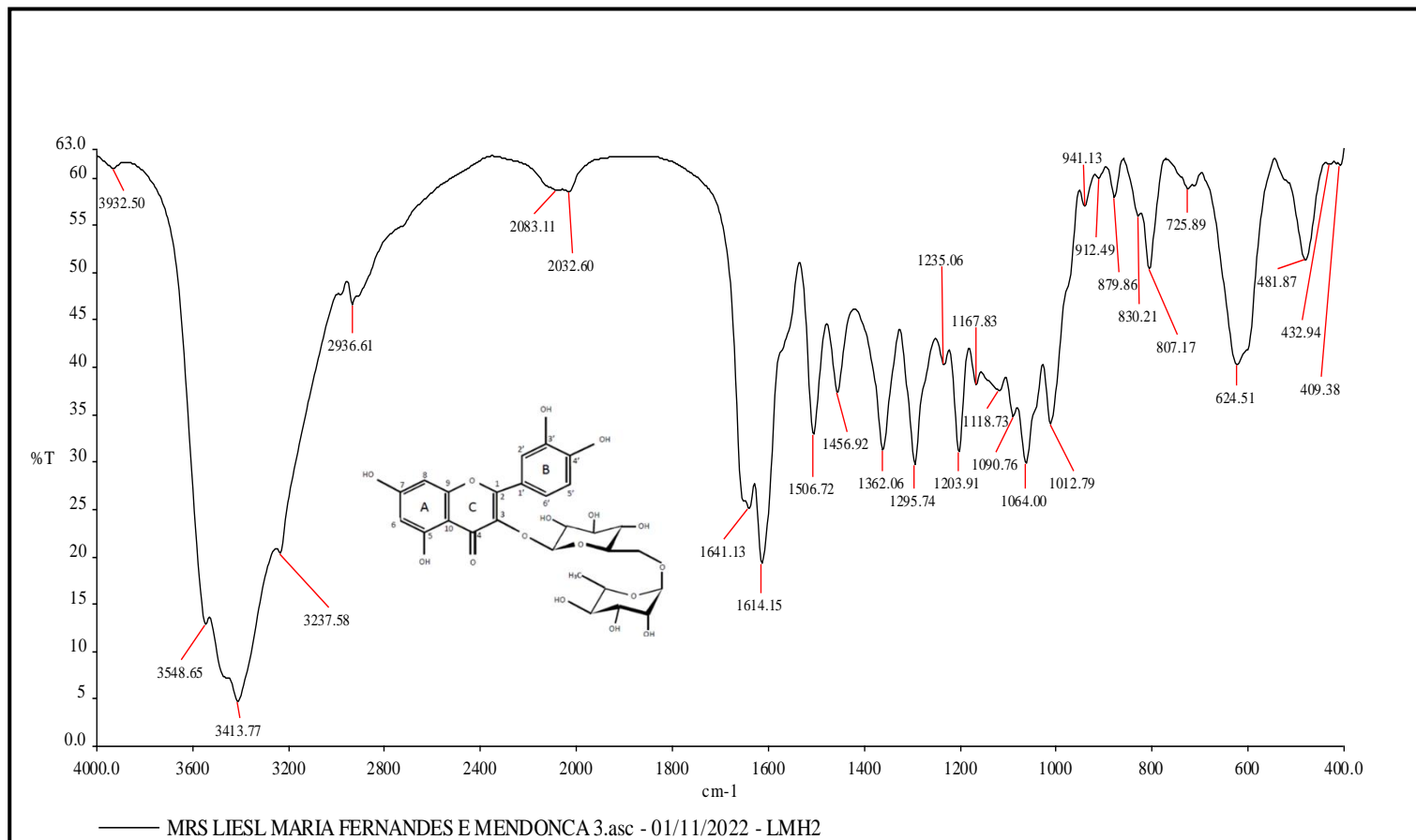
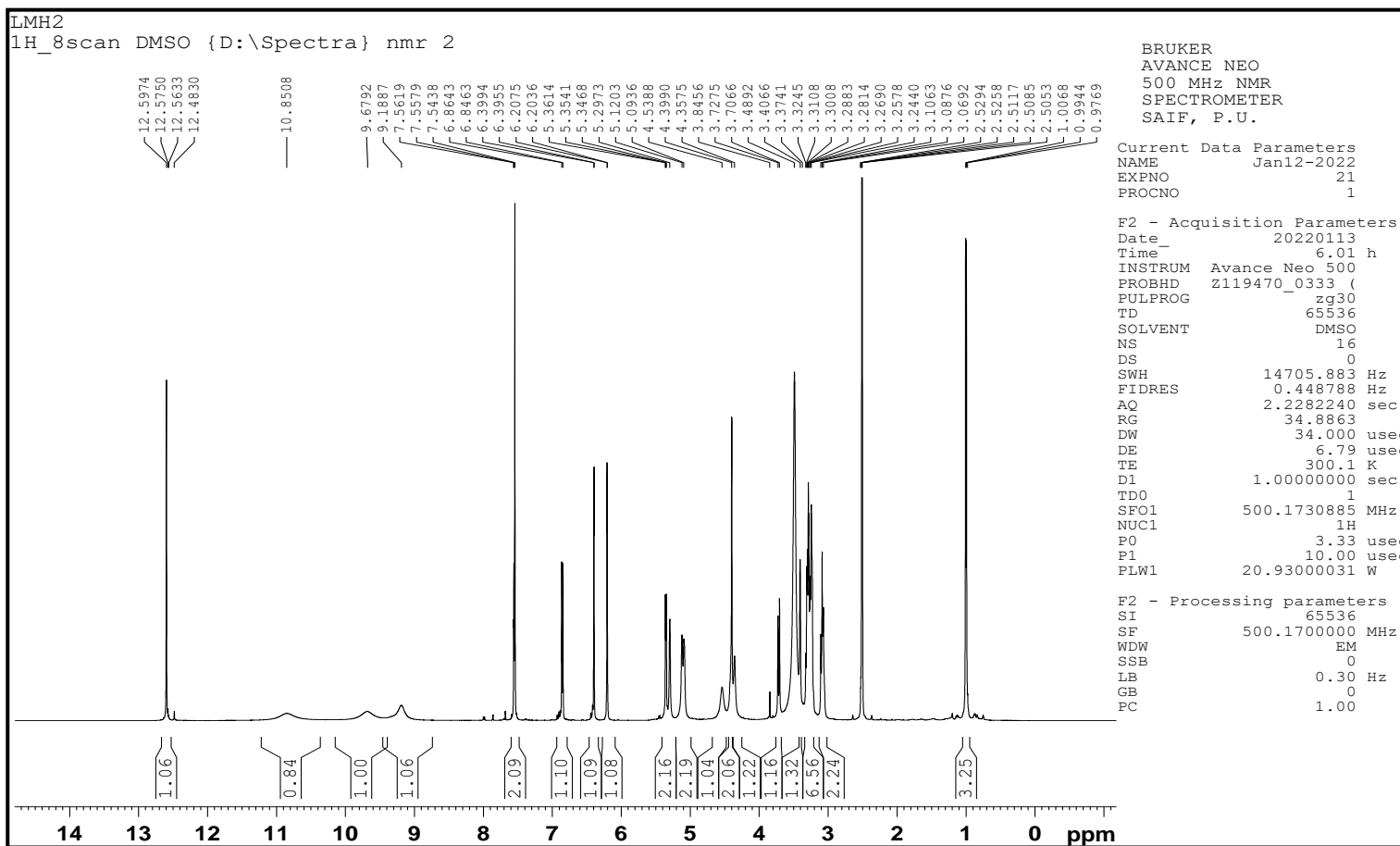
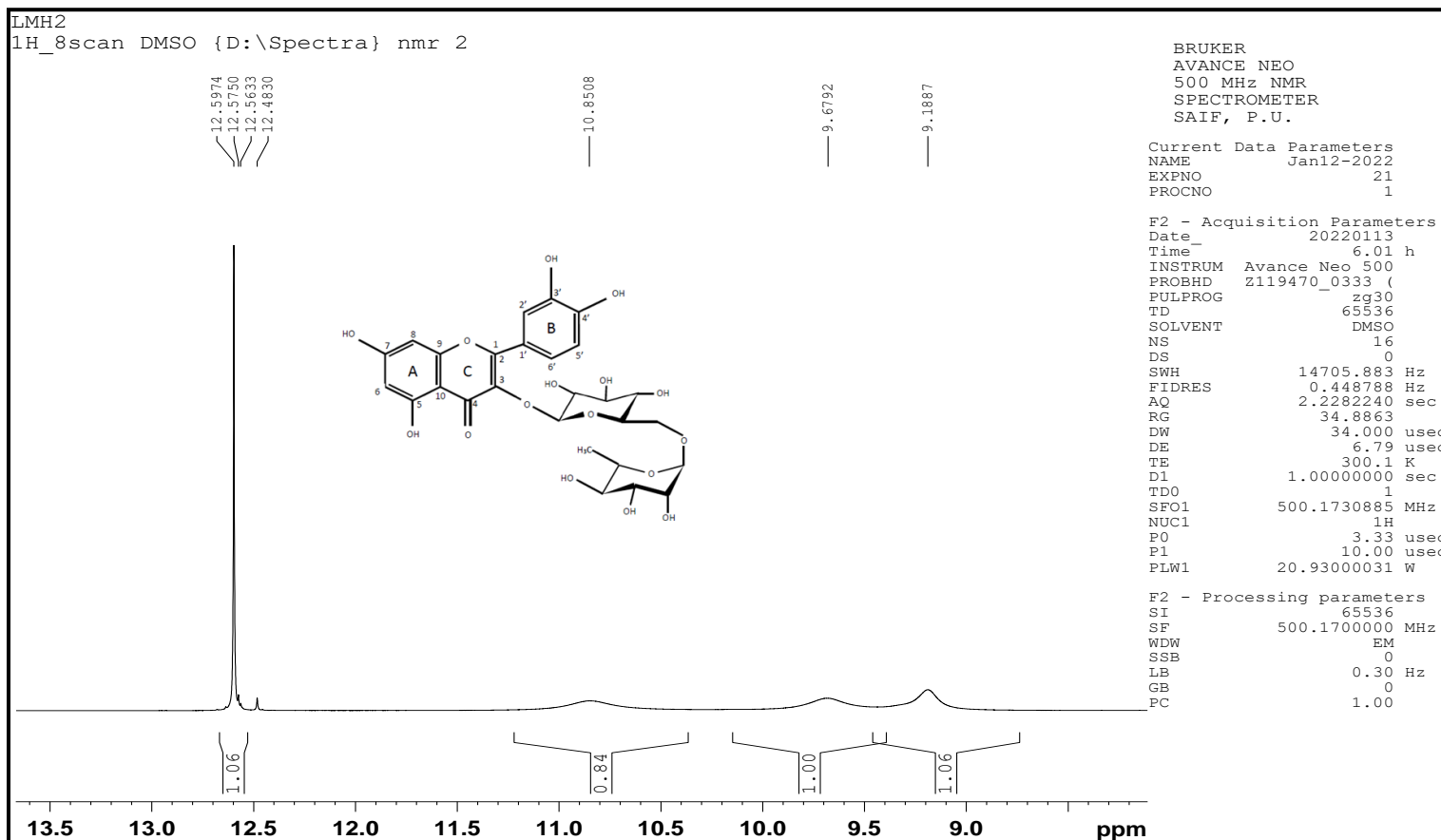
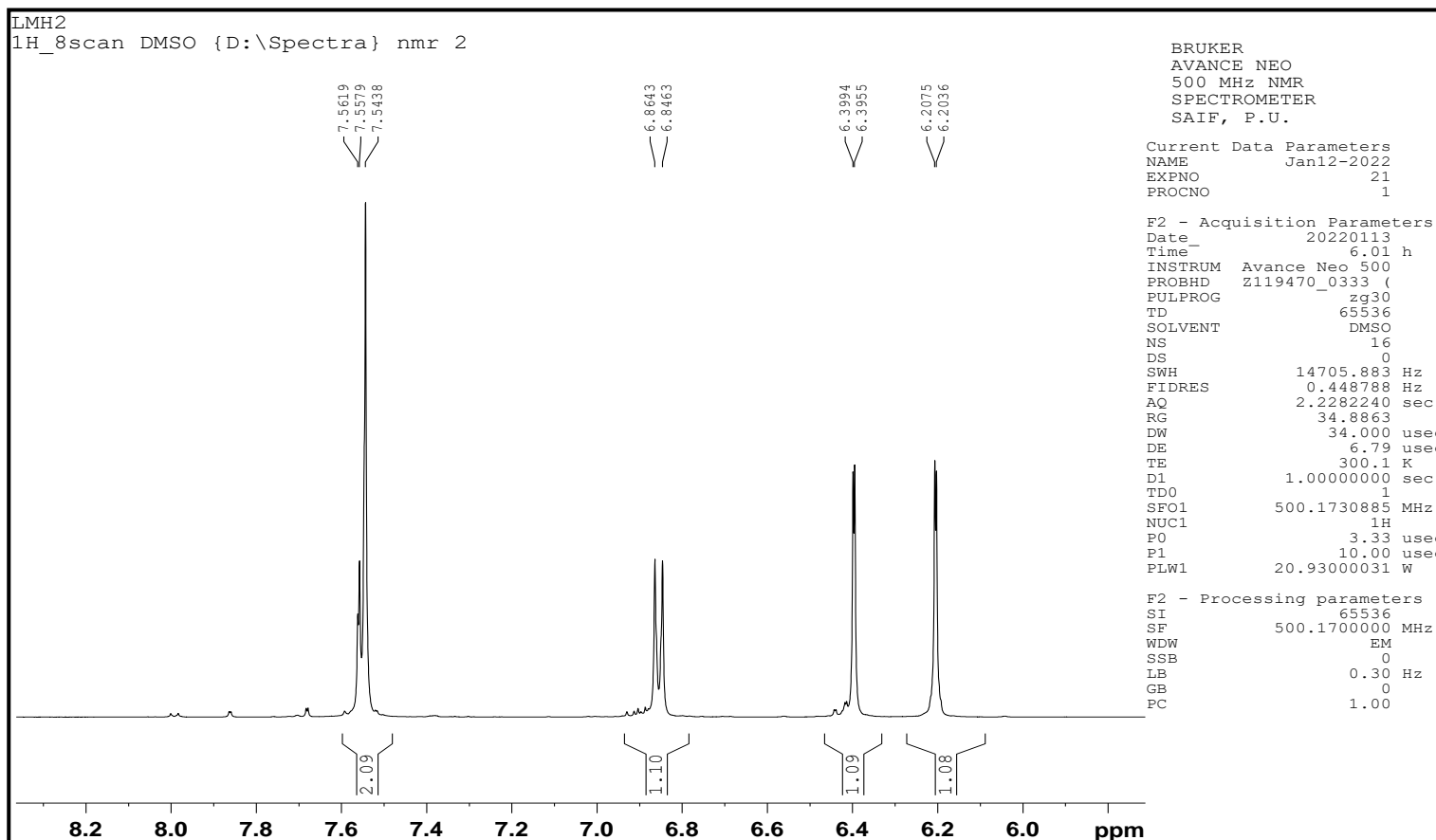
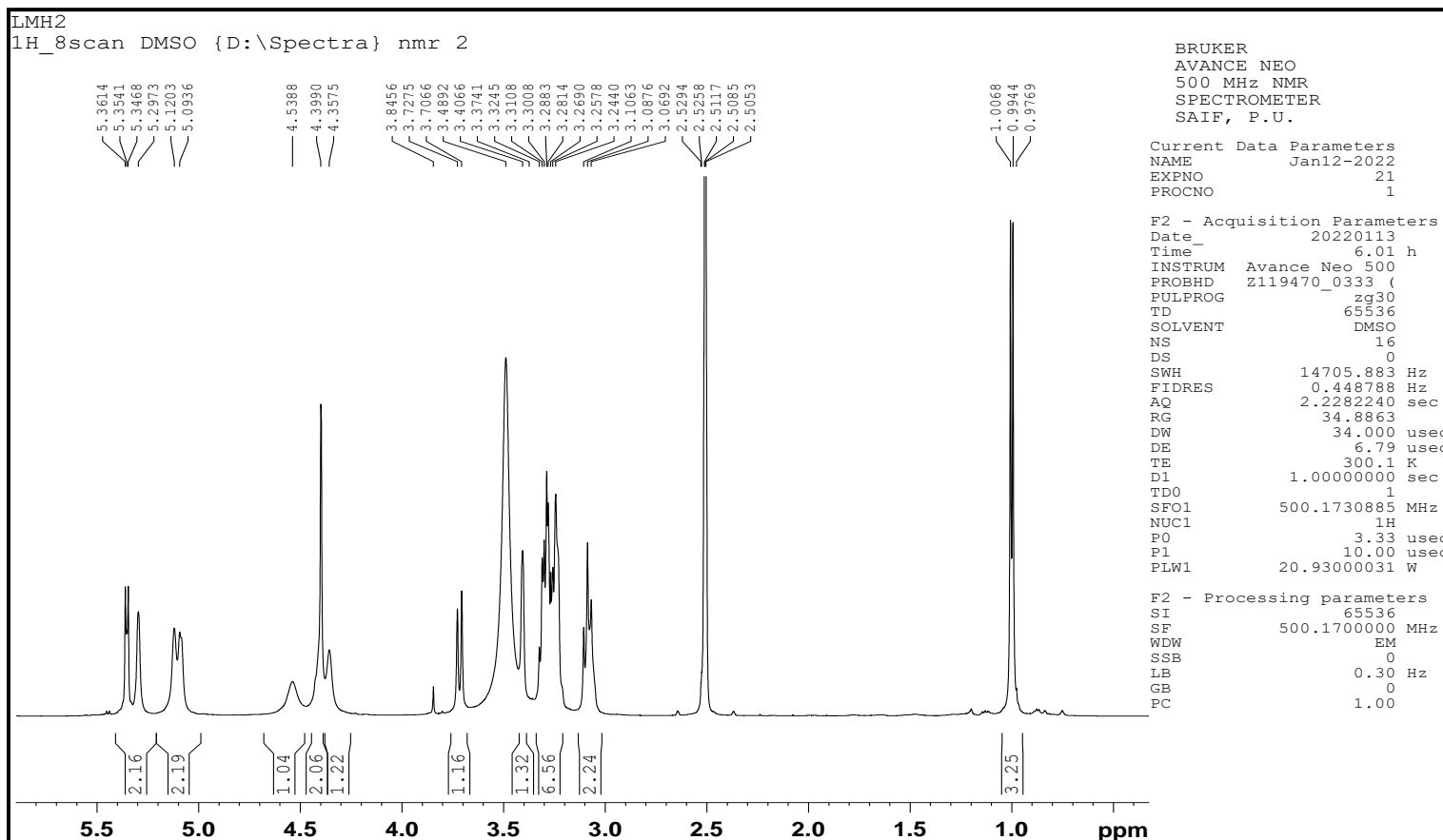


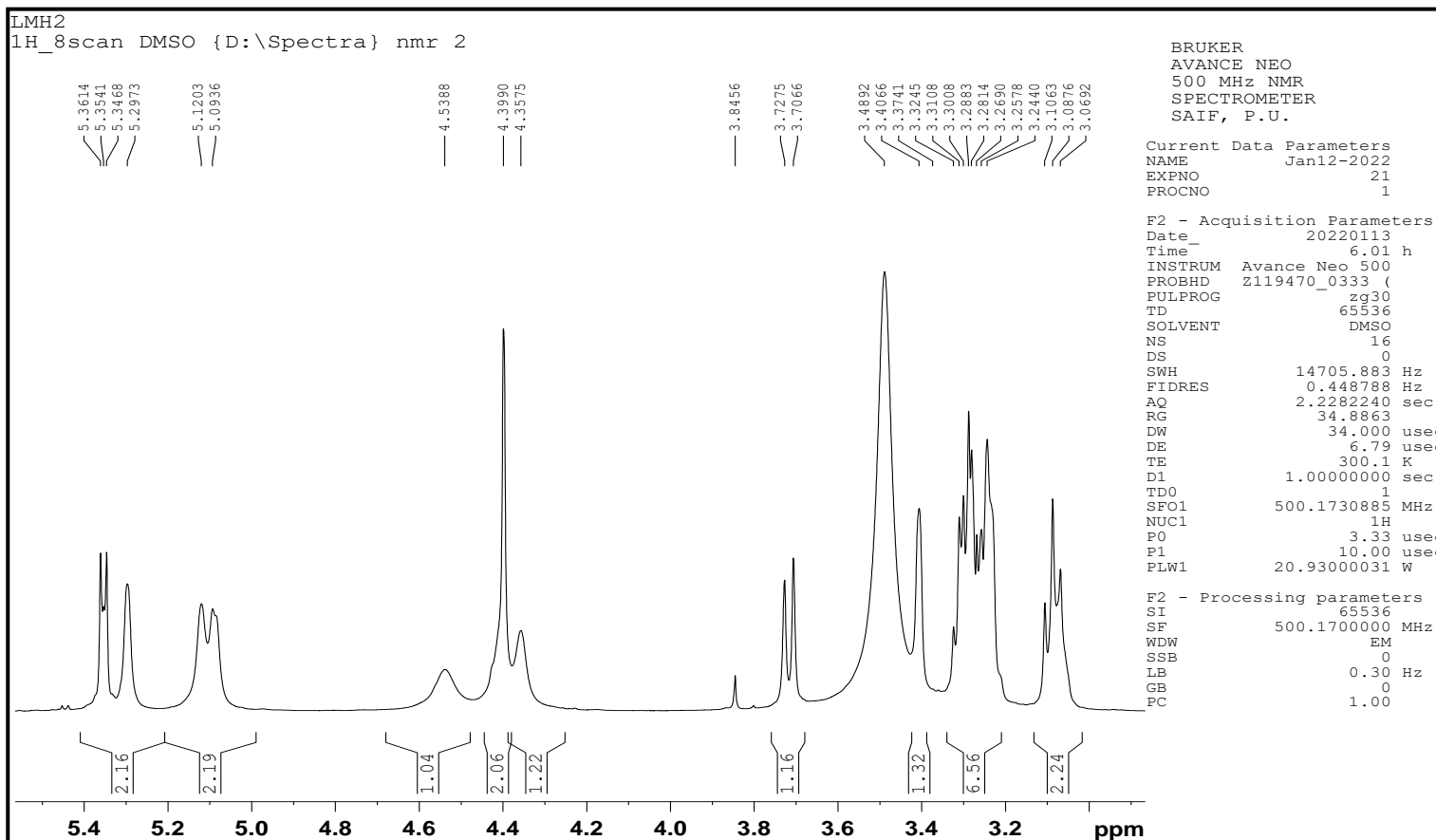
Figure 6.72: IR spectrum of LMH2 (Rutin).

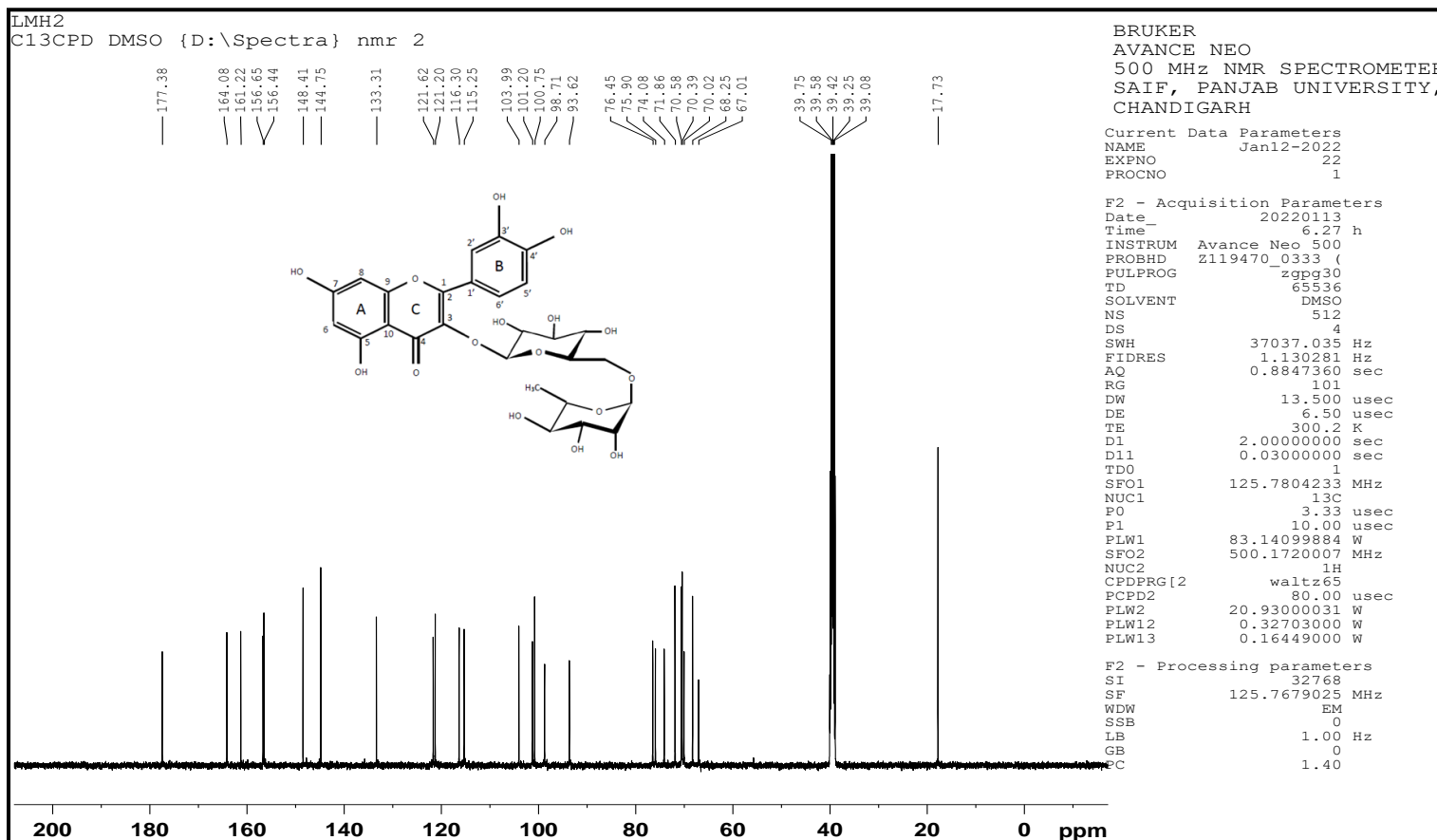
Figure 6.73: ^1H -NMR spectrum of LMH2 (Rutin).

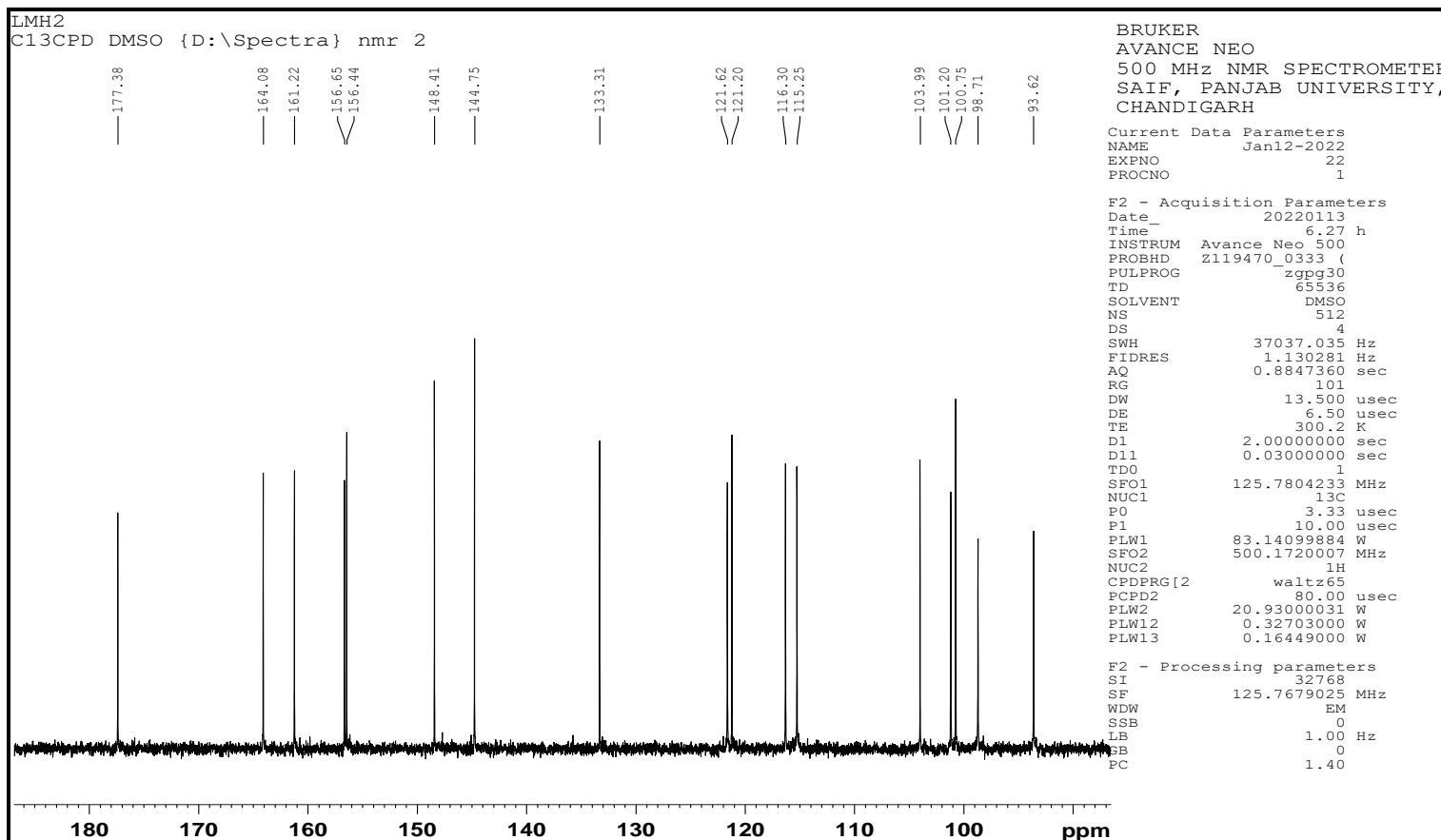
Figure 6.74: Resolution of ^1H -NMR spectrum of LMH2 (Rutin).

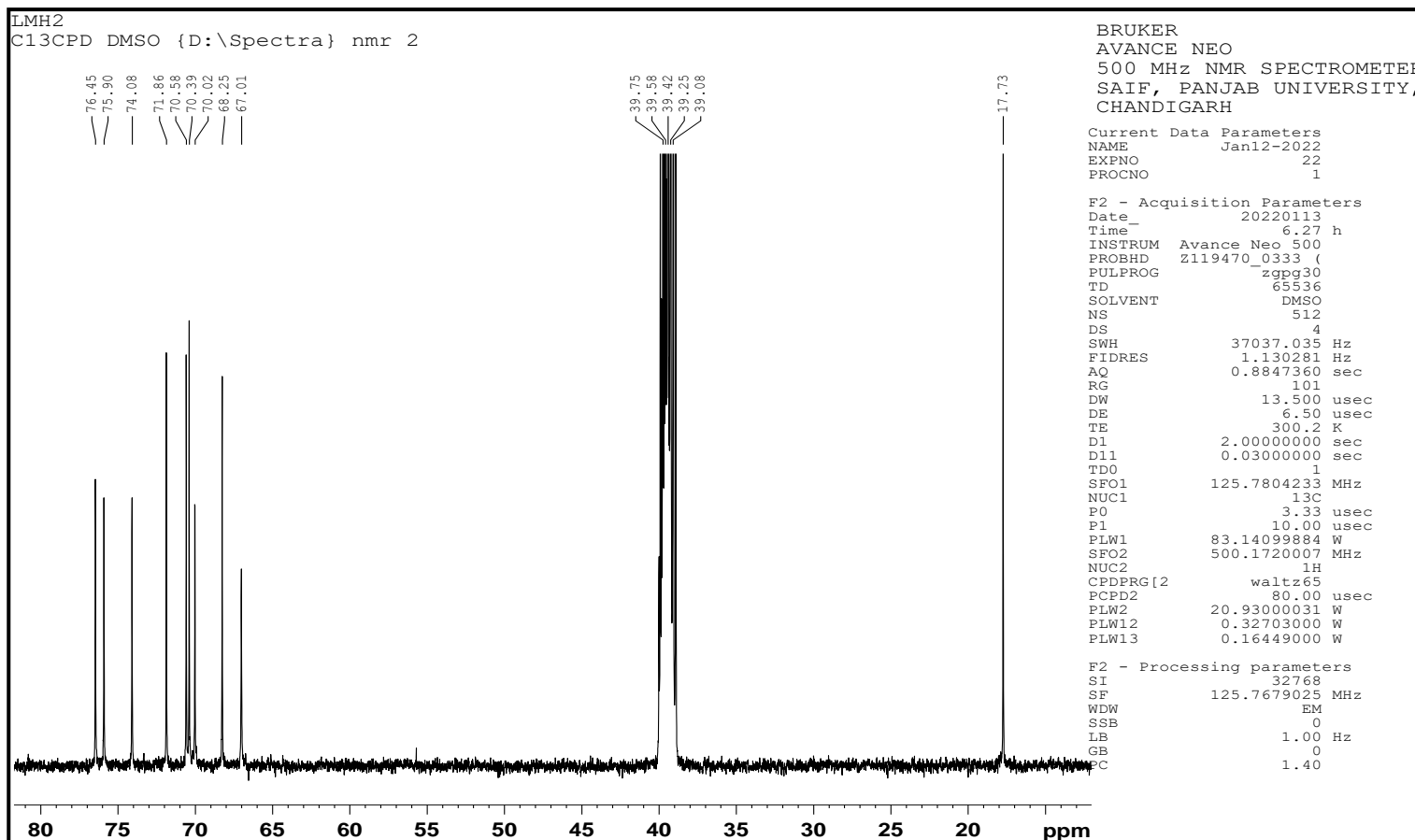
Figure 6.75: Resolution of ^1H -NMR spectrum of LMH2 (Rutin).

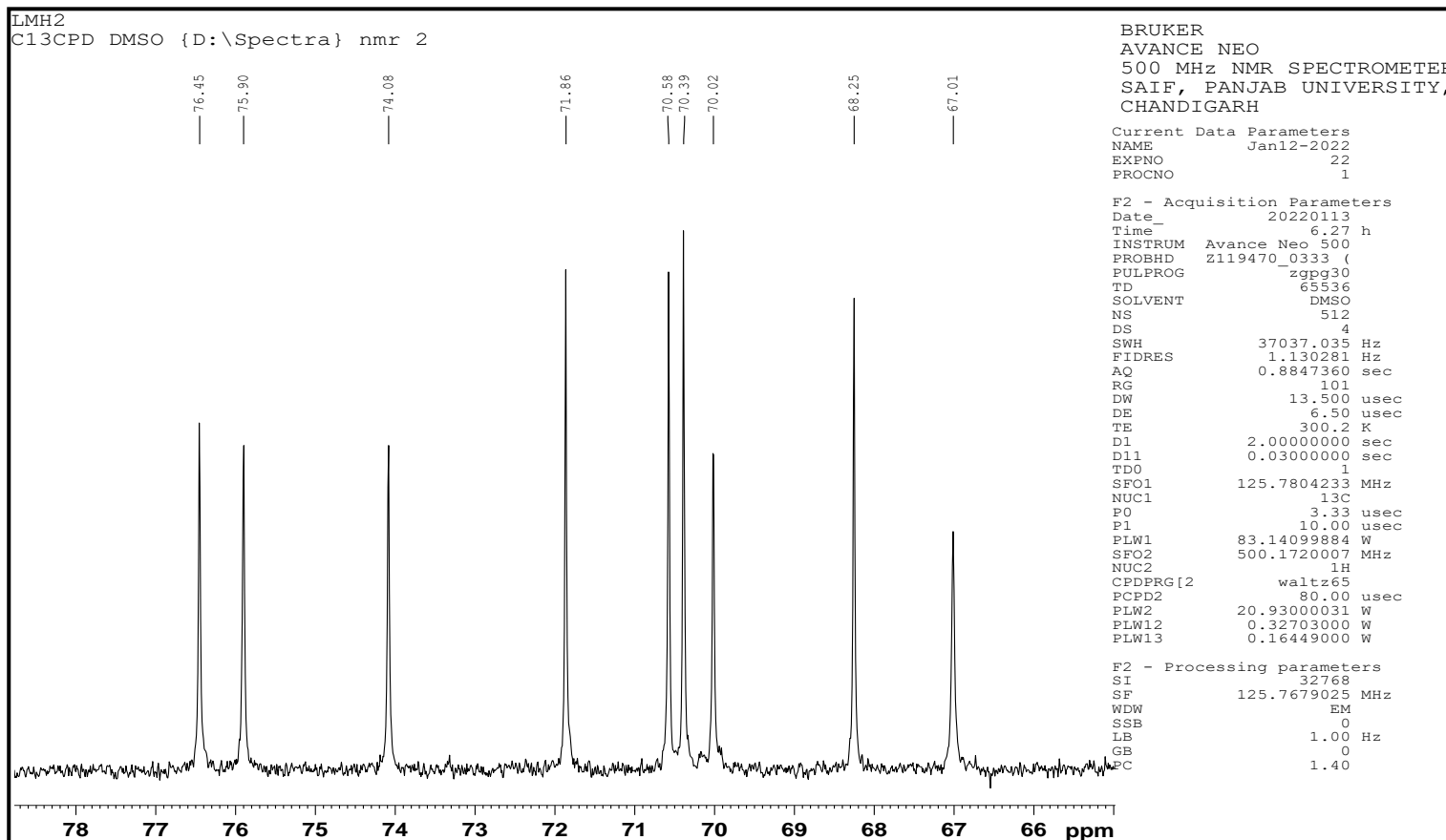
Figure 6.76: Resolution of ^1H -NMR spectrum of LMH2 (Rutin).

Figure 6.77: Resolution of ^1H -NMR spectrum of LMH2 (Rutin).



Figure 6.79: ^{13}C -NMR spectrum of LMH2 (Rutin).

Figure 6.80: Resolution of ^{13}C -NMR spectrum of LMH2 (Rutin).

Figure 6.81: Resolution of ^{13}C -NMR spectrum of LMH2 (Rutin).

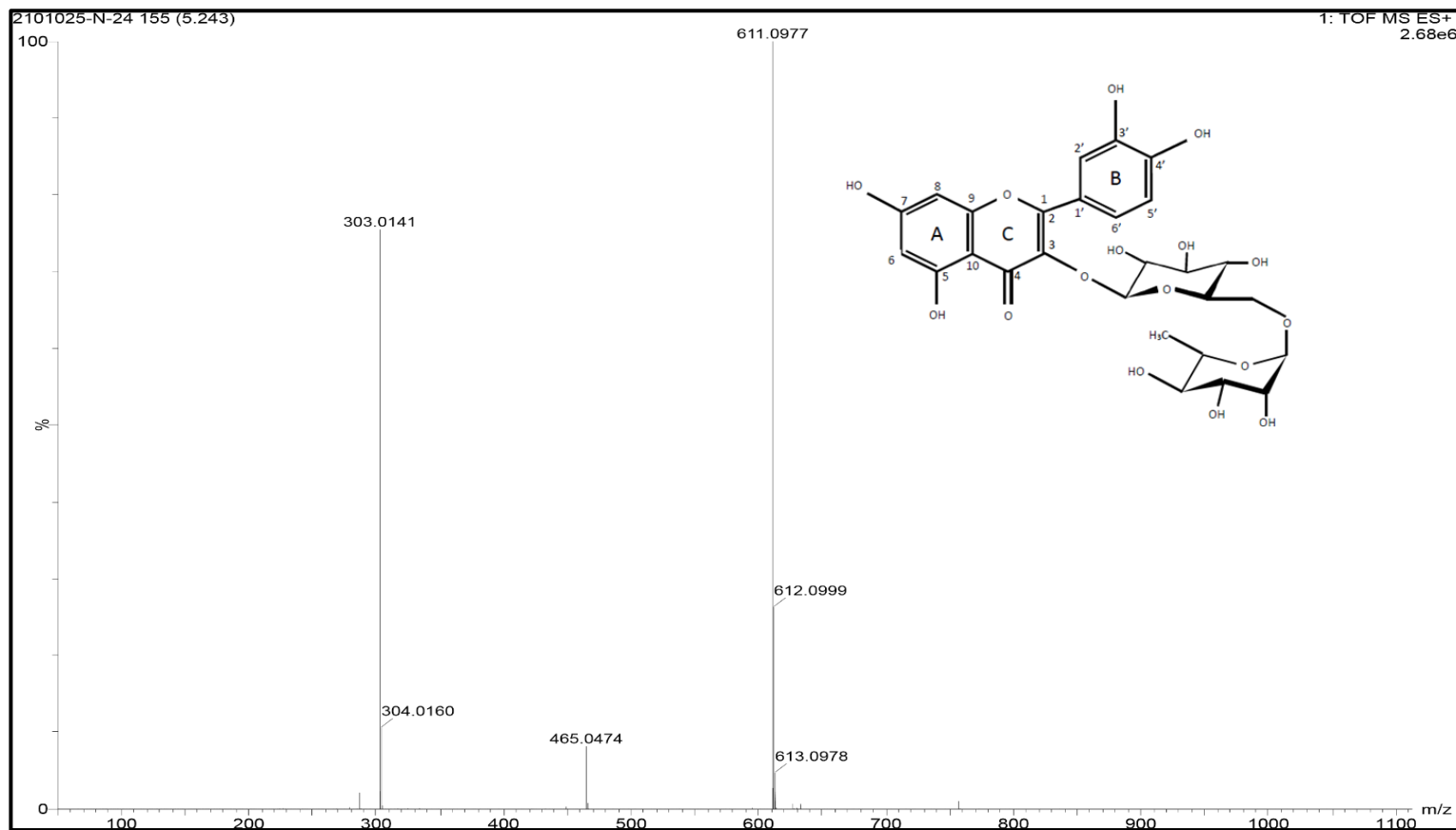


Figure 6.82: Mass spectrum of LMH2 (Rutin).

6.2.10.1.3. CHARACTERISATION OF COMPOUND LMH3

Physical parameters of the compound

Physical state Creamish - coloured compound

Melting point 254 °C (*lit.* 250 - 253 °C) [230]

The compound LMH3 gave a positive response for shinoda test for flavonoids.

Spectral characteristics of the compound

IR (KBr) 3468.50 cm⁻¹ (OH str.)
 1637.45 cm⁻¹ (C=O str.)
 1515.83 cm⁻¹ (C=C str. in aromatic ring)
 1382.34 cm⁻¹ (C-O str).

¹H-NMR and ¹³C-NMR Tables 6.54 and 6.55

Mass spectra (LC-MS)

LC-MS (*m/z*) 611.36 [M+H]⁺, other peaks appeared at
 302.05, 257.18, 242.45

Molecular formula C₂₈H₃₄O₁₅

Molecular weight 610.56 g/mol

From the m.p., IR, ¹H-NMR, ¹³C-NMR and mass spectral data, the compound was identified as Hesperidin.

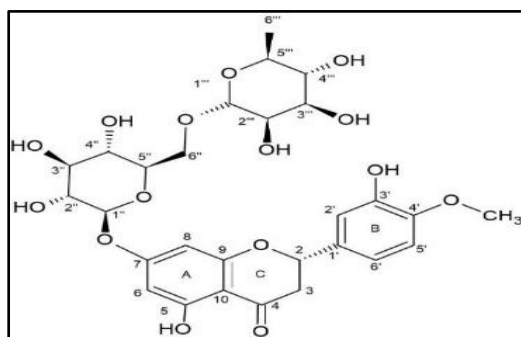


Figure 6.83: Structure of Hesperidin.

Table 6.54: ¹H-NMR data of the isolated compound LMH3.

Position	Hesperidin (DMSO-d ₆ , 400 MHz, δ ppm, J, Hz) Reported values ^[230]	LMH3 (DMSO-d ₆ , 400 MHz, δ ppm, J, Hz) Reported values
H-2	5.50 (dd, 1H, <i>J</i> = 12.2, 2.6 Hz)	5.521 (dd, 1H, <i>J</i> = 9.2, 2.8 Hz)
H-3a	3.09 - 3.20 (m, 1H)	3.099-3.163 (m, 2H)
H-3b	2.78 (dd, 1H, <i>J</i> = 17, 2.6 Hz)	2.798 (dd, 1H, <i>J</i> = 14, 2.8 Hz)
H-6	6.14 (d, 1H, <i>J</i> = 6.4 Hz)	6.143 (dd, 1H, <i>J</i> = 6.4, 2 Hz)
H-8	6.14 (d, 1H, <i>J</i> = 6.4 Hz)	6.143 (dd, 1H, <i>J</i> = 6.4, 2 Hz)
H-1'	4.53 (s, 1H)	4.520 (s, 1H)
H-2'	6.94 - 6.89 (m, 3H)	6.954 - 6.117 (m, 3H)
H-5'		
H-6'		
-OCH₃	3.78 (s, 3H)	3.774 (s, 3H)
H-1''	4.98 (d, 1H, <i>J</i> = 7.3 Hz)	4.983 (d, 1H, <i>J</i> = 7.2 Hz)
H-3''	4.05 - 4.14 (m, 1H)	4.587 - 4.452 (m, 1H)
H-4''	3.82 (br, s, 1H)	3.808 (s, 1H)
H-6''	4.59 (d, 1H, <i>J</i> = 3.5 Hz)	δ 4.598 (d, 1H, <i>J</i> = 4.4 Hz)
H-1'''	5.17 (t, 1H, <i>J</i> = 5.5 Hz)	5.179 (t, 1H, <i>J</i> = 5.6 Hz)
H-2'''	4.67 (d, 1H, <i>J</i> = 5.5 Hz)	4.674 (d, 1H, <i>J</i> = 5.2 Hz)
H-4'''	4.46 (d, 1H, <i>J</i> = 5.5 Hz)	4.467 (d, 1H, <i>J</i> = 6)
H-6'''-CH₃	1.09 (d, 3H, <i>J</i> = 6.1 Hz)	1.092 (d, 3H, <i>J</i> = 6.4 Hz)
Ar-OH-3'	9.08 (s, 1H)	9.082 (s, 1H)
Ar-OH-5	12.02 (s, 1H)	12.020 (s, 1H)

Table 6.55: ^{13}C -NMR data of the isolated compound LMH3.

Position	Hesperidin (DMSO- d_6 , 100 MHz, δ ppm) Reported values ^[230]	LMH3 (DMSO- d_6 , 100 MHz, δ , ppm) Spectral values
C-2	78.4	78.360
C-3	42.1	42.035
C-4	197.0	197.012
C-5	163.2	163.026
C-6	96.4	96.359
C-7	165.2	165.121
C-8	95.6	95.524
C-9	103.3	103.297
C-10	162.5	162.479
C-1'	130.9	130.884
C-2'	114.2	114.138
C-3'	146.5	146.439
C-4'	148.0	147.942
C-5'	112.1	112.012
C-6'	118.0	117.933
C-1''-R	99.5	99.426
C-2''	72.1	72.052
C-3''	75.6	75.506
C-4''	70.7	70.685
C-5''	76.3	76.257
C-6''	66.1	66.016
C-1'''	100.6	100.595

Position	Hesperidin (DMSO-d₆, 100 MHz, δ ppm) Reported values [230]	LMH3 (DMSO-d₆, 100 MHz, δ, ppm) Spectral values
C-2'''	69.6	69.569
C-3'''	70.3	70.252
C-4'''	73.0	72.970
C-5'''	68.3	68.301
C-6'''-CH₃	17.9	17.827
OCH₃	55.7	55.669

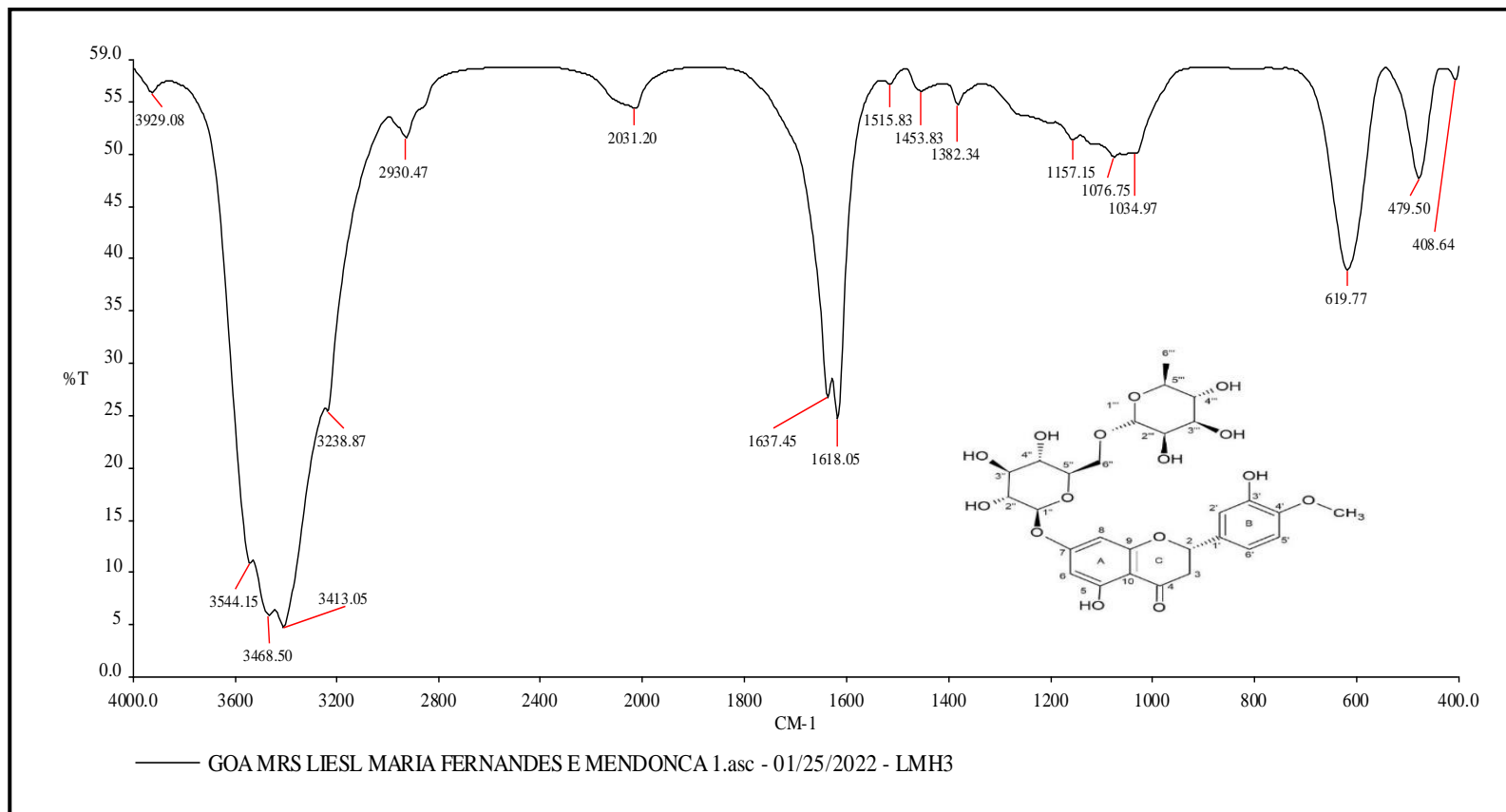


Figure 6.84: IR spectrum of LMH3 (Hesperidin).

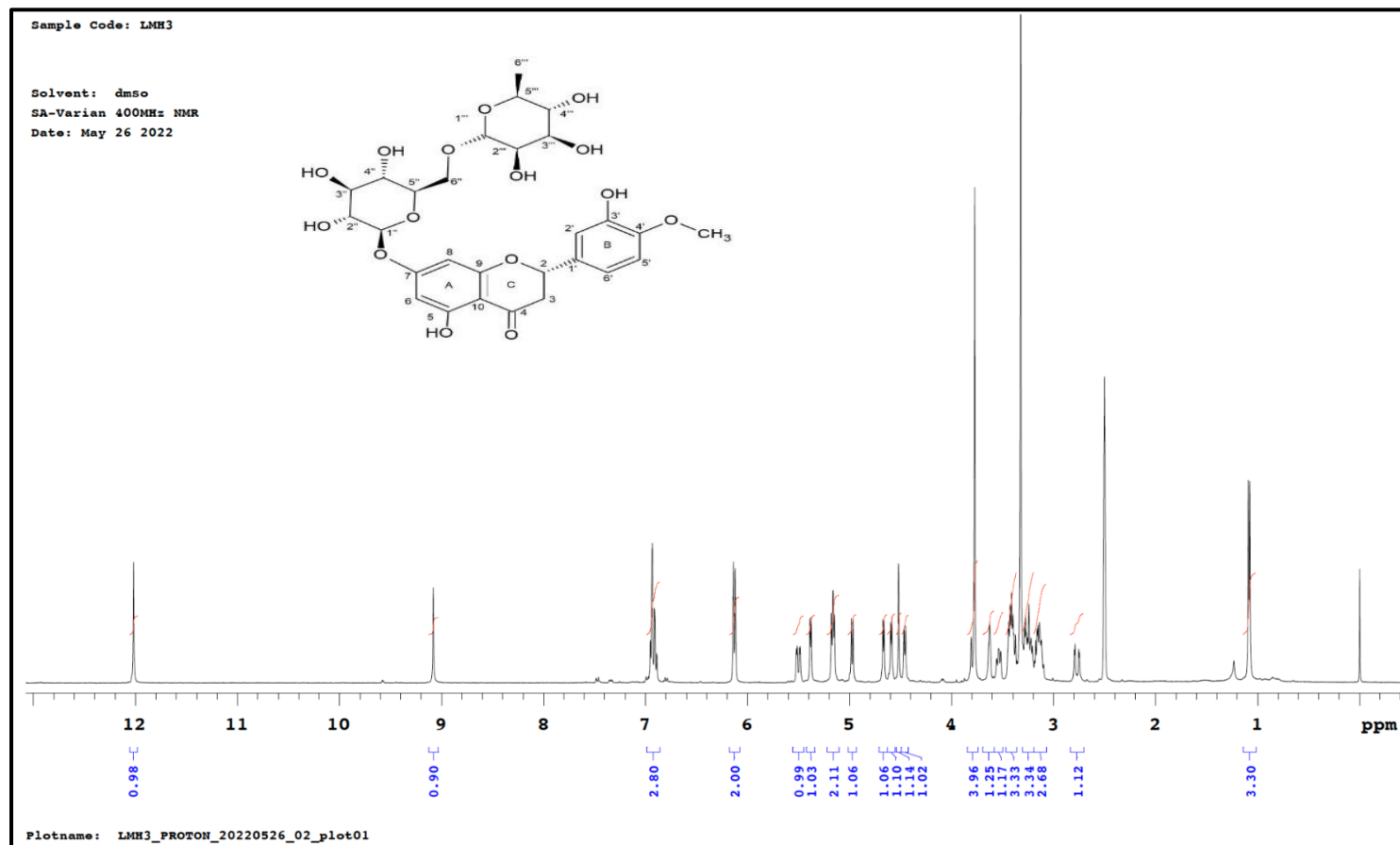


Figure 6.85: ^1H -NMR spectrum of LMH3 (Hesperidin).

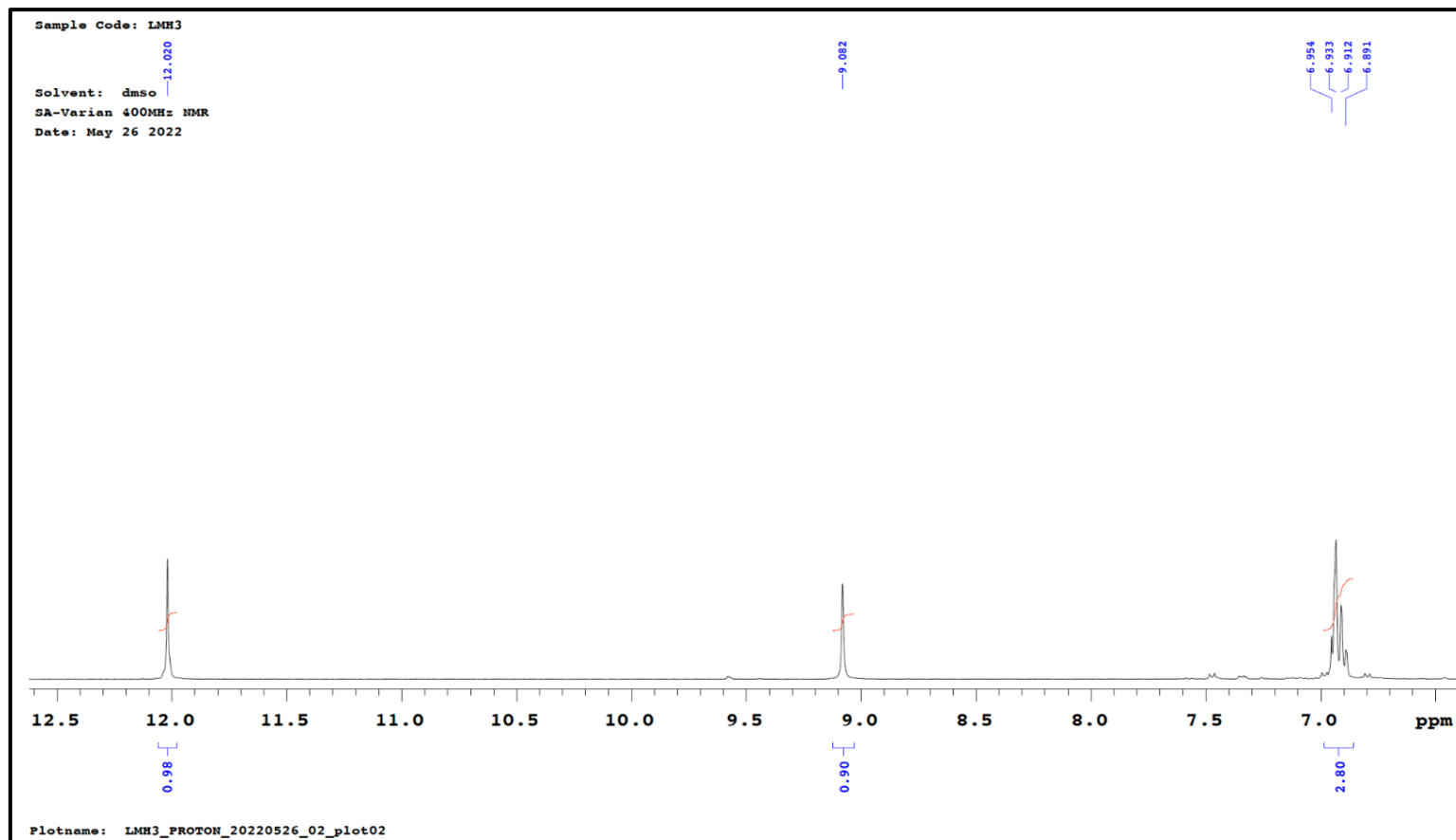


Figure 6.86: Resolution of ^1H -NMR spectrum of LMH3 (Hesperidin).

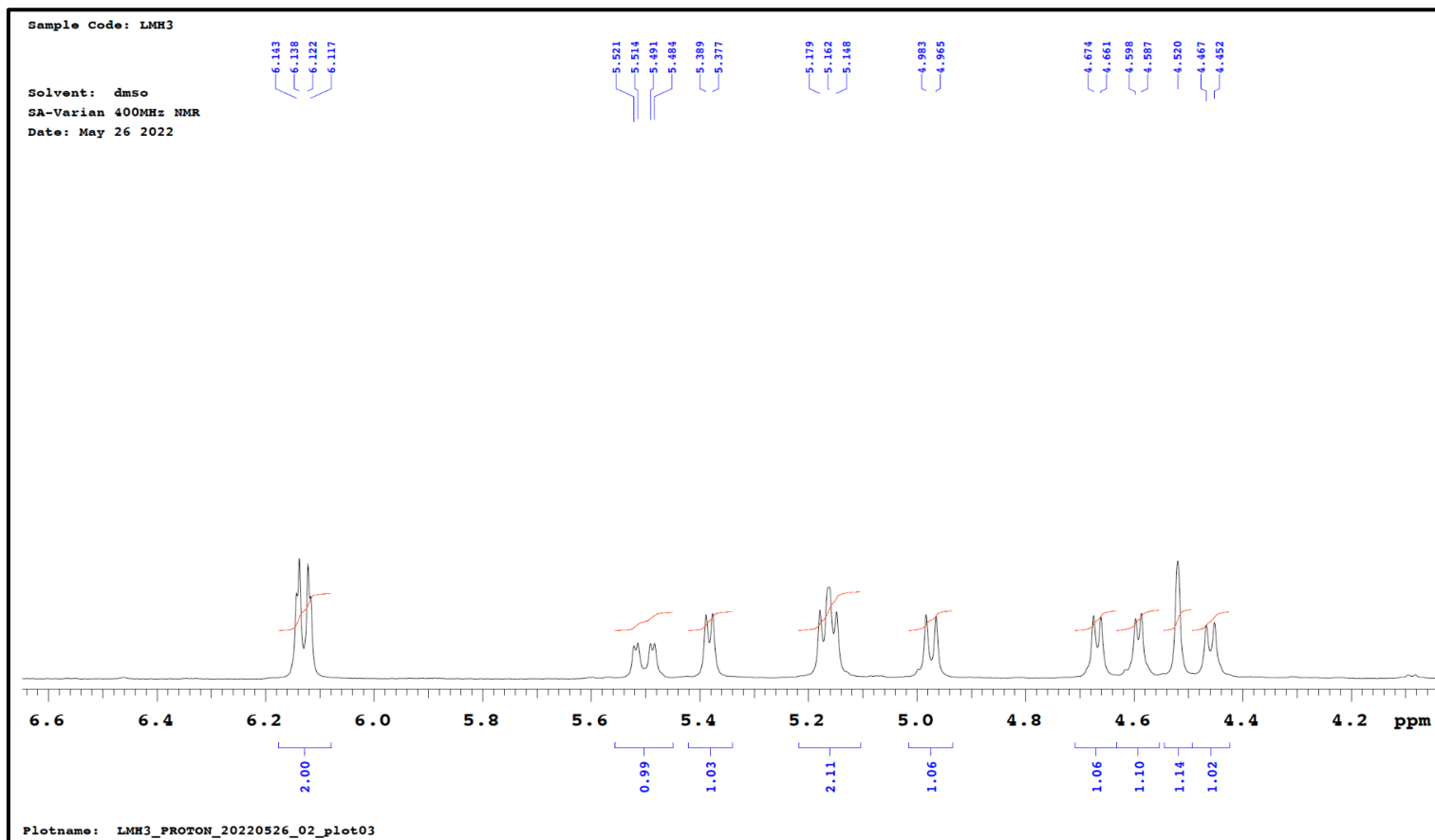


Figure 6.87: Resolution of ^1H -NMR spectrum of LMH3 (Hesperidin).

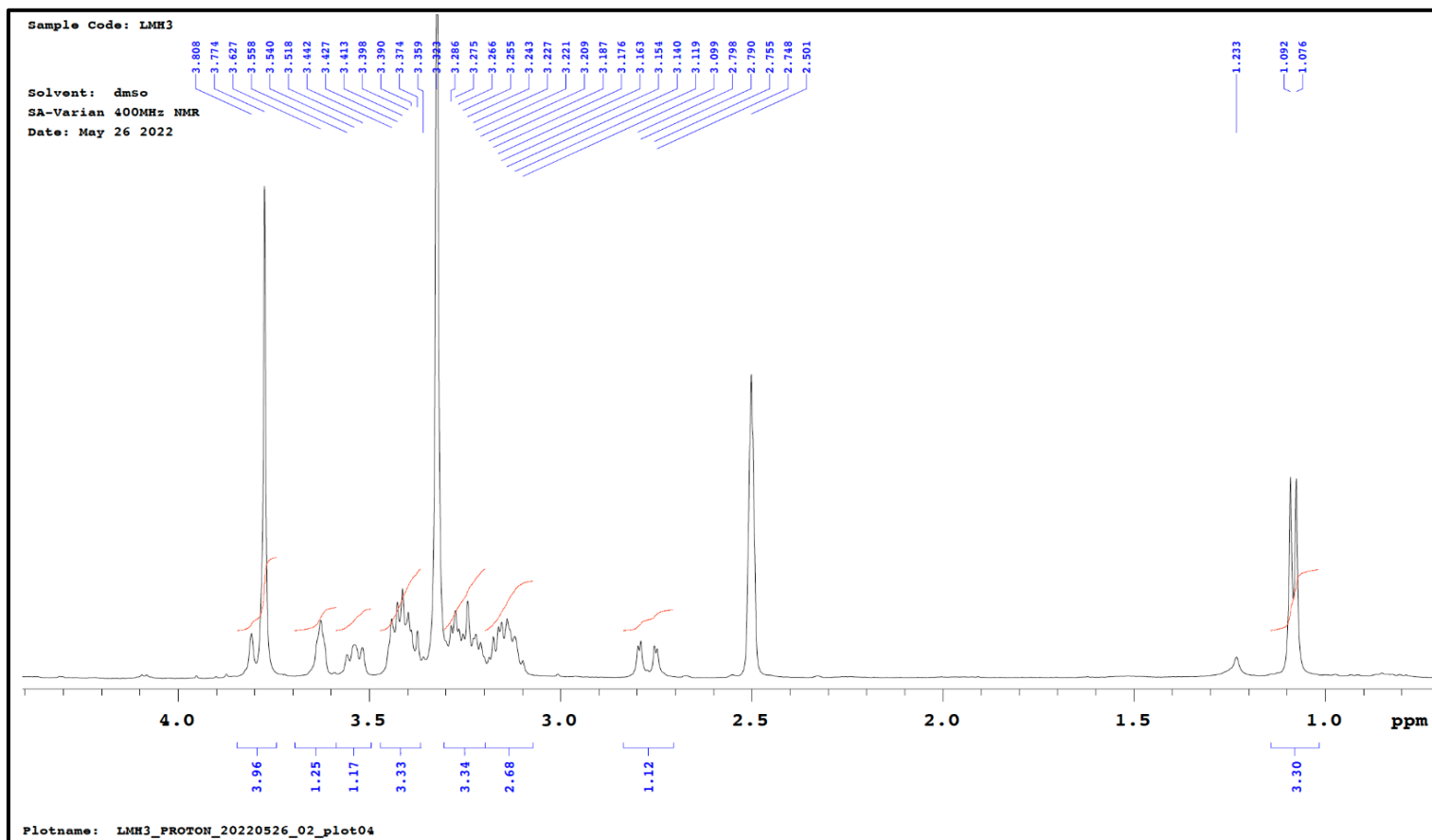
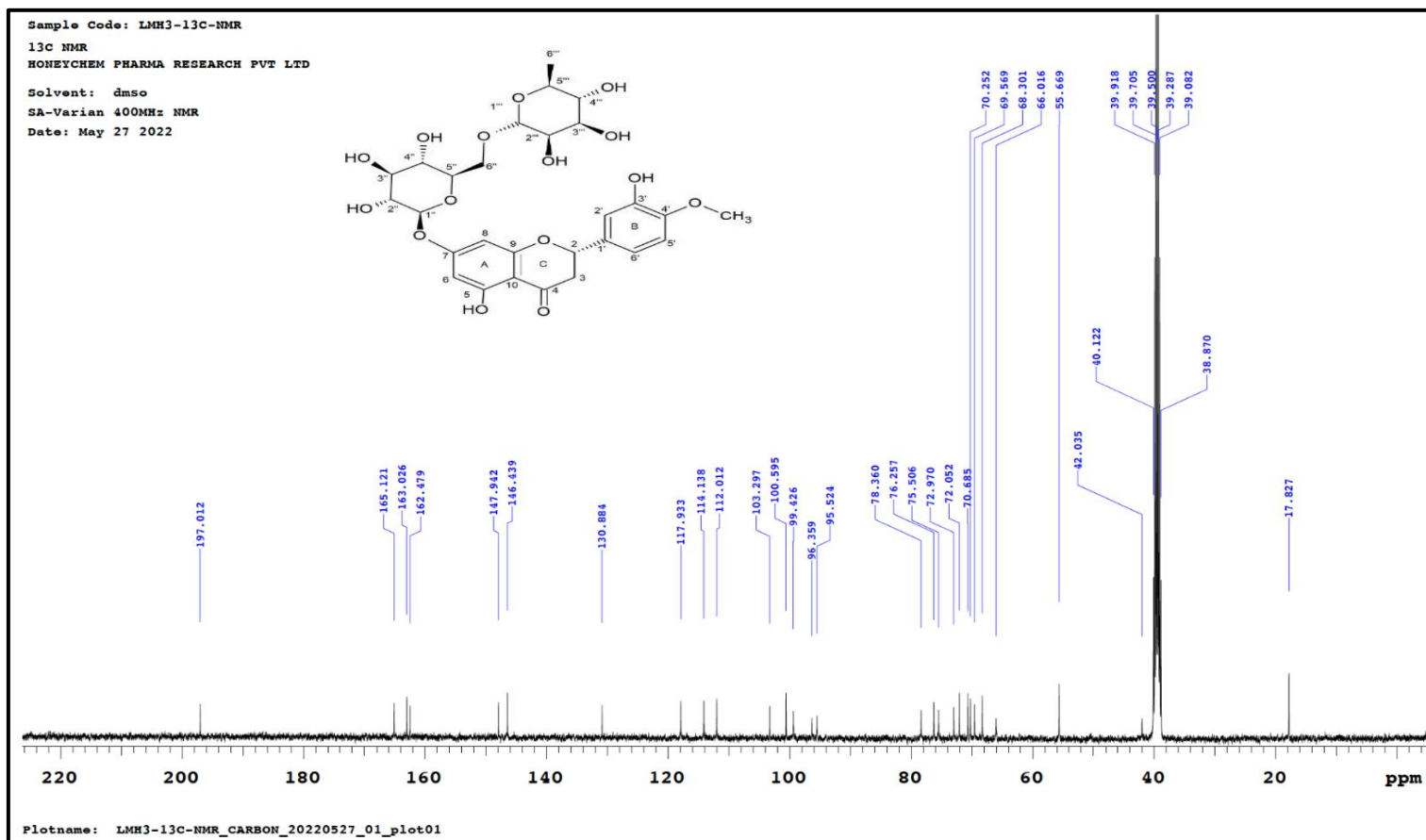


Figure 6.88: Resolution of ^1H -NMR spectrum of LMH3 (Hesperidin).

Figure 6.89: ¹³C-NMR spectrum of LMH3 (Hesperidin).

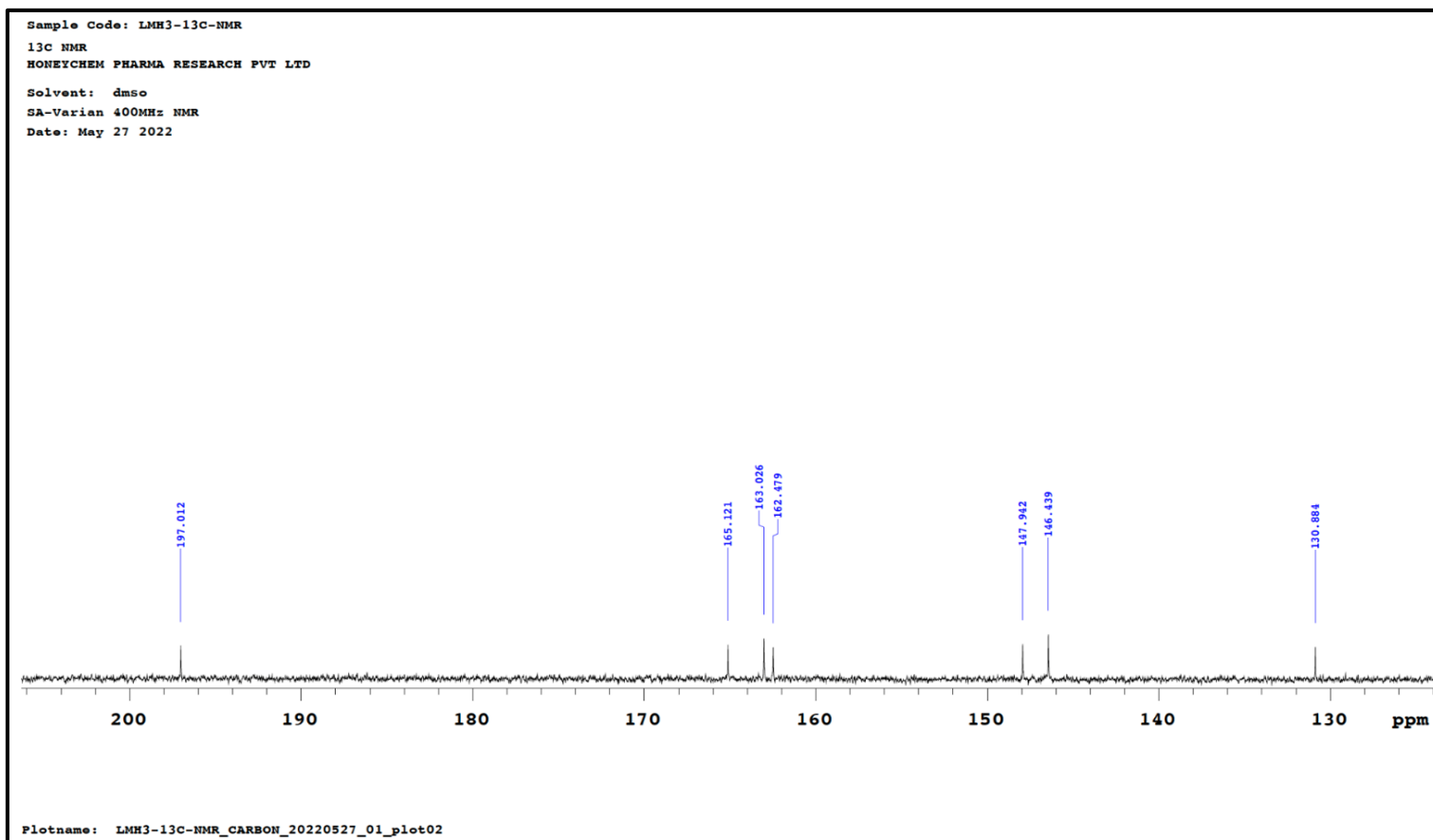


Figure 6.90: Resolution of ^{13}C -NMR spectrum of LMH3 (Hesperidin).

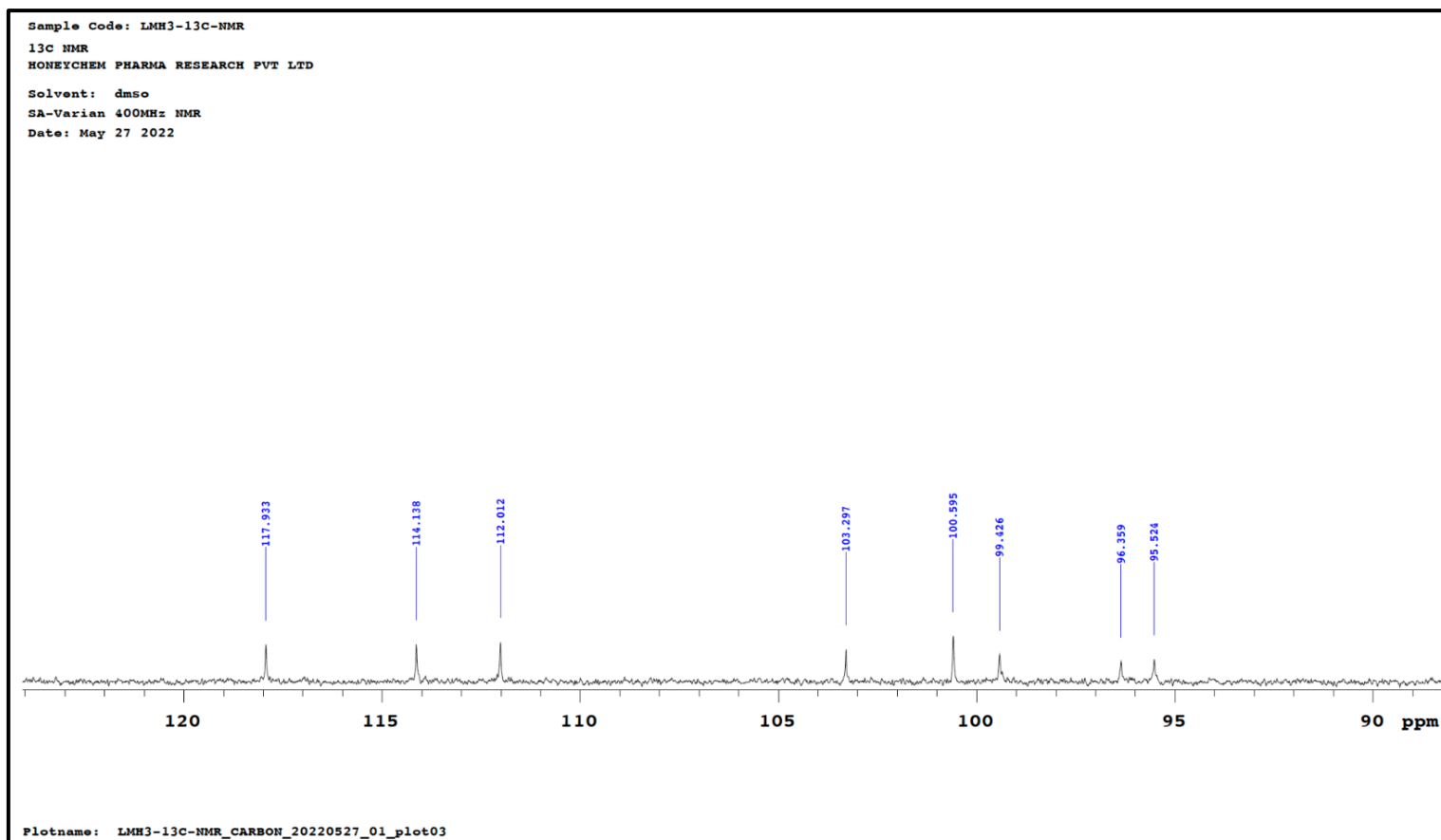


Figure 6.91: Resolution of ^{13}C -NMR spectrum of LMH3 (Hesperidin).

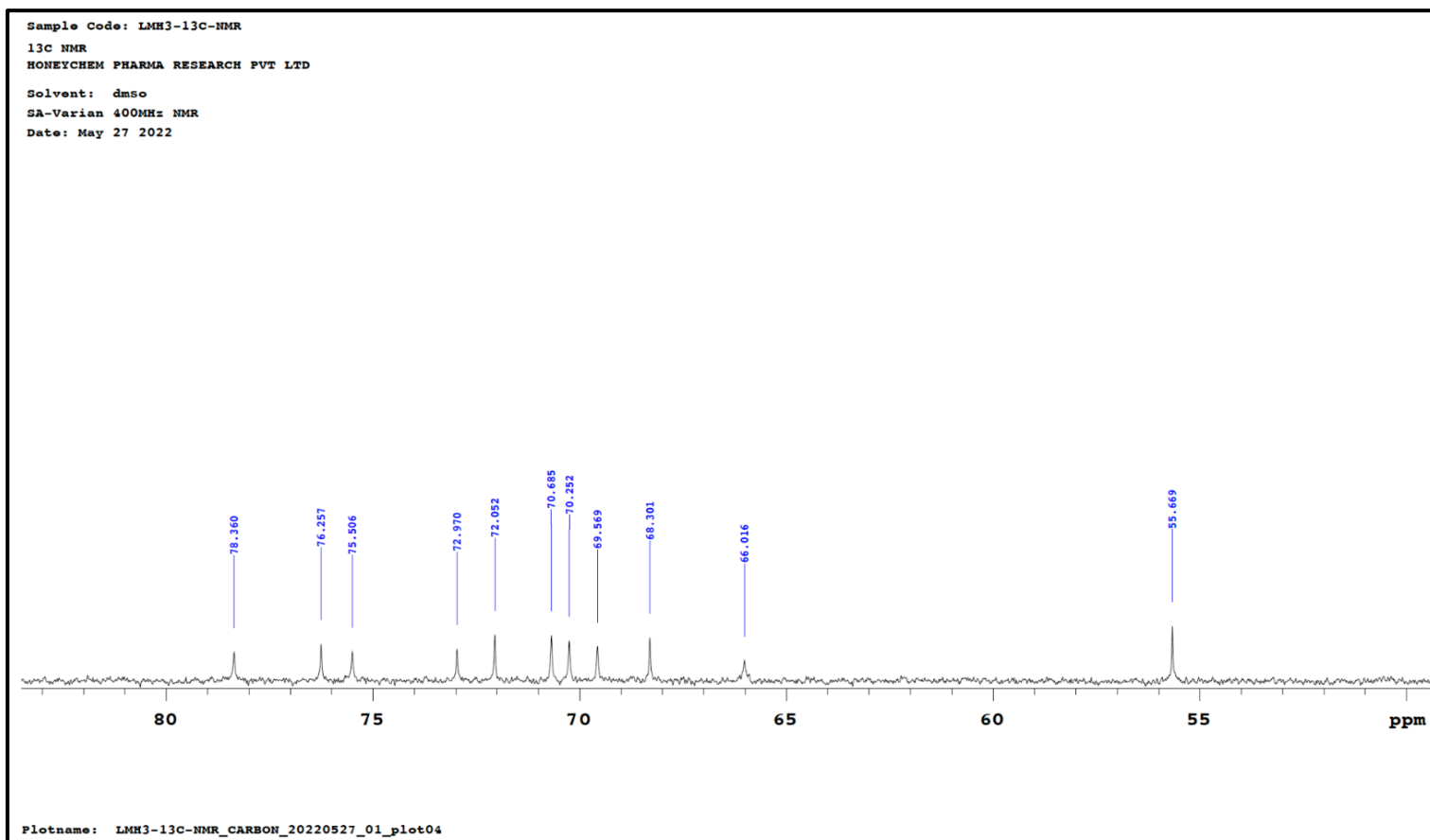


Figure 6.92: Resolution of ^{13}C -NMR spectrum of LMH3 (Hesperidin).

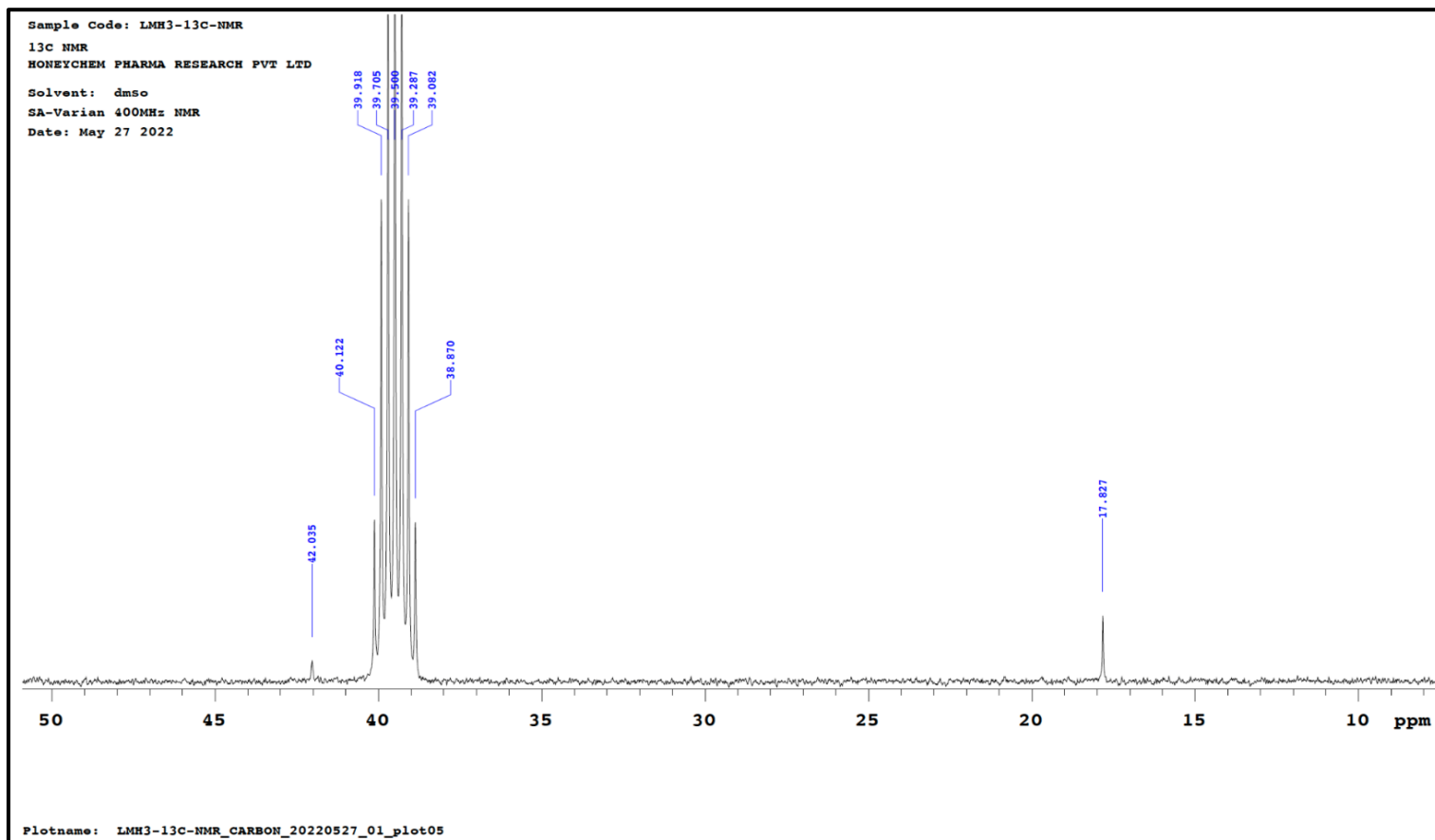


Figure 6.93: Resolution of ^{13}C -NMR spectrum of LMH3 (Hesperidin).

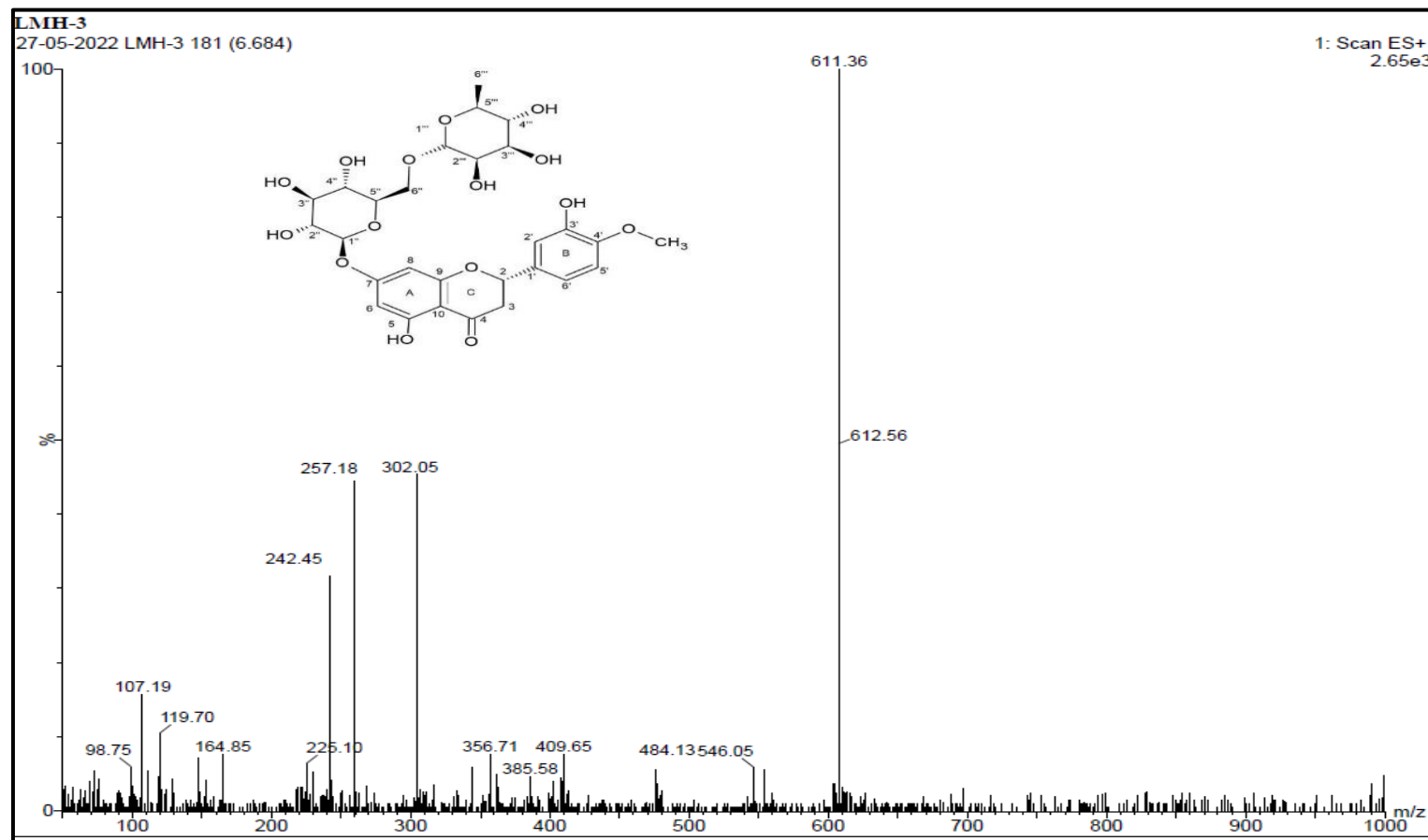


Figure 6.94: Mass spectrum of LMH3 (Hesperidin).

6.2.10.2. Isolation and characterisation of phytoconstituents from MFBF

The yield of the column fraction LMF obtained was 2.67 g. Purification of LMF by preparative HPLC led to the isolation of three compounds LMF1, LMF2, LMF3 and LMF4 that had yield of 21.3 mg (0.80 %), 142.6 mg (5.34 %), 21.1 mg (0.79 %) and 20.7 mg (0.78 %) respectively. The structural elucidation and characterization of the isolated compounds *viz.* LMF1, LMF2, LMF3 and LMF4 from MFBF is listed below.

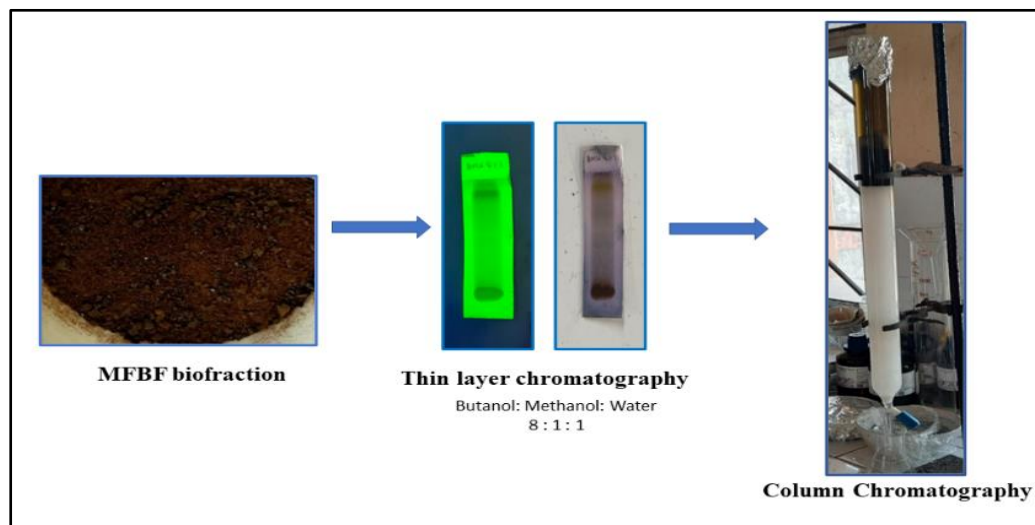


Figure 6.95: Isolation of phytoconstituents from MFBF.

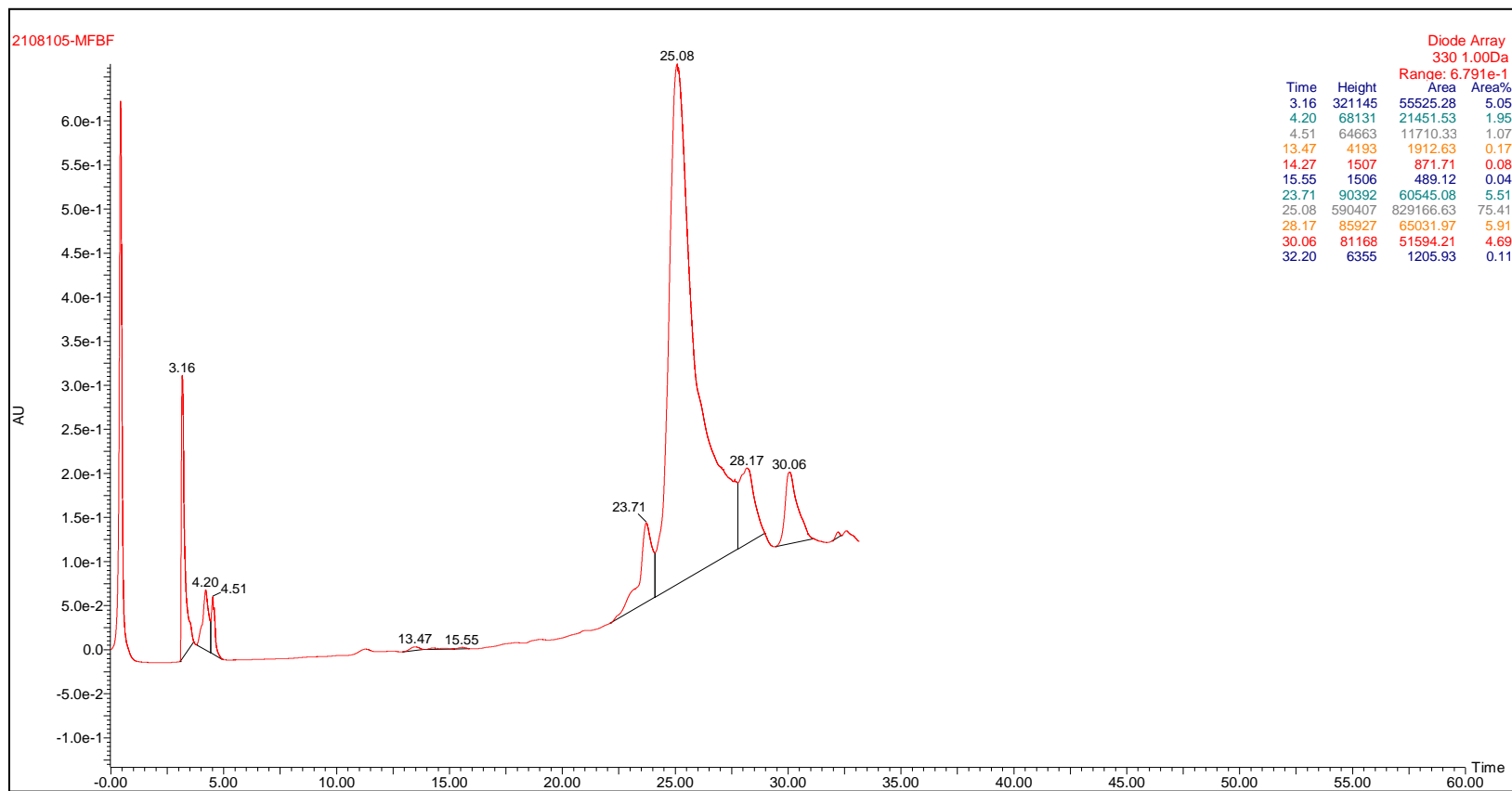


Figure 6.96: Preparative HPLC chromatogram of LMF (MFBF purified fraction).

6.2.10.2.1. CHARACTERISATION OF COMPOUND LMF1

Physical parameters of the compound

Physical state Amorphous yellow coloured compound

Melting point 180 °C (*lit.* 180 - 182 °C)^[78]

The compound LMF1 gave a positive response for shinoda test for flavonoids.

Spectral characteristics of the compound

IR (KBr) 3413.36 cm⁻¹ (OH str.)

2848.77 cm⁻¹ (C-H str.)

1662.44 cm⁻¹ (C=O str.)

1562.75 cm⁻¹ (C=C str. in Ar ring)

1320.12 cm⁻¹ (C-O str.)

¹H-NMR and ¹³C-NMR Tables 6.56 and 6.57

Mass spectra

LC-MS (*m/z*) 303.1495 [M+H]⁺, other peaks appeared at 257.1385, 229.1308, 201.1321, 153.0828, 137.0847

Molecular formula C₁₅H₁₀O₇

Molecular weight 302.24 g/mol

From the m.p., IR, ¹H-NMR, ¹³C-NMR and mass spectral data, the compound was identified as **Quercetin**.

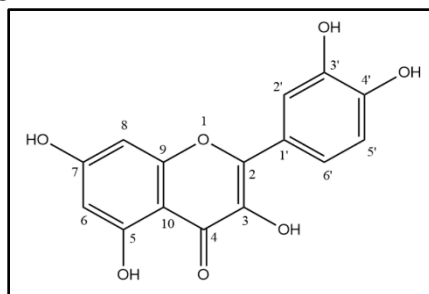


Figure 6.97: Structure of Quercetin.

Table 6.56: $^1\text{H-NMR}$ data of the isolated compound LMF1.

Position	Quercetin (DMSO- d_6 , 400 MHz, δ ppm, J , Hz) Reported values ^[231]	LMF1 (DMSO- d_6 , 500 MHz, δ ppm, J , Hz) Spectral values
H-6	6.21 (d, 1H, $J = 2$ Hz)	6.1948 (d, 1H, $J = 2.1$ Hz)
H-8	6.44 (d, 1H, $J = 2$ Hz)	6.4145 (d, 1H, $J = 2$ Hz)
OH-3	9.66 (s, 1H)	9.5395 (s, 1H)
OH-5	12.59 (s, 1H)	12.4929 (s, 1H)
OH-7	10.42 (s, 1H)	10.7687 (s, 1H)
H-2'	7.64 (d, 1H, $J = 2.2$ Hz)	7.6864 (d, 1H, $J = 2.2$ Hz)
H-5'	6.92 (d, 1H, $J = 8.5$ Hz)	6.9007 (d, 1H, $J = 8.5$ Hz)
H-6'	7.52 (dd, 1H, $J = 8.5, 2.2$ Hz)	7.5576 (dd, 1H, $J = 6.3, 2.2$ Hz)
OH-3'	9.30 (s, 1H)	9.3426 (s, 1H)
OH-4'	9.43 (s, 1H)	9.3426 (s, 1H)

Table 6.57: ^{13}C -NMR data of the isolated compound LMF1.

Position	Quercetin (DMSO-d ₆ , 100 MHz, δ ppm) Reported values ^[231]	LMF1 (DMSO-d ₆ , 125 MHz, δ ppm) Spectral values
C-2	147.2	146.71
C-3	134.6	135.63
C-4	179.4	175.74
C-5	160.2	160.63
C-6	99.6	98.09
C-7	165.2	163.80
C-8	94.8	93.26
C-9	158.1	156.04
C-10	104.2	102.92
C-1'	123.2	121.87
C-2'	117.4	114.97
C-3'	145.6	144.96
C-4'	148.6	147.60
C-5'	116.8	115.51
C-6'	121.5	119.88

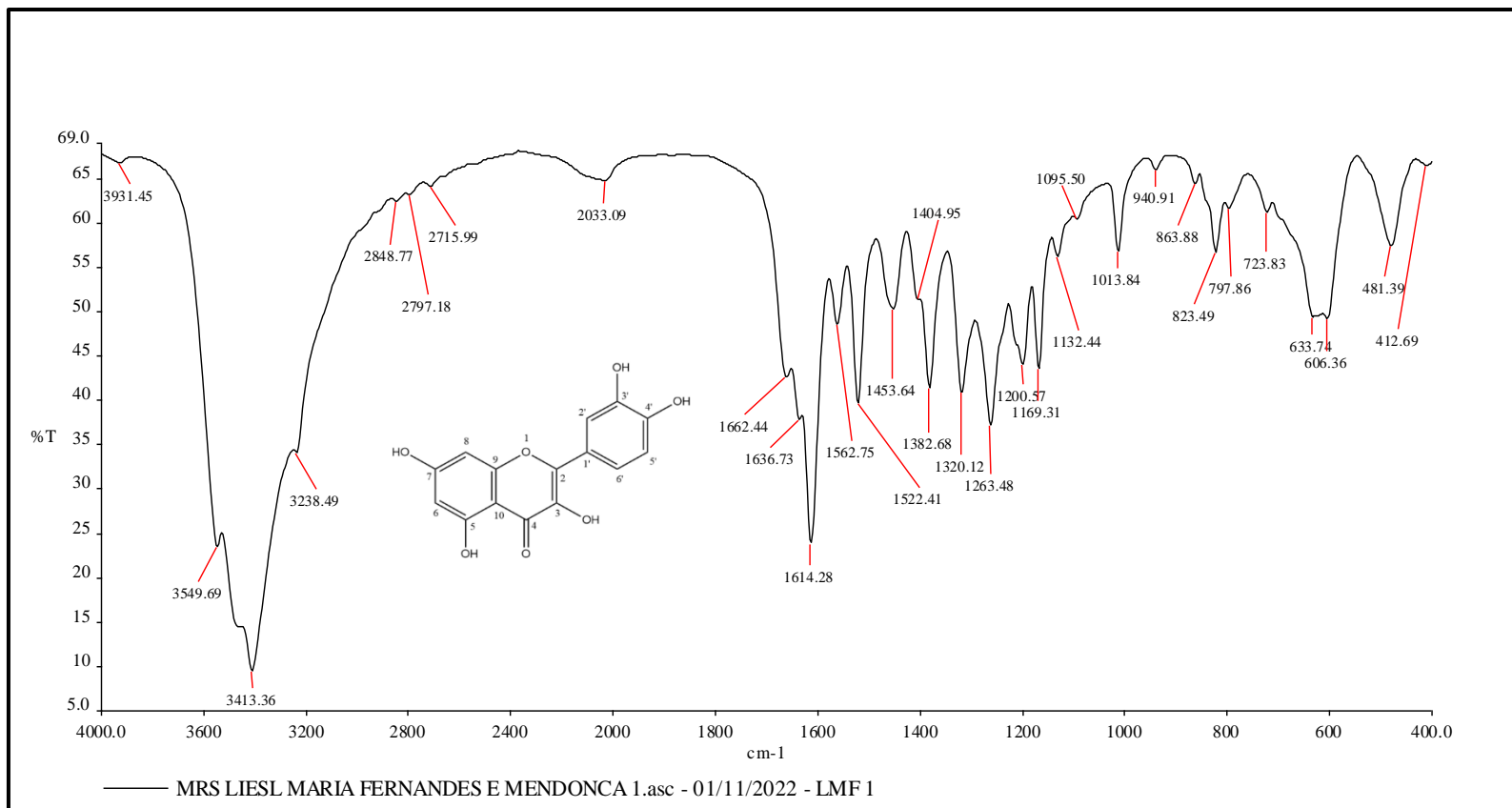
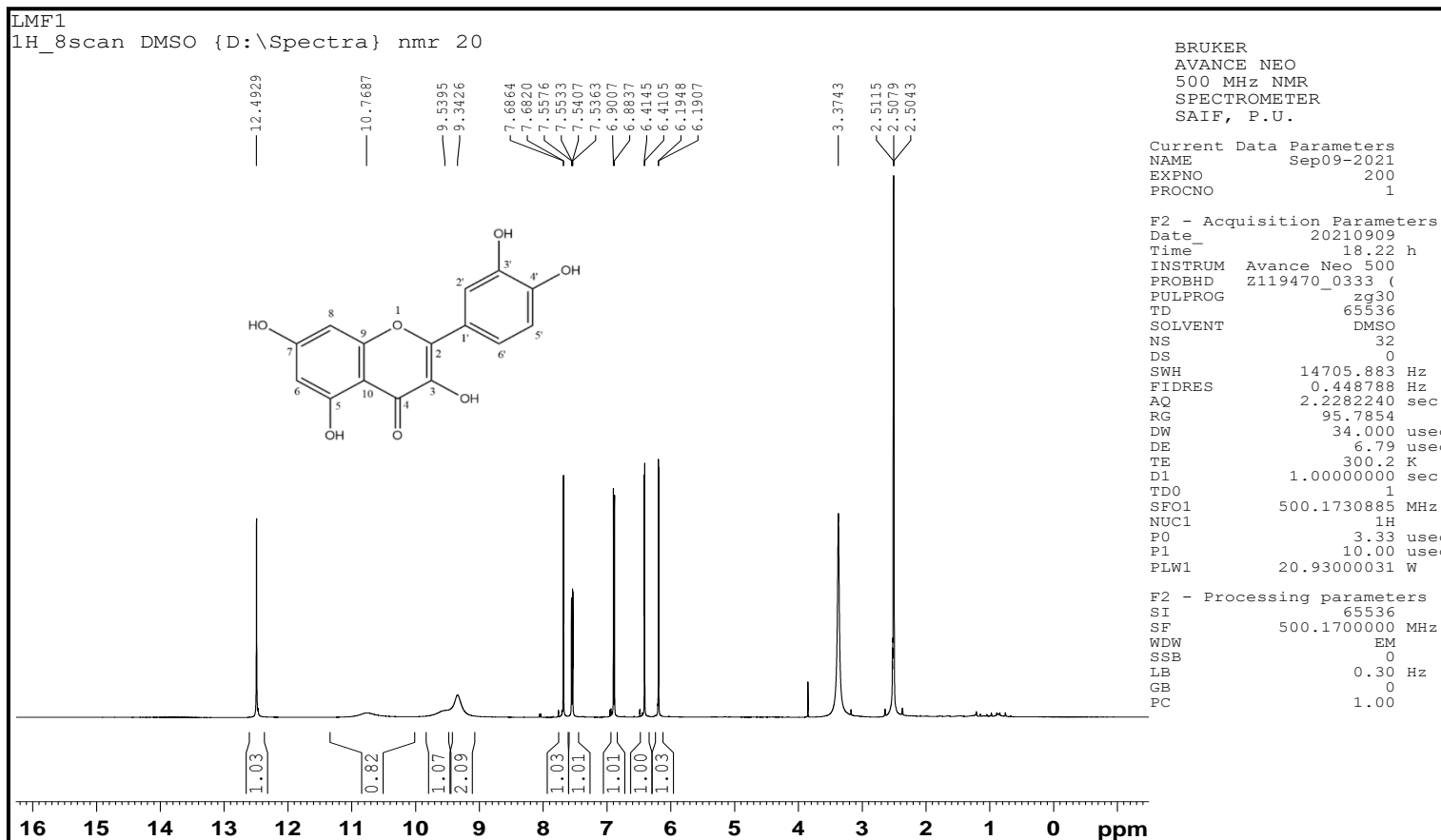
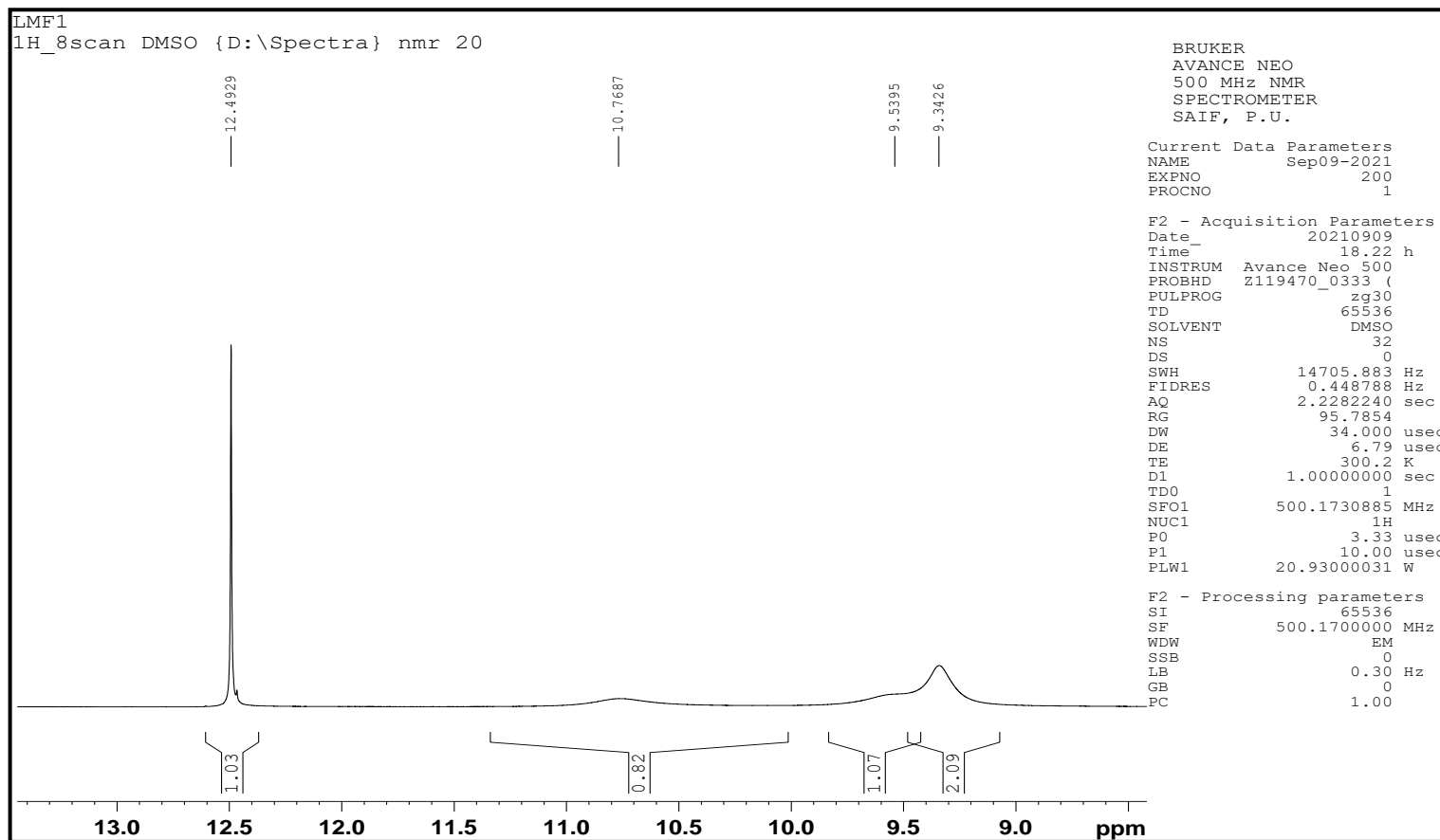
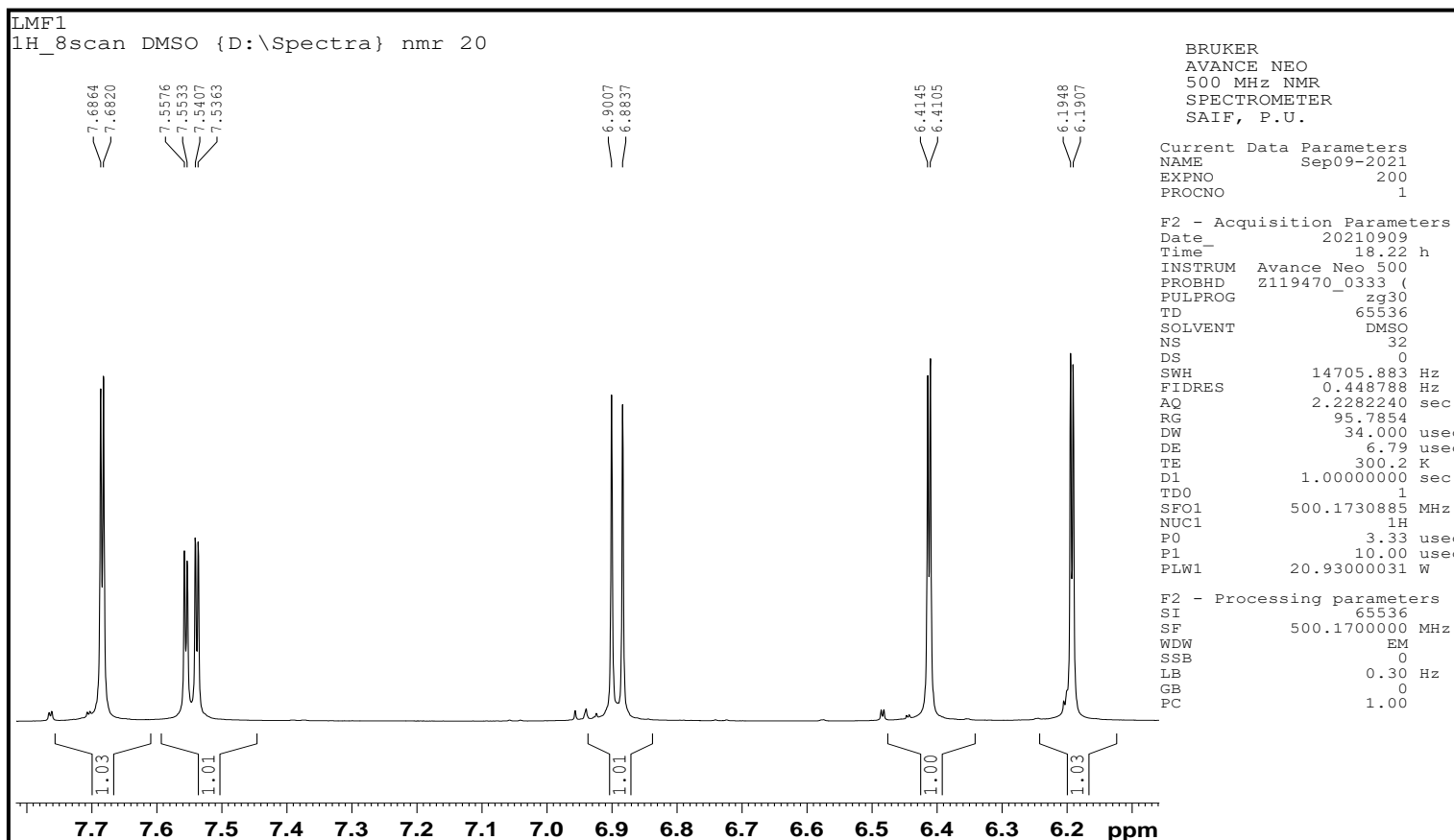
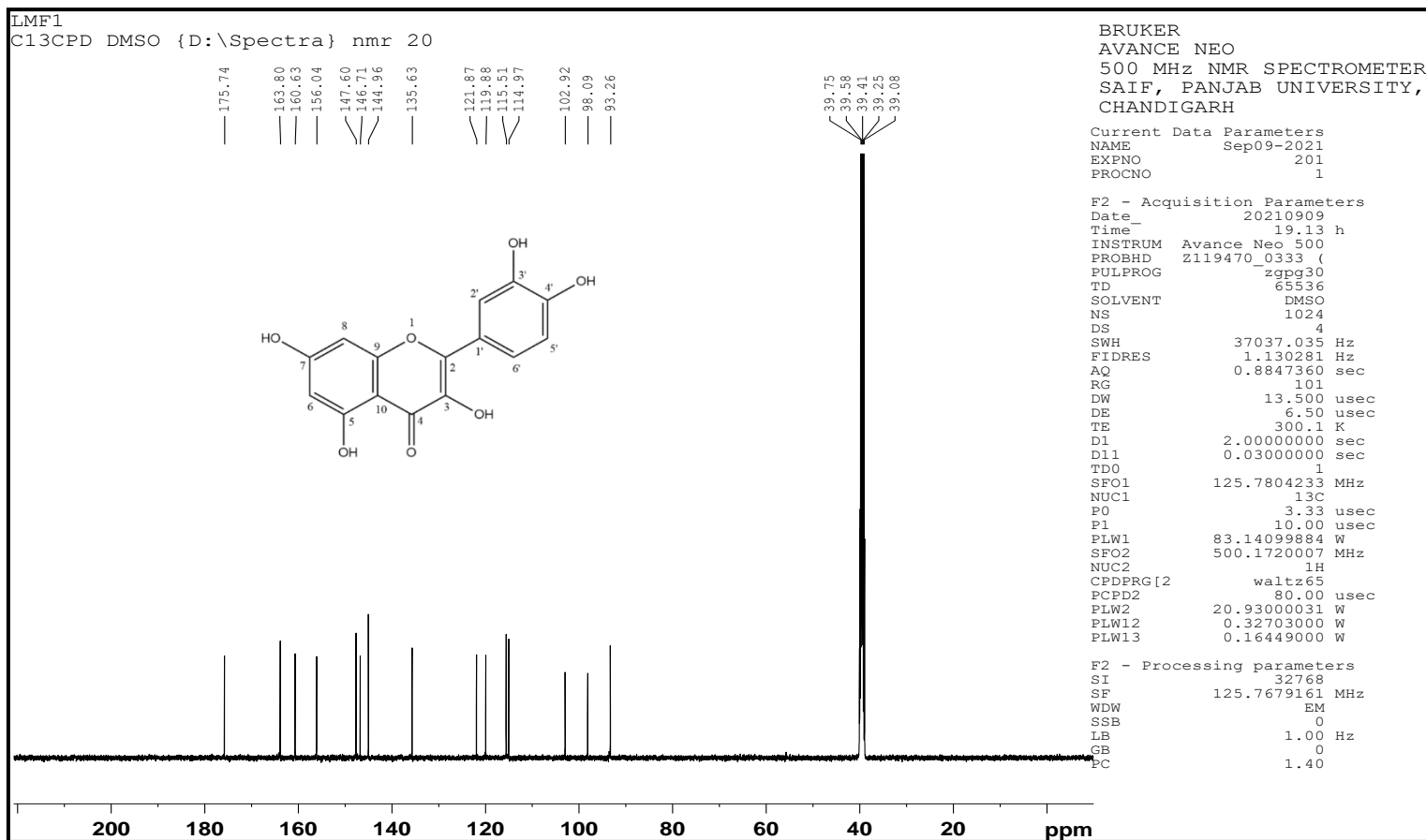


Figure 6.98: IR spectrum of LMF1 (Quercetin).

Figure 6.99: ¹H-NMR spectrum of LMF1 (Quercetin).

Figure 6.100: Resolution of ^1H -NMR spectrum of LMF1 (Quercetin).

Figure 6.101: Resolution of ^1H -NMR spectrum of LMF1 (Quercetin).

Figure 6.102: ^{13}C -NMR spectrum of LMF1 (Quercetin).

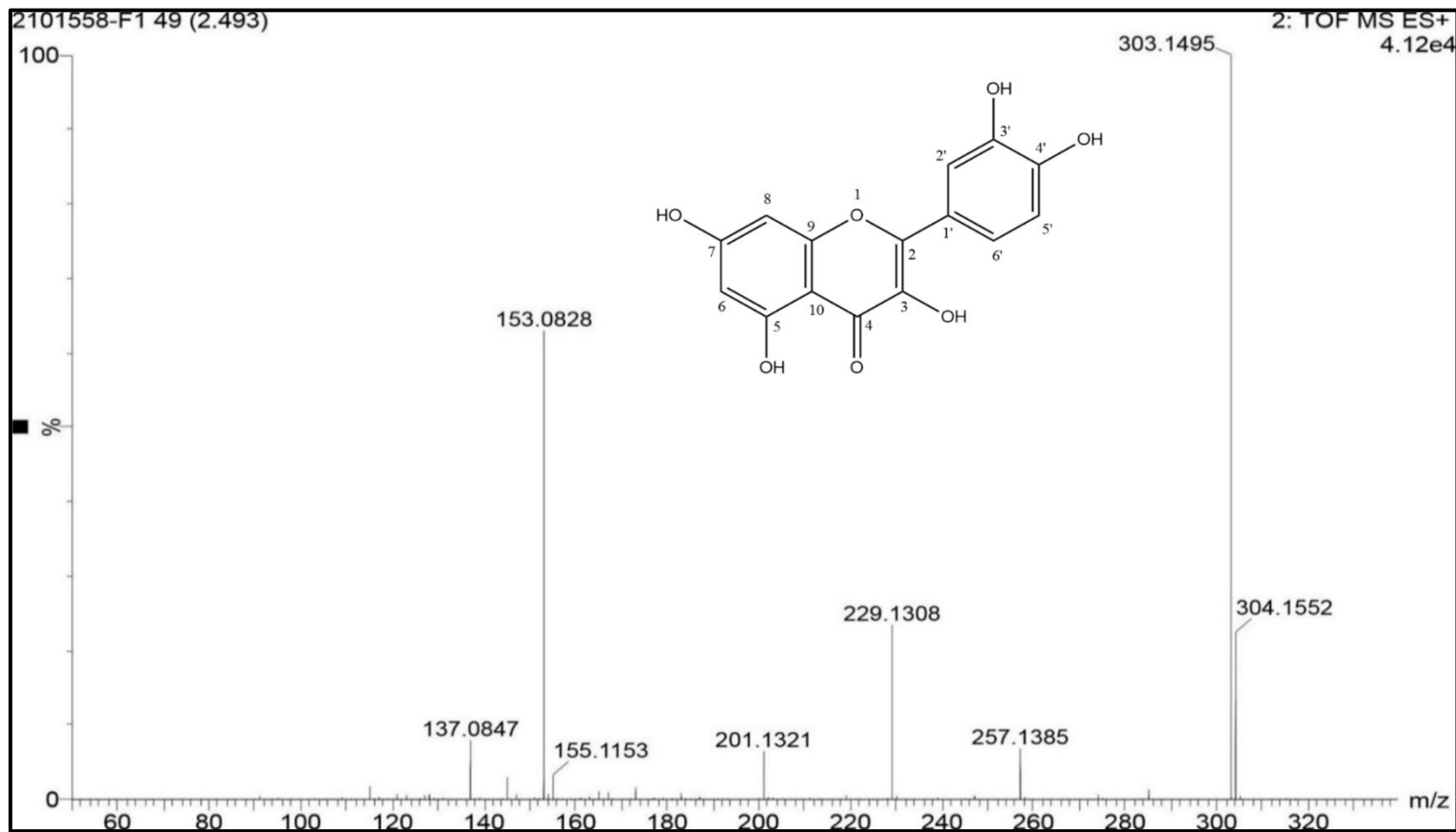


Figure 6.103: Mass spectrum of LMF1 (Quercetin).

6.2.10.2.2. CHARACTERISATION OF COMPOUND LMF2

Physical parameters of the compound

Physical state Yellowish coloured compound

Melting point 277 °C (*lit.* 276 - 278 °C) [232]

The compound LMF2 gave a positive response for shinoda test for flavonoids.

Spectral characteristics of the compound

IR (KBr) 3414.06 cm⁻¹ (OH str.)
 2815.01 cm⁻¹ (C-H str.)
 1661.20 cm⁻¹ (C=O str.)
 1570.59 cm⁻¹ (C=C str. in Ar ring)
 1382.24 cm⁻¹ (C-O str.)

¹H-NMR and ¹³C-NMR Tables 6.58 and 6.59**Mass spectra**

LC-MS (*m/z*) 287.1457 [M+H]⁺, other peaks appeared at 257.1320,
 229.1308, 153.0803

Molecular formula C₁₅H₁₀O₇**Molecular weight** 286.23 g/mol

From the m.p., IR, ¹H-NMR, ¹³C-NMR and mass spectral data, the compound was identified as **Kaempferol**.

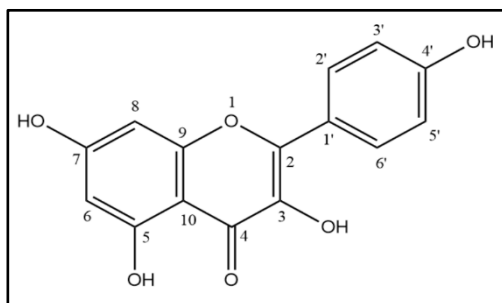
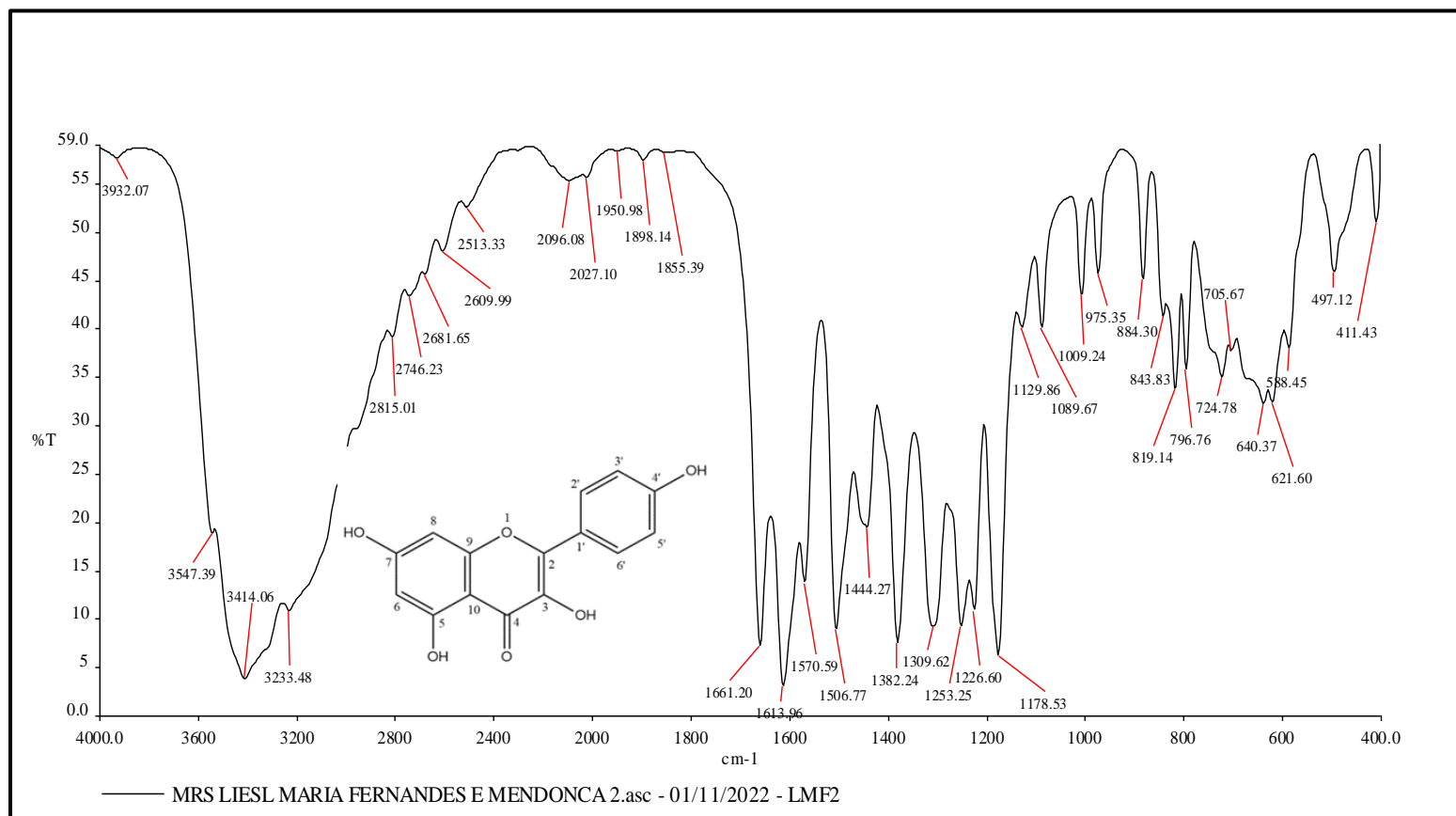
**Figure 6.104: Structure of Kaempferol.**

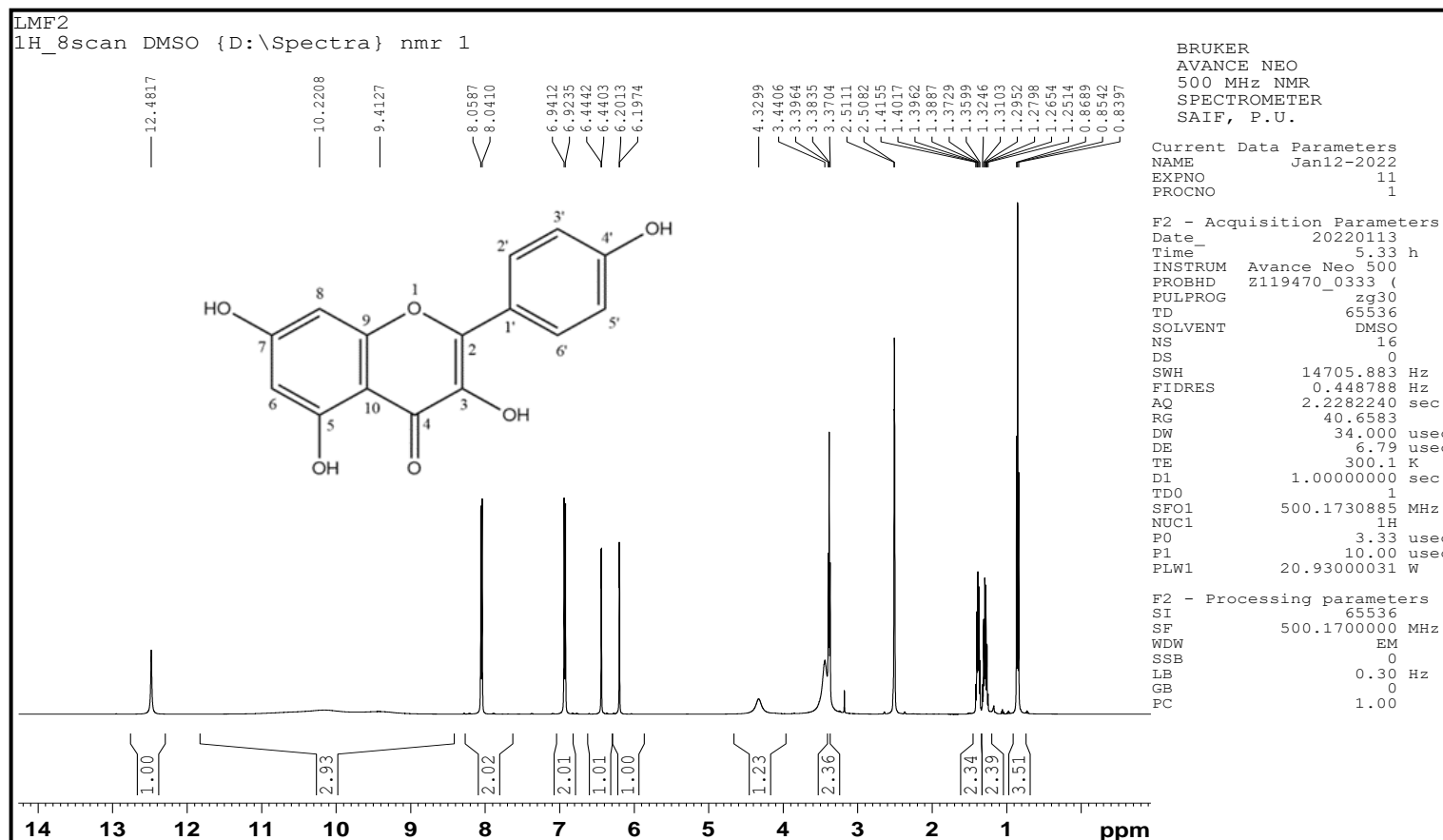
Table 6.58: ¹H-NMR data of the isolated compound LMF2.

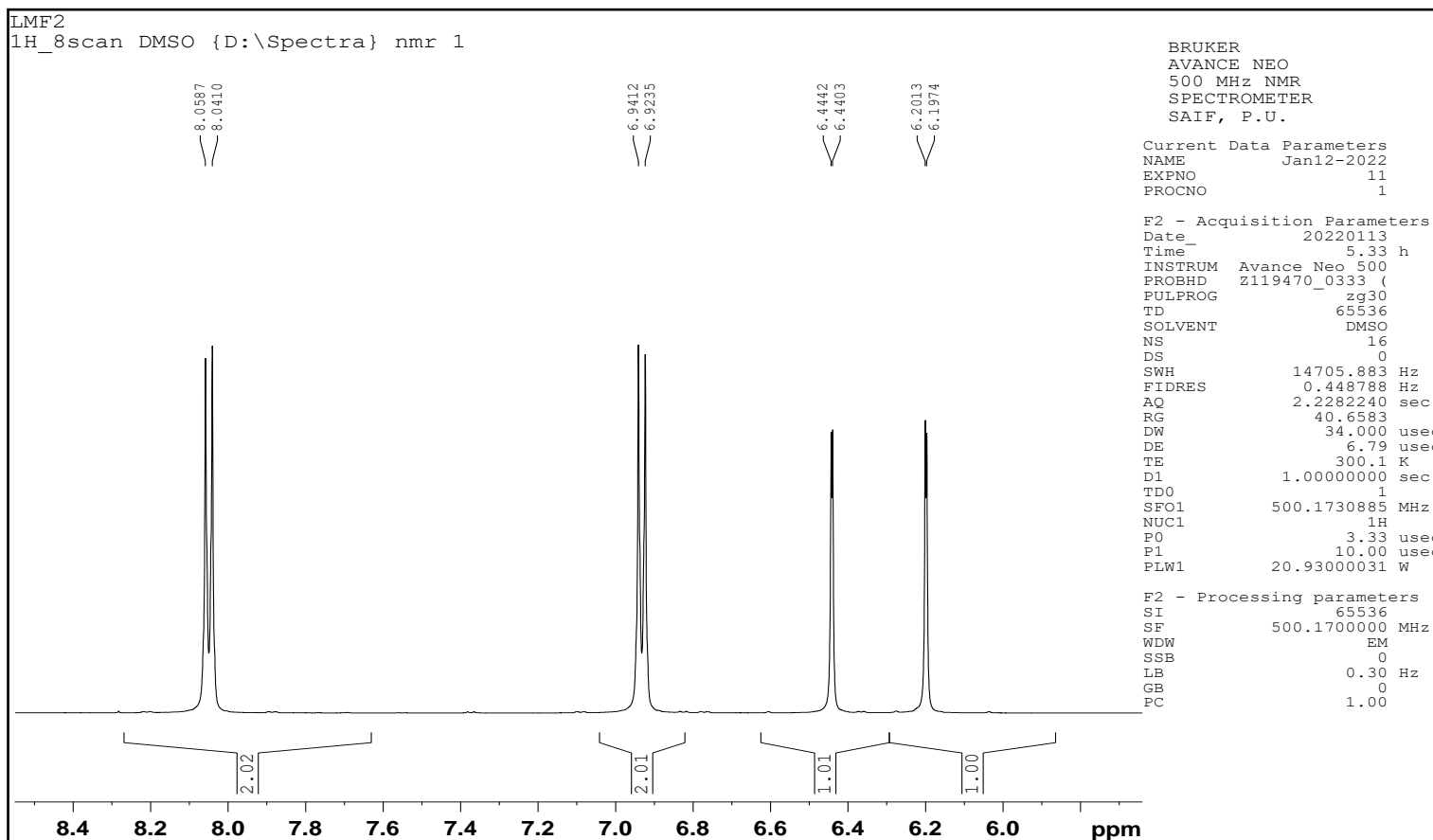
Position	Kaempferol (DMSO-d ₆ , 300 MHz, δ ppm, J, Hz) Reported values) ^[233]	LMF2 (DMSO-d ₆ , 500 MHz, δ ppm, J, Hz Spectral values)
H-6	6.11 (d, 1H, J = 2.0 Hz)	6.2013 (d, 1H, J = 2.0 Hz)
H-8	6.43 (d, 1H, J = 2.0 Hz)	6.4442 (d, 1H, J = 2.0 Hz)
H-2'	8.07 (d, 1H, J = 10.0 Hz)	8.0587 (d, 1H, J = 8.9 Hz)
H-3'	6.89 (d, 1H, J = 10.0 Hz)	6.9412 (d, 1H, J = 8.9 Hz)
H-5'	6.89 (d, 1H, J = 10.0 Hz)	6.9412 (d, 1H, J = 8.9 Hz)
H-6'	8.07 (d, 1H, J = 10.0 Hz)	8.0587 (d, 1H, J = 8.9 Hz)

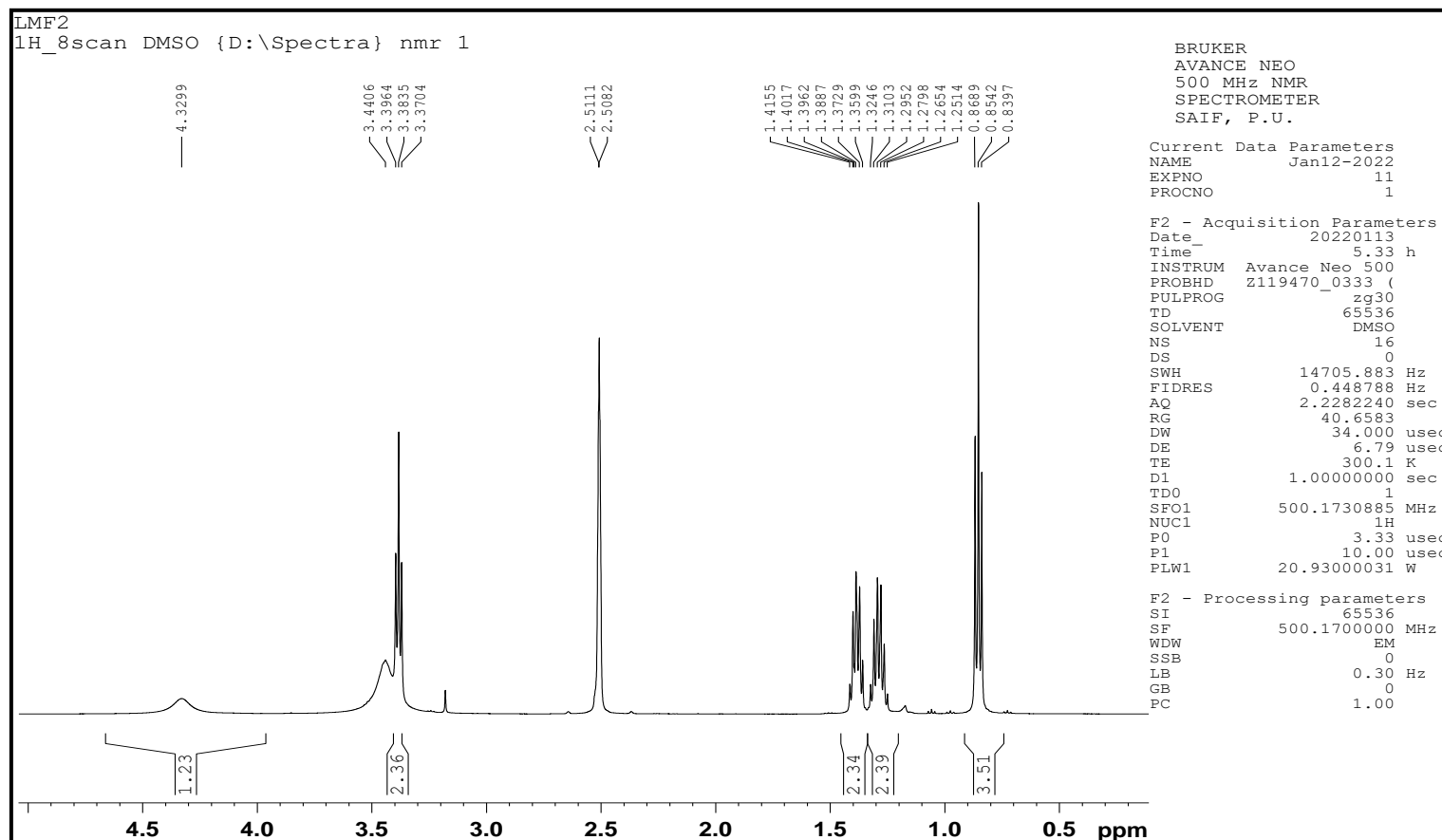
Table 6.59: ^{13}C -NMR data of the isolated compound LMF2.

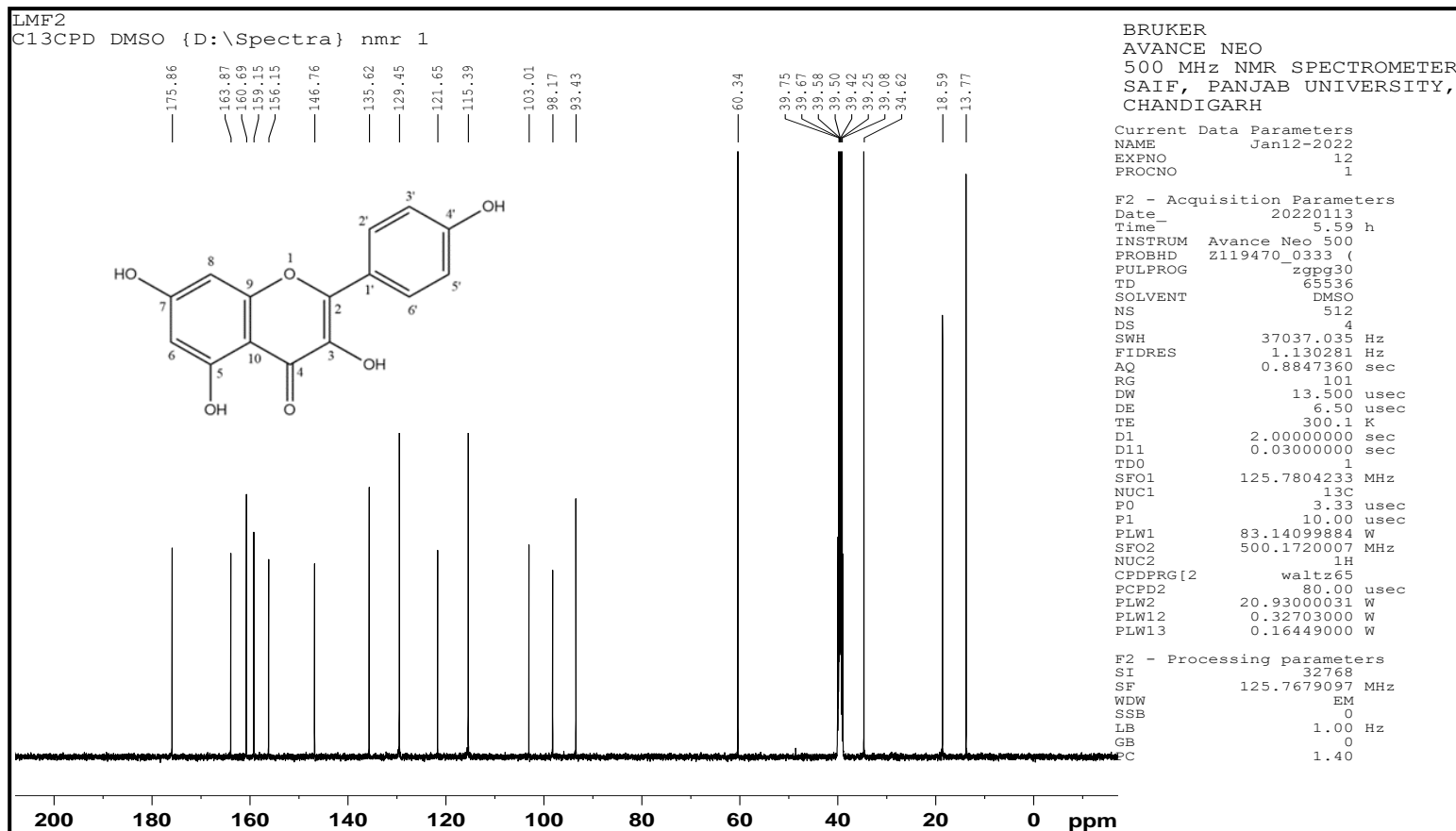
Position	Kaempferol (DMSO- d_6 , 100 MHz, δ , ppm) Reported values ^[233]	LMF2 (DMSO, 125 MHz, δ , ppm) Spectral values
C-2	146.7	146.76
C-3	135.8	135.62
C-4	175.9	175.86
C-5	156.5	156.15
C-6	98.5	98.17
C-7	163.9	163.87
C-8	93.5	93.43
C-9	161.1	160.69
C-10	103.5	103.01
C-1'	121.8	121.65
C-2'	129.6	129.45
C-3'	115.5	115.39
C-4'	159.6	159.15
C-5'	115.5	115.39
C-6'	129.6	129.45

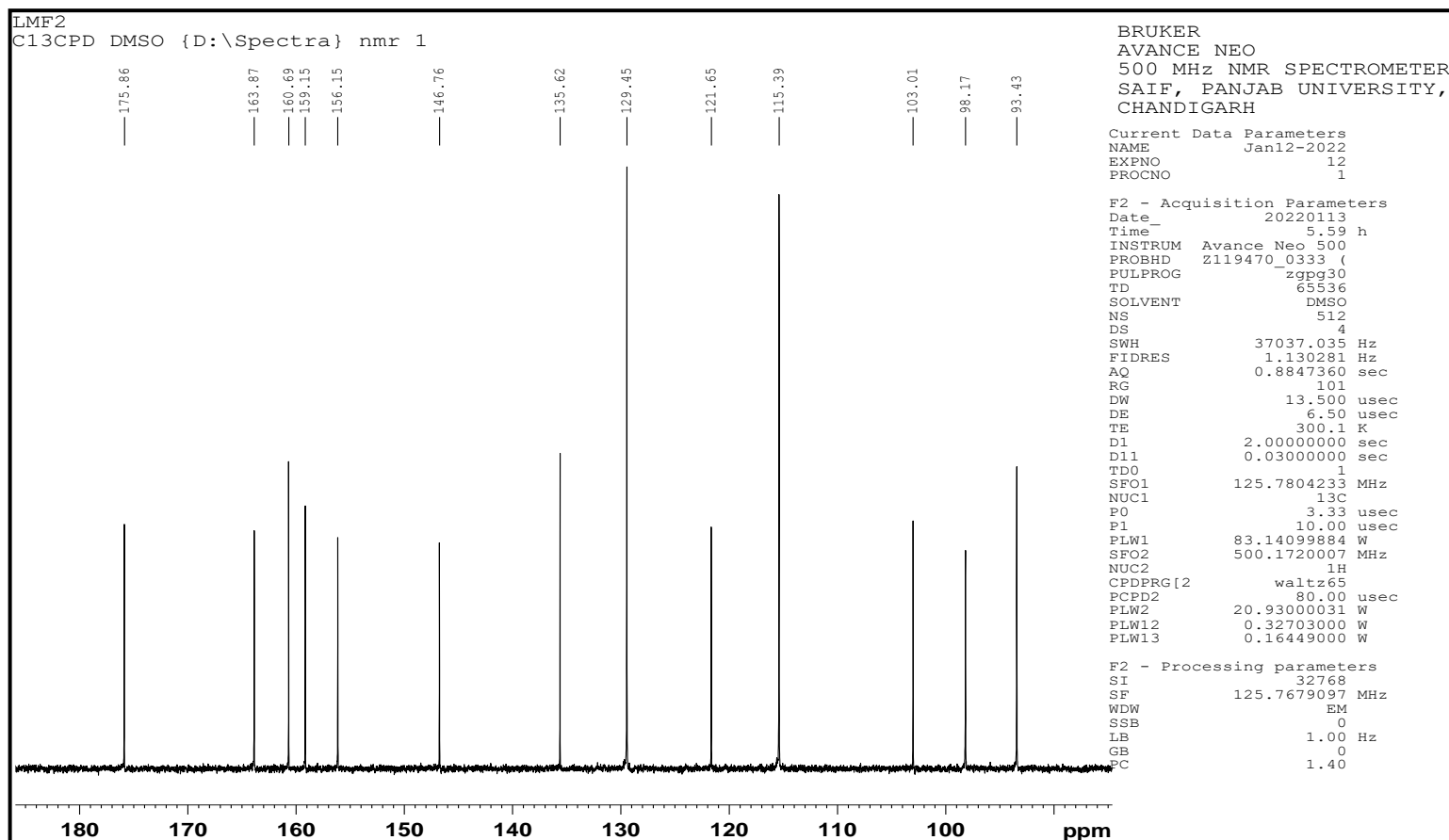
**Figure 6.105: IR spectrum of LMF2 (Kaempferol).**

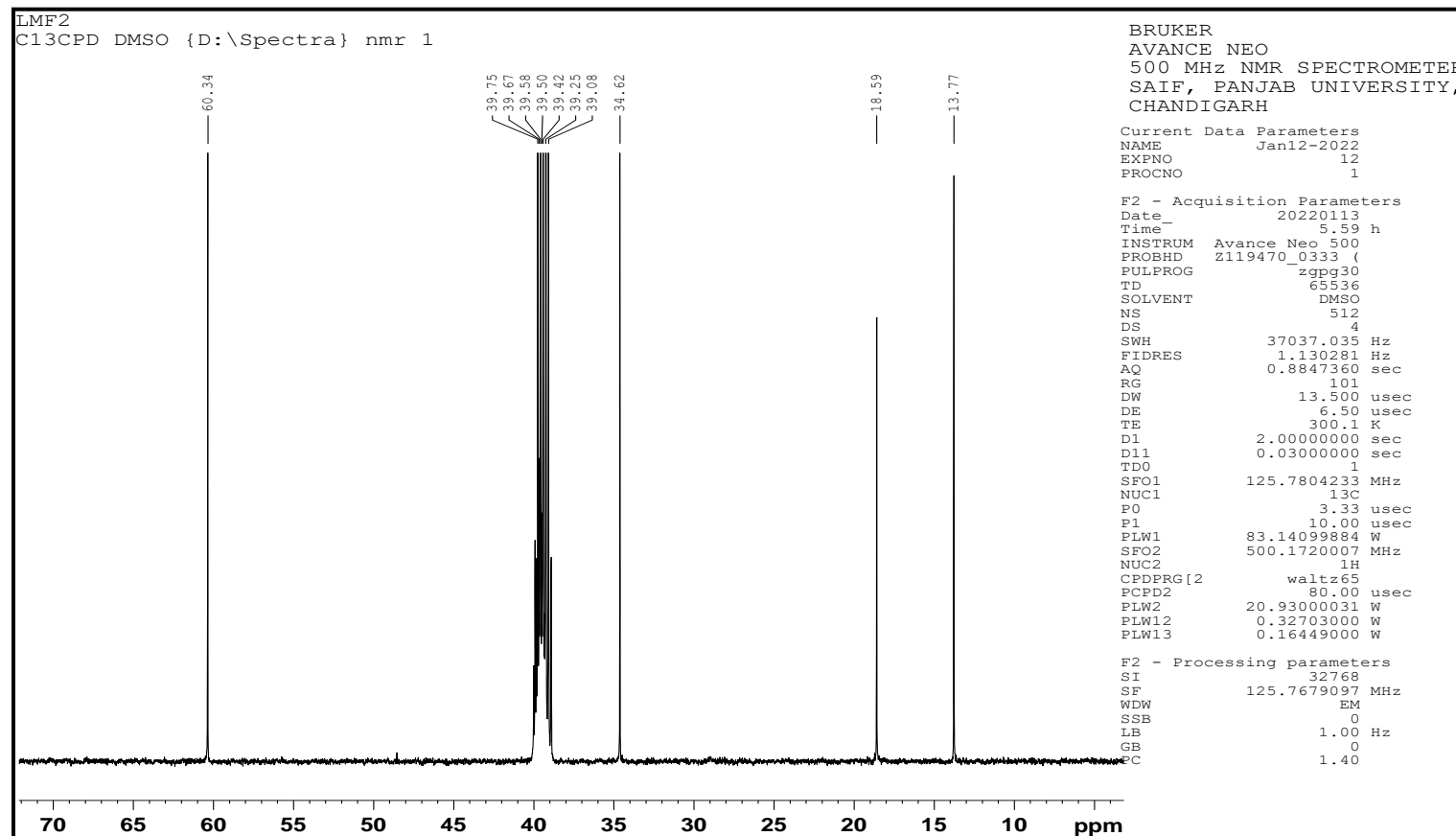
Figure 6.106: ^1H -NMR spectrum of LMF2 (Kaempferol).

Figure 6.107: Resolution of ^1H -NMR spectrum of LMF2 (Kaempferol).

Figure 6.108: Resolution of ^1H -NMR spectrum of LMF2 (Kaempferol).

Figure 6.109: ^{13}C -NMR spectrum of LMF2 (Kaempferol).

Figure 6.110: Resolution of ^{13}C -NMR spectrum of LMF2 (Kaempferol).

Figure 6.111: Resolution of ^{13}C -NMR spectrum of LMF2 (Kaempferol).

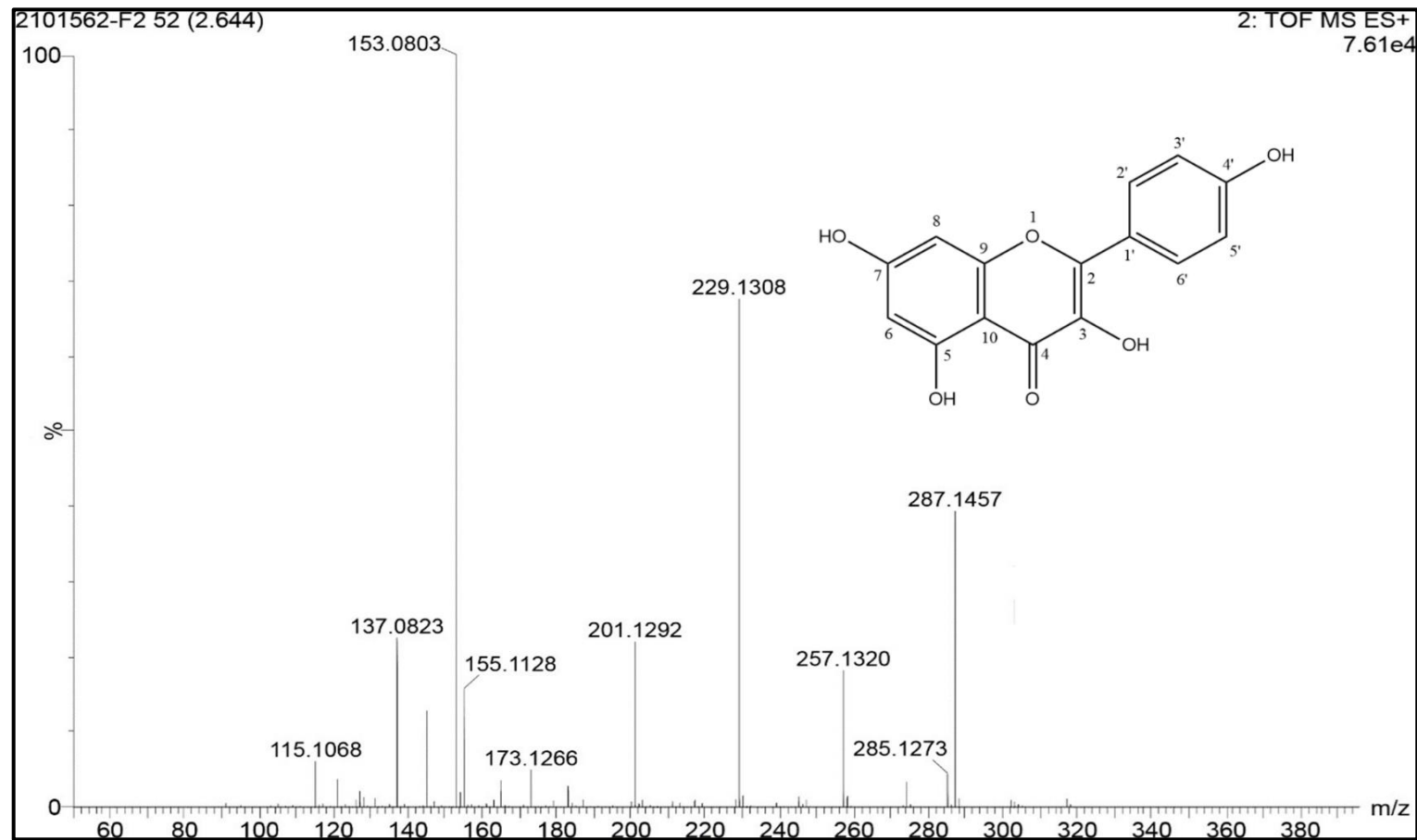


Figure 6.112: Mass spectrum of LMF2 (Kaempferol).

6.2.10.2.3. CHARACTERISATION OF COMPOUND LMF3

Physical parameters of the compound

Physical state Pale yellow amorphous compound

Melting point 186 °C (*lit.* 184 - 186 °C)^[78]

The compound LMF3 gave a positive response for shinoda test for flavonoids.

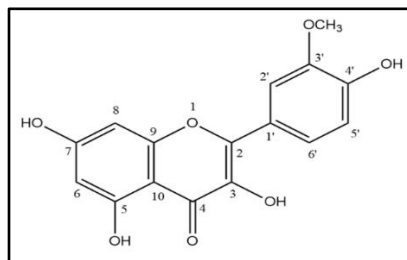
*Spectral characteristics of the compound***IR (KBr)** 3463.84 cm⁻¹ (br, OH str.)2918.69 cm⁻¹ (C-H str.)1635.08 cm⁻¹ (C=O str.)1468.42 cm⁻¹ (C=C str. in Ar ring)1386.79 cm⁻¹ (C-O str)¹H-NMR and ¹³C-NMR Tables 6.60 and 6.61**Mass spectra****LC-MS (m/z)** 317.1661 [M+H]⁺, other peaks appeared at 271.1510,
243.1498**Molecular formula** C₁₆H₁₂O₇**Molecular weight** 316.26 g/molFrom the m.p., IR, ¹H-NMR, ¹³C-NMR and mass spectral data, the compound was identified as **Isorhamnetin**.**Figure 6.113: Structure of Isorhamnetin.**

Table 6.60: ^1H -NMR data of the isolated compound LMF3.

Position	Isorhamnetin (DMSO- d_6 , 400 MHz, δ ppm, J , Hz) Reported values ^[231]	LMF3 (DMSO- d_6 , 400 MHz, δ ppm, J , Hz) Spectral values
H-6	6.21 (d, 1H, $J = 2.1$ Hz)	6.201 (d, 1H, $J = 2$ Hz)
H-8	6.42 (d, 1H, $J = 2.1$ Hz)	6.484 (d, 1H, $J = 2$ Hz)
OH-3	9.48 (s, 1H)	9.445 (s, 1H)
OH-5	12.52 (s, 1H)	12.473 (s, 1H)
OH-7	10.76 (s, 1H)	10.778 (s, 1H)
H-2'	7.68 (d, 1H, $J = 2.1$ Hz)	7.761 (d, 1H, $J = 2$ Hz)
H-5'	6.92 (d, 1H, $J = 8.5$ Hz)	6.954 (d, 1H, $J = 8.8$ Hz)
H-6'	7.58 (dd, 1H, $J = 8.5, 2.1$ Hz)	7.707 (dd, 1H, $J = 6.4, 2$ Hz)
OH-4'	9.74 (s, 1H)	9.751 (s, 1H)
OCH₃	3.76 (s, 1H)	3.847 (s, 3H)

Table 6.61: ^{13}C NMR of the isolated compound LMF3

Position	Isorhamnetin (DMSO-d ₆ , 100 MHz, δ , ppm – Reported values) ^[231]	LMF3 (DMSO-d ₆ , 100 MHz, δ , ppm – Spectral values)
C-2	156.8	148.792
C-3	134.8	135.803
C-4	176.8	175.863
C-5	160.4	160.665
C-6	99.0	98.188
C-7	165.6	163.891
C-8	93.8	93.573
C-9	157.4	156.140
C-10	104.1	103.009
C-1'	121.5	121.949
C-2'	115.4	111.693
C-3'	145.9	146.606
C-4'	148.8	147.342
C-5'	116.1	115.519
C-6'	121.4	121.699
OCH ₃	55.6	55.753

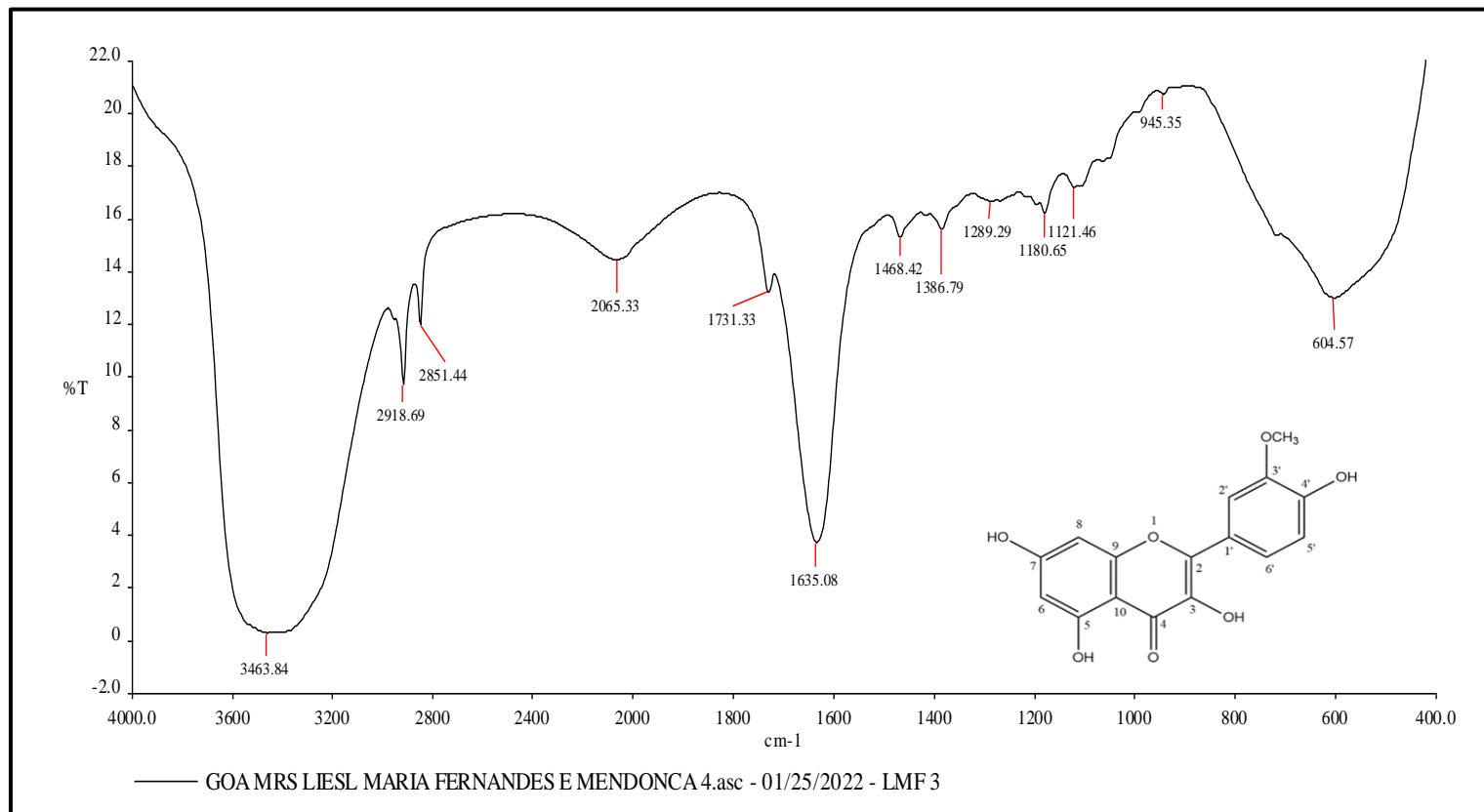
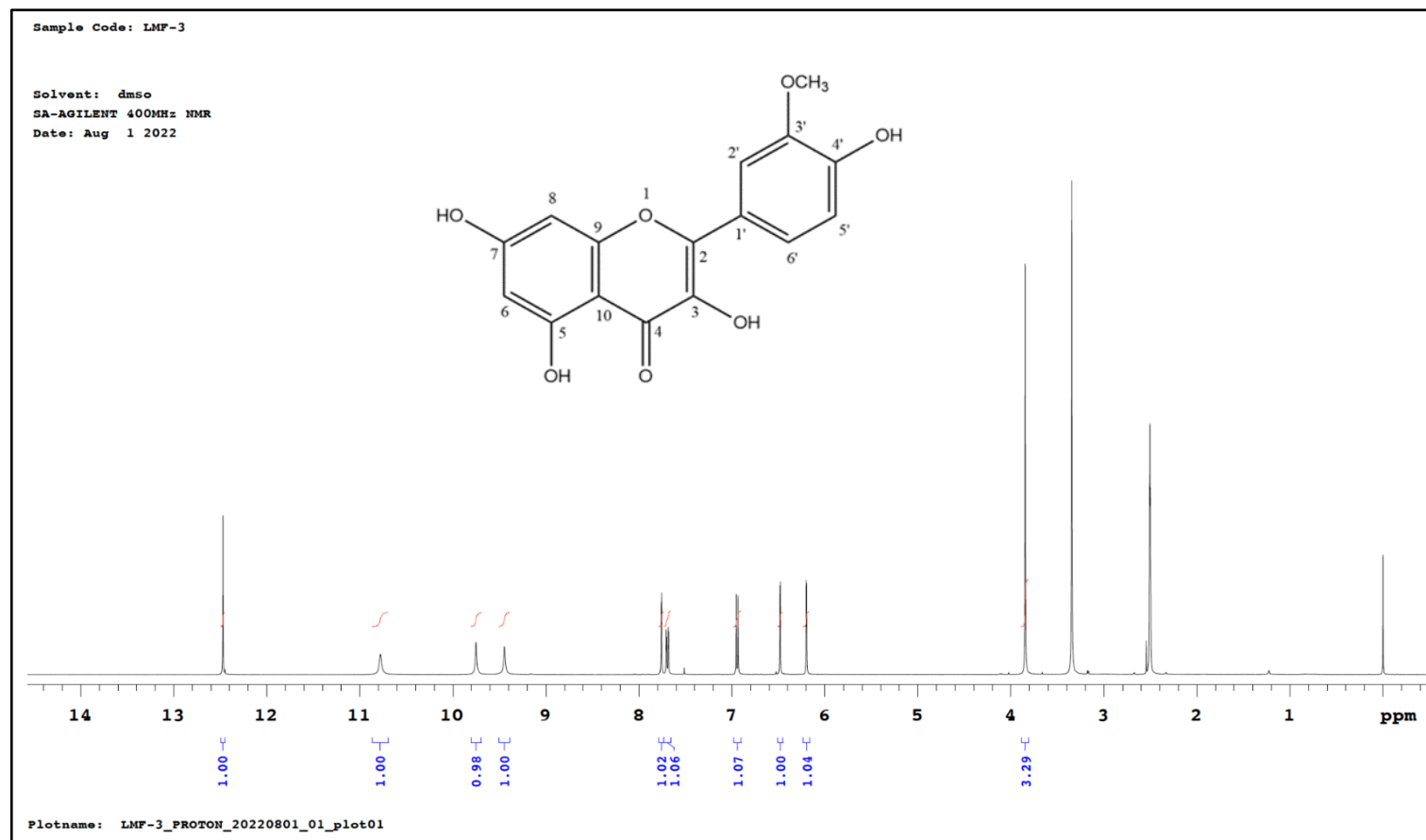


Figure 6.114: IR spectrum of LMF3 (Isorhamnetin).



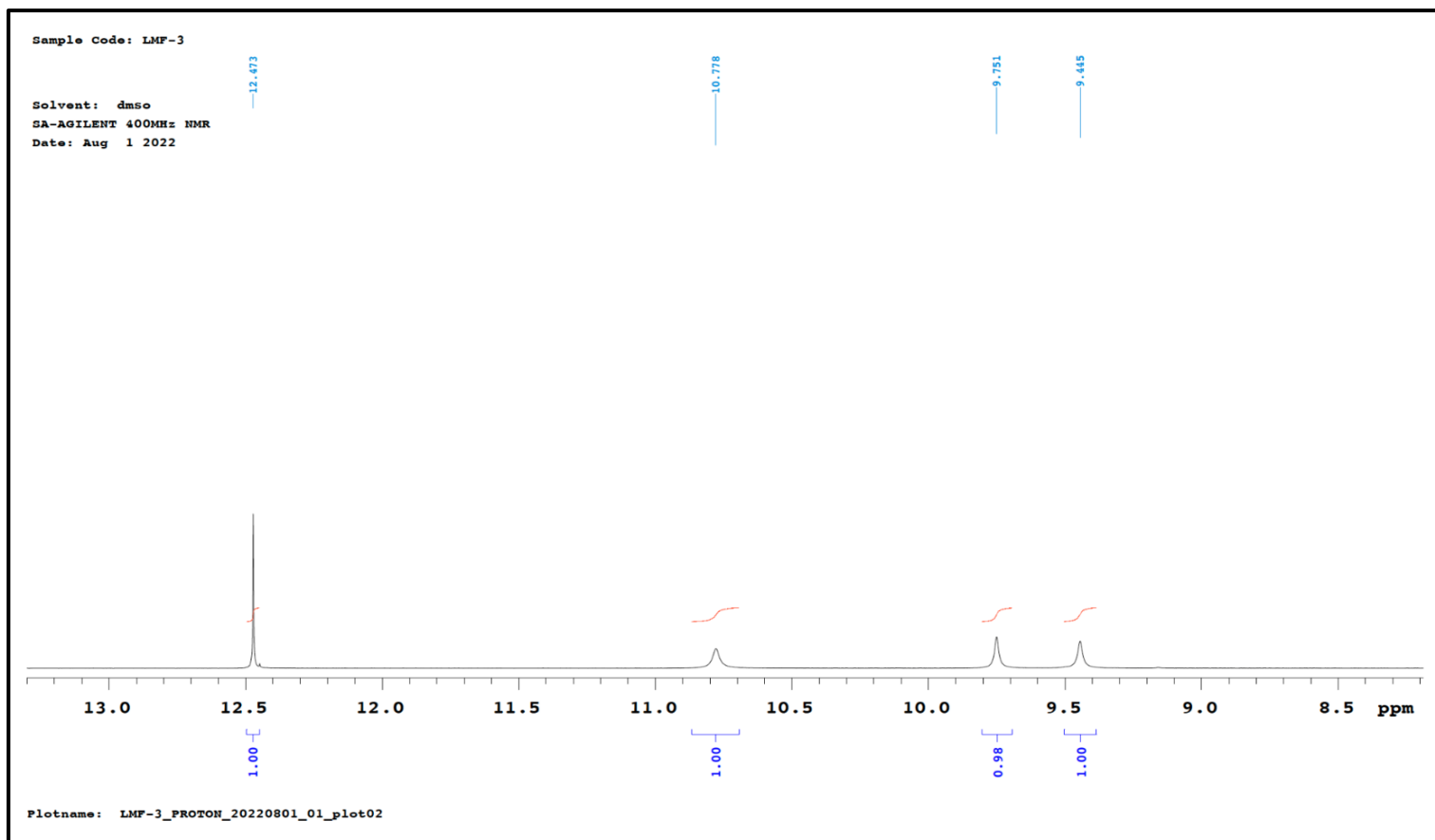


Figure 6.116: Resolution of ^1H -NMR spectrum of LMF3 (Isorhamnetin).

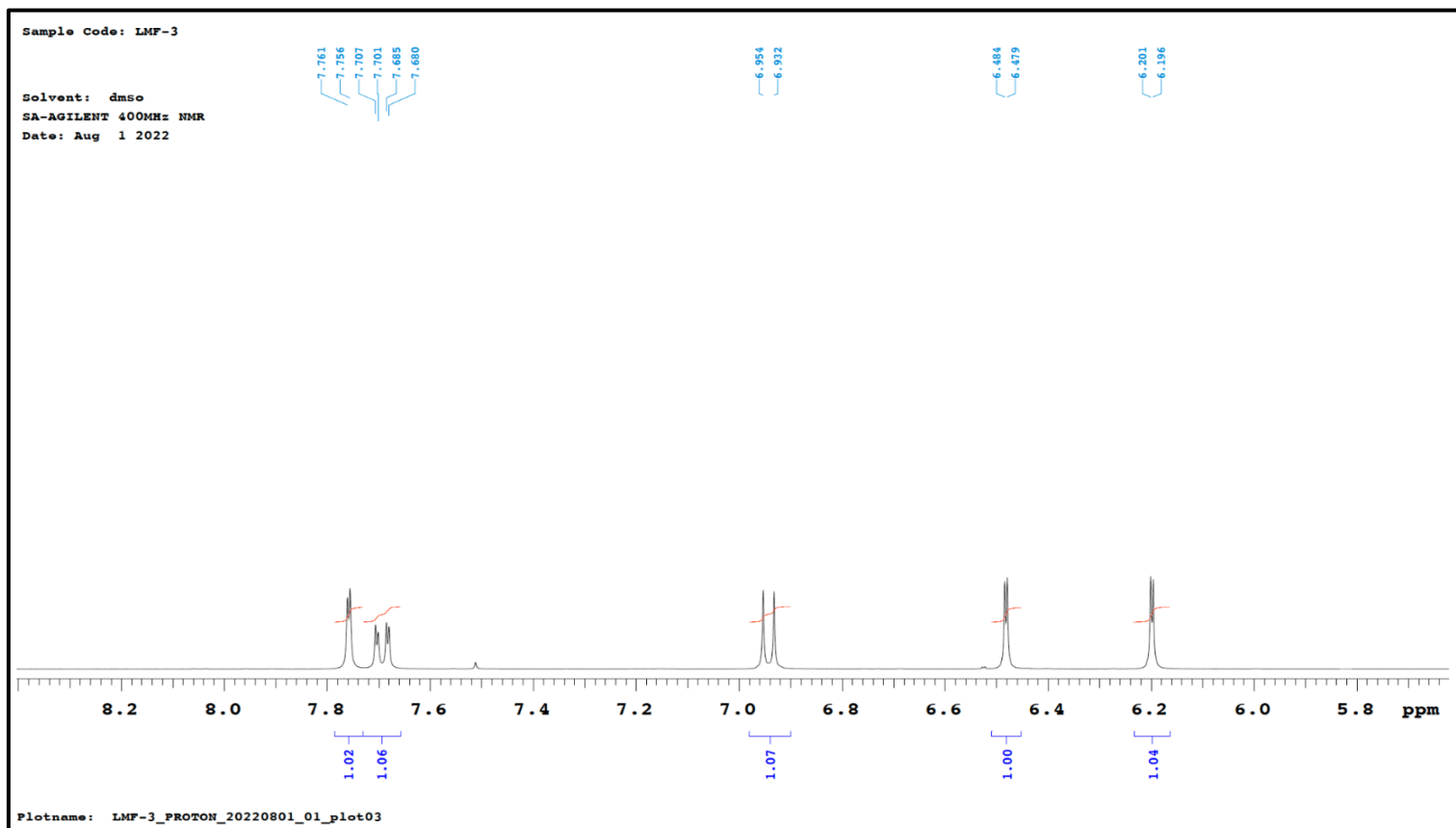


Figure 6.117: Resolution of ^1H -NMR spectrum of LMF3 (Isorhamnetin).

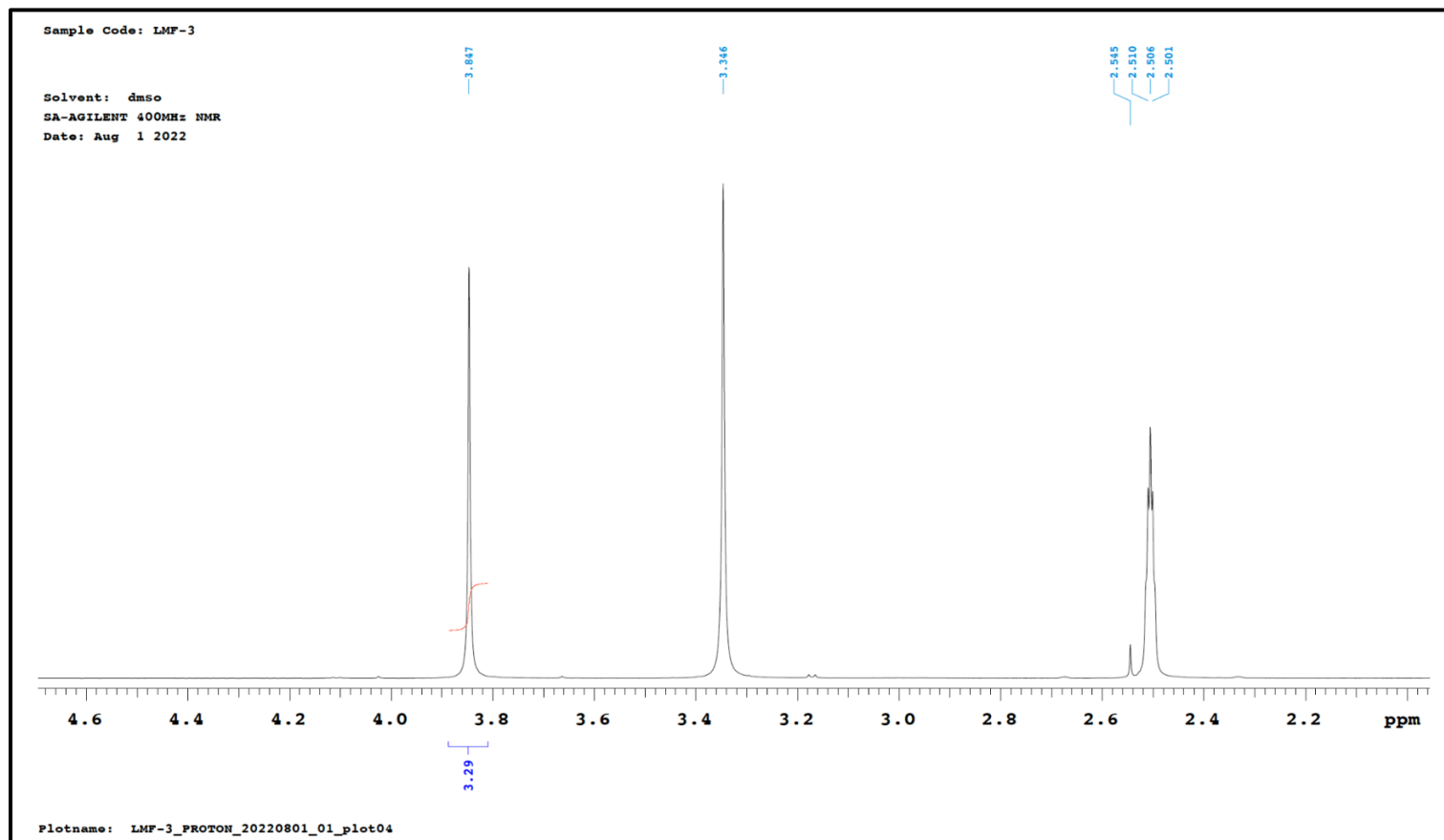
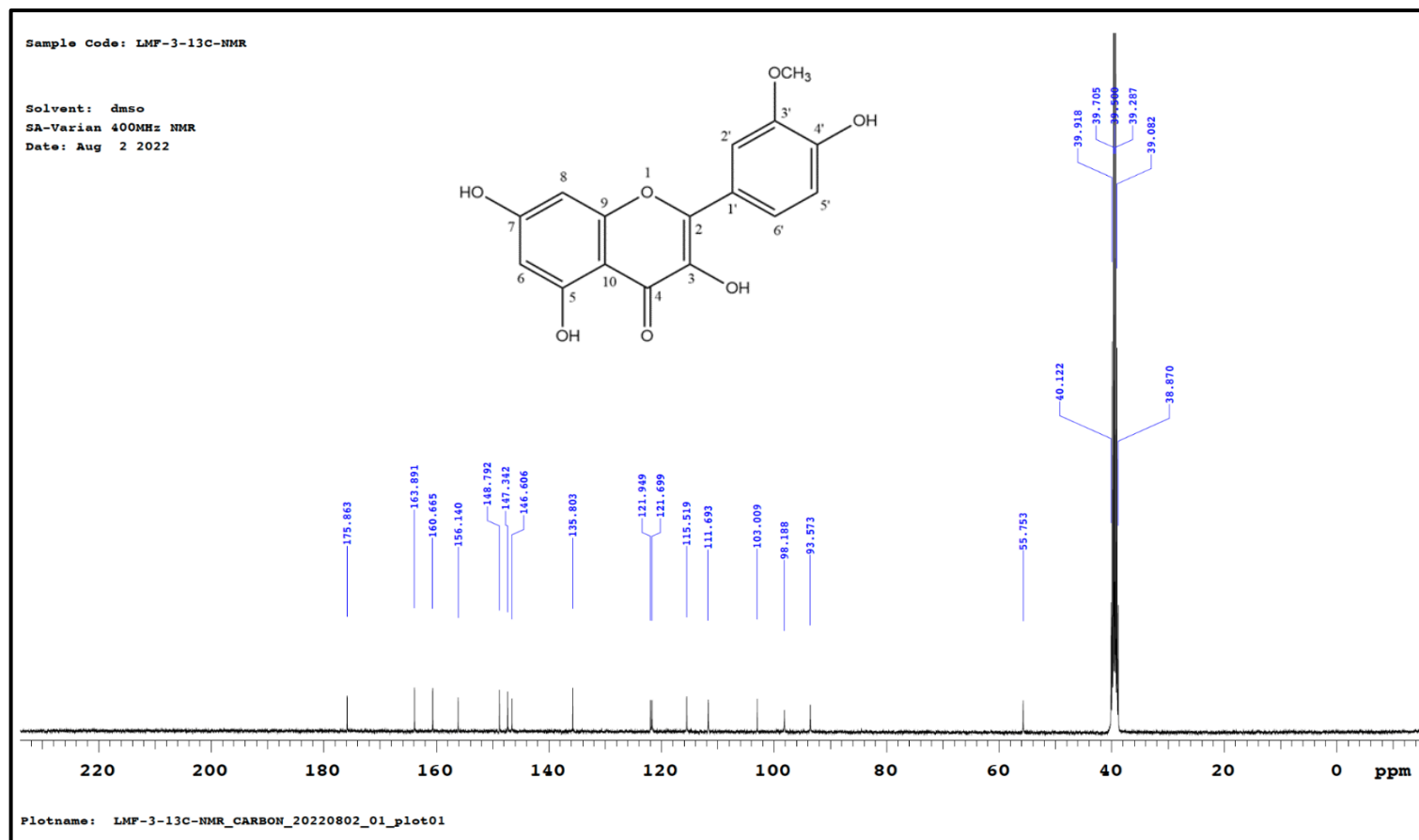


Figure 6.118: Resolution of ^1H -NMR spectrum of LMF3 (Isorhamnetin).

Figure 6.119: ^{13}C -NMR spectrum of LMF3 (Isorhamnetin).

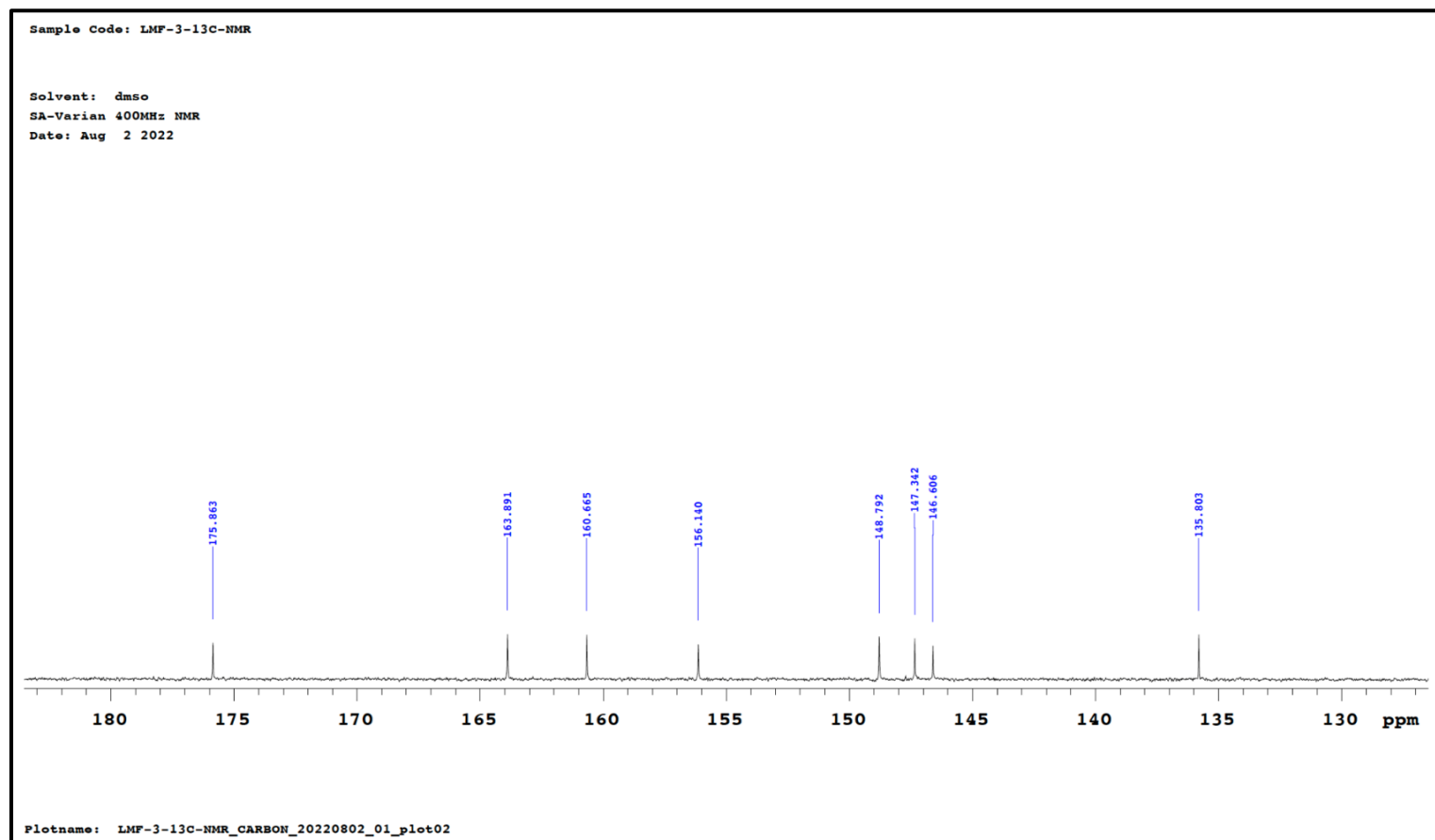


Figure 6.120: Resolution of ^{13}C -NMR spectrum of LMF3 (Isorhamnetin).

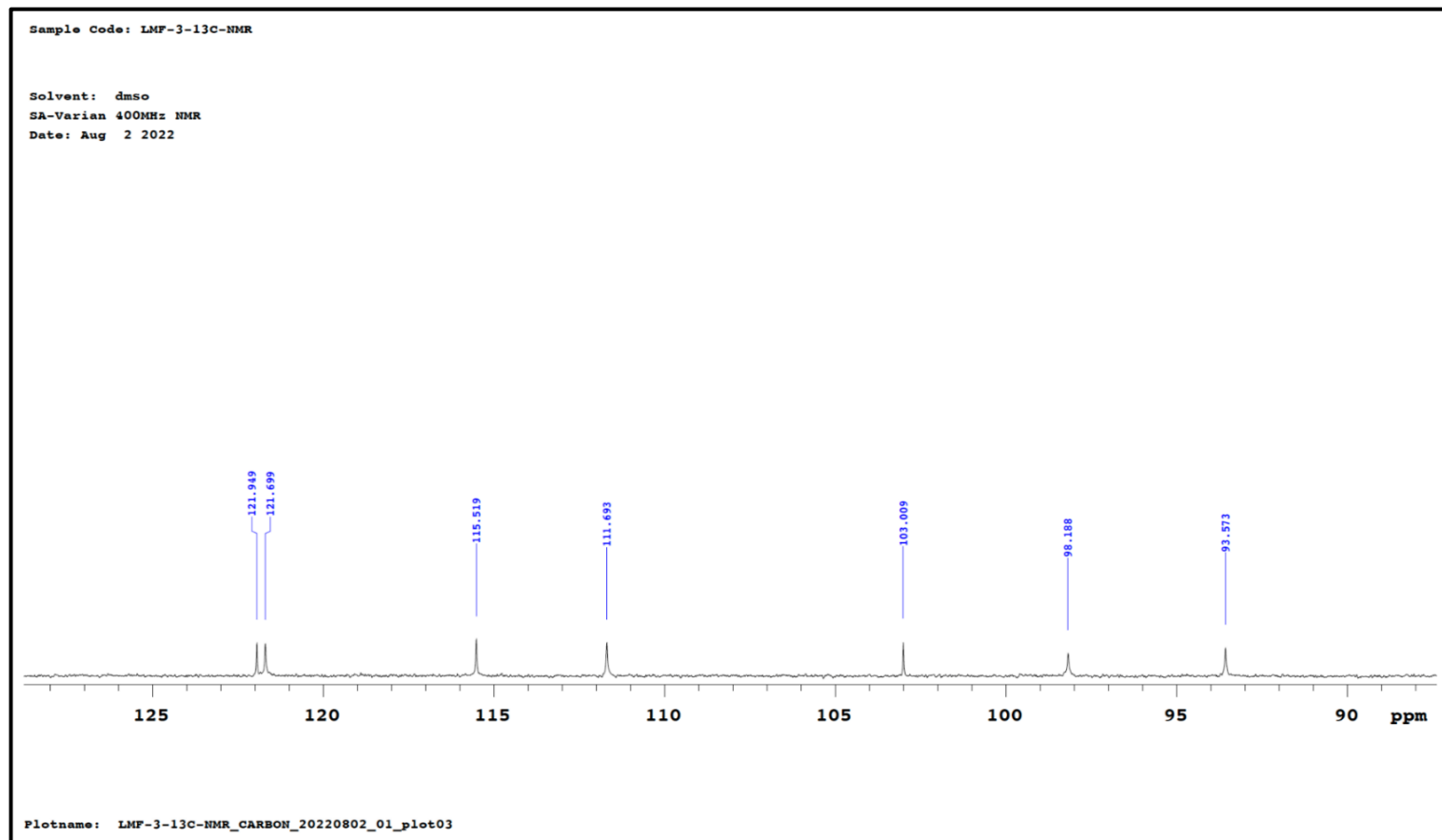


Figure 6.121: Resolution of ^{13}C -NMR spectrum of LMF3 (Isorhamnetin).

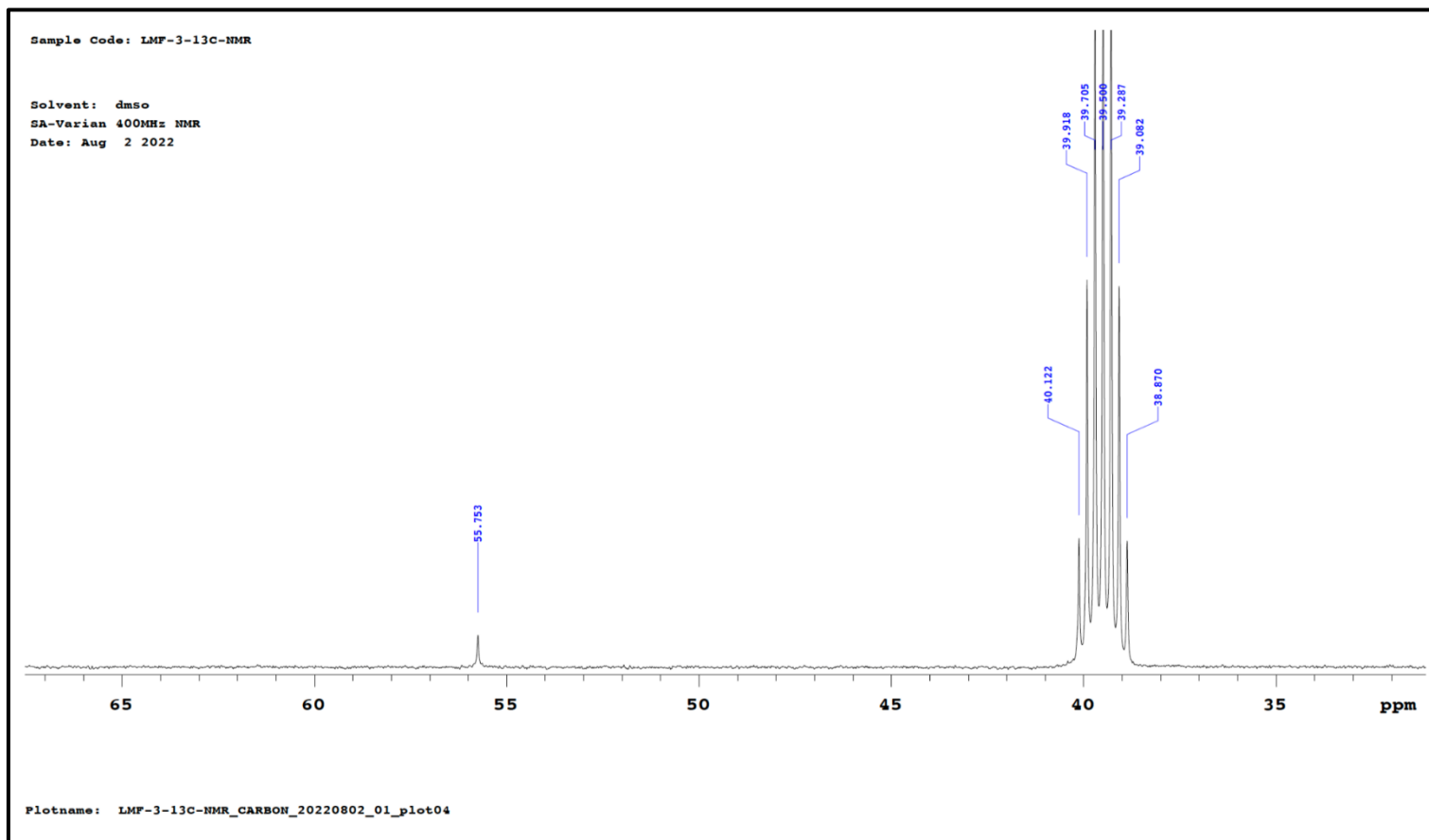


Figure 6.122: Resolution of ^{13}C -NMR spectrum of LMF3 (Isorhamnetin).

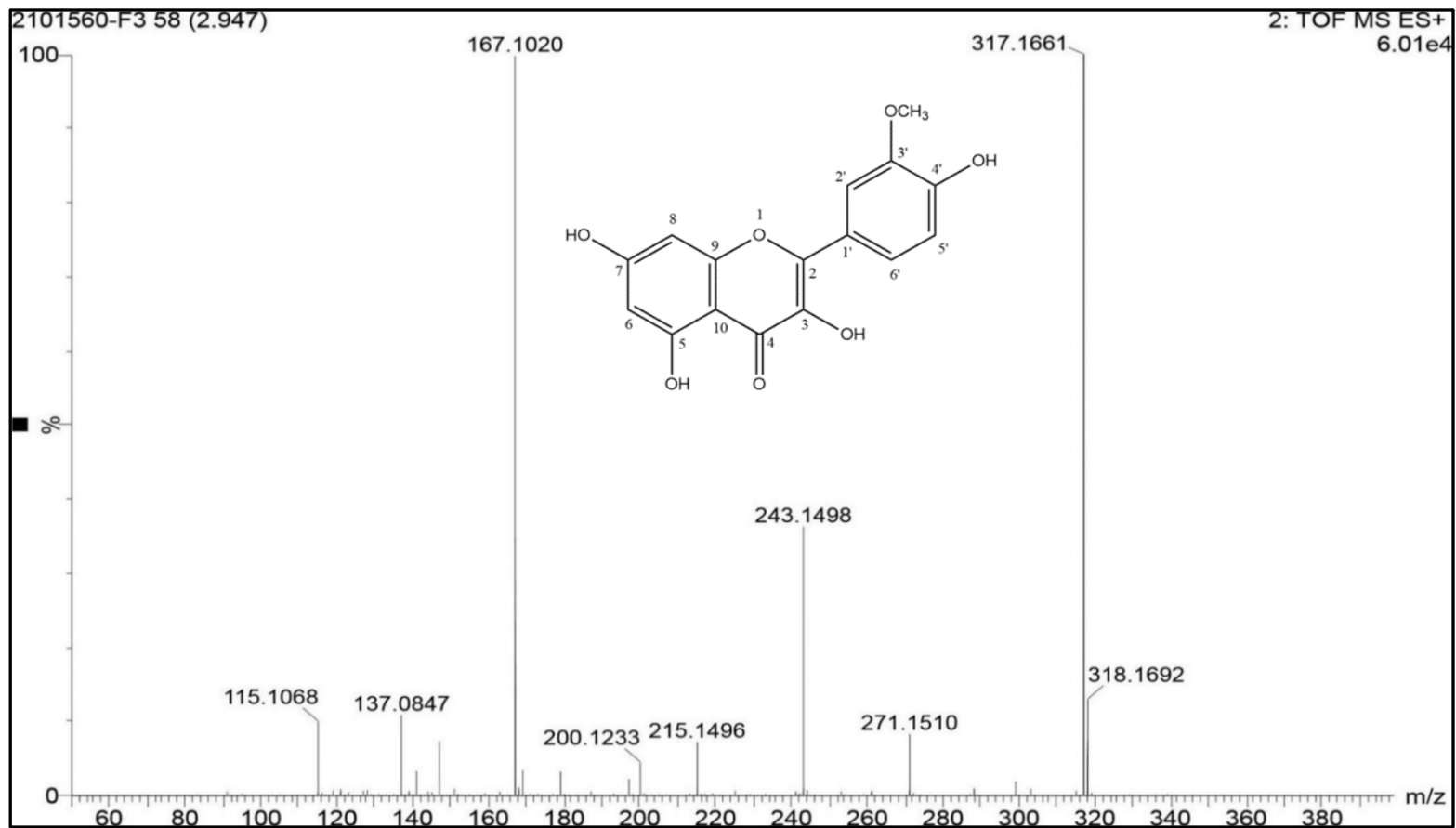


Figure 6.123: Mass spectrum of LMF3 (Isorhamnetin).

6.2.10.2.4. CHARACTERISATION OF COMPOUND LMF4

Physical parameters of the compound

Physical state Creamish white coloured compound

Melting point 213 °C (*lit.* 214 °C) [234]

The compound LMF4 gave a positive response for shinoda test for flavonoids.

Spectral characteristics of the compound

IR (KBr) 3413.80 cm⁻¹ (OH str.)
 2918.39 cm⁻¹ (C-H str.)
 1732.97m⁻¹ (C=O str.)
 1468.72 cm⁻¹ (C=C str. in Ar ring)
 1387.54 cm⁻¹ (C-O str.)

¹H-NMR and ¹³C-NMR Tables 6.62 and 6.63

Mass spectra

LC-MS (*m/z*) 333.6351 [M+H]⁺, other peaks appeared at 271.1935,
 211.5520, 169.5185, 125.8521

Molecular formula C₁₃H₁₆O₁₀

Molecular weight 332.26 g/mol

From the m.p., IR, ¹H-NMR, ¹³C-NMR and mass spectral data, the compound was identified as **β-Glucogallin**.

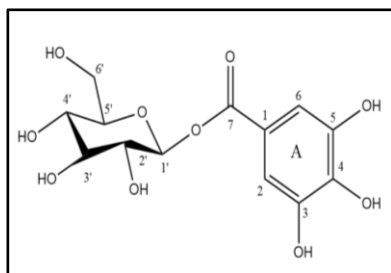


Figure 6.124: Structure of β-Glucogallin.

Table 6.62: ¹H-NMR data of the isolated compound LMF4.

Position	<i>β</i> -glucogallin (DMSO-d ₆ , 400MHz, δ ppm, <i>J</i> , Hz - Reported values) ^[235]	LMF4 (DMSO-d ₆ , 400 MHz, δ , ppm, <i>J</i> , Hz - Spectral values)
H-2	6.99 (s, 1H)	7.002 (s, 1H)
H-6	6.99 (s, 1H)	7.002 (s, 1H)
OH-3	9.32 (s, 1H)	9.217 (s, 3H)
OH-4	9.10 (s, 1H)	
OH-5	9.32 (s, 1H)	
H-1'	5.48 (d, 1H, <i>J</i> = 7.5 Hz)	5.515 (d, 1H, <i>J</i> = 7.6 Hz)
H-2'	3.2 - 3.7 (m, 6H)	3.197-3.323 (m, 4H)
H-3'		
H-4'		
H-5'		
H-6'		
H-6'		3.669 (d, 1H, <i>J</i> = 11.2 Hz), 3.473 (dd, 1H, <i>J</i> = 6.8, 5.6 Hz)
OH-2'	5.13 (s, 1H)	5.284 (s, 1H)
OH-3'	5.04 (s, 1H)	5.062 (s, 1H)
OH-4'	4.95 (s, 1H)	4.577 (s, 1H)
OH-6'	5.31 (s, 1H)	5.284 (s, 1H)

Table 6.63: ^{13}C -NMR data of the isolated compound LMF4.

Position	β -glucogallin (DMSO- d_6 , 100 MHz, δ , ppm) Reported values ^[236]	LMF4 (DMSO- d_6 , 100 MHz, δ , ppm) Spectral values
C-1	119.2	118.686
C-2	109.4	108.920
C-3	146.0	145.527
C-4	139.3	138.917
C-5	146.0	145.527
C-6	109.4	108.920
C-7	165.0	164.650
C-1'	95.0	94.403
C-2'	73.1	72.578
C-3'	77.1	76.578
C-4'	70.0	69.490
C-5'	78.3	77.852
C-6'	61.0	60.543

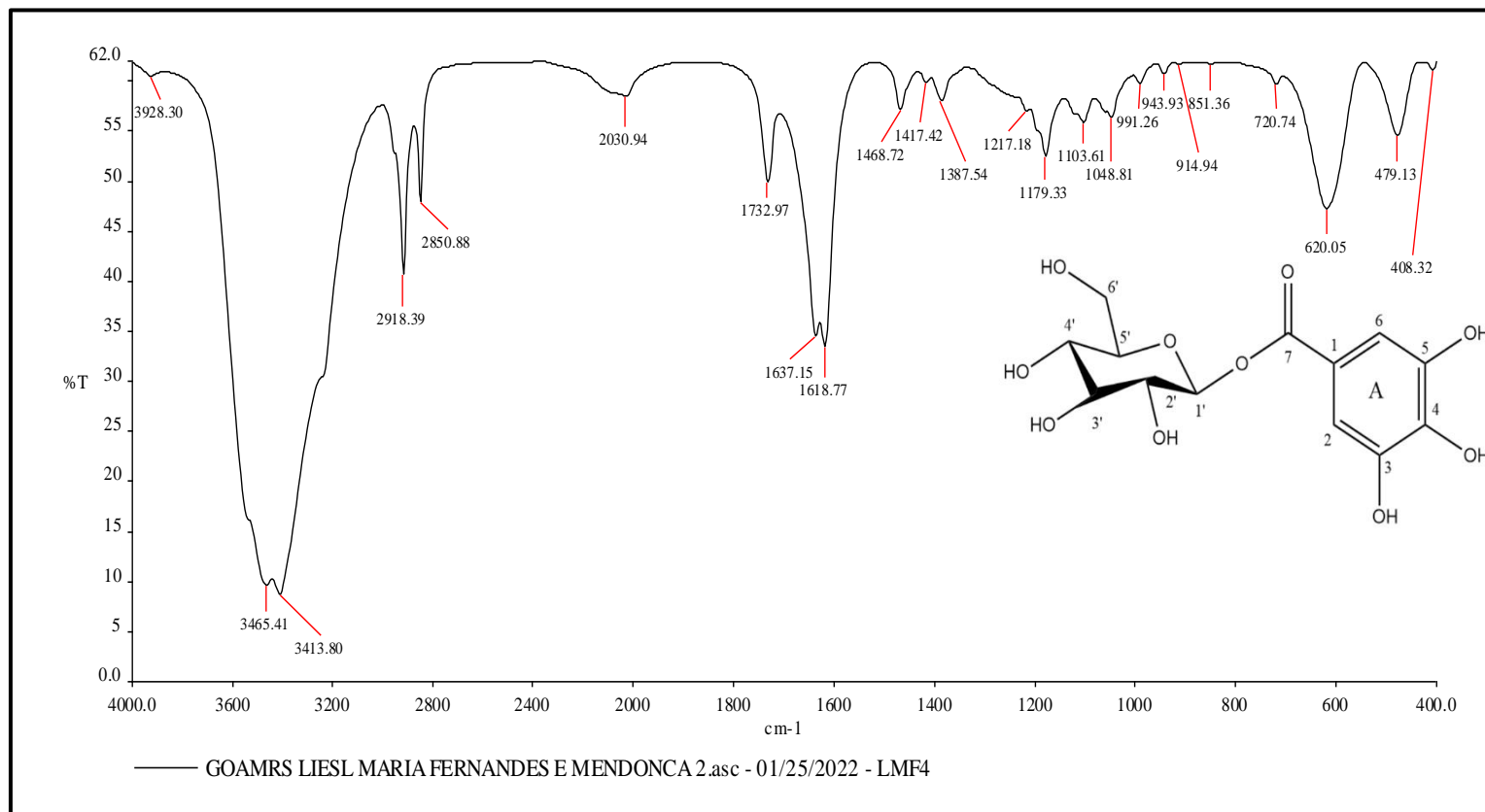


Figure 6.125: IR spectrum of LMF4 (β -Glucogallin).

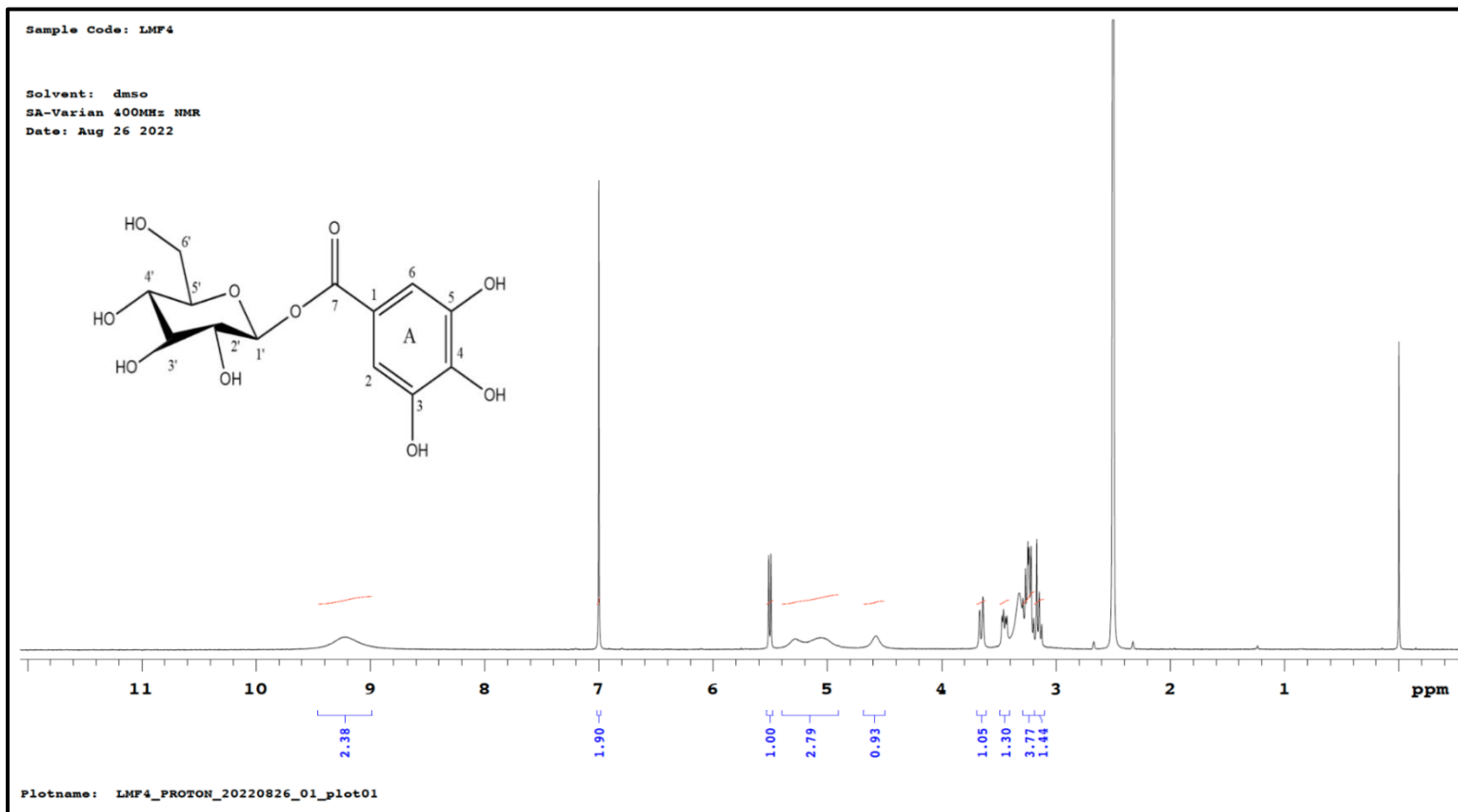


Figure 6.126: ^1H -NMR spectrum of LMF4 (β -Glucogallin).

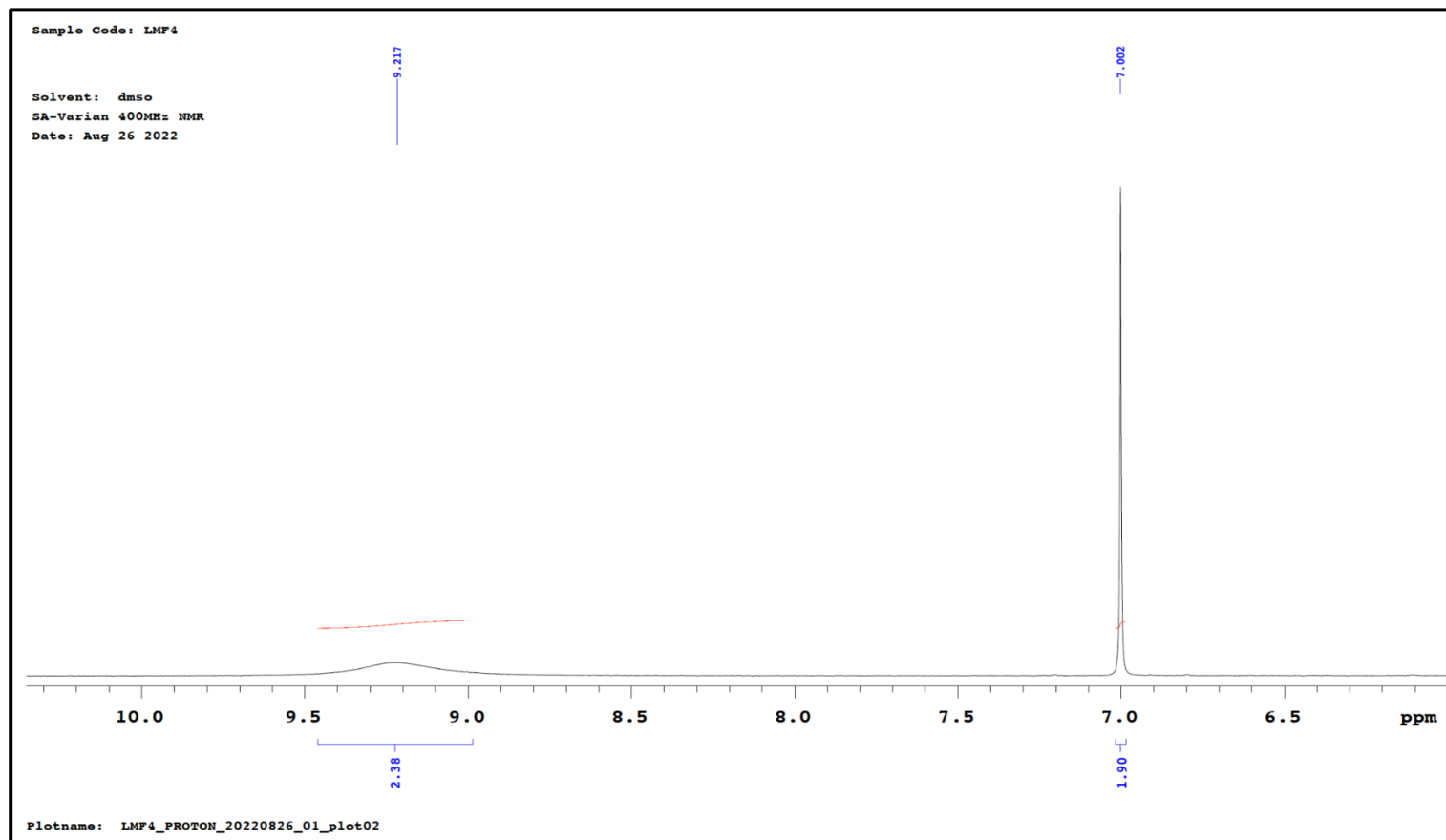


Figure 6.127: Resolution of $^1\text{H-NMR}$ spectrum of LMF4 (β -Glucogallin).

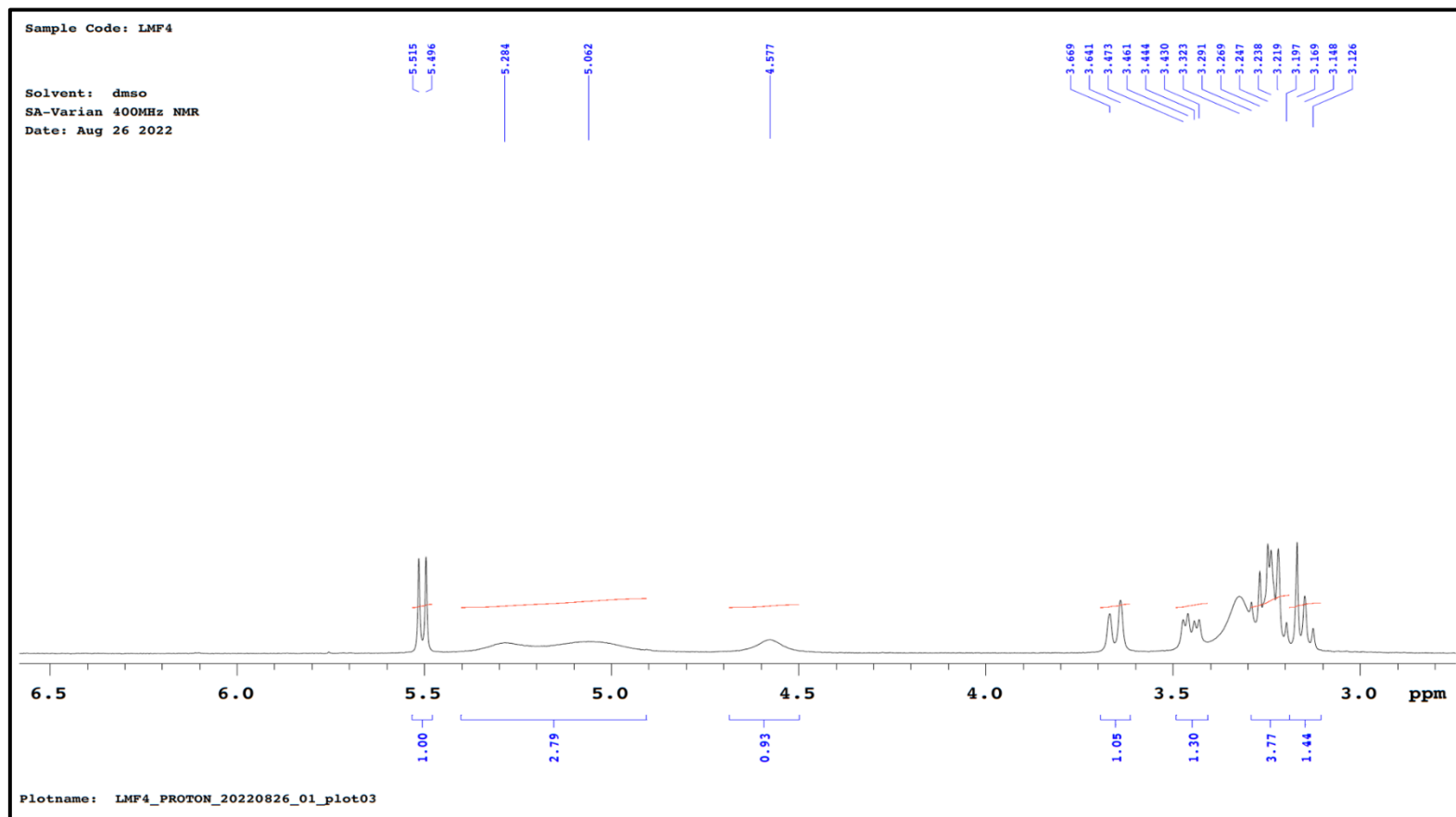


Figure 6.128: Resolution of ^1H -NMR spectrum of LMF4 (β -Glucogallin).

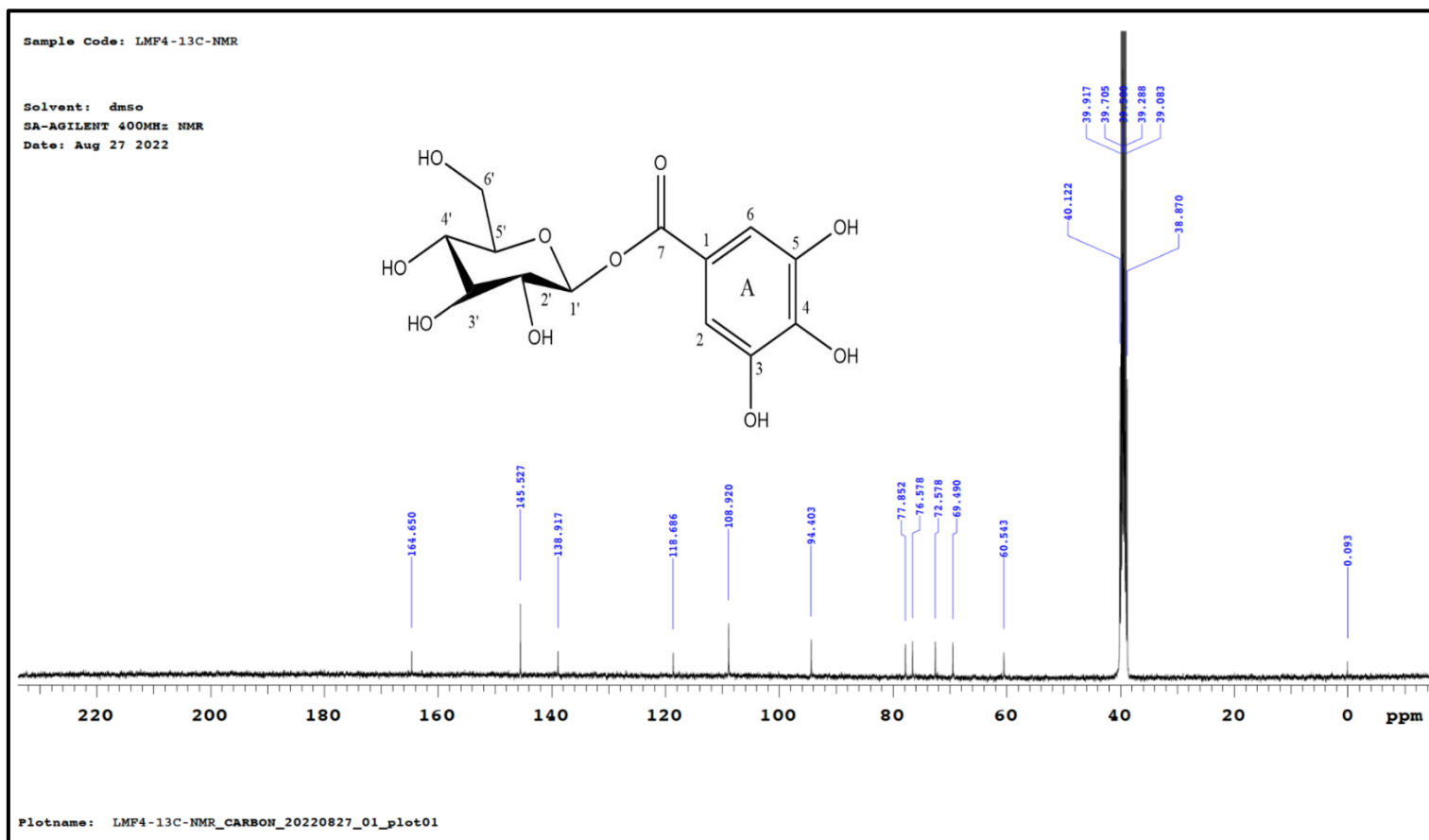


Figure 6.129: ^{13}C -NMR spectrum of LMF4 (β -Glucogallin).

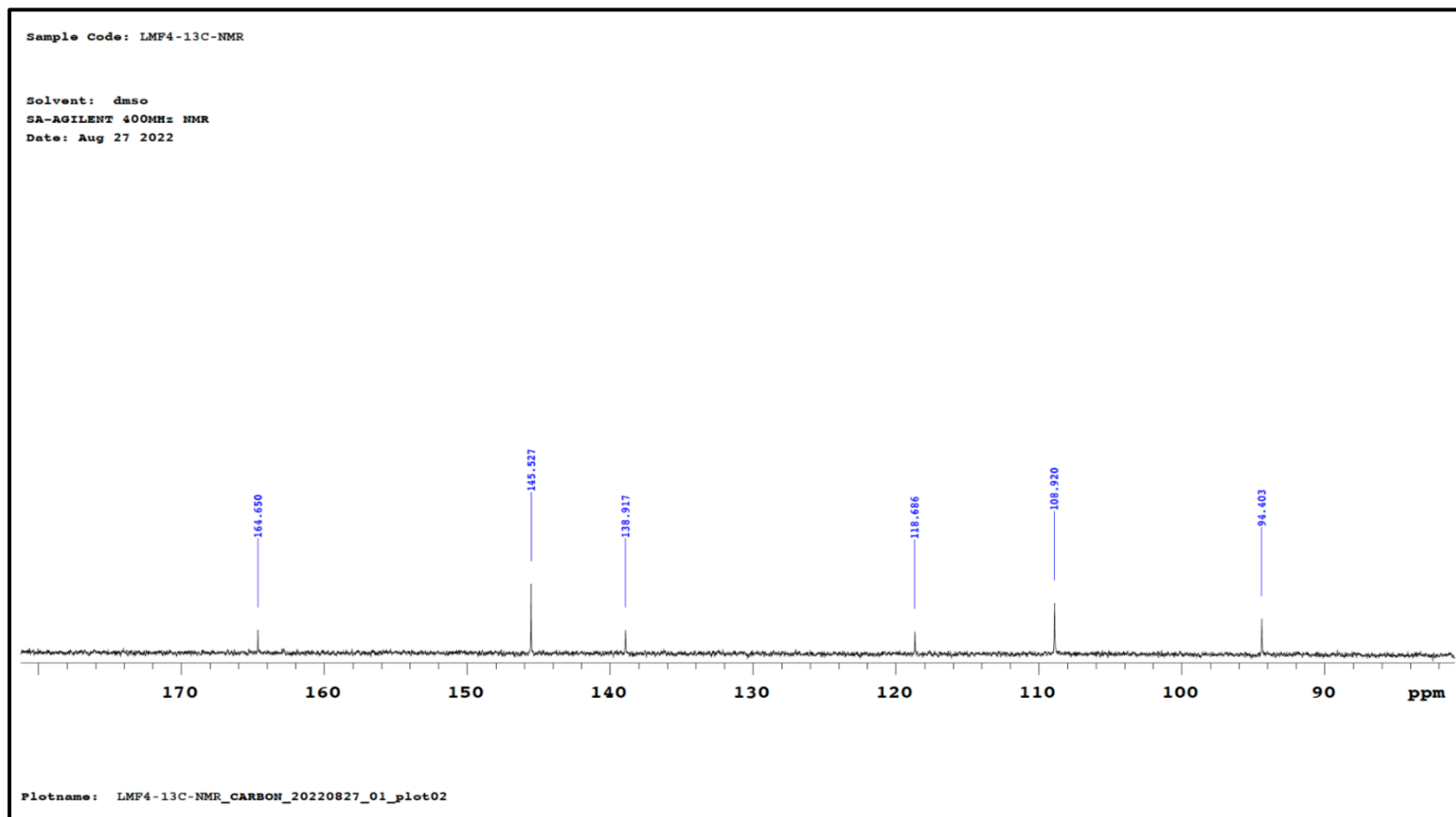


Figure 6.130: Resolution of ^{13}C -NMR spectrum of LMF4 (β -Glucogallin).

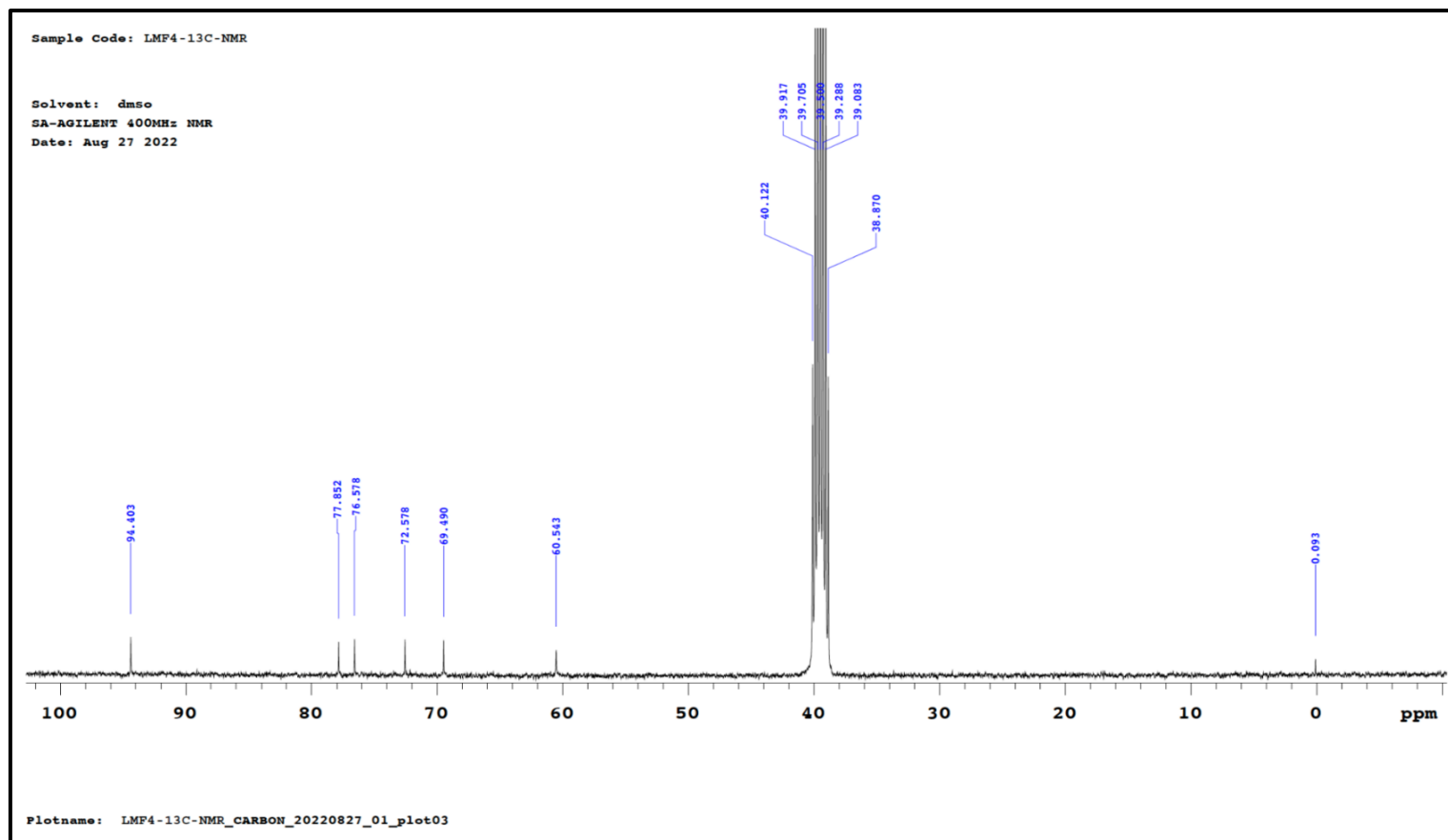


Figure 6.131: Resolution of ^{13}C -NMR spectrum of LMF4 (β -Glucogallin).

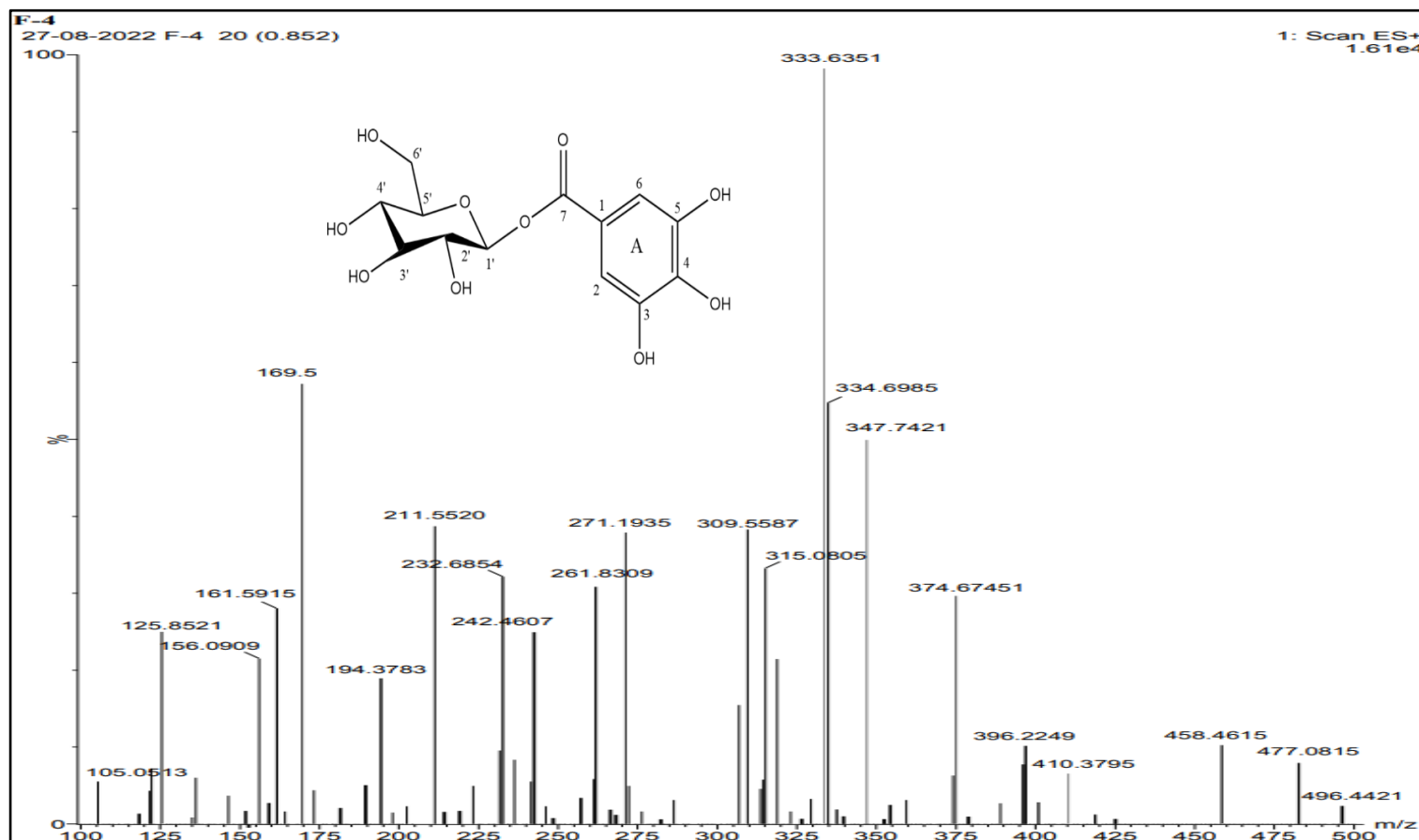


Figure 6.132: Mass spectrum of LMF4 (β -Glucogallin).

6.2.10.3. Isolation and characterisation of phytoconstituents from EFBF

The yield of the column fraction LME obtained was 1.92 g. Purification of LME by preparative HPLC led to the isolation of compound LME1 that had a yield of 37.06 mg (1.93 %). The structural elucidation and characterization of the isolated compound LME1, from EFBF is listed below.

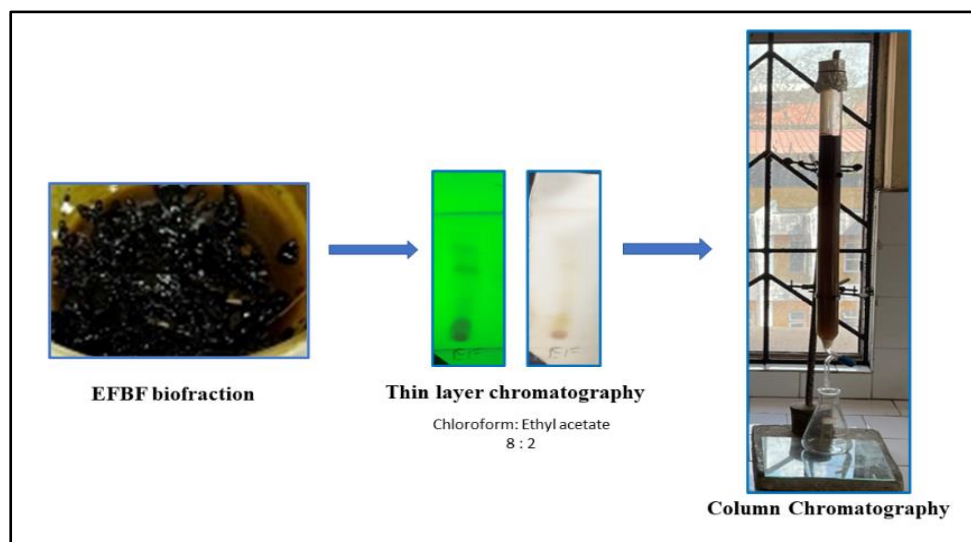


Figure 6.133: Isolation of phytoconstituent from EFBF.

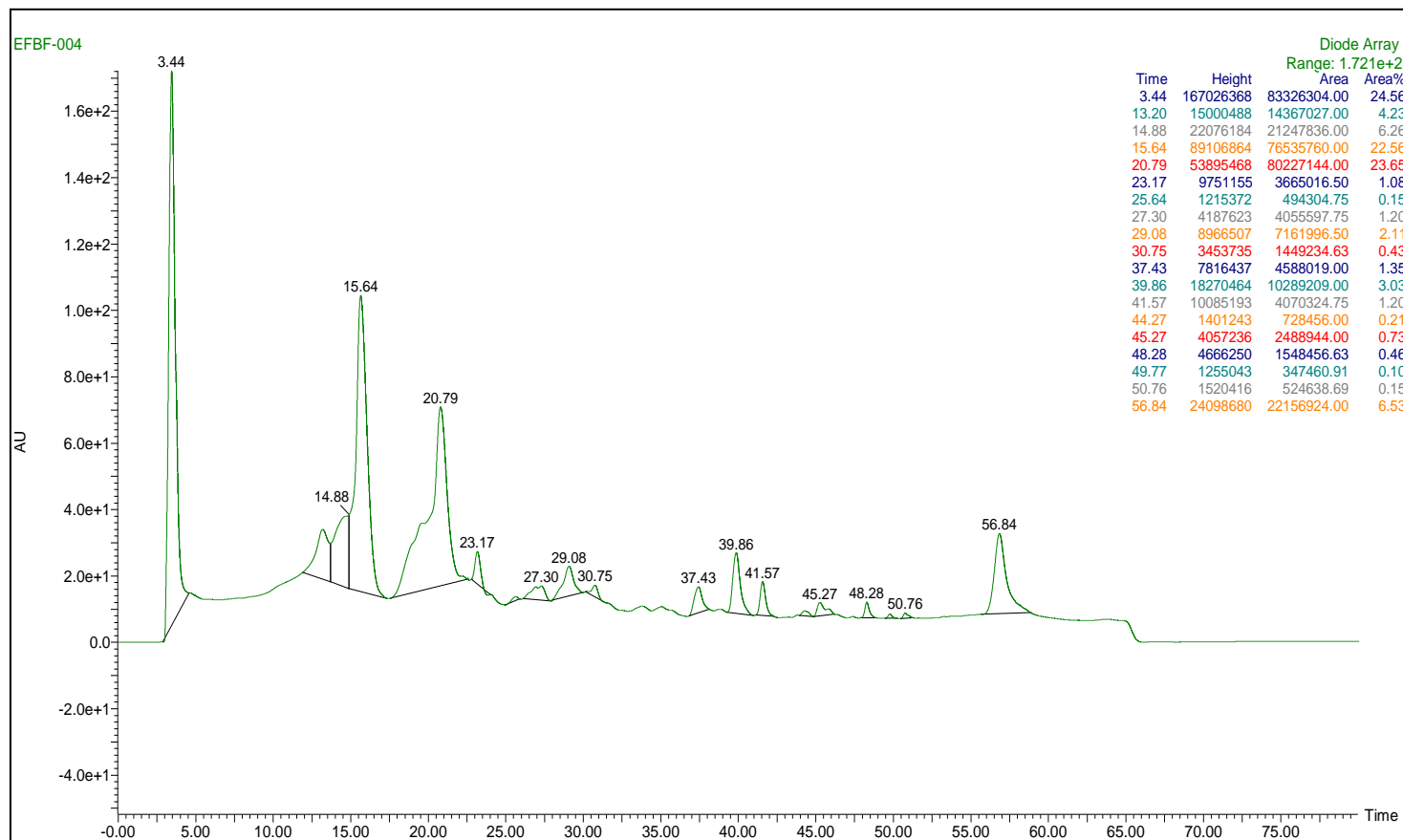


Figure 6.134: Preparative HPLC chromatogram of LME (EFBF purified fraction).

6.2.10.3.1. CHARACTERISATION OF COMPOUND LME1

Physical parameters of the compound

Physical state Yellow coloured compound

Melting point 179 °C (*lit.* 179 - 181 °C) [237]

The compound LME1 gave a positive response for shinoda test for flavonoids.

Spectral characteristics of the compound

IR (KBr) 3070 cm⁻¹ (O-H str.)
 2931 cm⁻¹ (C-H str.)
 1650 cm⁻¹ (C=O str.)
 1509 cm⁻¹ (C=C str.)
 1367 cm⁻¹ (C-O str)

¹H-NMR and ¹³C-NMR Tables 6.64 and 6.65**Mass spectra**

LC-MS (*m/z*) 359.15[M+H]⁺, other peaks appeared at 344.11, 329.11,
 314.02, 257.03

Molecular formula C₁₉H₁₈O₇**Molecular weight** 358.34 g/mol

From the m.p., IR, ¹H-NMR, ¹³C-NMR and mass spectral data, the compound was identified as **Gardenin B**.

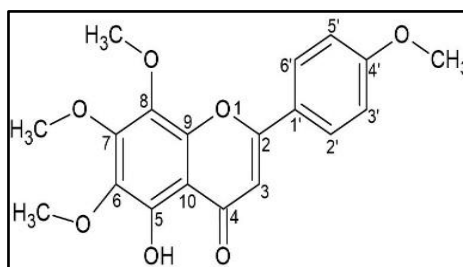
**Figure 6.135: Structure of Gardenin B**

Table 6.64: ¹H-NMR data of the isolated compound LME1.

Position	Gardenin B (DMSO-d₆, 500 MHz, δ ppm, <i>J</i>, Hz) Reported values ^[238]	LME1 (DMSO-d₆, 400 MHz, δ, ppm , <i>J</i>, Hz) Spectral values
H-3	6.954 (s, 1H)	6.998 (s, 1H)
OH-5	12.75 (s, 1H)	12.745 (s, 1H)
H-2'	8.046 (d, 1H, <i>J</i> = 9 Hz)	8.083 (d, 1H, <i>J</i> = 8.4 Hz)
H-3'	7.157 (d, 1H, <i>J</i> = 9 Hz)	7.187 (d, 1H, <i>J</i> = 8.8 Hz)
H-5'	7.157 (d, 1H, <i>J</i> = 9 Hz)	7.187 (d, 1H, <i>J</i> = 8.8 Hz)
H-6'	8.046 (d, 1H, <i>J</i> = 9 Hz)	8.083 (d, 1H, <i>J</i> = 8.4 Hz)
Ar-OCH₃	4.026 (s, 3H)	4.040 (s, 3H)
Ar-OCH₃	3.920 (s, 3H)	3.936 (s, 3H)
Ar-OCH₃	3.866 (s, 3H)	3.883 (s, 3H)
Ar-OCH₃	3.821 (s, 3H)	3.837 (s, 3H)

Table 6.65: ^{13}C -NMR data of the isolated compound LME1.

Position	Gardenin B (DMSO, 125 MHz, δ , ppm) Reported values ^[238]	LME1 (DMSO, 100 MHz, δ , ppm) Spectral values)
C-2	163.87	163.747
C-3	103.41	103.343
C-4	182.70	182.619
C-5	148.65	148.542
C-6	135.96	135.864
C-7	152.63	152.527
C-8	132.75	132.653
C-9	145.35	145.255
C-10	106.32	106.243
C-1'	122.81	122.746
C-2'	128.43	128.334
C-3'	114.87	114.775
C-4'	162.65	152.527
C-5'	114.87	114.775
C-6'	128.43	128.334
Ar-OCH3	60.67	60.558
Ar-OCH3	62.00	61.887
Ar-OCH3	61.59	61.477
Ar-OCH3	55.69	55.594

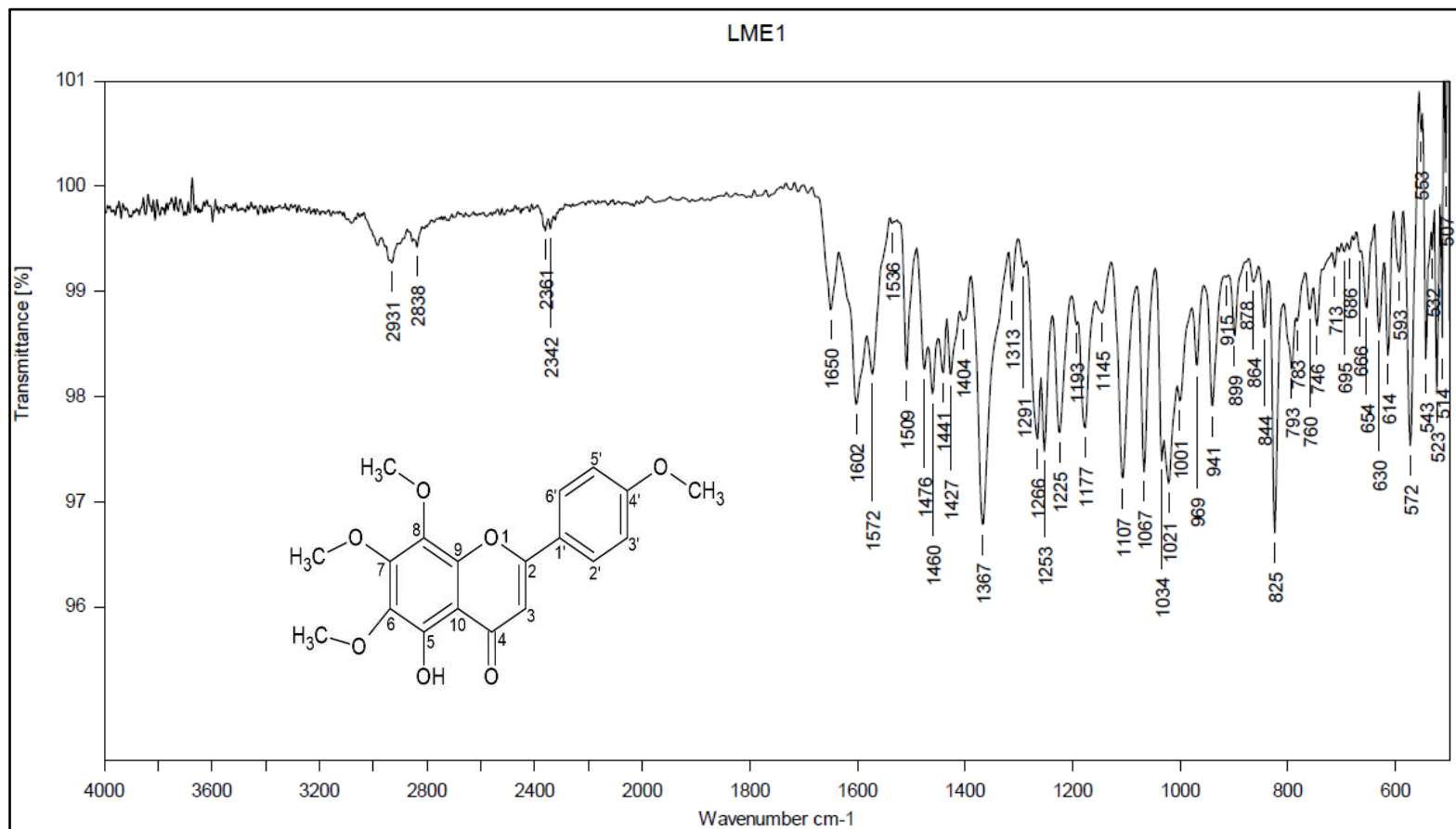
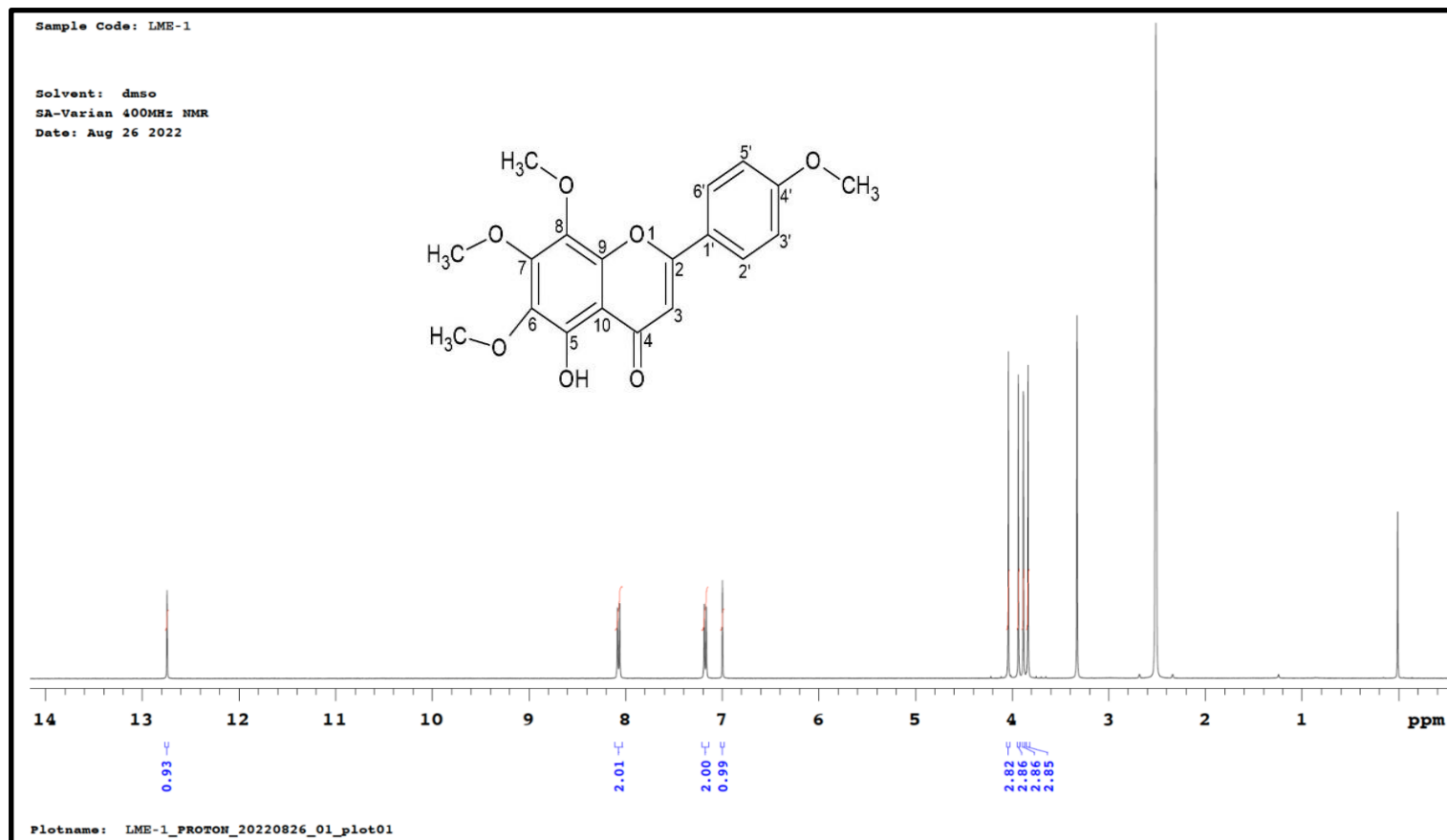


Figure 6.136: IR spectrum of LME1 (Gardenin B).

Figure 6.137: $^1\text{H-NMR}$ spectrum of LME1 (Gardenin B).

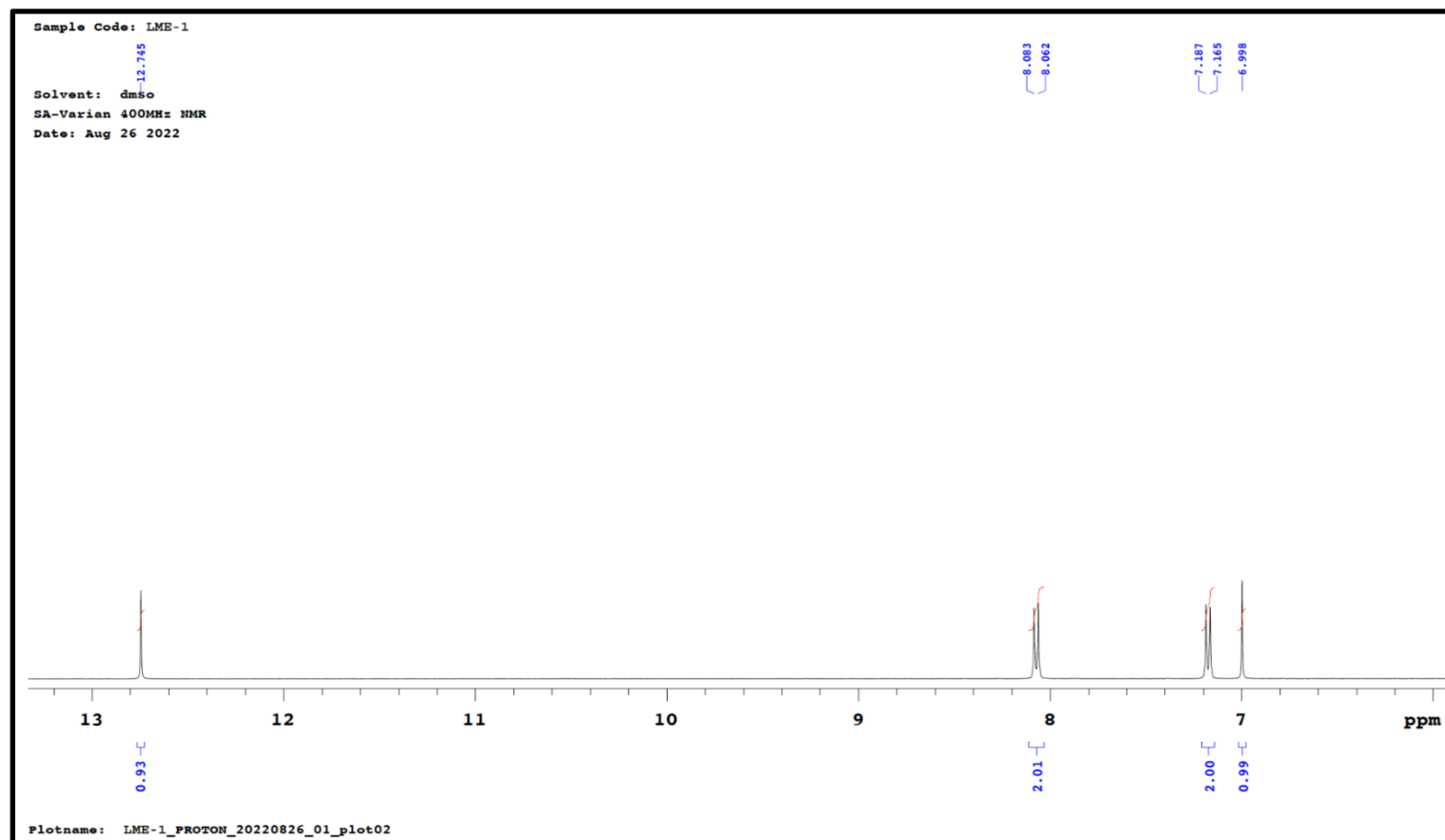


Figure 6.138: Resolution of ^1H -NMR spectrum of LME1 (Gardenin B).

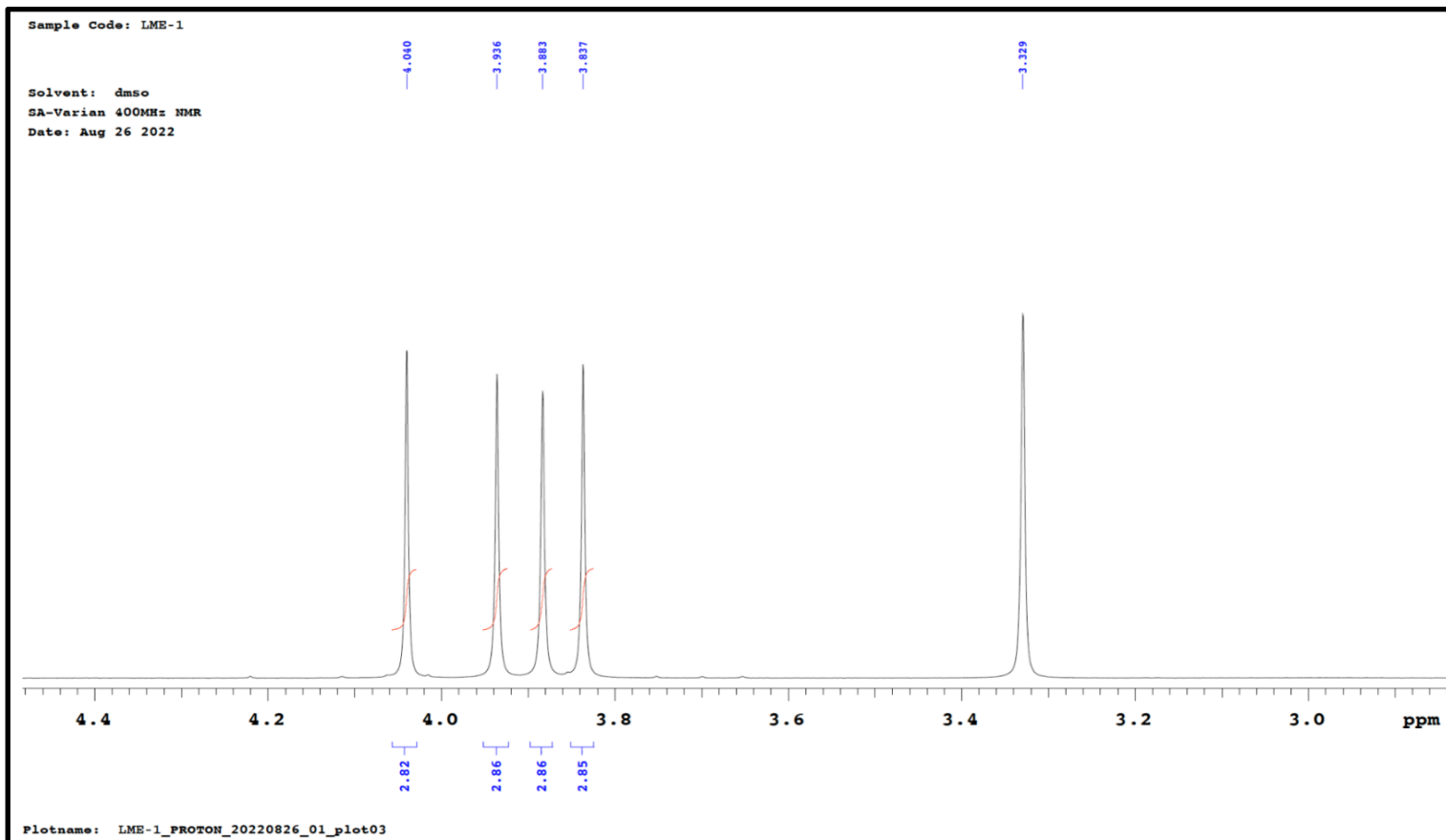
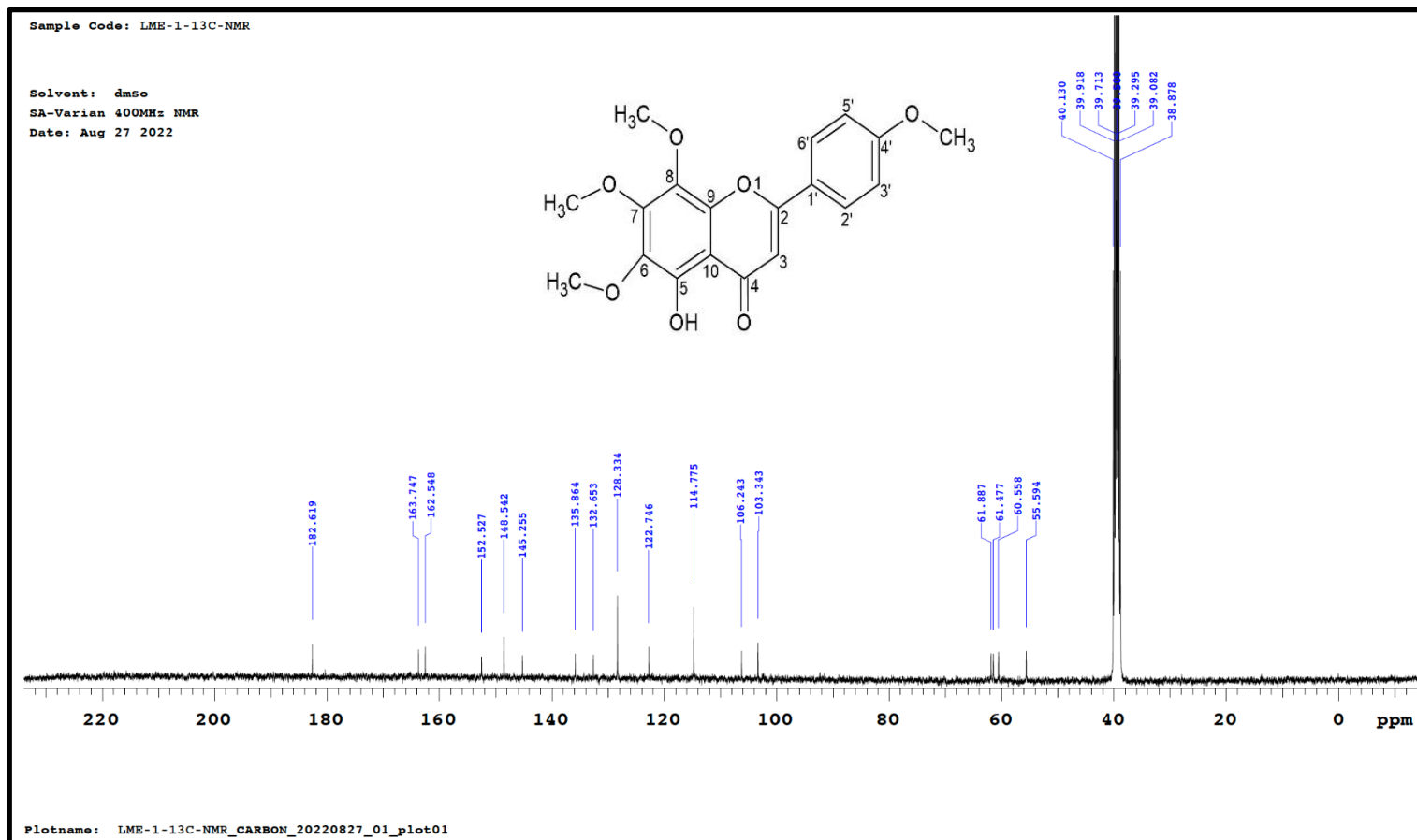


Figure 6.139: Resolution of ^1H -NMR spectrum of LME1 (Gardenin B).

Figure 6.140: ^{13}C -NMR spectrum of LME1 (Gardenin B).

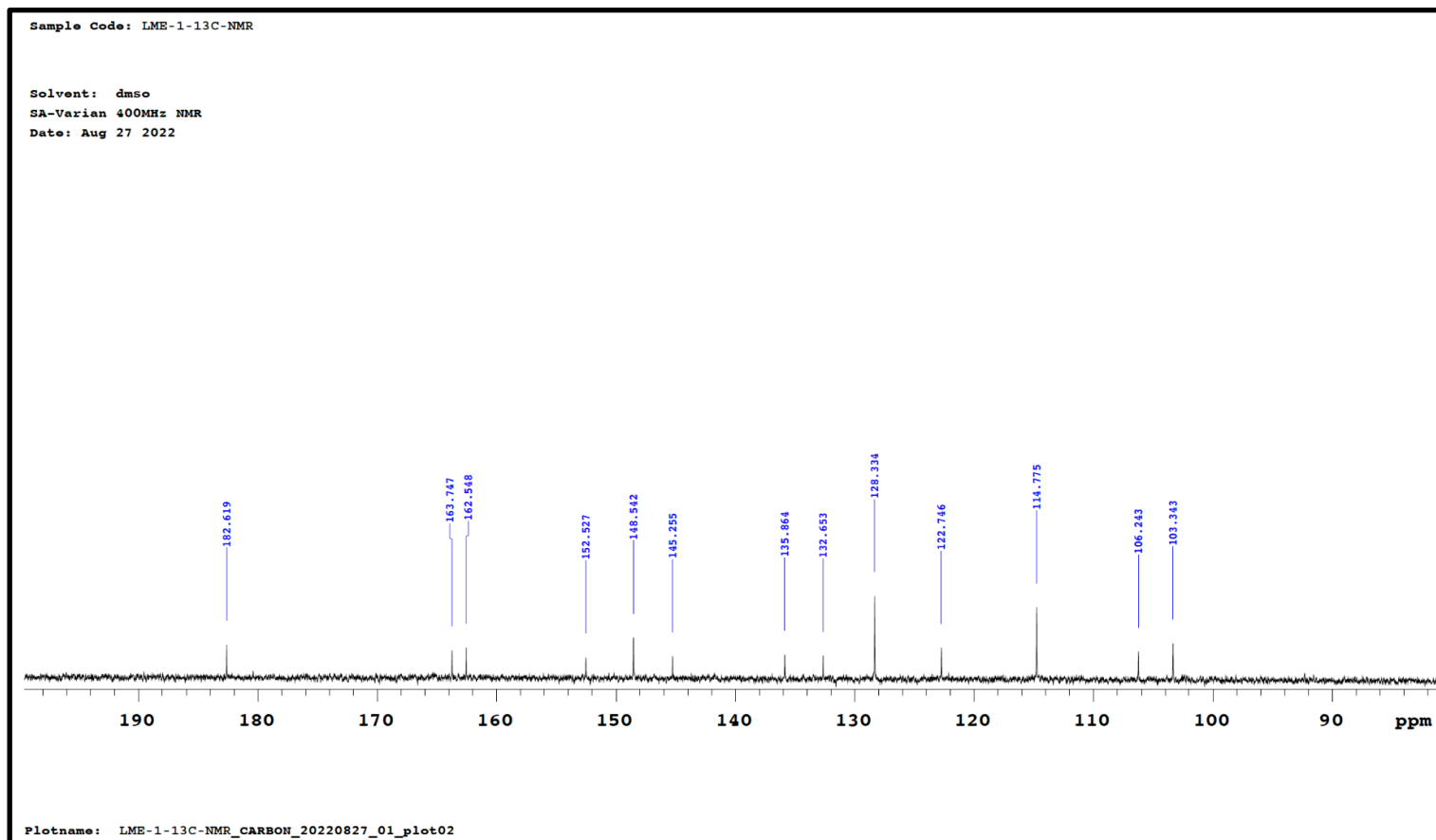


Figure 6.141: Resolution of ^{13}C -NMR spectrum of LME1 (Gardenin B).

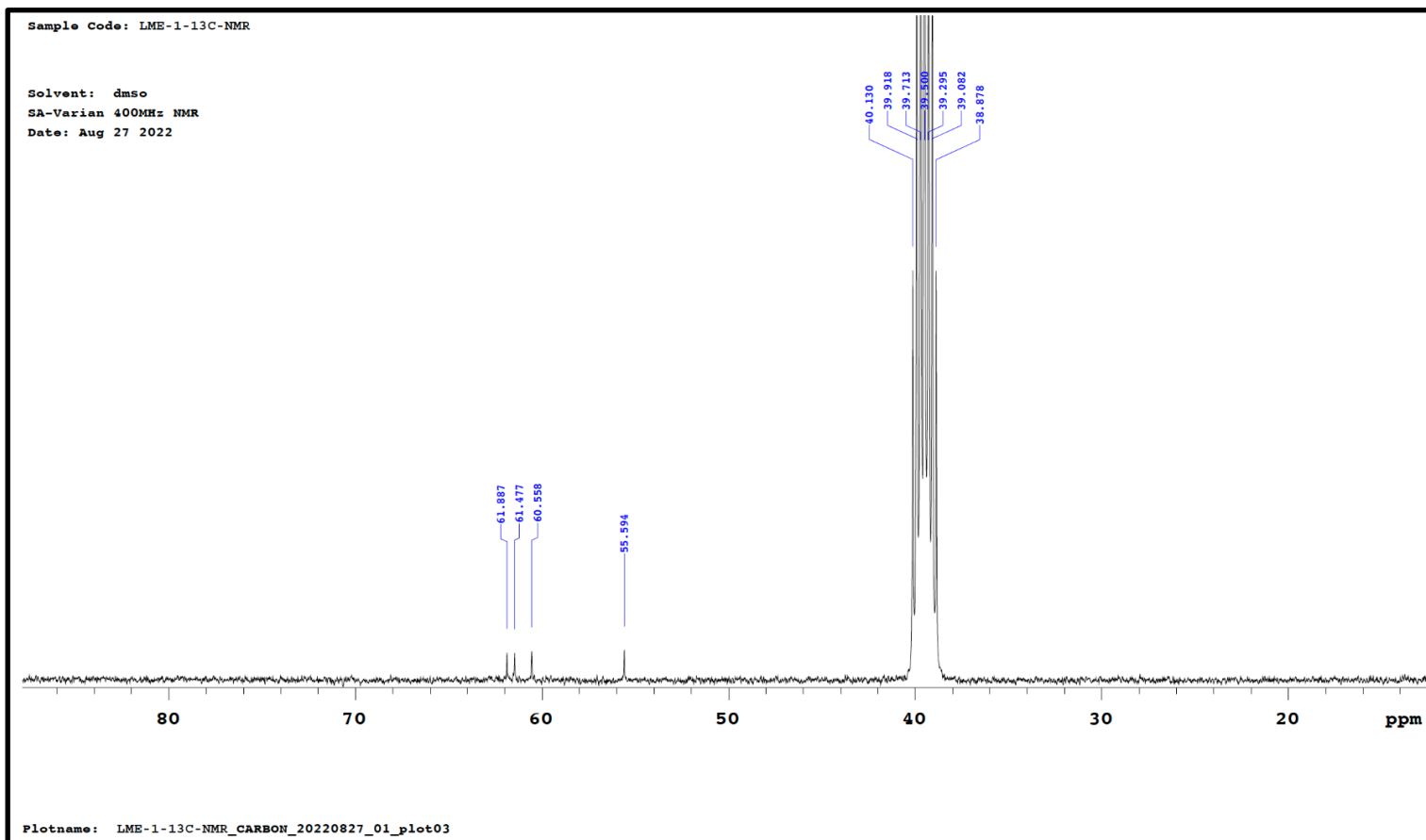


Figure 6.142: Resolution of ^{13}C -NMR spectrum of LME1 (Gardenin B).

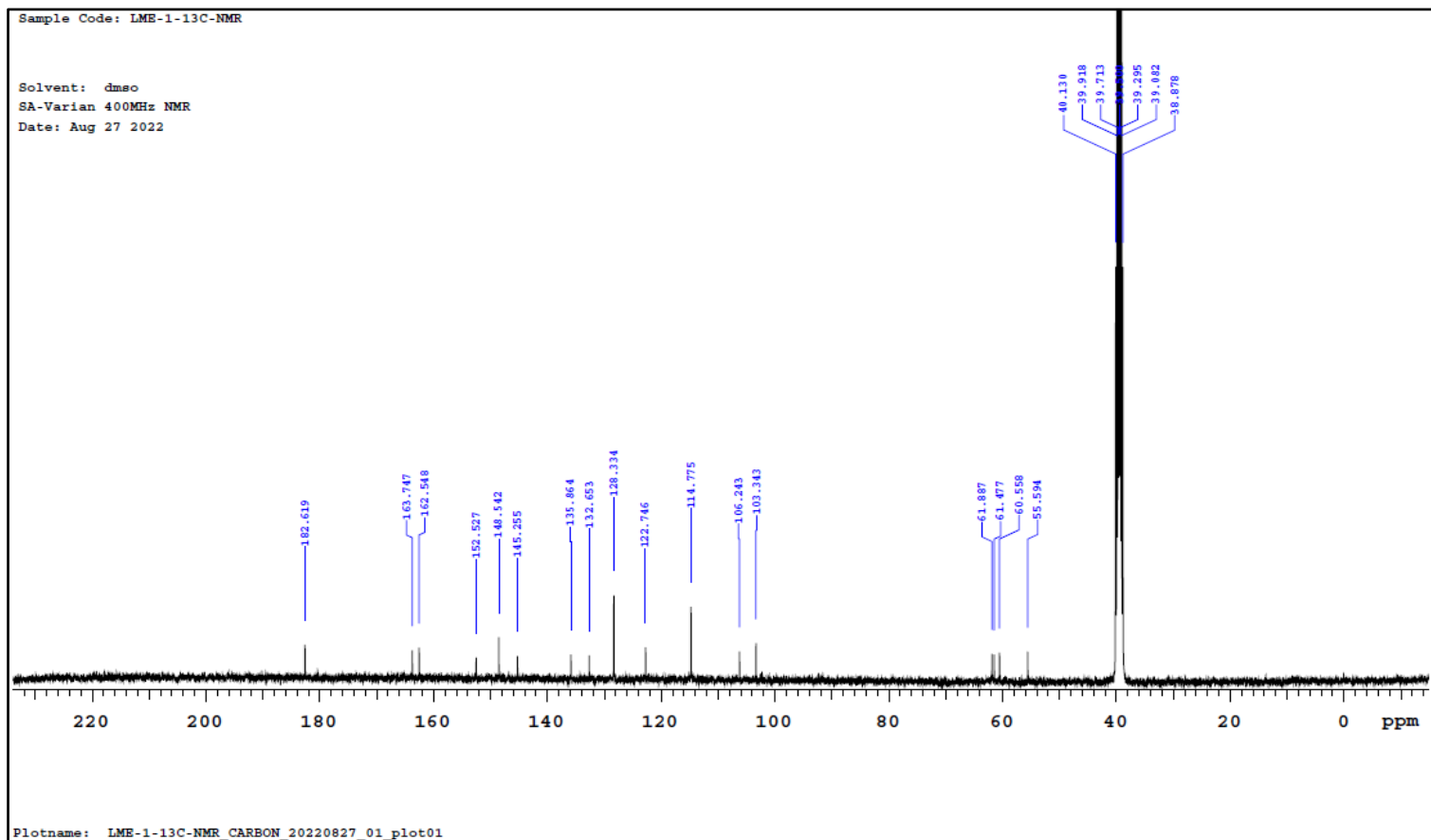


Figure 6.143: Resolution of ^{13}C NMR spectrum of LME1 (Gardenin B).

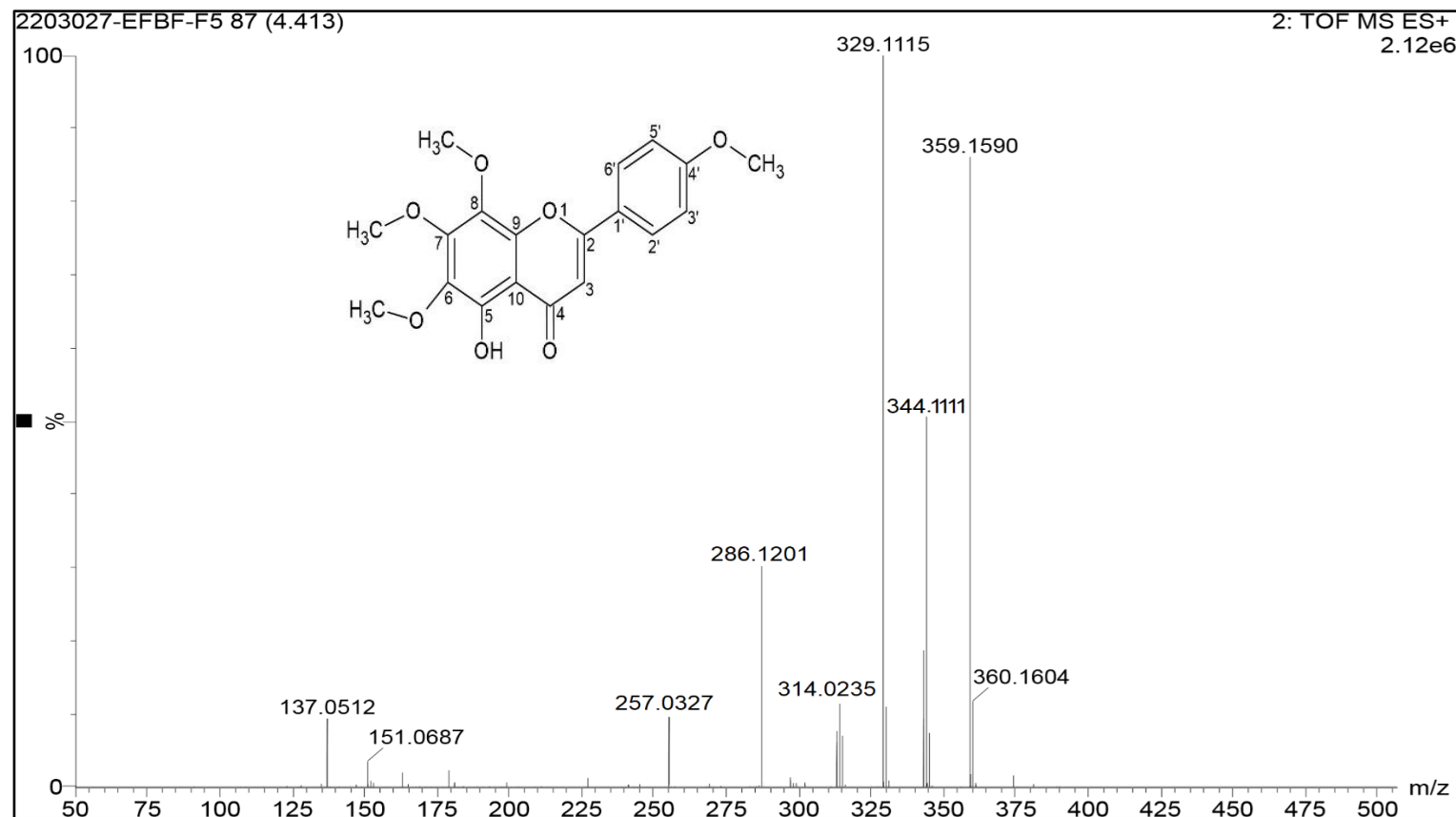
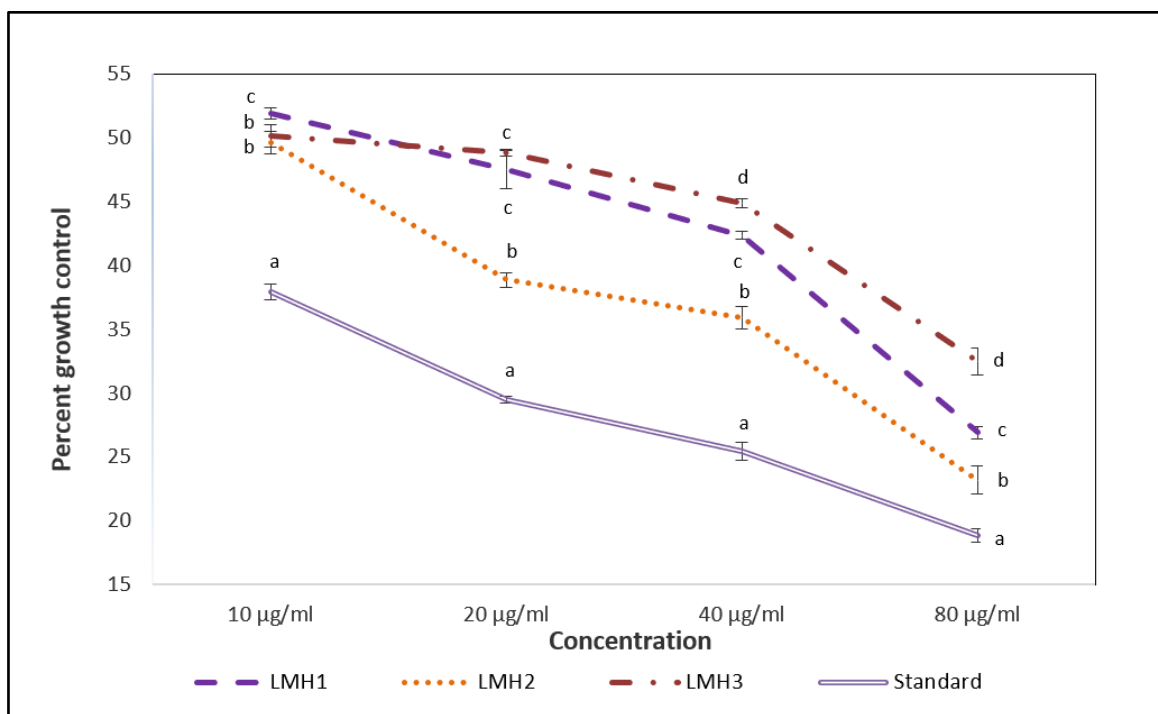


Figure 6.144: Mass spectrum of LME1 (Gardenin B).

6.2.11. *In vitro* anticancer activities of the isolated compounds

Each value is represented as the mean \pm SD (n = 3). Different superscript letters (a - d) are statistically significant (ANOVA, $p < 0.01$, and subsequent post hoc multiple comparisons with Duncan's test).

Figure 6.145: Antiproliferative activity of ITHE isolates against MCF-7 cell lines.

Table 6.66: Growth control of MCF-7 cell lines by ITHE isolates.

Experimental sample	GI ₅₀ (µg/mL)
LMH1 (Quercetrin)	19.64 \pm 0.20
LMH2 (Rutin)	8.06 \pm 2.17
LMH3 (Hesperidin)	15.84 \pm 2.87
Standard (Doxorubicin)	5.77 \pm 0.13

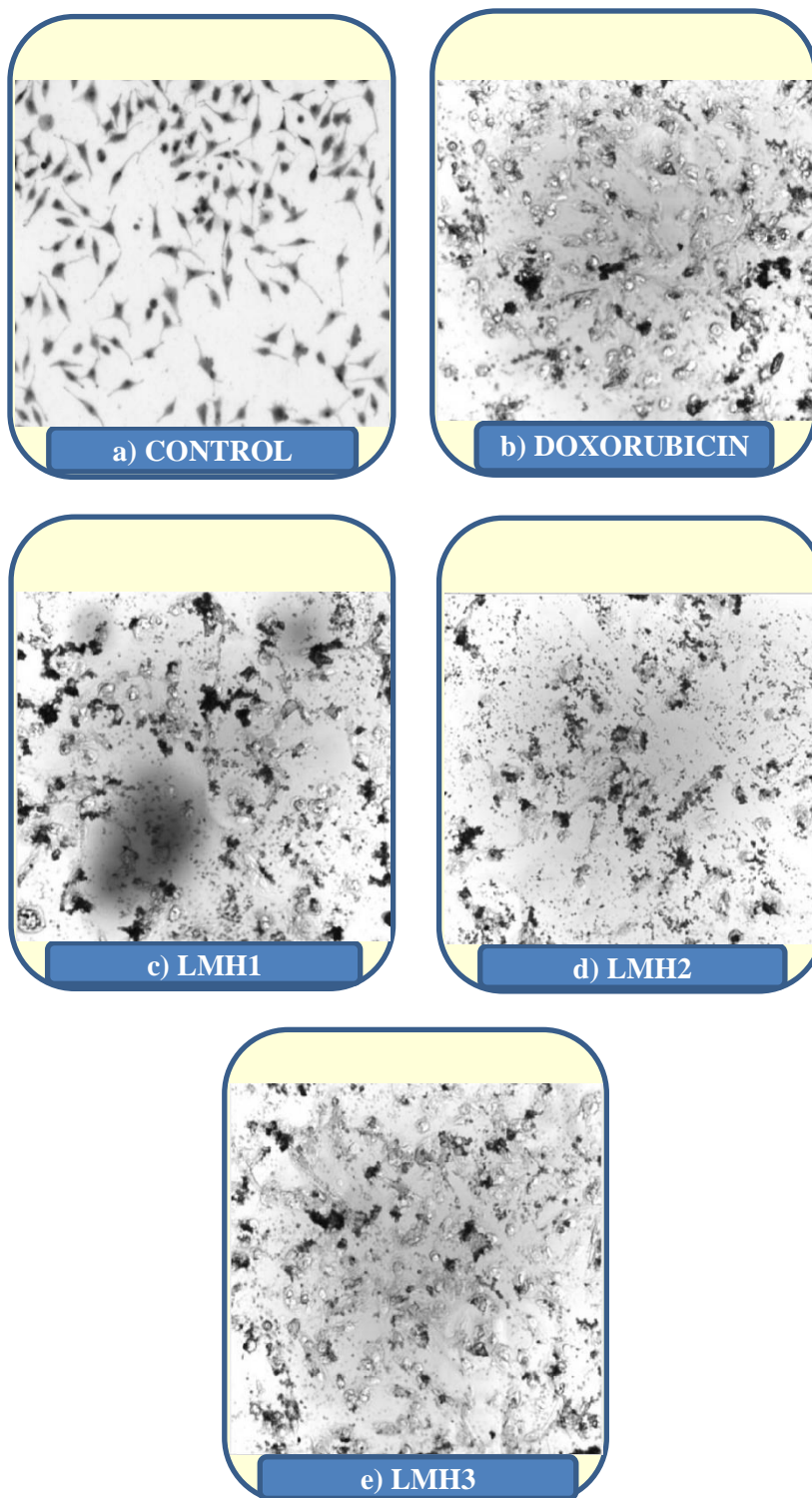
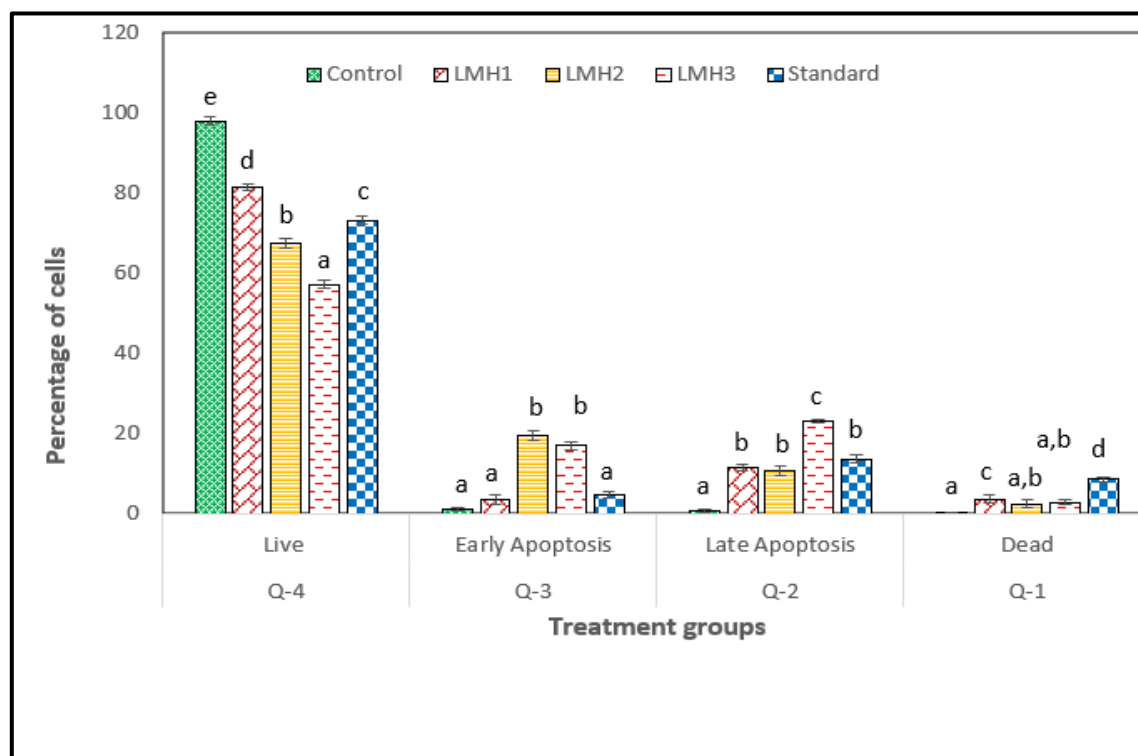


Figure 6.146: Morphological changes of MCF-7 cells treated with ITHE isolates.



Each value is represented as the mean \pm SD (n = 3). Within each stage, the means with different superscript letters (a - e) are statistically significant (ANOVA, $p < 0.001$, and subsequent post hoc multiple comparisons with Duncan's test).

Figure 6.147: Apoptosis activity of ITHE isolates against MCF-7 cell lines.

Table 6.67: Apoptosis analysis of ITHE isolates on MCF-7 cell lines.

Groups	Q-4 Live (%)	Q-3 Early Apoptosis (%)	Q-2 Late Apoptosis (%)	Q-1 Dead (%)
Control	98.07 \pm 0.87 ^e	1.12 \pm 0.35 ^a	0.71 \pm 0.48 ^a	0.13 \pm 0.05 ^a
LMH1	81.45 \pm 0.92 ^d	3.43 \pm 1.23 ^a	11.35 \pm 0.74 ^b	3.68 \pm 1.00 ^c
LMH2	67.42 \pm 1.30 ^b	19.56 \pm 1.24 ^b	10.68 \pm 1.15 ^b	2.39 \pm 1.08 ^{a,b}
LMH3	57.20 \pm 1.00 ^a	16.89 \pm 0.88 ^b	23.18 \pm 0.43 ^c	2.79 \pm 0.67 ^{a,b}
Standard (Doxorubicin)	73.20 \pm 0.96 ^c	4.81 \pm 0.83 ^a	13.67 \pm 1.02 ^b	8.58 \pm 0.65 ^d

Each value is represented as the mean \pm SD (n = 3). Within each stage, the means with different superscript letters (a - e) are statistically significant (ANOVA, $p < 0.001$, and subsequent post hoc multiple comparisons with Duncan's test).

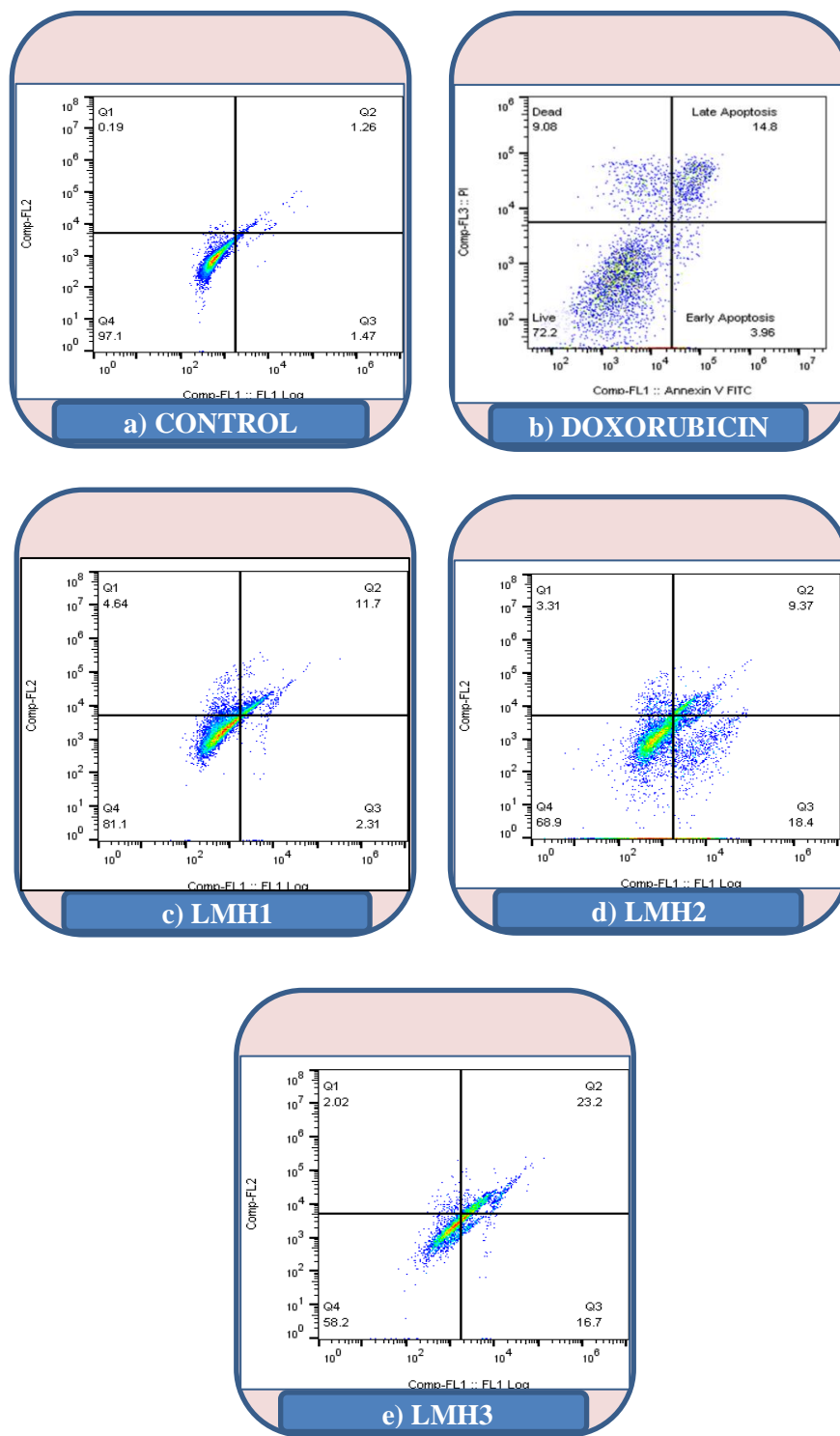
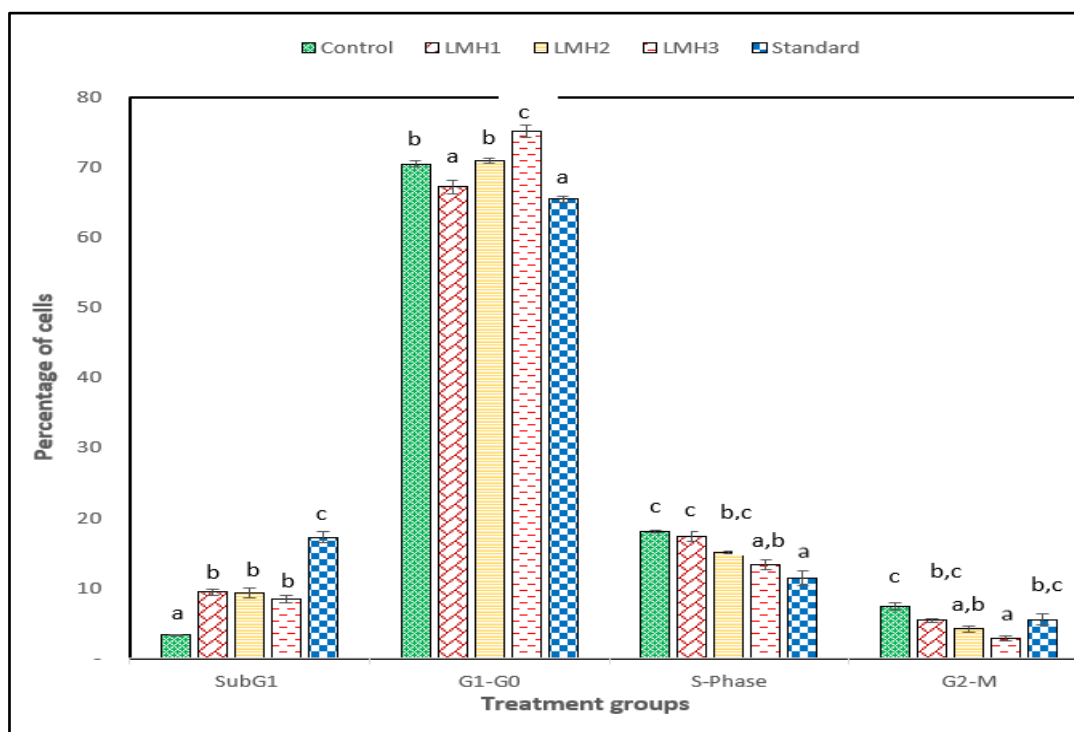


Figure 6.148: Apoptosis analysis of ITHE isolates against MCF-7 cell lines.



Each value is represented as the mean \pm SD (n = 3). Within each stage, the means with different superscript letters (a - c) are statistically significant (ANOVA, $p < 0.001$, and subsequent post hoc multiple comparisons with Duncan's test).

Figure 6.149: Cell cycle activity of ITHE isolates against MCF-7 cell lines.

Table 6.68: Cell cycle analysis of ITHE isolates on MCF-7 cell lines.

Groups	SubG ₁ (%)	G ₁ -G ₀ (%)	S-Phase (%)	G ₂ -M (%)
Control	3.28 \pm 0.13 ^a	70.56 \pm 0.42 ^b	18.08 \pm 0.21 ^c	7.33 \pm 0.52 ^c
LMH1	9.40 \pm 0.41 ^b	67.32 \pm 0.96 ^a	17.34 \pm 0.72 ^c	5.42 \pm 0.25 ^{b,c}
LMH2	9.31 \pm 0.68 ^b	71.02 \pm 0.41 ^b	15.09 \pm 0.15 ^{b,c}	4.15 \pm 0.45 ^{a,b}
LMH3	8.42 \pm 0.55 ^b	75.26 \pm 0.89 ^c	13.36 \pm 0.64 ^{a,b}	2.82 \pm 0.31 ^a
Standard (Doxorubicin)	17.27 \pm 0.74 ^c	65.52 \pm 0.38 ^a	11.42 \pm 1.10 ^a	5.49 \pm 0.79 ^{b,c}

Each value is represented as the mean \pm SD (n = 3). Within each stage, the means with different superscript letters (a - c) are statistically significant (ANOVA, $p < 0.001$, and subsequent post hoc multiple comparisons with Duncan's test).

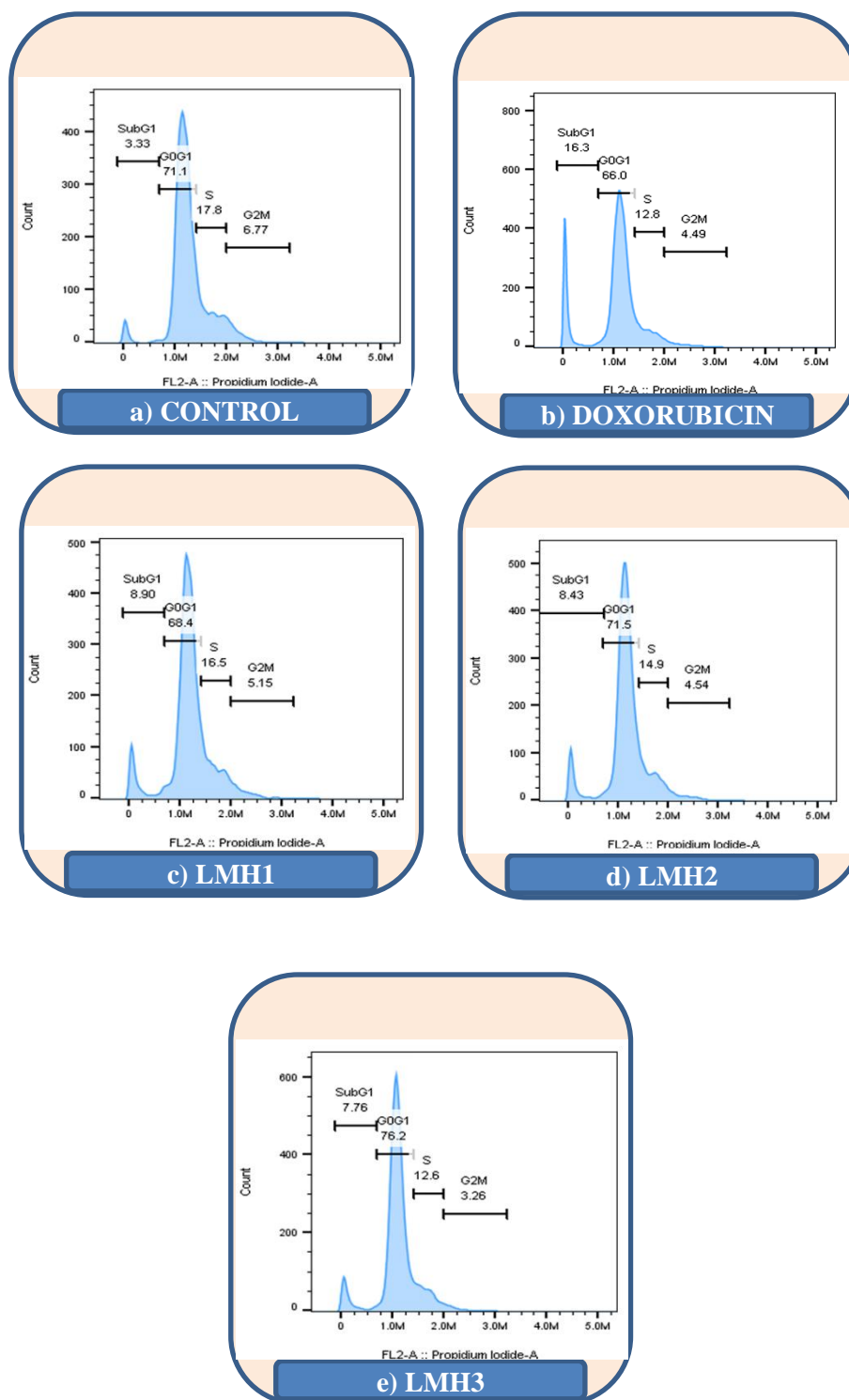
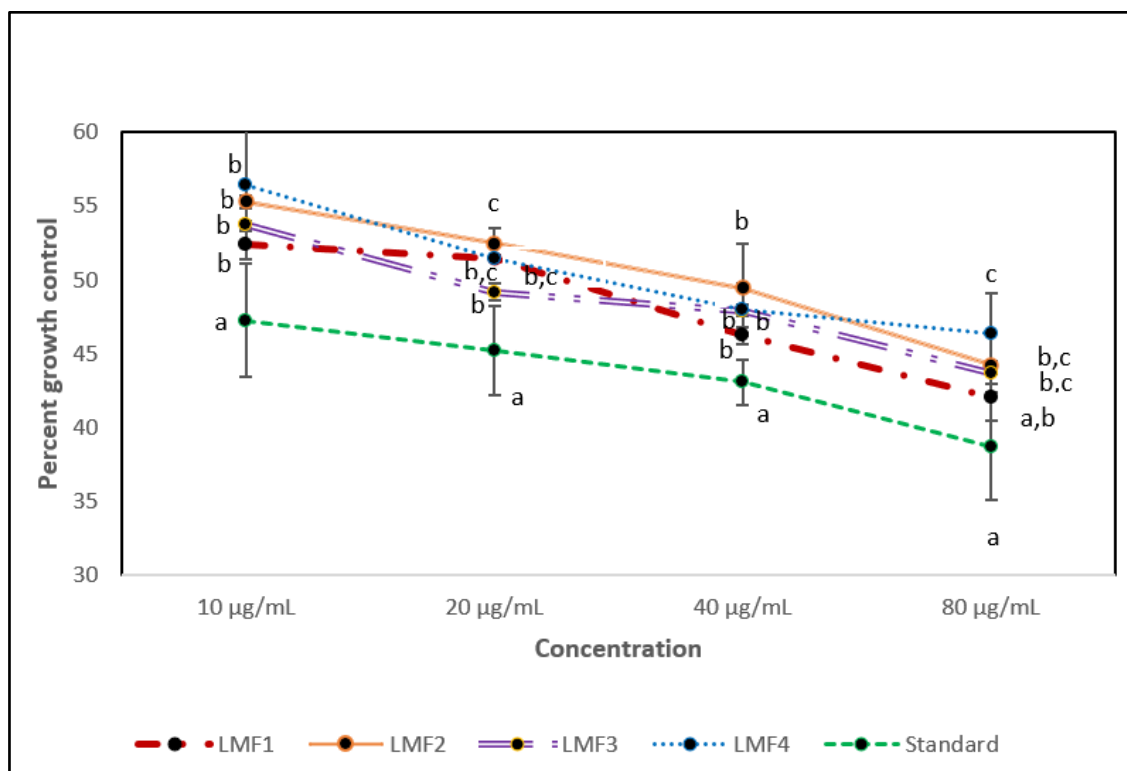


Figure 6.150: Cell cycle analysis of ITHE isolates against MCF-7 cell lines.



Each value is represented as the mean \pm SD (n = 3). Different superscript letters (a - c) are statistically significant (ANOVA, $p < 0.05$, and subsequent post hoc multiple comparisons with Duncan's test).

Figure 6.151: Antiproliferative assay of MFBF isolates against Hop-62 cell lines.

Table 6.69: Growth control of Hop-62 cell lines by EFBF isolates.

Experimental sample	GI ₅₀ (µg/mL)
LMF1 (Quercetin)	16.97 \pm 0.35
LMF2 (Kaempferol)	19.58 \pm 1.14
LMF3 (Isorhamnetin)	17.42 \pm 0.18
LMF4 (β-Glucogallin)	19.60 \pm 4.12
Standard (Doxorubicin)	10.63 \pm 0.90

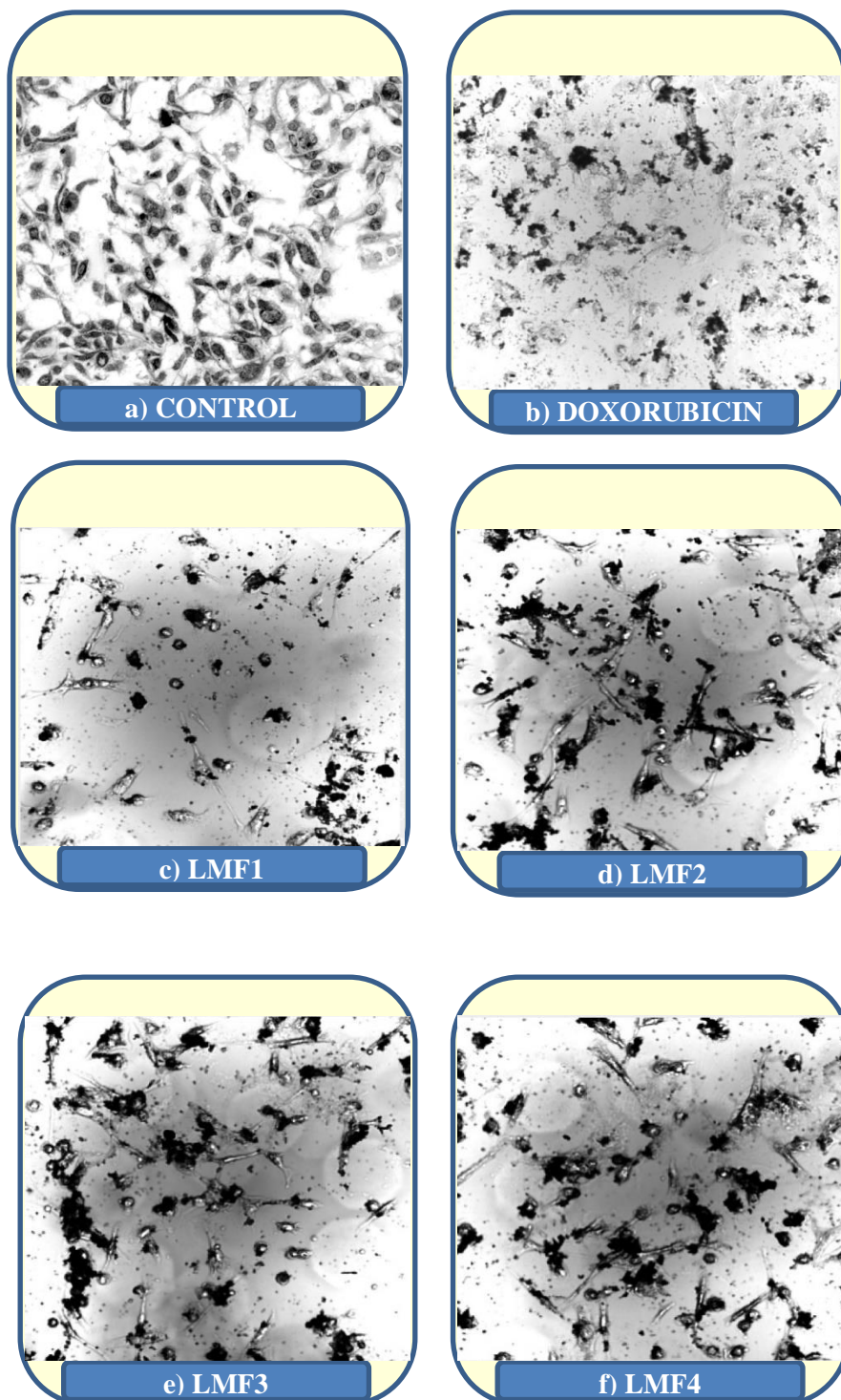
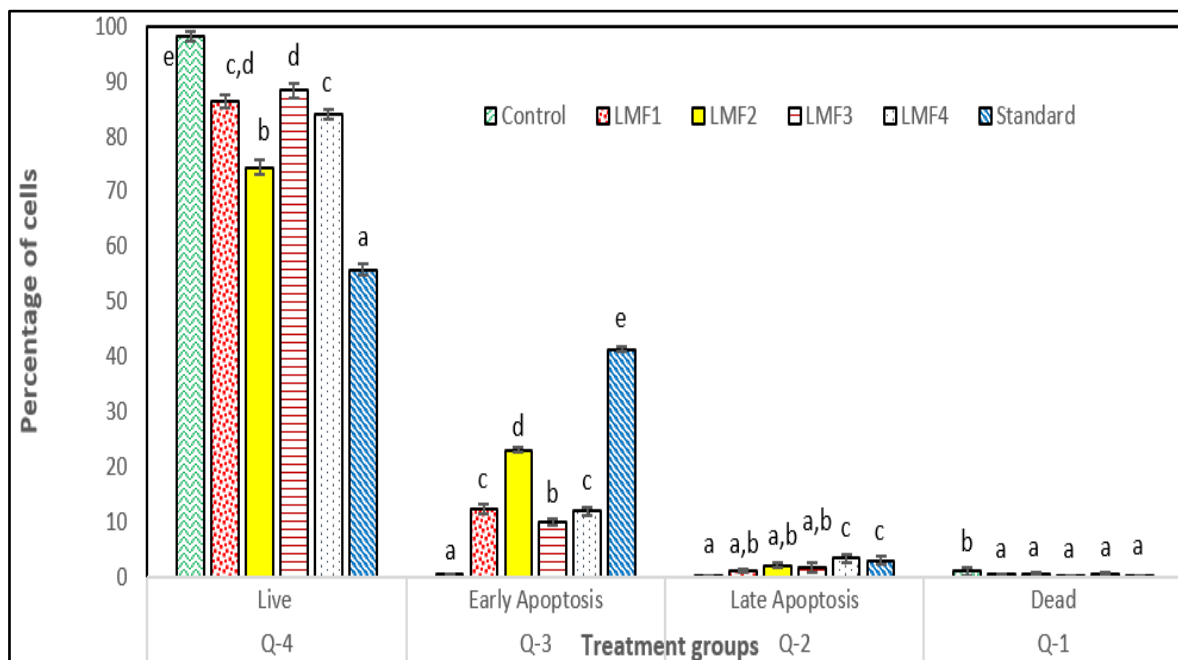


Figure 6.152: Morphological changes of Hop-62 cells treated with MFBF isolates.



Each value is represented as the mean \pm SD (n = 3). Different superscript letters (a - e) are statistically significant (ANOVA, $p < 0.01$, and subsequent post hoc multiple comparisons with Duncan's test).

Figure 6.153: Apoptosis activity of MFBF isolates against Hop-62 cell lines.

Table 6.70: Apoptosis analysis of MFBF isolates on Hop-62 cell lines.

Groups	Q-4 Live (%)	Q-3 Early Apoptosis (%)	Q-2 Late Apoptosis (%)	Q-1 Dead (%)
Control	98.27 \pm 0.87 ^e	0.43 \pm 0.07 ^a	0.28 \pm 0.06 ^a	1.02 \pm 0.82 ^b
LMF1	86.29 \pm 1.19 ^{c,d}	12.3 \pm 0.85 ^c	1.12 \pm 0.27 ^{a,b}	0.42 \pm 0.24 ^a
LMF2	74.38 \pm 1.28 ^b	23.03 \pm 0.37 ^d	2.11 \pm 0.55 ^{a,b}	0.51 \pm 0.37 ^a
LMF3	88.39 \pm 1.34 ^d	9.9 \pm 0.5 ^b	1.65 \pm 0.87 ^{a,b}	0.08 \pm 0.02 ^a
LMF4	84.05 \pm 0.8 ^c	11.98 \pm 0.73 ^c	3.44 \pm 0.74 ^c	0.51 \pm 0.36 ^a
Standard (Doxorubicin)	55.8 \pm 0.97 ^a	41.25 \pm 0.45 ^e	2.93 \pm 0.75 ^c	0.06 \pm 0.02 ^a

Each value is represented as the mean \pm SD (n = 3). Different superscript letters (a - e) are statistically significant (ANOVA, $p < 0.01$, and subsequent post hoc multiple comparisons with Duncan's test).

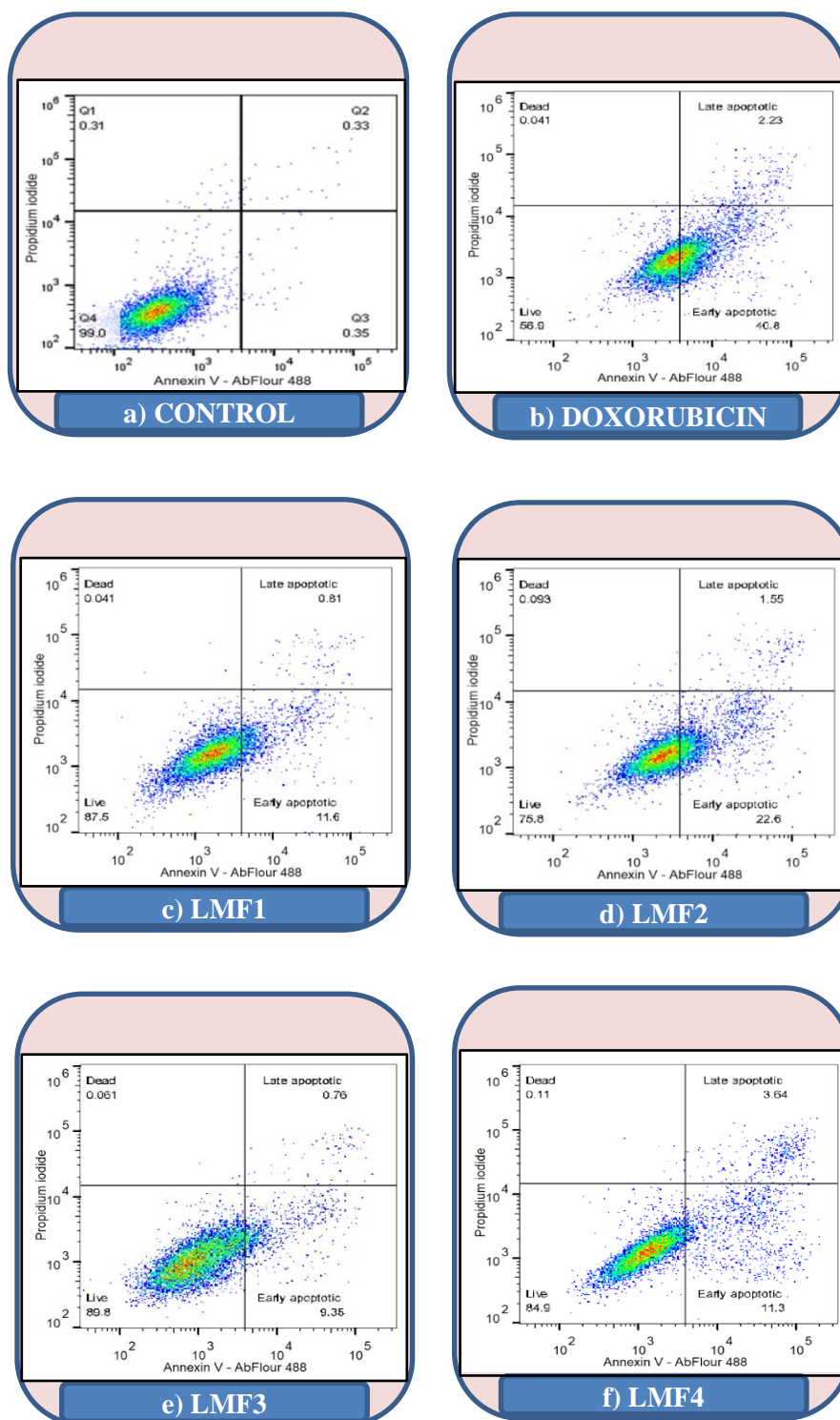
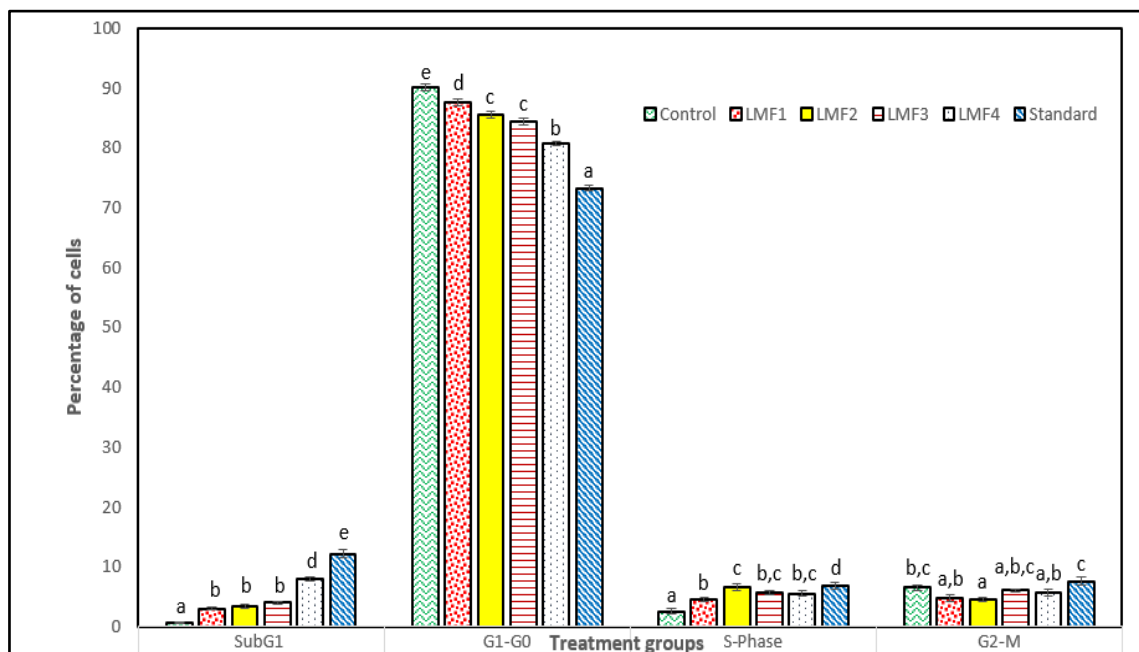


Figure 6.154: Apoptosis analysis of MFBF isolates against Hop-62 cell lines.



Each value is represented as the mean \pm SD (n = 3). Different superscript letters (a - e) are statistically significant (ANOVA, $p < 0.001$, and subsequent post hoc multiple comparisons with Duncan's test).

Figure 6.155: Cell cycle assay of MFBF isolates against Hop-62 cell lines.

Table 6.71: Cell cycle analysis of MFBF isolates on Hop-62 cell lines.

Groups	SubG1 (%)	G1-G0 (%)	S-Phase (%)	G2-M (%)
Control	0.68 \pm 0.13 ^a	90.13 \pm 0.55 ^e	2.57 \pm 0.52 ^a	6.55 \pm 0.4 ^{b,c}
LMF1	3.04 \pm 0.26 ^b	87.69 \pm 0.62 ^d	4.45 \pm 0.33 ^b	4.82 \pm 0.56 ^{a,b}
LMF2	3.32 \pm 0.34 ^b	85.57 \pm 0.56 ^c	6.55 \pm 0.57 ^c	4.52 \pm 0.43 ^a
LMF3	3.98 \pm 0.23 ^b	84.37 \pm 0.58 ^c	5.6 \pm 0.34 ^{b,c}	6.04 \pm 0.29 ^{a,b,c}
LMF4	8.04 \pm 0.36 ^d	80.75 \pm 0.36 ^b	5.54 \pm 0.4 ^{b,c}	5.67 \pm 0.63 ^{a,b}
Standard (Doxorubicin)	12.2 \pm 0.62 ^e	73.3 \pm 0.46 ^a	6.88 \pm 0.61 ^d	7.63 \pm 0.65 ^c

Each value is represented as the mean \pm SD (n = 3). Different superscript letters (a - e) are statistically significant (ANOVA, $p < 0.001$, and subsequent post hoc multiple comparisons with Duncan's test).

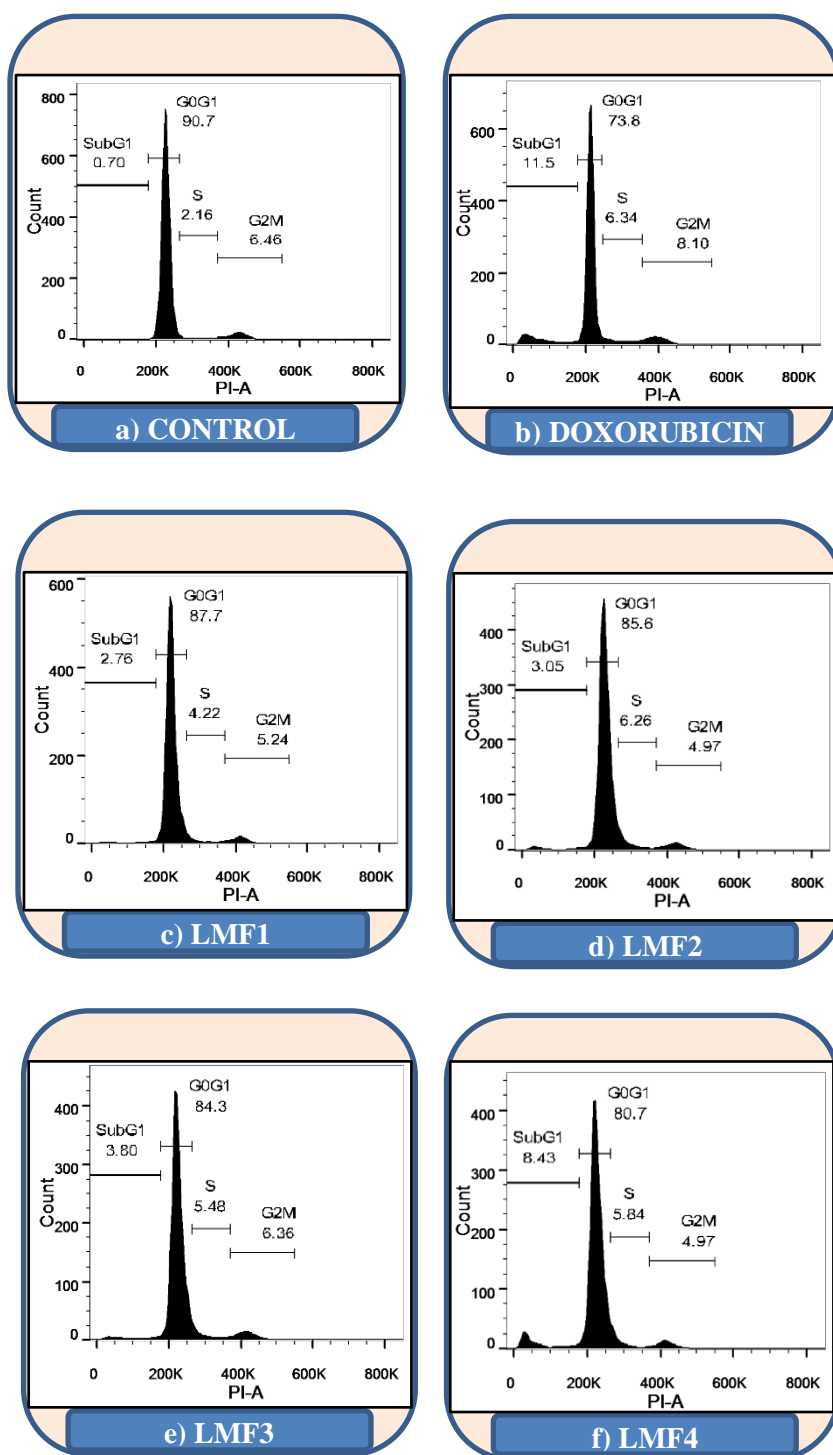
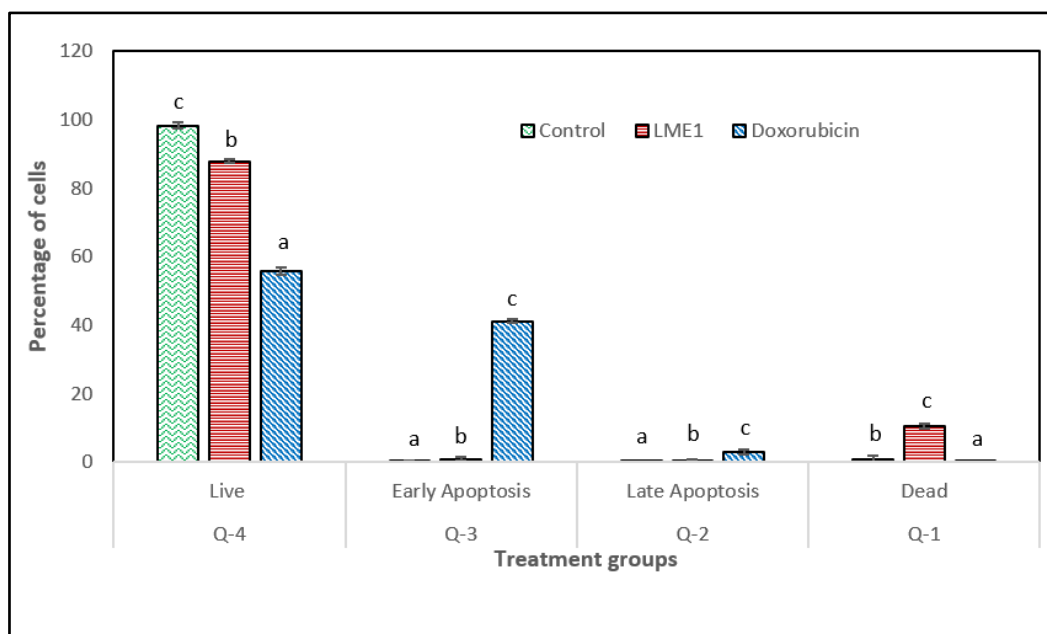


Figure 6.156: Cell cycle analysis of MFBF isolates against Hop-62 cell lines.

Table 6.72: Growth control of Hop-62 cell lines by EFBF isolate (LME1).

Experimental sample	GI ₅₀ (µg/mL)
LME1	21.91 ± 0.83
Standard (Doxorubicin)	10.63 ± 0.90

(Each value is stated as mean ± SD, n = 3, p < 0.01)

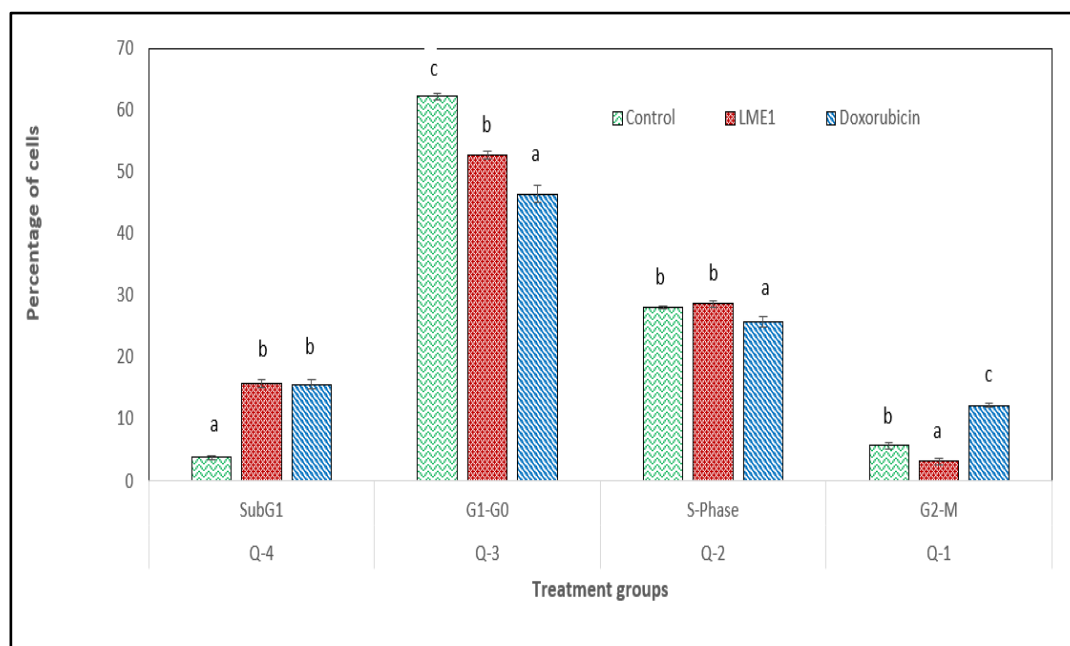


Each value is represented as the mean ± SD (n = 3). Different superscript letters (a - c) are statistically significant (ANOVA, p < 0.001, and subsequent post hoc multiple comparisons with Duncan's test).

Figure 6.157: Apoptosis activity of EFBF isolate (LME1) against Hop-62 cell lines.**Table 6.73: Apoptosis analysis EFBF isolate (LME1) on Hop-62 cell lines.**

Groups	Q-4 Live (%)	Q-3 Early Apoptosis (%)	Q-2 Late Apoptosis (%)	Q-1 Dead (%)
Control	98.27 ± 0.87 ^c	0.43 ± 0.07 ^a	0.28 ± 0.06 ^a	1.02 ± 0.82 ^b
LME1	87.79 ± 0.55 ^b	1.05 ± 0.46 ^b	0.60 ± 0.33 ^b	10.57 ± 0.79 ^c
Standard (Doxorubicin)	55.8 ± 0.97 ^a	41.25 ± 0.45 ^c	2.93 ± 0.75 ^c	0.06 ± 0.02 ^a

Each value is represented as the mean ± SD (n = 3). Different superscript letters (a - c) are statistically significant (ANOVA, p < 0.001, and subsequent post hoc multiple comparisons with Duncan's test).



Each value is represented as the mean \pm SD ($n = 3$). Different superscript letters (a - c) are statistically significant (ANOVA, $p < 0.001$, and subsequent post hoc multiple comparisons with Duncan's test).

Figure 6.158: Cell cycle activity of EFBF isolate (LME1) against Hop-62 cell lines.

Table 6.74: Cell cycle analysis of EFBF isolate (LME1) against Hop-62 cells.

Groups	SubG ₁ (%)	G ₁ -G ₀ (%)	S-Phase (%)	G ₂ -M (%)
Control	3.87 \pm 0.37 ^a	62.20 \pm 0.46 ^c	28.12 \pm 0.30 ^b	5.79 \pm 0.53 ^b
LME1	15.89 \pm 0.65 ^b	52.69 \pm 0.62 ^b	28.71 \pm 0.52 ^b	3.22 \pm 0.49 ^a
Standard (Cisplatin)	15.67 \pm 0.75 ^b	46.43 \pm 1.37 ^a	25.74 \pm 0.91 ^a	12.27 \pm 0.35 ^c

Each value is represented as the mean \pm SD ($n = 3$). Different superscript letters (a - c) are statistically significant (ANOVA, $p < 0.001$, and subsequent post hoc multiple comparisons with Duncan's test).

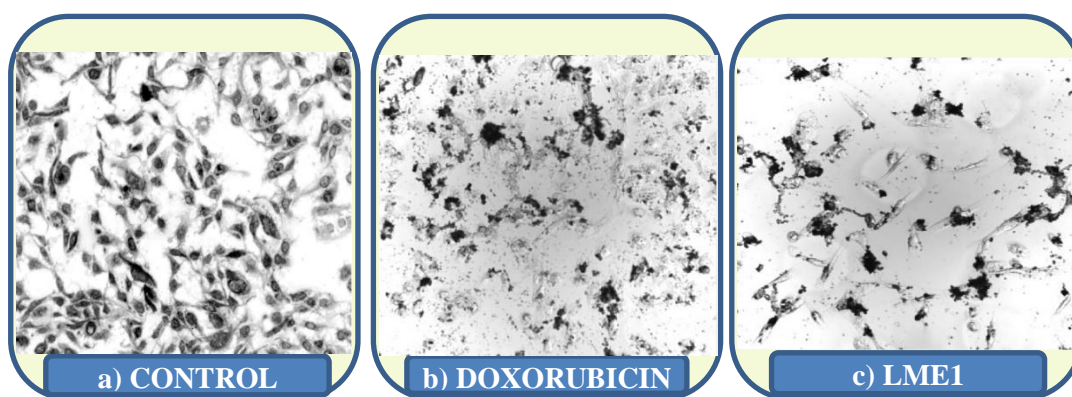


Figure 6.159: Morphological changes of Hop-62 cells treated with EFBF isolate (LME1).

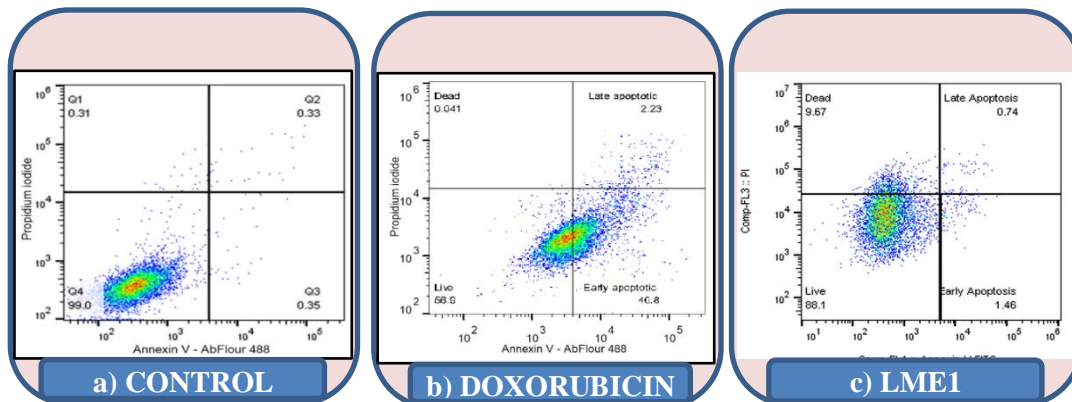


Figure 6.160: Apoptosis analysis of EFBF isolate (LME1) against Hop-62 cell lines.

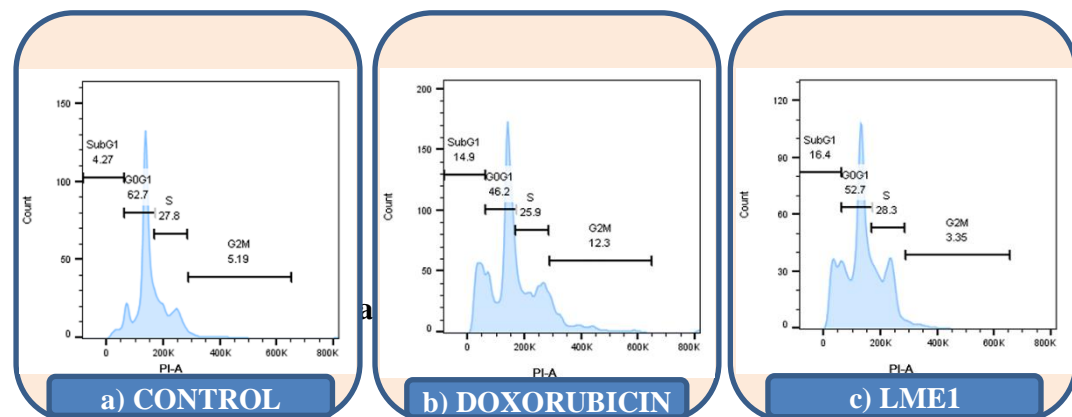
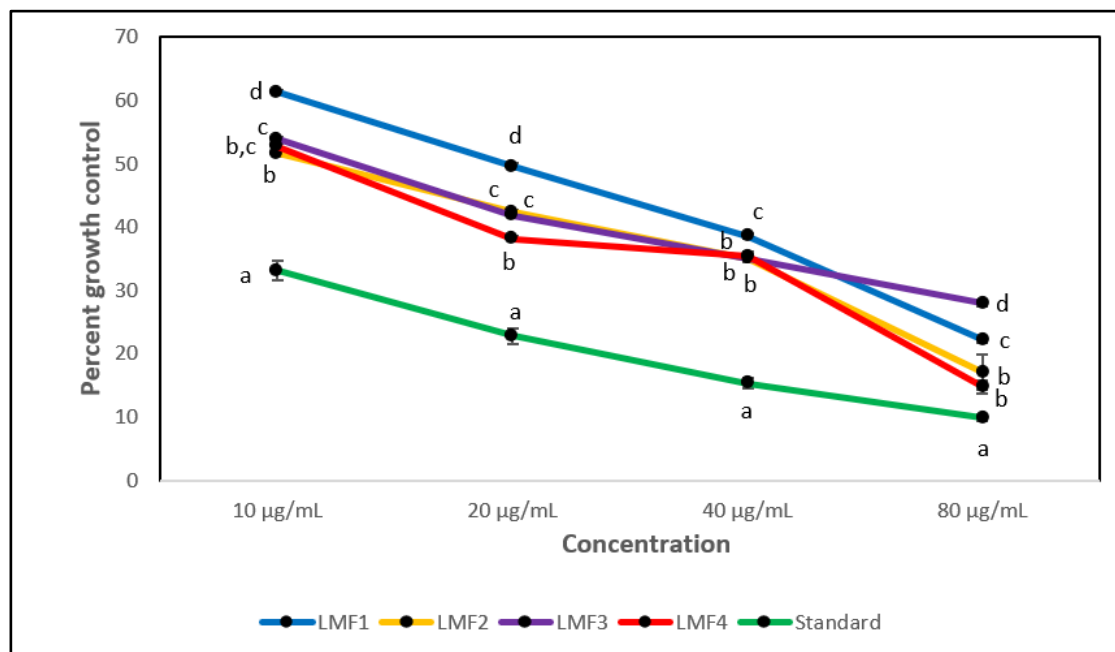


Figure 6.161: Cell cycle analysis of EFBF isolate (LME1) against Hop-62 cell lines.



Each value is represented as the mean \pm SD ($n = 3$). Within each stage, the means with different superscript letters (a - c) are statistically significant (ANOVA, $p < 0.01$, and subsequent post hoc multiple comparisons with Duncan's test).

Figure 6.162: Antiproliferative activity of MFBF isolates against HeLa cell lines.

Table 6.75: Growth control of HeLa cell lines by MFBF isolates.

Experimental sample	GI ₅₀ (µg/mL)
LMF1 (Quercetin)	15.92 \pm 0.32
LMF2 (Kaempferol)	11.41 \pm 0.09
LMF3 (Isorhamnetin)	12.31 \pm 0.10
LMF4 (β -Glucogallin)	10.03 \pm 0.67
Standard (Cisplatin)	1.29 \pm 0.10

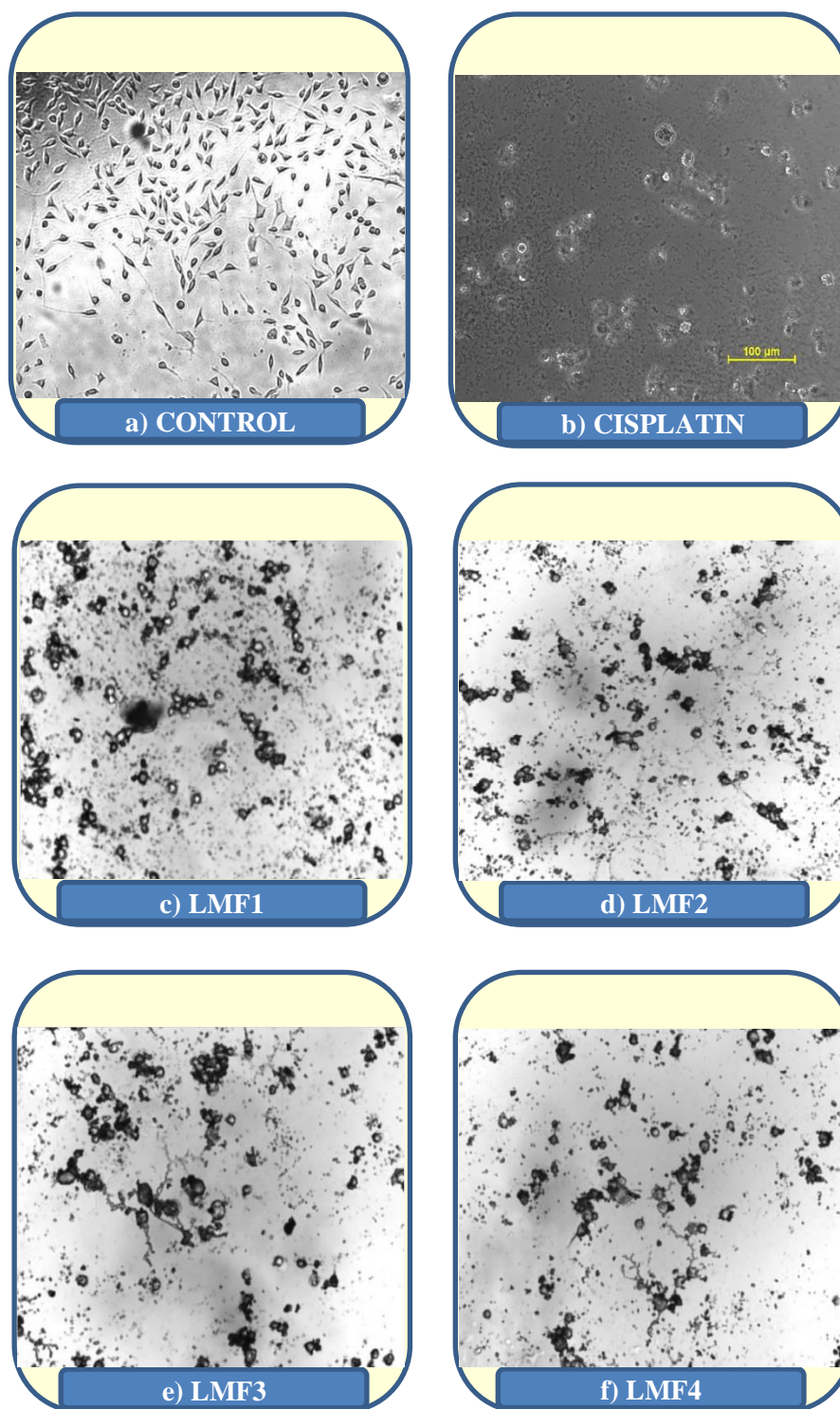
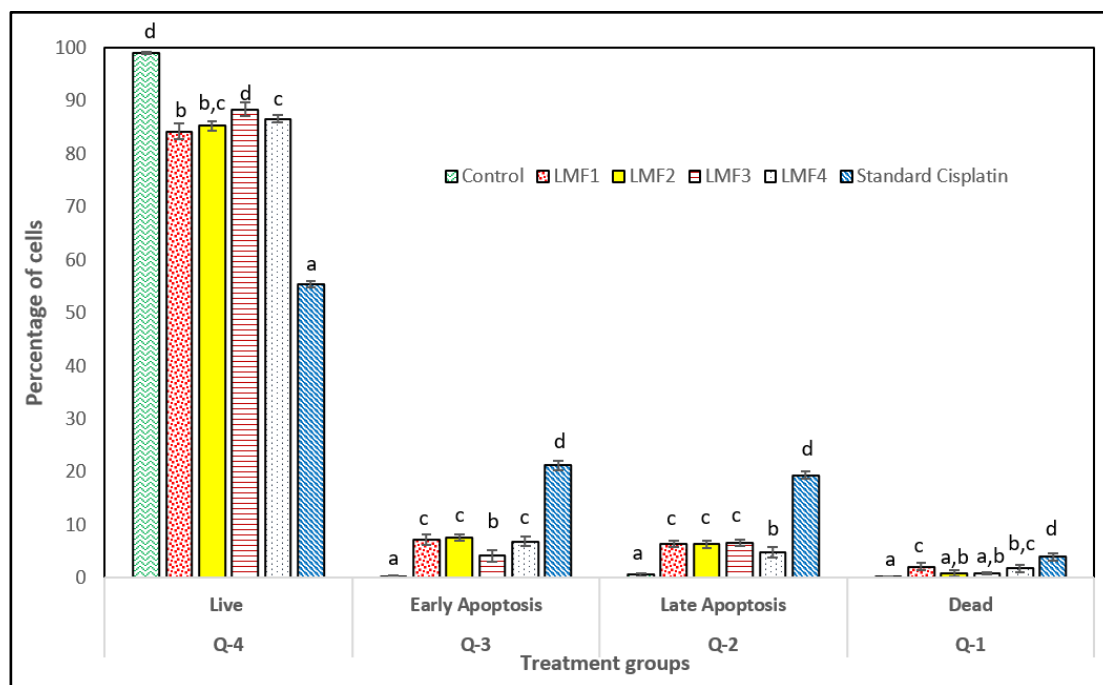


Figure 6.163: Morphological changes of HeLa cells treated with MFBF isolates.



Each value is represented as the mean \pm SD (n = 3). Different superscript letters (a - d) are statistically significant (ANOVA, $p \leq 0.001$, and subsequent post hoc multiple comparisons with Duncan's test).

Figure 6.164: Apoptosis activity of MFBF isolates against HeLa cell lines.

Table 6.76: Apoptosis analysis of MFBF isolated compounds on HeLa cell lines.

Groups	Q-4 Live (%)	Q-3 Early Apoptosis (%)	Q-2 Late Apoptosis (%)	Q-1 Dead (%)
Control	99.06 \pm 0.20 ^d	0.22 \pm 0.20 ^a	0.63 \pm 0.26 ^a	0.16 \pm 0.05 ^a
LMF1 (Quercetin)	84.17 \pm 1.5 ^b	7.28 \pm 1.00 ^c	6.47 \pm 0.59 ^c	2.1 \pm 0.67 ^c
LMF2 (Kaempferol)	85.21 \pm 0.87 ^{b,c}	7.60 \pm 0.66 ^c	6.31 \pm 0.77 ^c	0.91 \pm 0.60 ^{a,b}
LMF3 (Isorhamnetin)	88.35 \pm 1.2 ^d	4.16 \pm 1.07 ^b	6.62 \pm 0.6 ^c	0.86 \pm 0.15 ^{a,b}
LMF4 (Galloyl glucose)	86.54 \pm 0.69 ^c	6.88 \pm 0.86 ^c	4.82 \pm 1.06 ^b	1.76 \pm 0.64 ^{b,c}
Standard (Cisplatin)	55.40 \pm 0.66 ^a	21.23 \pm 0.85 ^d	19.37 \pm 0.76 ^d	3.99 \pm 0.72 ^d

Each value is represented as the mean \pm SD (n = 3). Different superscript letters (a - d) are statistically significant (ANOVA, $p \leq 0.001$, and subsequent post hoc multiple comparisons with Duncan's test).

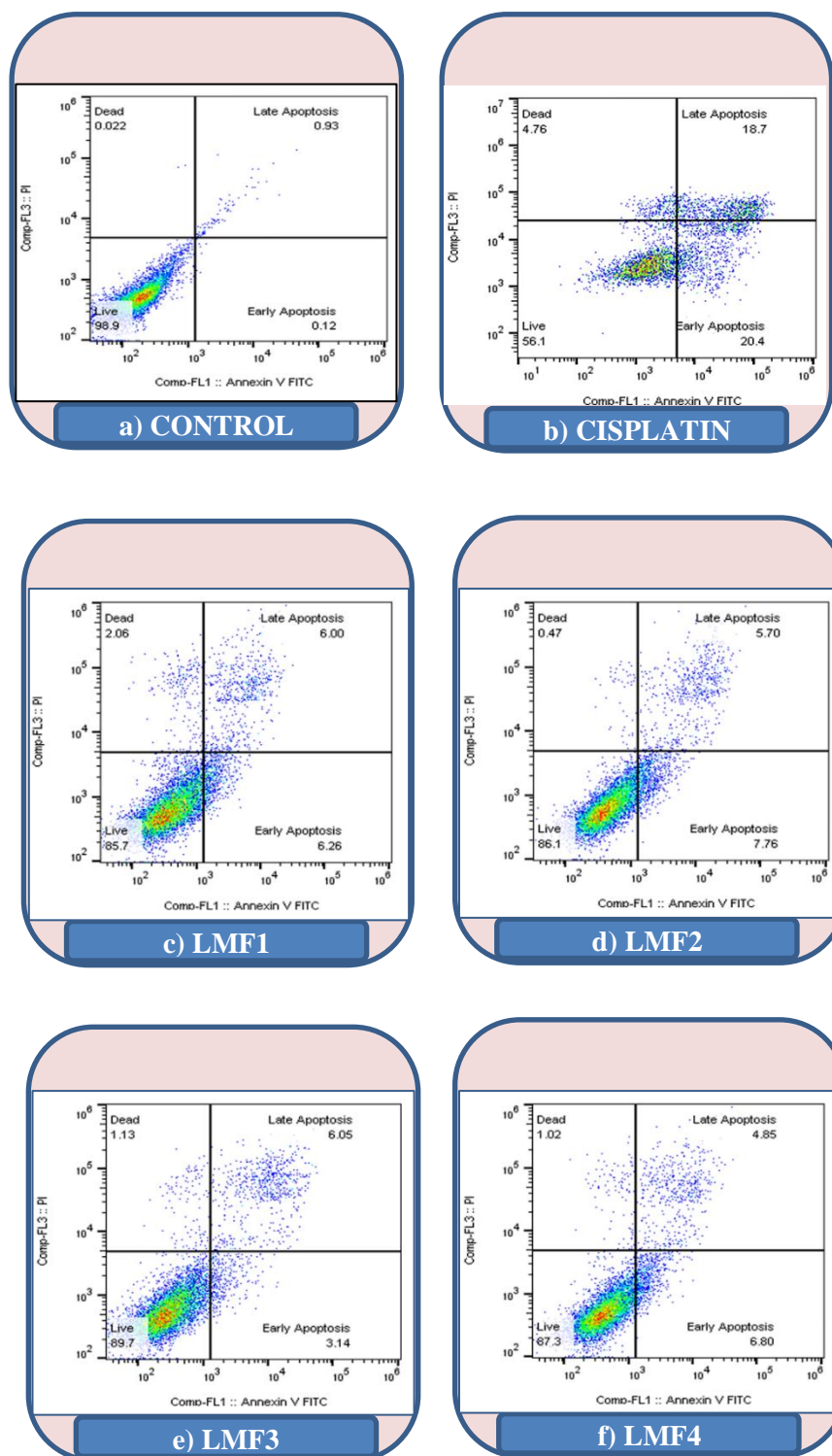
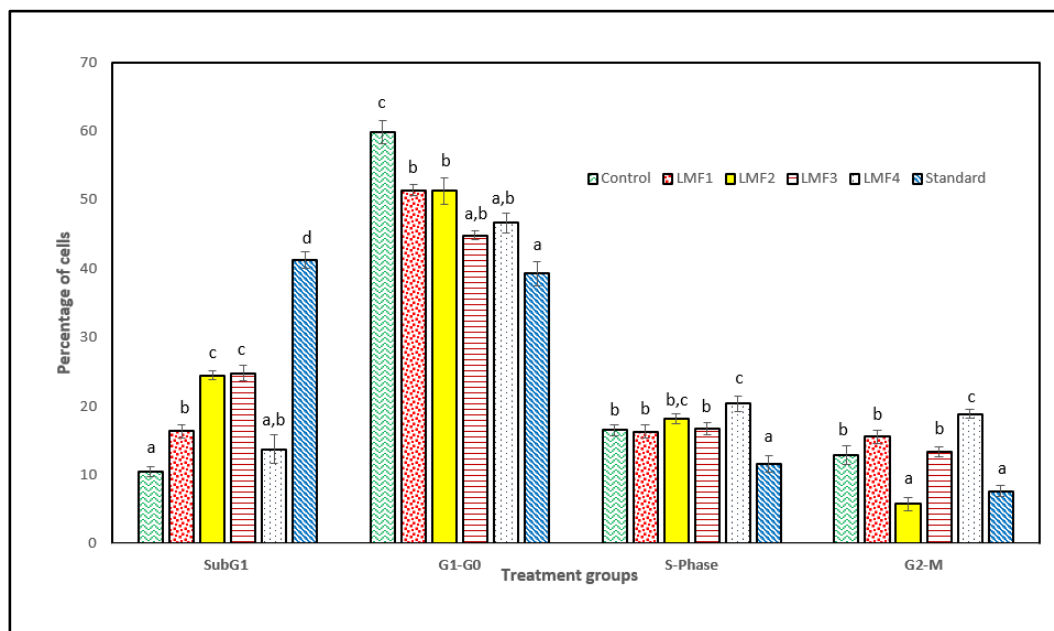


Figure 6.165: Apoptosis analysis of MFBF isolates against HeLa cell lines.



Each value is represented as the mean \pm SD (n = 3). Different superscript letters (a - d) are statistically significant (ANOVA, $p < 0.01$, and subsequent post hoc multiple comparisons with Duncan's test).

Figure 6.166: Cell cycle activity of MFBF isolates against HeLa cell lines.

Table 6.77: Cell cycle analysis of MFBF isolated compounds on HeLa cell lines.

Groups	SubG ₁ (%)	G ₁ -G ₀ (%)	S-Phase (%)	G ₂ -M (%)
Control	10.45 \pm 0.74 ^a	59.84 \pm 1.74 ^c	16.54 \pm 0.80 ^b	12.94 \pm 1.36 ^b
LMF1 (Quercetin)	16.33 \pm 1.01 ^b	51.4 \pm 0.83 ^b	16.31 \pm 0.94 ^b	15.53 \pm 0.98 ^b
LMF2 (Kaempferol)	24.48 \pm 0.64 ^c	51.32 \pm 1.93 ^b	18.20 \pm 0.75 ^{b,c}	5.81 \pm 0.98 ^a
LMF3 (Isorhamnetin)	24.79 \pm 1.07 ^c	44.83 \pm 0.70 ^{a,b}	16.73 \pm 0.88 ^b	13.42 \pm 0.71 ^b
LMF4 (Galloyl glucose)	13.70 \pm 2.08 ^{a,b}	46.62 \pm 1.4 ^{a,b}	20.34 \pm 1.14 ^c	18.88 \pm 0.65 ^c
Standard (Cisplatin)	41.25 \pm 1.25 ^d	40.57 \pm 3.04 ^a	11.64 \pm 1.18 ^a	7.65 \pm 0.74 ^a

Each value is represented as the mean \pm SD (n = 3). Different superscript letters (a - d) are statistically significant (ANOVA, $p < 0.01$, and subsequent post hoc multiple comparisons with Duncan's test).

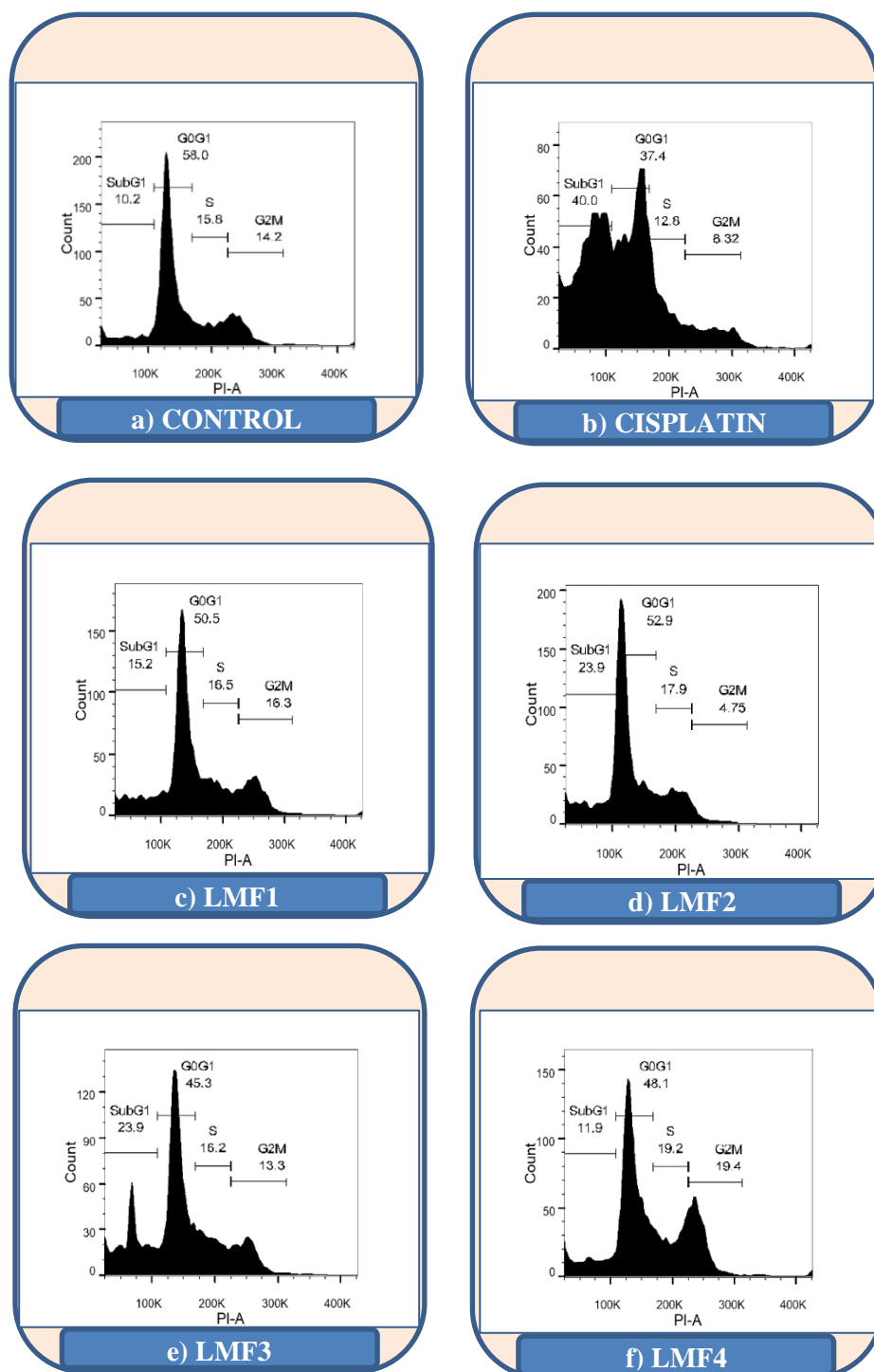
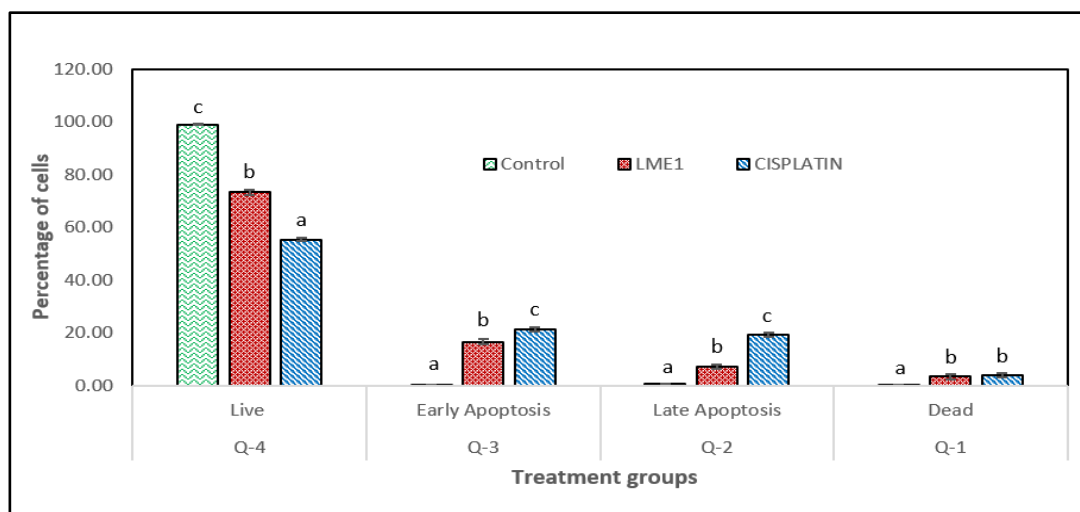


Figure 6.167: Cell cycle analysis of MFBF isolates against HeLa cell lines.

Table 6.78: Growth control of HeLa cell lines by EFBF isolate (LME1).

Experimental sample	GI ₅₀ (µg/mL)
LME1	16.69 ± 0.39
Standard (Cisplatin)	1.29 ± 0.10

(Each value is stated as mean ± SD, n = 3, p < 0.01)

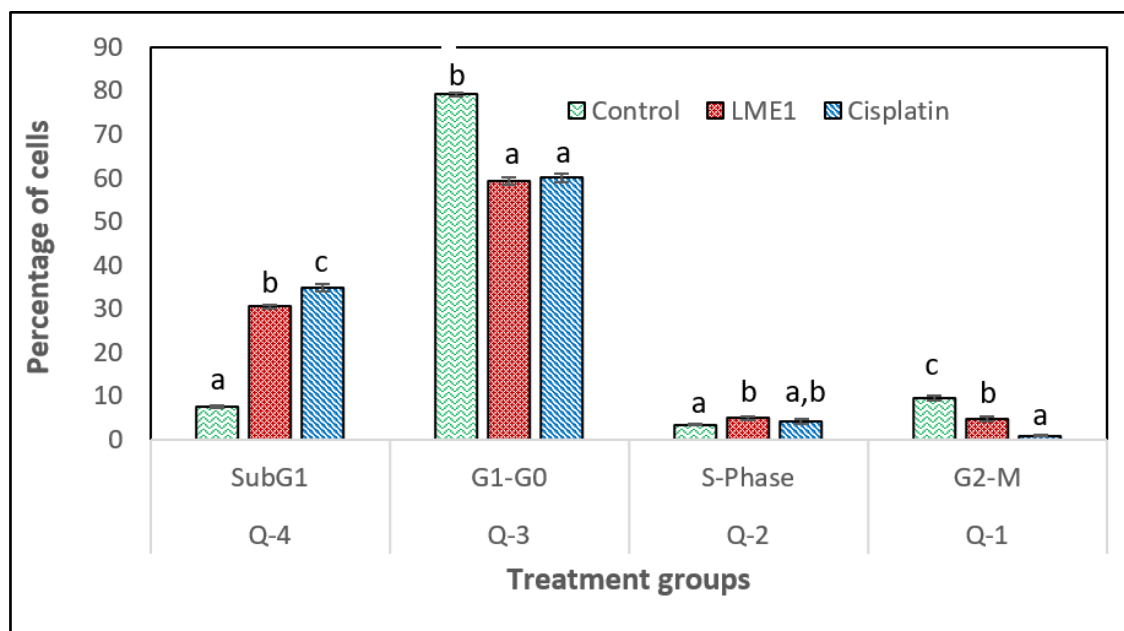


Each value is represented as the mean ± SD (n = 3). Different superscript letters (a - c) are statistically significant (ANOVA, p < 0.001, and subsequent post hoc multiple comparisons with Duncan's test).

Figure 6.168: Apoptosis activity of EFBF isolate (LME1) against HeLa cell lines.**Table 6.79: Apoptosis analysis of EFBF isolate (LME1) against HeLa cell lines.**

Groups	Q-4 Live (%)	Q-3 Early Apoptosis (%)	Q-2 Late Apoptosis (%)	Q-1 Dead (%)
Control	99.06 ± 0.20 ^c	0.22 ± 0.20 ^a	0.63 ± 0.26 ^a	0.16 ± 0.05 ^a
LME1	73.31 ± 0.91 ^b	16.53 ± 1.00 ^b	7.22 ± 0.86 ^b	3.40 ± 1.01 ^b
Standard (Cisplatin)	55.40 ± 0.66 ^a	21.23 ± 0.85 ^c	19.37 ± 0.76 ^c	3.99 ± 0.72 ^b

Each value is represented as the mean ± SD (n = 3). Different superscript letters (a - c) are statistically significant (ANOVA, p < 0.001, and subsequent post hoc multiple comparisons with Duncan's test).



Each value is represented as the mean \pm SD (n = 3). Different superscript letters (a - c) are statistically significant (ANOVA, $p < 0.001$, and subsequent post hoc multiple comparisons with Duncan's test).

Figure 6.169: Cell cycle activity of EFBF isolate (LME1) against HeLa cell lines.

Table 6.80: Cell cycle analysis of EFBF isolate (LME1) against HeLa cell lines.

Groups	SubG ₁ (%)	G ₁ -G ₀ (%)	S-Phase (%)	G ₂ -M (%)
Control	7.51 \pm 0.32 ^a	79.17 \pm 0.40 ^b	3.43 \pm 0.19 ^a	9.56 \pm 0.66 ^c
LME1	30.50 \pm 0.46 ^b	59.26 \pm 0.79 ^a	4.90 \pm 0.55 ^b	4.68 \pm 0.59 ^b
Standard (Cisplatin)	34.81 \pm 0.79 ^c	60.00 \pm 1.02 ^a	4.13 \pm 0.51 ^{a,b}	0.86 \pm 0.13 ^a

Each value is represented as the mean \pm SD (n = 3). Different superscript letters (a - c) are statistically significant (ANOVA, $p < 0.001$, and subsequent post hoc multiple comparisons with Duncan's test).

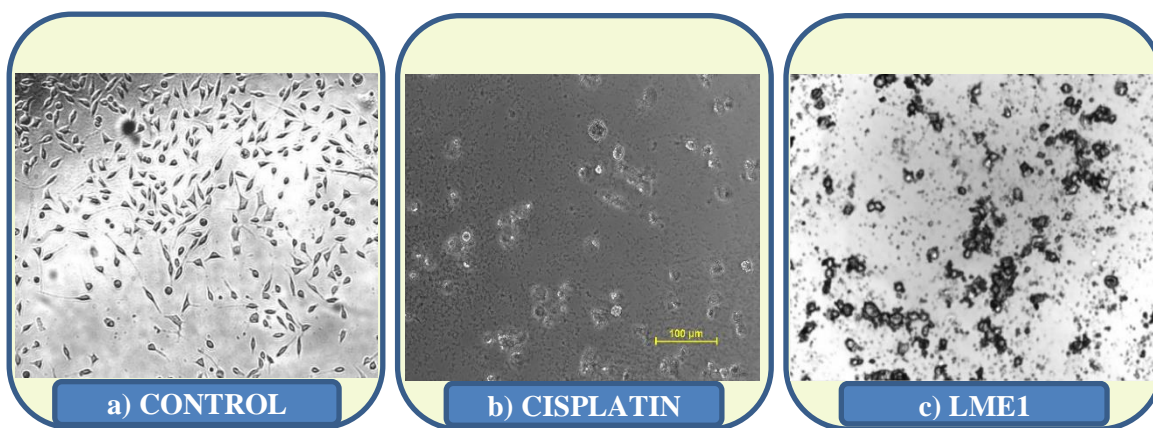


Figure 6.170: Morphological changes of HeLa cells treated with EFBF isolate (LME1).

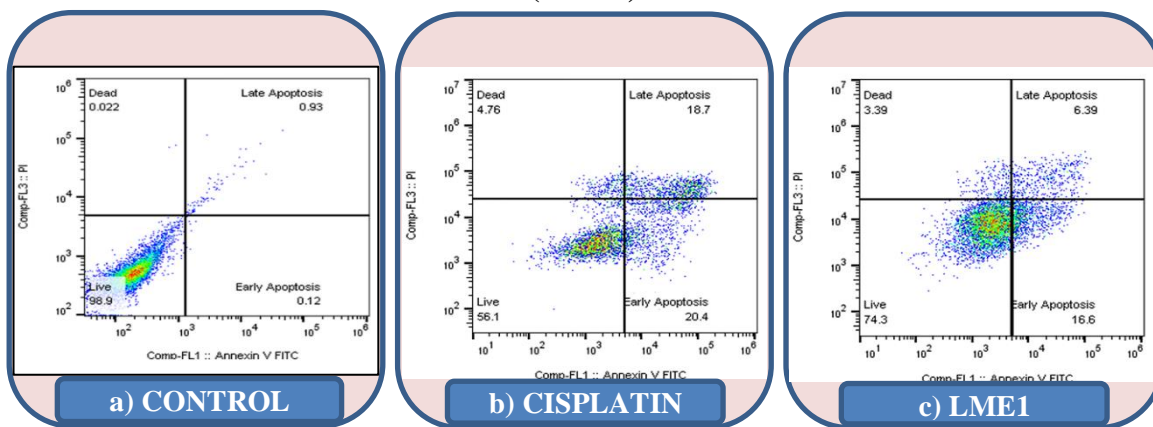


Figure 6.171: Apoptosis analysis of EFBF isolate (LME1) against HeLa cell lines.

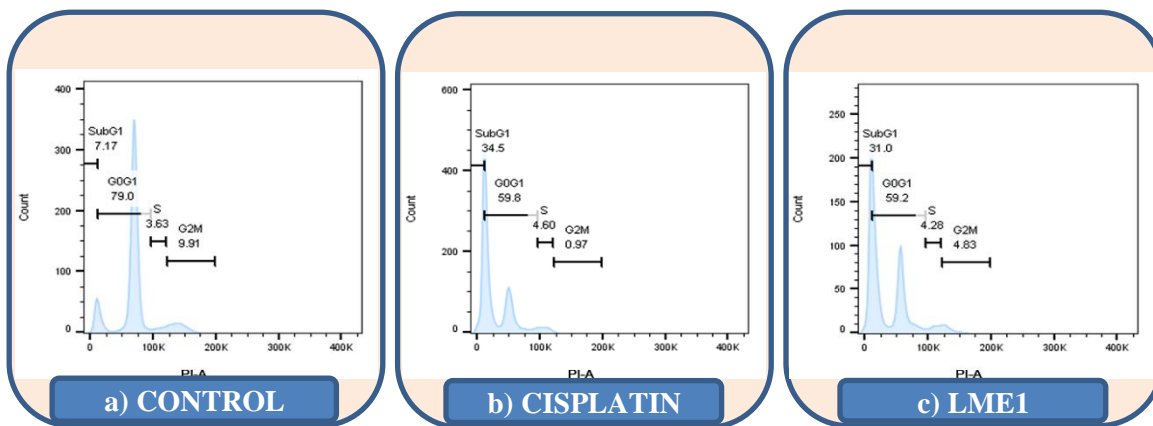
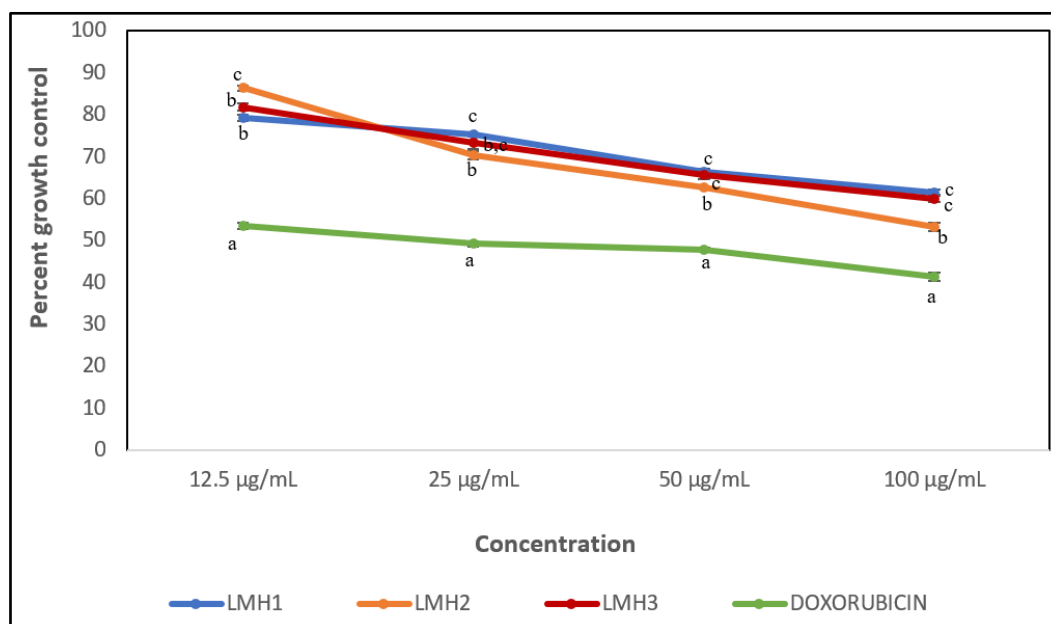


Figure 6.172: Cell cycle analysis of EFBF isolate (LME1) against HeLa cell lines.



Each value is represented as the mean \pm SD (n = 3). Within each stage, the means with different superscript letters (a - c) are statistically significant (ANOVA, $p < 0.01$, and subsequent post hoc multiple comparisons with Duncan's test).

Figure 6.173: Antiproliferative activity of ITHE isolates against normal cell lines.

Table 6.81: Growth control of normal cell lines by ITHE isolates.

Experimental sample	GI ₅₀ (µg/mL)
LMH1 (Quercetrin)	102.43 \pm 0.50
LMH2 (Rutin)	98.32 \pm 2.58
LMH3 (Hesperidin)	100.78 \pm 1.05
Standard (Doxorubicin)	19.42 \pm 0.30

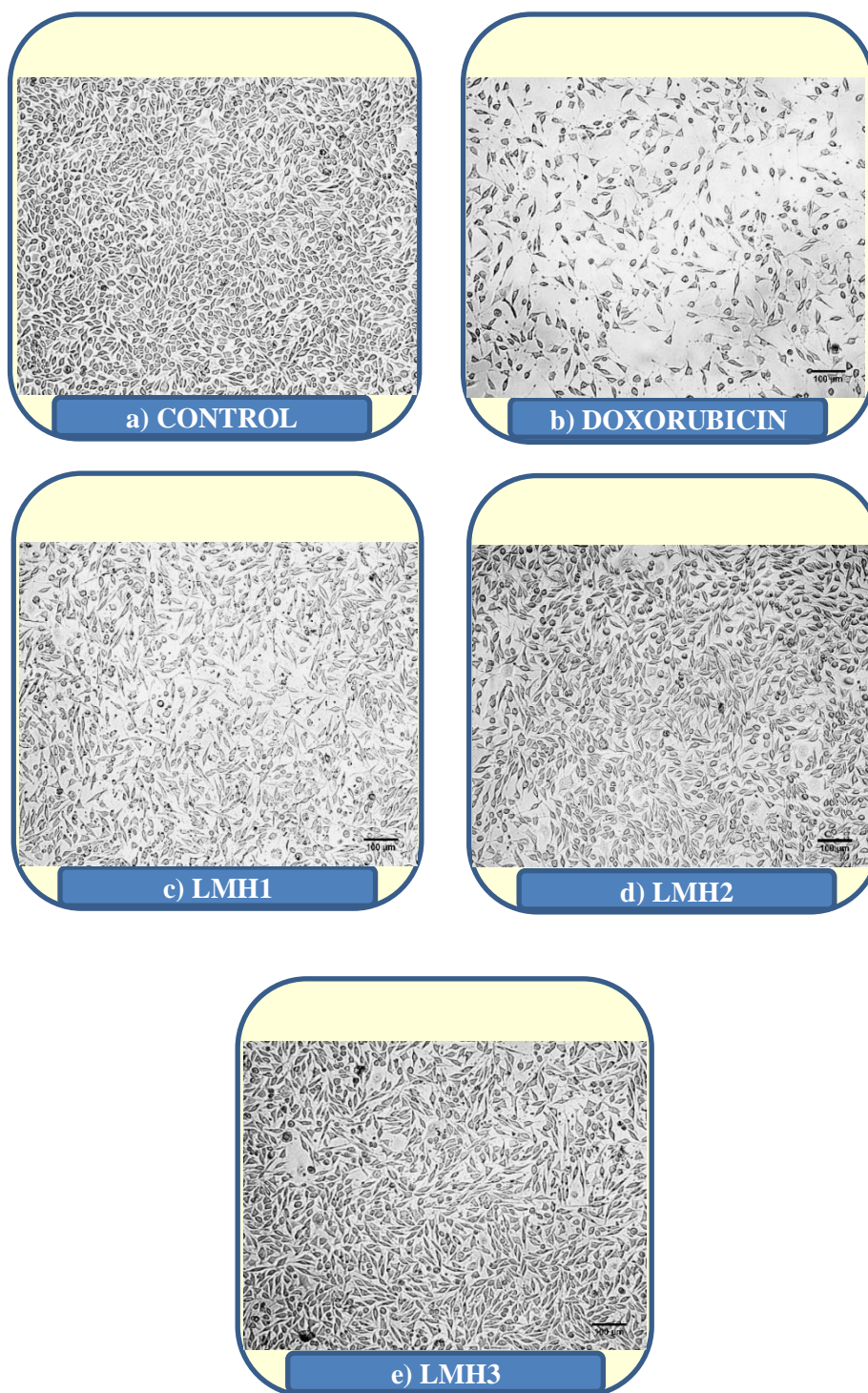
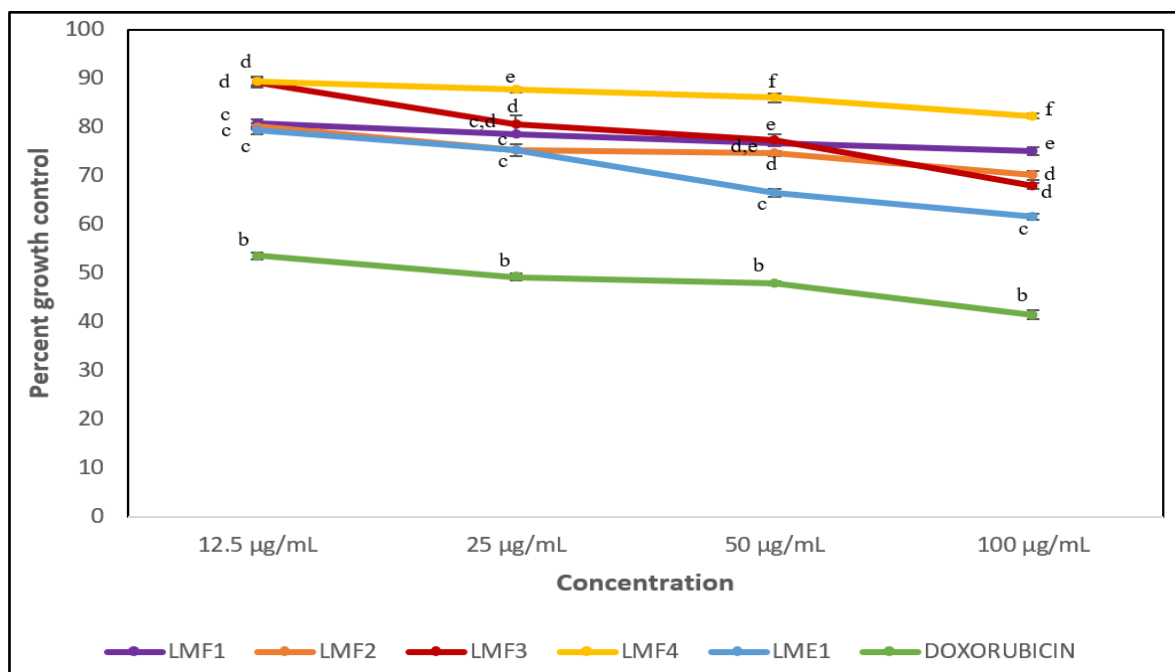


Figure 6.174: Morphological changes of normal cells treated with ITHE isolates.



Each value is represented as the mean \pm SD (n = 3). Within each stage, the means with different superscript letters are statistically significant (ANOVA, $p < 0.01$, and subsequent post hoc multiple comparisons with Duncan's test).

Figure 6.175: Antiproliferative activity of MFBF and EFBF isolates against normal cell lines.

Table 6.82: Growth control of normal cell lines by MFBF and EFBF isolates.

Experimental sample	GI ₅₀ (µg/mL)
LMF1 (Quercetin)	173.57 \pm 2.65
LMF2 (Kaempferol)	145.83 \pm 1.85
LMF3 (Isorhamnetin)	174.47 \pm 4.20
LMF4 (β -Glucogallin)	344.7 \pm 12.55
LME1 (Gardenin B)	142.43 \pm 0.50
Standard (Doxorubicin)	19.42 \pm 0.30

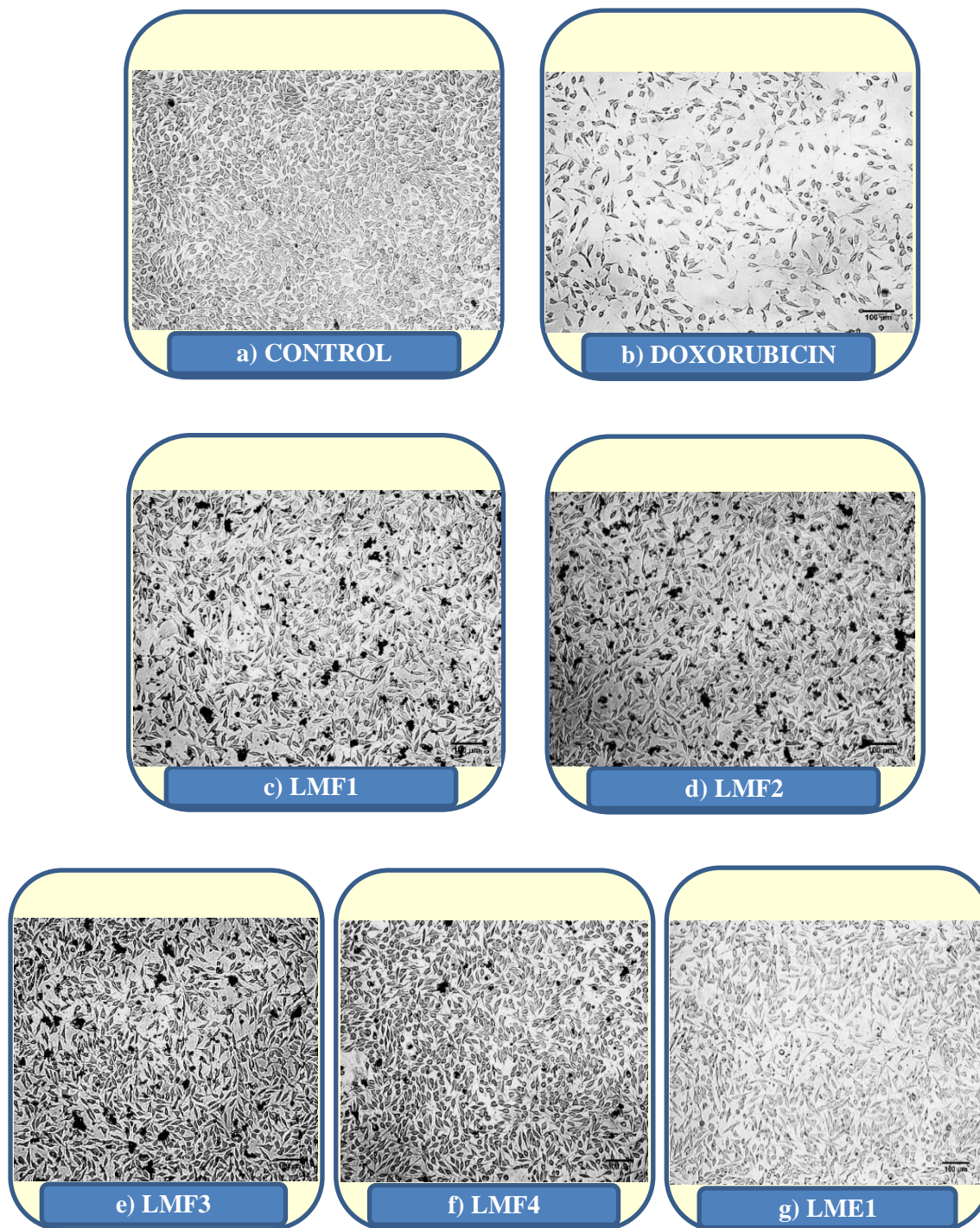
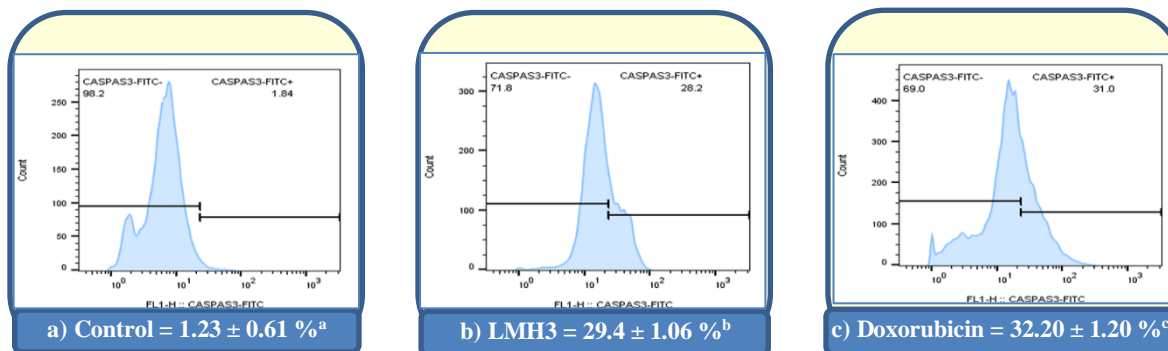
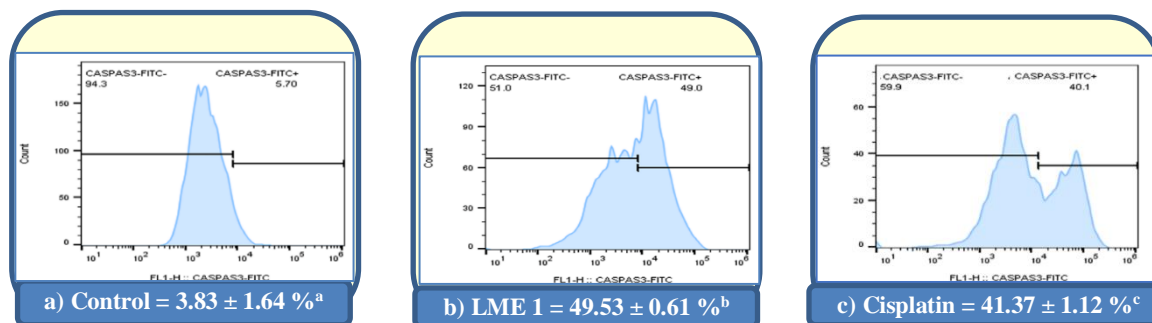


Figure 6.176: Morphological changes of normal cells treated with MFBF and EFBF isolates.

6.2.11.4. *In vitro* Caspase-3 activity

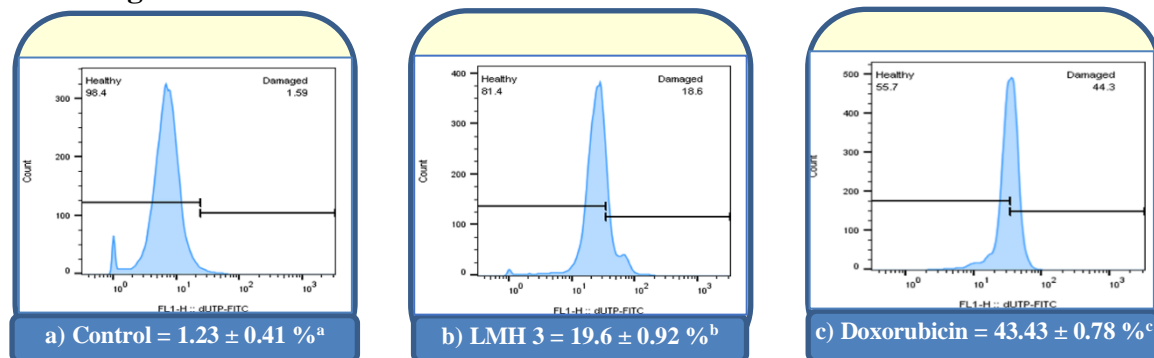
Each value is represented as the mean \pm SD (n = 3). Within each stage, the means with different superscript letters (a - c) are statistically significant (ANOVA, $p < 0.01$, and subsequent post hoc multiple comparisons with Duncan's test).

Figure 6.177: *In vitro* Caspase-3 activity of LMH-3 (Hesperidin) on MCF-7 cell lines.



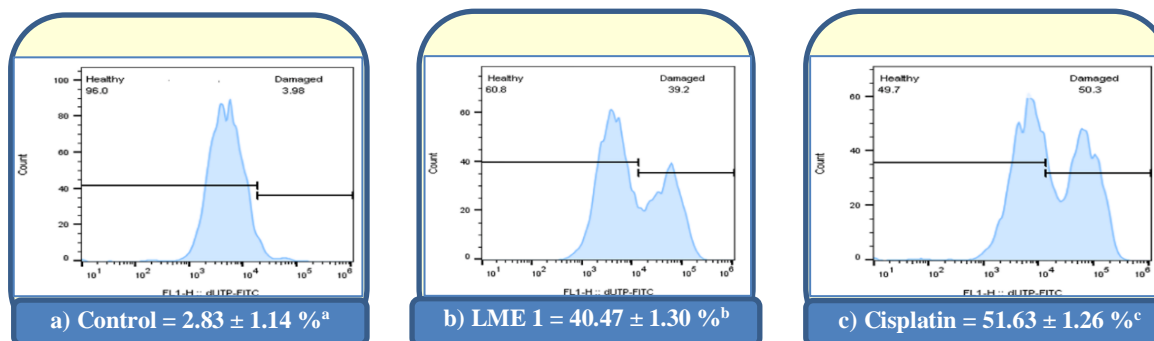
Each value is represented as the mean \pm SD (n = 3). Within each stage, the means with different superscript letters (a - c) are statistically significant (ANOVA, $p < 0.01$, and subsequent post hoc multiple comparisons with Duncan's test).

Figure 6.178: *In vitro* Caspase-3 activity of LME-1 (Gardenin B) on HeLa cell lines.

6.2.11.5. *In vitro* DNA fragmentation

Each value is represented as the mean \pm SD (n = 3). Within each stage, the means with different superscript letters (a - c) are statistically significant (ANOVA, $p < 0.01$, and subsequent post hoc multiple comparisons with Duncan's test).

Figure 6.179: *In vitro* DNA fragmentation of LMH-3 (Hesperidin) on MCF-7 cell lines.



Each value is represented as the mean \pm SD (n = 3). Within each stage, the means with different superscript letters (a - c) are statistically significant (ANOVA, $p < 0.01$, and subsequent post hoc multiple comparisons with Duncan's test).

Figure 6.180: *In vitro* DNA fragmentation of (Gardenin B) on HeLa cell lines.

6.2.11.6. GENE EXPRESSION

Table 6.83: Gene expression analysis using Real Time PCR.

Samples	Fold change in the gene expression		
	Bcl-2	P53	Bax
Control	1.00 ± 0.13 ^d	1.03 ± 0.38 ^a	1.00 ± 0.13 ^a
Cisplatin 1 µg	1.09 ± 0.14 ^d	0.89 ± 0.07 ^a	1.41 ± 0.19 ^a
Cisplatin 2 µg	0.83 ± 0.09 ^c	2.46 ± 0.18 ^a	1.51 ± 0.03 ^b
Cisplatin 3 µg	0.65 ± 0.13 ^b	6.65 ± 1.45 ^b	1.73 ± 0.03 ^b
LME1 8 µg	0.86 ± 0.33 ^c	8.65 ± 0.76 ^b	1.34 ± 0.09 ^a
LME1 16 µg	0.83 ± 0.12 ^c	9.66 ± 1.27 ^b	2.70 ± 0.32 ^c
LME1 24 µg	0.38 ± 0.01 ^a	13.99 ± 2.99 ^c	2.90 ± 0.34 ^c

(Each value is stated as mean ± SD, n = 3, $p < 0.01$)

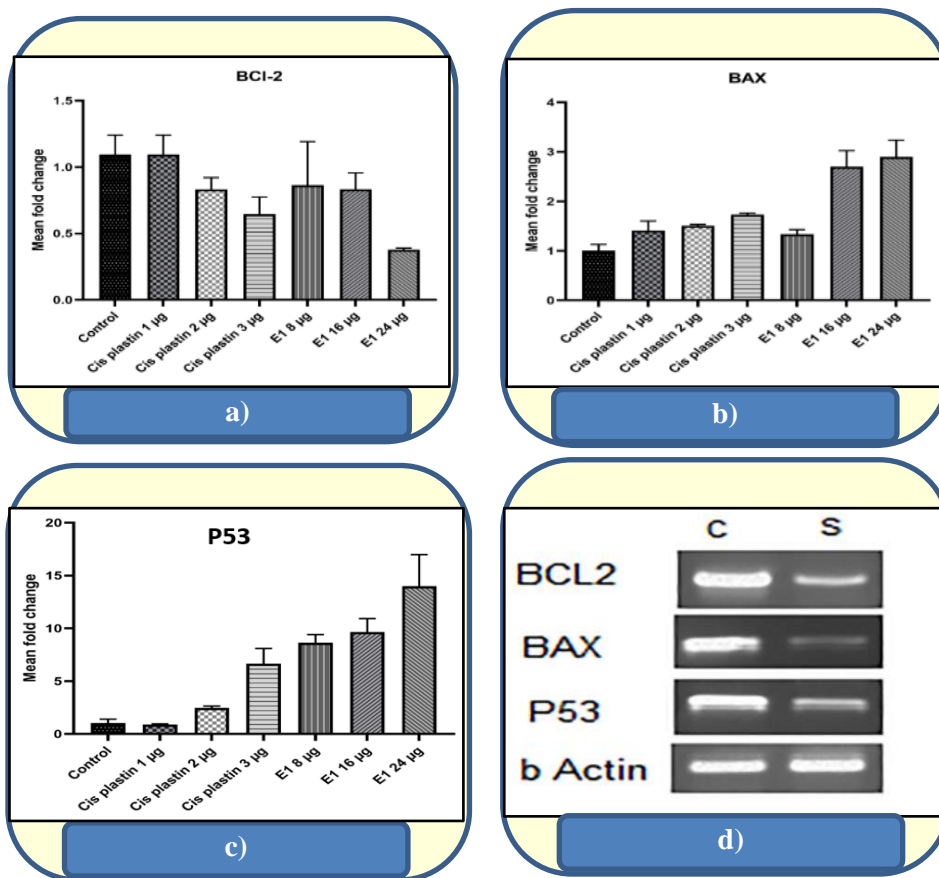
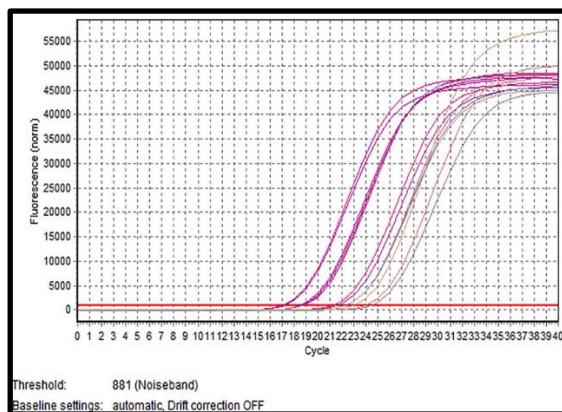
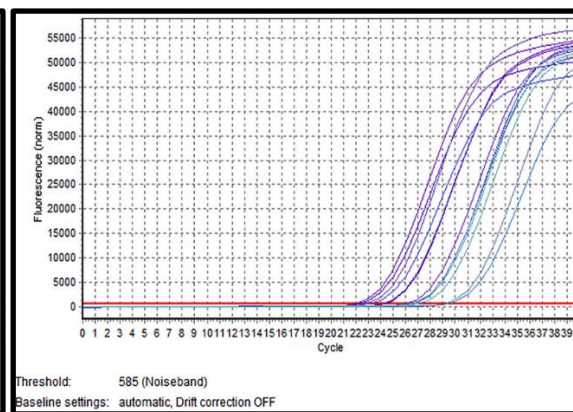


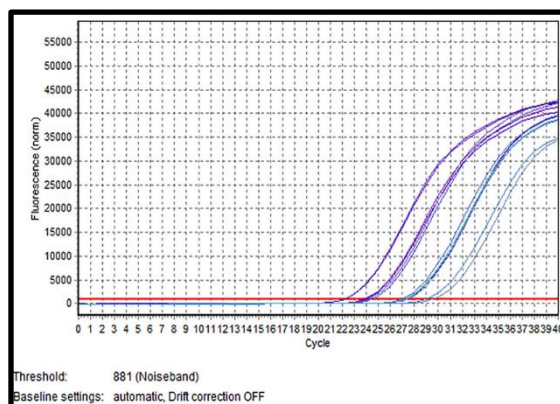
Figure 6.181: Effect of LME-1 on Bcl-2, p53, Bax gene expression in HeLa cells.



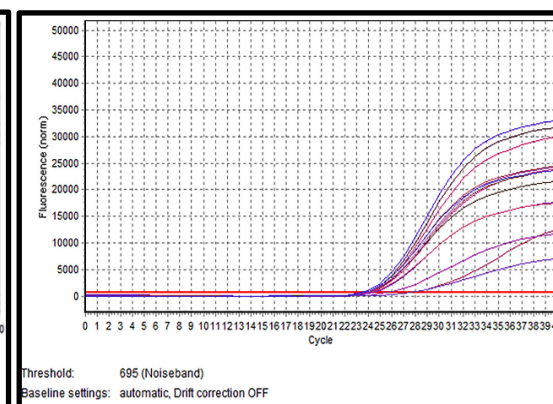
a) β -actin



b) Bax



c) Bcl-2



d) p53

Figure 6.182: Amplification plots of the genes expressed.

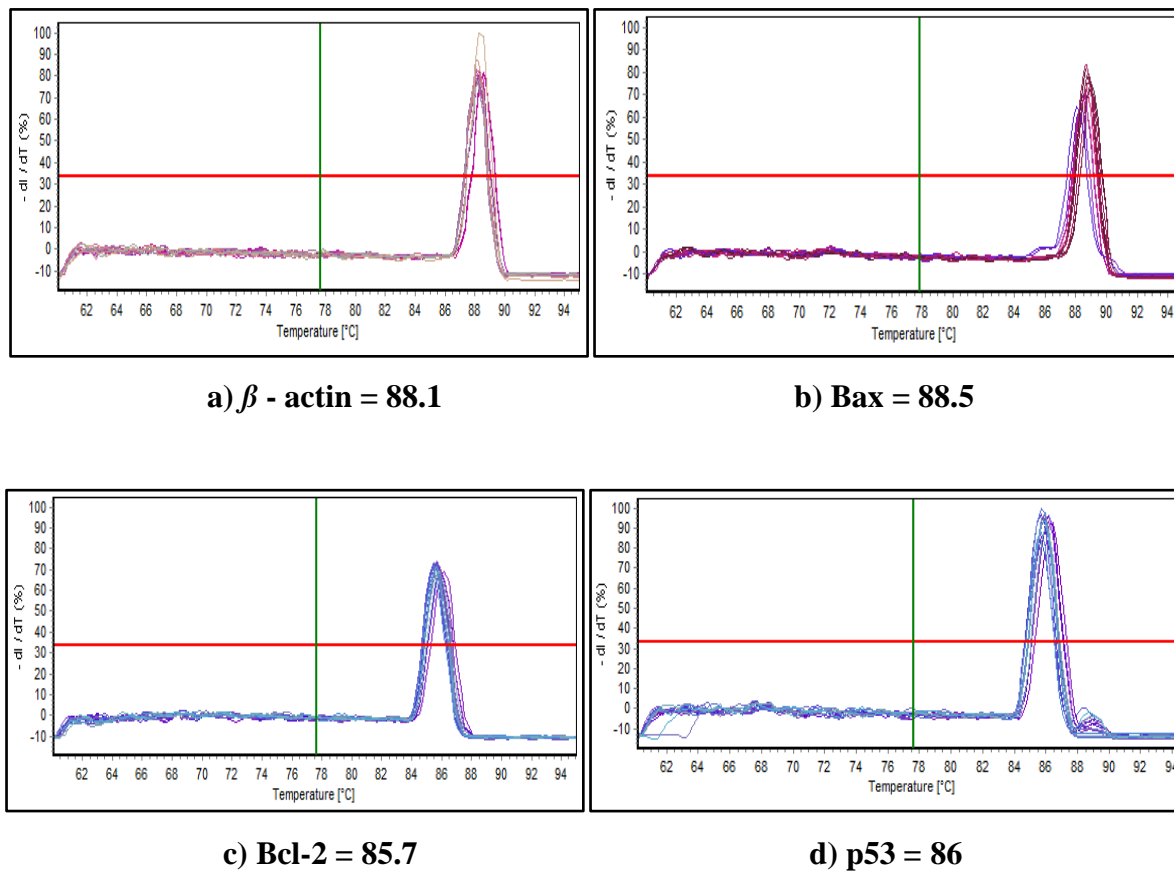


Figure 6.183: Melting temperatures of the reference and target genes.

6.2.12. *In silico* molecular docking studies

6.2.12.1. *In silico* molecular docking of isolated compounds with the active site of the Caspase-3 enzyme (PDB ID: 1QX3).

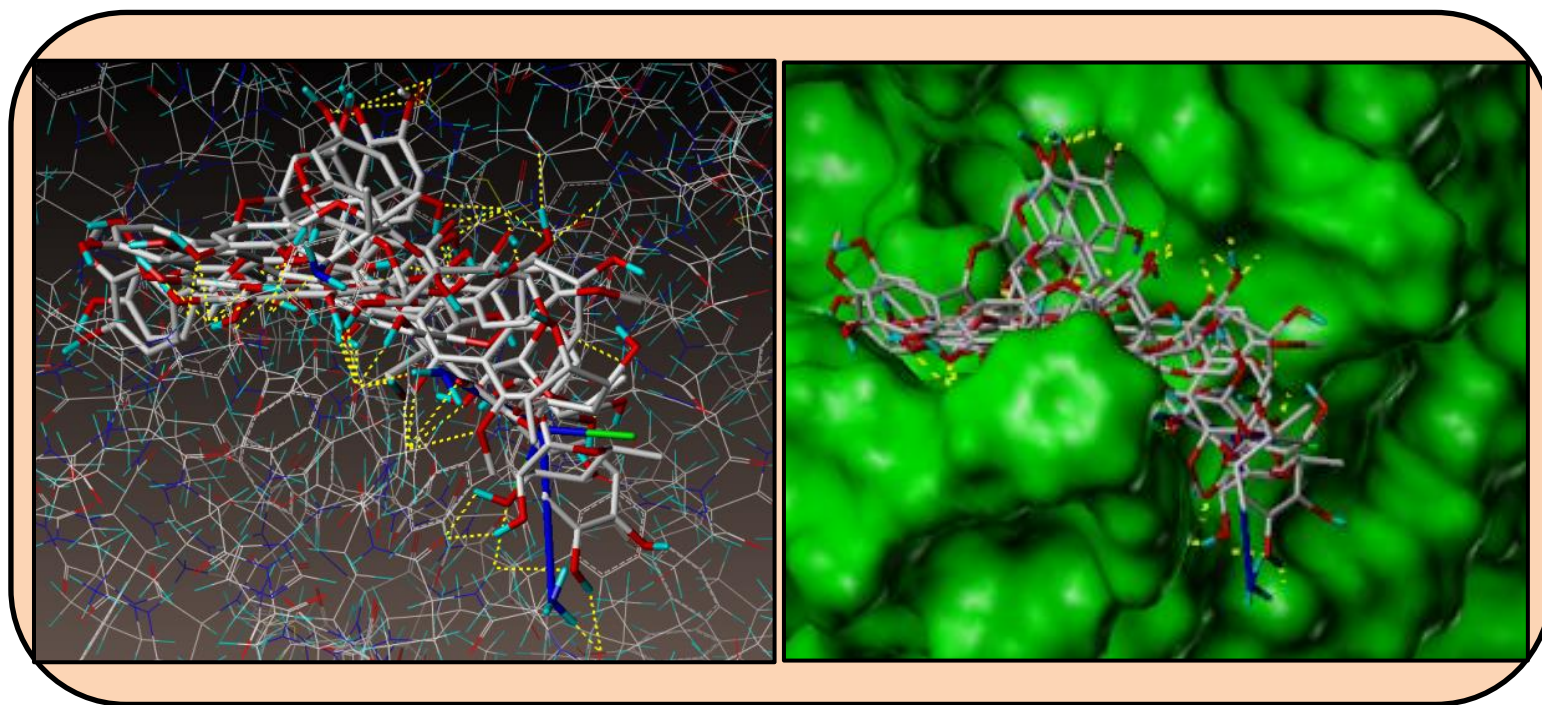


Figure 6.184: Docked view of all the compounds at the active site of the enzyme PDB ID: 1QX3.

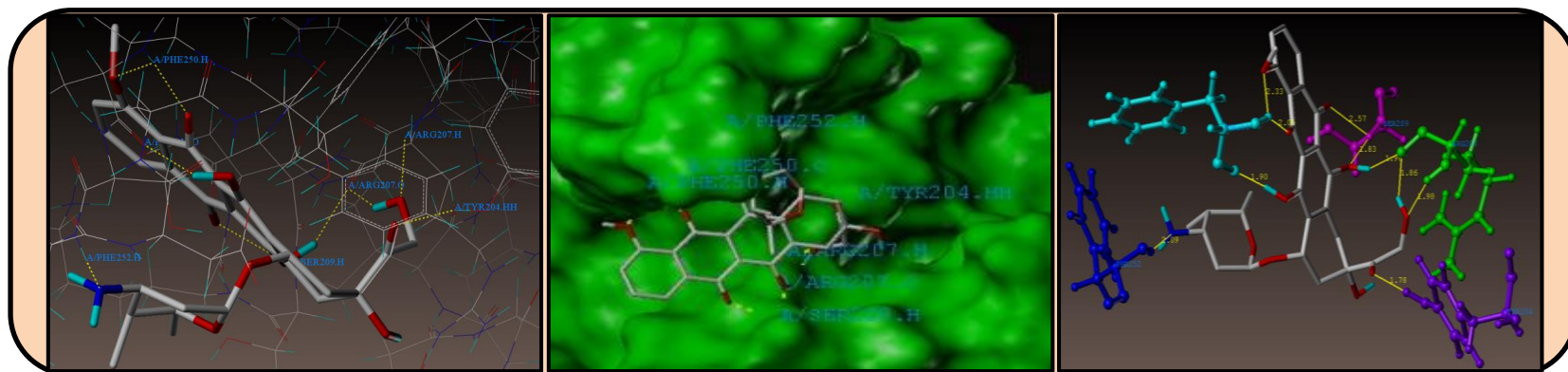


Figure 6.185: Interaction of Doxorubicin at the binding site of the enzyme (PDB ID: 1QX3).

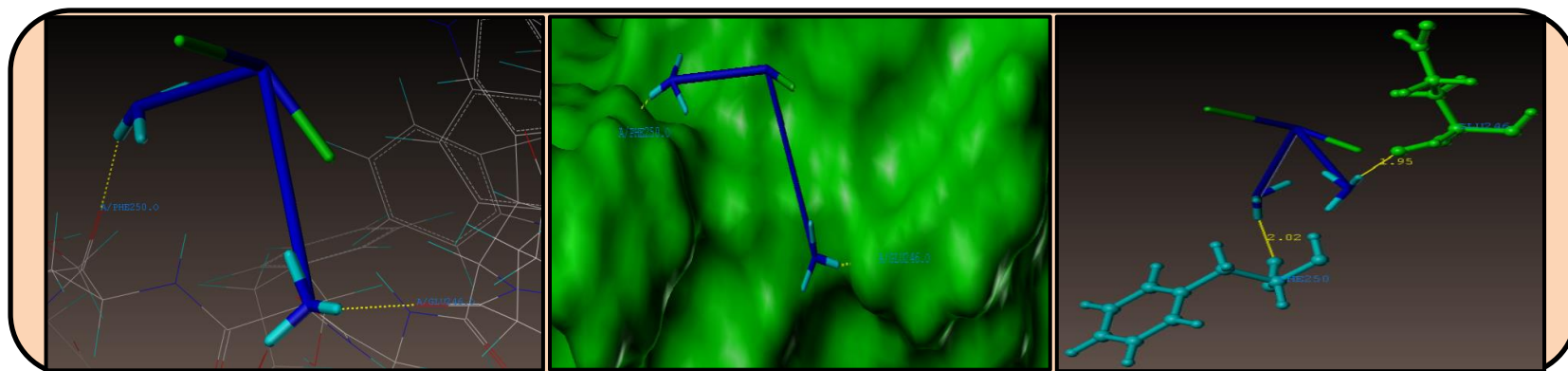
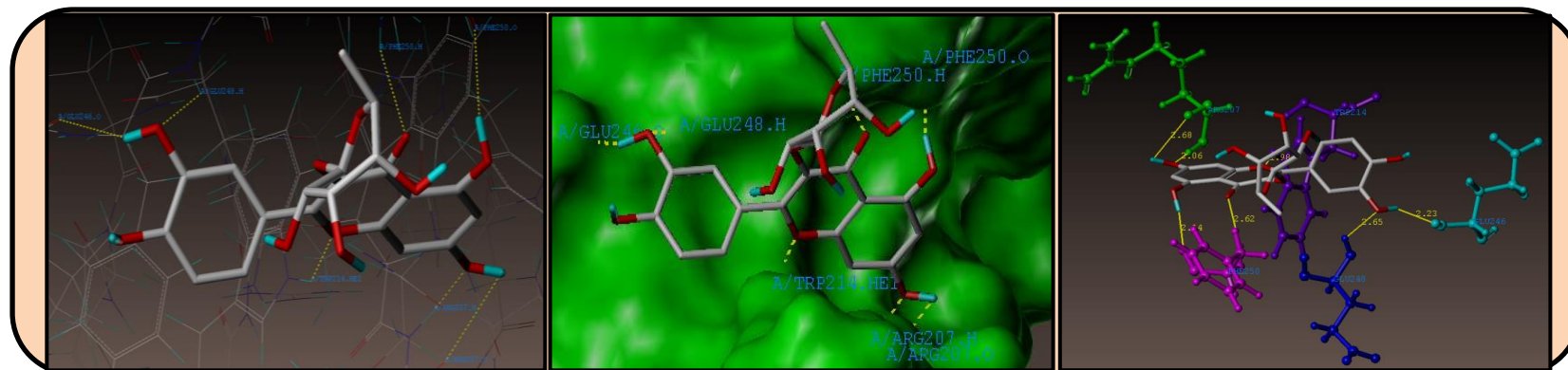


Figure 6.186: Interaction of Cisplatin at the binding site of the enzyme (PDB ID: 1QX3).



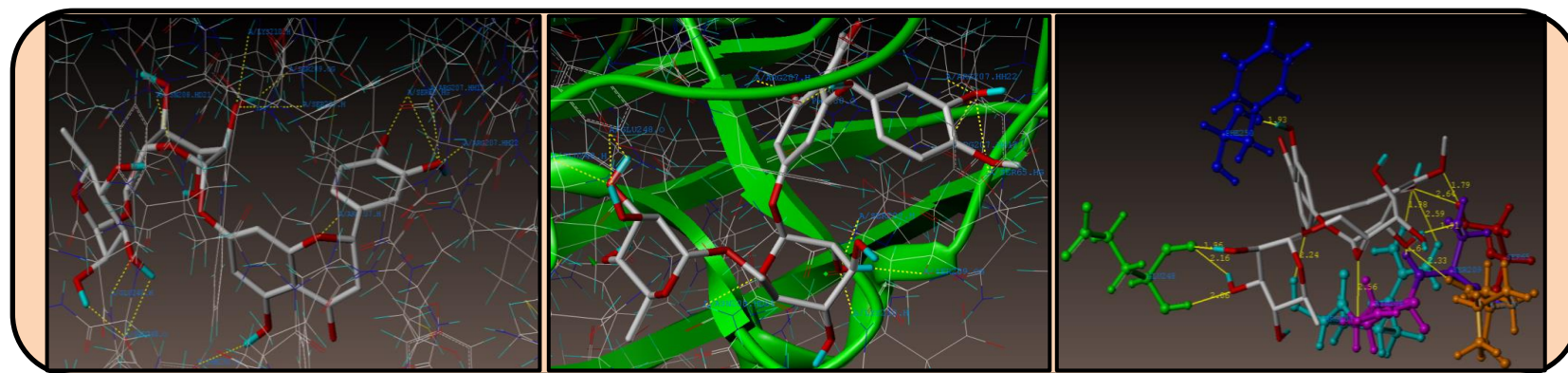
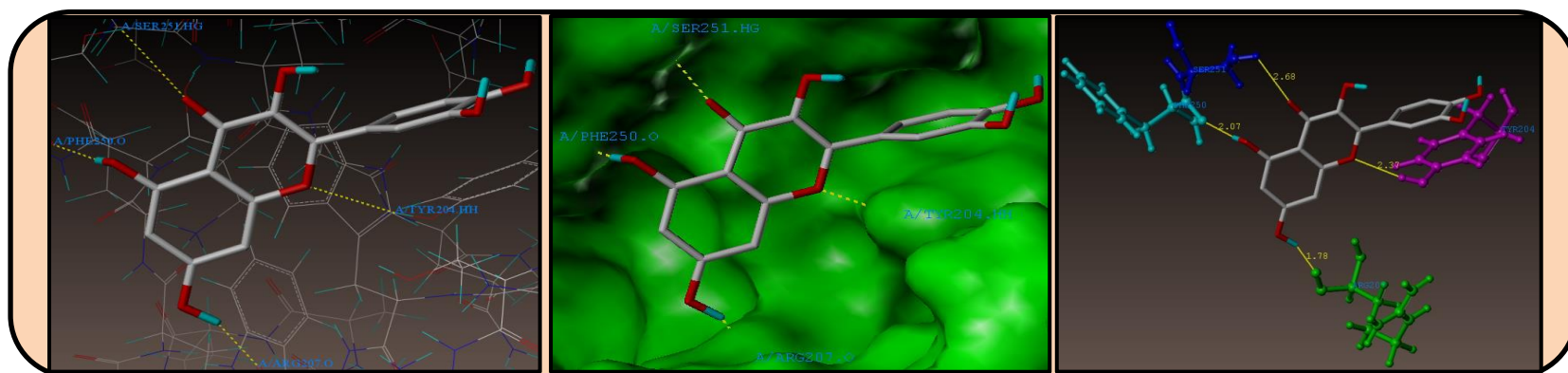


Figure 6.189: Interaction of LMH3 (Hesperidin) at the binding site of the enzyme (PDB ID: 1QX3).



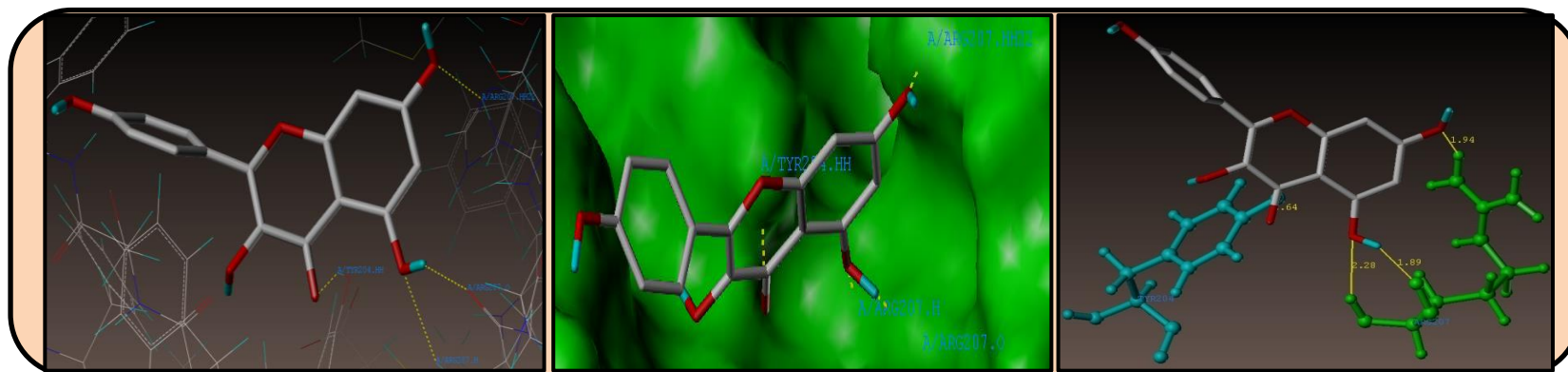


Figure 6.191: Interaction of LMF2 (Kaempferol) at the binding site of the enzyme (PDB ID: 1QX3).

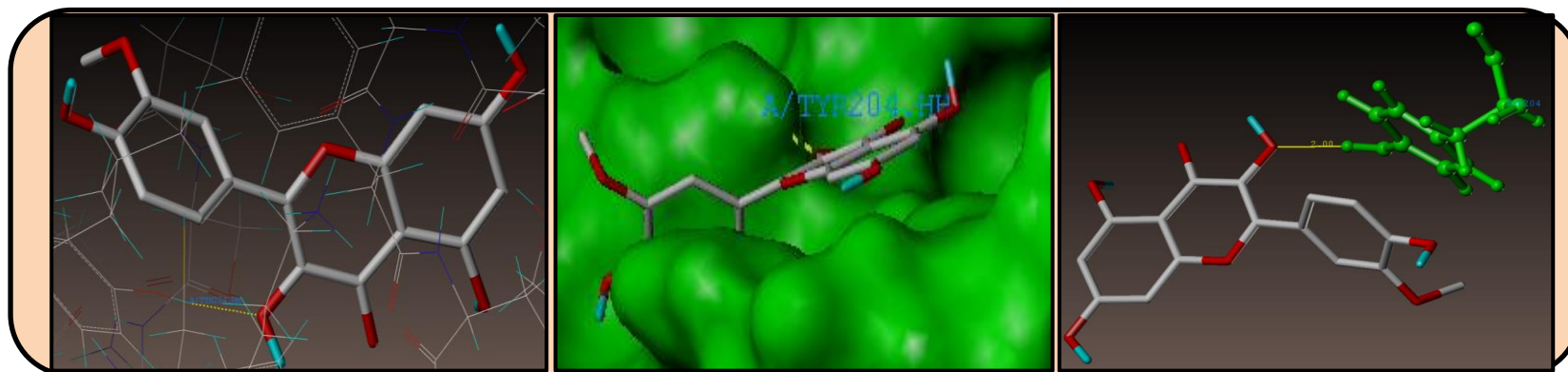


Figure 6.192: Interaction of LMF3 (Isorhamnetin) at the binding site of the enzyme (PDB ID: 1QX3).

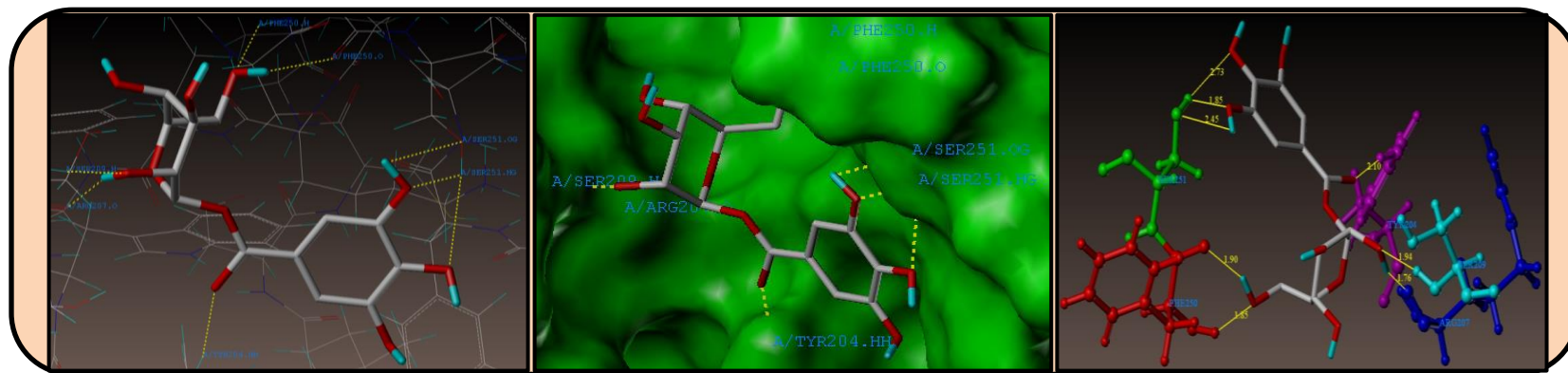


Figure 6.193: Interaction of LMF4 (β -Glucogallin) at the binding site of the enzyme (PDB ID: 1QX3).

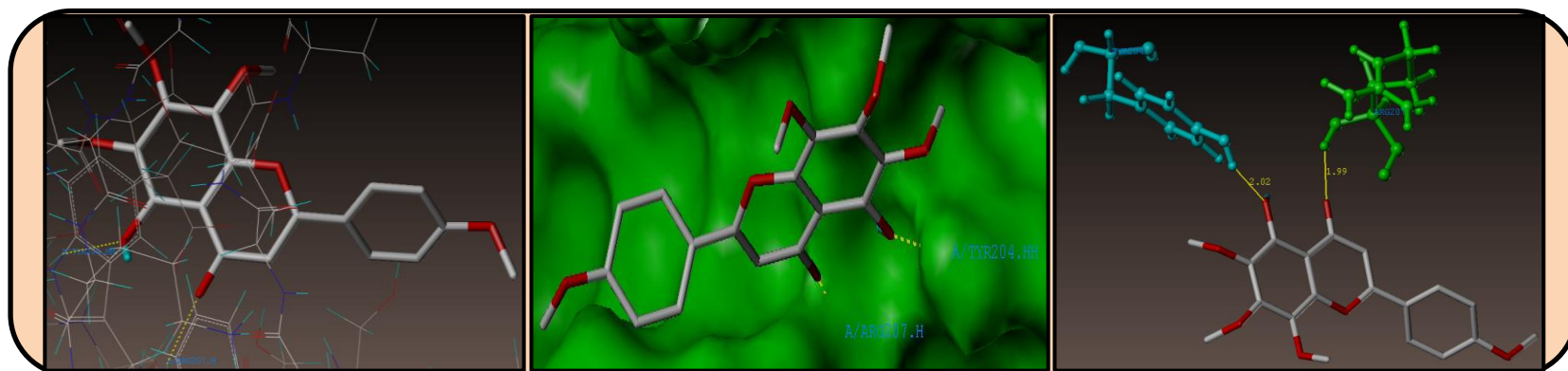


Figure 6.194: Interaction of LME1 (Gardenin B) at the binding site of the enzyme (PDB ID: 1QX3).

All the compounds were docked into the active site of enzyme as shown in Figure 6.184. The predicted binding energies of the compounds are listed in Table 6.84. The docking study revealed that all the compounds demonstrated encouraging docking activity for the enzyme, with consensus score in the range 7.00-2.65, indicating the summary of all forces of interaction between compounds and the enzyme. Most phytoconstituents displayed similar type of interactions with amino acid residues (PHE250, SER209, ARG207, TYR204) as those of standard drugs Doxorubicin and Cisplatin.

As depicted in the Figure 6.185, compound Doxorubicin makes ten hydrogen bonding interactions at the active site of the enzyme (PDB ID: 1QX3), among two bonding interactions raised from oxygen atom of methoxy group present on the 1st position of tetracene ring and oxygen atom of carbonyl group present on the 12th position of tetracene dione ring with hydrogen atom of PHE250 (CH₃O----H-PHE250, 2.33 Å; C=O----H-PHE250, 2.05 Å), hydrogen atom of hydroxyl group present on the 6th position of tetracene dione ring makes an interaction with oxygen atom of PHE250 (OH----O-PHE250, 1.90 Å), oxygen atom of carbonyl group present on the 5th position of tetracene dione ring makes an interaction with hydrogen atom of SER209 (C=O----H-SER209, 2.57 Å), oxygen atom of hydroxyl group present on the 11th position of tetracene dione ring makes an interaction with hydrogen atom of SER209 (HO----H-SER209, 2.57 Å), hydrogen atom of hydroxyl group present on the 11th position of tetracene dione ring makes an interaction with oxygen atom of ARG207 (OH----O-ARG207, 1.96 Å), hydrogen atom of 2-hydroxyacetyl group of tetracene dione ring makes an interaction with oxygen atom of ARG207 (OH----O-ARG207, 1.98 Å), oxygen atom of 2-hydroxyacetyl group of tetracene dione ring makes an interaction with hydrogen atom of ARG207 (HO----H-ARG207, 1.78 Å), oxygen atom of carbonyl group of 2-hydroxyacetyl group of tetracene dione ring makes an interaction with hydrogen atom of TYR204 (C=O----H-TYR204, 1.78 Å) and hydrogen atom amino group present on the 4th position of pyran ring makes an interaction with oxygen atom of PHE252

(-H---- O-PHE252, 2.09 Å).

As depicted in Figure 6.186, Cisplatin, makes two hydrogen bonding interactions at the active site of the enzyme (PDB ID: 1QX3), hydrogen atoms of both the amino groups makes hydrogen bonding interactions with GLU246 and PHE250 (-H----O-GLU246, 2.02 Å; -H----O-PHE250, 1.95 Å).

As depicted in Figure 6.187, Quercetrin, makes seven hydrogen bonding interactions at the active site of the enzyme (PDB ID: 1QX3), among them a bonding interaction raised from hydrogen atom of hydroxyl group present on 5th position of chromen-4-one ring with oxygen atom of PHE250 (-H----O-PHE250, 2.14 Å), oxygen atom of hydroxyl group present on 7th position of chromen-4-one ring makes an interaction with hydrogen atom of ARG207 (-O----H-ARG207, 2.06 Å), hydrogen atom of hydroxyl group present on 7th position of chromen-4-one ring makes an interaction with oxygen atom of ARG207 (-H----O-ARG207, 2.68 Å), hydrogen atom of hydroxyl group present on 3rd position of 3,4-dihydroxy phenyl ring present on the 2nd position of chromen-4-one ring makes an interaction with oxygen atom of GLU246 (-H----O-GLU246, 2.23 Å), oxygen atom present in the chromen-4-one ring makes an interaction with hydrogen atom of TYR214 (-O----H-TYR214, 1.98 Å), oxygen atom present at the 4th position of the chromen-4-one ring makes an interaction with hydrogen atom of PHE250 (-O----H-PHE250, 2.62 Å) and oxygen atom of hydroxyl group present on 3rd position of 3,4-dihydroxy phenyl ring present on the 2nd position of chromen-4-one ring makes an interaction with hydrogen atom of GLU248 (-O----H-GLU248, 2.65 Å).

As depicted in Figure 6.188, Rutin, makes ten hydrogen bonding interactions at the active site of the enzyme (PDB ID: 1QX3), among them a bonding interaction raised from oxygen atom of hydroxyl group present on the 3rd position of 3,4,-dihydroxy phenyl ring present at the 2nd position of chromen-4-one ring with hydrogen atom of PHE252 (-H----

O-PHE252, 2.48 Å), oxygen atom of hydroxyl group present on the 4th position of 3,4,-dihydroxy phenyl ring present at the 2nd position of chromen-4-one ring makes two interactions with hydrogen atoms of SER251 and ASP253 (-O----H-SER251, 2.12 Å; O---H-ASP253, 2.70 Å), oxygen atom of hydroxyl group present on the 3rd position of 3,4,5-trihydroxy-6-methyl pyran ring makes an interaction with hydrogen atom of PHE250 (O---H-PHE250, 2.48 Å), oxygen atom of hydroxyl group present on the 5th position of 3,4,5-trihydroxy pyran ring makes an interaction with hydrogen atom of PHE250 (O----H-PHE250, 2.02 Å), oxygen atom of hydroxyl group present on the 4th position of 3,4,5-trihydroxy-6-methyl pyran ring makes an interaction with hydrogen atom of TRP214 (O---H-TYR214, 2.01 Å), oxygen atom of hydroxyl group present on the 5th position of 3,4,5-trihydroxy-6-methyl pyran ring makes an interaction with hydrogen atom of ASN208 (O---H-ASN208, 2.04 Å), oxygen atom of hydroxyl group present on the 5th position of chromen-4-one ring makes an interaction with hydrogen atom of SER209 (O----H-SER209, 1.92 Å), hydrogen atom of hydroxyl group present on the 5th position of chromen-4-one ring makes an interaction with oxygen atom of ARG207 (H-----O-ARG207, 1.87 Å) and oxygen atom of hydroxyl group present on the 7th position of chromen-4-one ring makes an interaction with hydrogen atom of ARG207 (O-----H-ARG207, 2.14 Å).

As depicted in Figure 6.189, Hesperidin, makes thirteen hydrogen bonding interactions at the active site of the enzyme (PDB ID: 1QX3), among them a bonding interaction raised from hydrogen atom of hydroxyl group present on the 3rd position of 3,4,5-trihydroxy-6-methyl pyran ring with oxygen atom of GLU248 (-H---O-GLU248, 1.96 Å), hydrogen atom of hydroxyl group present on the 4th position of 3,4,5-trihydroxy-6-methyl pyran ring makes an interaction with oxygen atom of GLU248 (-H---O-GLU248, 2.16 Å), oxygen atom of hydroxyl group present on the 4th position of 3,4,5-trihydroxy-6-methyl pyran ring with hydrogen atom of GLU248 (-O----H-GLU248, 2.06 Å), oxygen atom present in the chromen-4-one ring makes an interaction with hydrogen atom of ARG207 (O-----H-ARG207, 2.24 Å), oxygen atom of hydroxyl group present on the 5th

position of chromen-4-one ring makes an interaction with hydrogen atom of PHE250 (O---H-PHE250, 1.93 Å), oxygen atom of hydroxyl group present on the 3rd position of phenyl ring which is present on the 2nd position of chromen-4-one ring makes three interactions with hydrogen atoms of SER65, ARG207 (HO-----O-SER65, 2.64 Å; HO-----O-ARG207, 2.59 Å; 1.98 Å), oxygen atom of hydroxyl group present on the 3rd position of 3,4,5-trihydroxy pyran ring makes interactions with hydrogen atoms of LYS210 and SER209 (-O---H-LYS210, 2.33 Å; O---H-SER209, 2.64 Å), hydrogen atom of hydroxyl group present on the 3rd position of 3,4,5-trihydroxy pyran ring makes an interaction with hydrogen atom of SER209 (-O---H-SER209, 1.91 Å), oxygen atom present in the 3,4,5-trihydroxy pyran ring makes an interaction with hydrogen atom of ASN208 (O---H-ASN208, 2.56 Å), and oxygen atom of methoxy group present on the 4th position of phenyl ring which is present on the 2nd position of chromen-4-one ring makes an interaction with hydrogen atom of SER65 (O-----H-SER65, 2.18 Å).

As depicted in Figure 6.190, Quercetin, makes four hydrogen bonding interactions at the active site of the enzyme (PDB ID: 1QX3), among them a bonding interaction raised from hydrogen atom of hydroxyl group present on 5th position of chromen-4-one ring with oxygen atom of PHE250 (-H---O-PHE250, 2.07 Å), hydrogen atom of hydroxyl group present on 7th position of chromen-4-one ring makes an interaction with oxygen atom of ARG207 (-H---O-ARG207, 1.78 Å), oxygen atom present at the 4th position of the chromen-4-one ring makes an interaction with hydrogen atom of SER251 (-O---H-SER251, 2.68 Å) and oxygen atom present in the chromen-4-one ring makes an interaction with hydrogen atom of TYR204 (-O---H-TYR204, 2.37 Å).

As depicted in Figure 6.191, Kaempferol, makes four hydrogen bonding interactions at the active site of the enzyme (PDB ID: 1QX3), oxygen atom of hydroxyl group present on the 5th position of chromen-4-one ring makes an interaction with hydrogen atom of ARG207 (O-----H-SRG207, 2.28 Å), hydrogen atom of hydroxyl group present on

the 5th position of chromen-4-one ring makes an interaction with oxygen atom of ARG207 (H-----O-ARG207, 1.89 Å), oxygen atom of hydroxyl group present on the 7th position of chromen-4-one ring makes an interaction with hydrogen atom of ARG207 (O-----H-ARG207, 1.94 Å) and oxygen atom present on the 4th position of chromen-4-one ring makes an interaction with hydrogen atom of TYR204 (O-----H-TYR204, 2.64 Å).

As depicted in Figure 6.192, Isorhamnetin, makes one hydrogen bonding interaction at the active site of the enzyme (PDB ID: 1QX3), oxygen atom of hydroxyl group present on the 3rd position of chromen-4-one ring makes an interaction with hydrogen atom of TYR204 (O-----H-TYR204, 2.00 Å).

As depicted in Figure 6.193, β -Glucogallin, makes eight hydrogen bonding interactions at the active site of the enzyme (PDB ID: 1QX3), among them one bonding interaction raised from hydrogen atom of hydroxyl group present on the 3rd position of pyran ring with oxygen atom of ARG207 (-H----O-ARG207, 1.76 Å), oxygen atom of hydroxyl group present on the 3rd position of pyran ring makes an interaction with hydrogen atom of SER209 (-O----H-SER209, 1.94 Å), oxygen atom of hydroxymethyl group present on the 6th position of pyran ring makes an interaction with hydrogen atom of PHE250 (-O---H-PHE250, 1.85 Å), hydrogen atom of hydroxymethyl group present on the 6th position of pyran ring makes an interaction with oxygen atom of PHE250 (-H----O-PHE250, 1.90 Å), oxygen atom of hydroxyl group present on the 3rd position of 3,4,5-trihydroxybenzoate ring makes an interaction with hydrogen atom of SER251 (-O----H-SER251, 1.85 Å), oxygen atom of hydroxyl group present on the 4th position of 3,4,5-trihydroxybenzoate ring makes an interaction with hydrogen atom of SER251 (-O----H-SER251, 2.73 Å), hydrogen atom of hydroxyl group present on the 3rd position of 3,4,5-trihydroxybenzoate ring makes an interaction with oxygen atom of SER251 (-H----O-SER251, 2.45 Å) and oxygen atom of benzoate ring makes an interaction with hydrogen atom of TYR204 (O-----H-TYR204, 2.10 Å).

As depicted in Figure 6.194, Gardenin B, makes two hydrogen bonding interactions at the active site of the enzyme (PDB ID: 1QX3), oxygen atom of hydroxyl group present on the 5th position of chromen-4-one ring makes an interaction with hydrogen atom of TYR204 (O-----H-TYR204, 2.02 Å) and oxygen atom present on the 4th position of chromen-4-one ring makes an interaction with hydrogen atom of ARG207 (O-----H-ARG207, 1.99 Å).

Docking studies with Surflex-Dock showed that almost all the compounds occupied the same binding sites as that of Doxorubicin.

Table 6.84: Surflex Docking score (Kcal/mol) of the isolated compounds with Caspase-3 enzyme.

Compounds	C Score ^a	Crash Score ^b	Polar Score ^c	D Score ^d	PMF Score ^e	G Score ^f	Chem Score ^g
Hesperidin	7.00	-2.11	7.65	-140.328	-50.789	-199.523	-29.359
Doxorubicin	6.64	-1.48	7.67	-107.866	-44.684	-159.470	-33.154
Rutin	5.10	-2.30	8.35	-105.300	-55.309	-73.564	-20.451
β -Glucogallin	4.38	-1.52	4.98	-86.212	-41.350	-103.296	-17.385
Isorhamnetin	4.04	-1.35	1.17	-92.566	-72.902	-120.428	-26.261
Quercetin	3.92	-1.42	2.86	-85.991	-66.160	-101.604	-25.821
Gardenin B	3.85	-0.98	2.16	-85.857	-41.600	-103.743	-22.672
Kaempferol	2.66	-0.78	2.48	-61.296	-61.701	-37.069	-18.879
Quercetrin	2.65	-1.61	3.95	-102.331	-53.925	-116.216	-28.692
Cisplatin	2.19	-0.20	2.79	-48.473	-7.581	-41.848	-14.351

^a C Score (Consensus Score) integrates a number of popular scoring functions for ranking the affinity of ligands bound to the active site of a enzyme/receptor and reports the output of total score.

^b Crash-score reveals the inappropriate penetration into the binding site. Crash scores close to 0 are favorable. Negative numbers indicate penetration.

^c Polar indicates the contribution of the polar interactions to the total score. The polar score may be useful for excluding docking results that make no hydrogen bonds.

^d D-score indicates the charge and van der Waals interactions between the protein and the ligand.

^e PMF-score indicates the Helmholtz free energies of interactions for protein-ligand atom pairs (Potential of Mean Force, PMF).

^f G-score shows hydrogen bonding, complex (ligand-protein), and internal (ligand-ligand) energies.

^g Chem-score points for H-bonding, lipophilic contact, and rotational entropy, along with an intercept term.

6.2.12.2. *In silico* molecular docking of isolated compounds with the active site of the BZD binding site of GABA-_A receptor (PDB ID: 6D6T).

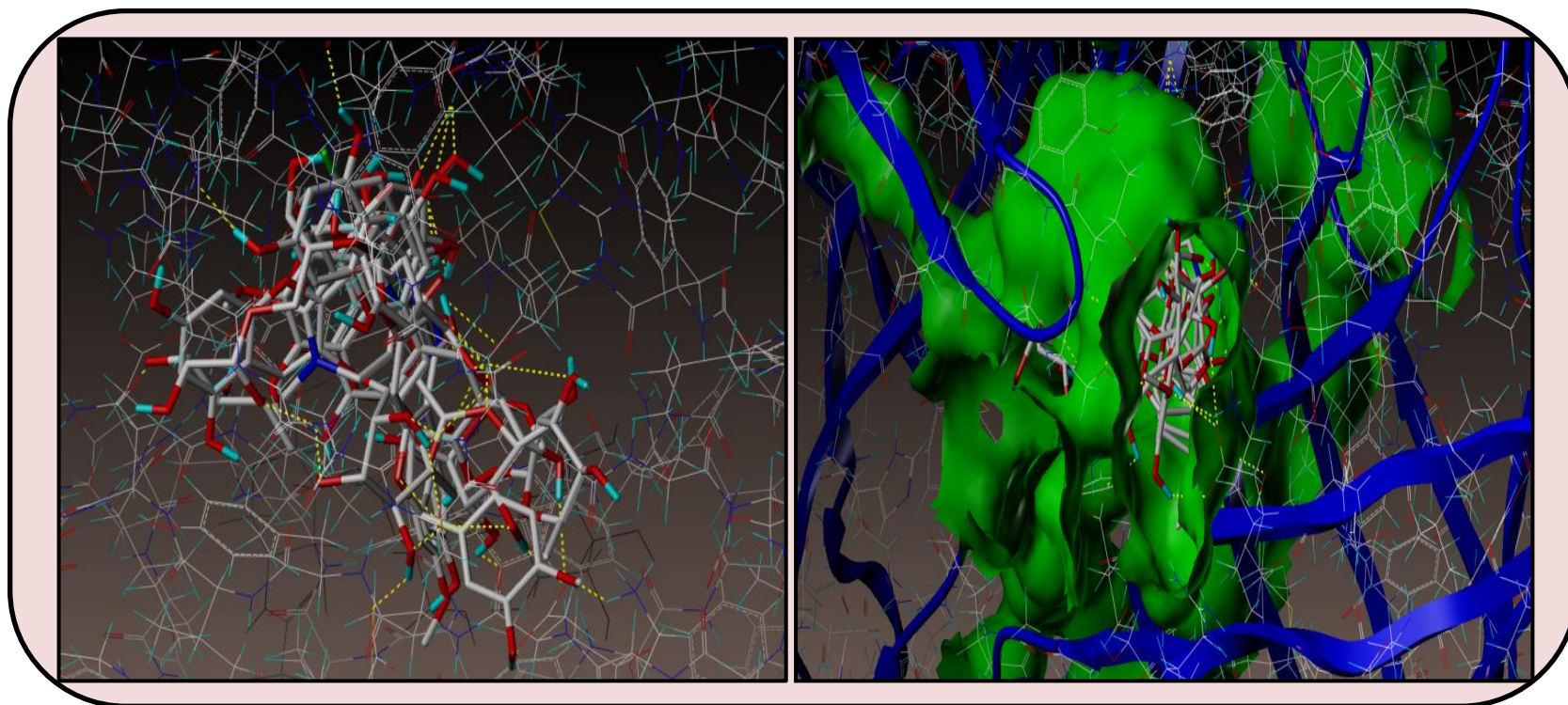


Figure 6.195: Docked view of all the compounds at the BZD binding site of GABA-_A receptor (PDB ID: 6D6T).

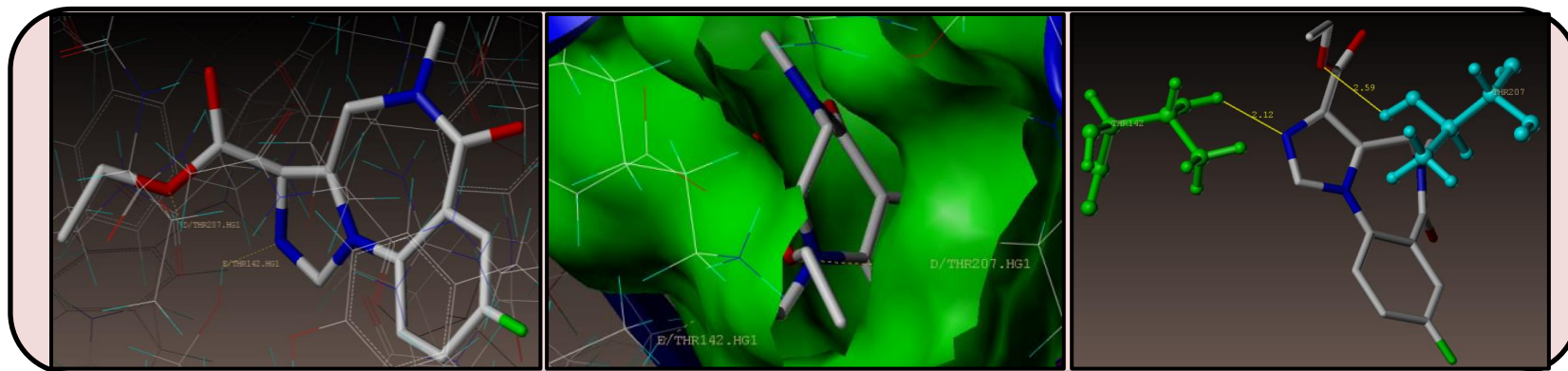


Figure 6.196: Interaction of Diazepam at the BZD binding site of the GABA-A receptor (PDB ID: 6D6T).

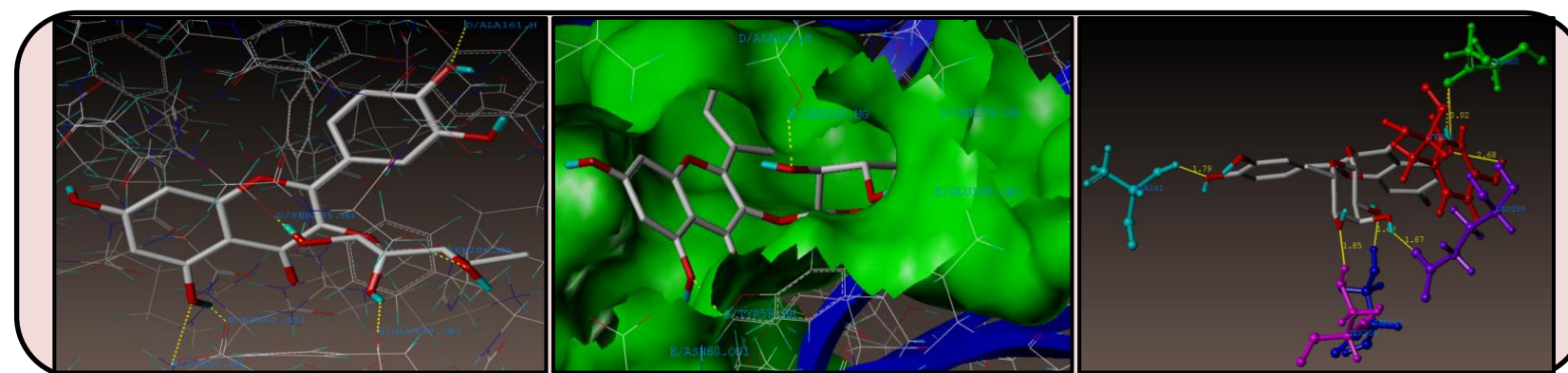


Figure 6.197: Interaction of LMH1 (Quercetin) at the BZD binding site of the GABA-A receptor (PDB ID: 6D6T).

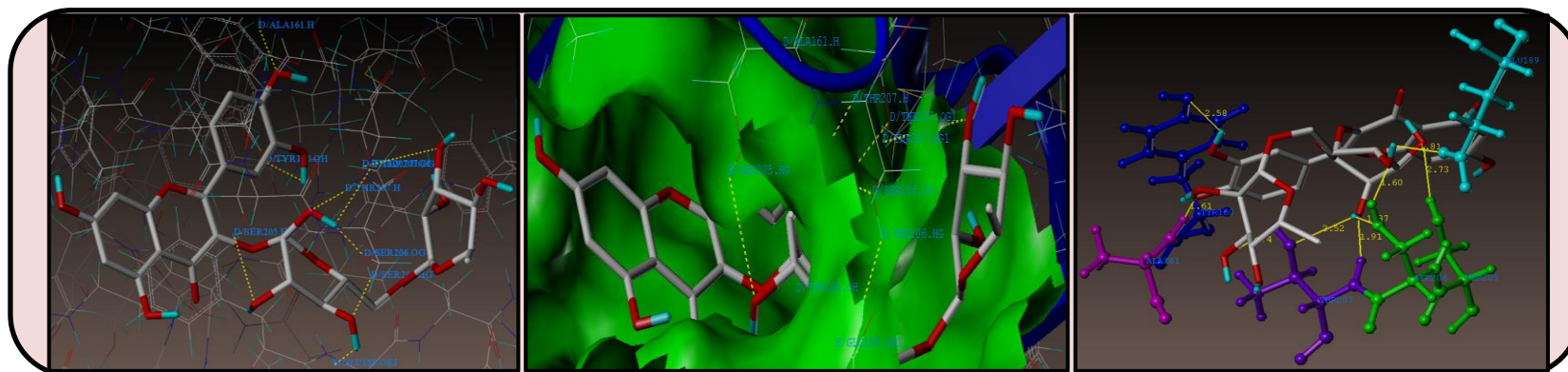


Figure 6.198: Interaction of LMH2 (Rutin) at the BZD binding site of the GABA_A receptor (PDB ID: 6D6T).

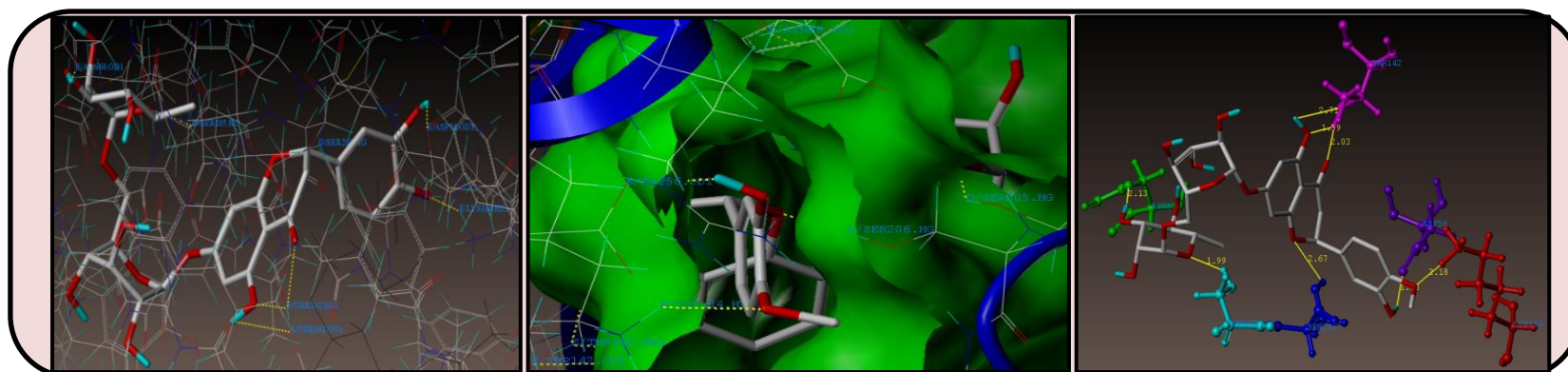


Figure 6.199: Interaction of LMH3 (Hesperidin) at the BZD binding site of the GABA_A receptor (PDB ID: 6D6T).

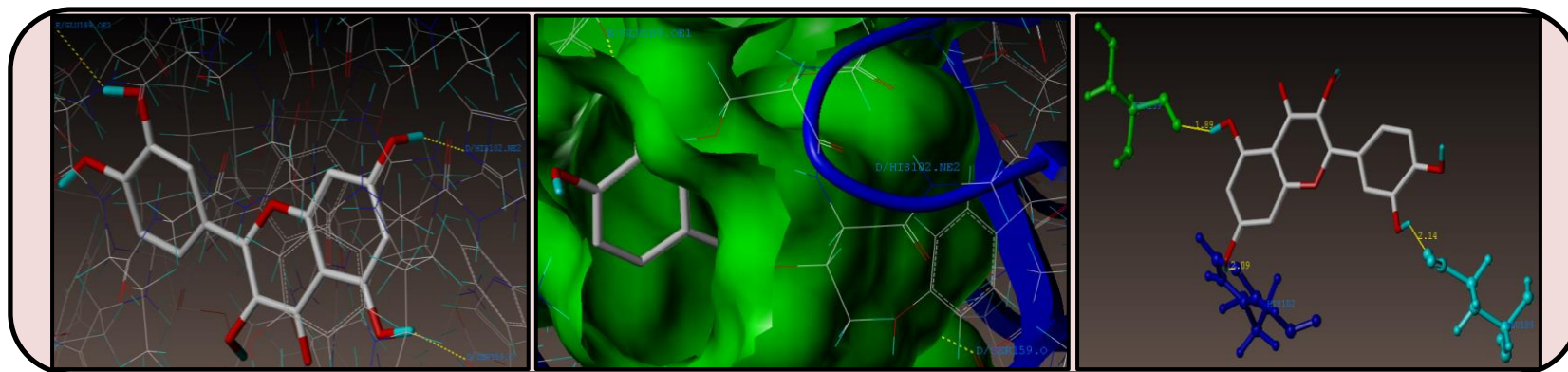


Figure 6.200: Interaction of LMF1 (Quercetin) at the BZD binding site of the GABA_A receptor (PDB ID: 6D6T).

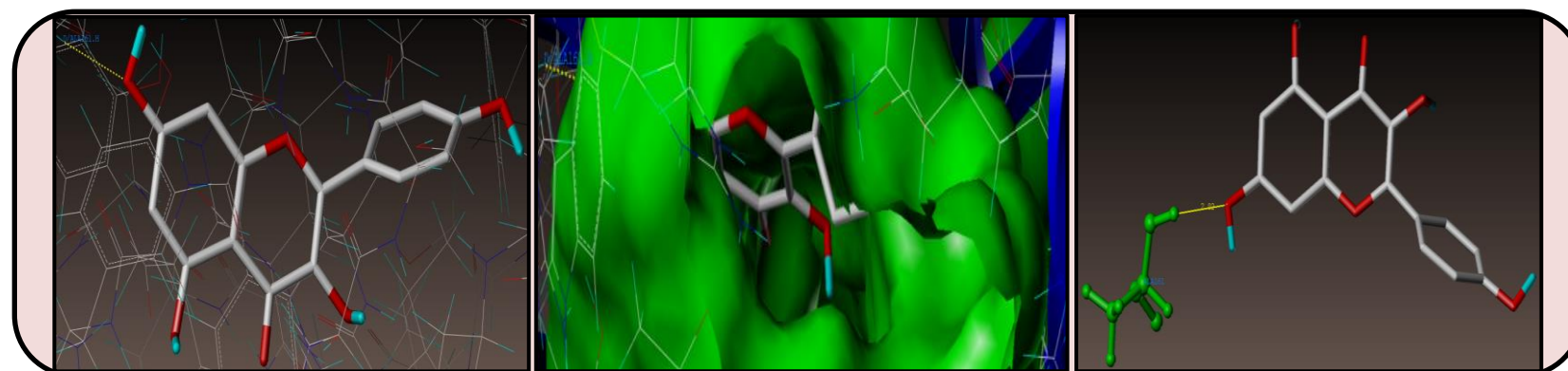


Figure 6.201: Interaction of LMF2 (Kaempferol) at the BZD binding site of the GABA_A receptor (PDB ID: 6D6T).

All the phytoconstituents were docked into the BZD binding site of the GABA_A receptor as shown in Figure 6.195. The predicted binding energies of the compounds are listed in Table 6.85. The docking study revealed that all the compounds have showed very good docking score against the enzyme.

As depicted in the Figure 6.196, Diazepam makes two hydrogen bonding interactions at the BZD binding site of the GABA_A receptor (PDB ID: 6D6T), among a bonding interaction raised from nitrogen atom present on the 3rd position of the ring with hydrogen atom of THR142 (-N---- H-THR142, E-Chain, 2.12 Å), and oxygen atom 3-carboxylate group makes an interaction with hydrogen atom of THR207 (-O---- H-THR207, D-Chain, 2.57 Å).

As depicted in Figure 6.197, Quercetrin, makes six hydrogen bonding interactions at the BZD binding site of the GABA_A (receptor PDB ID: 6D6T), among them a bonding interaction raised from hydrogen atom of hydroxyl group present on 5th position of chromen-4-one ring with oxygen atom of ASN60 (-H----O-ASN60, E-Chain, 2.02 Å), oxygen atom of hydroxyl group present on 5th position of chromen-4-one ring makes an interaction with hydrogen atom of TYR58 (-O----H-TYR58, E-Chain, 2.68 Å), oxygen atom of hydroxyl group present on the 3rd position of pyran ring makes an interaction with hydrogen atom of SER205 (O-----H-SER205, D-Chain, 1.68 Å), hydrogen atom of hydroxyl group present on the 4th position of pyran ring makes an interaction with oxygen atom of GLU189 (H-----O-GLU189, E-Chain, 1.87 Å), hydrogen atom of hydroxyl group present on the 5th position of pyran ring makes an interaction with oxygen atom of SER206 (H-----O-SER206, D-Chain, 1.85 Å), and oxygen atom of hydroxyl group present on 4th position of 3,4-dihydroxy phenyl ring present on 2nd position of chromen-4-one ring makes an interaction with hydrogen atom of ALA161 (-O----H-ALA161, D-Chain, 1.79 Å).

As depicted in Figure 6.198, Rutin, makes ten hydrogen bonding interactions at the BZD binding site of the GABA_A receptor (PDB ID: 6D6T), among them a bonding interaction raised from hydrogen atom of hydroxyl group present on the 3rd position of 3,4,-dihydroxy phenyl ring present at the 2nd position of chromen-4-one ring with oxygen atom of TYR160 (-H----O-TYR160, D-Chain, 2.58 Å), oxygen atom of hydroxyl group present on the 4th position of 3,4,-dihydroxy phenyl ring present at the 2nd position of chromen-4-one ring makes two interactions with hydrogen atoms of ALA161 and SER205 (-O----H-ALA161, D-Chain, 1.61 Å; O----H-SER205, D-Chain, 2.73 Å), hydrogen atom of hydroxyl group present on the 3rd position of 3,4,5-trihydroxy pyran ring makes two interactions with oxygen atoms of THR207 & SER206 (H-----O-THR207, D-Chain, 1.97 Å; H-----O-SER206, D-Chain, 1.87 Å), oxygen atom of hydroxyl group present on the 3rd position of 3,4,5-trihydroxy pyran ring makes an interaction with hydrogen atom of THR207 (O-----H-THR207, D-Chain, 2.52 Å), oxygen atom of hydroxyl group present on the 4th position of 3,4,5-trihydroxy pyran ring makes an interaction with hydrogen atom of SER205 (O----H-SER205, D-Chain, 1.60 Å), oxygen atom of hydroxyl group present on the 5th position of 3,4,5-trihydroxy pyran ring makes an interaction with hydrogen atom of SER206 (O----H-SER206, D-Chain, 1.60 Å), hydrogen atom of hydroxyl group present on the 5th position of 3,4,5-trihydroxy pyran ring makes an interaction with oxygen atom of GLU189 (H-----O-GLU189, E-Chain, 1.81 Å) and oxygen atom of hydroxyl group present on the 4th position of 3,4,5-trihydroxy-6-methyl pyran ring makes an interaction with hydrogen atom of THR207 (O-----H-THR207, D-Chain, 2.74 Å).

As depicted in Figure 6.199, Hesperidin, makes eight hydrogen bonding interactions at the BZD binding site of the GABA_A receptor (PDB ID: 6D6T), among them a bonding interaction raised from oxygen atom of hydroxyl group present on the 4th position of 3,4,5-trihydroxy tetrahydropyran ring with hydrogen atom of ASN60 (-O----H-ASN60, E-Chain, 2.13 Å), oxygen atom present in the pyran ring makes an interaction with hydrogen atom of SER205 (O-----H-SER205, D-Chain, 1.99 Å), oxygen atom of hydroxyl group present

on the 5th position of chromen-4-one ring makes an interaction with hydrogen atom of THR142 (O----- H-THR142, E-Chain, 1.59 Å), oxygen atom present at the 4th position of chromen-4-one ring makes an interaction with hydrogen atom of THR142 (O----- H-THR142, E-Chain, 2.03 Å), hydrogen atom of hydroxyl group present on the 5th position of chromen-4-one ring makes an interaction with oxygen atom of THR142 (OH----- O-THR142, E-Chain, 2.71 Å), oxygen atom present in the chromen-4-one ring makes an interaction with hydrogen atom of SER206 (O----- H-SER206, D-Chain, 2.67 Å), hydrogen atom of hydroxyl group present on the 3rd position of phenyl ring which is present on the 2nd position of chromen-4-one ring makes an interaction with oxygen atom of ASP56 (OH----- O-ASP56, E-Chain, 1.97 Å), oxygen atom of methoxy group present on the 4th position of phenyl ring which is present on the 2nd position of chromen-4-one ring makes an interaction with hydrogen atom of LYS184 (O-----H-LYS, E-Chain, 2.18 Å).

As depicted in Figure 6.200, Quercetin, makes three hydrogen bonding interactions at the BZD binding site of the GABA_A receptor (PDB ID: 6D6T), among them a bonding interaction raised from hydrogen atom of hydroxyl group present on 5th position of chromen-4-one ring with oxygen atom of SER159 (-H----O-SER159, D-Chain, 1.89 Å), hydrogen atom of hydroxyl group present on 7th position of chromen-4-one ring makes an interaction with oxygen atom of HIS102 (-H----O-HIS102, D-Chain, 2.09 Å), and hydrogen atom of hydroxyl group present on 3rd position of 3,4-dihydroxy phenyl ring present on the 2nd position of chromen-4-one ring makes an interaction with oxygen atom of GLU189 (-H----O-GLU189, E-Chain, 2.14 Å).

As depicted in Figure 6.201, Kaempferol, makes one hydrogen bonding interactions at the BZD binding site of the GABA_A receptor (PDB ID: 6D6T), hydrogen atom of hydroxyl group present on the 7th position of chromen-4-one ring makes an interaction with oxygen atom of ALA161 (O-----H-ALA161, D-Chain, 2.02 Å).

As depicted in Figure 6.202, Isorhamnetin, makes four hydrogen bonding interactions at the BZD binding site of the GABA_A receptor (PDB ID: 6D6T), among them a bonding interaction raised from hydrogen atom of hydroxyl group present on the 7th position of chromen-4-one ring with nitrogen atom of HIS102 (-H---N-HIS102, D-Chain, 2.14 Å), hydrogen atom of hydroxyl group present on the 5th position of chromen-4-one ring makes an interaction with oxygen atom of SER159 (O-----H-SER159, D-Chain, 1.80 Å), oxygen atom present at the 4th position of chromen-4-one ring makes an interaction with hydrogen atom of ALA161 (O-----H-ALA161, D-Chain, 2.15 Å), and hydrogen atom of hydroxyl group present on the 3rd position of chromen-4-one ring makes an interaction with oxygen atom of TYR160 (O-----H-TYR160, D-Chain, 2.37 Å).

As depicted in Figure 6.203, β -Glucogallin, makes seven hydrogen bonding interactions at the BZD binding site of the GABA_A receptor (PDB ID: 6D6T), among them three bonding interactions raised from hydrogen atoms of hydroxyl groups present on the 3rd, 4th and 7th positions of pyran ring with oxygen atom of ASP56 (-H---O-ASP56, E-Chain, 2.73 Å, 2.35 Å, 2.07 Å), oxygen atom of hydroxyl group present on the 7th position of pyran ring makes an interaction with hydrogen atom of SER206 (-O----H-SER206, D-Chain, 2.50 Å), oxygen atom present in the pyran ring makes an interaction with hydrogen atom of THR142 (O-----H-THR142, E-Chain, 2.02 Å), oxygen atom of carbonyl group of benzoate ring makes an interaction with hydrogen atom of THR142 (O----H-THR142, E-Chain, 2.29 Å), and oxygen atom of benzoate ring makes an interaction with hydrogen atom of THR207 (O-----H-THR207, D-Chain, 1.93 Å).

Table 6.85: Surflex Docking score (Kcal/mol) of isolated compounds with GABA-A receptor.

Compounds	C Score ^a	Crash Score ^b	Polar Score ^c	D Score ^d	PMF Score ^e	G Score ^f	Chem Score ^g
Gardenin	7.75	-1.04	0.00	-164.321	-98.029	-207.776	-31.710
Diazepam	6.05	-0.46	0.95	-107.328	-105.809	-204.434	-27.117
Hesperidin	5.85	-5.15	4.73	-225.877	-170.825	-323.542	-37.032
Isorhamnetin	5.77	-1.82	3.13	-133.449	-110.963	-158.473	-34.594
Kaempferol	5.61	-0.80	1.71	-126.404	-77.547	-112.670	-27.527
β -Glucogallin	5.19	-2.29	4.28	-138.464	-82.346	-202.341	-16.328
Rutin	2.21	-8.51	2.74	-234.490	-159.847	-283.168	-33.545
Quercetrin	6.57	-2.76	4.24	-164.646	-140.596	-197.598	-38.858
Quercetin	5.65	-1.01	3.41	-119.982	-115.801	-127.089	-31.992

^a C Score (Consensus Score) integrates a number of popular scoring functions for ranking the affinity of ligands bound to the active site of a enzyme/receptor and reports the output of total score.

^b Crash-score reveals the inappropriate penetration into the binding site. Crash scores close to 0 are favorable. Negative numbers indicate penetration.

^c Polar indicates the contribution of the polar interactions to the total score. The polar score may be useful for excluding docking results that make no hydrogen bonds.

^d D-score indicates the charge and van der Waals interactions between the protein and the ligand.

^e PMF-score indicates the Helmholtz free energies of interactions for protein-ligand atom pairs (Potential of Mean Force, PMF).

^f G-score shows hydrogen bonding, complex (ligand-protein), and internal (ligand-ligand) energies.

^g Chem-score points for H-bonding, lipophilic contact, and rotational entropy, along with an intercept term.



CHAPTER – VII

DISCUSSION

7. DISCUSSION

Plants and dietary foods rich in polyphenolics like flavonoids, tannins, gallic acid, etc., act as natural antioxidants that can improve health and reduce the risk of diseases.^[60] As reactive free radical scavengers, plant antioxidants help minimize oxidative stress, preserve cellular integrity, and maintain physiological functions and homeostasis in the human immune system.^[203] Antioxidants may help prevent or postpone the onset of degenerative diseases like cancer, cardiovascular disease, neural disorders, mild cognitive impairment, Alzheimer's, and Parkinson's disease.^[239] Naturally occurring polyphenolics have gained popularity due to their high antioxidant, anti-inflammatory and anti-carcinogenic potential that help reduce the risk of life-threatening diseases.^[240] The preliminary phytochemical investigations of the EEHE, EEBF and their biofractions revealed the presence of various phytoconstituents. Amongst the experimental samples screened, EEHE and EEBF showed the maximum phenolic content and flavonoid content, followed by ITHE and ITBF.

The results of the study illustrated the efficacy of EEHE and EEBF and their biofractions to scavenge the DPPH, hydrogen peroxide, nitric oxide and ABTS free radicals. The methanolic fraction of ethanolic extracts of *H. enneaspermus* (MFHE) exhibited significant antioxidant potential with IC₅₀ values of 21.10 ± 0.39 µg/mL and 25.99 ± 4.66 µg/mL as compared to the other treatments and was similar to the standard ascorbic acid with IC₅₀ values of 11.19 ± 1.09 µg/mL and 9.30 ± 0.26 µg/mL in DPPH and nitric oxide free radical scavenging assays, respectively. EFHE displayed substantial *in vitro* free radical scavenging activity in ABTS and hydrogen peroxide assay with IC₅₀ values of 40.38 ± 0.88 µg/mL and 99.11 ± 13.59 µg/mL, respectively, while ITHE showed considerable activity with IC₅₀ < 100 µg/mL in DPPH, NO and ABTS assays, as against the standard and other experimental samples tested ($p < 0.05$, Figure 6.1, Table 6.3).

The methanolic fraction of ethanolic extracts of *B. foveolata* (MFBF) exhibited significant ($p < 0.05$) free radical scavenging activity with IC_{50} values of 53.44 ± 0.83 $\mu\text{g/mL}$, 26.76 ± 0.75 $\mu\text{g/mL}$, 71.63 ± 0.19 $\mu\text{g/mL}$ and 52.01 ± 2.28 $\mu\text{g/mL}$ in DPPH, hydrogen peroxide, nitric oxide and ABTS radical scavenging assays respectively. EEBF also displayed significant activity ($p < 0.05$) with IC_{50} values of 19.04 ± 0.24 $\mu\text{g/mL}$, 43.96 ± 0.92 $\mu\text{g/mL}$, 65.85 ± 1.22 $\mu\text{g/mL}$ and 38.3 ± 1.51 $\mu\text{g/mL}$ against the DPPH, hydrogen peroxide, nitric oxide and ABTS free radicals respectively. ITBF and EFBF exhibited significant *in vitro* free radical scavenging activity with $IC_{50} < 100$ $\mu\text{g/mL}$ in all the assays ($p < 0.05$, Figure 6.2, Table 6.4). Antioxidant activity is attributed to the presence of hydroxyl groups of the flavonoid compounds. The hydroxyl groups help in the interaction with the binding site of the target and quench the free radicals. [241]

Column chromatography and preparative HPLC of ITHE led to the isolation of three compounds *viz.* LMH1, LMH2 and LMH3, the structures were elucidated and identified as Quercetrin, Rutin and Hesperidin, respectively by IR, $^1\text{H-NMR}$, $^{13}\text{C-NMR}$ and mass spectroscopic methods. MFBF led to the isolation of four compounds *viz.* LMF1, LMF2, LMF3 and LMF4 were structurally elucidated and characterised as Quercetin, Kampferol, Isorhamnetin and β -glucogallin, respectively, by spectroscopic methods. EFBF led to the isolation of LME1 and that was confirmed as Gardenin B. The structural elucidation and characterisation of each isolated compound has been explained in detail in section 6.2.10.

Tremendous research is being carried out to combat, alleviate symptoms, and cure patients suffering from debilitating diseases like cancer. However, current treatment approaches *viz.* chemotherapy or radiation therapy account for innumerable adverse effects, drug resistance, and increased financial burden to the patient community. [242] In cancer therapy, the focus lies on strategies that suppress tumour growth through cell cycle disturbance and activating a cascade of events, i.e. activation of caspases, inter-nucleosomal DNA fragmentation etc., resulting in induction of apoptosis or cell cycle arrest. [243]

Phytochemicals have a better safety profile and have demonstrated anticancer activity by inhibiting tumour cell proliferation, inducing apoptosis, suppressing cell cycle, metastasis, angiogenesis, etc. [62]

Secondary metabolites like flavonoids and phenolic compounds produced by plant cells have been shown to be effective against tumour cell proliferation. [244, 245] At the molecular level, flavonoids mainly initiate cell cycle arrest, promote down-regulation of mutant p53 protein, and inhibit tyrosine kinase, heat shock proteins or expression of Ras protein of cancerous cells, thus mediating their anticancer action. [246, 247] Apoptosis is important in regulating cell development, and its mitochondria-dependent pathway involves activation of the caspase family, which is mainly responsible for the cleavage of cellular proteins resulting in cell death. The Bcl-2 family also plays a crucial role in apoptosis, wherein Bcl-2 and Bcl-xL will prevent it, while Bax and Bad will promote it. Down-regulation of Bcl-2 and Bcl-xL facilitates apoptosis induced by chemotherapeutic agents. The protein p53 suppresses tumours and mediates several cellular responses, including G₁ cell cycle arrest, DNA damage repair and induction of apoptosis. [248,249] A cell cycle is regulated by activators and inhibitors that ensure normal cell growth. Its proliferation is fundamental to the development, maintenance of homeostasis, and replacement of dead or damaged cells and is mainly associated with four phases (Sub-G₁, G₁, S, G₂/M) of a cell cycle. [22]

To study the antiproliferative activity of the extracts, their biofractions, and isolated phytoconstituents against Hop-62 cells, the cancer cell viability was evaluated by Sulforhodamine B assay. Subsequently, the cycle distribution was investigated using flow cytometry by staining with Annexin V-FITC and/or Propidium Iodide for apoptosis and cell cycle arrest. Conceptually, annexin apoptosis utilizes Annexin V and PI dyes to investigate cells in early and late apoptosis. In early apoptosis, phosphatidylserine is transferred into the external surface of the cellular membrane, where it binds to annexin V-

FITC thus helping to identify apoptotic cells. Propidium iodide (PI) is a fluorescent nucleus dye, that is impermeable to live and apoptotic cells, but stains dead cells with red fluorescence and binds tightly to the nucleic acids in the cell. [250]

TFHE depicted significant growth inhibition of MCF-7 cells at GI_{50} value of $10.22 \pm 6.72 \mu\text{g/mL}$ ($p < 0.05$, Figure 6.3, Table 6.5). In comparison, EEHE and ITHE showed antiproliferative activity with GI_{50} values of $41.42 \pm 3.74 \mu\text{g/mL}$ and $64.37 \pm 7.07 \mu\text{g/mL}$ respectively and were further subjected to apoptosis and cell cycle analysis. After 24 h of treatment with EEHE, TFHE and ITHE, the MCF-7 cells displayed a reduction in size, as the cells underwent changes in morphology. Treatment with TFHE, caused the cells to become compact, comparable to the treatment with standard Doxorubicin, while EFHE and MFHE did not show significant changes in cell morphology (Figure 6.4). ITHE subjected to *in vitro* apoptotic and cell cycle studies, displayed that $11.31 \pm 0.82 \%$ cells were undergoing late apoptosis and $34.48 \pm 1.57 \%$ cells in necrosis. The results were compared with standard Doxorubicin, which exhibited $13.67 \pm 1.02 \%$ cells in late apoptosis and $8.58 \pm 0.65 \%$ in necrosis ($p < 0.001$, Figures 6.5 and 6.6, Table 6.6). In cell cycle analysis, ITHE arrested $13.99 \pm 1.65 \%$ cells in G_2/M phase, compared to control ($p \leq 0.001$, Figures 6.7 and 6.8, Table 6.7). All three isolated compounds of ITHE showed remarkable anti-proliferative activities with $GI_{50} < 20 \mu\text{g/mL}$, with cell size reduction and blebbing ($p < 0.01$, Figure 6.145 and 6.146, Table 6.66). It also exhibited significant apoptotic and cell cycle arrest abilities of MCF-7 cells. LMH3 (Hesperidin) exhibited growth inhibition at $GI_{50} = 15.84 \pm 2.81 \mu\text{g/mL}$, with $16.89 \pm 0.88 \%$, $23.18 \pm 0.43 \%$ and $2.79 \pm 0.67 \%$ cells in early apoptosis, late apoptosis and necrotic stages respectively, comparable to standard Doxorubicin ($p < 0.001$, Figure 6.147 and 6.148, Table 6.67). The isolated phytoconstituents increased the number of cells in the sub- G_1 phase indicating apoptotic cellular death ($p < 0.001$, Figure 6.149 and 6.150, Table 6.68). Amongst the extract EEBF and its biofractions tested against MCF-7 cells, TFBF indicated considerable growth inhibition of $GI_{50} = 73.50 \pm 11.96 \mu\text{g/mL}$ ($p < 0.01$, Figure 6.13, Table 6.10), with

cells shrinking in size and appearing rounder compared to the other experimental samples tested (Figure 6.14). The growth inhibition of MCF-7 cells by other biofractions of EEHE was $> 80 \mu\text{g/mL}$ and hence these samples were not subjected to molecular studies.

On Hop-62 cells, EEBF and biofractions showed substantial growth inhibition. TFBF, EEBF, EFBF and MFBF exhibited antiproliferative activity, with GI_{50} values of $23.7 \pm 2.54 \mu\text{g/mL}$, $54.8 \pm 3.08 \mu\text{g/mL}$, $74.4 \pm 5.43 \mu\text{g/mL}$, and $84.9 \pm 1.45 \mu\text{g/mL}$ respectively ($p < 0.01$, Figure 6.15, Table 6.11). The Hop-62 cells depicted a decrease in cell size and morphology as compared to the control, after 24 h of treatment with EEBF and its biofractions (Figure 6.16). In the apoptosis study, MFBF confirmed $42.24 \pm 0.57 \%$ cells undergoing early apoptosis, while $4.61 \pm 0.88 \%$ in late apoptosis and $0.61 \pm 0.40 \%$ in necrosis stage, comparable to the standard Doxorubicin (Figure 6.17 and 6.18, Table 6.12). Cell cycle analysis depicted that MFBF showed a significant increase in cells from $0.68 \pm 0.13 \%$ to $11.95 \pm 0.33 \%$ in the sub- G_1 phase and $2.57 \pm 0.52 \%$ to $7.35 \pm 0.39 \%$ in S-phase, while decrease in cells from $90.13 \pm 0.55 \%$ to $75.08 \pm 0.79 \%$ in the $\text{G}_1\text{-G}_0$ phase and $6.55 \pm 0.40 \%$ to $5.63 \pm 0.27 \%$ in the $\text{G}_2\text{-M}$ phase as against the control ($p < 0.001$, Figure 6.19 and 6.20, Table 6.13), indicating that it induces apoptosis and cell cycle arrest of Hop-62 cells in the S phase. Apoptosis and cell cycle study of EFBF on Hop-62 cells, exhibited $36.42 \pm 1.15 \%$ cells in early and $6.71 \pm 0.5 \%$ cells in late apoptotic stages, arresting the cells in S-phase. All four MFBF isolates exhibited significant antiproliferative activity against Hop-62 cells, with shrinkage in cell size ($p < 0.05$, Figure 6.151 and 6.152, Table 6.69). Apoptosis study of the MFBF isolates at their GI_{50} concentrations showed that LMF2 (Kaempferol) induced significant activity with $23.03 \pm 0.37 \%$ cells in early apoptosis, $2.11 \pm 0.55 \%$ cells in late apoptosis and $0.51 \pm 0.37 \%$ cells in necrotic stage, as compared to the standard Doxorubicin ($p < 0.01$, Figure 6.153 and 6.154, Table 6.70). In cell cycle analysis, all the compounds exhibited an increased number of cells in the sub- G_1 phase while a reduced number of cells in the $\text{G}_1\text{-G}_0$ phase as compared to the control, thus indicating induction of apoptosis-mediated cell death. The percentage of cells in the S-

phase had increased from 2.57 ± 0.52 % to 4.45 ± 0.33 %, 6.55 ± 0.57 %, 5.60 ± 0.34 % and 5.54 ± 0.40 % with quercetin, kaempferol, isorhamnetin and β -Glucogallin respectively, with a decrease in cellular percentage in G₂-M phase, arresting the cells at the S-phase checkpoint ($p < 0.001$, Figure 6.155 and 6.156, Table 6.71). LME1 (Gardenin B), isolated from EFBF, demonstrated substantial antiproliferative activity with $GI_{50} = 21.91 \pm 0.83$ μ g/mL on Hop-62 cells ($p < 0.01$, Figure 6.159, Table 6.72). It induced necrosis of 10.57 ± 0.78 % cells, ($p < 0.001$, Figure 6.157 and 6.160, Table 6.73) with 15.89 % Hop-62 cells arrested in sub-G₁ phase ($p < 0.001$, Figure 6.158 and 6.161, Table 6.74). Amongst the extract EEHE and its biofractions tested against Hop-62 cells, TFHE and MFHE indicated considerable growth inhibition of $GI_{50} = 63.50 \pm 8.34$ μ g/mL and 58.5 ± 9.86 μ g/mL respectively, compared to the other experimental samples tested, while the extract EEHE and other biofractions displayed growth control at concentrations above 80 μ g/mL ($p < 0.01$, Figures 6.9 and 6.10, Table 6.8).

On the HeLa cell lines, EEBF, TFBF, and EFBF confirmed antiproliferative activity with $GI_{50} < 10$ μ g/mL, while MFBF showed $GI_{50} = 76.4 \pm 3.08$ μ g/mL as compared to the standard Cisplatin with $GI_{50} < 10$ μ g/mL ($p < 0.05$, Figure 6.21, Table 6.14). Upon treatment with EEBF and its biofractions, the HeLa cells reduced in size, and underwent significant changes in morphology. The cells became rounder and compact, which were comparable to the treatment with standard Cisplatin (Figure 6.22). EFBF subjected to apoptosis assay, exhibited significant activity with 11.09 ± 0.91 % cells in early apoptosis, while 16.38 ± 0.83 % in late apoptosis and 10.96 ± 0.85 % in necrosis stage, which was comparable to the standard Cisplatin. It was observed that Cisplatin exhibited 21.23 ± 0.85 % cells in early apoptosis, while 19.37 ± 0.76 % in late apoptosis and 3.99 ± 0.72 % in necrosis stage ($p < 0.001$, Figures 6.23 and 6.24, Table 6.15). EFBF caused HeLa cell cycle arrest in G₂-M phase and 23.62 ± 0.92 % cells in Sub-G₁ stage representing its apoptotic mode of action EEBF, TFBF and MFBF also induced profound apoptotic activity, against HeLa cell lines with accumulation of > 22 % cells in sub-G₁ phase ($p < 0.001$, Figures

6.25 and 6.26, Table 6.16). LME-1 (Gardenin B) isolated from EFBF, demonstrated antiproliferative activity on the HeLa cells with GI_{50} value of $16.69 \pm 0.39 \mu\text{g/mL}$ ($p < 0.01$, Figure 6.170, Table 6.78). It displayed significant apoptotic activity with $16.53 \pm 1.00 \%$ cells in early apoptosis and $7.22 \pm 0.86 \%$ cells in late apoptosis, and $3.40 \pm 1.01 \%$ in necrosis stages ($p < 0.001$, Figure 6.168 and 6.171, Table 6.79) producing cell cycle arrest in S-phase ($p < 0.001$, Figure 6.169 and 6.172, Table 6.80). MFBF isolates LMF 4 (β -Glucogallin) and LMF2 (Kaempferol) indicated remarkable antiproliferative activity against HeLa cell lines, with GI_{50} values of $10.03 \pm 0.67 \mu\text{g/mL}$ and $11.41 \pm 0.09 \mu\text{g/mL}$ respectively, while LMF 3 (Isorhamnetin) and LMF1 (Quercetin) inhibited cell growth at $12.31 \pm 0.10 \mu\text{g/mL}$ and $15.92 \pm 0.32 \mu\text{g/mL}$ respectively ($p < 0.01$, Figure 6.162 and 6.163, Table 6.75). All the compounds isolated from MFBF, induced apoptosis in $> 10 \%$ cells after 24 h of treatment ($p \leq 0.001$, Figure 6.164 and 6.165, Table 6.76), with accumulation of most cells in sub-G1 phase, compared to the control ($p < 0.01$, Figure 6.166 and 6.167, Table 6.77). However, EEHE and its biofractions (Figure 6.11 and 6.12, Table 6.9), did not show antiproliferative activity below $80 \mu\text{g/mL}$, indicating less antiproliferative potential against cervical cancer, and hence were not considered for apoptosis and cell cycle analysis.

EEHE, its biofractions (Figures 6.27 and 6.28, Table 6.17), EEBF, its biofractions (Figures 6.29 and 6.30, Table 6.18) and the isolated compounds (Figures 6.173, 6.174, 6.175, and 6.176, Tables 6.81 and 6.82) did not show signs of toxicity against the normal cells tested, indicating their safety against non-cancerous cells. The phytoconstituents may activate pro-Caspases or cause up-regulation of pro-apoptotic genes like Bax, p53 etc. or down-regulation of expression of anti-apoptotic genes like Bcl-2, cyclinD1, which could facilitate apoptosis and/or trigger cell cycle arrest. ^[242]

To investigate the mechanism and detailed intermolecular interactions between the phytoconstituents, molecular docking studies were performed on the crystal structure of

Human caspase-3 using the surflex-dock programme of Sybyl-X 2.0 software. All the compounds demonstrated consensus scores in the range of 7.00-2.65, indicating the summary of all forces of interaction between ligands and the active site of the enzyme. The studied compounds exhibited the same type of interaction with amino acid residues (THE250, SER209, ARG207, TYR204) as that of the standard doxorubicin drug. The detailed intermolecular interactions of the individual compounds with the Human caspase-3 enzyme, have been explained in section 6.2.12.1.

The characteristics of apoptosis were also further confirmed by *in vitro* activation of caspase-3 enzyme and determination of the DNA ladder which is a result of DNA fragmentation and indicative of late stage of apoptosis. *In vitro*, caspase-3 activation studies and DNA fragmentation studies revealed that amongst the compounds isolated from *H. enneaspermus*, LMH3 (Hesperidin) significantly upregulated caspase-3 activity in 29.40 ± 1.06 % cells and caused DNA fragmentation in 19.60 ± 0.92 % HeLa cells, comparable to standard drug Doxorubicin used, thus clearly demonstrating its apoptotic mechanism of action ($p < 0.01$, Figure 6.177 and 6.179). Amongst the compounds isolated from *B. foveolata* Dalzell., LME1 (Gardenin B) significantly upregulated caspase-3 activity in 49.53 ± 0.61 % cells and caused DNA fragmentation in 40.47 ± 1.30 % HeLa cells comparable to standard drug Cisplatin ($p < 0.01$, Figure 6.178 and 6.180). The effect of LME1 on Bcl-2 gene expression on Hela cells was investigated by RT-PCR technique. LME1 at doses of 8 μ g, 16 μ g and 24 μ g significantly downregulated Bcl-2 gene expression and upregulated p53 and Bax genes comparable to the standard Cisplatin ($p < 0.01$, Figure 6.181, Table 6.83).

Plant extracts have been proven to be strong candidates in the treatment of various types of cancer via modulating apoptotic pathway. The major mechanism involves the activation of apoptotic proteins intrinsically and extrinsically and induction of DNA damage. Additionally, studies demonstrated that phytoconstituents like phenolics,

flavonoids, tannins, nitrogen-containing compounds and triterpenes have good anticancer potential. Isoflavones like daidzein, genistein etc., inhibit proliferation and induce apoptosis of cancer cells; epigallocatechin gallate, a polyphenolic catechin suppresses growth and angiogenesis while increasing apoptosis; flavonols (quercetin, kaempferol etc.) and phytochemicals like resveratrol, lignans and curcumin possess antiproliferative activities.^[242, 251] From the earlier reports, it was observed that Quercetin induced apoptosis of cancer cells by up-regulating the expression of the Bax gene and down-regulating the expression of Bcl-2. Kaempferol was reported to have anticancer properties by inhibiting cell proliferation, inducing cell cycle arrest and apoptosis, and suppressing cell invasion and migration in diverse cancers, e.g., colorectal cancer, breast cancer, melanoma and hepatoma. Isorhamnetin has been reported to induce apoptosis and arrest the cell cycle at the G₂/M phase or S-phase in different cancer cells, depending on the type of cancer cell line. In one study, Gardenin B-induced cell death in human leukemia cells involving significant induction of multiple caspases viz. caspase-2, caspase-3, caspase-8 and caspase-9 activities. Thus, the anticancer activity of the extracts, biofractions and isolated compounds from the selected plants may be attributed primarily to the flavonoid mode of apoptotic action, without inflammation of neighbouring cells.^[242,252-255]

In vivo acute toxicity studies of the ethanolic extract of *H. enneaspermus* (EEHE) confirmed that it was safe up to 5000 mg/Kg BW.^[65] The acute toxicity study trials conducted on rats treated with ethanolic extract of *B. foveolata* (EEBF) administered up to a dose level of 5000 mg/Kg revealed that no adverse or clinical toxicity was observed in any of the study group of animals. Hence EEBF was confirmed to be safe up to 5000 mg/Kg BW. The extracts EEHE and EEBF and their biofractions ITHE and ITBF were further subjected to *in vivo* antianxiety efficacy studies at doses of 100, 200 and 400 mg/Kg BW.

In vivo anxiolytic analysis of different doses of EEHE, ITHE, EEBF and ITBF was performed using behavioural animal models viz. EPM, LDT, MCT, Holeboard and

Optovarimex tests, 1 h after drug administration and 2 h post-self-isolation. The screening models used were traditional and accepted models, regularly employed to screen anxiety-modulating drugs. Furthermore, the isolation of rats individually in cages 2 h before the experiment enhanced fear and anxiety-like behaviour when placed in the animal models.

The EPM model takes advantage of the conflict between the rodents' natural desire to explore and their apprehension of heights and open areas. However, the LDT and MCT models explore the conflict between the desire to investigate new environments and the aversion to open bright and mirrored spaces. An increase in the number of entries in the lightbox or mirrored chamber, with an increase in time spent in the lightbox or mirrored chamber, indicates anxiolytic activity. The HBT and Optovarimex models analyzed the exploratory and locomotor activities of the rats and correlated with the anxiogenic or anxiolytic potential of the therapy. The more the exploratory behaviour of the animal, the lesser the anxiety. Conversely, the animal is more anxious if it does not show signs of exploration, head dips or locomotor activity.^[211-217]

The repeated dosing with EEHE, ITHE, EEBF, and ITBF demonstrated considerable anxiolytic potential in rats using the various screening models, through the 30-day trial. ITHE and ITBF, at doses of 400 mg/kg BW, demonstrated a significant reduction in anxiety levels in all experimental models, comparable to standard Diazepam.

There was a significant increase in exploratory activity observed in EPM, compared to the rats in the control group during the respective treatment weeks (T2, T3, T4 and T5). The number of open-arm entries in the elevated plus maze apparatus exhibited an increasing trend from the second week of treatment with EEHE and ITHE, at 100, 200 and 400 mg/Kg BW. A significant increase in the number of open arm entries was observed in the fifth week of treatment with all three doses of EEHE and ITHE as compared to the control. In the fifth week of treatment, EEHE at 100, 200 and 400 mg/Kg exhibited 6.34 ± 4.37 , 10.06

± 4.85 and 15.39 ± 3.54 number of open arm entries respectively. While, ITHE at 100, 200 and 400 mg/Kg exhibited 10.61 ± 4.92 , 12.59 ± 4.77 and 18.41 ± 8.95 respectively. There was nearly a three-fold increase in number of open arm entries observed from the first to the fifth week of treatment with EEHE and ITHE. EEBF at all doses produced a considerable increase in open arm entries in the EPM from the first to the fourth week of treatment. ITBF at 100, 200 and 400 mg/Kg exhibited a dose dependent increase in open arm entries from the second week till the fifth weeks of treatment with over triple the number of entries observed from the first to fifth week with 100 mg/Kg and 400 mg/Kg BW of ITBF. ITBF at 400 mg/kg BW demonstrated 16.28 ± 9.80 open arm entries, in the fifth week of treatment. EEHE, ITHE, EEBF and ITBF were able to increase the percent time spent by the rats in the open arm. A significant dose dependent increase in percentage of time spent in open arm was observed with EEHE in the third, fourth and the fifth weeks of treatment as compared to the control, while ITHE displayed an increase in the fourth and fifth weeks of treatment ($p < 0.05$). EEBF at all doses produced a substantial dose dependent response in increased percent time spent in open arms in all weeks of treatment. ITBF at all doses were also found to exhibit an increase in percent time in open arm from first to last weeks of treatment (Figures 6.31- 6.34, Tables 6.22 - 6.25).

In the LDT, EEHE, ITHE, EEBF, and ITBF revealed substantial exploration by the rats in the lightbox area with increased number of lightbox entries and percent time spent in light box, from the second to the fifth weeks of treatment. In the fourth and fifth weeks of treatment, EEHE depicted significant increase ($p < 0.05$) in the number of light box entries, as compared to the control, with the highest number of 7.17 ± 1.13 and 9.83 ± 3.93 entries observed with EEHE 100 and 200 mg/Kg BW in fourth week of treatment and 10.33 ± 3.14 light box entries with EEHE 400 mg/Kg BW in fifth week of treatment. ITHE at 400 mg/kg BW exhibited an increased number (9.67 ± 3.44) of light chamber entries, in the fifth week of treatment. Also, a dose dependent activity was observed with all its three doses in the third to fifth weeks of treatment. EEBF and ITBF at 100, 200 and 400 mg/Kg

demonstrated an increase in number of light box entries from the second week onwards. EEBF at 400 mg/Kg BW displayed 7.50 ± 3.15 , 8.37 ± 3.22 and 10.83 ± 2.36 number of light box entries in the third, fourth and fifth weeks respectively. ITBF at 400 mg/kg BW demonstrated highest number of light chamber entries (18.11 ± 9.34). EEHE and ITHE at all doses displayed a significant increase in the percentage of time spent in light box in a dose dependent manner as compared to the control at the third, fourth and fifth week of the treatment. EEBF and ITBF also displayed an increase in the percentage of time spent in light box from second week till the fifth week, with a dose dependent activity observed in the fifth week of treatment. The behavioural analysis confirmed that the extracts exhibited anxiolytic activity in the LDT model ($p < 0.05$, Figures 6.35- 6.38, Tables 6.26 - 6.29).

MCT is based on an approach-avoidance conflict between exploring novel environments and avoiding the mirror chamber since the ability to recognize itself in the mirror is absent in most animals. The animal is afraid looking at itself in the mirror, as it perceives it to be another animal and this behaviour is reflected in the reduced number of mirror chamber entries and duration of time spent in the mirror chamber. EEHE did not produce a significant increase in the number of mirror chamber entries as compared to the control. However, it was observed that, ITHE at doses of 100, 200 and 400 mg/Kg BW produced a dose-dependent increase in mirror chamber entries in the first, third and fifth weeks of treatment. In the fifth week of treatment, ITHE at 400 mg/kg BW displayed highest number of entries in the mirror chamber i.e. 17.55 ± 4.64 . EEBF at 100, 200 and 400 mg/kg BW depicted a slight increase in number of mirror chamber entries, in a dose dependent in the first week of treatment. ITBF at 100, 200 and 400 mg/kg BW revealed a dose dependent increase in the number of mirror entries in the third week of treatment. ITBF 400 mg/Kg exhibited an increasing trend of 8.75 ± 3.37 , 11.45 ± 3.88 and 15.52 ± 8.16 number of mirror entries from the third to the fifth week respectively. Similar to the increase in number of mirror chamber entries, ITHE at the three respective doses produced increased percent time spent in the open arm in a dose dependent manner during the five-

week trial period. The percent time spent in the mirror chamber by the groups treated with EEBF and ITBF gradually increased by the third to the fifth weeks of treatment, indicating extended anxiolytic effect over a period ($p < 0.05$, Figures 6.39- 6.42, Tables 6.30 - 6.33).

The HBT measures anxiety, neophilia and emotional behaviour in rodents. Head dipping is commonly defined as when the rodent puts its head into the hole with its ears immersed. In the first two weeks of experimentation, there were few number of head dips and exploration, which gradually increased from the third to the fifth week of treatment with EEHE and in the fifth week of treatment with ITHE. A dose dependent increase in number of head dips was observed with ITHE 100, 200 and 400 mg/Kg BW in the third and fifth weeks of treatment. In the third week of treatment, ITHE at a dose 400 mg/kg BW exhibited 17.67 ± 5.21 number of head dips which increased to 32.83 ± 5.45 numbers in the hole board test, depicting increased neophilic activity. EEBF and ITBF did not exhibit a considerable increase in head dips in the first two weeks of treatment. Moreover, a gradual increase in head dips was observed by the fourth week, which was subsequently reduced in the fifth week of treatment. However, ITBF at 400 mg/Kg BW depicted an increase in head dip count in the third to the fifth week with significant neophilic activity of 17.33 ± 6.02 and 21.71 ± 11.27 head dips observed in fourth and fifth weeks respectively, as compared to the control ($p < 0.05$, Figures 6.43, 6.44, Tables 6.34, 6.35).

The Optovarimex or autotrack apparatus measures locomotor activity in rodents. The distance travelled and ambulatory time of the animals treated with EEHE, ITHE, EEBF and ITBF were evaluated at the end of each week of treatment, for five weeks. Overall, all three doses of the extracts did not exhibit significant decrease in locomotor activity in the first two weeks of experimentation. However, an eventual reduction in locomotor activity was observed in the third, fourth and fifth weeks of treatment as compared to the control, indicating CNS depressant action. ITHE at 400 mg/kg caused significant reduction ($p < 0.05$) in the distance travelled by the rats in the autotrack apparatus with $505.00 \pm$

130.22 cm compared to the control (1107.33 ± 178.86 cm) and standard Diazepam (562.83 ± 69.11) in the fifth week of treatment. ITBF at 200 and 400 mg/kg caused reduction in the distance travelled from the first week onwards. ITBF exhibited decrease in distance travelled with 586.67 ± 134.50 cm and 691.83 ± 104.30 cm comparable to the standard Diazepam (653.60 ± 72.48) in the third week of treatment. The ambulatory time of rats treated with EEHE, ITHE, EEBF and ITBF at doses of 100, 200 and 400 mg/Kg BW, reduced gradually till the fifth week of treatment ($p < 0.05$, Figures 6.45- 6.48, Tables 6.36 - 6.39).

From the *in vivo* antianxiety studies, it was confirmed that EEHE, ITHE, EEBF and ITBF possessed anxiolytic activity which developed gradually over a period of weeks and was more apparent after three to five weeks of treatment in the behavioural models. ITHE and ITBF at doses of 400 mg/Kg BW, displayed considerable anxiolytic activity during the 30-day trial period. Hence the groups of rats (VIII and XIV) treated with these biofractions were subjected to isolation of brain and estimation of levels of neurotransmitters and antioxidant enzymes expressed in the sectioned brain tissue homogenates.

The development of anxiety disorders comprises changes in various brain regions, which coordinate cognitive, autonomic, motor, and endocrine systems. The cerebral cortex, hippocampus, cerebellum, pons, and medulla oblongata were analysed due to their reported involvement in anxiety and behavioural disorders. Numerous neurotransmitters serve as channels for communication between these components. In anxiety disorders, several neurotransmitter systems are affected. These changes primarily involve baseline neurotransmitter levels, receptor expression and signaling, and enzymatic modulation in various brain areas. Studies have shown that specific neuropeptides and neurotransmitters, including monoamines (NE, DA, and 5-HT), amino acids (L-glutamate, GABA, and glycine), steroids (cortisol), and cholecystokinin, can generate anxiety. ^[256]

GABA (Gamma-aminobutyric acid) is a major inhibitory transmitter that calms neurons and is primarily found in the cerebellum, brainstem etc. GABA has been demonstrated to reduce anxiety and stress and increase the production of alpha waves in the brain. These are accompanied by increased relaxation. The neurotransmitter Glutamate functions in providing a physiological equilibrium with GABA. GABA and glutamate account for 90 % of all neurotransmissions. One of the causes of anxiety could be an imbalance in the GABA-Glutamate homeostasis (for example, glutamate excitotoxicity). The fundamental function of the glutamate pathway is associated with anxiety conditions and stress response. Increased levels of glutamate were observed in the hippocampus and other regions of the brain. Chronic state of stress releases glucocorticoids, which can damage hippocampal and other brain cells due to increased glutamate levels and excitotoxicity. [48]

ITHE, ITBF, and diazepam treatment restored the normal levels of glutamate, indicating the presence of various phytoconstituents in ITHE and ITBF that affect the glutamatergic pathway. Previous studies have shown that acute and repetitive immobilisation, social isolation and cold stress decrease GABA levels in the cortex, hypothalamus, and olfactory bulb regions. [257,258] In the stress control group, GABA levels were reduced in the cortex, hippocampus, and brain stem. The alteration in the expression of the GABA-synthesising enzymes, particularly glutamic acid decarboxylases, may have promoted GABAergic activity. [38,48]

ITHE potentiated GABA levels in the cerebral cortex ($143.87 \pm 8.16 \mu\text{g/g}$), hippocampus ($162.02 \pm 9.40 \mu\text{g/g}$), cerebellum ($177.00 \pm 7.75 \mu\text{g/g}$), followed by pons, medulla oblongata and the remaining tissue homogenate. ITBF at 400 mg/Kg significantly potentiated GABA levels ($p < 0.01$) as compared to the control in all sections of the brain with highest levels observed in the pons and medulla oblongata section ($127.27 \pm 5.62 \mu\text{g/g}$), hippocampus ($124.87 \pm 7.79 \mu\text{g/g}$) and remaining collective tissue homogenate

(124.17 ± 11.47 µg/g) (Figure 6.57, Table 6.48).

The biofractions also significantly reduced glutamate levels in the hippocampus with ITHE and ITBF exhibiting 361.75 ± 6.72 µg/g and 397.67 ± 7.36 µg/g levels respectively, comparable to standard Diazepam that exhibited reduction in glutamate levels to 328.00 ± 7.11 µg/g from the stress control group that depicted glutamate levels of 608.51 ± 11.34 µg/g. The glutamate levels were also reduced in the pons and medulla oblongata, cerebellum, and other regions of the brain ($p < 0.01$, Figure 6.58, Table 6.49).

Medicinal plants like *Ginkgo biloba*, *Centella asiatica*, *Melissa officinalis* etc. exhibited similar anxiolytic activity. An extensive study on Valerian revealed that its extract could cause CNS depressant action, by increasing the GABA levels in the brain. GABA, in large quantities, can cause a sedative effect. Natural herbs/herbal mixtures that act synergistically promise an effective remedy for anxiety. This suggests that the extracts relieve anxiety symptoms potentially due to phytoconstituents that impact the GABAergic pathway [63,259].

Stressful procedures led to a decrease in the levels of 5-HT and DA in the brain. [258,260] ITHE and ITBF 400 mg/kg treatment resulted in a significant increase in the levels of DA, 5-HT and NE in all regions of the brain, compared to stress control animals. ITHE 400 mg/kg significantly increased the levels of nor adrenaline in the hippocampal tissue homogenate (359.74 ± 6.85 ng/g), while ITBF 400 mg/kg also increased nor adrenaline levels to 327.39 ± 8.29 from 161.84 ± 7.52 ng/g as observed in the stress control group. ITHE and ITBF 400 mg/Kg were also found to increase the levels of nor adrenaline in the pons and medulla oblongata, cerebral cortex and cerebellum almost comparable to the standard diazepam ($p < 0.01$, Figure 6.54, Table 6.45).

The neurotransmitter dopamine levels in the brain were significantly increased by

ITHE 400 mg/Kg BW as compared to the control. Highest levels of dopamine were observed in the cerebellum (291.31 ± 7.46), followed by collective tissue homogenates (276.58 ± 5.40 ng/g), cerebral cortex (267.96 ± 4.59 ng/g), pons and medulla oblongata and hippocampal homogenates. ITBF 400 mg/Kg BW, remarkably increased the dopamine levels in the cerebellum (336.73 ± 8.95 ng/g), followed by other regions. The dopamine levels were significantly higher than that exhibited by Diazepam (205.86 ± 8.27 ng/g) in the cerebellum ($p < 0.01$, Figure 6.55, Table 6.46). The neurotransmitter serotonin levels were significantly increased in the hippocampal tissue homogenates by ITHE 400 mg/Kg (355.50 ± 6.78 ng/g), and ITBF 400 mg/Kg (371.21 ± 4.52 ng/g) as compared to the control and standard that exhibited serotonin levels of 186.95 ± 6.68 ng/g and 211.27 ± 11.44 ng/g respectively ($p < 0.01$, Figure 6.56, Table 6.47).

Thus, the overall results indicate that ITHE and ITBF at 400 mg/kg BW demonstrated a significant increase in expression of GABA levels in the cerebral cortex, hippocampus, pons, medulla oblongata and cerebellum as compared to the control and other treatments. These biofractions also affected the neurotransmission of NE, 5-HT, and DA and reduced glutamate neurotransmitter levels in the brain. As the ITHE and ITBF fractions were enriched with flavonoids and the compounds isolated from these included Quercetin, rutin and Hesperidin from ITHE and Quercetin, Kaempferol, Isorhamnetin and Galloyl glucose and Gardenin - B from ITBF. Flavonoids are known for their antianxiety effects. Benzodiazepine receptors activation by flavonoids has been proposed for the antianxiety responses produced by different flavonoids. The literature survey reveals that most of these compounds have anxiolytic potential. Quercetin, Kaempferol, and Gallic acid have been previously reported for their anxiolytic activity. ^[41,56,261,262]

During oxidative stress, antioxidant levels are reduced, which contributes to a variety of disorders. Antioxidants in the brain may be beneficial in reducing oxidative damage of the neuronal cells with the maintenance of cellular integrity. Glutathione is a

key antioxidant involved in the cellular defense of the body. Other important antioxidant enzymes include catalase, superoxide dismutase etc. In healthy cells and tissue, 90 % of the total glutathione is present in the reduced form (GSH). The enzyme glutathione reductase is responsible for the conversion of glutathione from the oxidized state to the reduced state by NADPH. [17]

Glutathione reductase maintains the supply of reduced glutathione, antioxidant defense, redox balance, regulation of various proteins, and nucleotide metabolism. Glutathione peroxidase maintains the integrity of the blood-brain barrier (BBB). It scavenges and inactivates the hydrogen and lipid peroxides, thereby protecting the body against oxidative stress. Glutathione-S-transferase detoxifies toxic substances, e.g. drugs and carcinogens, xenobiotics etc. and prevents their interaction with vital nucleic acids and cellular protein. Catalases oxidize ethanol to acetaldehyde within the brain and remove H₂O₂ by forming H₂O and O₂ by catalytic reaction. SOD reduces the effect of superoxide radicals by converting superoxide to less harmful peroxide. [15-17]

Glutathione levels depleted in stress control group of rats were elevated in groups. Diazepam (2 mg/kg) showed significantly ($p < 0.05$) higher glutathione levels. Levels of GSH enzymes viz., glutathione s-transferase, glutathione peroxidase and glutathione reductase were also significantly elevated ($p < 0.05$) in ITHE and ITBF treated groups of rats as compared to the control.

Elevated levels of Glutathione-S-transferase were observed in the hippocampal homogenates after treatment with ITHE 400 mg/Kg (15.69 ± 2.14 U/mg of protein) and ITBF 400 mg/Kg (13.17 ± 1.45 U/mg of protein) as compared to stress control and diazepam group of rats i.e. 9.58 ± 1.70 U/mg of protein and 13.47 ± 2.83 U/mg of protein respectively ($p < 0.05$, Figure 6.51, Table 6.42). Glutathione peroxidase levels were potentiated in the cerebral cortex and pons and medulla oblongata. In the cerebral cortex,

ITHE 400 mg/Kg elevated the levels to 0.07 ± 0.01 U/mg of protein, while ITBF 400 mg/Kg elevated the glutathione peroxidase levels to 0.06 ± 0.02 U/mg of protein, compared to the stress control group that exhibited levels of 0.04 ± 0.02 U/mg of protein. ITHE and ITBF increased the glutathione peroxidase levels to 0.06 ± 0.02 and 0.04 ± 0.01 U/mg of protein respectively, in the pons and medulla oblongata tissue homogenates ($p < 0.05$, Figure 6.52, Table 6.43). Glutathione reductase enzyme levels were significantly increased in all regions of the brain tissue homogenates ($p < 0.05$), as compared to the control, with highest levels observed in the pons and medulla oblongata tissue homogenates. ITHE and ITBF elevated the glutathione reductase levels to 3.67 ± 0.31 and 3.29 ± 0.35 U/mg of protein respectively in these regions ($p < 0.05$, Figure 6.53, Table 6.44).

Catalase and superoxide dismutase endogenous antioxidant enzymes which neutralize free radicals also demonstrated increased levels in ITHE, ITBF and Diazepam ($p < 0.05$) treated groups. ITHE at 400 mg/Kg significantly increased ($p < 0.05$) the levels of catalase enzymes as compared to the control, in all the regions of the brain. Highest levels of catalase were observed in the cerebral cortex (11.45 ± 1.01 U/mg of protein) and hippocampal tissue (10.79 ± 2.46 U/mg of protein) homogenates post treatment with ITHE. ITBF depicted elevated levels of catalase in the cerebral cortex (10.39 ± 1.92 U/mg of protein) and hippocampal tissue (9.94 ± 2.96 U/mg of protein) homogenates ($p < 0.05$, Figure 6.49, Table 6.40). Superoxide dismutase enzyme levels were also significantly elevated ($p < 0.05$) in all the regions of the brain in the ITHE and ITBF treatment groups as compared to the control, with highest levels observed in the hippocampal and cerebellum tissue homogenates (Figure 6.50, Table 6.41).

Thus, by potentiating the endogenous antioxidant levels like SOD, catalase, glutathione peroxidase, glutathione reductase, glutathione-s-transferase etc., ITHE and ITBF may aid in modulating oxidative stress and combating anxiety. The therapeutic virtues may be attributed to the presence of flavonoids. ^[263,264]

Long-term stress is thought to indirectly disrupt the benzodiazepine-GABA receptors. Most of the physiological actions of GABA are produced by GABA_A receptors in the brain, where 17-20 % of all neurons are GABAergic. The GABA_A receptors are targets for several drugs, viz. agonists, partial agonists, inverse agonists and antagonists of GABA. The binding of the agonist to the receptor site or modulatory sites of the GABA_A receptors subunits increases the opening of the chloride ion channel in response to GABA. The influx of chloride ions through the ion channels hyperpolarises the membrane, thereby producing an inhibitory effect and facilitating anxiolysis.^[38, 48]

In silico molecular docking analysis was performed to observe the detailed intermolecular interactions of the phytoconstituents isolated from both the plants with the GABA_A receptor. The phytoconstituents isolated from the fractions displaying significant activity were docked with the BZD binding site of the human GABA_A receptor alpha1-beta2-gamma2 subtype to deduce the mechanism of action. Docking studies with Surflex-Dock showed that the compounds occupied the same binding sites as that of standard Diazepam. All the compounds exhibited consensus scores in the range of 7.75 - 5.65, indicating the summary of all forces of interaction between ligands and the receptor, showing the same type of interaction with amino acid residues (THR207, THR142) as that of standard drug. The detailed intermolecular interactions of the individual compounds with the Human GABA_A receptor, have been explained in section 6.2.10.2. Thus, from this evaluation, it can be corroborated that the anxiolytic effect of the biofractions may be attributed to the flavonoids present which primarily act by modulating the GABA_A-BZD-Cl⁻ ion channel receptor to mediate the inhibitory effect, through hyperpolarisation of the neuronal cells caused due to influx of Cl⁻ ions.

Thus the antioxidant, anticancer and anxiolytic activities of the extracts and biofractions of *H. enneaspermus* and *B. foveolata* may be accredited to the phytoconstituents, chiefly flavonoids present in them^[265].



CHAPTER – VIII

CONCLUSION

8. CONCLUSION

Plants have been used in traditional medicine systems for health and therapeutic benefits. The World Health Organisation (WHO) states that herbal medicines still play a key role in medical treatment in developing nations. As an alternative approach, complementary and alternative medicines are gaining popularity, especially in developing countries, due to their safety profile, cultural acceptability and being used to manage various pathological conditions. Numerous studies indicate that combining conventional therapies with natural products, provide better efficacy, additive or synergistic therapeutic benefits with reduced side effects, and drug resistance.

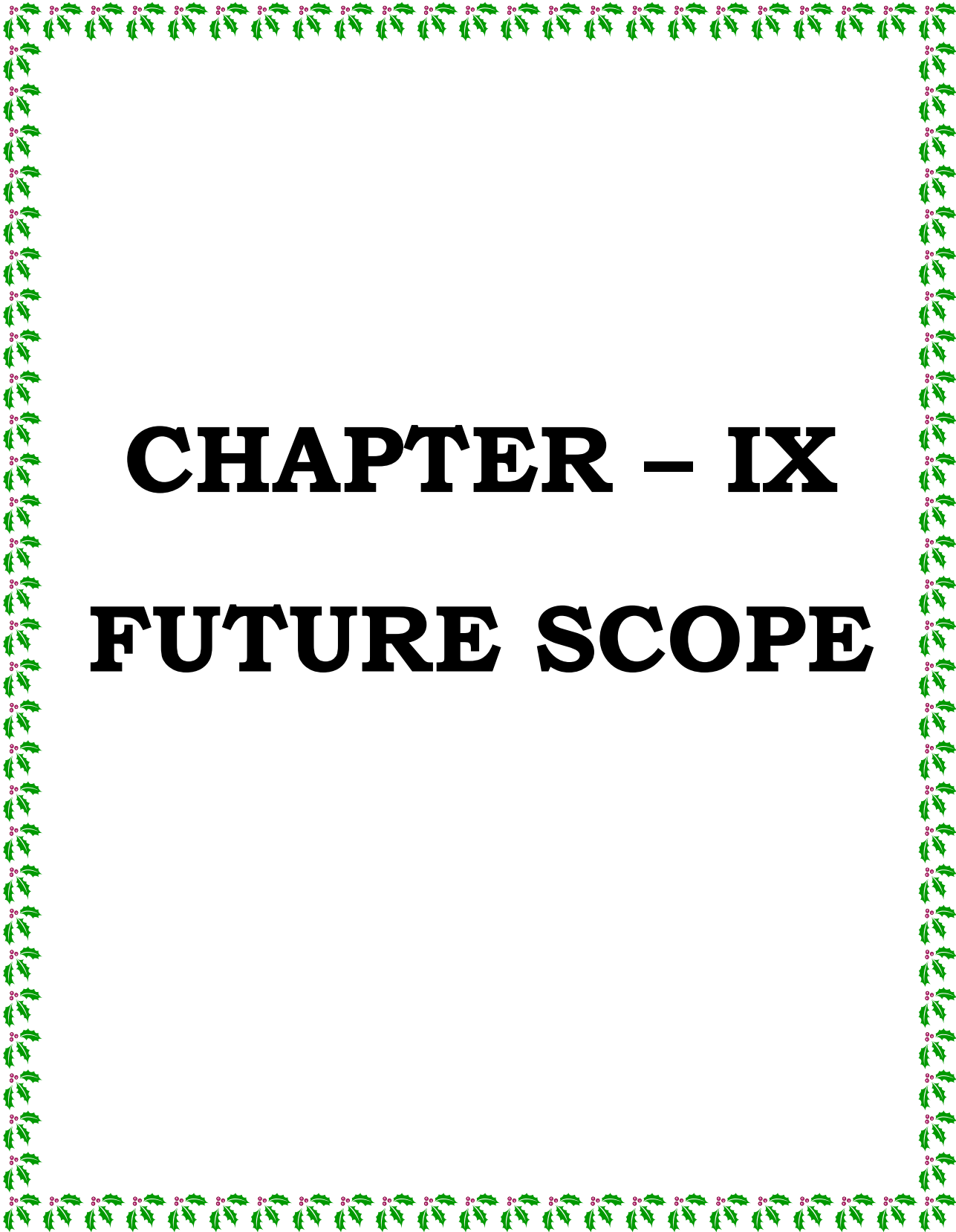
The phytochemical and pharmacological investigation of the selected plants *H. enneaspermus* and *B. foveolata* revealed that these plants are rich reservoirs of potential phytoconstituents with substantial amounts of flavonoids and phenolics, and have displayed prominent antioxidant, anticancer and antianxiety properties. The ethanolic extracts and biofractions of *H. enneaspermus* and *B. foveolata* demonstrated significant antioxidant activities in the *in vitro* DPPH, H₂O₂, NO and ABTS free radical scavenging assays, accrediting this property to the presence of phenolics and flavonoids.

The *in vitro* anticancer activity was evaluated using antiproliferative, apoptotic, cell cycle and gene expression analysis. The ethanolic extract, biofractions and three isolated compounds *viz.* quercetrin, rutin and hesperidin from *H. enneaspermus* demonstrated remarkable cytotoxic activity against breast cancer (MCF-7) cells and hence may be promising agents for mammary tumor therapy. The ethanolic extract, biofractions and five compounds *viz.* quercetin, kaempferol, isorhamnetin, β -glucogallin and Gardenin B isolated from *B. foveolata* exhibited remarkable cytotoxic activity against cervical cancer (HeLa) and lung cancer (Hop-62) cell lines and hence may be considered as potential therapeutic candidates to alleviate cervical and lung cancer by apoptotic mechanisms. Additionally, activation of caspases (caspase-3), DNA fragmentation, downregulation of Bcl-2 gene and

upregulation p53 and Bax genes expression validate the claim. Since apoptosis causes cellular death by non-inflammatory processes, the enriched bioactive components of *H. enneaspermus* and *B. foveolata* may be regarded as safe and effective therapeutics for cancer therapy.

The *in vivo* antianxiety study demonstrated anxiolytic activity of *H. enneaspermus* and *B. foveolata*, with the probable mechanism of action using five well-established animal models (EPM, LDT, MCT, HBT, AT), estimation of neurotransmitters and enzymes and *in silico* docking studies. The insoluble toluene biofractions of ethanolic extracts of *H. enneaspermus* and *B. foveolata* revealed a significant reduction in anxiety in most animal models. Reduced GABA and increased glutamate levels were observed in the hippocampal, cerebral cortex, cerebellum, pons, medulla oblongata regions of the brain, following chronic exposure to stressful environments thus triggering anxiety, neuronal damage, and oxidative stress. However, treatment with ITHE and ITBF for a month resulted in mitigation of anxiety, by increasing the levels of GABA, attenuating glutamate, and potentiating other neurotransmitters (GABA, NE, 5-HT, DA) and antioxidant enzymes in the brain. The 30-day treatment with the ITHE and ITBF at 400 mg/kg BW, produced a considerable increase in monoamines and GABA neurotransmitter levels, suggesting that their anxiolytic effects are mainly and plausibly mediated by activation of GABAergic receptor complex and influx of Cl⁻ ions thereby leading to hyperpolarization of neuronal cells.

The flavonoid compounds isolated from *H. enneaspermus* and *B. foveolata* exhibited significant *in silico* intermolecular interactions and docking scores with the Caspase-3 enzyme and GABA-A receptor, highlighting the anticancer and anxiolytic modes of action at the molecular level. The enriched phytoconstituents of *H. enneaspermus* and *B. foveolata* have exhibited the ability to modulate oxidative stress, mitigating cancer, anxiety thereby aiding in improving patient's quality of life. Thus, the study effectively concludes that the selected plants are rich medicinal reservoirs with potential health benefits.



CHAPTER – IX

FUTURE SCOPE

9. FUTURE PROSPECTIVE

The present study enlightened the development of therapeutic drugs using traditional and modern knowledge for the treatment of cancer and anxiety.

However, the following aspects can be explored in the future to confirm their significance in treating these ailments.

1. To undertake standardization and quality control studies of *H. enneaspermus* and *B. foveolata* extracts, biofractions and isolated compounds as per international guidelines.
2. To promote cultivation, cell culture techniques and use of other scientific approaches to save the species of *H. enneaspermus* and *B. foveolata*, as *H. enneaspermus* is a seasonal plant and *B. foveolata* is an endangered species.
3. Preparation of different formulations based on the synergistic effect of the phytoconstituents and confirming their efficacy.
4. Structural modification of the isolated compounds with enhanced pharmacological and biological properties and further compare and evaluate the efficacy.
5. Preclinical study using animal models for validating anticancer activity.
6. Clinical trials in patients suffering from breast, cervical and lung cancer and anxiety.
7. Marketing the formulations in various dosage forms and promoting the drugs internationally.



CHAPTER – X

REFERENCES

10. REFERENCES

1. Hostettmann K, Marston A. Twenty years of research into medicinal plants: results and perspectives. *Phytochem. Rev.* 2002; 1:275-85. DOI: 10.1023/A:1026046026057.
2. Fridlender M, Kapulnik Y, Koltai H. Plant derived substances with anti-cancer activity: from folklore to practice. *Front. Plant Sci.* 2015;6:799. DOI: 10.3389/fpls.2015.00799.
3. Salmerón-Manzano E, Garrido-Cardenas JA, Manzano-Agugliaro F. Worldwide research trends on medicinal plants. *Int. J. Environ. Res. Public Health.* 2020;17(10):3376. DOI: 10.3390/ijerph17103376.
4. Jamshidi-Kia F, Lorigooini Z, Amini-Khoei H. Medicinal plants: Past history and future perspective. *J. Herbm. Pharmacol.* 2017;7(1):1-7. DOI: 10.15171/jhp.2018.01.
5. Phillipson JD. Phytochemistry and medicinal plants. *Phytochemistry.* 2001;56(3):237-43. DOI: 10.1016/S0031-9422(00)00456-8.
6. Sen S, Chakraborty R. Toward the integration and advancement of herbal medicine: a focus on traditional Indian medicine. *Botanics.* 2015;5:33-44.
7. Sofowora A. Research on medicinal plants and traditional medicine in Africa. *J Altern. Complement. Med.* 1996;2(3):365-72. DOI: 10.1089/acm.1996.2.365.
8. Taylor JL, Rabe T, McGaw LJ, Jäger AK, VanStaden J. Towards the scientific validation of traditional medicinal plants. *Plant Growth Regul.* 2001;34:23-37.
9. Saxena M, Saxena J, Nema R, Singh D, Gupta A. Phytochemistry of medicinal plants. *J. Pharmacogn. Phytochem.* 2013;1(6):168-82. DOI: 10.1089/acm.1996.2.365
10. Azwanida NN. A review on the extraction methods use in medicinal plants, principle, strength and limitation. *Med. Aromat. Plants.* 2015;4(3):1000196.
11. Kamdem JP, Adeniran A, Boligon AA, Klimaczewski CV, Elekofehinti OO, Hassan W, *et al.* Antioxidant activity, genotoxicity and cytotoxicity evaluation of lemon balm

- (*Melissa officinalis* L.) ethanolic extract: Its potential role in neuroprotection. *Ind. Crops Prod.* 2013;51:26-34. DOI: 10.1016/j.indcrop.2013.08.056.
12. Pham-Huy LA, He H, Pham-Huy C. Free radicals, Antioxidants in disease and health. *Int. J. Biomed. Sci.* 2008;4(2):89-96.
 13. Mohan H. Textbook of pathology. 7th ed. India: Jaypee Brothers Medical Publishers; 2015.
 14. Sundaram SS, Shukla AK. Free radicals versus antioxidants. Potential therapeutic applications of nano-antioxidants. Singapore: Springer; 2021. p.28-30.
 15. Aravind P, Prasad MN, Malec P, Waloszek A, Strzałka K. Zinc protects *Ceratophyllum demersum* L. (free-floating hydrophyte) against reactive oxygen species induced by cadmium. *J. Trace Elem. Med. Biol.* 2009;23(1):50-60. DOI: 10.1016/j.jtemb.2008.10.002.
 16. Prasad AS, Bao B, Beck FW, Kucuk O, Sarkar FH. Antioxidant effect of zinc in humans. *Free Radic. Biol. Med.* 2004;37(8):1182-90. DOI: 10.1016/j.freeradbiomed.2004.07.007.
 17. Jayakumar T, Thomas PA, Sheu JR, Geraldine P. *In vitro* and *in vivo* antioxidant effects of the oyster mushroom *Pleurotus ostreatus*. *Food Res. Int.* 2011;44(4):851-61. DOI: 10.1016/j.foodres.2011.03.015.
 18. World health organization. <https://www.who.int/news-room/fact-sheets/detail/cancer>. (Date accessed: 1st December 2021)
 19. Banu S, Ramakrishnaiah TN. Screening of *Garcinia cambogia* for *in-vitro* anti-cancerous activity against colon adenocarcinoma cell line. *Res. J. Pharmacogn. Phytochem.* 2018;10(4):272-6. DOI: 10.5958/0975-4385.2018.00043.2.
 20. Hanahan D, Weinberg RA. Hallmarks of cancer: the next generation. *Cell.* 2011;144(5):646-74. DOI: 10.1016/j.cell.2011.02.013.
 21. Weiss RA. Multistage carcinogenesis. *Br. J. Cancer.* 2004;91(12):1981-2.
 22. Kumar V, Abbas AK, Aster JC. Robbins & Cotran Pathologic Basis of Disease. 10th ed. Philadelphia: Elsevier; 2021.

23. Medeiros B, Allan AL. Molecular mechanisms of breast cancer metastasis to the lung: clinical and experimental perspectives. *Int. J. Mol. Sci.* 2019;20(9):2272. DOI: 10.3390/ijms20092272.
24. Abdulkareem IH. Aetio-pathogenesis of breast cancer. *Niger Med J.* 2013;54(6):371-75. DOI: 10.4103/0300-1652.126284.
25. Minna JD, Roth JA, Gazdar AF. Focus on lung cancer. *Cancer cell.* 2002;1(1):49-52. DOI: 10.1016/S1535-6108(02)00027-2.
26. Ibeanu OA. Molecular pathogenesis of cervical cancer. *Cancer Biol. Ther.* 2011;11(3):295-306. DOI: 10.4161/cbt.11.3.14686.
27. Zahra K, Patel S, Dey T, Pandey U, Mishra SP. A study of oxidative stress in cervical cancer-an institutional study. *Biochem. Biophys. Rep.* 2021;25:100881. DOI: 10.1016/j.bbrep.2020.100881.
28. Sosa V, Moliné T, Somoza R, Paciucci R, Kondoh H, LLeonart ME. Oxidative stress and cancer: an overview. *Ageing Res. Rev.* 2013;12(1):376-90. DOI: 10.1016/j.arr.2012.10.004.
29. Rosen EM, Fan S, Pestell RG, Goldberg ID. BRCA1 gene in breast cancer. *J. Cell Physiol.* 2003;196(1):19-41. DOI: 10.1002/jcp.10257.
30. Shao C, Folkard M, Held KD, Prise KM. Estrogen enhanced cell-cell signalling in breast cancer cells exposed to targeted irradiation. *BMC cancer.* 2008;8:1-9.
31. Cavalieri E, Chakravarti D, Guttenplan J, Hart E, Ingle J, Jankowiak R, *et al.* Catechol estrogen quinones as initiators of breast and other human cancers: implications for biomarkers of susceptibility and cancer prevention. *Biochim. Biophys. Acta Rev. Cancer.* 2006;1766(1):63-78. DOI: 10.1016/j.bbcan.2006.03.001.
32. Pratt JA. The neuroanatomical basis of anxiety. *Pharmacol. Ther.* 1992;55(2):149-81. DOI: 10.1016/0163-7258(92)90014-Q.
33. Kumar D, Bhat ZA, Kumar V, Raja WY, Shah MY. Anti-anxiety activity of *Stachys tibetica* Vatke. *Chin. J. Nat. Med.* 2013;11(3):240-4. DOI: 10.1016/S1875-5364(13)60022-9.

34. Mortazavi M, Kalani N, Marzouni HZ, Kooti W, Ali-Akbari S. Effect of hydroalcoholic extract of *rosmarinus officinalis* L. leaf on anxiety in mice. J Evid Based Complementary Altern Med. 2016;21(4):NP85-90. DOI: 10.1016/S1875-5364(13)60022-9.
35. Gupta V, Bansal P, Kohli K, Ghaiye P. Development of economic herbal based drug substitute from *Citrus paradisi* (Grape fruit) for existing anti-anxiety drug modules. Nat. Prod. Chem. Res. 2014;1:2. DOI: 10.4172/2329-6836.S1-001.
36. Nikfarjam M, Bahmani M, Heidari-Soureshjani S. Phytotherapy for anxiety in Iran: A review of the most important anti-anxiety medicinal plants. J. Chem. Pharm. Sci. 2016;9(3):1235-41.
37. Manikkoth S, Damodar S, Sequeira M, Samuel K. Anti-anxiety activity of *Eucalyptus tereticornis* n-hexane extract in Wistar albino rats. Int. J. Basic Clinical Pharmacol. 2017;6(3):577-80. DOI: 10.18203/2319-2003.ijbcp20170816.
38. Sahoo S, Kharkar P, Sahu N. Anxiolytic activity of *Psidium guajava* in mice subjected to chronic restraint stress and effect on neurotransmitters in brain. Phytother. Res. 2021;35(3):1399-415. DOI: 10.1002/ptr.6900.
39. Gupta V, Bansal P, Kumar S, Sannd R, Rao MM. Therapeutic efficacy of Phytochemicals as anti-anxiety-a review. J. Pharm. Res. 2010;3(1):174-9.
40. Canteras NS, Resstel LB, Bertoglio LJ, de Pádua Carobrez A, Guimaraes FS. Neuroanatomy of anxiety. Behav. Neurobiol. Anxiety. 2010;77-96. DOI: 10.1007/7854_2009_7.
41. Sachan A, Kumar S, Singh H, Shankar P, Kumar D, Sachan AK, *et al.* Potential anti-anxiety effect of *Mucuna pruriens* in experimental model of Swiss albino mice. Pharmacol. Toxicol. Biomed. Rep. 2015;1(1):20-23.
42. Brambilla P, Perez J, Barale F, Schettini G, Soares JC. GABAergic dysfunction in mood disorders. Mol. Psychiatry. 2003;(8):721-37. DOI: 10.1038/sj.mp.4001362.
43. Owens DF, Kriegstein AR. Is there more to GABA than synaptic inhibition?. Nat. Rev. Neurosci. 2002;3(9):715-27. DOI: 10.1038/nrn919.

44. Li C, Lei Y, Tian Y, Xu S, Shen X, Wu H, *et al.* The etiological contribution of GABAergic plasticity to the pathogenesis of neuropathic pain. *Mol. Pain.* 2019;15:1-13. DOI: 10.1177/1744806919847366.
45. Farrant M, Nusser Z. Variations on an inhibitory theme: phasic and tonic activation of GABA_A receptors. *Nat. Rev. Neurosci.* 2005;6(3):215-29. DOI:10.1038/nrn1625.
46. Liu GX, Liu S, Cai GQ, Sheng ZJ, Cai YQ, Jiang J, *et al.* Reduced aggression in mice lacking GABA transporter subtype 1. *J. Neurosci. Res.* 2007;85(3):649-55. DOI: 10.1002/jnr.21148.
47. Bormann J. The 'ABC' of GABA receptors. *Trends Pharmacol Sci.* 2000;21(1):16-9. DOI: 10.1016/S0165-6147(99)01413-3.
48. Rang HP, Dale MM, Ritter JM, Flower RJ. *Rang and Dale's Pharmacology.* 6th ed. USA: Churchill Livingstone Elsevier; 2007.
49. Goodman and Gillman. *The Pharmacological basis of therapeutics.* 13th ed. New York: Mc Graw Hill; 2017.
50. Fritschy JM, Benke D, Mertens S, Oertel WH, Bachi T, Mohler H. Five subtypes of type A gamma-aminobutyric acid receptors identified in neurons by double and triple immunofluorescence staining with subunit-specific antibodies. *Proc. Natl. Acad. Sci.* 1992;89(15):6726-30. DOI: 10.1073/pnas.89.15.6726.
51. Korpi ER, Sinkkonen ST. GABA_A receptor subtypes as targets for neuropsychiatric drug development. *Pharmacol. Ther.* 2006;109(1-2):12-32. DOI: 10.1016/j.pharmthera.2005.05.009.
52. Nuss P. Anxiety disorders and GABA neurotransmission: a disturbance of modulation. *Neuropsychiatr. Dis. Treat.* 2015:165-75.
53. Katzung BG, Vanderah TW. *Basic and Clinical Pharmacology.* 15th ed. New York: Mc Graw Hill; 2018.
54. Razavi BM, Zargarani N, Hosseinzadeh H. Anti-anxiety and hypnotic effects of ethanolic and aqueous extracts of *Lippia citriodora* leaves and verbascoside in mice. *Avicenna J. Phytomedicine.* 2017;7(4):353.

55. Liu X, Zhu W, Guan S, Feng R, Zhang H, Liu Q, *et al.* Metabolomic analysis of anti-hypoxia and anti-anxiety effects of Fu Fang Jin Jing Oral Liquid. PLoS One. 2013;8(10):e78281. DOI: 10.1371/journal.pone.0078281.
56. Kaur D, Shri R, Kamboj A. Evaluation of anti-anxiety effect of *Brassica oleracea* L. extracts in experimental animals. Pharmacogn. J. 2017;9(5). DOI:10.5530/pj.2017.5.101.
57. López-Rubalcava C, Estrada-Camarena E. Mexican medicinal plants with anxiolytic or antidepressant activity: Focus on preclinical research. J. Ethnopharmacol. 2016;186:377-91. DOI: 10.1016/j.jep.2016.03.053.
58. Hajhashemi V, Rabbani M, Ghanadi A, Davari E. Evaluation of antianxiety and sedative effects of essential oil of *Ducrosia anethifolia* in mice. Clinics. 2010;65:1037-42. DOI: 10.1590/S1807-59322010001000020.
59. Al-Snafi AE, Talab TA, Majid WJ. Medicinal plants with central nervous activity- An overview. IOSR J. Pharm. 2019;9(3):52-102.
60. Greenwell M, Rahman PK. Medicinal plants: their use in anticancer treatment. Int. J. Pharm. Sci. Res. 2015;6(10):4103. DOI: 10.13040/IJPSR.0975-8232.6(10).4103-12.
61. Ferdous UT, Balia Yusof ZN. Insight into potential anticancer activity of algal flavonoids: current status and challenges. Molecules. 2021 Nov 13;26(22):6844. DOI: 10.3390/molecules26226844.
62. Balabhaskar R, Vijayalakshmi K. Evaluation of anticancer activity of ethanol extract of *Bauhinia tomentosa* linn. on A549, human lung carcinoma cell lines. Res. J. Pharm. Technol. 2019;12(6):2748-52. DOI:10.5958/0974-360X.2019.00460.8.
63. Valcheva-Kuzmanova S, Eftimov M, Belcheva I, Belcheva S, Tashev R. Anti-anxiety effect of Aronia melanocarpa fruit juice administered subchronically to rats. Farmacia. 2016;64(3):367-71.
64. Gupta V, Bansal P, Kohli K, Ghaiye P. Development of economic herbal based drug substitute from *Citrus paradisi* (Grape fruit) for existing anti-anxiety drug modules.

- Nat Prod Chem Res S. 2014;1:2. DOI:10.4172/2329-6836.S1-001.
65. Rajsekhar PB, Bharani RA, Angel KJ, Ramachandran M, Rajsekhar SP. *Hybanthus enneaspermus* (L) F. Muell: A phytopharmacological review on herbal medicine. J. Chem. Pharm. Res. 2016;8(1):351-5.
66. Ramya AK, Devika R. Current Pharmacological Impacts and Perspective of *Hybanthus enneaspermus* (Linn.) F. Muell. Pharmacogn. Res. 2022;14(4). DOI: 10.5530/pres.14.4.51.
67. Patel DK, Kumar R, Sairam K, Hemalatha S. *Hybanthus enneaspermus* (L.) F. Muell: a concise report on its phypharmacological aspects. Chin. J. Nat. Med. 2013;11(3):199-206. DOI: 10.1016/S1875-5364(13)60017-5.
68. Chandru G, Jayakumar K, Navaneethakannan D. Effect of raw extract of *Hybanthus enneaspermus* (L.) F. Muell. on the fertility test in female mice (*Mus musculus* L). World Sci. News. 2017(65):160-70.
69. India biodiversity portal. <https://indiabiodiversity.org/species/show/33144>. Accessed on 28th January 2018.
70. Efloraofindia. Database of plants of Indian subcontinent. <https://sites.google.com/site/efloraofindia/species/m-z/v/violaceae/hybanthus/hybanthus-enneaspermus>. Accessed on 28th January 2018.
71. Bandyopadhyay S, Thothathri K, Sharma BD. The genus *Bauhinia* L. (Leguminosae: Caesalpinioideae) in India. J. Econ. Taxon. Bot. 2005;29(4):763-801.
72. Bandyopadhyay S. Neotypification of *Bauhinia foveolata* (Leguminosae:Caesalpinioideae). J. Jpn. Bot. 2011;86:169.
73. India biodiversity portal. <https://indiabiodiversity.org/species/show/264728>. Accessed on 21st February 2018.
74. Botanical Journal of the Linnean society. <https://academic.oup.com/botlinnean/articleabstract/13/67/185/2926368?redirectedFrom=fulltext>. Accessed on 28th February 2021.

75. Efloraofindia. Database of plants of Indian subcontinent. <https://sites.google.com/site/efloraofindia/species/a/f/fabaceae/piliostigma/bauhinia-foveolata>. Accessed on 05th September 2022.
76. Valke D. Flickr. https://www.flickr.com/photos/dinesh_valke/4102054571. Accessed on 16th March 2022.
77. Filho VC. Chemical composition and biological potential of plants from the genus *Bauhinia*. *Phytother. Res.* 2009;23(10):1347-54. DOI: 10.1002/ptr.2756.
78. Habbu PV, Miskin N, Kulkarni VH, Bhat P, Joshi A, Bhandarkar A, *et al.* Isolation, characterization, and cytotoxic studies of secondary metabolites from the leaves of *Bauhinia foveolata* Dalzell: An endemic tree from the Western Ghats, India. *J. Appl. Pharm. Sci.* 2020;10(3):135-48. DOI: 10.7324/JAPS.2020.103018.
79. Mohanty R, Nayak M, Sekar T, Thirunavoukkarasu M. Adsorption of Selenium and Lanthanum by Agrobacterium-mediated hairy roots of *Hybanthus enneaspermus* (L.) F. Muell: A Greener phytoremediation strategy. *Bull. Environ. Contam. Toxicol.* 2023;110(2):54. DOI: 10.1007/s00128-023-03694-9.
80. Sathish S, Vasudevan V, Karthik S, Pavan G, Siva R, Manickavasagam M. Precursor feeding enhances L-Dopa production in hairy root culture of *Hybanthus enneaspermus* (L.) F. Muell. *Biologia.* 2023;10:1-1. DOI: 10.1007/s11756-022-01308-z.
81. Maheswari P, Sugapriya S, Krishnaveni N, Senthil TS. Investigation of pure and CuO-and ZnO-Loaded TiO₂ nanocomposites prepared by modified hydrothermal cum green synthesis (*Hybanthus enneaspermus* extract) method for photocatalytic and antioxidant applications. *Braz. J. Phys.* 2022;52(4):142. DOI: 10.1007/s13538-022-01112-9.
82. Sathish S, Vasudevan V, Karthik S, Ajithan C, Siva R, Parthasarathy SP, *et al.* Impact of silver nanoparticles on the micropropagation of *Hybanthus enneaspermus* and assessment of genetic fidelity using RAPD and SCoT markers. *Plant Cell, Tissue and Organ Cult.* 2022;151(2):443-9. DOI: 10.1007/s11240-022-02350-0.

83. Al-Owaisi A, Al-Sadi AM, Al-Sabahi JN, Sathish Babu SP, Al-Harrasi MM, Hashil Al-Mahmooli I, *et al.* *In vitro* detoxification of aflatoxin B1 by aqueous extracts of medicinal herbs. *All Life*. 2022; 15(1):314-24. DOI: 10.1080/26895293.2022.2049900.
84. Katta A, Murugan M. A study on protective effect of *Piper longum* and *Hybanthus enneaspermus* on glucose induced diabetic cataract in cultured goat lens. *Biomedicine*. 2022; 42(2):236-40. DOI:10.51248/.v42i2.1103.
85. Sankareswaran M. *In Silico* molecular docking analysis of anti HIV-1 Rt from Indian medicinal plant *Hybanthus enneaspermus*. *Indian J. Nat. Sci.* 2021;12(65):29704-12.
86. Kumari CS, Logeshwari B. *In silico* and *In vitro* evaluation of anti-urolithiatic activity of ethanolic extract of *Hybanthus enneaspermus* (Linn.) F. Muell. *Int. J. Pharm. Res. Appl.* 2021;6(2)548-60.
87. Suchithra MR, Bhuvanewari S, Sampathkumar P, Dineshkumar R, Chithradevi K, Madhumitha R, *et al.* *In vitro* study of antioxidant, antidiabetic and antiurolithiatic activity of synthesized silver nanoparticles using stem bark extracts of *Hybanthus enneaspermus*. *Biocatal. Agric. Biotechnol.* 2021;38:102-09.
88. Du Q, Huang YH, Bajpai A, Frosig-Jorgensen M, Zhao G, Craik DJ. Evaluation of the *in vivo* aphrodisiac activity of a cyclotide extract from *Hybanthus enneaspermus*. *J. Nat. Prod.* 2020;83:3736-43. DOI: 10.1021/acs.jnatprod.0c01045.
89. Nivethitha S, Arivarasu L, Rajeshkumar S. Cytotoxic and antioxidant potential of *Hybanthus enneaspermus* mediated silver nanoparticles. *Plant cell biotechnol. Mol. Biol.* 2020;26:104-10.
90. Sathish S, Vasudevan V, Karthik S, Elayaraja D, Pavan G, Ajithan C, *et al.* Elicitors induced L-Dopa accumulation in adventitious root cultures of *Hybanthus enneaspermus* (L.) F. Muell. *Vegetos.* 2020;33:304-12. DOI: 10.1007/s42535-020-00108-7.
91. Patel DK. Evaluation of antidiabetic, antioxidant and nephroprotective activity of flavonoid rich fraction of *Hybanthus enneaspermus* in diabetic rats: *In-silico*

- molecular docking studies for SOD, Catalase, GPx, xanthine oxidase and NF-KB. Nephrol. Dial. Transplant. 2020;35:142-P0995. DOI: 10.1093/ndt/gfaa142.P0995.
92. Amrithaa B, Rajeshkumar S. Anti-inflammatory and anti-microbial activity of *Hybanthus enneaspermus* mediated silver nanoparticles. Plant Cell Biotechnol. Mol. Biol. 2020;30:104-08.
93. Patel DK. Evaluation of Flavonoid rich extract of *Hybanthus enneaspermus* in Streptozotocin-nicotinamide induced diabetic rats through measurement of antioxidant enzymes (superoxide dismutase, catalase, and thiobarbituric acid reactive substance), liver glycogen and lipid parameters in liver tissue. Gut Liver. 2019;13(6)2;13.
94. Patel DK. Investigation of aldose reductase inhibitory potential of phytoconstituents rich principles from the whole plant of *Hybanthus enneaspermus* (Linn) F. Muell. Gut Liver. 2019;13(6):210-13.
95. Shekhawat MS, Manokari M. *In vitro* multiplication, micromorphological studies and *ex vitro* rooting of *Hybanthus enneaspermus* (L.) F. Muell. - a rare medicinal plant. Acta Bot Croat. 2018;77(1):80-7. DOI: 10.1515/botcro-2017-0012.
96. Aigbe FR, Ameh D, Salako OA, Adeyemi OO. An evaluation of the analgesic action of aqueous leaves extract of *Hybanthus enneaspermus* linn. F. Muell (Violaceae) in rodents. Unilag J. Med. Sci. Technol. 2016;4(2):1-3.
97. Muthu AK. Isolation and characterization of active components derived from whole plant of *Ionidium suffruticosum* (Ging.). Int. J. Chem. Pharm. Sci. 2017;8(1):51-6.
98. Afolabi AO, Alagbonsi IA, Aliyu JA. Pharmacological mechanisms involved in the analgesia induced by ethanol extract of *Hybanthus enneaspermus* leaves. J Pain Res. 2017;10:1997-2002. DOI: 10.2147/JPR.S141981.
99. Jayanthi K, Kavitha K, Jayanthi J, Ragunathan MG, Kumaran T. Quantitative analysis of total phenolic and flavonoid compounds of ethanolic extracts of stem and root of *Hybanthus enneaspermus* (L.) F. Muell. World J. Pharm. Res. 2017;6(17):767-73. DOI: 10.20959/wjpr201717-10371.

100. Chenniappan K, Murugan K. Therapeutic and fertility restoration effects of *Ionidium suffruticosum* on sub-fertile male albino Wistar rats: effects on testis and caudal spermatozoa. Pharm Biol. 2017;55(1):946-57. DOI: 10.1080/13880209.2016.1278453.
101. Jaikumar K, Sheik NMN, Marimuthu S, Anantha PS, Anand D, Saravanan P. *In vitro* anticancer activity of ethanolic leaf extract of *Hybanthus enneaspermus* L., against Hep-2 Cell line. Indo Am. J. Pharm. Res. 2016;6(12): 7254-9.
102. Anupa MP, Chinju S, Murugan M. Qualitative phytochemical screening, and *in vitro* antioxidant activity of *Hybanthus enneaspermus*. Int. J. Pharmacogn. Phytochem. Res. 2016;8(6):1046-9.
103. Suman TY, Radhika SR, Rajasree C, Jayaseelan R, Regina Mary S, Gayathri L, *et al.* GC-MS analysis of bioactive components and biosynthesis of silver nanoparticles using *Hybanthus enneaspermus* at room temperature evaluation of their stability and its larvicidal activity. Environ. Sci. Pollut. Res. 2016;23(3):2705-14. DOI: 10.1007/s11356-015-5468-5.
104. Behera PR, Jena RC, Das A, Thirunavoukkarasu M, Chand PK. Genetic stability and coumarin content of transformed rhizoclones and regenerated plants of a multi-medicinal herb, *Hybanthus enneaspermus* (L.) F. Muell. Plant Growth Regul. 2016;80(2):103-114. DOI: 10.1007/s10725-016-0145-3.
105. Thiru A, Ashokan K, ChandraMohan S, Rajakrishnan B. Regulation of ROS defense system by *Hybanthus enneaspermus* in CCl₄ induce cardiac damage. Pak. J. Pharm. Sci. 2015;28(4):1397-9.
106. Sundaram S, Radhakrishnan A, Kanniappan GV, Bhaskaran SK, Palanisamy CP, Kannappan P. Comparative study on antioxidant activity of crude and alkaloid extracts of *Hybanthus enneaspermus* (L.) F. Muell. Anal. Chem. Lett. 2015;5(5):291-9. DOI: 10.1080/22297928.2015.1135076.
107. Velayutham P, Karthi C. GC-MS Profile of *in vivo*, *in vitro*, and fungal elicited *in vitro* leaves of *Hybanthus enneaspermus* (L.) F. Muell. Int. J. Pharm. Pharm. Sci.

- 2015;7(1):260-7.
108. Afolabi AO, Oluwakanmi ET, Salahdeen HM, Oyekunle AO, Alagbonsi IA. Antinociceptive effect of ethanolic extract of *Hybanthus enneaspermus* leaf in rats. Br. J. Med. Med. Res. 2014;4(1):322-30. DOI: 10.9734/BJMMR/2014/4217.
 109. Ragavan B, Rex Dab. Studies on Phytochemicals, antioxidant, and cytotoxicity effect of *H. enneaspermus*. Int. J. Pharm. Pharm. Sci. 2014;6(6):567-72.
 110. Vamsi K, Bholla PK. Antibacterial activity of *Hybanthus enneaspermus* against *Enterococcus faecalis* a root canal organism. Int. J. Dent. Sci. Res. 2014;2(6C):14-6. DOI: 10.12691/ijdsr-2-6C-4.
 111. Patel DK, Krishnamurthy S, Hemalatha S. Evaluation of glucose utilization capacity of bioactivity guided fractions of *Hybanthus enneaspermus* and *Pedalium murex* in isolated rat hemidiaphragm. J Acute Dis. 2013;2(1):33-6. DOI: 10.1016/S2221-6189(13)60091-8.
 112. Vetrivelvan S, Suganya V, Muthuramu T. Antihyperlipidemic activity of hydroalcoholic extract of *Hybanthus enneaspermus*. Asian J. Phytomed. Clin. Res. 2013;1(1):27-33.
 113. Mozhi MT, Swarnalatha S, Sakthivel P, Manigandan LS, Jayabharat A, Suresh Kumar P. Anti-allergic and analgesic activity of aerial parts of *Hybanthus enneaspermus*. Int. Res. J. Pharm. 2013;4(6):243-8. DOI: 10.7897/2230-8407.04655.
 114. Sadasivam SK, Ismail M, Thameezan AN, Naveenkumar K, Rayees-Ifham MDS. *In vitro* antimicrobial activity and phytochemical analysis of leaves of *Ionidium Suffruticosum* (Ging). Int. J. Biotechnol. Allied Fields. 2013;1(10):452-9.
 115. Kumar ACK, Devivani G, Sharmila VG, Mounika P, Johnson K, Satheesh Kumar. D; *In vitro* antioxidant activity of aqueous extract of *Ionidium Suffruticosum* (Ging). entire plant. J. Glob. Trends Pharm Sci. 2013;4(1):1034-8.
 116. Olubajo AF, Adefunke AO, Olubusola IB, Ibilola OB. Experimental evaluation of the impact of maternal consumption of aqueous leaf extract of *Hybanthus*

- enneaspermus* on pregnancy in Sprague Dawley rats. Afr. J Tradit. Complement. Altern. Med. 2013;10(2):283-91. DOI: 10.4314/ajtcam.v10i2.13.
117. Nathiya S, Selvi SR. Anti-infertility effect of *Hybanthus enneaspermus* on endosulfan induced toxicity in male rats. Int. J Med. Biosci. 2013;2(1):28-32.
118. Mishra PK, Subhangkar N, Abhishek D. Wound healing activity of different extracts of *Hybanthus enneaspermus* Muell. in albino rats. Pharm. Chem. 2012;11(3):32-9.
119. Sailaja G, SK HB, Meenabai M, Kamala K, Suman B, Venkataswamy M, Kedam TR. Regulation of Acrylamide induced μ -class glutathione-S-transferases in mice testis by the treatment of *Hybanthus enneaspermus* active principles. J. Appl. Pharm. Sci. 2012;2(8):203-9. DOI: 10.7324/JAPS.2012.2836.
120. Anand T, Kalaiselvan A, Gokulakrishnan K. *Hybanthus enneaspermus* is a potent regulator for membrane bound enzymes in mitochondria on carbon tetrachloride induced oxidative stress in rats. Int. J. Drug Dev. Res. 2012;4(3):259-62.
121. Vuda M, D'Souza R, Upadhya S, Kumar V, Rao N, Kumar V, *et al.* Hepatoprotective and antioxidant activity of aqueous extract of *Hybanthus enneaspermus* against CCl₄-induced liver injury in rats. Exp. Toxicol Pathol. 2012;64(7-8):855-9. DOI: 10.1016/j.etp.2011.03.006.
122. Satheeshkumar D, Kottai Muthuand A, Manavalan R. *In vivo* antioxidant and lipid peroxidation effect of whole plant of *Ionidium suffruticosum* (Ging.) in rats fed with high fat diet. Asian J Pharm. Clin. Res. 2012;5(2):132-5.
123. Muthu AK, Dharmarajan SK. Comparative evaluation of flavone from *Mucuna pruriens* and coumarin from *Ionidium suffruticosum* for hypolipidemic activity in rats fed with high fat diet. Lipids Health Dis. 2012;11(1):1-6. DOI: 10.1186/1476-511X-11-126.
124. Anand T, Gokulakrishnan K. GC - MS analysis and anti-microbial activity of bioactive components of *Hybanthus enneaspermus*. Int. J. Pharm. Pharm. Sci. 2012;4(3):456-60.

125. Anand T, Gokulakrishnan K. Phytochemical and FTIR analysis of *Hybanthus enneaspermus* using UV, GC-MS. ISOR J. Pharm. 2012;2(3):520-4.
126. Arumugam N, Kandasamy S, Sekar M. *In vitro* antifungal activity of *Hybanthus enneaspermus* F. Muell. Int. J. Pharm. Pharm. Sci. 2012;4(2):594-6.
127. Sahoo SP, Subudhi BB, Ramchandran S, Dhanraju MD, Kumaraswamy B. Evaluation of anti-ulcer and anti-secretory activity of *Hybanthus enneaspermus*. Int. J. Pharm. Res. Allied Sci. 2012;1(4):85-8.
128. Radhika S, Smila KH, Mutheshilan R. Cardioprotective activity of *Hybanthus enneaspermus* (Linn.) on isoproterenol induced rats. Indian J. Fundam. Appl. Life Sci. 2011;1(3):90-7.
129. Thyagaraju K, Haseena BS, Meena BM, Pallavi C. Suppression of paracetamol toxicity by antioxidant principles of *Hybanthus enneaspermus* (L.) G. Muell in mice blood and liver. Int. J. Pharm. Pharm. Sci. 2011;3(4):90-4.
130. Patel DK, Kumar R, Prasad SK, Sairam K, Hemalatha S. Antidiabetic and *in vitro* antioxidant potential of *Hybanthus enneaspermus* (Linn) F. Muell in streptozotocin - induced diabetic rats. Asian Pac. J. Trop. Biomed. 2011;1(4):316-22. DOI: 10.1016/S2221-1691(11)60051-8.
131. Ramamoorthy J, Meera R, Devi P, Sabarmathy. Phytochemical investigation and anti-inflammatory activity of *Ionodium suffruticosum*. Asian J. Biochem. Pharm. Res. 2011;1(2):142-147.
132. Kannan CS, Kumar AS, Amudha P. Evaluation of anxiolytic activity of hydroalcoholic extract of *Hybanthus enneaspermus* Linn. in swiss albino mice. Int. J. Pharm. Pharm. Sci. 2011;3:121-5.
133. Arumugam N, Sasikumar K, Himaja M, Sekar M. Antifungal activity of *Hybanthus enneaspermus* on wet clothes. Int. J. Res. Ayurveda Pharm. 2011;2(4):1184-5.
134. Awobajo FO, Olatunji-Bello II. Hypoglycemic activities of aqueous and methanol leaf extract of *Hybanthus enneaspermus* and *Paquetina nigricense* on normal and alloxan induced diabetic female Sprague Dawley rats. J. Phytol. 2010;2(2):1-9.

135. Kar DM, Maharana L, Rout SP. CNS activity of aerial parts of *Hybanthus enneaspermus* Mull. Pharmacologyonline. 2010;3:959-81.
https://www.researchgate.net/publication/216412991_CNS_Activity_of_aerial_parts_of_Hybanthus_enneaspermus_Mull. Accessed on 10th May 2017.
136. Tripathy S, Sahoo SP, Pradhan D, Sahoo S, Satapathy DK. Evaluation of anti-arthritic potential of *Hybanthus enneaspermus*. Afr. J. Pharm. Pharmacol. 2009;3(12):611-4.
137. Setty M, Narayanaswamy VB, Sreenivasan KK, Shirwaikar A. Free radical scavenging and nephroprotective activity of *Hybanthus enneaspermus* (L) F. Muell. Pharmacologyonline. 2007;2:158-71.
https://www.researchgate.net/publication/288808563_Free_radical_scavenging_and_nephroprotective_activity_of_Hybanthus_enneaspermus_L_FMuell. Accessed on 25th November 2018.
138. Narayanswamy VB, Setty MM, Malini S, Shirwaikar A. Preliminary aphrodisiac activity of *Hybanthus enneaspermus* in rats. Pharmacologyonline. 2007;1:152-61.
https://www.researchgate.net/publication/51504585_Hemalatha_S_Evaluation_of_phytochemical_and_antioxidant_activities_of_the_different_fractions_of_Hybanthus_enneaspermus_Linn_F_MuellViolaceae. Accessed on 17th May 2017.
139. Weniger B, Lagnika L, Vonthron-Sénécheau C, Adjobimey T, Gbenou J, Moudachirou M, *et. al.* Evaluation of ethnobotanically selected Benin medicinal plants for their *in vitro* antiplasmodial activity. J. Ethnopharmacol. 2004;90(2-3):279-84. DOI: <https://doi.org/10.1016/j.jep.2003.10.002>.
140. Hemalatha S, Wahi AK, Singh PN, Chansouria JP. Anticonvulsant and free radical scavenging activity of *Hybanthus enneaspermus*: A preliminary screening. Indian J. Tradit. Knowl. 2003;2(4):383-8.
141. Gamit SB, Sapra P, Vasava MS, Solanki HA, Patel H, Rajani D. Antimicrobial and antimalarial activities of some selected ethno-medicinal plants used by tribal communities of Tapi district, Gujarat, India. Int. Res. J. Pharm. 2018;9(10):151-6. DOI: 10.7897/2230-8407.0910243.

142. Khanna T, Dave A, Purani S, Vedamurthy J, Jivani D, Robin P. *Bauhinia variegata* Bark Extract: Assessment of its Anti-proliferative and Apoptotic Activities on A549 and H460 Lung Cancer Cell Lines. *J. Nat. Remedies*. 2022;175-95. DOI: 10.18311/jnr/2022/28740.
143. Chávez-Bustos EA, Morales-González A, Anguiano-Robledo L, Madrigal-Santillán EO, Valadez-Vega C, Lugo-Magaña O, *et al.* *Bauhinia forficata* Link, antioxidant, genoprotective, and hypoglycemic activity in a murine model. *Plants*. 2022;11(22):3052. DOI: 10.3390/plants11223052.
144. Phonghanpot S, Jarintanan F. Antiproliferative, antibacterial, and antioxidant activities of *Bauhinia strychnifolia* Craib aqueous extracts in gut and liver perspective. *BMC Complement. Med. Ther.* 2021;21:1-12. DOI: 10.1186/s12906-021-03448-2.
145. Vijayan R, Joseph S, Mathew B. Anticancer, antimicrobial, antioxidant, and catalytic activities of green-synthesized silver and gold nanoparticles using *Bauhinia purpurea* leaf extract. *Bioprocess Biosyst. Eng.* 2019;42:305-19. DOI: 10.1007/s00449-018-2035-8.
146. Santos M, Fortunato RH, Spotorno VG. Analysis of flavonoid glycosides with potential medicinal properties on *Bauhinia uruguayensis* and *Bauhinia forficata* subspecies *pruinosa*. *Nat. Prod. Res.* 2019;33(17):2574-8. DOI: 10.1080/14786419.2018.1460826.
147. Sharmila G, Muthukumaran C, Sandiya K, Santhiya S, Pradeep RS, Kumar NM, *et al.* Biosynthesis, characterization, and antibacterial activity of zinc oxide nanoparticles derived from *Bauhinia tomentosa* leaf extract. *J. Nanostructure Chem.* 2018;8:293-9. DOI: 10.1007/s40097-018-0271-8.
148. Pandey S. *In vivo* antitumor potential of extracts from different parts of *Bauhinia variegata* Linn. against b16f10 melanoma tumour model in c57bl/6 mice. *Appl. Cancer Res.* 2017;37(1):1-4. DOI: 10.1186/s41241-017-0039-3.

149. Rahman MA, Akhtar J, Arshad M. Evaluation of cytotoxic potential and apoptotic effect of a methanolic extract of *Bauhinia racemosa* Lam. against a human cancer cell line, HeLa. Eur. J. Integr. Med. 2016;8(4):513-8. DOI: 10.1016/j.eujim.2016.02.004.
150. Sharma AK, Sharma UK, Pandey AK. Protective effect of *Bauhinia variegata* leaf extracts against oxidative damage, cell proliferation and bacterial growth. Proc. Natl. Acad. Sci. India Sect B Biol. Sci. 2015;87:45-51. DOI: 10.1007/s40011-015-0578-x.
151. Garbi MI, Osman EE, Kabbashi AS. Anticancer activity of *Bauhinia rufescens* (Lam.) leaf extracts on MCF-7 human breast cancer cells. J. Med. Plants Stud. 2015;3(5):103-6.
152. Ajiboye AT, Musa MD, Otun KO, Jimoh AA, Bale AT, Lawal SO, *et al.* The studies of antioxidant and antimicrobial potentials of the leaf extract of *Bauhinia monandra* plant. Nat. Prod. Chem. Res. 2015;3(4):1000180. DOI: 10.4172/2329-6836.1000180.
153. Kumar S, Bhat KI. Apoptosis and flowcytometric studies of *Bauhinia variegata* bark extract. Asian J. Pharm. Clin. Res. 2014;7(1):45-7.
154. Jatav N, Ganeshpurkar A, Gupta N, Ayachi C, Ramhariya R, Bansal D, *et al.* Nootropic potential of *Bauhinia variegata*: A systematic study on murine model. Arch. Med. Health Sci. 2014;2(1):29. DOI: 10.4103/2321-4848.133792.
155. Jash SK, Roy R, Gorai D. Bioactive constituents from *Bauhinia variegata* Linn. Int. J Pharm. Biomed. Res. 2014;5(2):51-4.
156. Chaudhari MG, Joshi BB, Mistry KN. *In vitro* anti-diabetic and anti-inflammatory activity of stem bark of *Bauhinia purpurea*. Bull. Pharm. Med. Sci. 2013;1(2):139-50.
157. Kuo YH, Yeh MH. Chemical constituents of heartwood of *Bauhinia purpurea*. J. Chin. Chem. Soc. 1997;44(4):379-83. DOI: 10.1002/jccs.199700056.
158. Kang SC, Sowndhararajan K. Free radical scavenging activity from different extracts of leaves of *Bauhinia vahlii* Wight & Arn. Saudi J. Biol Sci. 2013;20(4):319-25. DOI: 10.1016/j.sjbs.2012.12.005.

-
159. Jain R, Yadav N, Bhagchandani T, Jain SC. A new pentacyclic phenol and other constituents from the root bark of *Bauhinia racemosa* Lamk. Nat. Prod. Res. 2013;27(20):1870-6. DOI: 10.1080/14786419.2013.771351.
160. Santos FJ, Lima SG, Cerqueira GS, Citó AM, Cavalcante AA, Marques TH, *et al.* Chemical composition and anxiolytic-like effects of the *Bauhinia platypetala*. Rev. Bras. Farmacogn. 2012;22:507-16. DOI: 10.1590/S0102-695X2012005000018.
161. Annegowda HV, Mordi MN, Ramanathan S, Hamdan MR, Mansor SM. Effect of extraction techniques on phenolic content, antioxidant and antimicrobial activity of *Bauhinia purpurea*: HPTLC determination of antioxidants. Food Anal. Methods. 2012;5:226-33. DOI: 10.1007/s12161-011-9228-y.
162. Cavalcanti EM, Bonafé C, Silva MG, Gerenutti M. Properties of *Bauhinia forficata* Link in rats: Behavioral evaluations. Pharmacologyonline. 2011;2:205-11. <https://pharmacologyonline.silae.it/files/archives/2011/vol2/022.marli.pdf>. Accessed on 19th July 2020.
163. Zakaria ZA, Rofiee MS, Teh LK, Salleh MZ, Sulaiman MR, Somchit MN. *Bauhinia purpurea* leaves' extracts exhibited *in vitro* antiproliferative and antioxidant activities. Afr. J. Biotechnol. 2011;10(1):65-74. DOI: 10.5897/AJB10.1354.
164. Zakaria ZA, Hisam EA, Rofiee MS, Norhafizah M, Somchit MN, Teh LK, *et al.* *In vivo* antiulcer activity of the aqueous extract of *Bauhinia purpurea* leaf. J. Ethnopharmacol. 2011;137(2):1047-54. DOI: 10.1016/j.jep.2011.07.038.
165. Ananth KV, Asad M, Kumar NP, Asdaq SM, Rao GS. Evaluation of wound healing potential of *Bauhinia purpurea* leaf extracts in rats. Indian J. Pharm. Sci. 2010;72(1):122. DOI: 10.4103/0250-474X.62250.
166. Lakshmi BV, Neelima N, Kasthuri N, Umarani V, Sudhakar M. Protective effect of *Bauhinia purpurea* on gentamicin-induced nephrotoxicity in rats. Indian J. Pharm. Sci. 2009;71(5):551. DOI: 10.4103/0250-474X.58196.

167. Shreedhara CS, Vaidya VP, Vagdevi HM, Latha KP, Muralikrishna KS, Krupanidhi AM. Screening of *Bauhinia purpurea* Linn. for analgesic and anti-inflammatory activities. Indian J. Pharmacol. 2009;41(2):75-9. DOI: 10.4103/0253-7613.51345.
168. Agrawal RC, Pandey S. Evaluation of anticarcinogenic and antimutagenic potential of *Bauhinia variegata* extract in Swiss albino mice. Asian Pac. J. Cancer Prev. 2009;10(5):913-6.
169. Rajkapoor B, Murugesh N, Rama Krishna D. Cytotoxic activity of a flavanone from the stem of *Bauhinia variegata* Linn. Nat. Prod. Res. 2009;23(15):1384-9. DOI: 10.1080/14786410802553752.
170. Jain R, Saxena U, Rathore K, Jain SC. Bioactivities of polyphenolics from the roots of *Bauhinia racemosa*. Arch. Pharm. Res. 2008;31:1525-9. DOI: 10.1007/s12272-001-2145-7.
171. Kaewamatawong R, Kitajima M, Kogure N, Takayama H. Flavonols from *Bauhinia malabarica*. J. Nat. Med. 2008;62:364-5. DOI: 10.1007/s11418-008-0249-9.
172. Boonphong S, Puangsombat P, Baramée A, Mahidol C, Ruchirawat S, Kittakoop P. Bioactive compounds from *Bauhinia purpurea* possessing antimalarial, antimycobacterial, antifungal, anti-inflammatory, and cytotoxic activities. J. Nat. Prod. 2007;70(5):795-801. DOI: 10.1021/np070010e.
173. Aderogba MA, Ogundaini AO, Eloff JN. Isolation of two flavonoids from *Bauhinia monandra* (Kurz) leaves and their antioxidative effects. Afr J. Tradit Complement Altern Med. 2006;3(4):59-65.
174. Gupta M, Mazumder UK, Kumar RS, Kumar TS. Antitumor activity and antioxidant role of *Bauhinia racemosa* against Ehrlich ascites carcinoma in Swiss albino mice. Acta Pharmacol Sin. 2004;25:1070-6. DOI: 10.22159/ajpcr.2018.v11i4.23968.
175. Rajkapoor B, Jayakar B, Murugesh N. Antitumour activity of *Bauhinia variegata* against Ehrlich ascites carcinoma induced mice. Pharm. Biol. 2003;41(8):604-7. DOI: 10.1080/13880200390501947.

176. Rajkapoor B, Jayakar B, Murugesh N. Antitumour activity of *Bauhinia variegata* on Dalton's ascitic lymphoma. *J. Ethnopharmacol.* 2003;89(1):107-9. DOI: 10.1016/S0378-8741(03)00264-2.
177. Yadava RN, Tripathi P. A novel flavone glycoside from the stem of *Bauhinia purpurea*. *Fitoterapia.* 2000;71(1):88-90. DOI: 10.1016/S0367-326X(99)00114-8.
178. Talebi M, Talebi M, Farkhondeh T, Kopustinskiene DM, Simal-Gandara J, Bernatoniene J, *et al.* An updated review on the versatile role of chrysin in neurological diseases: Chemistry, pharmacology, and drug delivery approaches. *Biomed. Pharmacother.* 2021;141:111906. DOI: 10.1016/j.biopha.2021.111906.
179. Yazan R, Fadzelly AB, Azlen-Che R, Kartinee KN, Johnson S, Yuan-Han T, *et al.* Methyl gallate isolated from *Mangifera pajang* kernel induces proliferation inhibition and apoptosis in MCF-7 breast cancer cells via oxidative stress. *Asian Pac. J. Trop. Biomed.* 2022;12(4):175-84. DOI: 10.4103/2221-1691.340562.
180. Farrag IM, Belal A, Al Badawi MH, Abdelhady AA, Abou Galala FM, El-Sharkawy A, *et al.* Antiproliferative, apoptotic effects and suppression of oxidative stress of quercetin against induced toxicity in lung cancer cells of rats: *In vitro* and *in vivo* study. *J. Cancer.* 2021;12(17):5249. DOI: 10.7150/jca.52088.
181. Razack S, Kandikattu HK, Venuprasad MP, Amruta N, Khanum F, Chuttani K, *et al.* Anxiolytic actions of *Nardostachys jatamansi* via GABA benzodiazepine channel complex mechanism and its biodistribution studies. *Metab. Brain Dis.* 2018; 33(5):1533-49. DOI: 10.1007/s11011-018-0261-z.
182. Singh J, Kumar A, Sharma A. Antianxiety activity guided isolation and characterization of Bergenin from *Caesalpinia digyna* Rottler roots. *J. Ethnopharmacol.* 2017;195:182-7. DOI: 10.1016/j.jep.2016.11.016.
183. Pemminati S, Gopalakrishna HN, Swati B, Shreyasi C, Pai MR, Nair V. Antianxiety effect of aqueous extract of fruits of *Embllica officinalis* (EO) on acute and chronic administration in rats. *J. Pharm. Res.* 2010;3(2):219-33.

184. Latha K, Rammohan B, Sunanda BP, Maheswari MU, Mohan SK. Evaluation of anxiolytic activity of aqueous extract of *Coriandrum sativum* Linn. in mice: A preliminary experimental study. *Pharmacogn. Res.* 2015;7(5s). DOI: 10.4103/0974-8490.157996.
185. Dutt V, Dhar VJ, Sharma A. Antianxiety activity of *Gelsemium sempervirens*. *Pharm. Biol.* 2010;48(10):1091-6. DOI: 10.3109/13880200903490521.
186. Kumar S, Sharma A. Anti-anxiety activity studies of various extracts of *Turnera aphrodisiaca* Ward. *J. Herb. Pharmacother.* 2005;5(4):13-21. DOI: 10.1080/J157v05n04_02.
187. Bhandari SS, Kabra MP. To evaluate anti-anxiety activity of thymol. *J of Acute Dis.* 2014;3(2):136-40. DOI: 10.1016/S2221-6189(14)60030-5.
188. Sahoo S, Brijesh S. Anxiolytic activity of *Coriandrum sativum* seeds aqueous extract on chronic restraint stressed mice and effect on brain neurotransmitters. *J Funct. Foods.* 2020;68:103884. DOI: 10.1016/j.jff.2020.103884.
189. Houghton P, Raman A. *Laboratory handbook for the fractionation of natural extracts.* 1st ed. New York: Springer Science & Business Media; 2012.
190. Khandelwal KR. *Practical Pharmacognosy techniques and experiments.* 20th ed. India: Nirali Prakashan; 2010.
191. Trease GE, Evans WC. *Trease and Evan's Textbook of Pharmacognosy.* 13th ed. London: Cambridge University Press; 2009.
192. Chakraborty P, Sharma S, Chakraborty S, Siddapurand A, Abraham J. Cytotoxicity and Antimicrobial Activity of *Ipomoea batatas*. *Res. J. Pharm. Technol.* 2018;11(7):2741-6. DOI: 10.5958/0974-360X.2018.00506.1.
193. Oliveira AMFO, Pinheiro L, Pereira CKS, Matias W, Gomes R, Chaves OS Souza, *et al.* Total phenolic content and antioxidant activity of some Malvaceae family species. *Antioxidants.* 2012;1(1):33-43. DOI: 10.3390/antiox1010033.
194. Meda A, Lamien CE, Romito M, Millogo J, Nacoulma OG. Determination of the total phenolic, flavonoid and proline contents in Burkina Fasan honey, as well as their

- radical scavenging activity. Food chem. 2005;91(3):571-7. DOI: 10.1016/j.foodchem.2004.10.006.
195. Chanda S, Dave R. *In vitro* models for antioxidant activity evaluation and some medicinal plants possessing antioxidant properties: An overview. Afr. J. Microbiol. Res. 2009;3(13):981-96.
196. Ghagane SC, Puranik SI, Kumbar VM, Nerli RB, Jalalpure SS, Hiremath MB, *et al.* *In vitro* antioxidant and anticancer activity of *Leea indica* leaf extracts on human prostate cancer cell lines. Integr. Med. Res. 2017;6(1):79-87. DOI: 10.1016/j.imr.2017.01.004.
197. Chen Z, Bertin R, Froidi G. EC₅₀ estimation of antioxidant activity in DPPH assay using several statistical programs. Food Chem. 2013;138(1):414-20. DOI: 10.1016/j.foodchem.2012.11.001.
198. Raju DC, Victoria TD, Biji N, Nikitha G. Evaluation of antioxidant potential of ethanolic extract of *Centella asiatica* L. Res. J. Pharm. Technol. 2015;8(9):1289-93. DOI: 10.5958/0974-360X.2015.00234.6.
199. Ruch RJ, Cheng SJ, Klaunig JE. Prevention of cytotoxicity and inhibition of intercellular communication by antioxidant catechins isolated from Chinese green tea. Carcinogenesis. 1989;10(6):1003-8. DOI: 10.1093/carcin/10.6.1003.
200. Boora F, Chirisa E, Mukanganyama S. Evaluation of nitrite radical scavenging properties of selected Zimbabwean plant extracts and their phytoconstituents. J. Food Process. 2014;2014. DOI: 10.1155/2014/918018.
201. Krishnaveni M, Santhoshkumar J. Secondary metabolite, antioxidant, phytonutrient assay of essential oil from dry *Coriandrum sativum* seed black variety. Res. J. Pharm. Technol. 2016;9(7):853. DOI: 10.5958/0974-360X.2016.00161.X.
202. Praveen D, Chowdary PR, Thanmayi G, Poojitha G, Aanandhi MV. Antioxidant and analgesic activity of leaf extracts of *Artocarpus heterophyllus*. Res. J. Pharm. Technol. 2016;9(3):257-61. DOI: 10.5958/0974-360X.2016.00047.0.

203. Seena H, Kannappan N, Kumar PM. *In vitro* antioxidant and anticancer activity of methanolic extract of *Alangium salvifolium subsp. hexapetalum* (Wangerin). Res. J. Pharm. Technol. 2020;13(8):3715-9. DOI: 10.5958/0974-360X.2020.00657.5.
204. Prior RL, Wu X, Schaich K. Standardized methods for the determination of antioxidant capacity and phenolics in foods and dietary supplements. J Agric. Food Chem. 2005;53(10):4290-302. DOI: 10.1021/jf0502698.
205. Salama ZA, Aboul-Enein AM, Gaafar AA, Asker MS, Aly HF, Ahmed HA. *In-vitro* antioxidant, antimicrobial and anticancer activities of banana leaves (*Musa acuminata*) and olive leaves (*Olea europaea L.*) as by products. Res. J. Pharm. Technol. 2020;13(2):687-96. DOI: 10.5958/0974-360X.2020.00132.8.
206. Keepers YP, Pizao PE, Peters GJ, Van Ark-Otte J, Winograd B, Pinedo HM. Comparison of the sulforhodamine B protein and tetrazolium (MTT) assays for *in vitro* chemosensitivity testing. Eur. J. Cancer. 1991;27(7):897-900. DOI: 10.1016/0277-5379(91)90142-Z.
207. Vichai V, Kirtikara K. Sulforhodamine B colorimetric assay for cytotoxicity screening. Nat. Protoc. 2006;1(3):1112-6. DOI: 10.1038/nprot.2006.179.
208. Bhagwat DA, Swami PA, Nadaf SJ, Choudhari PB, Kumbar VM, More HN, *et al.* Capsaicin loaded solid SNEDDS for enhanced bioavailability and anticancer activity: *in vitro*, *in silico*, and *in vivo* characterization. J. Pharm. Sci. 2021;110(1):280-91. DOI: 10.1016/j.xphs.2020.10.020.
209. Pozarowski P, Grabarek J, Darzynkiewicz Z. Flow cytometry of apoptosis. Curr. Protoc. Cell Biol. 2003;18.8.1-33. DOI: 10.1002/0471143030.cb1808s21.
210. OECD. Guidelines for the Testing of Chemicals. Acute oral toxicity - acute toxic class method. Organization for Economic Co-operation and Development. Test number: 423; 2001.
211. Sinnathambi A, Mazumder PM, Lohidasan S, Thakurdesai P. Dopaminergic effect of *Alstonia scholaris* Linn. R. Br. in experimentally induced anxiety. Biomed Aging Pathol. 2013;3(2):51-7. DOI: 10.1016/j.biomag.2013.04.001.

212. Guillén-Ruiz G, Cueto-Escobedo J, Hernández-López F, Rivera-Aburto LE, Herrera-Huerta EV, Rodríguez-Landa JF. Estrous cycle modulates the anxiogenic effects of caffeine in the elevated plus maze and light/dark box in female rats. *Behav. Brain Res.* 2021;413:113469. DOI: 10.1016/j.bbr.2021.113469.
213. Walf AA, Paris JJ, Frye CA. Chronic estradiol replacement to aged female rats reduces anxiety-like and depression-like behavior and enhances cognitive performance. *Psychoneuroendocrinology.* 2009;34(6):909-16. DOI: 10.1016/j.psyneuen.2009.01.004.
214. Paterson NE, Iwunze M, Davis SF, Malekiani SA, Hanania T. Comparison of the predictive validity of the mirror chamber and elevated plus maze tests in mice. *J. Neurosci. Methods.* 2010;188(1):62-70. DOI: 10.1016/j.jneumeth.2010.02.005.
215. Brown GR, Nemes C. The exploratory behaviour of rats in the hole-board apparatus: is head-dipping a valid measure of neophilia? *Behav. Process.* 2008;78(3):442-8. DOI: 10.1016/j.beproc.2008.02.019.
216. Vogel HG. *Drug discovery and evaluation - pharmacological assays.* 2nd ed. Germany: Springer; 2002.
217. Kulkarni SK. *Practical Pharmacology and Clinical Pharmacy.* 1st ed. India: Vallabh Publications; 2008.
218. Shaikh S, Desai PV. Effect of CoO nanoparticles on the enzyme activities and neurotransmitters of the brain of the mice "*Mus musculus*". *Curr Trends Clin Toxicol.* 2018;2018(1):1-8. DOI: 10.1016/J.JOBAZ.2015.12.003.
219. Wagner H, Bladt S. *Plant drug analysis - A thin layer chromatography atlas.* 2nd ed. Berlin: Springer sciences; 1996.
220. Crowley LC, Waterhouse NJ. Detecting cleaved caspase-3 in apoptotic cells by flow cytometry. *Cold Spring Harb. Protoc.* 2016;2016(11):pdb-rot087312. DOI: 10.1101/pdb.prot087312.
221. Darzynkiewicz Z, Galkowski D, Zhao H. Analysis of apoptosis by cytometry using TUNEL assay. *Methods.* 2008;44(3):250-4. DOI: 10.1016/j.ymeth.2007.11.008.

222. Hummon AB, Lim SR, Difilippantonio MJ, Ried T. Isolation and solubilization of proteins after TRIzol® extraction of RNA and DNA from patient material following prolonged storage. *Biotechniques*. 2007;42(4):467-72. DOI: 10.2144/000112401.
223. Protein Data bank. <https://www.rcsb.org/pdb>. Accessed on 10th June 2022.
224. Gasteiger J, Marsili M. Iterative partial equalization of orbital electronegativity—a rapid access to atomic charges. *Tetrahedron*. 1980;36(22):3219-28. DOI: 10.1016/0040-4020(80)80168-2.
225. Tripos International., 2012. Sybyl-X (Version 2.0). Tripos International. St. Louis, MO, USA.
226. O'Neil MJ. The Merck index: An encyclopedia of chemicals, drugs, and biologicals. 15th ed. United Kingdom: Royal Society of Chemistry RSC Publishing; 2013.
227. Darwish RS, Shawky E, Hammada HM, Harraz FM. Peroxidase inhibitory and antioxidant constituents from *Juniperus L.* species guided by HPTLC-bioautography and molecular docking studies. *Nat Prod Res*. 2021;35:4653-7. DOI: 10.1080/14786419.2019.1700249.
228. Ashok PK, Saini B. HPLC analysis and isolation of rutin from stem bark of *Ginkgo biloba L.* *J. Pharmacogn. Phytochem*. 2013;2(4):68-71.
229. Fathiazad F, Delazar A, Amiri R, Sarker SD. Extraction of flavonoids and quantification of rutin from waste tobacco leaves. *Iran J. Pharm. Res*. 2010;20(3):222-7.
230. Victor MM, David JM, Cortez MV, Leite JL, Da Silva GS. A high-yield process for extraction of hesperidin from orange (*citrus sinensis L.* osbeck) peels waste, and its transformation to diosmetin, A valuable and bioactive flavonoid. *Waste Biomass Valorization*. 2021;12:313-20. DOI: 10.1007/s12649-020-00982-x.
231. Manivannan R, Shopna R. Isolation of quercetin and isorhamnetin derivatives and evaluation of anti-microbial and anti-inflammatory activities of *Persicaria glabra*. *Nat. Prod. Sci*. 2015;21(3):170-15.

232. Rajput MS, Mathur V, Agrawal P, Chandrawanshi HK, Pilaniya U. Fibrinolytic activity of kaempferol isolated from the fruits of *Lagenaria siceraria* (Molina) Standley. Nat. Prod. Res. 2011; 25(19):1870-5. DOI: 10.1080/14786419.2010.540760.
233. Liu C, Chen J, Wang J. A novel kaempferol triglycoside from flower buds of *Panax quinquefolium*. Chem. Nat. Comp. 2009;45:808-810. DOI: 10.1007/s10600-010-9500-1.
234. El Ansari MA, Reddy KK, Sastry KN, Nayudamma Y. Polyphenols of *Mangifera indica*. Phytochemistry. 1971;10(9):2239-41. DOI:10.1016/S0031-9422(00)97234-0.
235. Wu TS, Chang FC, Wu PL, Kuoh CS, Chen IS. Constituents of leaves of *Tetradium glabrifolium*. J Chin Chem Soc. 1995;42(6):929-34. DOI: 10.1002/jccs.199500128.
236. Puppala M, Ponder J, Suryanarayana P, Reddy GB, Petrash JM, LaBarbera DV. 2012. The isolation and characterization of β -glucogallin as a novel aldose reductase inhibitor from *Embllica officinalis*. PloS one. 7(4):e31399. DOI: 10.1371/journal.pone.0031399.
237. Parmar VS, Bisht KS, Sharma SK, Jain R, Taneja P, Singh S, *et al.* Highly oxygenated bioactive flavones from *Tamarix*. Phytochemistry. 1994;36(2):507-11. DOI: 10.1016/S0031-9422(00)97104-8.
238. Li S, Lo CY, Ho CT. Hydroxylated polymethoxyflavones and methylated flavonoids in sweet orange (*Citrus sinensis*) peel. J. Agric. Food Chem. 2006;54(12):4176-85. DOI: 10.1021/jf060234n.
239. Alam MN, Bristi NJ, Rafiquzzaman M. Review on *in vivo* and *in vitro* methods evaluation of antioxidant activity. Saudi Pharm. J. 2013;21(2):143-52. DOI: 10.1016/j.jsps.2012.05.002.
240. Zakaria ZA, Rofiee MS, Teh LK, Salleh MZ, Sulaiman MR, Somchit MN. *Bauhinia purpurea* leaves' extracts exhibited *in vitro* antiproliferative and antioxidant activities. Afr. J. Biotechnol. 2011;10(1):65-74. DOI: 10.5897/AJB10.1354.

241. Zuo AR, Dong HH, Yu YY, Shu QL, Zheng LX, Yu XY, *et al.* The antityrosinase and antioxidant activities of flavonoids dominated by the number and location of phenolic hydroxyl groups. *Chin. Med.* 2018;13:1-2. DOI: 10.1186/s13020-018-0206-9.
242. Abotaleb M, Samuel SM, Varghese E, Varghese S, Kubatka P, Liskova A, *et al.* Flavonoids in cancer and apoptosis. *Cancers.* 2018;11(1):28. DOI: 10.3390/cancers11010028.
243. Swarnalatha Y. Isolation of flavonoids and their anticancer activity from *Sphaeranthus amaranthoides* in A549 cell line. *Res. J. Pharm. Technol.* 2015;8(4):462-67. DOI: 10.5958/0974-360X.2015.00077.3.
244. Ali G, Neda G. Flavonoids and phenolic acids: Role and biochemical activity in plants and human. *J. Med. Plant. Res.* 2011;5(31):6697-703. DOI: 10.5897/JMPR11.1404.
245. Wang Y, Qian J, Cao J, Wang D, Liu C, Yang R, *et al.* Antioxidant capacity, anticancer ability and flavonoids composition of 35 citrus (*Citrus reticulata* Blanco) varieties. *Molecules.* 2017;22(7):1114. DOI: 10.3390/molecules22071114.
246. Kumar S, Pandey AK. Chemistry and biological activities of flavonoids: an overview. *Sci. World J.* 2013;2013. DOI: 10.1155/2013/162750.
247. Ghafouri-Fard S, Shoorei H, Sasi AK, Taheri M, Ayatollahi SA. The impact of the phytotherapeutic agent quercetin on expression of genes and activity of signaling pathways. *Biomed. Pharmacother.* 2021;141:111847. DOI: 10.1016/j.biopha.2021.111847.
248. Li Q, Ren FQ, Yang CL, Zhou LM, Liu YY, Xiao J, *et al.* Anti-proliferation effects of isorhamnetin on lung cancer cells *in vitro* and *in vivo*. *Asian Pac. J. Cancer Prev.* 2015;16(7):3035-42.
249. Elmore S. Apoptosis - A review of programmed cell death. *Toxicol Pathol.* 2007;35(4):495-516. DOI: 10.1080/01926230701320337.

250. Engeland MV, Van den Eijnde SM, Aken TV, Vermeij-Keers C, Ramaekers FC, Schutte B, *et al.* Detection of apoptosis in ovarian cells *in vitro* and *in vivo* using the annexin V-affinity assay. *Ovarian Cancer*. 2001;669-77.
251. Israel BE, Tilghman SL, Parker-Lemieux K, Payton-Stewart F. Phytochemicals: Current strategies for treating breast cancer. *Oncol. Lett.* 2018;15(5):7471-8. DOI: 10.3892/ol.2018.8304.
252. Farrag IM, Belal A, Al Badawi MH, Abdelhady AA, Abou Galala FM, El-Sharkawy A, *et al.* Antiproliferative, apoptotic effects and suppression of oxidative stress of quercetin against induced toxicity in lung cancer cells of rats: *In vitro* and *in vivo* study. *J. Cancer*. 202;12(17):5249-59. DOI: 10.7150/jca.52088.
253. Wang F, Wang L, Qu C, Chen L, Geng Y, Cheng C, *et al.* Kaempferol induces ROS-dependent apoptosis in pancreatic cancer cells via TGM2-mediated Akt/mTOR signaling. *BMC Cancer*. 2021;21(1):1-1. DOI: 10.1186/s12885-021-08158-z.
254. Park C, Cha HJ, Choi EO, Lee H, Hwang-Bo H, Ji SY, *et al.* Isorhamnetin induces cell cycle arrest and apoptosis via reactive oxygen species-mediated AMP-activated protein kinase signaling pathway activation in human bladder cancer cells. *Cancers*. 2019;11(10):1494. DOI: 10.3390/cancers11101494.
255. Cabrera J, Saavedra E, Del Rosario H, Perdomo J, Loro JF, Cifuentes DA, *et al.* Gardenin B-induced cell death in human leukemia cells involves multiple caspases but is independent of the generation of reactive oxygen species. *Chem.Biol. Interact.* 2016;256:220-7. DOI: 10.1016/j.cbi.2016.07.016.
256. Aparecida Gelfuso E, Santos Rosa D, Lúcia Fachin A, Renata Mortari M, Olimpio Siqueira Cunha A, Oliveira Belebony R. Anxiety: a systematic review of neurobiology, traditional pharmaceuticals and novel alternatives from medicinal plants. *CNS Neurol. Disord.* 2014;13(1):150-65.
257. Schiavone S, Sorce S, Dubois-Dauphin M, Jaquet V, Colaianna M, Zotti M, *et al.* Involvement of NOX2 in the development of behavioral and pathologic alterations in

- isolated rats. Biol. Psychiatry. 2009;66(4):384-92. DOI: 10.1016/j.biopsych.2009.04.033.
258. Dimonte S, Sikora V, Bove M, Morgese MG, Tucci P, Schiavone S, *et al.* Social isolation from early life induces anxiety-like behaviors in adult rats: Relation to neuroendocrine and neurochemical dysfunctions. Biomed. Pharmacother. 2023;158:114181. DOI: 10.1016/j.biopha.2022.114181.
259. Savage K, Firth J, Stough C, Sarris J. GABA-modulating phytomedicines for anxiety: A systematic review of preclinical and clinical evidence. Phyther. Res. 2018;32(1):3-18. DOI: 10.1002/ptr.5940.
260. Ahmad A, Rasheed N, Banu N, Palit G. Alterations in monoamine levels and oxidative systems in frontal cortex, striatum, and hippocampus of the rat brain during chronic unpredictable stress. Stress. 2010;13(4):356-65. DOI: 10.3109/10253891003667862.
261. Bhutada P, Mundhada Y, Bansod K, Ubgade A, Quazi M, Umathe S, *et al.* Reversal by quercetin of corticotrophin releasing factor induced anxiety and depression like effect in mice. Prog. NeuroPsychopharmacol. 2010;34(6):955-60. DOI: 10.1016/j.pnpbp.2010.04.025.
262. Dhingra D, Chhillar R, Gupta A. Antianxiety like activity of gallic acid in unstressed and stressed mice - possible involvement of nitriergic system. Neurochem. Res. 2012;37:487-94. DOI: 10.1007/s11064-011-0635-7.
263. Ali G, Neda G. Flavonoids and phenolic acids: Role and biochemical activity in plants and human. J. Med. Plant. Res. 2011;5(31):6697-703. DOI: 10.5897/JMPR11.1404.
264. Ko YH, Kim SK, Lee SY, Jang CG. Flavonoids as therapeutic candidates for emotional disorders such as anxiety and depression. Arch. Pharm Res. 2020;43:1128-43. DOI: 10.1007/s12272-020-01292-5.
265. Ullah A, Munir S, Badshah SL, Khan N, Ghani L, Poulson BG, *et al.* Important flavonoids and their role as a therapeutic agent. Molecules. 2020;25(22):5243. DOI: 10.3390/molecules25225243.







ANNEXURES



ANNEXURE - I

ANNEXURE – I

AUTHENTICATION OF *HYBANTHUS ENNEASPERMUS* SPECIMEN.

 निस्केयर NISCAIR	 सीएसआईआर - राष्ट्रीय विज्ञान संचार एवं सूचना स्रोत संस्थान CSIR-NATIONAL INSTITUTE OF SCIENCE COMMUNICATION AND INFORMATION RESOURCES (वैज्ञानिक एवं औद्योगिक अनुसंधान परिषद्) (Council of Scientific and Industrial Research) डॉ. के. एस. कृष्णन् मार्ग, नई दिल्ली 110 012 Dr. K. S. KRISHNAN MARG, (Near Pusa Gate), NEW DELHI 110 012 14, सत्संग विहार मार्ग, नई दिल्ली 110 067 14, SATSANG VIHAR MARG, NEW DELHI 110 067
<u>RAW MATERIAL HERBARIUM AND MUSEUM, DELHI (RHMD)</u>	
Ref. No.-NISCAIR/RHMD/Consult/2017/3101-50	24/08/2017
<u>CERTIFICATE FOR CRUDE DRUG SAMPLE AUTHENTICATION</u>	
<p>This is to certify that whole plants sample of <i>Hybanthus enneaspermus</i>, Ratan Purush, Spade Flower, received from Ms. Liesl Maria Fernandes vide letter No. Nil dated 16th August 2017 for authentication has been found correct as whole plants of <i>Hybanthus enneaspermus</i> (L.) F. Muell. which is commonly known as Ratanpurush and Spade Flower. The identification has been done on the basis of macroscopic studies of the sample followed by detailed scrutiny of literature and matching the sample with authentic samples deposited in the Raw Material Herbarium and Museum, Delhi (RHMD).</p>	
<p>Identification pertains to the quantity/quality of specimen/sample(s) received in RHMD. This certificate is not issued for any judicial purpose.</p>	
 (Mr. RS Jayasomu) Senior Principal Scientist Head, RHMD	 (Dr. Sunita Garg) Emeritus Scientist, CSIR-NISCAIR sunitag@niscair.res.in; sunita.niscair@gmail.com Ph.: +91-11-25846001; 25846301. Ext. 263
Ms. Liesl Maria Fernandes Goa College of Pharmacy 18 th June Road Panaji-Goa	



ANNEXURE – II

ANNEXURE – II

AUTHENTICATION OF *BAUHINIA FOVEOLATA* SPECIMEN.

Dr. Satyanarayan S. Hebbar

Lecturer

Department of Biology

Government P.U. College,

R.N. Shetty Stadium

Dharwad - 580008,

Karnataka INDIA

MOB: 9448922821

Email: sshebbar12@gmail.com

Date: 10.01.2018

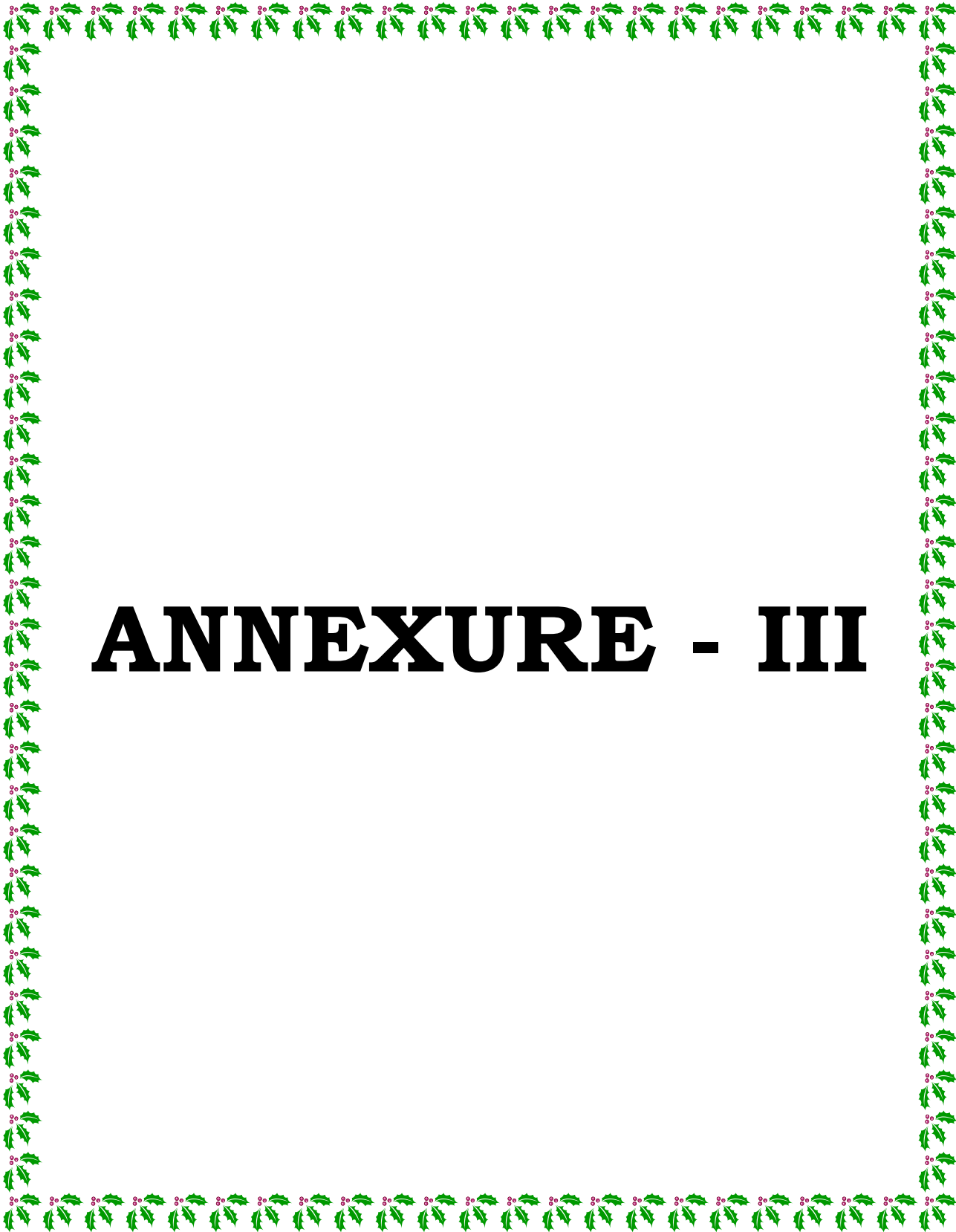
Sub: Authentication of plant material submitted

This is to certify that the plant material submitted by Ms. Liesl Maria Fernandes, Goa College of Pharmacy, Panajim Goais identified as *Bauhinia foveolata* Dalzell belonging to the family Leguminosae. Voucher specimen of the same has been deposited in our herbarium with accession no. GCPDOP-07.



Dr. Satyanarayan S. Hebbar




Dr. S. S. Hebbar
Lecturer in Biology
Govt. P.U. College
Dharwad-580 008.

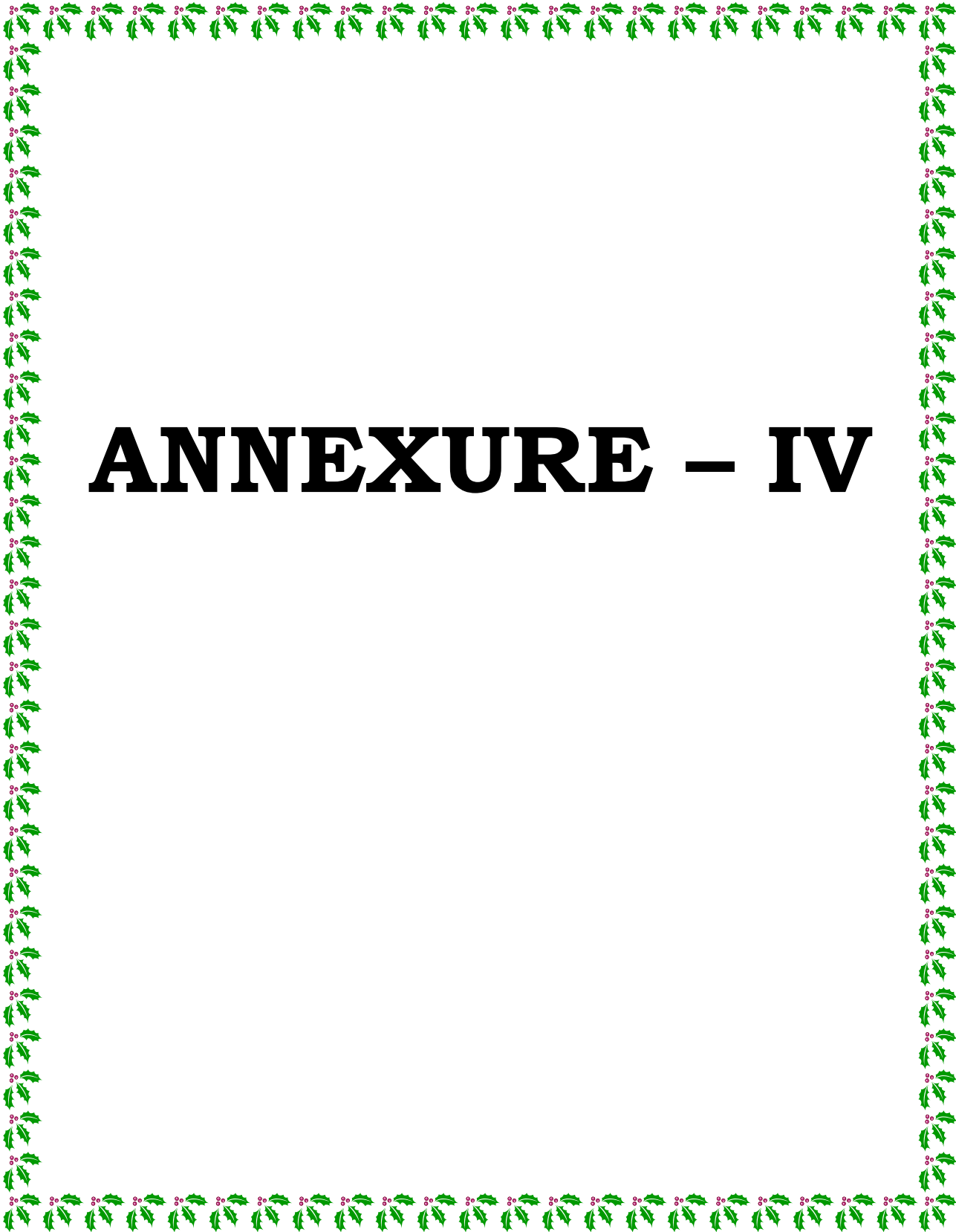


ANNEXURE - III

ANNEXURE – III

INSTITUTIONAL ANIMAL ETHICS COMMITTEE APPROVAL FOR ANXIOLYTIC
ACTIVITY STUDIES

Goa College of Pharmacy Department of Pharmacology Institutional Animal Ethics Committee (611/02/c/CPSCEA)			
<u>Certificate</u>			
<p>This is to certify that the project proposal no. GCP/IAEC/2020/08 entitled "Phytochemical and Pharmacological investigations of <i>Hybanthus enneaspermus</i> Linn. and <i>Bauhinia foveolata</i> Dalzell" submitted by Mrs. Liesl Maria Fernandes e Mendonça has been approved/recommended by the Institutional Animals Ethics Committee of Goa College of Pharmacy, Panaji Goa in its meeting held on 11.02.2021 and <u>78</u> Wistar Albino rats have been sanctioned under this.</p>			
Authorized by	Name	Signature	Date
Chairman:	Dr. Madhusudan P. Joshi		11/2/21
Member Secretary:	Smt. Asmita S. Arondekar		11.02.2021
Main Nominee of CPCSEA:	Dr. Viswanatha Swamy A.H.M.		11.02.2021
GCP/IAEC/2020/08			
9			



ANNEXURE – IV

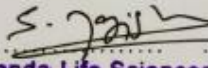
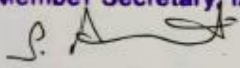
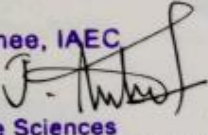
ANNEXURE – IV

INSTITUTIONAL ANIMAL ETHICS COMMITTEE APPROVAL FOR ACUTE TOXICITY STUDIES

Skanda Life Sciences

CERTIFICATE

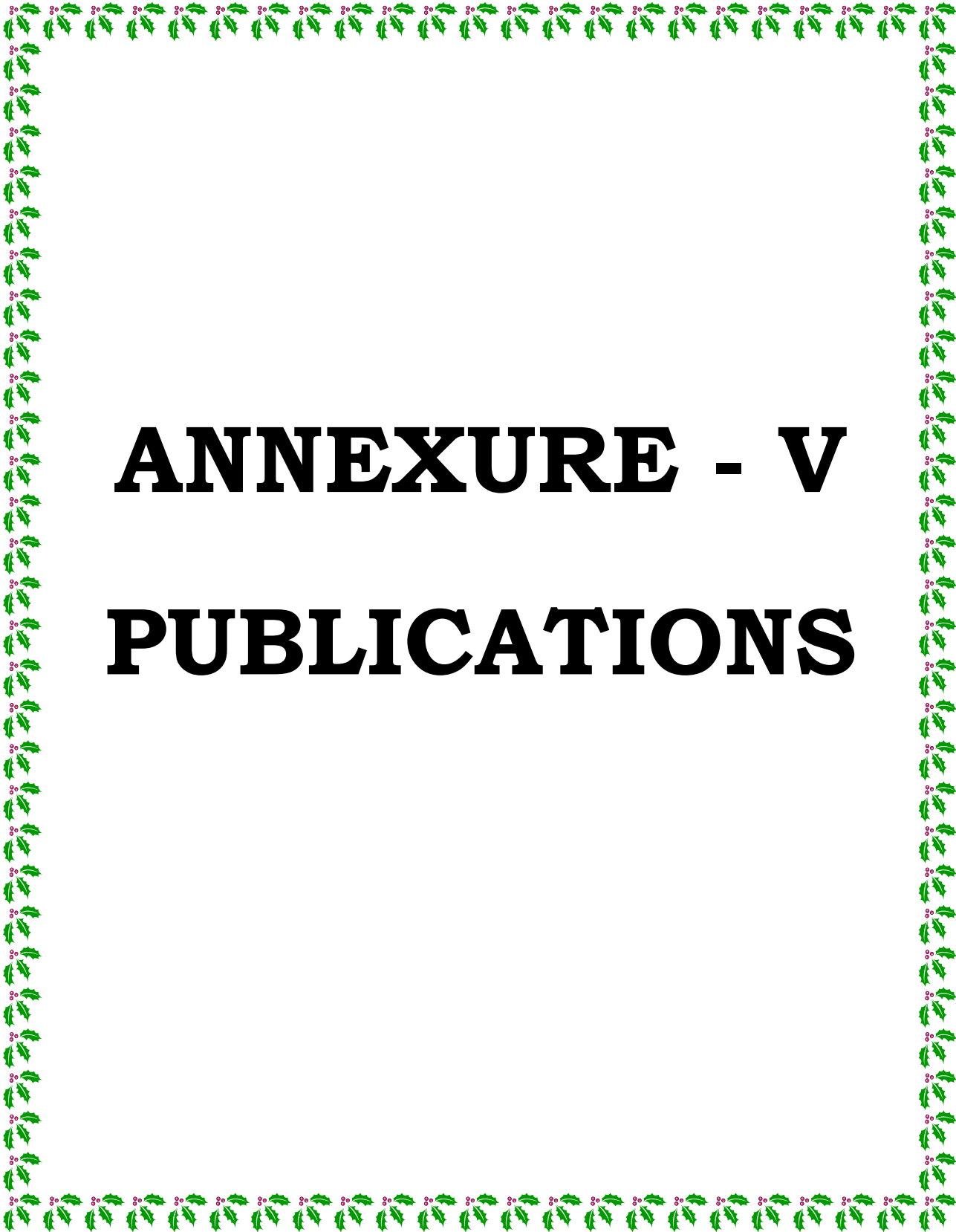
This is to certify that the project proposal no. IAEC-SLS-2021-037 entitled Acute oral toxicity study of test sample in rats submitted by Dr. Channabasava R has been approved / recommended by the IAEC of Skanda Life Sciences (Organization) in its meeting dated 28th July 2021 and has been sanctioned 225 Rat Sprague dawley Female (animals) under this proposal for a duration of next 12 months.

Authorized by	Name	Signature	Date
Chairman:	<u>Dr. Yogisha S</u>	Chairperson, IAEC  Skanda Life Sciences	09/08/2021
Member secretary	<u>Dr. Anand S</u>	Member Secretary, IAEC  Skanda Life Sciences	09/08/2021
Main Nominee of CPCSEA:	<u>Dr. J. Anbu</u>	Main Nominee, IAEC  Skanda Life Sciences	25/8/2021

(Kindly make sure that minutes of the meeting duly signed by all the participants are maintained by Office)

Page 7 of 9

IAEC-SLS-2021-037



ANNEXURE - V

PUBLICATIONS

ANNEXURE V

**PUBLICATIONS -
MANUSCRIPT CONTRIBUTIONS FROM THE THESIS**

MANUSCRIPT PUBLISHED/ACCEPTED FOR PUBLICATION

1. Fernandes e Mendonça LM, Joshi AB, Bhandarkar AV, Joshi H. 2021. Evaluation of antioxidant property and anticancer prospective of the leaf extract and biofractions of *Bauhinia foveolata* Dalzell - A native of the Indian Western Ghats. Int. J. Res Pharm Sci. 12(3):1886-94. <https://doi.org/10.26452/ijrps.v12i3.4789>
2. Fernandes e Mendonça LM, Joshi AB, Bhandarkar AV, Joshi H, Joshi S. 2023. Phytoconstituents from *Piliostigma foveolatum* (Dalzell) Thoth. leaves induce anti-proliferative effect, apoptosis and cell cycle arrest in Hop-62 cells. Nat. Prod. Res. 1-5. <https://doi.org/10.1080/14786419.2023.2197228> (Taylor and Francis, Impact Factor : 2.488)
3. Manuscript titled “Antioxidant, Antiproliferative, Pro-apoptotic and cell cycle arrest properties of crude extract and biofractions of *Hybanthus enneaspermus* Linn. to combat breast cancer.” authored by Liesl Maria Fernandes e Mendonca, Arun Bhimrao Joshi, Anant Bhandarkar, Himanshu Joshi. has been accepted on 18th November 2022 for publication in Research Journal of Pharmacy and Technology in the Year 2023, Volume 16, issue 9 of the journal.

MANUSCRIPT COMMUNICATED

1. Potential anxiolytic therapeutics from *Hybanthus enneaspermus* Linn.: A phytochemical, *in vivo* and *in silico* evaluation. Liesl Maria Fernandes e Mendonca, Arun Bhimrao Joshi, Anant Bhandarkar, Shamshad Shaikh, Samantha Fernandes, Himanshu Joshi, Srinivas Joshi.

MANUSCRIPT IN PREPARATION

1. Polymethoxyflavone Gardenin B isolated from *Bauhinia foveolata* Dalzell. leaves arrest cervical cancer cells. Liesl Maria Fernandes e Mendonca, Arun Bhimrao Joshi, Anant Bhandarkar, Himanshu Joshi.



Evaluation of antioxidant property and anticancer prospective of the leaf extract and biofractions of *Bauhinia foveolata* Dalzell – A native of the Indian Western Ghats

Liesl Maria Fernandes e Mendonça^{*1}, Arun B. Joshi², Anant V. Bhandarkar², Himanshu Joshi³

¹Department of Pharmacology, Goa College of Pharmacy, 18th June Road, Panaji, Goa – 403001 India

²Department of Pharmacognosy and Phytochemistry, Goa College of Pharmacy, 18th June Road, Panaji, Goa – 403001 India

³Department of Pharmacology, College of Pharmacy, Graphic Era Hill university, Bhimtal campus, Uttarakhand – 263156 India

Article History:

Received on: 03 Mar 2021

Revised on: 01 Apr 2021

Accepted on: 09 Apr 2021

Keywords:

DPPH (2,2-diphenyl-1-picrylhydrazyl),
Hydrogen peroxide,
MCF-7 cells,
Nitric oxide,
Sulforhodamine B

ABSTRACT



The current study was designed to evaluate the antioxidant and anticancer potential of ethanolic leaf extract of *Bauhinia foveolata* Dalzell. (EEBF) and its toluene, ethyl acetate and methanolic biofractions viz., TFBB, EBBF and MBBF. Phytoconstituents were screened by adopting established procedures. Total phenolic and flavonoid content were assessed spectrophotometrically. *In vitro* antioxidant activity was assayed using DPPH (2,2-diphenyl-1-picrylhydrazyl), hydrogen peroxide and nitric oxide as free radicals, whereas anticancer activity was evaluated using sulforhodamine B assay. EEBF showed maximum phenolic content of 49.12 ± 0.31 mg GAE/g and flavonoidal content of 28.75 ± 0.42 mg QUE/g, than its biofractions. EEBF showed considerable antioxidant activity with $IC_{50} = 19.04 \pm 0.24$ μ g/mL and $IC_{50} = 65.85 \pm 1.22$ μ g/mL when compared to the standards Ascorbic acid ($IC_{50} = 12.06 \pm 0.05$ μ g/mL) and Gallic acid ($IC_{50} = 64.65 \pm 0.72$ μ g/mL) in DPPH and nitric oxide scavenging assays, respectively. MBBF showed significant activity with $IC_{50} = 26.76 \pm 0.75$ μ g/mL in hydrogen peroxide scavenging assay compared to the standard Gallic acid ($IC_{50} = 76.60 \pm 1.31$ μ g/mL). TFBB showed favourable growth inhibition of MCF-7 cells with $GI_{50} = 73.5 \pm 11.96$ μ g/mL when compared to other samples screened ($GI_{50} > 80$ μ g/mL) as against the standard Adriamycin ($GI_{50} < 10$ μ g/mL) in SRB assay. The therapeutic virtues of EEBF and MBBF as free radical scavengers and TFBB as an antiproliferative may be attributed to the phenolics, flavonoids, steroids and triterpenoids present.

*Corresponding Author

Name: Liesl Maria Fernandes e Mendonça

Phone: +91-9822185432

Email: lieslpharma@gmail.com

ISSN: 0975-7538

DOI: <https://doi.org/10.26452/ijrps.v12i3.4789>

Production and Hosted by

Pharmascope.org

© 2021 | All rights reserved.

INTRODUCTION

Reactive free radicals contribute to oxidative stress in the living cells by damaging the lipids, proteins, DNA and other macromolecular components (Pham-Huy *et al.*, 2008). Altered cellular changes and excitotoxicity play a specific feature in the pathogenesis of degenerative diseases like cancer, cardiovascular diseases, neurodegenerative disorders, cataract and inflammation (M. *et al.*, 2020). Cancer is a life-threatening disease that can potentially diminish the quality of life of an individual. Breast cancer is a growing concern nowa-

days, as it is a leading cause of cancer-related mortalities amongst women worldwide (Malvia *et al.*, 2017; Mathur *et al.*, 2020). It can be clinically sub-classified based on the underlying molecular mechanisms viz., gene expression and receptor status (estrogen receptor [ER], progesterone receptor [PR], human epidermal growth factor receptor 2 [HER2]) and proliferation status (Medeiros and Allan, 2019). Constant research is being carried out to identify agents that may help alleviate the symptoms and treat breast cancer.

Consumption of antioxidant-rich food helps to minimize the chances of the development of degenerative diseases (Do *et al.*, 2014). Potential free radical scavengers may thus help reduce cell death.

Plants rich in essential phytoconstituents are being extensively investigated for their medicinal potential to treat various ailments. Several species of the genus *Bauhinia* are widely distributed across Africa, Asia and South America and have been used frequently in folk medicine to treat different kinds of pathologies (Filho, 2009). *Bauhinia foveolata* Dalzell. (family Leguminosae) is usually found along the Western Ghats of India. The tree is dioecious and grows to a height of about 30 meters. Leaves are suborbicular to broadly ovate and pubescent beneath numerous closely situated fine pits within areolae of reticulations (Bandyopadhyay *et al.*, 2005). The synonyms of *B. foveolata* are *Bauhinia lawii* Baker and *Piliostigma foveolatum* (Dalzell) Thoth, and its common name is Pore leaved *Bauhinia*. Its leaves are possibly the largest among all *Bauhinia* species found in India, and its scientific name *foveolata* is due to the presence of minute pores (foveoli) on the underside of the leaves (Bandyopadhyay *et al.*, 2005; Habbu *et al.*, 2020). Very few studies have been documented on *B. foveolata* Dalzell. A recent study reported the isolation of quercetin and odoratin-7-glucoside from butanol fraction of ethanolic leaf extract of *B. foveolata* that exhibited cytotoxicity towards the human colon cancer cell lines, HT-29 and HCT-15 (Habbu *et al.*, 2020). The acetone and ethyl acetate extracts of *B. foveolata* bark reported antibacterial and antimalarial activities, respectively (Gamit *et al.*, 2018). The commonly found species of *Bauhinia* in India have reported antioxidant, antimicrobial and cytotoxic effects (Mishra *et al.*, 2013; Vijayan *et al.*, 2019).

Thus, the current study was focused on evaluating the antioxidant and anticancer potential of the ethanolic leaf extract of *B. foveolata* Dalzell. (EEBF) and its toluene, ethyl acetate and methanol soluble fractions, i.e., TFBF, EFBF and MFBF by *in vitro* assays.

MATERIALS AND METHODS

Chemicals and reagents

High purity analytical grade solvents and chemicals were used for the study. Folin ciocalteu reagent, aluminum chloride, DPPH, sodium nitroprusside, ferrous ammonium sulfate, and sulphanilamide were purchased from Molychem (Mumbai, India). 1,10-phenanthroline and hydrogen peroxide solution were purchased from Merck (Bangalore, India). Naphthyethylene diamine was procured from Qualigens (Mumbai, India). Reference standards were procured from Sigma-Aldrich (St. Louis, Mo., USA).

Instrumentation

A double beam UV-Vis spectrophotometer (LABINDIA Analytical UV 3092) was used for spectroscopic analysis.

Plant material

Fresh leaves of *B. foveolata* were collected from the forests of Dandeli, Karnataka – India, in the months of August-September 2017. They were washed to remove the extraneous matter and then dried. Dr. Satyanarayan S. Hebbar, Department of Botany, Government Pre university college, Dharwad, Karnataka, authenticated the specimen (GCPDOP-07) which was then deposited in the Department.

Preparation of experimental samples

The experimental samples consisted of the ethanolic leaf extract of *B. foveolata* (EEBF) and its three biofractions viz., toluene soluble fraction of EEBF (TFBF), ethyl acetate soluble fraction of EEBF (EFBF) and methanol soluble fraction of EEBF (MFBF).

Preparation of the ethanolic leaf extract of *B. foveolata* (EEBF)

1.5 kg of powdered leaves were defatted by refluxing with 3.5 L of Petroleum ether thrice. The defatted drug (900g) was refluxed with absolute ethanol (4.5L) for 90 minutes, thrice. The alcoholic extract was filtered using the Whatmann filter paper (No.1). The solvent from the extract was distilled off using a rotary evaporator and air-dried to yield the dry extract (79.14g). The ethanolic extract of *B. foveolata* (EEBF) was stored at 4°C until further processed.

Preparation of biofractions of EEBF

20 g of EEBF was refluxed successively with toluene, ethyl acetate and methanol and filtered using Whatmann filter paper (No.1). The solvent was distilled off using a rotary evaporator and the toluene, ethyl acetate and methanol soluble fractions of the

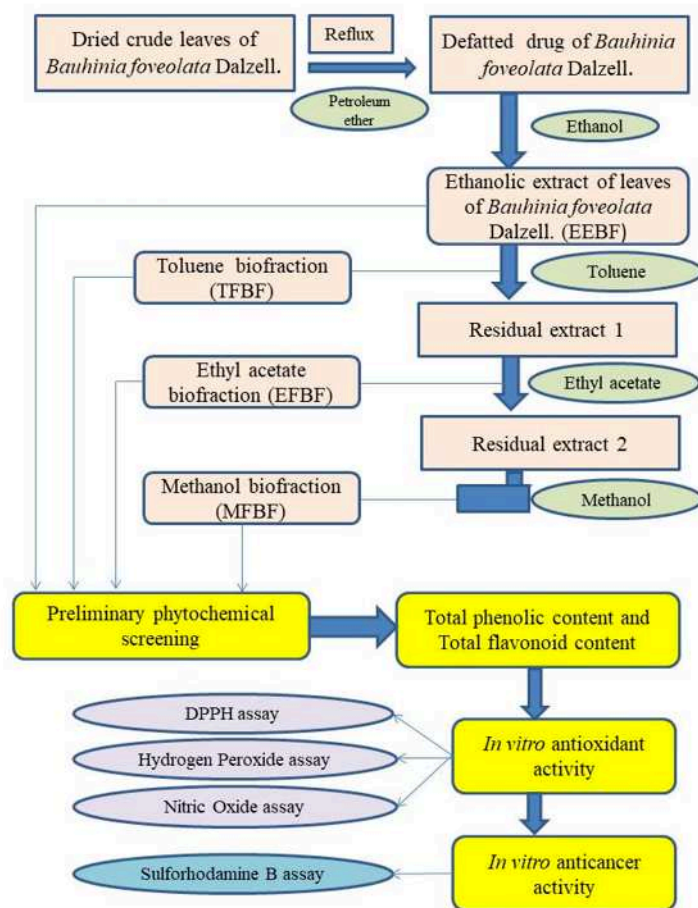


Figure 1: Schematic representation of the process.

ethanolic leaf extract of *B. foveolata* viz., TFBF (5.14g), EFBF (3.36g) and MFBF (6.91g) were successively obtained and stored at 4°C until further used (Figure 1).

Qualitative phytochemical screening

The experimental samples (EEBF, TFBF, EFBF and MFBF) were screened to detect the phytoconstituents present by adopting standard procedures (Khandelwal, 2010).

QUANTITATIVE PHYTOCHEMICAL ANALYSIS

The total phenolic content, total flavonoid content, *in vitro* antioxidant and anticancer activities were carried out with slight modifications to the referenced procedures.

Total Phenolic Content

The total phenolic content of the experimental samples was determined using the Folin-Ciocalteu's method (Oliveira et al., 2012). The intensity of blue colour formed due to the polyphenol content in different concentrations (10 - 1000 µg/mL) of experimental samples was measured at 760 nm using UV-

Visible spectrophotometer. Various concentrations (10-100 µg/mL) of gallic acid were used to plot the standard curve. The total phenolic content of EEBF and its biofractions were expressed as mg of GAE/g of samples.

Total Flavonoid content

The total flavonoid content of the experimental samples was estimated using the aluminum chloride colorimetry method (Meda et al., 2005). The reactions of varying concentrations (10 - 1000 µg/mL) of experimental samples were analyzed at an absorbance of 415nm using a UV-VIS spectrophotometer. The standard graph was plotted with a series of concentrations (10-100 µg/mL) of quercetin on the X-axis and absorbance on the Y-axis. The total flavonoid content of EEBF and its biofractions was determined from the standard graph and expressed as mg of QUE equivalents/g of samples.

In vitro antioxidant activity

The *in vitro* antioxidant activity of the selected experimental samples (EEBF, TFBF, EFBF and MFBF) was measured using the DPPH, hydrogen peroxide and nitric oxide radical scavenging

methods.

DPPH (2,2-diphenyl-1-picrylhydrazyl) radical scavenging assay

The radical scavenging assay of the selected samples was studied using DPPH free radicals (Chanda and Dave, 2009). The absorbances of the reaction mixtures that consisted of 1 mL of DPPH in methanol (0.3 mM), 1 mL of varying concentrations of experimental samples (10 - 1000 $\mu\text{g/mL}$) or standard drug Ascorbic acid (2 - 20 $\mu\text{g/mL}$) and 1 mL of methanol, was measured at 517 nm using a UV-Visible spectrophotometer, after incubation for 30 min in the dark, at room temperature. The percentage of DPPH scavenged was calculated by using the formula,

$$\% \text{ DPPH scavenged} = \left[\frac{\text{Absorbance of control} - \text{Absorbance of sample}}{\text{Absorbance of control}} \right] \times 100$$

Hydrogen peroxide radical scavenging assay

In this assay, the reaction mixture consisted of 0.3mL of ferrous ammonium sulfate (1 mM), different concentrations of experimental samples (10 - 100 $\mu\text{g/mL}$) or standard drug Gallic acid (10 - 100 $\mu\text{g/mL}$), 0.1 mL of hydrogen peroxide (5 mM) and 1.5 mL of 1,10-phenanthroline (1mM) (Mukhopadhyay et al., 2016). After appropriate incubation, the absorbance of the reaction mixture was analysed at a wavelength of 510 nm using a UV-Visible spectrophotometer. The percentage of hydrogen peroxide free radical scavenged was calculated by using the formula

$$\% \text{ H}_2\text{O}_2 \text{ scavenged} = \left[\frac{\text{Absorbance of sample}}{\text{Absorbance of control}} \right] \times 100$$

Nitric oxide radical scavenging (NO) assay

The amount of nitric oxide free radical scavenged by the treatment groups was determined (Boora et al., 2014). The absorbance of the reaction mixtures that consisted of 1mL of sodium nitroprusside solution with 1 mL of different concentrations of experimental samples (10 - 1000 $\mu\text{g/mL}$) or standard drug Gallic acid (10 - 100 $\mu\text{g/mL}$), incubated in the dark at 25°C for 180 min, successively treated with 2mL of freshly prepared Griess reagent and further incubated for 20 min was measured using a UV-Visible spectrophotometer at a wavelength of 540 nm.

The percentage of free radical nitric oxide scavenged was calculated by using the formula,

$$\% \text{ Nitric Oxide scavenged} = \left[\frac{\text{Absorbance of control} - \text{Absorbance of sample}}{\text{Absorbance of control}} \right] \times 100$$

In vitro anticancer activity

The *in vitro* anticancer activity of the experimental samples was determined using SRB assay (Lopez et al., 2018; Skehan et al., 1990; Vichai and Kirtikara, 2006). RPMI 1640 media containing 10% fetal bovine serum along with 2mM L-glutamine were used to grow the MCF-7 cell lines, which were further inoculated into 96 well microtiter plates in 100 μL at plating densities of 1×10^3 cells/well and incubated at 37°C, 5% CO_2 , 95% air and 100% relative humidity for 24 h before addition of experimental samples (EEBF and its biofractions) or standard drug Adriamycin. Standard drug and experimental samples were solubilized in dimethyl sulfoxide at 100mg/mL and diluted with water. Varying concentrations of 10 $\mu\text{g/mL}$, 20 $\mu\text{g/mL}$, 40 $\mu\text{g/mL}$ and 80 $\mu\text{g/mL}$ of each experimental sample or standard drug were added to the microtiter wells and incubated at 37°C for 48 h. The assay was concluded by addition of cold trichloroacetic acid. About 50 μL of trichloroacetic acid (30%w/v) was added to fix the cells in situ and incubated at 4°C for 60 min. After incubation, cells were washed, air-dried and stained with sulforhodamine B (SRB) for 20 mins and then washed with 1% acetic acid to remove excess stain. Tris buffer (10 mmol/L) was used to dissolve the bound sulforhodamine B and absorbance was measured on a plate reader at a wavelength of 540 nm. The average absorbance of test and control well was calculated and the percentage growth of MCF-7 cells was expressed using the formula,

$$\% \text{ growth} = \left[\frac{\text{Absorbance of test well}}{\text{Absorbance of control wells}} \right] \times 100$$

Statistical analysis

Analyses were performed in triplicate observations and recorded. Data was documented as mean value \pm standard deviation (SD). Calculation of IC_{50} and GI_{50} values were done using GraphPad Prism version 7.3. Statistical analysis was done using IBM® SPSS version 23.0 statistical software (IBM Corporation, New York, USA). One way Analysis of Variance (ANOVA) was used to measure statistical significance along with Duncan's multiple test ($P < 0.05$ for antioxidant activity and < 0.001 for anticancer activity).

RESULTS

Preliminary phytochemical analysis

The ethanolic leaf extract of *B. foveolata* (EEBF) and its experimental biofractions have confirmed the presence of alkaloids, flavonoids, tannins and phenolic compounds. Steroids and triterpenoids were present in EEBF and its toluene biofraction (Table 1).

Table 1: Preliminary phytochemical analysis of ethanolic leaf extract of *B. foveolata* and its biofractions.

Sr. No.	Phytochemical constituents	EEBF	TFBF	EFBF	MFBF
1.	Alkaloids	+ve	+ve	+ve	+ve
2.	Glycosides	+ve	-ve	-ve	+ve
3.	Saponins	+ve	-ve	-ve	+ve
4.	Carbohydrates	+ve	-ve	-ve	+ve
5.	Flavanoids	+ve	+ve	+ve	+ve
6.	Proteins	+ve	-ve	-ve	+ve
7.	Tannins and Phenolics	+ve	+ve	+ve	+ve
8.	Resins	-ve	-ve	-ve	-ve
9.	Steroids And Triterpenoids	+ve	+ve	-ve	-ve
10.	Starch	-ve	-ve	-ve	-ve

Where -ve indicates absent, +ve indicates present.

Table 2: Total phenolic content by Folin-ciocalteu method and Total flavonoid content by aluminum chloride method.

Method	EEBF	TFBF	EFBF	MFBF
Total phenolic content (mg GAE/g)	49.12±0.31	3.27±0.35	21.01±0.35	25.65±0.21
Total flavonoid content (mg QUE/g)	28.75±0.42	1.14±0.28	11.12±0.46	14.83±0.31

Each value is expressed as mean ± SD (n=3).

Table 3: *In vitro* antioxidant activity - DPPH, hydrogen peroxide and nitric oxide free radical scavenging activity.

Free radical scavenging assay	IC ₅₀ values (µg/mL)				
	Standard	EEBF	TFBF	EFBF	MFBF
DPPH	12.06±0.05 ^a	19.04±0.24 ^b	391.5±3.32 ^c	68.39±0.27 ^d	53.44±0.83 ^c
H ₂ O ₂	76.60±1.31 ^a	43.96 ±0.92 ^d	71.45±1.03 ^b	64.66±0.43 ^c	26.76±0.75 ^e
NO	64.65±0.72 ^a	65.85±1.22 ^a	569.67±4.19 ^c	288.67±10.61 ^b	71.63±0.19 ^a

Each value is articulated as the mean ± SD (n= 3). Within each row, the means with different superscript letters are statistically significant (ANOVA, $P < 0.05$, and subsequent post hoc multiple comparisons with Duncan's test).

Table 4: *In vitro* anticancer activity on human breast cancer cell line MCF-7

Experimental sample/standard	% Control Growth of MCF-7 cell lines			
	10 µg/mL	20 µg/mL	40 µg/mL	80 µg/mL
EEBF	92.2±3.59 ^b	91.6±6.16 ^b	85.5±3.77 ^c	74.7±11.45 ^b
TFBF	88.9±9.13 ^b	82.1±6.50 ^b	67.8±5.57 ^b	47.0±10.67 ^b
EFBF	93.5±5.70 ^b	93.3±10.5 ^{bc}	90.7±10.2 ^c	67.1±9.4 ^b
MFBF	104.7±3.89 ^b	111.1±8.72 ^c	114.9±4.72 ^d	115.4±8.09 ^c
Standard (Adriamycin)	-61.2±5.26 ^a	-64.9±2.34 ^a	-50.5±6.98 ^a	-18.8±21.17 ^a

Each value is expressed as the mean ± SD (n =3). Within each column, the means with different superscript letters are statistically significant (ANOVA, $P < 0.001$, and subsequent post hoc multiple comparisons with Duncan's test).

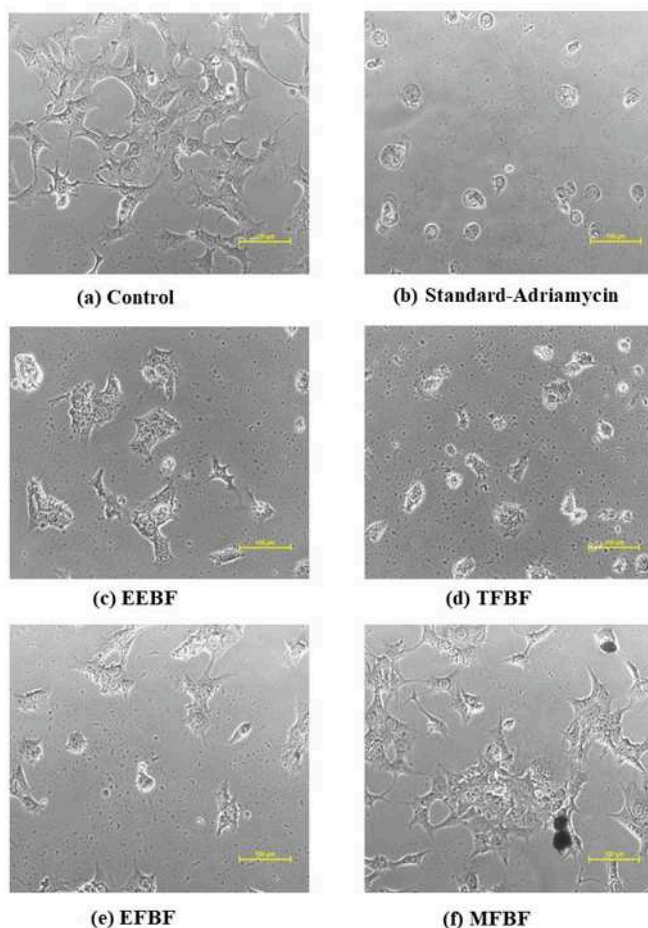


Figure 2: Morphology of (a) control and (b-f) treatment groups of standard and experimental samples at a concentration of $80\mu\text{g}/\text{mL}$ against MCF7 breast cancer cells.

Estimation of the total phenolic and total flavonoid content

The ethanolic leaf extract of *B. foveolata* (EEBF) has reported the highest phenolic and flavonoid content, followed by its methanolic biofraction, as depicted in Table 2.

Determination of *in vitro* free radical scavenging activity

The results of the *in vitro* free radical scavenging activities performed using DPPH, hydrogen peroxide and nitric oxide free radicals have been listed in Table 3. IC_{50} value indicates the concentration of the sample, at which 50% of the free radicals are scavenged.

Determination of *in vitro* anticancer activity

The percent growth control of MCF-7 breast cancer cells observed with the selected experimental samples and standard drug Adriamycin by sulforhodamine B (SRB) assay, have been noted in Table 4. The morphological characteristics of MCF-7 breast cancer cells when treated with $80\mu\text{g}/\text{mL}$ of standard drug Adriamycin and each experimental sam-

ple have been illustrated in Figure 2.

DISCUSSION

Antioxidants are beneficial in reducing oxidative damage to cells and improving an individual's quality of life by preventing or postponing the onset of degenerative diseases like cancer, cardiovascular disease, neural disorders, Alzheimer's disease, mild cognitive impairment and Parkinson's disease (Alam *et al.*, 2013). Oxidative damage to cells may be attributed to the presence of free radicals and antioxidants limit this damage by donating electrons to free radicals and neutralizing them (Lalhinglui and Jagetia, 2018). Endogenous and exogenous antioxidants play an important role in preventing oxidative stress (Bouayed and Bohn, 2010). Plants, vegetables and fruits have been known to be a source of exogenous antioxidants that include phenolics, carotenoids, anthocyanins and tocopherols (Altemimi *et al.*, 2017; Kasote *et al.*, 2015).

The preliminary phytochemical investigations of

the experimental samples of ethanolic leaf extracts of *B. foveolata* Dalzell. (EEBF) and its bio fractions viz. TFBF, EFBF and MFBF revealed the presence of various phytoconstituents. Naturally occurring polyphenolics have gained popularity due to the high antioxidant, anti-inflammatory and anti-carcinogenic potential that help reduce the risk of life-threatening diseases (Zakaria et al., 2011). Flavonoids, tannins and phenolic compounds exhibit antioxidant activity mainly due to their redox properties, since they behave as reducing agents, hydrogen donating agents or singlet oxygen quenching agents (Medini et al., 2014; Patel et al., 2011). Folin ciocalteau method and aluminum chloride method were used to quantitatively estimate the phenolic and flavonoid contents, respectively. EEBF showed the maximum phenolic content and flavonoid content as compared to its biofractions. *In vitro* antioxidant activity was assessed using three radicals viz. DPPH (2,2-diphenyl-1-picrylhydrazyl), hydrogen peroxide and nitric oxide. A lower IC₅₀ value indicates higher scavenging ability of the extract and hence better antioxidant activity (Brighente et al., 2007). DPPH, hydrogen peroxide and nitric oxide free radical scavenging assays were selected as the models to study the *in vitro* antioxidant activity of the ethanolic leaf extract and biofractions of *B. foveolata* Dalzell., as they are ideal methods to screen natural products (Alam et al., 2013; Parul et al., 2013). EEBF has exhibited significant ($p < 0.05$) antioxidant potential in DPPH and nitric oxide radical scavenging methods. Interestingly, the methanolic biofraction (MFBF) displayed significant *in vitro* antioxidant potential in hydrogen peroxide free radical scavenging assay. The antioxidant activity of EEBF and MFBF may thus be attributed to the presence of phenolics and flavonoids.

The anticancer properties of natural foods are possibly due to the additive and synergistic effects of various phytochemicals (Mates et al., 2011). Steroids have the potential to act as cytostatic (antiproliferative) and cytotoxic anticancer agents. Steroidal hormones like estrogen, progesterone and androgen play a crucial role in developing secondary sexual characteristics in females and males. Breast cancer and other steroidal hormone related carcinogenesis mainly occur due to accelerated cell proliferation. Steroidal anticancer drugs act as antihormonal antiproliferative through enzyme inhibition (steroid sulfatase inhibitors, aromatase inhibitors (AI), hydroxysteroid dehydrogenase inhibitors) or receptor inhibition (antiestrogens, antiprogestins). Their cytotoxic action is mainly exhibited by naturally occurring or

semisynthetic compounds through non-hormonal targets (Gupta et al., 2013). Natural triterpenes have proved to possess anti-oxidative, anticancer and chemopreventive effects and show cytotoxicity against tumor cells with low activity towards normal cells (Chudzik et al., 2015).

In vitro anticancer activity was assessed by sulforhodamine B (SRB) assay, using MCF-7 breast cancer cell lines. Amongst the experimental samples subjected to *in vitro* anticancer activity, TFBF showed satisfactory growth inhibition of MCF-7 cells at GI₅₀=73.5+11.96 µg/mL. TFBF was found to be substantively rich in steroids and triterpenoids. Thus, the antiproliferative property of TFBF could be attributed to the presence of steroids, triterpenoids that may also have synergetic effects with other phytoconstituents present.

CONCLUSIONS

The study effectively concludes that the ethanolic leaf extract of *B. foveolata* Dalzell. (EEBF) and its methanolic biofraction (MFBF) have encouraging antioxidant activity as EEBF substantially scavenged DPPH and nitric oxide, while MFBF considerably neutralized hydrogen peroxide free radicals *in vitro*. Notably, the toluene biofraction effectively inhibited the growth of MCF-7 human breast cancer cells in sulforhodamine B assay, thus demonstrating its antiproliferative potential against breast cancer. However, further phytochemical and pharmacological investigation of EEBF and its biofractions are desirable to determine the active compounds and deduce their mechanisms of action.

ACKNOWLEDGEMENT

The contributors are thankful to Anticancer drug screening facility (ACDSF), Advanced Centre for Treatment, Research & Education in Cancer, (ACTREC) at Tata Memorial Centre, Navi Mumbai, India, for carrying out the *in vitro* anticancer activity. The contributors are also grateful to Dr. Satyanarayan S. Hebbar for the authentication of the tree leaf sample and the Principal of Goa College of Pharmacy, Government of Goa, for providing the facilities to perform the research.

Conflict of Interest

The authors declare that they have no conflict of interest for this study.

Funding Support

The authors declare that they have no funding support for this study.

REFERENCES

- Alam, M. N., Bristi, N. J., Rafiquzzaman, M. 2013. Review on *in vivo* and *in vitro* methods evaluation of antioxidant activity. *Saudi Pharmaceutical Journal*, 21(2):143–152.
- Altemimi, A., Lakhssassi, N., Baharlouei, A., Watson, D., Lightfoot, D. 2017. Phytochemicals: Extraction, Isolation, and Identification of Bioactive Compounds from Plant Extracts. *Plants*, 6(4):42–42.
- Bandyopadhyay, S., Thothathri, K., Sharma, B. D. 2005. The genus *Bauhinia* L. (Leguminosae: Caesalpinioideae) in India. *Journal of Economic and Taxonomic Botany*, 29(4):763–801.
- Boora, F., Chirisa, E., Mukanganyama, S. 2014. Evaluation of Nitrite Radical Scavenging Properties of Selected Zimbabwean Plant Extracts and Their Phytoconstituents. *Journal of Food Processing*, 2014:1–7.
- Bouayed, J., Bohn, T. 2010. Exogenous Antioxidants—Double-Edged Swords in Cellular Redox State: Health Beneficial Effects at Physiologic Doses versus Deleterious Effects at High Doses. *Oxidative Medicine and Cellular Longevity*, 3(4):228–237.
- Brighente, I. M. C., Dias, M., Verdi, L. G., Pizzolatti, M. G. 2007. Antioxidant Activity and Total Phenolic Content of Some Brazilian Species. *Pharmaceutical Biology*, 45(2):156–161.
- Chanda, S., Dave, R. 2009. *In vitro* models for antioxidant activity evaluation and some medicinal plants possessing antioxidant properties: An overview. *African Journal of Microbiology Research*, 3(13):981–996.
- Chudzik, M., Korzonek-Szlacheta, I., Król, W. 2015. Triterpenes as Potentially Cytotoxic Compounds. *Molecules*, 20:1610–1625.
- Do, Q. D., Angkawijaya, A. E., Tran-Nguyen, P. L., Huynh, L. H., Soetaredjo, F. E., Ismadji, S., Ju, Y.-H. 2014. Effect of extraction solvent on total phenol content, total flavonoid content, and antioxidant activity of *Limnophila aromatica*. *Journal of Food and Drug Analysis*, 22(3):296–302.
- Filho, V. C. 2009. Chemical composition and biological potential of plants from genus *Bauhinia*. *Phytotherapy Research*, 23(10):1347–1354.
- Gamit, S. B., Sapra, P., Vasava, M. S., Solanki, H. A., Patel, H., Rajani, D. 2018. Antimicrobial and antimalarial activities of some selected ethnomedicinal plants used by tribal communities of tapi district, gujarat, india. *International Research Journal Of Pharmacy*, 9(10):151–156.
- Gupta, A., Kumar, B. S., Negi, A. S. 2013. Current status on development of steroids as anticancer agents. *The Journal of Steroid Biochemistry and Molecular Biology*, 137:242–270.
- Habhu, P. V., Miskin, N., Kulkarni, V. H., Bhat, P., Joshi, A., Bhandarkar, A., Kulkarni, S., Dixit, S. R., Vaijanathappa, J. 2020. Isolation, characterization, and cytotoxic studies of secondary metabolites from the leaves of *Bauhinia foveolata* Dalzell: An endemic tree from the Western Ghats. *India. Journal of Applied Pharmaceutical Science*, 10(03):135–148.
- Kasote, D. M., Katyare, S. S., Hegde, M. V., Bae, H. 2015. Significance of Antioxidant Potential of Plants and its Relevance to Therapeutic Applications. *International Journal of Biological Sciences*, 11(8):982–991.
- Khandelwal, K. R. 2010. Practical Pharmacognosy. *Techniques and Experiments*. 20th Edn. Nirali Prakashan.
- Lalhminghlui, K., Jagetia, G. C. 2018. Evaluation of the free-radical scavenging and antioxidant activities of Chilauni, *Schima wallichii* Korth *in vitro*. *Future Science OA*, 4(2):FSO272–FSO272.
- Lopez, D., Cherigo, L., de Sedas, A., Spadafora, C., Martinez-Luis, S. 2018. Evaluation of antiparasitic, anticancer, antimicrobial and hypoglycemic properties of organic extracts from Panamanian mangrove plants. *Asian Pacific Journal of Tropical Medicine*, 11(1):32–32.
- M., M. N., P., C. J., C., O. Y., D., S. R., L., D. C., A., F. L. 2020. Evaluation of antioxidant potential and total phenolic content of exotic fruits grown in Colombia. *Journal of Applied Pharmaceutical Science*, 10(09):50–58.
- Malvia, S., Bagadi, S. A., Dubey, U. S., Saxena, S. 2017. Epidemiology of breast cancer in Indian women. *Asia-Pacific Journal of Clinical Oncology*, 13(4):289–295.
- Mates, J. M., Segura, J. A., Alonso, F. J., Marquez, J. 2011. Anticancer Antioxidant Regulatory Functions of Phytochemicals. *Current Medicinal Chemistry*, 18(15):2315–2338.
- Mathur, P., Sathishkumar, K., Chaturvedi, M., Das, P., Sudarshan, K. L., Santhappan, S., Nallasamy, V., John, A., Narasimhan, S., Roselind, F. S. 2020. Cancer Statistics, 2020: Report From National Cancer Registry Programme, India. *JCO Global Oncology*, 6(6):1063–1075.
- Meda, A., Lamien, C. E., Romito, M., Millogo, J., Nacoulma, O. G. 2005. Determination of the total phenolic, flavonoid and proline contents in Burkina Fasan honey, as well as their radical scavenging activity. *Food Chemistry*, 91(3):571–577.

- Medeiros, B., Allan, A. L. 2019. Molecular Mechanisms of Breast Cancer Metastasis to the Lung: Clinical and Experimental Perspectives. *International Journal of Molecular Sciences*, 20(9):2272–2272.
- Medini, F., Fellah, H., Ksouri, R., Abdelly, C. 2014. Total phenolic, flavonoid and tannin contents and antioxidant and antimicrobial activities of organic extracts of shoots of the plant *Limonium delicatulum*. *Journal of Taibah University for Science*, 8(3):216–224.
- Mishra, A., Sharma, A. K., Kumar, S., Saxena, A. K., Pandey, A. K. 2013. *Bauhinia variegata* Leaf Extracts Exhibit Considerable Antibacterial, Antioxidant, and Anticancer Activities. *BioMed Research International*, 2013:1–10.
- Mukhopadhyay, D., Dasgupta, P., Roy, D. S., Palchoudhuri, S., Chatterjee, I., Ali, S., Dastidar, S. G. 2016. A Sensitive *In vitro* Spectrophotometric Hydrogen Peroxide Scavenging Assay using 1,10-Phenanthroline. *Free Radicals and Antioxidants*, 6:124–132.
- Oliveira, A. M. F. D., Pinheiro, L. S., Pereira, C. K. S., Matias, W., Gomes, R., Chaves, O. S., Souza, M. D. F. V. D., Almeida, R. N. D. 2012. Simões de Assis, T. 2012. Total phenolic content and antioxidant activity of some Malvaceae family species. *Antioxidants*, 1(1):33–43.
- Parul, R., Kundu, S. K., Saha, P. 2013. *In vitro* nitric oxide scavenging activity of methanol extracts of three Bangladeshi medicinal plants. *The Pharma Innovation- Journal*, 1(12):83–88.
- Patel, D. K., Kumar, R., Prasad, S. K., Hemalatha, S. 2011. *Pedalium murex* Linn (Pedaliaceae) fruits: a comparative antioxidant activity of its different fractions. *Asian Pacific Journal of Tropical Biomedicine*, 1(5):395–400.
- Pham-Huy, L. A., He, H., Pham-Huy, C. 2008. Free radicals, antioxidants in disease and health. *International journal of biomedical science*, 4(2):3614697–3614697.
- Skehan, P., Storeng, R., Scudiero, D., Monks, A., McMahon, J., Vistica, D., Warren, J. T., Bokesch, H., Kenney, S., Boyd, M. R. 1990. New Colorimetric Cytotoxicity Assay for Anticancer-Drug Screening. *JNCI Journal of the National Cancer Institute*, 82(13):1107–1112.
- Vichai, V., Kirtikara, K. 2006. Sulforhodamine B colorimetric assay for cytotoxicity screening. *Nature Protocols*, 1(3):1112–1116.
- Vijayan, R., Joseph, S., Mathew, B. 2019. Anticancer, antimicrobial, antioxidant, and catalytic activities of green-synthesized silver and gold nanoparticles using *Bauhinia purpurea* leaf extract. *Bioprocess and Biosystems Engineering*, 42(2):305–319.
- Zakaria, Z. A., Rofiee, M. S., Teh, L. K., Salleh, M. Z., Sulaiman, M. R., Somchit, M. N. 2011. *Bauhinia purpurea* leaves' extracts exhibited *in vitro* antiproliferative and antioxidant activities. *African Journal of Biotechnology*, 10(1):65–74.



Phytoconstituents from *Piliostigma foveolatum* (Dalzell) Thoth. leaves induce antiproliferative effect, apoptosis, and cell cycle arrest in Hop-62 cells

Liesl Maria Fernandes e Mendonça^a, Arun Bhimrao Joshi^b, Anant Bhandarkar^b, Himanshu Joshi^c and Shrinivas Joshi^d

^aDepartment of Pharmacology, Goa College of Pharmacy, Panaji, Goa, India; ^bDepartment of Pharmacognosy and Phytochemistry, Goa College of Pharmacy, Panaji, Goa, India; ^cDepartment of Pharmacology, College of Pharmacy, Graphic Era Hill University, Bhimtal Campus, Bhimtal, Uttarakhand, India; ^dDepartment of Pharmaceutical Chemistry, S.E.T.'s College of Pharmacy, Dharwad, Karnataka, India

ABSTRACT

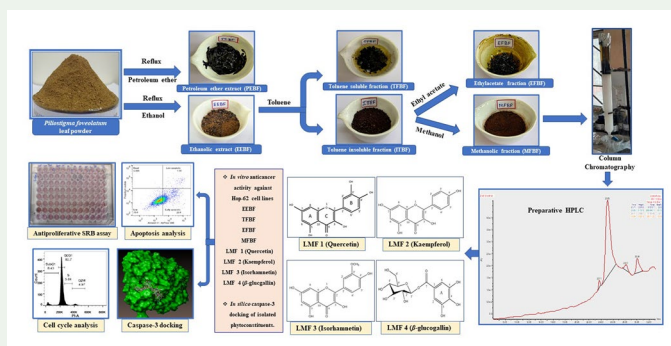
The study evaluated the therapeutic potential of ethanolic leaf extract of *Piliostigma foveolatum* (Dalzell) Thoth. (EEBF), its toluene, ethylacetate, methanol soluble fractions (*viz.* TFBF, EFBF, MFBF), and isolated phytoconstituents against lung cancer. Four compounds were isolated from MFBF by column chromatography and preparative HPLC. Structures were elucidated by IR, ¹³C-NMR, ¹H-NMR, mass spectroscopy and identified as Quercetin, Kaempferol, Isorhamnetin, and β -glucogallin. EEBF and its biofractions exhibited remarkable antiproliferative activity with $GI_{50} < 85 \mu\text{g/mL}$, while isolated Quercetin, Kaempferol, Isorhamnetin, and β -Glucogallin displayed GI_{50} values of $56.15 \pm 1.16 \mu\text{M}$, $68.41 \pm 3.98 \mu\text{M}$, $55.08 \pm 0.57 \mu\text{M}$ and $58.99 \pm 12.39 \mu\text{M}$ respectively. MFBF demonstrated significant apoptotic activity with $42.24 \pm 0.57\%$ cells in early and $4.61 \pm 0.88\%$ cells in late apoptosis comparable to standard Doxorubicin. Kaempferol exhibited $23.03 \pm 0.37\%$ cells in early and $2.11 \pm 0.55\%$ cells in late apoptosis, arresting Hop-62 cells in S-phase. *In silico* molecular docking, revealed that isolated constituents effectively bound to the same binding site of caspase-3 as Doxorubicin, highlighting their apoptotic mode of action.

ARTICLE HISTORY


Received 26 December 2022
Accepted 25 March 2023

KEYWORDS

Phytoconstituents;
preparative HPLC;
antiproliferative;
apoptosis; Hop-62;
caspase-3



CONTACT Liesl Maria Fernandes e Mendonça  lieslpharma@gmail.com

 Supplemental data for this article can be accessed online at <https://doi.org/10.1080/14786419.2023.2197228>.

© 2023 Informa UK Limited, trading as Taylor & Francis Group

1. Introduction

Lung cancer continues to be an alarming pandemic contributing to several co-morbidities, loss of millions of lives with 1.80 million deaths reported worldwide in 2020 (Thandra et al. 2021). Therapeutics from herbal sources are being continuously screened as prospective anticancer agents with an aim of improving the quality of life of the individual undergoing cancer treatment. Several plant species of the genus *Bauhinia* have been used in folk medicine to treat different kinds of pathologies and possess a variety of pharmacological activities viz. antioxidant, antimicrobial and cytotoxic effects (Negi et al. 2012; Rahman et al. 2016; Vijayan et al. 2019). *Piliostigma foveolatum* (Dalzell) Thoth. (Syn. *Bauhinia foveolata* Dalzell.) belonging to the family Fabaceae, is a tropical tree found along the lush semi-evergreen forests of the Indian Sahyadris (Bandyopadhyay et al. 2005). It has large porous leaves and is endemic to the Indian western ghats (Habhu et al. 2020). Limited research has been carried out on this species with key developments relating to antibacterial activity against *Streptococcus pyogenes* and antimalarial activity against *Plasmodium falciparum* by the acetone fraction and ethyl acetate extract respectively (Gamit et al. 2018), exploration of the cytotoxic principles of odoratin-7-glucoside and quercetin against HT-29 and HCT-15 human colon cancer cell lines (Habhu et al. 2020) and toluene fraction of the ethanolic leaf extract against MCF-7 human breast cancer cells with significant *in vitro* antioxidant activities (Mendonça et al. 2021). Based on the presence of substantial amounts of flavonoids and phenolics in *Piliostigma foveolatum* (Dalzell) Thoth, its antioxidant profile, and its ability to inhibit the proliferation of cancerous cells in breast, the current study was undertaken to evaluate and explore the anti-proliferative, apoptotic and cell cycle arrest potential of the ethanolic leaf extract of *Piliostigma foveolatum* (Dalzell) Thoth. (EEBF), its toluene (TFBF), ethyl acetate (EFBF) and methanol (MFBF) soluble biofractions along with the isolated phytoconstituents against lung cancer using Hop-62 cell lines.

2. Results and discussion

The yield of the ethanolic leaf extract of *Piliostigma foveolatum* (Dalzell) Thoth. was reported to be 151.29g while that of its biofractions TFBF, EFBF and MFBF were 27.99g, 13.79g and 28.68g respectively. The phytochemical analysis reported by Mendonça et al. 2021, revealed that the leaf extract and its methanolic biofraction contained considerable amounts of flavonoids, alkaloids, glycosides, tannins, phenolics etc. Since MFBF exhibited a remarkable ability to scavenge the DPPH, nitric oxide, and hydrogen peroxide free radicals, it was further subjected to liquid chromatography-mass spectroscopy.

Column chromatography resulted in the isolation of column fraction LMF, which upon further purification by preparative HPLC led to the isolation of four compounds LMF1, LMF2, LMF3 and LMF4 (Supplementary material, Figure S1), the yields of which were 21.1 mg, 242.6 mg, 21.7 mg, and 19.1 mg respectively. The structures of the isolated compounds were elucidated by IR, ¹H-NMR, ¹³C-NMR and mass spectroscopic methods and identified as Quercetin (LMF1), Kaempferol (LMF2), Isorhamnetin (LMF3) and β -glucogallin (Syn. 1-O-galloyl- β -D-glucose) (LMF4) respectively. The spectral data of the isolated compounds has been listed in the supplementary material.

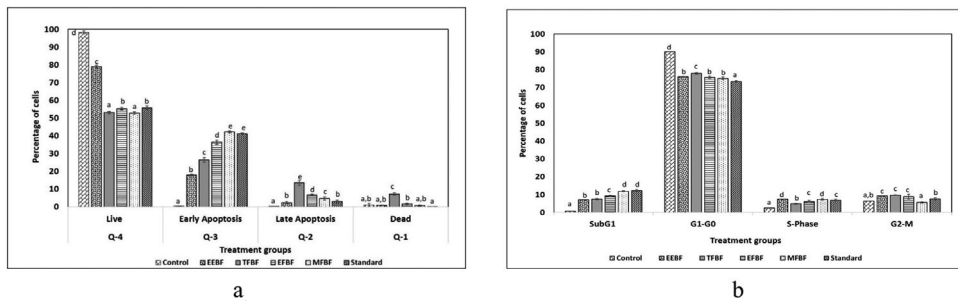


Figure 1. Apoptosis (a) and cell cycle (b) analysis of EEBF and biofractions against Hop-62 cells.

In vitro anticancer activity of the leaf extract, its biofractions, and isolated phytoconstituents was evaluated using the Sulforhodamine B antiproliferative assay and subsequently investigated for apoptosis and cell cycle arrest using flow cytometry after staining with Annexin V-FITC and/or Propidium Iodide.

TFBF, EEBF, EFBF and MFBF exhibited substantial antiproliferative activity against the Hop-62 cells, with GI_{50} values of $23.7 \pm 2.54 \mu\text{g/mL}$, $54.8 \pm 3.08 \mu\text{g/mL}$, $74.4 \pm 5.43 \mu\text{g/mL}$, and $84.9 \pm 1.45 \mu\text{g/mL}$ respectively. Treatment with EEBF and its biofractions at their GI_{50} concentrations, induced apoptosis of Hop-62 cells. MFBF exhibited $42.24 \pm 0.57\%$ cells in early apoptosis, while $4.61 \pm 0.88\%$ in late apoptosis and $0.61 \pm 0.40\%$ in necrosis stage, that was comparable to standard Doxorubicin (Figures 1 and S19). Cell cycle analysis depicted that MFBF showed a significant increase in cells from $0.68 \pm 0.13\%$ to $11.95 \pm 0.33\%$ in the sub- G_1 phase and $2.57 \pm 0.52\%$ to $7.35 \pm 0.39\%$ in S-phase, while decrease in cells from $90.13 \pm 0.55\%$ to $75.08 \pm 0.79\%$ in the G_1 - G_0 phase and $6.55 \pm 0.40\%$ to $5.63 \pm 0.27\%$ in the G_2 -M phase as against the control (Figures 1 and S20), indicating that it induces apoptosis and cell cycle arrest of Hop-62 cells in the S phase.

Amongst the isolated phytoconstituents investigated, all four compounds *viz.* LMF1 (Quercetin), LMF2 (Kaempferol), LMF3 (Isorhamnetin) and LMF4 (β -glucogallin) displayed significant Hop-62 cell antiproliferative activity with GI_{50} values of $56.15 \pm 1.16 \mu\text{M}$, $68.41 \pm 3.98 \mu\text{M}$, $55.08 \pm 0.57 \mu\text{M}$ and $58.99 \pm 12.39 \mu\text{M}$ respectively as against the standard doxorubicin with GI_{50} value of $19.49 \pm 1.70 \mu\text{M}$. Apoptosis study of the isolated compounds at their GI_{50} concentrations showed that all compounds induced substantial apoptotic activity. LMF2 (Kaempferol) exhibited considerable apoptotic activity with $23.03 \pm 0.37\%$ cells experiencing early apoptosis, $2.11 \pm 0.55\%$ cells in late apoptosis and $0.51 \pm 0.37\%$ cells in necrotic stage (Figures 2 and S21), as compared to other compounds tested. In cell cycle analysis, all the compounds showed an increase in the number of cells in the sub- G_1 phase, while a decrease in the number of cells in the G_1 - G_0 phase as compared to the control, thus indicating induction of apoptosis-mediated cell death. The percentage of cells in the S-phase had increased from $2.57 \pm 0.52\%$ to $4.45 \pm 0.33\%$, $6.55 \pm 0.57\%$, $5.60 \pm 0.34\%$ and $5.54 \pm 0.40\%$ with quercetin, kaempferol, isorhamnetin and β -glucogallin respectively, with a decrease in cellular percentage in G_2 -M phase (Figures 2 and S22). It can hence be inferred that the isolated constituents contribute to the cell cycle arrest at the S-phase checkpoint.

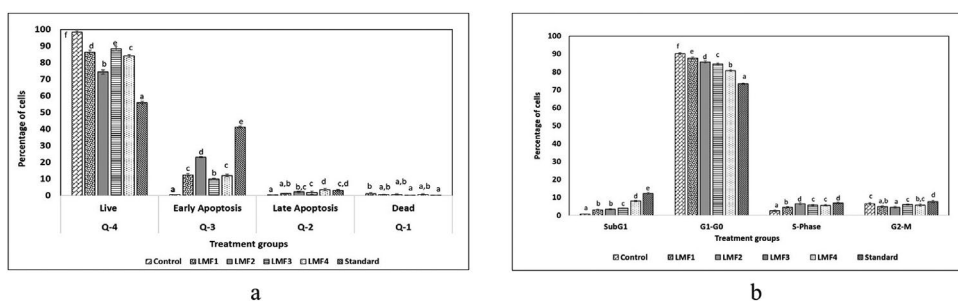


Figure 2. Apoptosis (a) and cell cycle (b) analysis of MFBF isolates against Hop-62 cells.

Thus, the phytoconstituents may have induced activation of caspase-3, caspase-7, caspase-6, caspase-9, or caused up-regulation of pro-apoptotic genes like Bax, p53 etc. or down-regulation of expression of anti-apoptotic genes like Bcl-2, cyclinD1, which could facilitate apoptosis and/or trigger cell cycle arrest (Goda et al. 2021).

In silico molecular docking studies were performed to investigate the probable mechanism of action and intermolecular interactions of the isolated compounds with the crystal structure of human caspase-3 enzyme (PDB ID 1QX3, 1.90 Å, X-ray Diffraction), using the surflex-dock programme of sybyl-X 2.0 software. Surflex-Dock studies revealed that all four isolated compounds showed the same type of interaction with amino acid residues (PHE250, SER209, ARG207, TYR204) of the active site of the human caspase-3 enzyme, as that of the standard drug doxorubicin (Figure S23). The detailed intermolecular interactions of all isolated compounds and standard drug doxorubicin has been elaborately explained in the [supplementary data](#), while the predicted binding energies of the compounds are listed in [Table S9](#). All the compounds exhibited a significant docking score against the enzyme, with a consensus score in the range 4.38–2.66, indicating the summary of all forces of interaction between compounds and the enzyme. Quercetin demonstrated a consensus score of 3.92, while kaempferol, isorhamnetin and β -glucogallin exhibited a consensus score of 2.66, 4.04 and 4.38 respectively as against doxorubicin, that displayed a consensus score of 6.64 ([Table S9](#)) indicating their apoptotic mode of action *via* the caspase pathway (Eom et al. 2005).

Since apoptosis causes cellular death by non-inflammatory processes, the enriched bioactive components of *Piliostigma foveolatum* (Dalzell) Thoth. leaves may be regarded as safe and effective therapeutics for lung cancer therapy (Tilekar et al. 2020).

3. Experimental

The materials and methods adopted for the study have been described in the [Supplementary material](#).

4. Conclusion

The extract, biofractions and phytoconstituents quercetin, kaempferol, isorhamnetin and β -glucogallin isolated from MFBF have shown to possess significant anti-proliferative effects against Hop-62 cells *via* apoptotic and cell cycle arrest pathways, accrediting these as potential therapeutic candidates in management of lung cancer.

Acknowledgements

The authors are thankful to Dr. Satyanarayan S. Hebbar for the authentication of the leaf sample, Principal of Goa College of Pharmacy, Government of Goa and authorities of Central research laboratory, Maratha Mandal's NGH Institute of dental sciences and research center- Belagavi, Honeychem Pharma Pvt. Ltd.- Bengaluru and Sophisticated Analytical Instrumentation Facility, Punjab University-Chandigarh for facilitating the research.

Disclosure statement

The authors declare no conflicts of interest.

Funding

The author(s) reported there is no funding associated with the work featured in this article.

References

- Bandyopadhyay S, Thothathri K, Sharma BD. 2005. The genus *Bauhinia* L. (Leguminosae: caesalpinioideae) in India. *J Econ Taxon Bot.* 29(4):763–801.
- Eom YW, Kim MI, Park SS, Goo MJ, Kwon HJ, Sohn S, Kim WH, Yoon G, Choi KS. 2005. Two distinct modes of cell death induced by doxorubicin: apoptosis and cell death through mitotic catastrophe accompanied by senescence-like phenotype. *Oncogene.* 24(30):4765–4777.
- Gamit SB, Sapra P, Vasava MS, Solanki HA, Patel H, Rajani D. 2018. Antimicrobial and antimarial activities of some selected ethno-medicinal plants used by tribal communities of Tapi district, Gujarat, India. *Int Res J Pharm.* 9(10):151–156.
- Goda MS, Nafie MS, Awad BM, Abdel-Kader MS, Ibrahim AK, Badr JM, Eltamany EE. 2021. *In vitro* and *in vivo* studies of anti-lung cancer activity of *Artemesia judaica* L. crude extract combined with LC-MS/MS metabolic profiling, docking simulation and HPLC-DAD quantification. *Antioxidants.* 11(1):17.
- Habbu PV, Miskin N, Kulkarni VH, Bhat P, Joshi A, Bhandarkar A, Kulkarni S, Dixit SR, Vaijanathappa J. 2020. Isolation, characterization, and cytotoxic studies of secondary metabolites from the leaves of *Bauhinia foveolata* Dalzell: an endemic tree from the Western Ghats, India. *J Appl Pharm Sci.* 10(3):135–148.
- Mendonça LM, Joshi AB, Bhandarkar AV, Joshi H. 2021. Evaluation of antioxidant property and anticancer prospective of the leaf extract and biofractions of *Bauhinia foveolata* Dalzell - A native of the Indian Western Ghats. *Int J Res Pharm Sci.* 12(3):1886–1894.
- Negi A, Sharma N, Singh MF. 2012. Spectrum of pharmacological activities from *Bauhinia variegata*: a review. *J Pharm Res.* 5(2):792–797.
- Rahman MA, Akhtar J, Arshad M. 2016. Evaluation of cytotoxic potential and apoptotic effect of a methanolic extract of *Bauhinia racemosa* Lam. against a human cancer cell line, HeLa. *Eur J Integr Med.* 8(4):513–518.
- Thandra KC, Barsouk A, Saginala K, Aluru JS, Barsouk A. 2021. Epidemiology of lung cancer. *Contemp Oncol.* 25(1):45–52.
- Tilekar K, Upadhyay N, Jänsch N, Schweipert M, Mrowka P, Meyer-Almes FJ, Ramaa CS. 2020. Discovery of 5-naphthylidene-2, 4-thiazolidinedione derivatives as selective HDAC8 inhibitors and evaluation of their cytotoxic effects in leukemic cell lines. *Bioorg Chem.* 95:103522.
- Vijayan R, Joseph S, Mathew B. 2019. Anticancer, antimicrobial, antioxidant, and catalytic activities of green-synthesized silver and gold nanoparticles using *Bauhinia purpurea* leaf extract. *Bioprocess Biosyst Eng.* 42(2):305–319.

Date: November 18, 2022

Research Journal of Pharmacy and Technology

Paper ID:22726053524366880

Author's Name:Liesl Maria Fernandes e Mendonca, Arun Bhimrao Joshi, Dr. Anant Bhandarkar, Himanshu Joshi

Paper Title: Antioxidant, Antiproliferative, Pro-apoptotic and cell cycle arrest properties of crude extract and biofractions of Hybanthus enneaspermus Linn. to combat breast cancer.



Acceptance of Manuscript

With reference to your article titled '**Antioxidant, Antiproliferative, Pro-apoptotic and cell cycle arrest properties of crude extract and biofractions of Hybanthus enneaspermus Linn. to combat breast cancer.**' Author by **Liesl Maria Fernandes e Mendonca, Arun Bhimrao Joshi, Dr. Anant Bhandarkar, Himanshu Joshi**. We wish to bring to your kind notice the following:

- We acknowledge the receipt of the above mentioned article.
- The above mentioned article has been sent to the reviewer of expert comments.
- The above mentioned article have been accepted for publication in Year : 2023 , Vol : 16 , Issue : 9 of the journal.

Thanking you for submission of manuscript.

Yours sincerely,



(Signature)
Editor in Chief

Note: -

1. To verify the originality of this certificate please visit the following link:

http://www.anpublication.org/Download_Acceptance.aspx?PID=22726053524366880



ANNEXURE - VI

PRESENTATIONS

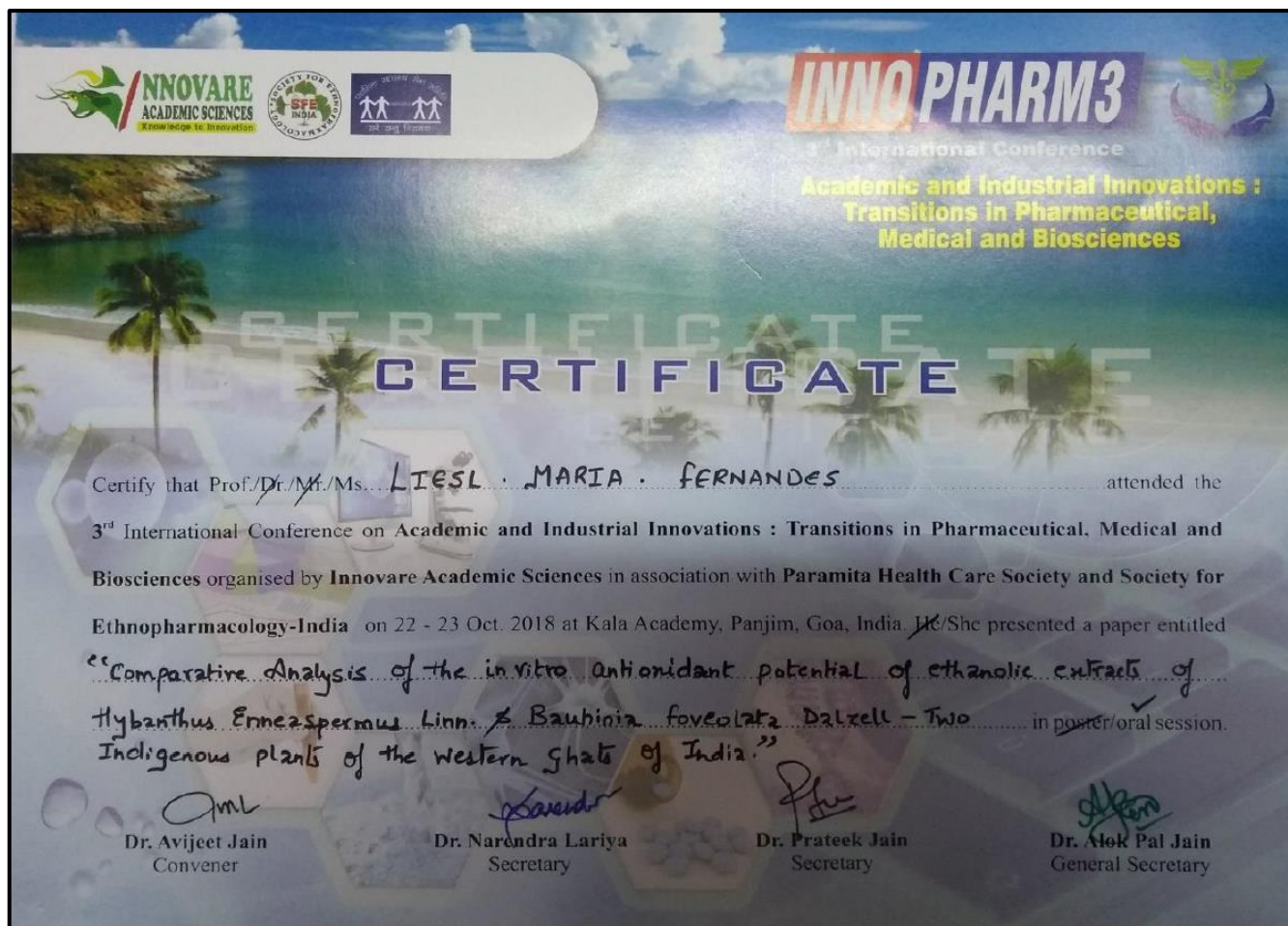
ANNEXURE VI

PRESENTATIONS - ABSTRACTS PUBLISHED AT INTERNATIONAL CONFERENCES

1. Oral presentation titled ‘Comparative analysis of the *in vitro* antioxidant potential of ethanolic extracts of *Hybanthus enneaspermus* Linn. and *Bauhinia foveolata* Dalzell.- two indigenous plants of the Western Ghats of India’ at the 3rd International Conference on Academic and Industrial Innovations: Transitions in Pharmaceutical, medical and biosciences (INNOPHARM3) organized by Innovare Academic sciences in association with Paramita healthcare society and society for Ethnopharmacology India on 22nd and 23rd October 2018 at Kala Academy, Panaji-Goa.
2. Research showcase poster presentation titled “Free radical scavenging activity of ethanolic leaf extract of *Bauhinia foveolata* Dalzell. and its biofractions” during 3rd Annual International Conference on Intellectual Property conducted by G-CEIP and Goa College of Pharmacy on 15th and 16th November 2018 at Goa College of Pharmacy, Panaji- Goa.
3. Research showcase poster presentation titled “*In vitro* anticancer activity of *Bauhinia foveolata* Dalzell against HOP-62 cell lines” at the 6th Annual International Conference on Intellectual Property Rights to be held on 1st and 2nd December, 2021, organized by GCEIP and Goa College of Pharmacy, at Goa College of Pharmacy, Panaji.
4. Oral presentation on “Anxiolytic activity of *Hybanthus enneaspermus* Linn. and its effect on antioxidant enzymes and neurotransmitters on rats’ brain” at the 9th International conference on Society of Ethnopharmacology held from 22nd - 24th April 2022 at JSS College of Pharmacy, Mysuru, JSSAHER, Karnataka, India.
5. Best paper in oral presentation on the topic titled “Isolation, characterization, *in silico* and *in vitro* anti-breast cancer evaluation of phytoconstituents from *Hybanthus enneaspermus* Linn. at the International Conference on Medicinal Plants, Health and

Quality Life - 2022, held on 25th and 26th November 2022 at Graphic Era Hill University, GEHU, Bhimtal, India. Recipient of the travel grant award for significant contribution to the field of pharmaceutical research.









G-CEIP



Certificate of Participation

Presented to

LEISL M.F. MENDONCA

**in recognition of your participation in the
"Research Showcase Presentation (RSP)" at the
6th Annual International Conference on IPR
Global Trends in IPR: Patenting & Beyond !!**

TITLED: "IN VITRO ANTICANCER ACTIVITY OF BAUHINIA FOVEOLATA D AGAINST HOP-62 CELL LINES"
held on December 1-2, 2021 at Goa College of Pharmacy, Panaji-Goa

Umesh Banakar

Umesh Banakar, Ph.D.
Professor

Dr. Gopal Krishna Rao

Dr. Gopal Krishna Rao
Principal



